Digitized by the Internet Archive
in 2023 with funding from
Kahle/Austin Foundation

https://archive.org/details/contributionsfro0007unse_a9r6

Carnegie Institution of Washington

CONTRIBUTIONS

FROM THE

MOUNT WILSON SOLAR OBSERVATORY

VOLUME VII

NOS. 124–147

WITH NINETEEN PLATES

SEPTEMBER, 1916—FEBRUARY, 1918

B

UNIVERSITY OF ARIZONA
LIBRARY

v. 7

CONTENTS

NO. PAGE

124. THE VARIATIONS IN SPECTRAL TYPE OF TWENTY CEPHEID VARIABLES. *Harlow Shapley* 1

125. PRELIMINARY OBSERVATIONS OF THE SPECTRA OF CALCIUM AND IRON WHEN PRODUCED BY CATHODO-LUMINESCENCE. *Arthur S. King and Edna Carter* 21

126. STUDIES BASED ON THE COLORS AND MAGNITUDES IN STELLAR CLUSTERS. FOURTH PAPER: THE GALACTIC CLUSTER MESSIER 11. *Harlow Shapley* 29

127. HIND'S VARIABLE NEBULA N.G.C. 1555. *Francis G. Pease* . . 47

128. THE COLOR-CURVE OF XZ CYGNI. *Martha Betz Shapley* . . 51

129. ON THE DISTRIBUTION OF STARS IN TWELVE GLOBULAR CLUSTERS. *Francis G. Pease* 59

130. A STUDY WITH THE ELECTRIC FURNACE OF THE ANOMALOUS DISPERSION OF METALLIC VAPORS. *Arthur S. King* . . . 79

131. THE RELATIONSHIP OF STELLAR MOTIONS TO ABSOLUTE MAGNITUDE. *Walter S. Adams and Gustaf Strömberg* 95

132. PHOTOGRAPHS OF NEBULAE WITH THE 60-INCH REFLECTOR 1911–1916. *Francis G. Pease* 109

133. STUDIES BASED ON THE COLORS AND MAGNITUDES IN STELLAR CLUSTERS. FIFTH PAPER: COLOR-INDICES OF STARS IN THE GALACTIC CLOUDS. *Harlow Shapley* 141

134. A METHOD OF INVESTIGATING THE STARK EFFECT FOR METALS, WITH RESULTS FOR CHROMIUM. *J. A. Anderson* . . . 153

135. A DETERMINATION OF THE GALACTIC CONDENSATION FROM CERTAIN ZONES OF THE "ASTROGRAPHIC CATALOGUE." *Frederick H. Seares* 167

136. THE PHOTOGRAPHIC DETERMINATION OF STELLAR PARALLAXES WITH THE 60-INCH REFLECTOR. SECOND SERIES. *Adriaan van Maanen* 189

137. THE ELIMINATION OF POLE-EFFECT FROM THE SOURCE FOR SECONDARY STANDARDS OF WAVE-LENGTH. *Charles E. St. John and Harold D. Babcock* 231

175584

CONTENTS

NO. PAGE

138. THE PRINCIPLE OF GENERALIZED RELATIVITY AND THE DISPLACEMENT OF FRAUNHOFER LINES TOWARD THE RED. *Charles E. St. John* 261

139. THE SPIRAL OF OBSCURATION. *Frederick H. Seares* 279

140. NOTES ON THE COLOR-CURVE AND LIGHT-ELEMENTS OF W URSAE MAJORIS. *Harlow Shapley and J. van der Bilt* 285

141. SOLAR HYDROGEN "BOMBS." *Ferdinand Ellerman* 295

142. THE LUMINOSITIES AND PARALLAXES OF FIVE HUNDRED STARS. *Walter S. Adams and A. H. Joy* 299

143. BAXANDALL'S EXPLANATION OF AN "ABNORMAL" SOLAR SPECTRUM. *George E. Hale* 327

144. A DETERMINATION OF THE SOLAR MOTION AND THE STREAM-MOTION FROM RADIAL VELOCITIES AND ABSOLUTE MAGNITUDES OF STARS OF LATE SPECTRAL TYPES. *Gustaf Strömberg* 333

145. NOTE ON THE CEPHEID VARIABLE SU CASSIOPEIAE. *Walter S. Adams and Harlow Shapley* 365

146. RADIAL VELOCITY AND ABSOLUTE MAGNITUDE: COMMENTS ON PROFESSOR PERRINE'S ARTICLE. *Walter S. Adams and Gustaf Strömberg* 371

147. ON THE PARALLAXES AND THE MOTION OF THE BRIGHTER GALACTIC HELIUM STARS BETWEEN GALACTIC LONGITUDES 150° AND 216°. *J. C. Kapteyn* 375

LIST OF PLATES

NO. FACING PAGE

I. Hind's Variable Nebula N.G.C. 1555 50

II. Four Successive Exposures on Messier 13 . . . 63

III. Anomalous Dispersion of Titanium Lines 83

IV. Anomalous Dispersion of λ 4227 of Calcium and of Three Chromium Lines at Four Stages of Decreasing Temperatures, Showing Inverted Effect for λ 4227 at Highest Temperature 83

V. Anomalous Dispersion in Line and Band Spectra; (*a*) Manganese Lines $\lambda\lambda$ 4031–35; (*b*) D Lines (Low Vapor-Density), Showing Inversion of Effect Due to Higher Temperature; (*c*) Opposite Effects Produced Simultaneously for Calcium Lines K and λ 4227; (*d*) Anomalous Dispersion for "Cyanogen" Band with Principal Head at λ 3883 83

VI. (*a*) N.G.C. 1501; (*b*) N.G.C. 1535; (*c*) N.G.C. 2022; (*d*) N.G.C. 2371–2; (*e*) and (*f*) N.G.C. 2392 . . . 110

VII. (*a*) N.G.C. 6309; (*b*) N.G.C. 6543; (*c*) N.G.C. 6818; (*d*) N.G.C. 7008; (*e*) N.G.C. 7009; (*f*) N.G.C. 7662 . 110

VIII. (*a*) N.G.C. 1579; (*b*) N.G.C. 4449 110

IX. (*a*) N.G.C. 205; (*b*) N.G.C. 278; (*c*) N.G.C. 1068; (*d*) N.G.C. 1068; (*e*) N.G.C. 972; (*f*) N.G.C. 2681 110

X. (*a*) N.G.C. 2841; (*b*) N.G.C. 2976; (*c*) N.G.C. 2403 . . 110

XI. (*a*) N.G.C. 3115; (*b*) N.G.C. 3593; (*c*) N.G.C. 4216; (*d*) N.G.C. 4567–8; (*e*) N.G.C. 4594 110

XII. N.G.C. 4736. Exposure *a*, 5^{m}; *b*, 10^{m}; *c*, 20^{m}; *d*, 40^{m}; *e*, 225^{m} 110

XIII. (*a*) N.G.C. 5383; (*b*) N.G.C. 5383; (*c*) N.G.C. 5544–5; (*d*) N.G.C. 5746; (*e*) N.G.C. 5866 110

XIV. (*a*) N.G.C. 6070; (*b*) N.G.C. 6555; (*c*) N.G.C. 7217 . . 110

XV. Stark Effect. (*a*) Hγ; (*b*) Chromium Groups $\lambda\lambda$ 5005, 5027, 5055; (*c*) Chromium Groups at $\lambda\lambda$ 4098, 4111, 4129; (*d*) Chromium Groups at $\lambda\lambda$ 5276, 5298, 5329; (*c′*, *d′*) Drawings Representing Groups in *c* and *d*, A–B being the Negative Glow, C the Surface of the Cathode 164

LIST OF PLATES

NO. FACING PAGE

XVI. Distribution of Luminosity in 12-mm, 5-amp Pfund Arc (*a*) and in International Arc (*b*) with Superposed Images of Defining Diaphragm. Arc Lamp for Precision Observations 237

XVII. Comparative Sharpness of Lines from International Arc (*a*) and Proposed Arc (*b*); 15-mm Etalon . . . 252

XVIII. (*a*) and (*b*) Appearance of the Hα Line in an Active Sun-Spot Region, Showing the Bands of "Bombs" and the Distortions of the Line; (*c*) Spectrum of a "Bomb" (Close to the Dark Hα Line) Superposed on the Spectrum of a Facula; (*d*) Appearance of Reversals in an Active Region 297

XIX. Variation with Temperature of Lines in Furnace Spectrum of Strontium; (*a*) Barium Arc; (*b–e*) Furnace Spectra of Strontium; (*f*) Strontium Arc 322

Contributions from the Mount Wilson Solar Observatory, No. 124
Reprinted from the *Astrophysical Journal*, Vol. XLIV, pp. 273–291, 1916

THE VARIATIONS IN SPECTRAL TYPE OF TWENTY CEPHEID VARIABLES

By HARLOW SHAPLEY

A considerable amount of material relative to the spectral types of variable stars of the Cepheid class has been accumulated at the Mount Wilson Observatory during the past year, chiefly with the aid of the 10-inch photographic telescope. Earlier work on some of these stars at the Lick, Harvard College,[1] and Pulkova Observatories had shown or suggested variations in certain characteristics of the spectra. The data collected in the present paper, however, indicate that distinct changes in spectral type, accompanying regularly the periodic variations in light and apparent velocity, constitute one of the general and fundamental properties of Cepheid variables. A statement of the Cepheid problem at the time it was taken up at Mount Wilson is outlined in *Contribution* No. 92,[2] together with a summarized account of the most relevant previous work. The significance of spectral variations in the interpretation of variability in light and velocity is noted in the same article and in subsequent papers on the light-curves and spectra of Cepheid variables.[3] The following pages will be devoted to the observations of the spectra of individual stars.

A list of all the Cepheids for which definite variations of spectral type have been observed is given in Table I. The positions in the second and third columns are from *Harvard Annals*, **56**, No. 6, Table VIII. The data for the light-variations are taken from the same source except that the magnitudes for RT Aurigae are by

---

[1] See, for instance, the remark by Miss Cannon on the spectrum of δ Cephei in *Harvard Annals*, **56**, 110, 1912.

[2] *Astrophysical Journal*, **40**, 448, 1914.

[3] *Mt. Wilson Contr.*, Nos. 104, 112; *Astrophysical Journal*, **42**, 148, 1915; **43**, 217, 1916; *Mt. Wilson Communications*, Nos. 14, 21, 22, 27; *Proceedings of the National Academy of Sciences*, **1**, 452, 1915; **2**, 132, 136, 208, 1916.

Kiess,[1] those for RR Lyrae by Shapley,[2] and those for RS Boötis and XZ Cygni from Hartwig's *Ephemeris*.[3] Precise information as to the maximum magnitude and range of variation of these stars, even of the much observed brighter ones, is unfortunately not available.[4] Widely differing values are given in the catalogues by different observers. The uncertainty arises partly from probable irregularities in the variations, but chiefly because most of the light-observations have been naked-eye comparisons with stars for which various estimates of magnitudes have been adopted. The values in the fourth and fifth columns, therefore, serve in most cases only to indicate approximately the visual brightness and range of light-change. The point is of some importance in that it shows the

TABLE I

LIST OF SPECTRAL VARIABLES

STAR	R.A. 1900	DECL. 1900	VISUAL LIGHT		PERIOD	SPECTRAL VARIATION	NO. OF PHOTOGRAPHS
			Maximum	Range			
TU Cassiopeiae..	$0^{h}20^{m}9$	$+50°44'$	$7^{M}2$	$1^{M}4$	$2^{d}139$	F1–F8	5
SU Cassiopeiae..	2 43.0	+68 28	5.9	0.4	1.950	A8–F5	24
SZ Tauri......	4 31.4	+18 20	7.2	0.5	3.149	A9–F7	13
T Monocerotis.	6 19.8	+ 7 8	5.7	1.1	27.012	F5–G2	9
RT Aurigae.....	6 22.1	+30 34	5.1	0.9	3.728	A7–G1	30
W Geminorum.	6 29.2	+15 24	6.7	0.8	7.916	F2–G1	9
RS Boötis......	14 29.2	+32 11	9.2	1.0	0.377	B8–F0	13
X Sagittarii...	17 41.3	−27 48	4.4	0.6	7.012	F1–G5	24
Y Ophiuchi....	17 47.3	− 6 7	6.1	0.4	17.113	F5–G3	8
W Sagittarii...	17 58.6	−29 35	4.3	0.8	7.595	A8–G2	25
Y Sagittarii...	18 15.5	−18 54	5.4	0.8	5.773	F4–G4	10
RR Lyrae......	19 22.3	+42 36	6.8	0.9	0.567	B9–F2	17
U Aquilae.....	19 24.0	− 7 15	6.2	0.7	7.024	F6–G2	4
XZ Cygni......	19 30.4	+56 10	8.7	0.6	0.467	A0–A6	2
U Vulpeculae..	19 32.3	+20 7	6.5	1.1	7.990	F7–G5	8
SU Cygni......	19 40.8	+29 1	6.2	0.8	3.846	A6–F7	17
η Aquilae.....	19 47.4	+ 0 45	3.7	0.8	7.176	A8–G5	29
S Sagittae....	19 51.5	+16 22	5.5	0.6	8.382	F4–G3	18
T Vulpeculae..	20 47.2	+27 52	5.5	0.6	4.436	A9–G1	17
δ Cephei.....	22 25.4	+57 54	3.5	0.8	5.366	F0–G2	46

---

[1] *Laws Observatory Bulletin*, No. 23, 1915.

[2] *Mt. Wilson Contr.*, No. 112; *Astrophysical Journal*, **43**, 217, 1916.

[3] *Vierteljahrsschrift der Astronomischen Gesellschaft*, **49**, 287, 301, 1914.

[4] Exceptions are δ Cephei, RR Lyrae, and perhaps a few others. See note to Table VIII below.

futility of attempting at present to study the relation of range in light to range in spectral variation. The data are sufficient, however, to show the relation of spectral type to period (which had already been noted for a larger number of stars on the basis of the Harvard classification),[1] although in a number of cases the extreme range of spectrum is not recorded when observations near maximum or minimum light are wanting.

Of the 328 photographs of spectra used in deriving the results for the stars in Table I, 311 were made by the writer with the 10-inch portrait lens and objective prism. The remainder were made with the 60-inch reflector—13 by Mr. Pease and 4 by Mr. Adams. For nearly all the work with the 10-inch, a 15° prism is employed. The refracting edge is set perpendicular to the hour circle, and the spectrum, drifting in right ascension, is widened as desired by adjusting the driving clock. For some of the brighter variables, a small 30° prism was used on a few nights in conjunction with the 15° prism. Such instances are designated by the note "45°" in the columns of remarks in Tables III–XIX. Except in the cases noted, all photographs are on Seed "27" plates.

With the single prism the dispersion is $H\beta - H\varepsilon = 5.2$ mm; for the two prisms $H\beta - H\varepsilon = 12$ mm. The uncertainty of a determination of spectral type with the lower dispersion is one- or two-tenths of a spectral interval, but there may be a small systematic difference between my classification and that made at Harvard. So far as possible, however, the choice of criteria for type has been based upon the classifications of the *Draper Catalogue*.

In preparing the material for tabular presentation, all the spectra were classified before phases were computed. This procedure lessens the possibility of errors of prejudice where small changes are concerned. Only two or three discordant results remained after some errors of identification were eliminated, and such discordances may be due to irregularities in the variations or to erroneous light-elements.

As remarked in earlier papers, the changes observed in the spectra of these stars are between known, normal types. No peculiarities appear other than those to be expected in the spectra of stars of very high luminosity. Possible exceptions are the spectrum of W Geminorum, also noted at Harvard,[1] and the occasional unequal sharpness of the hydrogen lines in spectra made during increasing light. With high dispersion other peculiarities may appear, as, for instance, those indicated in the special study of δ Cephei.[2]

---

[1] *Mt. Wilson Contr.*, No. 92, p. 16; *Astrophysical Journal*, **40**, 463, 1914.

Continuous and periodic changes of spectral type are shown distinctly for fifteen of the stars over several epochs of maximum, and are definitely indicated for the remainder of the list. No Cepheid variable observed has failed to show variability of spectrum. Upon the basis of this result we may believe that for the two or three thousand variable stars which belong to the same class similar disturbances of the radiating surfaces underlie similar periodic oscillations in light and spectral type.

The variation in spectrum of a Cepheid is undoubtedly as important a part of the phenomenon as the fluctuation in light; moreover, it should be as definite a method of detecting a star's peculiar variability as the measures of magnitude. By collecting the classifications of spectrum into normals (using the period that defines the variation in light) and plotting the mean spectrum against phase, we may obtain a curve closely similar to the curves of variation in magnitude and velocity. Such a curve is shown for δ Cephei in Fig. 1, based upon the data in Table II. It differs in form from the light-curve on a later page in certain respects—the spectrum falls away from its maximum (bluest) value more rapidly than the light falls from its maximum, and the change from red to blue spectrum at the end of minimum light is frequently abrupt. To some extent this latter result probably reflects the oscillation in the time of the rise to maximum light, which has been shown to be conspicuous for several Cepheids.

The changes in the spectrum of RR Lyrae are discussed in *Contribution* No. 112. Data for RS Boötis are given by Pease in *Publications of the Astronomical Society of the Pacific*, **26**, 256,

---

[1] *Harvard Annals*, **55**, 38, 1907.

[2] *Mt. Wilson Communications*, No. 22; *Proceedings of the National Academy of Sciences*, **2**, 136, 1916.

1914.[1] The observations of XZ Cygni by Adams will be published elsewhere. For the other seventeen stars listed in Table I the variations are detailed in the accompanying series of tables and figures.

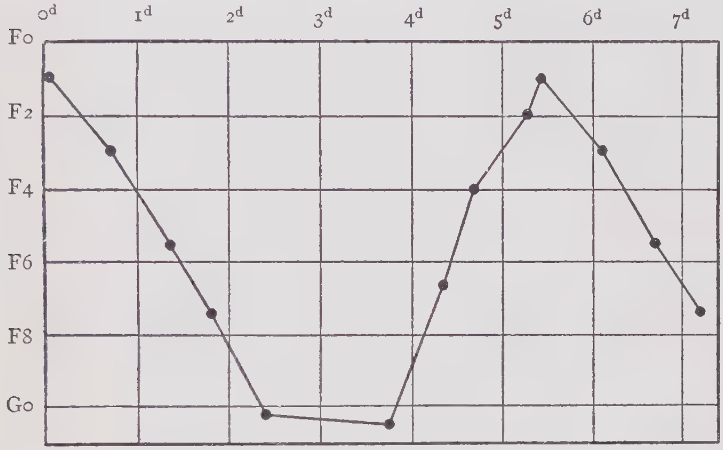

FIG. 1.—The curve of spectral variation of δ Cephei

TABLE II

SPECTRAL VARIATION OF δ CEPHEI

Mean Phase	Mean Spectrum	Number Spectra	Weight
+0.d04	F1.0	7	12
0.74	F3.0	6	11
1.36	F5.6	5	8
1.82	F7.5	4	8
2.40	G0.2	4	8
3.76	G0.5	4	8
4.37	F6.7	4	7
4.72	F4.0	5	10
5.29	F1.9	7	14

---

[1] A later curve of the spectral variation is shown in *Contribution* No. 112 and *Communication* No. 21.

TABLE III

TU CASSIOPEIAE

Max.=J.D. $2419302.12+2^{\mathrm{d}}139\cdot E$*

Plate	Date	P.S.T.	Duration	Phase	Spectrum	Remarks
	1916					
71......	Feb. 2	$9^{\mathrm{h}}21^{\mathrm{m}}$	13^{m}	$1^{\mathrm{d}}048$	F6	Faint
85......	5	9 46	18	1.926	F0:	Faint
100......	6	8 44	25	0.744	F1	
		9 04	16	0.758	F2	
108......	7	7 46	37	1.704	F8	

---

* *Vierteljahrsschrift der Astronomischen Gesellschaft*, **49**, 334, 1914. The visual range given by Hartwig is $1^{\mathrm{M}}1$.

TABLE IV

SU CASSIOPEIAE

Max.=J.D. $2417287.30+1^{\mathrm{d}}9498\cdot E$*

Plate	Date	P.S.T.	Duration	Phase	Spectrum	Remarks
	1915					
48......	Dec. 9	$12^{\mathrm{h}}04^{\mathrm{m}}$	8^{m}	$0^{\mathrm{d}}051$	F1	
	1916					
61......	Jan. 31	8 23	10	0.253	F0:	Out of focus
		36	10	0.262	F0:	
		46	10	0.269	F0:	
62......	31	10 36	11	0.345	F3	Poor plate, wind
		46	11	0.352	F4	
		56	6	0.359	F2:	
70......	Feb. 2	8 55	6	0.325	F5:	
		9 05	12	0.332	F5	
81......	5	6 56	15	1.292	A9	
		7 09	10	1.301	A8	
87*b*.....	5	11 42	11	1.491	F2	
		50	5	1.497	F0:	Bad seeing
		59	10	1.503	F0	
101......	6	9 34	12	0.453	F2	
		46	8	0.461	F1	
		53	4	0.466	F1	
109......	7	8 27	12	1.406	A9	
		39	10	1.415	F0	
		52	15	1.424	F2	
110......	7	9 09	14	1.435	F1	Clouds
		24	14	1.446	F0	
		42	21	1.458	F0	

---

* The phases are computed with the elements derived by Müller and Kempf (*Astronomische Nachrichten*, **173**, 307, 1907). The agreement with spectral type is not good, but the difficulty probably is attributable to inaccurate light-elements rather than to an anomalous relation between spectrum and light-variations. Using the later elements by Parkhurst (*Astrophysical Journal*, **28**, 279, 1908):

$$\text{Max.}=\text{J.D. } 2417287.30+1^{\mathrm{d}}9490\cdot E,$$

the agreement is equally bad; but with an intermediate period, $1^{\mathrm{d}}94935$, the representation is all that could be expected when the small range and the quality of the observations are considered. Direct observations of the brightness of the spectral images on the plates in Table IV verify the supposition that the light-elements are erroneous.

TABLE V

SZ TAURI

Max.=J.D. $2410000.60+3^d1487\cdot E$*

Plate	Date	P.S.T.	Duration	Phase	Spectrum	Remarks
26......	1915 Nov. 14	9^h46^m	180^m	0^d356	F2	Overexposed
59......	Dec. 12	14 59	60	0.235	F0	
		15 39	7	0.262	A9	
63......	1916 Jan. 31	11 08	5	2.844	F3:	High wind
		18	10	2.851	F4	
64......	31	13 11	8	2.929	F0:	Field low
		22	10	2.937	F2	
88......	Feb. 5	12 20	17	1.597	G	Faint
97......	6	6 36	3	2.358	F6	
		42	7	2.362	F7	
102......	6	10 02	3.5	2.501	F5	
		21	30	2.514	F6	
113......	7	12 16	33	0.446	F0	

* Leavitt, *Harvard Circulars*, No. 186, p. 2, 1914.

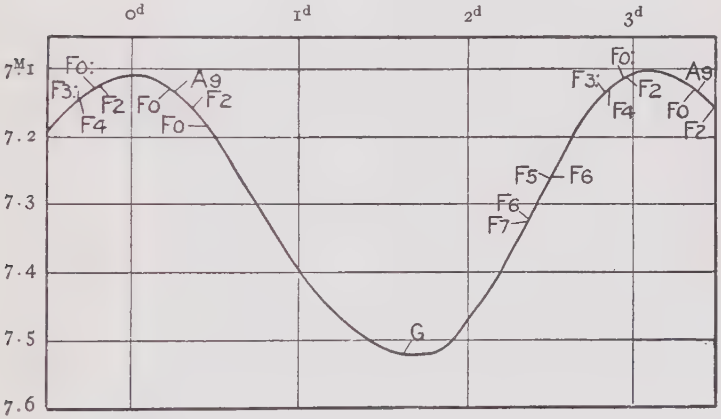

FIG. 2.—SZ Tauri. Mean light-curve by Miss Leavitt (*op. cit.*). An increase of five seconds in the length of the period (a change well within the uncertainty of the light-elements) would place the plotted spectral observations a fourth of a day earlier and harmonize better with the light-curve.

TABLE VI

T MONOCEROTIS

Max. = J.D. $2409633.63+27\overset{\text{d}}{.}0122\cdot E$*

Plate	Date	P.S.T.	Duration	Phase	Spectrum	Remarks
	1916					
78......	Feb. 2	$13^{h}34^{m}$	10^{m}	$26\overset{\text{d}}{.}193$	F8	
		45	10	26.201	F8	
89......	5	13 06	20	2.162	F6	Wind
111......	7	11 02	25	4.076	F6	Clouds
114......	7	12 54	33	4.153	F7	Clear
121......	Apr. 7	8 41	30	9.953	G2	
160......	25	9 26	5	0.972	F5	Wind
169......	27	8 54	16	2.950	F6	
174......	28	8 58	29	3.953	F8	Clouds

* Yendell, *Astronomical Journal*, **16**, 149, 1896.

TABLE VII

RT AURIGAE

Max. = J.D. $2417173.459+3\overset{\text{d}}{.}72806\cdot E$*

Plate	Date	P.S.T.	Duration	Phase	Spectrum	Remarks
	1916					
65......	Jan. 31	$13^{h}38^{m}$	4^{m}	$0\overset{\text{d}}{.}839$	F2	
		46	10	0.844	F2	
67......	Feb. 1	6 31	10	1.542	F7	Plate fogged
		41	10	1.549	F5	
77......	2	12 56	10	2.810	F7	Haze
		13 03	4	2.815	G0	
		11	10	2.820	F9	
90......	5	13 47	11	2.117	G0	
		57	10	2.124	G1	
104......	6	11 38	12	3.027	G0	
112......	7	11 28	13	0.292	A8	
		38	5	0.299	A8	
119......	Mar. 30	11 14	9	0.090	A7	
		22	8	0.095	A8	
120*a*.....	Apr. 7	7 35	7	0.481	F0	
120*b*.....	7	7 48:	4:	0.490:	A9	Time uncertain
		55	8	0.495	A9	
122......	7	9 10	17	0.547	F1	
145......	9	10 04	7	2.585	F8	
		11	6	2.590	F8	
146......	9	10 21	10	2.597	F7	Faint
159......	25	9 01	8	3.629	F0	
		08	5	3.634	F1	
		11	2	3.636	A9	
167......	26	7 30	3	0.838	F4	Strong twilight
168......	27	7 24	10	1.834	F8:	Faint
170......	27	9 15	12	1.911	F9	
		24	5	1.917	F8	
175......	28	9 21	12	2.916	F7	
		38	21	2.927	F6	

* Kiess, *Laws Observatory Bulletin*, No. 23, 1915.

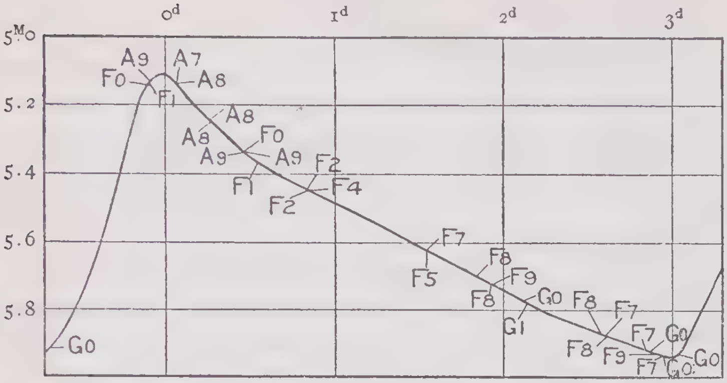

FIG. 3.—RT Aurigae. Mean visual light-curve by Kiess (*op. cit.*), neglecting supposed oscillations in the descending branch.

TABLE VIII

W GEMINORUM

Max. = J.D. $2413266.34 + 7^d.91603 \cdot E$*

Plate	Date	P.S.T.	Duration	Phase	Spectrum	Remarks
	1916					
78......	Feb. 2	13^h34^m	10^m	$7^d.422$	F2	Haze
		45	10	7.429	F2	
89......	5	13 06	20	2.486	F7:	Wind; faint
103......	6	11 16	20	3.410	G	Faint
111......	7	11 02	25	4.400	F6:	Clouds
114......	7	12 54	33	4.478	G0	Clear
121......	Apr. 7	8 41	30	0.974	F4	
169......	27	8 54	16	5.151	G1	
174......	28	8 58	29	6.153	F3	Haze

* *Vierteljahrsschrift der Astronomischen Gesellschaft*, 49, 334, 1914. The visual range in Table I is $0^M.8$; according to Hartwig it is $1^M.3$, and from unpublished observations made at Utrecht and generously placed at my disposal by Dr. Van der Bilt it appears to be less than $0^M.4$.

TABLE IX

X Sagittarii

Max.=J.D. 2403169.93+$7^{d}.01190$·E*

Plate	Date	P.S.T.	Duration	Phase	Spectrum	Remarks
	1916					
69......	Feb. 1	$17^{h}34^{m}$	3^{m}	$0^{d}.052$	F2	Dawn
		38	5	0.055	F3	
96......	5	17 36	7	4.053	G	Dawn
130......	Apr. 7	15 49	10	2.872	F8	
		57	5	2.878	F8	
		16 03	6	2.882	F6:	
140......	8	13 22	7	3.770	F8:	
156......	9	15 39	14	4.865	F8	Wratten "M" plate
158......	9	16 24	10	4.897	F8	Wratten "M" plate
164......	25	15 43	10	6.844	F1	
		50	5	6.849	F1	
183......	28	14 14	4	2.770	F7	
		20	9	2.774	F6	
187......	July 9	11 36	13	4.542	G1	
		48	8	4.550	G1	
198......	28	9 51	10	2.433	F4	45°
205......	29	10 00:	10	3.439:	F8:	45°, faint
219*a*.....	30	10 10	23	4.446	G5	45°, faint
220......	30	10 52	20	4.475	G4	45°, faint
236......	31	11 47	38	5.513	F5	45°
244......	Aug. 1	8 59	26	6.397	F1	45°, Hγ sharp
256......	2	11 42	34	0.498	F	45°, faint
261......	3	8 03	8	1.346	F3	
		16	18	1.355	F2	

* Hellerich, *Dissertation*, p. 9 (Bonn, 1913).

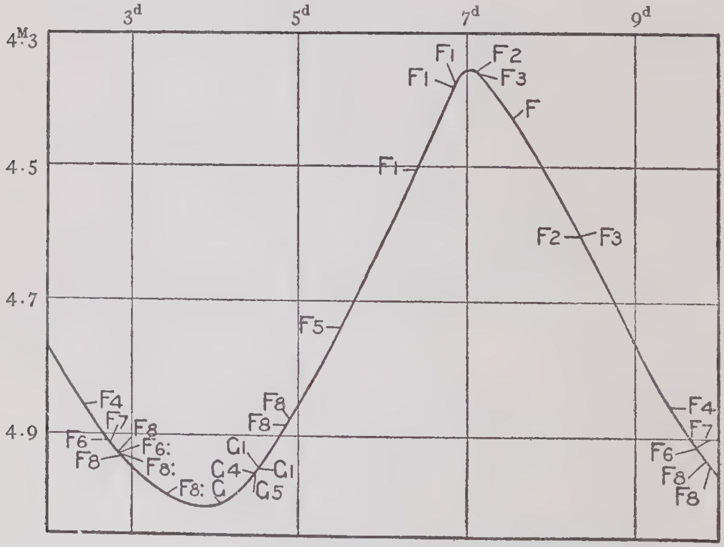

Fig. 4.—X Sagittarii. Mean light-curve by E. C. Pickering (*Harvard Annals*, 46, 155, 1903).

TABLE X

Y Ophiuchi

Max.=J.D. 2408697.25+$17\overset{d}{.}1130\cdot E$*

Plate	Date	P.S.T.	Duration	Phase	Spectrum	Remarks
	1916					
68	Feb. 1	$17^{h}14^{m}$	7^{m}	$14\overset{d}{.}35$	G0	Field low
		23	10	14.35	F8:	Weak
94	5	16 22	21	1.20	F5	Field low
		40	15	1.21	F7	
131	Apr. 7	16 16	5	11.85	G2	Dawn
		22	10	11.86	G3	
139	8	13 00	9	12.72	G	Field low
181*a*	28	13 26	10	15.62	F6	

* Hellerich, *op. cit.*, p. 11.

TABLE XI

W Sagittarii

Max.=J.D. 2403198.88+$7\overset{d}{.}594386\cdot E$*

Plate	Date	P.S.T.	Duration	Phase	Spectrum	Remarks
	1916					
96	Feb. 5	$17^{h}36^{m}$	7^{m}	$6\overset{d}{.}267$	F5:	Dawn
130	Apr. 7	15 49	10	7.438	F0	
		57	5	7.444	F0	
		16 03	6	7.448	A9	
140	8	13 22	7	0.742	F2	
		31	2	0.748	F1	Narrow
		40	5	0.754	F2	
156	9	15 39	14	1.837	F4	Wratten "M" plate
158	9	16 24	10	1.868	F4	Wratten "M" plate
164	25	15 43	10	2.651	F5	
		50	5	2.656	F6	
183	28	14 14	4	5.589	G0	
		20	9	5.593	G2	
187	July 9	11 36	13	1.535	F6	
		48	8	1.544	F6	
198	28	9 51	10	5.274	G1	45°
205	29	10 00:	10	6.280	F8	45°, time uncertain
219*a*	30	9 58:	1:	7.278:	A8	45°, time uncertain
		10 10	23	7.287	F0	
220	30	10 52	20	7.316	A9	45°
236	31	11 47	38	0.760	F1	45°
244	Aug. 1	8 59	26	1.643	F3	45°
256	2	11 42	34	2.756	F6	45°, faint
261	3	8 03	8	3.604	F9	
		16	18	3.613	F9	

* Hellerich, *op. cit.*, p. 9.

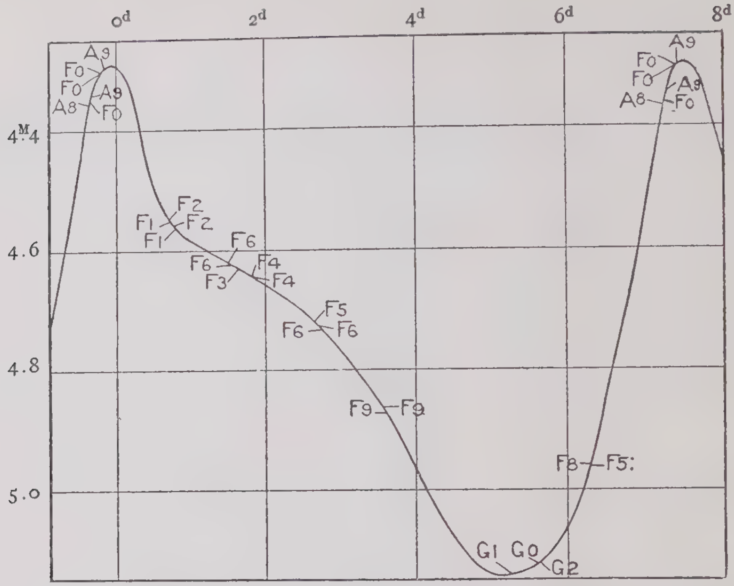

FIG. 5.—W Sagittarii. Mean light-curve by E. C. Pickering (*Harvard Annals*, 46, 155, 1903).

TABLE XII

Y SAGITTARII

Max.=J.D. $2410175.08+5^{d}773268\cdot E$*

Plate	Date	P.S.T.	Duration	Phase	Spectrum	Remarks
	1916					
130......	Apr. 7	$15^{h}49^{m}$	10^{m}	$2^{d}448$	G0	
		57	5	2.453	F8:	Diffuse
		16 03	6	2.458	F8	
140......	8	13 22	7	3.346	G2	
164......	25	15 43	10	3.124	G:	Wind; diffuse
183......	28	14 14	4	0.289	F4	
		20	9	0.293	F4	
187......	July 9	11 36	13	2.900	F8	Moon near field
		48	8	2.908	G	
261......	Aug. 3	8 16	18	4.668	G4	

* Hellerich, *op. cit.*, p. 10.

TABLE XIII

U AQUILAE

Max. = J.D. $2410170.325+7^{\mathrm{d}}.02387\cdot E$*

Plate	Date	P.S.T.	Duration	Phase	Spectrum	Remarks
	1916					
142......	Apr. 8	$15^{\mathrm{h}}33^{\mathrm{m}}$	15^{m}	$3^{\mathrm{d}}.992$	G2	
181*b*.....	28	13 48	12	2.847	F6	Diffuse
191......	July 10	10 06	17	5.455	F8	
230......	31	8 14	17	5.305	F6	

* *Vierteljahrsschrift der Astronomischen Gesellschaft*, **49**, 335, 1914.

TABLE XIV

U VULPECULAE

Max. = J.D. $2414200.253+7^{\mathrm{d}}.98950\cdot E$*

Plate	Date	P.S.T.	Duration	Phase	Spectrum	Remarks
	1916					
128......	Apr. 7	$14^{\mathrm{h}}38^{\mathrm{m}}$	21^{m}	$2^{\mathrm{d}}.573$	F7	
		54	8	2.584	F7:	Narrow
141......	8	14 30	27	3.567	G4	Diffuse
152......	9	13 46	20	4.537	G4:	Faint
153......	9	14 14	15	4.556	G0	
161......	25	13 31	12	4.547	G5	
178......	28	12 25	20	7.501	F8p	Hβ strong
211......	July 29	14 50	22	3.728	G5	Difficult

* *Vierteljahrsschrift der Astronomischen Gesellschaft*, **49**, 335, 1914.

TABLE XV

SU CYGNI

Max. = J.D. $2414202.820+3^{\mathrm{d}}.845612\cdot E$*

Plate	Date	P.S.T.	Duration	Phase	Spectrum	Remarks
	1916					
128......	Apr. 7	$14^{\mathrm{h}}38^{\mathrm{m}}$	21^{m}	$2^{\mathrm{d}}.383$	F6	
		54	8	2.394	F7	Drift in declination
141......	8	14 30	27	3.377	A6	
152......	9	13 46	20	0.501	F1	
		58	5	0.510	F0:	Narrow
161......	25	13 31	12	1.108	F3	
178......	28	12 25	20	0.217	A8	
184*b*.....	July 9	9 42	15	2.883	F5	
		56	11	2.892	F5:	
188......	10	8 21	10	3.826	A6	
		38	24	3.838	A7	
211......	29	14 33	12	0.011	A8	
		50	22	0.023	A9	
216......	30	8 34	17	0.637	F4	
231......	31	8 38	21	1.640	F6	
258......	Aug. 2	13 26	21	0.119	A8	
262......	3	8 40	20	0.920	F2	

* Luizet, *Astronomische Nachrichten*, **173**, 196, 1906.

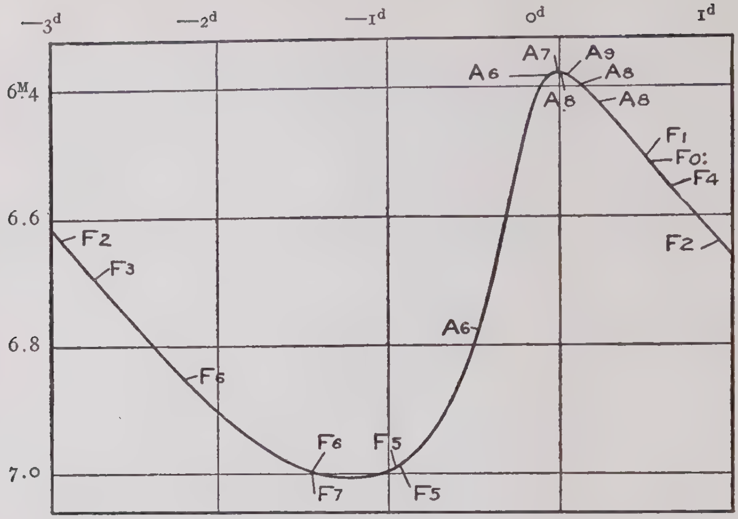

FIG. 6.—SU Cygni. Mean light-curve from observations made at Utrecht; data furnished in manuscript by Dr. Van der Bilt.

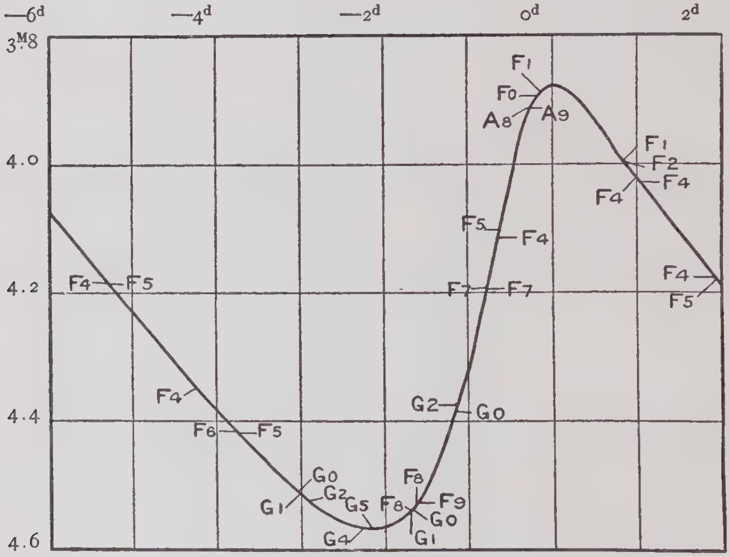

FIG. 7.— η Aquilae. Mean light-curve from observations made at Utrecht; data furnished in manuscript by Dr. Van der Bilt.

TABLE XVI

η AQUILAE

Max.=J.D. 2396168.732+7^{d}176382·E*

Plate	Date	P.S.T.	Duration	Phase	Spectrum	Remarks
	1916					
142	Apr. 8	$15^{h}33^{m}$	15^{m}	7^{d}053	F0	
		44	5	7.061	F1	
162	25	13 40	3	3.418	F5	
		43	2	3.420	F6	
172*b*	27	14 40	3	5.460	G0	
		42	2	5.461	G1	
181*b*	28	13 40	4	6.418	F7:	Diffuse
		48	12	6.424	F7	
184*a*	July 9	9 16	7	5.471	F8	
		21	4	5.474	F8	
		26	5	5.478	F9	
190	10	9 45	15	6.491	F4	Hγ very sharp
191	10	10 06	17	6.506	F5	
196	28	8 49	10	2.923	F4	45°
210	29	13 44	9	4.128	G0	45°
		54	11	4.135	G1	
213	29	15 43	10	4.210	G2	
215	30	8 12	5	4.897	G4	
		17	4	4.901	G5	
230	31	8 02	5	5.890	G0	
		14	17	5.899	G2	
243	Aug. 1	8 20	2	6.903	A8	45°
		31	12	6.910	A9	
254	2	9 47	10	0.787	F1	45°
		10 01	18	0.797	F2	Hγ very sharp
259*b*	2	14 04	7	0.966	F4	
		12	7	0.971	F4	
269	3	13 00	5	1.921	F5	45°
		08	11	1.926	F4	

---

* Hellerich (*op. cit.*, p. 6) finds that the elements derived by Luizet (*Astronomische Nachrichten*, **163**, 361, 1903) are satisfactory without the use of the harmonic term adopted by the latter.

TABLE XVII

S Sagittae

Max.=J.D. 2409863.324+8^d.381613·E*

Plate	Date	P.S.T.	Duration	Phase	Spectrum	Remarks
	1916					
144......	Apr. 8	16^{h}18^m	11^m	2^d.433	F5	Dome
		26	6	2.438	F6	Diffuse
153......	9	14 14	15	3.347	F9	
172*a*.....	27	14 28	7	4.593	G1	
		34	5	4.597	G2	
179......	28	12 42	9	5.519	G3	
		50	5	5.525	G2	
184*c*.....	July 9	10 12	10	1.981	F7	
		20	6	1.987	F6	
		24	3	1.990	F6:	Narrow
189......	10	9 07	26	2.936	F8	
		24	6	2.948	F7	
212......	29	15 11	12	5.426	G2	
227......	30	15 16	27	6.429	G	45°, faint
233*b*.....	31	9 38	10	7.194	F6	Wind
		44	1	7.199	F5	
237......	31	12 41	51	7.322	F6	45°
259*a*.....	Aug. 2	13 50	15	0.488	F4	Very thick

* *Vierteljahrsschrift der Astronomischen Gesellschaft*, 49, 335, 1914.

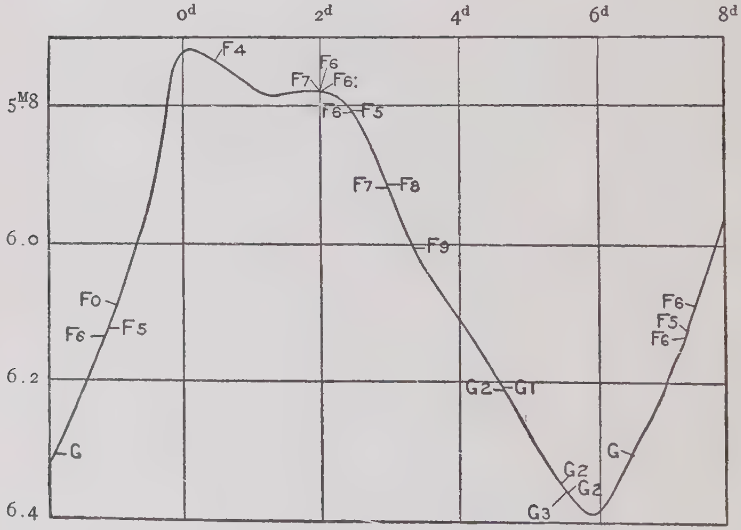

Fig. 8.—S Sagittae. Mean light-curve by Gore as reduced by Luizet (*Astronomische Nachrichten*, 168, 349, 1905).

TABLE XVIII

T VULPECULAE

Max.=J.D. $2409849.04+4\overset{d}{.}435521 \cdot E$*

Plate	Date	P.S.T.	Duration	Phase	Spectrum	Remarks
	1916					
154......	Apr. 9	$14^{h}31^{m}$	10^{m}	$3\overset{d}{.}918$	F4	
		40	7	3.924	F5	
163......	25	13 54	7	2.150	G1	
		14 00	5	2.154	G0	Faint
171......	27	14 12	8	4.162	F0	
		18	3	4.167	A9	
180......	28	13 02	8	0.679	F4	
		10	9	0.685	F3	
186*a*.....	July 9	10 56	9	1.623	F6	
192......	10	10 26	3	2.602	F7	
		33	8	2.607	F8	
214......	29	15 56	12	4.089	F2	Hδ very faint
217......	30	8 52	3	0.359	F0	Hδ stronger
		9 00	11	0.365	F0	
233*a*.....	31	9 22	15	1.380	F5	
260......	Aug. 2	14 20	3:	3.587:	F6	Time uncertain
		40	9	3.601	F6	Thick

---

* Hellerich, *op. cit.*, p. 7.

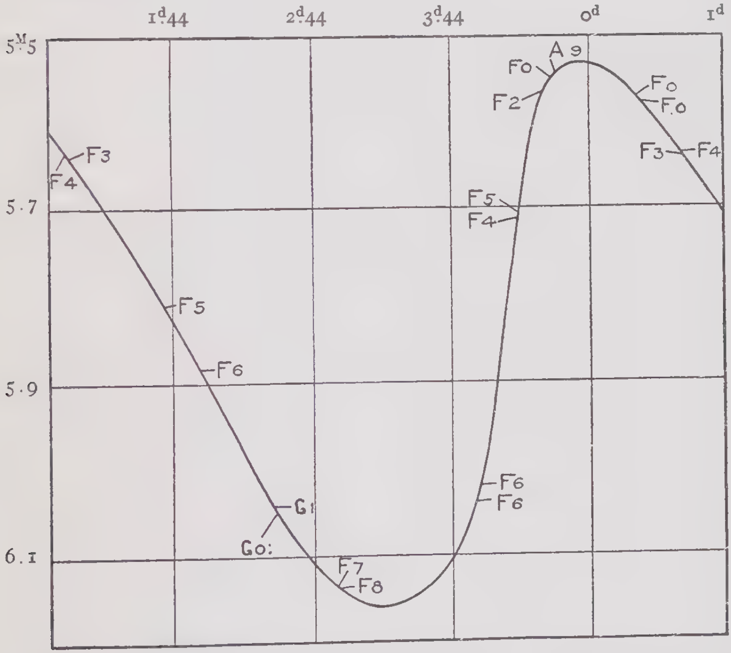

FIG. 9.—T Vulpeculae. Mean light-curve by E. C. Pickering (*Harvard Annals*, **46**, 156, 1903).

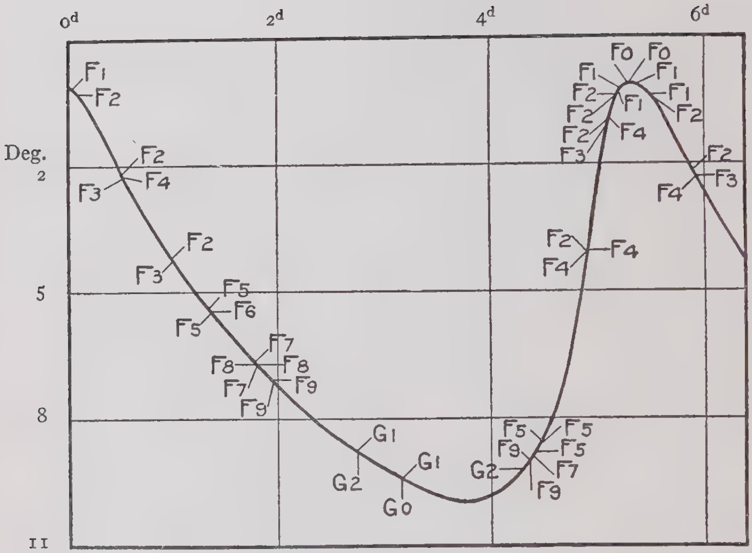

FIG. 10.—δ Cephei. Mean light-curve by Luizet (*op. cit.*). The curve printed in *Popular Astronomy*, 25, 355, 1916, has been revised and supplemented by later data.

TABLE XIX

δ CEPHEI

Max. = J.D. $2393659.856 + 5^{d}.366386 \cdot E$*

Plate	Date	P.S.T.	Duration	Phase	Spectrum	Remarks
	1915					
γ 4571...	Dec. 23	$7^{h}04^{m}$	225^{m}	$4^{d}.294$	G2	60-inch reflector
γ 4578...	24	14 07	120	5.254	F4	60-inch reflector
	1916					
60......	Jan. 31	7 28	5	0.379	F	Bad focus
66......	Feb. 1	6 59	4	1.359	F5	Haze
		7 02	1	1.361	F5	
		04	3	1.362	F6:	
		14	4	1.369	F6	
80......	5	6 28	3	5.338	F :	Clouds
		32	3	5.341	F1	
		34	3	5.342	F0	
83......	5	8 18	2	0.048	F1	
		20	2	0.049	F2	
98......	6	7 10	10	1.001	F5:	Seed "23" plate
		18	5	1.006	F5:	Faint
107......	7	7 06	12	1.998	F9	Seed "23" plate
		16	5	2.005	F9	
143......	Apr. 8	16 02	8	4.340	F9	
		07	2	4.343	F9	
157......	9	16 02	5	5.340	F2	Wratten "M" plate
		10	10	5.345	F1	
165......	25	16 02	5	5.241	F2	Seed "23" plate
		06	3	5.244	F2	
		11	6	5.247	F3	
173......	27	14 48	1.5	1.823	F8	Bad seeing
		50	1	1.824	F7	
		51	1	1.825	F8	
		52	2	1.826	F7	
182......	28	14 04	5	2.792	G1	Seed "23" plate
		07	2	2.794	G2	
186*b*.....	July 9	11 10	1	4.908	F4	
		14	2	4.911	F4	
		18	5	4.914	F2	
193......	10	10 45	6	0.525	F2	
		48	1	0.527	F3	
		52	4	0.530	F4	
218......	30	9 26	8	4.371	F7	45°
		36	12	4.378	F5	
		44	3	4.383	F5:	
219*b*.....	30	11 12	5	4.444	F5	45°
		19	8	4.449	F5	
232......	31	9 02	5	5.354	F0	Seed "23" plate
		06	3	5.357	F1	
245......	Aug. 1	9 28	9	1.006	F3	45°
		34	4	1.010	F2	
271......	3	14 14	11	3.204	G0	45°
		23	8	3.210	G1	

---

* Luizet, *Annales de l'Université de Lyon*, Nouvelle Série, Fascicule 33, 1912.

MOUNT WILSON SOLAR OBSERVATORY
September 1916

Contributions from the Mount Wilson Solar Observatory, No. 125
Reprinted from the *Astrophysical Journal*, Vol. XLIV, pp. 303–310, 1916

PRELIMINARY OBSERVATIONS OF THE SPECTRA OF CALCIUM AND IRON WHEN PRODUCED BY CATHODO-LUMINESCENCE

By ARTHUR S. KING and EDNA CARTER

The excitation of a vapor to luminescence by means of a stream of cathode rays directed into it furnishes a source different from those in which the radiation is produced by high temperature or by the conduction of a current through the vapor. The purpose of the present investigation was to study the peculiarities of the spectrum given by the cathode-ray excitation for certain elements having groups of lines known to show different behavior in the ordinary sources.

The possibility of producing spectra in this way was shown by Hertz,[1] who obtained the stronger mercury lines, and by Lewis,[2] who examined the spectra of several of the more easily vaporized metals, the vapor being produced by heating the substance in a hard glass tube by means of a flame and directing a stream of cathode rays into the tube. In each case a spectrum of what seemed to be the more fundamental lines of the element was observed. The present writers have been aided by valuable suggestions from Professor Lewis, obtained during a discussion of the problem.

The heating effects regularly observed in X-ray tubes since the introduction of tungsten targets made it appear feasible to work with some of the more refractory metals by heating them with a concentrated stream of cathode particles. When brought to luminescence the vapor in the cathode stream could then be observed at a sufficient distance from the heated surface to avoid the direct effects of high temperature.

The first apparatus constructed was a modified X-ray bulb, with concave cathode and disk anode in the usual positions. The cathode stream was directed vertically downward upon an anti-cathode consisting of a tungsten dish containing metallic calcium, supported on the end of a silica tube passing into the bulb through the end opposite the cathode. When the bulb was pumped out to a vacuum sufficient to give in air a parallel spark 10–15 cm long, the calcium was readily vaporized and the pencil of cathode rays above the dish showed, when observed visually with a small spectroscope, a spectrum containing a considerable number of lines. The lines H, K, and λ 4227 were photographed with a 1-meter concave grating.

---

[1] *Wiedemanns Annalen*, **19**, 809, 1883.

[2] *Astrophysical Journal*, **16**, 31, 1902.

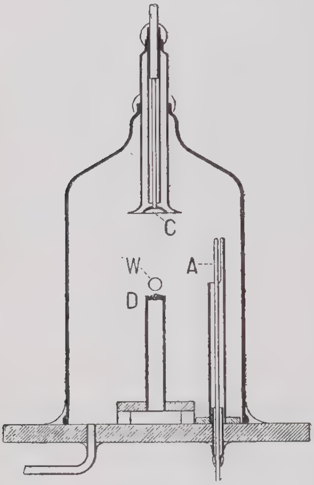

FIG. 1

A more substantial apparatus was then made from a bell-jar supported on a thick glass plate, as shown in Fig. 1. The cathode *C* is 25 mm in diameter, concave to such a degree as to focus the rays at 9.5 cm when the spark crosses a parallel air-gap of 15 cm. It is screwed to an aluminum rod passing through the top of the bell-jar, while a flaring glass tube around the electrode protects the wall of the jar from the cathode discharge. The anode *A* is a vertical aluminum rod 5 mm in diameter, passing through the glass base and inclosed by a glass tube, the inner side of which is cut away for a length of 4 cm below the end of the rod in order to expose the anode and at the same time protect the wall of the jar. The anti-cathode *D* is supported by a silica tube of 15 mm bore, held vertically by being set in a glass plate resting on the base plate. This tube holds at its top either a tungsten dish containing calcium or a shallow iron dish with iron filings. The dish in each case is at the focus of the cathode and is several centimeters away from the direct discharge between anode and cathode. As the experiments of Lewis with metals and with nitrogen[1] showed clearly the possibility of bringing gases outside the path of the conduction current to luminescence by cathode rays, no special examination of this point was made during the present investigation. A tube through the base-plate for the pump connection and a side tube inserted at the opening *W* in the bell-jar and closed by a quartz window completed the fittings. The joints in the apparatus were cemented either with sealing-wax or with an odorless black wax of nearly the same consistency. The discharge was obtained from a large induction coil driven by an electrolytic interrupter of the Simon type, which, when the vacuum was sufficiently high, gave little inverse current.

---

[1] *Astrophysical Journal*, 17, 258, 1903.

When calcium was vaporized by the cathode stream, the vapor immediately absorbed the residue of air—an effect noted by Saunders[1]—which made the vacuum so high that the discharge would not pass until a little air was admitted. The lumps of metallic calcium were found to be almost consumed by the discharge, which could not be closely watched on account of an opaque deposit that blackened all parts of the chamber except the window toward the spectrograph. The iron was raised only to a white heat, the filings not being fully fused. However, sufficient iron vapor was given off in the high vacuum to enable the cathode rays to yield a spectrum. In focusing the light on the spectrograph, the image of the metal anti-cathode was kept well off the slit, the light photographed coming from the cathode stream about a centimeter above the heated metal.

As the experiments will be discontinued for a short time, pending the installation of apparatus which may be expected to give much stronger effects, the following results are presented in the belief that they are typical of what such a discharge will yield. The spectra were photographed in the first order of a 1-meter concave grating, the scale being 1 mm = 17 A. The metallic lines were very sharp and the measurements for identification usually agreed with the published values within 0.02 A. Two reasonably strong spectrograms were obtained for calcium, in which the 26 lines listed in Table I were identified. These were supported by three weaker photographs giving the same effects for such lines as appeared. Three photographs of the iron spectrum were made, which were also concordant in the effects shown. While the 42 iron lines obtained are a small fraction from the rich region between λ 3400 and λ 4400, they show the class of lines which appear under these conditions.

---

[1] *Ibid.*, **40**, 377, 1914.

RESULTS

Calcium.—Table I gives a comparison of the relative intensities of the lines in the luminescence spectrum and in that of the arc in air. An arc spectrum of very short exposure on the same kind of film was used in order to obtain a general intensity comparable with that of the spectrum excited by the cathode discharge. In the fourth column is entered the symbol used by Saunders[1] to denote the series to which the line belongs.

TABLE I

LUMINESCENCE SPECTRUM OF CALCIUM

λ (Exner and Haschek)	Arc in Air	Luminescence Spectrum	Series	λ (Exner and Haschek)	Arc in Air	Luminescence Spectrum	Series
3179.50....	1	1	P_1	4283.20...	15	....	p
3181.43....	trace	trace	P_1	4289.50...	15	....	T
3350.25....	2	....	T_1	4299.18...	10	....	T
3361.95....	4	....	T_1	4302.70...	20	1	p
3624.19....	4	....	T_1	4307.90...	15	....	......
3630.87....	8	2	T_1	4318.80...	15	....	T
3644.53....	15	4	T_1	4355.50...	2	7	SL_3
3706.18....	1	4	P_2	4425.60...	20	3	T_1
3737.06....	2	8	P_2	4435.17...	30	8	T_1
3933.81....	80	40	PH	4435.88...	8	1	T_1
3949.10....	1	....	T_2	4455.00...	40	15	T_1
3957.22....	4	trace	T_2	4456.10...	10	1	T_1
3968.63....	60	30	PH	4527.35...	3	8	SL_2
3973.91....	6	2	T_2	4578.88...	3	....	t
4093.00....	1	....	t	4581.77...	6	1	t
4095.30....	2	....	t	4586.22...	8	2	t
4098.9.....	4	....	t	4685.35...	trace	5	......
4108.60....	trace	4	SL_3	4878.38...	3	4	SL_3
4226.90....	100R	400	SL_1	5041.83...	1	1	SL_2
4240.61....	1	4	SL_2				

In the luminescence spectrum, the lines H, K, and λ 4227 are much the strongest, and perhaps the most striking feature is the phenomenal intensity, combined with sharpness, of λ 4227. In the arc and furnace, even in vacuum, this line widens and reverses more strongly than any other line in the calcium spectrum. Its intensity, so far as this can be based on widening, has seemed a reliable indication of the vapor-density of the source. When excited by cathode rays in the present experiments, a strong central maximum is present with apparently no tendency toward reversal. This is illustrated by the fact that while the grating used does not usually give perceptible ghosts, even of very strong lines, the first-order ghosts of λ 4227 are now of about the same intensity as the H line. Apparently we have here a low vapor-density, resulting in an extremely narrow line, combined with other conditions highly favorable for the production of λ 4227. The strength of λ 4227 is the only resemblance to the furnace spectrum. The luminescence spectrum brings out strongly H and K and the enhanced pair λ 3706 and λ 3737. The latter have not been obtained in the furnace, and H and K are weak in the furnace as compared with the arc. λ 3159.01, belonging to the same series as the first two lines in Table I, is probably present, but blends with the diffuse head of a nitrogen band.

---

[1] *Astrophysical Journal*, **32**, 154, 1910.

Another noteworthy feature of the luminescence spectrum is the weakness of the group of six lines near λ 4300, of which only the strongest, λ 4302.70, was photographed. This group is one of the least variable in the usual sources, including the furnace at different temperatures.

Table I shows further that the series triplets are uniformly weak in the cathode discharge as compared with the arc, while the members of the "single-line" (SL) series of Saunders are much stronger than in the arc. Some of these, such as λ 4108.60, are diffuse in the arc in air, and are rendered more distinct by any of the vacuum sources, but this does not account for the high relative intensity obtained here. Saunders[1] has recently placed λ 4227 also in a single-line series, of which the other members are in the ultra-violet.

If a general feature of this discharge is an excitation of the more fundamental vibrations, as the experiments of Lewis seemed to indicate, the several series, consisting of single lines, of pairs, and of triplets, respectively, are of increasing complexity in their vibrations, since they are arranged in this order in the facility with which they are given by the cathode luminescence.

---

[1] *Ibid.*, 43, 234, 1916.

There is no evidence that new lines are produced by the cathode discharge and, with the exception of certain nitrogen bands referred to later on, all lines in the luminescence spectrum have been identified with known lines of calcium.

TABLE II

Luminescence Spectrum of Iron

λ (Rowland)	Int.	λ (Rowland)	Int.
3440.762	4	3767.341	trace
3441.155		3813.100	trace
3570.273	3	3815.987	1
3581.349	10	3820.586	4
3609.008	1	3824.591	2
3618.919	1	3826.027	2
3631.605	1	3834.364	1
3647.988	1	3840.580	trace
3680.069	trace	3856.524	3
3687.610	trace	3860.055	15
3705.708	1	3878.720	2
3720.084	20	3886.434	5
3722.729	1	3920.410	1
3727.778	trace	3923.054	1
3735.014	7	3928.075	1
3737.281	12	3930.450	1
3745.717	8	4045.975	1
3748.408	4	4308.081	trace
3749.631	4	4325.939	trace
3758.375	2	4383.720	2
3763.945	1	4404.927	trace

Iron.—The list of iron lines identified, with their estimated intensities, is given in Table II. Their general characteristic is that they are the strongest lines in the flame, furnace, arc, and spark spectra. Hemsalech and De Watteville[1] observed all of the lines listed in Table II, and a few others in the oxyhydrogen flame. Although considerable differences in relative intensity appear between the flame and the cathode excitation, the latter seeming stronger in the ultra-violet, we cannot tell how far differences in contrast and in the treatment of plates may account for the variations observed. The strongest lines of the luminescence spectrum

[1] *Comptes Rendus*, **146**, 962, 1908.

are also the strongest in the flame, but many very faint luminescence lines are given as of considerable strength in the flame.

The furnace material available, part of which has not been published, shows that the lines of Table II appear at low temperatures, below 2000° C., and reverse readily at temperatures above 2300°. They would be placed usually in Class II of the furnace classification. In the arc and the condensed spark these are among the strongest lines, reversing readily with high vapor-density. The strongest lines of the luminescence spectrum, λλ 3581, 3720, 3737, 3860, are of great strength in all of the usual sources. The lines most characteristic of the furnace and the enhanced lines of the spark are, however, absent from the luminescence spectrum. While this may be due in some degree to the general weakness of the latter in the photographs obtained, it can at least be said that such lines do not dominate the spectrum, as they do in the sources favorable to them. A fair statement would be that the lines thus far obtained are those of an under-exposed arc spectrum of iron. When more lines are photographed we may expect, among various groups, differences similar to those occurring in the calcium spectrum.

Band spectrum of nitrogen.—The following nitrogen bands appeared on the photographs of the luminescence spectrum:

Positive Pole Bands	Negative Pole Bands
3158.9	3581.5
3371.2	3914.4
3536.5	4236.3
3576.9	4278.0
3755.2	4708.6
3804.9	
4059.0	

While no attempt was made to locate closely the region of production, the appearance of the bands under these conditions is in harmony with the conclusions of Lewis,[1] that the negative pole bands are produced by the impact of cathode rays, while the positive pole bands are given in all parts of the chamber. The concentration of the cathode discharge should favor the negative bands, and this is borne out by the fact that they are much the stronger. The heads of the positive pole bands appear as diffuse lines, while the negative bands λ 3914 and λ 4278 are strong enough to show considerable structure. These bands present the curious appearance of fading out a short distance from the head and then continuing again. This was observed by Deslandres[1] to be peculiar to low pressures, and to result from the suppression under these conditions of one of the series of lines composing the band, only a few of the first members of this series appearing, while at atmospheric pressure the full structure is present.

---

[1] *Astrophysical Journal*, **17**, 258, 1903.

SUMMARY

1. A method, applicable to a wide variety of elements, has been developed for the production of metallic spectra through the luminescence excited by cathode rays.

2. The spectrum of calcium in this discharge consists of lines present in the arc, but differing in relative intensities from the arc and other sources. The lines of the several single-line series are strongest, followed by the lines occurring in pairs, while the triplet series are relatively faint.

3. The iron lines thus far obtained belong to what appears to be the fundamental group in the iron spectrum, strong in all of the usual sources. Lines characteristic of the low-temperature sources and of the spark are absent.

4. Bands of the positive and negative pole spectra of nitrogen have been photographed, the negative bands having high intensity.

Mount Wilson Solar Observatory
October 9, 1916

---

[1] *Comptes Rendus*, **139**, 1174, 1904.

Contributions from the Mount Wilson Solar Observatory, No. 126
Preprinted from the *Astrophysical Journal*, Vol. XLV, 1917

STUDIES BASED ON THE COLORS AND MAGNITUDES IN STELLAR CLUSTERS

FOURTH PAPER: THE GALACTIC CLUSTER MESSIER 11

By HARLOW SHAPLEY

Of the many striking stellar clusters in the great galactic clouds extending through Ophiuchus, Sagittarius, and Scorpio, none has received as much attention as Messier 11,[1] the very rich open aggregation of stars in the small constellation of Scutum Sobieski. Discovered by Kirch two hundred and thirty-five years ago, it has since been observed and described by nearly all students of clusters, nebulae, and comets.[2] In 1836–1839 a catalogue of micrometrically determined positions of 184 of its stars was undertaken by Lamont at Munich.[3] Thirty years later Helmert at Hamburg repeated the measures, forming a catalogue of 200 stars and comparing his results with those of the earlier astronomer.[4] The favorable length of the interval since the work of Lamont and the serviceable check by Helmert's later catalogue led Stratonoff at Tachkent in Turkestan to redetermine in 1896 with the more accurate methods then available the relative position of the stars, and to deduce proper motions for the cluster as a whole and for its individual members.[5] To accomplish this the positions were measured on photographic plates, not only for the stars in the cluster, but for several hundred stars outside its bounds. The 861 objects, whose co-ordinates to the hundredth of a second of arc are tabulated by Stratonoff, include practically all the stars in an area of 700 square minutes which are brighter than a certain magnitude (near the limit of his plates). That the comparison of his positions with those of sixty years earlier gave only negative results for proper motion does not detract from the value of the work, for his result indicates the great distance of the stars involved, and the new measures of position afford a much sounder basis for the future investigation of motions. Stratonoff also determined the photographic magnitudes; but since his values are based on estimates of brightness taken from the *B.D.* catalogue, no especial accuracy is claimed for them.

---

[1] Messier 11 = h.2019 = G.C.4437 = N.G.C.6705; position for 1900 (from *Harvard Annals*, **60**, 214, 1908), $\alpha=18^{h}\,45^{m}.7$, $\delta=-6^\circ 23'$; galactic longitude = 355°, galactic latitude $=-3^\circ$. The conspicuous bright star in the south-following edge of the cluster is Lalande 35043 = B.D. −6°4929, etc.

[2] For instance, see the paper by Barnard in *Monthly Notices*, **57**, 15, 1896, and the descriptive and historical notes by Miss Clerke, *The System of the Stars*, p. 229 (London, 1905).

[3] *Annalen der königlichen Sternwarte bei München*, **17**, 305.

[4] *Publicationen der Hamburger Sternwarte*, No. 1, 1874.

[5] *Publications de l'Observatoire astronomique et physique de Tachkent*, No. 1, 1899.

The present study of colors and magnitudes in Messier 11 was undertaken chiefly because of the cluster's low galactic latitude and its position with reference to the star clouds of the southern Milky Way. The open cluster discussed in the preceding paper of this series,[1] Messier 67, is situated in galactic latitude +34°. Its constituency differs little from the non-cluster stars of that neighborhood, and the conclusion was reached that, unlike the globular clusters, it is nothing more than a condensation in an ordinary stellar field. The faint stars in that locality are of the redder color-classes, in agreement with Seares's result for the North Polar stars,[2] galactic latitude +28°. A different result might be anticipated for stars in Messier 11 and for the fainter members of the rich galactic cloud which forms its background. The determination of color-classes in such regions thus contributes directly to the problem of the extent of the Milky Way, and bears as well on the relation of open stellar groups to the surrounding clouds of stars.[3]

The large angular distance of Messier 11 from the reference field of standard magnitudes at the North Pole has made it difficult to secure good intercomparison photographs, and it has been necessary to reject many plates without measurement, either because of deformed images, or because of marked differences in the seeing in the directions of the cluster field and the North Pole. The plates finally adopted and used for the determination of magnitudes are described in Table I. The time and hour-angle for each plate refer to the middle of the exposure on the cluster.

---

[1] *Mt. Wilson Contr.*, No. 117, 1916.

[2] *Ibid.*, No. 81; *Astrophysical Journal*, **39**, 361, 1914.

[3] Excellent photographs by Barnard of the star clouds in the region of Messier 11 are published in *Lick Observatory Publications*, **11**, 1915.

TABLE I

LIST OF PLATES

Plate Number	Date, G.M.T.	Kind of Plate	Number of Exposures	Exposure Time	Hour-Angle	Extinction Correction
2467.....	1915, June 7.965	Iso	3	10^m	$23\overset{\circ}{.}5$ W	$+0\overset{M}{.}06$
2468.....	7.960	Seed 27	3	2	21.5 W	+0.11
2638.....	Aug. 16.804	Iso	3	5	34 W	+0.02
2639.....	16.803	Seed 27	3	2	33 W	+0.06
3180.....	1916, July 5.710	Iso	2	10	40 E	0.00
3181.....	5.704	Seed 27	3	1	42 E	−0.02
3235.....	8.753	Iso	3	15	22 E	+0.06
3236.....	8.746	Seed 27	3	3*	25 E	+0.11

* Duration of exposure on cluster uncertain; the measures on Polar Standards rejected and scale of plate and zero point determined by comparisons with results from other Seed 27 plates.

The method of measurement and reduction is sufficiently indicated in the preceding papers.[1] In order to abbreviate the catalogue of magnitudes, the residuals are omitted and a brief discussion of them is given in Tables II and III. An error in the timing of one exposure on Plate 3236 (not discovered until the plates were measured) made it necessary to determine the scale from the results of the other Seed 27 plates. To do this the mean magnitudes in the eighth column of Table II were plotted against the scale-readings for the corresponding stars on Plate 3236, and the resulting curve was employed to determine magnitudes for all stars measured on that plate.

The residuals for the different plates in Tables II and III are the deviations (in hundredths of a magnitude) from the tabulated means after the systematic deviations at the bottom of the table have been applied. The stars included in these two tables are chiefly near the center and are the most difficult in the cluster. The average errors for the more distant stars are appreciably smaller. The tabulated residuals show that no important errors are present. For one plate, which showed diversely irregular images for the more

[1] *Mt. Wilson Contr.*, Nos. 115, 116, 117.

TABLE II

Residuals for Photographic Magnitudes

Star	Plate 2468		Plate 2639		Plate 3181		Mean of Three Plates	Plate 3236		Mean of All Plates*
	Mag.	Res.	Mag.	Res.	Mag.	Res.		Mag.	Res.	
449	14.37	− 4	14.18	−10	14.21	+ 1	14.25	14.43	+13	14.30
452	......	.....	12.71	+12	12.46	− 5	......	12.66	+ 5	12.61
459	14.27	+12	13.88	−14	13.79	−15	13.98	14.21	+17	14.04
462	12.84	− 6	12.79	+ 2	12.63	− 6	12.75	12.90	+11	12.79
466	13.90	− 7	13.77	− 7	......	.....	......	13.90	+ 4	13.86
466*a*	14.89	− 7	14.87	+ 4	......	.....	......	14.78	− 7	14.85
472	13.06	+10	12.84	+ 1	12.71	− 4	12.87	12.80	− 5	12.85
472*a*	15.74	+ 3	15.67	+ 9	15.39	−11	15.60	15.60	0	15.60
476	13.09	−18	13.15	+ 1	13.25	+19	13.16	13.14	− 2	13.16
491	12.37	− 8	12.38	+ 6	......	.....	......	12.28	− 6	12.34
501	12.07	0	12.11	+17	11.71	−15	11.96	11.95	− 1	11.96
503	14.76	+13	14.40	−10	14.48	+ 6	14.55	14.44	− 8	14.52
516	12.20	− 6	12.12	− 1	......	.....	......	12.13	− 2	12.15
517	13.73	+12	13.48	0	13.29	−11	13.50	13.49	− 1	13.50
520	15.13	− 8	14.96	−12	15.03	+ 3	15.04	15.28	+18	15.10
520*a*	15.40	−13	15.53	+13	15.39	+ 7	15.44	15.38	− 4	15.42
523	12.44	+ 8	12.30	+ 7	12.02	−13	12.25	12.23	− 2	12.25
523*a*	15.50	0	15.30	− 7	15.33	+ 4	15.38	15.43	+ 4	15.39
524	14.13	− 2	13.92	−10	14.00	+ 6	14.02	14.11	+ 7	14.04
533	13.57	+ 1	......	.....	13.24	−11	......	13.53	+ 8	13.45
533′	14.43	+10	14.11	− 9	14.16	+ 4	14.23	14.16	− 6	14.22
534	12.67	−14	12.82	+14	......	.....	......	12.61	− 9	12.70
538	......	.....	12.62	+ 8	12.50	+ 4	......	12.55	− 1	12.56
538*a*	14.60	+10	14.23	−14	14.23	− 6	14.35	14.48	+ 9	14.39
539	13.30	−11	......	.....	13.10	−10	......	13.49	+19	13.30
542	14.23	+ 8	13.84	−18	......	.....	......	14.04	0	14.04
542*a*	15.00	+13	14.51	−23	......	.....	......	14.78	+ 2	14.76
543	15.19	−22	15.49	+21	15.23	+ 3	15.30	......	.....	15.30
544	12.07	− 1	......	.....	11.71	−16	......	12.13	+16	11.97
551	12.77	+ 5	12 59	0	12.46	− 5	12.61	12.63	+ 2	12.61
553	15.09	+ 4	14.91	− 1	14.91	+ 7	14.97	14.84	−10	14.94
554	14.06	+ 1	......	.....	13.90	+ 6	......	13.85	− 9	13.94
556	13.90	+13	13.66	− 2	13.54	− 2	13.70	13.53	−13	13.66
558	14.56	+ 3	......	.....	14.41	+ 9	......	14.29	−13	14.42
562	14.53	−14	......	.....	14.65	+19	......	14.49	− 7	14.56
565	13.84	+ 7	13.68	+ 4	13.54	− 2	13.69	13.57	− 9	13.66
570*a*	15.65	+16	15.41	+ 5	15.22	− 6	15.43	15.23	−15	15.38
572	13.47	+ 4	13.36	+ 6	13.14	− 8	13.32	13.33	+ 1	13.32
572*a*	15.43	−24	15.67	+13	15.51	+ 5	15.54	15.64	+ 8	15.56
581	11.90	− 5	......	.....	11.72	− 2	......	11.91	+ 7	11.84
582	......	.....	14.26	− 3	14.29	+ 8	......	14.39	+ 8	14.31
586	13.93	+10	13.68	− 2	13.58	− 4	13.73	13.71	− 1	13.72
589	15.22	0	15.19	+10	15.06	+ 5	15.16	14.95	−16	15.11
593	13.90	− 9	13.95	+ 9	13.72	− 6	13.86	13.93	+ 5	13.88
593*a*	15.53	− 5	15.49	+ 4	15.41	+ 4	15.48	15.43	− 4	15.47
600	14.43	+13	14.04	−13	14.21	+12	14.23	14.08	−11	14.19
600*a*	15.97	−10	15.91	− 3	16.16	+30	16.01	15.81	−15	15.96
604*a*	15.87	+ 8	15.59	− 7	15.49	− 9	15.65	15.76	+ 8	15.68
607	13.64	+ 9	13.41	− 1	13.26	− 8	13.44	......	.....	13.44
622	14.37	−13	......	.....	14.56	+27	......	14.25	−14	14.39
No. of values	47		42		43			48		
Av. dev	±0.085		±0.079		±0.085			±0.076		
Syst. dev	+0.11		−0.02		−0.10			....		

---

* In some cases these means differ slightly from the final mean photographic magnitudes in the catalogue, because of the application of the systematic corrections derived with the aid of this table.

distant stars, only images near the center were measured; and for Plate 3235 the relatively long exposure of 15 minutes made impossible the accurate measurement of the brighter stars.

TABLE III

RESIDUALS FOR PHOTO-VISUAL MAGNITUDES

STAR	PLATE 2467		PLATE 2638		PLATE 3180		PLATE 3235		MEAN PV. MAG.	COLOR-INDEX
	Mag.	Res.	Mag.	Res.	Mag.	Res.	Mag.	Res.		
449	14.19	+ 1	14.16	+ 2	14.26	+ 2	14.20	− 4	14.20	+0.10
457	13.18	−10	13.36	+12	13.25	− 9	13.40	+ 6	13.30	+0.36
459	13.77	+ 1	13.56	−16	13.80	− 2	14.00	+18	13.78	+0.26
462*a*	14.66	+ 6	14.53	− 3	14.63	− 3	14.66	0	14.62	+0.39
472*a*	14.64	+ 3	14.57	0	14.73	+ 6	14.57	−10	14.63	+0.97
474	14.04	+12	14.17	+19	14.00	− 8	13.96	−12	14.04	+0.40
481	13.68	− 8	13.71	− 1	13.84	+ 2	13.89	+ 7	13.78	+0.10
485	13.97	−11	14.14	+10	14.07	− 7	14.21	+ 7	14.10	+0.44
492	13.72	− 2	13.76	+ 6	13.80	0	13.74	− 6	13.76	+0.34
502	13.97	− 6	13.92	− 7	14.10	+ 1	14.21	+12	14.05	+0.19
503	14.24	+ 5	14.23	+ 8	14.33	+ 8	14.04	−21	14.21	+0.31
513	14.22	+ 2	14.05	−11	14.29	+ 3	14.32	+ 6	14.22	+0.24
514	14.76	+ 5	14.61	− 6	14.83	+ 6	14.72	− 5	14.73	+0.40
520	14.47	+ 6	14.29	− 8	14.60	+13	14.35	−12	14.43	+0.67
520*a*	14.84	− 2	14.88	+ 8	15.04	+14	14.69	−21	14.86	+0.57
522	12.96	− 6	12.99	+ 1	13.03	− 5	13.18	+10	13.04	+0.57
523*a*	14.96	+ 5	14.79	− 8	14.91	− 6	15.06	+ 9	14.93	+0.46
524	14.00	+ 8	13.77	−11	13.95	− 3	14.04	+ 6	13.94	+0.10
532	14.06	+ 1	14.11	+10	14.10	− 1	14.00	−11	14.07	+0.03
533′	14.13	+ 3	14.03	− 3	14.13	− 3	14.20	+ 4	14.12	+0.10
538*a*	14.17	−14	14.31	+ 4	14.42	+ 5	14.42	+ 5	14.33	+0.06
543	14.90	+ 6	14.76	− 4	14.84	− 6	14.93	+ 3	14.86	+0.34
553	14.76	+11	14.53	− 8	14.63	− 8	14.77	+ 6	14.67	+0.27
452	12.08	+21	11.70	−13	11.89	− 8	......	.....	11.89	+0.76
461	12.74	+ 1	12.65	− 4	12.86	+ 3	......	.....	12.75	+0.43
462	12.23	+ 1	12.18	0	12.32	0	......	.....	12.24	+0.55
472	12.31	− 1	12.33	+ 5	12.39	−3	......	.....	12.34	+0.52
476	12.34	0	12.33	+ 3	12.42	− 2	......	.....	12.36	+0.80
477	12.65	− 3	12.72	+ 8	12.72	− 6	......	.....	12.70	+0.54
482	13.04	0	12.99	− 1	13.16	+ 2	......	.....	13.06	+0.43
486	12.31	−12	12.44	+ 5	12.59	+ 6	......	.....	12.45	+0.40
491	11.21	−10	11.41	+14	11.36	− 5	......	.....	11.33	+1.00
493	12.01	+11	11.76	−10	12.00	0	......	.....	11.92	+0.63
498	12.71	+ 2	12.59	− 6	12.83	+ 4	......	.....	12.71	+0.50
516	11.42	− 6	11.65	+21	11.42	−16	......	.....	11.50	+0.62
523	11.45	− 6	11.33	−14	11.81	+20	......	.....	11.53	+0.72
534	11.26	+ 1	11.16	− 5	11.40	+ 5	......	.....	11.27	+1.40
538	12.05	+ 2	11.98	− 1	12.11	− 2	......	.....	12.05	+0.55
551	12.11	+ 3	12.05	+ 1	12.15	− 3	......	.....	12.10	+0.52
No. of values	39		39		39		23			
Syst. dev.										
>13 Mag.	−0.02		−0.06		+0.04		+0.04			
<13 Mag.	−0.02		−0.06		+0.08		....			
Av. dev.	±0.052		±0.071		±0.053		±0.087			

With a few exceptions, all the magnitudes of the main catalogue (Table IV) depend upon at least two plates. The numbers in the first column are those assigned by Stratonoff. Stars marked with an asterisk are omitted from the statistical discussion, either because neighboring images are so close that the Eberhard effect may have influenced their magnitudes, or because of uncertainty in the measures. Except for close groups and double stars, the general concentration of images on the plates used is not sufficient to cause fear of perceptible errors from the Eberhard effect or similar phenomena. The residuals give no evidence of a differential effect of this kind between the plates; and, even for stars nearly in contact, whatever errors enter affect mainly magnitudes and not colors, for the densities of the stellar images on the two kinds of plates are closely comparable. In choosing stars for statistical discussion, however, liberal exclusion was made wherever possibility of such systematic errors was suspected. The results tabulated in Tables VI and VII should, therefore, be completely free from systematic or accidental errors depending on stellar condensation.

The numbers with postscript letters in Tables II, III, and IV refer to objects not listed by Stratonoff—those with appended Greek letters indicating the components of double or triple stars, and those with italic letters referring either to close faint companions or merely to neighboring uncatalogued stars of a photovisual brightness comparable with that of the stars catalogued. Using Stratonoff's stars for reference points, identification positions of the postscript stars were determined by measurements with a millimeter scale on enlarged positives. The right ascensions and declinations so obtained are listed in Table V. For positions of the Stratonoff stars reference must be made to the Tachkent catalogue.

As a matter of convenience in discussing colors and magnitudes, the cluster was divided into several concentric regions. The numbers in the second column of Table IV refer to these divisions, Region 1 including all stars within $0'.5$ from the center, Region 2 including all stars between $0'.5$ and $1'.0$, Region 3 those between $1'.0$ and $1'.5$, etc. The star at the point adopted as center of the cluster is No. 462, for which the position for 1900 is:

$$\text{R.A.} = 18^{h}\ 45^{m}\ 42^{s}.75, \qquad \text{Dec.} = -6^{\circ}\ 23'\ 12''.8.$$

TABLE IV

PHOTOMETRIC CATALOGUE OF 458 STARS IN MESSIER 11

No.	Region	Pg. Mag.	Pv. Mag.	Color-Index	No.	Region	Pg. Mag.	Pv. Mag.	Color-Index
204...	7	13.38	13.12	+0.26	253..	5	14.50	14.31	+0.19
205...	9	13.86	13.76	+0.10	257..	6	15.26	14.84	+0.42
206...	7	14.50	14.34	+0.16	258*.	5	14.24	13.86	+0.38
207...	8	12.75	12.24	+0.51	258*a*.	5	15.80	15.00	+0.80
208...	7	14.39	13.98	+0.41	260*.	6	14.06	13.72	+0.34
210...	8	14.76	14.58	+0.18	261*.	7	14.40	14.19	+0.21
211...	7	12.26	11.62	+0.64	262..	7	13.54	13.31	+0.23
212...	9	13.68	13.61	+0.07	263..	5	14.82	14.69	+0.13
213...	7	14.37	14.08	+0.29	264..	5	14.82	14.62	+0.20
214...	7	13.48	13.18	+0.30	265*.	7	13.34	13.32	+0.02
217...	8	14.70	14.54	+0.16	266*.	6	13.89	13.53	+0.36
218...	8	14.42	14.20	+0.22	266*a*.	6	15.24	14.82	+0.42
219...	6	14.64	14.54	+0.10	266*b*.	6	15.17	13.44	+1.73
221...	6	13.07	12.86	+0.21	267..	5	13.26	12.78	+0.48
224...	6	13.56	13.58	−0.02	267*a*.	5	14.76	13.30	+1.46
225...	6	13.78	13.64	+0.14	267*b**	5	15.20	14.70	+0.50
226*..	8	14.09	13.76	+0.33	268..	6	14.46	14.25	+0.21
226*a*..	7	14.40	14.50	−0.10	272..	5	13.76	13.36	+0.40
226*b*..	7	14.90	13.46	+1.44	273..	4	13.00	12.54	+0.46
226*c*..	8	15.38	13.50	+1.88	273*a*.	4	15.41	14.91	+0.50
227...	6	12.06	11.31	+0.75	274..	5	14.32	14.12	+0.20
229...	6	13.57	13.48	+0.09	275..	7	14.86	14.72	+0.14
230...	6	14.82	14.71	+0.11	276..	7	14.43	14.26	+0.17
232...	6	12.22	11.89	+0.33	277..	8	14.54	14.28	+0.26
233α*.	6	14.52	12.40	....	278..	4	14.32	14.11	+0.21
233β*.	6	14.68		....	280..	7	13.01	11.92	+1.09
234*..	8	14.57	14.36	+0.21	283..	4	14.08	13.92	+0.16
236...	6	13.07	12.61	+0.46	284..	5	14.49	14.26	+0.23
237...	7	11.74	11.02	+0.72	285..	4	13.08	12.38	+0.70
238...	8	14.58	14.32	+0.26	287..	4	14.56	14.28	+0.28
239...	5	13.24	13.13	+0.11	287*a*.	4	15.23	14.69	+0.54
240...	5	13.21	11.81	+1.40	288..	4	12.75	12.13	+0.62
242...	5	14.00	14.16	−0.16	291..	6	14.82	14.50	+0.32
243...	8	14.07	13.92	+0.15	292*.	4	13.22	12.80	+0.42
245...	5	12.15	11.89	+0.26	293*.	4	12.56	11.71	+0.85
247...	7	13.12	11.07	+2.05	293*a**	5	15.29	14.76	+0.53
248*..	5	14.64	14.48:	+0.16:	296..	5	13.89	13.64	+0.25
248α*.	5	15.50	14.17:	+1.33:	296*a*.	5	14.86	14.70	+0.16
249...	6	13.92	13.80	+0.12	297..	4	12.44	11.68	+0.76
249*a*..	5	15.28	14.82	+0.46	298..	4	13.91	13.63	+0.28
249*b*..	5	15.14	14.56	+0.58	300..	6	12.28	11.86	+0.42
250...	5	13.08	12.60	+0.48	301..	6	15.16	14.64	+0.52
251...	6	13.34	13.12	+0.22	302..	4	15.24	14.77	+0.47
251*a*..	5	15.11	14.82	+0.29	303..	4	14.69	14.55	+0.14
252...	7	13.08	11.12	+1.96	307..	5	14.20	14.02	+0.18

TABLE IV—*Continued*

No.	Region	Pg. Mag.	Pv. Mag.	Color-Index	No.	Region	Pg. Mag.	Pv. Mag.	Color-Index
308*..	4	14.96	14.65	+0.31	358..	3	13.84	13.66	+0.18
310...	4	13.04	12.52	+0.52	359..	3	14.33	14.25	+0.08
310a..	3	15.60	14.34	+1.26	360*.	4	14.62	14.25	+0.37
314...	5	14.28	14.16	+0.12	362..	5	13.68	13.28	+0.40
315...	4	14.48	14.19	+0.29	363..	3	14.00	13.86	+0.14
317*..	6	14.36:	14.14	+0.22:	364..	4	12.73	11.44	+1.29
320...	5	14.84	14.67	+0.17	365*.	3	13.32	12.55	+0.77
321...	6	14.86	14.56	+0.30	366..	3	13.02	12.52	+0.50
322*..	6	13.46:	13.12	+0.34:	368..	3	14.08	13.60	+0.48
323*..	4	13.54	12.82	+0.72	369*.	3	14.44	13.76	+0.68
323a*.	4	14.66	14.51	+0.15	370*.	3	15.04	14.64	+0.40
324...	4	13.80	13.70	+0.10	372*.	3	14.56	14.10	+0.46
324a..	4	15.07	14.76	+0.31	373..	2	14.86	14.68	+0.18
325...	3	13.04	12.48	+0.56	374..	2	14.46	14.10	+0.36
328...	3	14.11	13.84	+0.27	375..	3	12.54	11.97	+0.57
329...	3	14.65	14.30	+0.35	376..	4	14.10	13.58	+0.52
330...	4	14.66	14.26	+0.40	376a.	4	15.11	14.78	+0.33
330a..	4	15.84	14.68	+1.16	377..	4	13.64	13.27	+0.37
331...	4	12.24	11.14	+1.10	378..	2	14.18	13.87	+0.31
333...	6	14.06	13.86	+0.20	379..	4	14.76	14.31	+0.45
334...	3	14.18	13.95	+0.23	380..	3	14.49	14.16	+0.33
335...	3	15.24	14.84	+0.40	381..	4	12.44	11.81	+0.63
336...	3	12.08	11.29	+0.79	381a.	4	15.29	14.27	+1.02
336a..	3	15.26	14.66	+0.60	383..	4	14.12	14.04	+0.08
337...	4	14.61	14.24	+0.37	384..	6	14.58	14.52	+0.06
338...	4	13.36	12.90	+0.46	385..	5	12.96	12.18	+0.78
338a..	5	15.60	15.00	+0.60	386..	5	14.64	14.37	+0.27
341...	3	12.42	11.78	+0.64	387..	3	12.84	11.30	+1.54
342...	3	13.22	11.47	+1.75	389..	2	14.67	14.36	+0.31
343...	4	14.18	13.74	+0.44	391..	2	13.18	12.76	+0.42
344...	5	13.23	12.62	+0.61	392..	3	15.04	14.74	+0.30
345...	4	12.06	11.32	+0.74	393..	3	13.54	13.18	+0.36
345a..	4	15.30	14.80	+0.50	394..	2	14.16	13.92	+0.24
346...	3	12.82	12.46	+0.36	394a.	2	15.34	15.00	+0.34
347...	4	13.32	11.74	+1.58	395*.	5	12.19	11.31	+0.84
348...	4	14.84	14.60	+0.24	396..	3	15.16	14.92	+0.24
348a..	4	15.13	14.62	+0.51	397..	4	14.98	14.62	+0.36
350...	6	14.42	14.40	+0.02	397a.	5	15.68	15.02	+0.66
351...	5	13.45	13.06	+0.39	398..	2	13.84	13.51	+0.33
352...	5	13.69	13.32	+0.37	400*.	3	14.68	14.28	+0.40
353...	3	13.68	13.31	+0.37	402..	4	13.06	12.53	+0.53
354...	6	14.55	14.52	+0.03	403..	3	13.53	13.24	+0.29
355...	3	14.49	14.04	+0.45	404..	3	14.36	14.02	+0.34
356*..	4	12.60	11.94	+0.66	405..	7	13.18	12.93	+0.25
357...	5	14.78	14.52	+0.26	406..	6	14.99	14.70	+0.29

TABLE IV—*Continued*

No.	Region	Pg. Mag.	Pv. Mag.	Color-Index	No.	Region	Pg. Mag.	Pv. Mag.	Color-Index
407	3	11.93	11.02	+0.91	456	3	12.30	11.44	+0.86
408	3	13.00	12.52	+0.48	456*a*	3	15.01	14.64	+0.37
409	2	13.74	13.11	+0.63	457*	1	13.66	13.30	+0.36
410*	5	14.80	14.18	+0.62	458	2	14.09	13.84	+0.25
411	1	14.04	13.84	+0.20	459	1	14.04	13.78	+0.26
411*a*	2	15.42	15.10	+0.32	460	2	12.97	12.63	+0.34
412	2	13.54	12.18	+1.36	460*a*	3	15.50	14.90	+0.60
414*	3	13.96	13.54	+0.42	461	2	13.18	12.75	+0.43
417*	5	14.64	14.13	+0.51	461*a*	2	15.59	14.90	+0.69
419	3	15.36	14.80	+0.56	462	1	12.79	12.24	+0.55
419*a*	4	15.00	14.72	+0.28	462*a*	1	15.01	14.62	+0.39
420	2	13.42	13.28	+0.14	464	3	13.94	13.74	+0.20
420*a*	3	15.43	14.99	+0.44	465	3	13.12	12.62	+0.50
421	3	13.13	12.60	+0.53	466*	1	13.82	13.34	+0.48
421*a**	3	15.42	14.56:	+0.86:	466*a**	1	14.82	13.40	+1.42
422*	3	13.22	12.66	+0.56	467	4	15.14	14.64	+0.50
423	1	13.46	11.83	+1.63	468	4	13.91	13.62	+0.29
424	6	12.72	12.23	+0.49	468*a*	4	15.10	14.67	+0.43
425	2	12.62	12.12	+0.50	469	2	13.78	13.42	+0.36
426*	3	13.21	12.67	+0.54	470*	1	14.48	13.85	+0.63
427	1	13.26	11.80	+1.46	471	4	12.62	12.04	+0.58
428*	2	14.89	14.30	+0.59	472	1	12.86	12.34	+0.52
430	4	13.32	12.88	+0.44	472*a*	1	15.60	14.63	+0.97
431	1	12.55	12.11	+0.44	474*	1	14.44	14.04	+0.40
431*a*	1	16.00	15.28	+0.72	475	6	14.42	14.40	+0.02
432*	1	13.64	13.32	+0.32	476	1	13.16	12.36	+0.80
433	2	13.79	12.16	+1.63	477*	2	13.24	12.70	+0.54
436	4	14.12	13.74	+0.38	480	5	13.52	13.28	+0.24
437*	3	11.46	10.69	+0.77	481	2	13.88	13.78	+0.10
438*	2	14.84	14.38:	+0.46:	482*	2	13.49	13.06	+0.43
439	6	13.64	13.49	+0.15	483	6	14.32	14.23	+0.09
440*	5	14.18	14.10	+0.08	484	4	14.15	13.89	+0.26
442*	5	14.00	13.82	+0.18	485	1	14.54	14.10	+0.44
443	5	13.58	13.32	+0.26	486	1	12.85	12.45	+0.40
444	4	14.61	14.25	+0.36	487	2	12.39	11.59	+0.80
445	1	12.74	12.42	+0.32	488	6	14.52	14.51	+0.01
445*a*	1	15.24	14.78	+0.46	489	3	13.40	12.91	+0.49
446	3	13.58	13.27	+0.31	490*	3	13.12	12.62	+0.50
447	2	14.06	13.64	+0.42	490*a**	3	14.56	14.08	+0.48
448	5	14.02	13.94	+0.08	491*	2	12.33	11.33	+1.00
449	1	14.30	14.20	+0.10	492	1	14.10	13.76	+0.34
451	6	13.09	12.84	+0.25	493	2	12.55	11.92	+0.63
452	1	12.65	11.89	+0.76	494	3	12.32	11.47	+0.85
454	6	12.66	12.16	+0.50	494*a*	3	15.14	14.80	+0.34
455	6	14.84	14.62	+0.22	495*	2	12.42	11.59	+0.83

TABLE IV—*Continued*

No.	Region	Pg. Mag.	Pv. Mag.	Color-Index	No.	Region	Pg. Mag.	Pv. Mag.	Color-Index
496α*.	3	14.70	13.87	+0.83	540*.	3	12.08	11.02	+1.06
496β*.	3	13.14	12.36	+0.78	541..	5	14.35	14.16	+0.19
496γ*.	3	14.80	13.76	+1.04	542*.	2	14.00	13.61	+0.39
497...	3	14.82	14.43	+0.39	542*a**	2	14.74	14.00	+0.74
498...	1	13.21	12.71	+0.50	543..	2	15.20	14.86	+0.34
499*..	5	13.50	13.22	+0.28	544..	3	11.97	11.35	+0.62
501...	4	11.96	11.11	+0.85	545*.	2	9.3:	8.5	+0.8:
502...	2	14.24	14.05	+0.19	546*.	4	13.47	12.68	+0.79
503*..	2	14.52	14.21	+0.31	548*.	4	12.23	11.32	+0.91
504*..	3	12.31	11.94	+0.37	551..	2	12.62	12.10	+0.52
505*..	2	12.80	11.92	+0.88	552..	6	14.20	14.28	−0.08
507*..	3	13.02	11.81	+1.21	553..	2	14.94	14.67	+0.27
508...	6	13.23	12.93	+0.30	553*a*.	2	15.77	15.12	+0.65
509*..	2	13.28	12.46	+0.82	554..	3	13.93	13.84	+0.09
513*..	2	14.46	14.22	+0.24	555*.	3	14.74	12.91	+1.83
514...	2	15.13	14.73	+0.40	556..	4	13.66	13.50	+0.16
515...	7	14.09	14.08	+0.01	556*a*.	4	16.17	15.08	+1.09
516...	3	12.12	11.50	+0.62	557..	4	13.56	11.50	+2.06
517...	2	13.50	13.07	+0.43	557*a*.	5	15.14	14.85	+0.29
519...	4	13.30	12.88	+0.42	557*b*.	5	15.14	14.68	+0.46
519*a*..	4	15.56	15.00	+0.56	558..	3	14.42	14.32	+0.10
520...	2	15.10	14.43	+0.67	558*a*.	4	16.68	14.68	+2.00
520*a*..	2	15.43	14.86	+0.57	559*.	3	15.08	14.38	+0.70
522...	2	13.61	13.04	+0.57	560*.	3	12.80	11.11	+1.69
523...	3	12.25	11.53	+0.72	561*.	2	14.78	13.92	+0.86
523*a*..	3	15.39	14.93	+0.46	562..	3	14.55	14.28	+0.27
524...	2	14.04	13.94	+0.10	563..	2	13.12	12.61	+0.51
525*..	3	12.08	11.14	+0.94	563*a*.	3	15.48	15.01	+0.47
525*a**.	3	14.58	14.21	+0.37	564*.	3	14.28	13.40:	+0.88:
526...	4	13.63	13.06	+0.57	564*a**	2	15.36	14.56	+0.80
526*a**.	4	15.41	14.66	+0.75	564*b**	3	15.36	14.52	+0.84
528...	7	13.54	13.48	+0.06	565..	4	13.66	13.62	+0.04
529...	5	13.48	13.36	+0.12	567..	3	14.61	14.40	+0.21
532...	3	14.10	14.07	+0.03	568*.	3	13.31	12.16	+1.15
532*a*..	4	15.47	14.76	+0.71	568*a**	3	15.46	14.67	+0.79
533...	3	13.44	13.22	+0.22	569..	6	13.26	12.96	+0.30
533*a*..	3	15.93	14.92	+1.01	570*.	4	13.20	12.87	+0.33
533′..	2	14.22	14.12	+0.10	570*a*.	5	15.38	14.69	+0.69
534*..	2	12.67	11.27	+1.40	571*.	3	13.16	12.16	+1.00
536...	5	14.58	14.22	+0.36	572..	4	13.33	12.94	+0.39
536*a*..	5	15.37	14.80	+0.57	572*a*.	4	15.54	14.96	+0.58
538...	2	12.60	12.05	+0.55	573..	3	13.13	12.74	+0.39
538*a*..	2	14.39	14.33	+0.06	573*a*.	3	15.34	14.88	+0.46
539...	3	13.29	11.31	+1.98	574..	3	12.94	12.41	+0.53
539*a**.	3	15.50	14.57	+0.93	576*.	3	12.39	11.65:	+0.74:

TABLE IV—*Continued*

No.	Region	Pg. Mag.	Pv. Mag.	Color-Index	No.	Region	Pg. Mag.	Pv. Mag.	Color-Index
576*a**	3	14.30	14.02:	+0.28:	614*a**	5	16.12	14.12	+2.00
577	4	12.22	11.44	+0.78	615	4	13.92	13.70	+0.22
579α*	4	14.72	14.81	−0.09	616	6	13.89	13.66	+0.23
579β*	4	14.38	13.73	+0.65	617	8	13.25	12.78	+0.47
579*a*	4	15.32	14.90	+0.42	618	7	14.09	13.84	+0.25
580*	3	14.34	14.06	+0.28	619	5	13.86	13.36	+0.50
581	4	11.85	11.08	+0.77	620	7	13.33	13.06	+0.27
581*a*	4	14.56	14.35	+0.21	621	7	14.10	13.80	+0.30
582	4	14.35	14.32	+0.03	622	4	14.39	13.78	+0.61
583	6	13.84	13.69	+0.15	622*a*	4	15.36	14.78	+0.58
585	3	14.05	13.76	+0.29	623	5	13.83	13.62	+0.21
586	4	13.73	13.60	+0.13	623*a*	5	16.00	15.10	+0.90
588	3	15.14	14.88	+0.26	624	4	14.04	14.00	+0.04
588*a*	4	15.30	15.00	+0.30	630	5	13.54	13.52	+0.02
589	4	15.11	14.73	+0.38	631	7	12.46	11.94	+0.52
590	3	13.04	11.20	+1.84	633	8	13.37	13.18	+0.19
591	7	14.64	14.15	+0.49	634	6	13.46	13.22	+0.24
592*	5	14.22	13.88	+0.34	635	5	13.23	13.01	+0.22
593	3	13.88	13.58	+0.30	637	7	15.08	14.69	+0.39
593*a*	3	15.47	14.92	+0.55	638	5	14.88	14.72	+0.16
594	4	13.28	12.80	+0.48	639	6	14.64	14.44	+0.20
596	6	14.43	14.10	+0.33	640*	6	13.12:	13.04:	+0.08:
597	7	12.78	11.92	+0.86	643	6	15.08	14.60	+0.48
598	4	13.02	11.46	+1.56	644	5	14.30	13.94	+0.36
598*a*	4	15.40	14.73	+0.67	645	7	15.15	14.67	+0.48
599	5	12.40	11.80	+0.60	647	5	12.66	11.98	+0.68
600	5	14.19	13.97	+0.22	648	6	13.54	13.16	+0.38
600*a*	5	15.96	15.00	+0.96	649*	5	14.77	14.32	+0.45
601*	8	11.69	10.68:	+1.01:	650	6	14.54	14.58	−0.04
602	4	14.02	13.80	+0.22	652	8	13.16	12.81	+0.35
603	7	12.83	12.14	+0.69	653	6	13.52	13.12	+0.40
604	4	13.34	12.94	+0.40	654	6	13.36	11.92	+1.44
604*a*	3	15.68	14.90	+0.78	655	6	14.97	14.62	+0.35
606	4	13.72	13.31	+0.41	656	7	14.31	13.67	+0.64
606*a*	4	16.38	15.57	+0.81	657	6	14.49	14.04	+0.45
607	4	13.48	13.34	+0.14	658	6	14.28	13.93	+0.35
608	5	14.45	14.23	+0.22	660	6	14.39	14.14	+0.25
609	5	13.21	11.20	+2.01	662	7	12.47	12.00	+0.47
610	4	13.48	13.27	+0.21	663	6	11.90	11.22	+0.68
610*a*	4	15.52	14.84	+0.68	664	7	12.79	12.30	+0.49
610*b*	4	15.26	14.54	+0.72	666	8	13.45	12.01	+1.44
611	4	13.39	12.95	+0.44	668	7	14.82	14.64	+0.18
612	6	14.82	14.58	+0.24	670	7	13.92	13.60	+0.32
613	4	14.15	13.99	+0.16	671	7	13.66	13.40	+0.26
614*	5	15.48	14.62	+0.86	672	6	12.50	12.12	+0.38

TABLE IV—*Continued*

No.	Region	Pg. Mag.	Pv. Mag.	Color-Index	No.	Region	Pg. Mag.	Pv. Mag.	Color-Index
674...	7	13.28	11.84	+1.44	680..	7	13.58	12.84	+0.74
675...	7	13.62	13.30	+0.32	681..	6	14.90	14.51	+0.39
677...	8	15.17	14.76	+0.41	682..	9	13.05	12.72	+0.33
679...	6	15.10	14.66	+0.44	685..	7	14.92	14.62	+0.30

NOTES TO THE CATALOGUE

Star	
233.	Components not separated on isochromatic plates.
248.	Components not separated on Seed 27 plates.
421*a*.	A close double, components unequal.
461.	Chosen as central star by Stratonoff.
462.	Position of this star adopted as center of cluster; it is 32″ south of No. 461.
470.	Close double, components not separately measured.
545.	This bright star, B.D.−6°4929, is No. 1 in the catalogues of Lamont and Helmert, and is the star upon which the Mount Wilson plates were centered. It is a minute of arc distant from the center of the cluster, and probably is not physically connected with the group. The star is too bright for accurate measurement on photographs taken with the full aperture of the 60-inch reflector. The visual magnitude according to the *B.D.* catalogue is 8.8, and, according to Lamont and to Helmert, 9.0 and 8.6, respectively. Stratonoff's photographic magnitude, which, however, is based on visual standards, is 8.6. No proper motion has been detected in this or in any of the reference stars (Stratonoff, *op. cit.*, p. 24).
555.	May be variable. About half a magnitude fainter July 8, 1916, than June 7, 1915. The value of the color-index given in the table is of the right order.
560.	Close double, components not separately measured.
570.	Close double, components not separately measured.
640.	A close double; components equally bright, both photographically and photo-visually but not separately measured.

The arrangement of the material in Tables VI and VII follows that of the analogous tables in preceding contributions.[1] The 14 stars fainter than photo-visual magnitude 15.0 are excluded from Table VII. In the region covered, which is a square 6′ on a side with star No. 462 as center, all stars brighter than 15.0 are included. The cluster itself is apparently limited to a little more than half of this area, and is also limited chiefly to the brighter magnitudes here considered. The density of the stars fainter than magnitude 14.0 or 14.5 is little, if any, greater in the cluster than outside, and there

---

[1] Tables XII and XIII of *Mt. Wilson Contr.*, No. 116, and Tables VII and VIII of No. 117.

TABLE V

Positions of Postscript Stars

Star	R.A. 1900	Decl. 1900	Star	R.A. 1900	Decl. 1900
226*a*	$18^{h}45^{m}31^{s}.8$	−6°21′12″	494*a*	$18^{h}45^{m}44^{s}.0$	−6°24′39″
226*b*	32.8	21 4	496α	43.9	21 51
226*c*	32.3	20 30	496β	44.0	21 52
233α	32.6	23 18	496γ	44.1	21 53
233β	32.6	23 20	519*a*	45.3	24 46
248*a*	33.4	22 55	520*a*	44.4	23 28
249*a*	34.9	21 58	523*a*	45.9	22 16
249*b*	34.7	22 4	525*a*	45.2	24 33
251*a*	34.3	24 28	526*a*	45.5	21 38
258*a*	34.5	24 16	532*a*	46.0	21 57
266*a*	34.7	21 32	533*a*	45.1	24 18
266*b*	34.8	21 37	536*a*	46.5	21 29
267*a*	34.8	23 37	538*a*	45.5	23 2
267*b*	34.2	23 55	539*a*	46.0	24 19
273*a*	35.3	23 10	542*a*	45.9	23 25
287*a*	37.0	24 13	553*a*	46.3	22 57
293*a*	36.2	22 5	556*a*	46.6	22 6
296*a*	37.0	21 39	557*a*	45.9	25 6
310*a*	37.3	23 40	557*b*	46.4	25 3
323*a*	37.6	21 55	558*a*	47.5	24 26
324*a*	38.2	22 6	563*a*	46.8	22 57
330*a*	37.2	24 9	564*a*	46.6:	23 16
336*a*	38.2	22 32	564*b*	46.8	23 18
338*a*	37.7	21 23	568*a*	46.8	23 47
345*a*	38.2	24 54	570*a*	48.1	21 41
348*a*	38.7	21 32	572*a*	47.6	21 43
376*a*	38.9	24 46	573*a*	47.3	22 58
381*a*	39.7	24 41	576*a*	47.5	22 34
394*a*	40.9	22 48	579α	47.5	24 47
397*a*	40.5	21 17	579β	47.6	24 45
411*a*	41.3	22 53	579*a*	47.1	24 50
419*a*	41.3	24 50	581*a*	47.5	23 26
420*a*	41.9	22 11	588*a*	48.6	22 42
421*a*	41.9	24 22	593*a*	48.2	23 50
431*a*	41.2	23 29	598*a*	48.6	22 47
445*a*	41.8	22 54	600*a*	48.4	21 24
456*a*	42.9	22 4	604*a*	48.3	23 30
460*a*	42.6	24 19	606*a*	49.5	22 17
461*a*	42.2	22 31	610*a*	50.0	22 46
462*a*	42.6	23 17	610*b*	50.2	22 33
466*a*	42.9	23 25	614*a*	49.4	21 54
468*a*	43.9	24 57	622*a*	50.0	23 36
472*a*	43.2	23 30	623*a*	50.2	24 48
490*a*	44.1	24 15			

TABLE VI

FREQUENCY OF COLORS AND MAGNITUDES

DISTANCE FROM CENTER	LIMITS OF PV. MAG.	COLOR-CLASS							ALL COLORS
		b	*a*0–*a*4	*a*5–*a*9	*f*	*g*	*k*	*m*	
0′.0 to 1′.0	11.0–11.5								
	11.5–12.0				2	1	1	1	5
	12.0–12.5			1	7	1	1	1	11
	12.5–13.0			1	4				5
	13.0–13.5		1	1	3				5
	13.5–14.0		2	7	1				10
	14.0–14.5		4	2	2				8
	14.5–15.0		1	3	4	1			9
	≥15.0			2	2				4
1.0 to 2.0	11.0–11.5				5	5	3	3	16
	11.5–12.0				6		1	1*	8
	12.0–12.5			1	5				6
	12.5–13.0			2	14				16
	13.0–13.5		1	7	2				10
	13.5–14.0		9	11	4				24
	14.0–14.5		6	12	3	1	1		23
	14.5–15.0		1	11	23	2		1	38
	≥15.0			1	2	2			5
2.0 to 3.0	11.0–11.5				2			1†	3
	11.5–12.0			2	3		2		7
	12.0–12.5			1	3				4
	12.5–13.0			4	4				8
	13.0–13.5		4	8	4		1	1	18
	13.5–14.0	1	5	7					13
	14.0–14.5	2	7	9	1				19
	14.5–15.0	1	9	11	10				31
	≥15.0				2	3			5
≥3.0	11.0–11.5				1			2‡	3
	11.5–12.0				2	2	1		5
	12.0–12.5				4		1		5
	12.5–13.0			3	2				5
	13.0–13.5		2	6			1		9
	13.5–14.0		3	3	2			1	9
	14.0–14.5		3	4	1				8
	14.5–15.0	1	4	2	2				9
	≥15.0								0
All of cluster	11.0–11.5				8	5	3	6	22
	11.5–12.0			2	13	3	5	2	25
	12.0–12.5			3	19	1	2	1	26
	12.5–13.0			10	24				34
	13.0–13.5		8	22	9		2	1	42
	13.5–14.0	1	19	28	7			1	56
	14.0–14.5	2	20	27	7	1	1		58
	14.5–15.0	2	15	27	39	3		1	87
	≥15.0			3	6	5			14
	All magnitudes....	5	62	122	132	18	13	12	364

* Color-Index = +2.06. † Color-Index = +2.01. ‡ Contains one star with color-index of +2.05.

TABLE VII

Distance and Color Class

Distance from Center	Quantity	Color-Class						All Colors
		a0–a4	*a5–a9*	*f*	*g*	*k*	*m*	
0'.0 to 0'.5	No. stars...	1	5	8 (1)	2	1	1	18
	Av. Pv. mag.	14.20	13.68	12.83	13.50	11.80	11.83	13.10
	Av. C. I....	+0.10	+0.30	+0.51	+0.88	+1.46	+1.63	+0.59
0.5 to 1.0	No. stars...	7	10	15 (4)	1	1	1	35
	Av. Pv. mag.	14.03	13.92	13.21	11.59	12.18	12.16	13.47
	Av. C. I....	+0.12	+0.31	+0.53	+0.80	+1.36	+1.63	+0.45
1.0 to 1.5	No. stars...	6	23	24 (8)	4	2	3	62
	Av. Pv. mag.	14.00	13.91	13.29	12.21	12.82	11.33	13.41
	Av. C. I....	+0.10	+0.30	+0.56	+0.91	+1.40	+1.86	+0.53
1.5 to 2.0	No. stars...	11	20	38 (12)	5	3	2*	79
	Av. Pv. mag.	13.87	14.02	13.46	13.26	11.55	13.09	13.56
	Av. C. I....	+0.11	+0.30	+0.55	+1.04	+1.48	+2.03	+0.53
2.0 to 2.5	No. stars...	13†	19	14 (5)	0	2	1	49
	Av. Pv. mag.	14.12	13.85	13.39	....	12.56	11.20	13.68
	Av. C. I....	+0.11	+0.27	+0.55	....	+1.43	+2.01	+0.39
2.5 to 3.0	No. stars...	16‡	23	13 (2)	0	1	1	54
	Av. Pv. mag.	14.15	13.72	13.30	....	11.92	13.44	13.71
	Av. C. I....	+0.06	+0.28	+0.49	....	+1.44	+1.73	+0.32
3.0 to 3.5	No. stars...	7§	13	11 (5)	2	2	2‖	37
	Av. Pv. mag.	14.29	13.61	12.76	11.92	12.65	11.10	13.21
	Av. C. I....	+0.09	+0.29	+0.57	+0.98	+1.44	+2.00	+0.53
≥3.5	No. stars...	6	5	3 (0)	0	1	1	16
	Av. Pv. mag.	13.93	13.67	13.26	....	12.01	13.50	13.58
	Av. C. I....	+0.14	+0.28	+0.46	....	+1.44	+1.88	+0.44
All of cluster	No. stars...	67	118	126 (38)	14	13	12	350
	Av. Pv. mag.	14.07	13.83	13.27	12.68	12.20	12.04	13.50
	Av. C. I....	+0.10	+0.29	+0.54	+0.96	+1.44	+1.88	+0.467

* Color-indices are +2.00 and +2.06.
† Contains one star with color-index of −0.16.
‡ Contains three stars with color-indices of −0.08, −0.04, and −0.02.
§ Contains one star with color-index of −0.10.
‖ Contains one star with color-index of +2.05.

is no evidence on any of the photographs of the existence of the highly concentrated background of faint stars that is typical of truly globular clusters. In fact, the cluster is apparently a condensation, on a rich background, of 150 or 200 stars whose magnitudes are between 11.0 and 14.5. The distribution (number of stars per square minute for successive regions) is illustrated in Fig. 1.

No conspicuous difference in average color or average magnitude is evident between the center of the cluster and the outermost region. In this similarity of cluster stars to the non-cluster stars in the immediate neighborhood, the conditions here are like those in Messier 67, the open cluster discussed in the foregoing paper. The result supports the hypothesis that open clusters are an integral part of the galactic system and in most characteristics differ little from their environment.

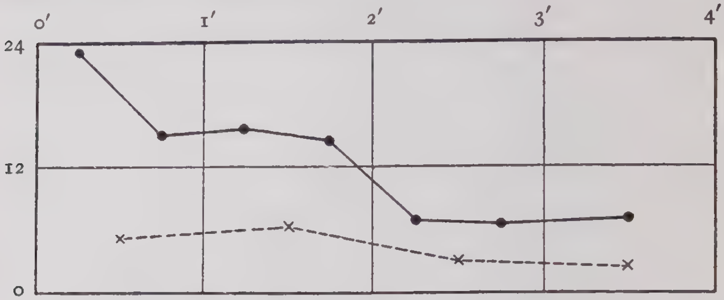

FIG. 1.—Distribution of stars in Messier 11. Full line, all stars brighter than pv. mag. 15.0; broken line, stars between pv. mag. 14.0 and 15.0.

Ordinates: Number of stars per square minute
Abscissae: Distance from center of the cluster

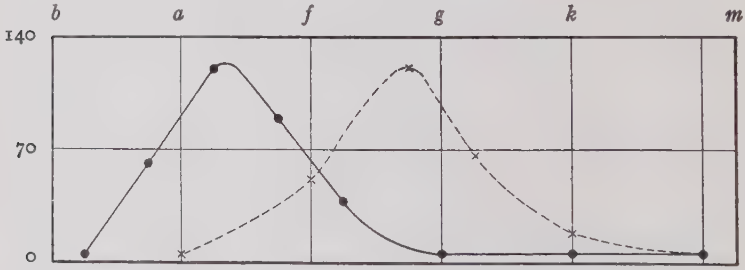

FIG. 2.—Relative frequency of colors. Full line, Messier 11; broken line, Messier 67. Ordinates: Numbers of stars. Abscissae: Color classes

Curves of relative frequency of colors are shown in Fig. 2. The data for Messier 67 are taken from Table VII of *Contribution* No. 117. The distribution of color-classes is seen to be totally different in the two open groups. The color-index of maximum frequency is about $0^{M}.6$ bluer for the cluster in the star clouds than for the one of higher galactic latitude. Moreover, the small color-indices in Messier 11 are not confined to the cluster itself and its immediate surroundings, but occur throughout that region of the sky. The point will be treated further in the following paper of this series, which deals with the colors in several parts of the surrounding galactic clouds.

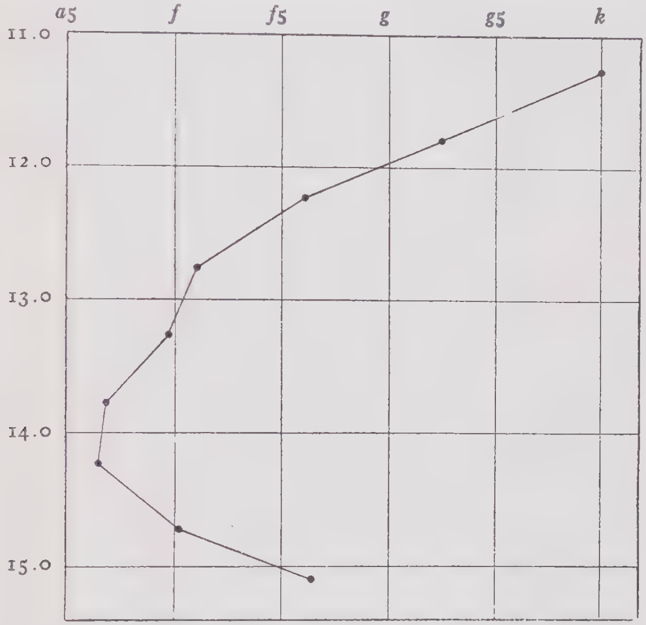

FIG. 3.—Relation between color and luminosity in Messier 11

Ordinates: Color classes. Abscissae: Apparent magnitudes

In the same paper will appear a discussion of the decrease of brightness with decreasing color-index—a point wherein Messier 11 bears a resemblance to the Hercules cluster. For the present the average color-index for successive intervals of magnitude is shown in Table VIII, and a plot of the results appears in Fig. 3. To supplement the lower part of the curve, provisional color-indices of a number of faint stars have been determined from Plates 3235 and 3236. For 34 objects the average photo-visual magnitude is 15.34, and the average color-index +1.03; but because of a selection, uncertain in amount, of some stars peculiarly red and others peculiarly blue, the result for this group of fainter stars is not of high weight.

TABLE VIII

MAGNITUDE AND AVERAGE COLOR

Interval of Pv. Mag.	Number of Stars	Mean Pv. Mag.	Mean C.I.
11.0 to 11.5..	22	11.26	+1.20
11.5 to 12.0..	25	11.80	+0.90
12.0 to 12.5..	26	12.22	+0.64
12.5 to 13.0..	34	12.75	+0.44
13.0 to 13.5..	42	13.25	+0.39
13.5 to 14.0..	56	13.75	+0.27
14.0 to 14.5..	58	14.23	+0.26
14.5 to 15.0..	87	14.71	+0.41
>15.0..	14	15.09	+0.66

SUMMARY

1. A catalogue has been made of the photographic and photovisual magnitudes of 458 stars within four minutes of arc of the center of the open galactic cluster Messier 11, which is situated in one of the densest star clouds in the sky. Although considerable difficulty was experienced in obtaining satisfactory series of plates, the average probable error of a resulting color-index does not exceed a tenth of a magnitude.

2. It seems probable that the cluster proper is composed of not more than 200 stars, nearly all of which are brighter than magnitude 14.5. The diameter of the group appears to be less than five minutes of arc.

3. In absolute values and frequency of color-indices, the stars in the cluster are not unlike the stars in its neighborhood; but they average half a magnitude bluer than those of the same magnitude in and near the open cluster Messier 67. The galactic latitude of the latter is +34°, of the former −3°.

4. The presence of small color-indices among the faint stars in this low galactic region must have a significant bearing on the extent of the Milky Way.

MOUNT WILSON SOLAR OBSERVATORY
November 1916

Contributions from the Mount Wilson Solar Observatory, No. 127
Reprinted from the *Astrophysical Journal*, Vol. XLV, 1917

HIND'S VARIABLE NEBULA N.G.C. 1555[1]

By FRANCIS G. PEASE

Hind's variable nebula N.G.C. 1555[2] lies close to the irregular variable star T Tauri. Since December 1911 seven negatives of this object have been made from time to time with the 60-inch reflector. The length of the exposures, which were on Seed 27 plates, has usually been about three hours.

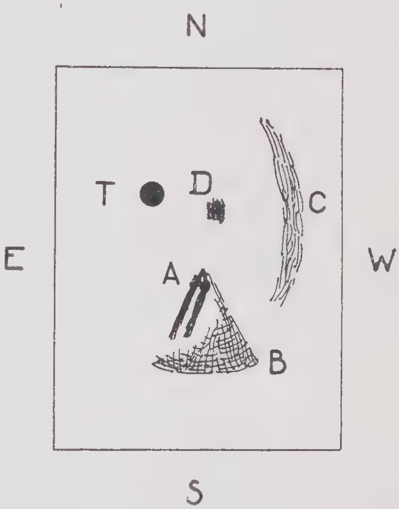

Fig. 1.—T Tauri and Hind's variable nebula.

The most prominent feature is a fan-shaped bit of nebulosity, whose apex lies 220°, 25″ southwest of T Tauri and points a little to the west of the variable (Fig. 1). Two knots at *A*, each with a streamer running to the south, are the brightest parts of the nebula. The sides of the fan include an angle of 70° and are about one minute of arc in length. The nebulosity at *B* is never strong, but on some plates shows distinct detail. A curved streamer *C* lying to the west of *T* is also relatively faint and at times only portions of it show. A knot appears at *D* and varies in size and intensity. A nebulous wing of irregular intensity extends from the variable star about 7″ to the south. There is evidence of very faint extended nebulosity filling the whole starless region about T Tauri. Such details as can be seen on the photographs are roughly sketched in

---

[1] Position for 1860: $\alpha = 4^h\ 13^m\ 48^s$, $\delta = +19^\circ\ 11'.2$. N.G.C. 1554, which precedes No. 1555 by 15^s and is $0'.2$ south, is sometimes referred to as Hind's variable nebula, probably because of the note on p. 225 of the *First Index Catalogue*.

Fig. 2. The luminosity at *E*, *F*, *G*, and *H* is strongest on plate No. 55, although it is also visible in varying degrees on the other plates of the series. The regions I and K appear dark on the plates.

Below is a brief description of the appearance of the nebula on each plate. The brightness of T Tauri is about the same on all the photographs excepting Nos. 180 and 181, upon which it is about a magnitude fainter. Although both the star and the nebula increased in brightness during the interval separating Plates 181 and 217, the data now available do not establish a parallelism between the fluctuation of the two objects.

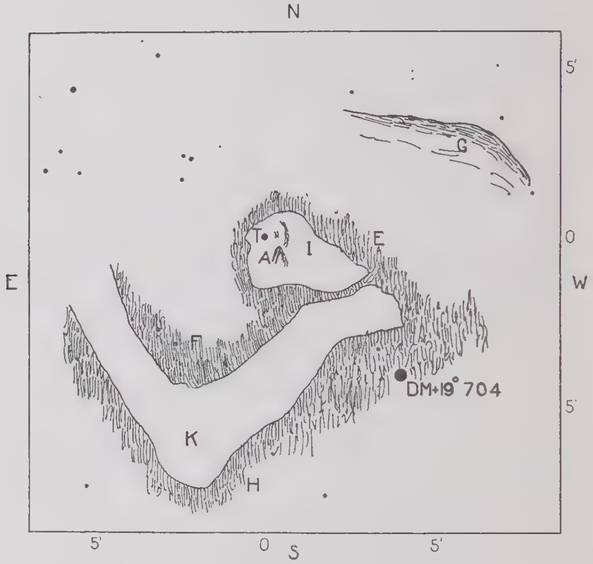

FIG. 2.—Faint nebulosity surrounding T Tauri and Hind's variable nebula

Plate No. 55, 1911, December 25, exposure 3^h 39^m. Nebula diffuse in outline.

T strong.

A knots strong; wings to south medium.

B and *C* very faint.

D medium intensity.

Plate No. 180, 1913, January 8, exposure 20^m.
T faint; has wing on south side, no other detail visible.

Plate No. 181, 1913, February 3, exposure $2^h\ 30^m$. Nebula fan-shaped; contrast stronger than No. 55.
T faint; has strong wing on south side.
A knots stronger than in No. 55; wings to south medium.
B very faint.
C and *D* missing.

Plate No. 217, 1913, September 28, exposure 3^h. Nebula fan-shaped; sharp detail and strong contrast; the nebula is appreciably stronger in intensity than on No. 181.
T same as No. 55.
A knots about same as in No. 181; wings to south medium and longer.
B shows detail; medium intensity.
C faint.
D trace.

Plate No. 226, 1913, October 27, exposure $3^h\ 30^m$. Nebula fan-shaped; detail softer.
T strong; shows wing on south side.
A knots blend with wings; northern half strong.
B west edge only visible; medium intensity.
C very faint.
D faint.

Plate No. 230, 1913, November 25, exposure 3^h. Nebula fan-shaped; same as No. 226.
T strong; wing on south side stronger than in No. 226.
A weaker than No. 226; point strongest; left wing strong, right weak; cross-bar halfway down.
B details; medium intensity.
C missing.
D trace.

Plate No. 280, 1916, November 27, exposure 3^h. Whole region embracing *A*, *T*, and *C* filled with diffuse nebulosity.
T strong.
A diffuse knot, appreciably weaker than on No. 226.

Mr. Adams finds that the spectrum of T Tauri is of type Md with additional bright lines, and that the parallax is of the order of

0″.05 to 0″.10. Since the bright lines of the spectrum appear to extend beyond the dark lines, they are evidently due to the surrounding nebulosity.

In Plate I are shown enlargements of photographs Nos. 181, 217, and 280. The enlargement and contrast necessary for purposes of reproduction have emphasized the grain of the photographs, but the changes in form and intensity of the nebula are clearly visible.

Mount Wilson Solar Observatory
January 1917

PLATE I

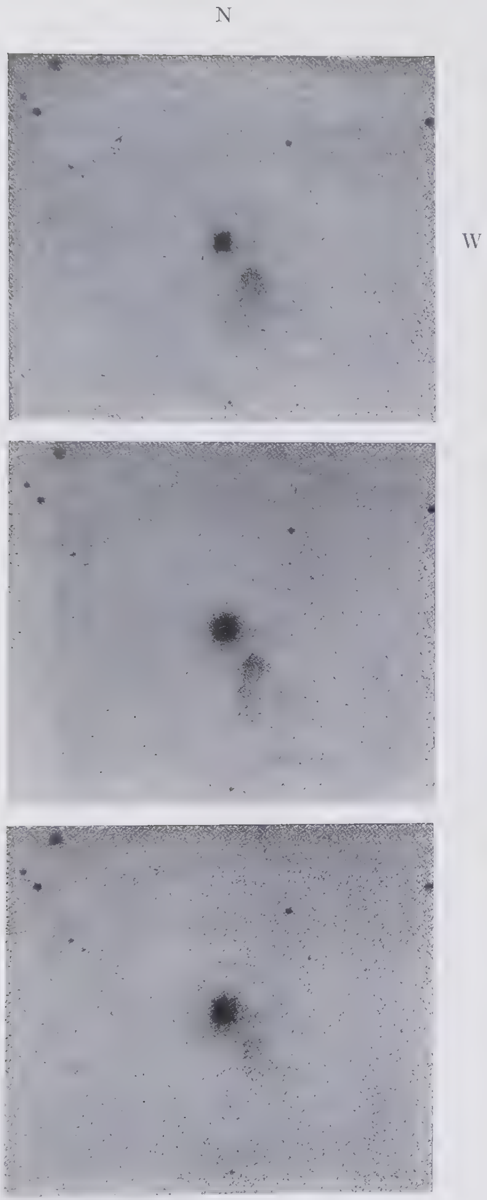

No. 181
1913, Feb. 3

No. 217
1913, Sept. 28

No. 280
1916, Nov. 27

HIND'S VARIABLE NEBULA N.G.C. 1555

Exposures about 3^h with the 60-inch reflector
Enlargement 4.5, Scale 1 mm = 6.″1

Contributions from the Mount Wilson Solar Observatory, No. 128
Reprinted from the *Astrophysical Journal*, Vol. XLV, pp. 182–188, 1917

THE COLOR-CURVE OF XZ CYGNI

By MARTHA BETZ SHAPLEY

The progressive change of spectral type throughout the period of light-variation, recently found for Cepheid variables, denotes a synchronous and continuous change of color-index. As detailed studies of spectral variation will be possible for only the brighter stars, the color-curves afford the best means of inferring the changes in spectral class of the fainter Cepheids, particularly of those with half-day periods. As yet only one or two variables of this type have definitive color-curves. A further contribution to the subject is made in the present paper, which deals with the photographic and photo-visual light-curves of XZ Cygni,[1] a cluster-type variable with unusually rapid change of light.

Ninety-five multiple-exposure photographs, of which 50 are on Seed "27" and 45 on Cramer "Instantaneous Iso" plates, were obtained by Mr. Seares and Mr. Shapley, and kindly placed at my disposal. The plates are described in Tables I and II. An asterisk after the number in the first column indicates that in addition to the exposures on the field of the variable, the plate was also exposed on the field of the North Polar Standards to determine the magnitudes of the comparison stars. For such plates the number after the comma in the sixth column refers to the exposures on the Pole. The magnitude in the fifth column is the mean deduced from all the exposures on one plate. The light-elements used in computing phases are those of Enebo as corrected by Martin and Plummer:[2]

$$\text{Maximum} = \text{J. D. } 2417201.2542 + 0^{d}.466586 \cdot E$$

which represent the Mount Wilson observations with sufficient accuracy.

---

[1] XZ Cygni = B.D. + 56°2257 = A.Oe. 19376 = A.G. Helsingfors 10573. The position for 1900.0 from *Hamburger Astronomische Abhandlungen*, 1, No. 3, p. 95, 1909, is: R.A. = $19^{h}\ 30^{m}\ 24^{s}.92$, Dec. = $56^{\circ}10'22''.8$.

[2] *Monthly Notices*, **74**, 226, 1914.

Because of the great difference in the brightness of the available comparison stars, diaphragms, as indicated in the seventh column, were employed to make the images comparable with those of the variable. The duration of exposure was one minute for the Seed "27" and three minutes for the Isochromatic plates.

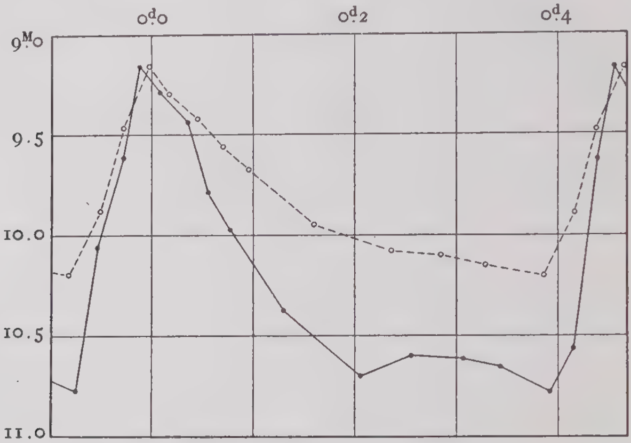

FIG. 1.—Mean photo-visual (broken line) and photographic light-curves of XZ Cygni

The methods of measurement and reduction were those generally employed in photometry with the 60-inch reflector.[1] The North Polar plates yield photographic and photo-visual magnitudes for the comparison stars as shown in Table III. For these determinations, Plates 1904, 1926, 1939, 2860, and 1911, 1927, 1954, 2861 were not used because of the distorted images of polar stars.

The observations in Tables I and II were combined into normals in order of phase, generally four in a group, giving the data of Table IV. Plotting the mean magnitudes against phase, we have the light-curves represented in Fig. 1. Whatever irregularities exist in the shape of the maximum at different epochs and in the color-change are necessarily obscured in a mean curve; and the period of XZ Cygni is too long to permit a determination of the complete color-variation at a single epoch.

---

[1] Seares, *Mt. Wilson Contr.*, No. 80; *Astrophysical Journal*, **39**, 307, 1914.

TABLE I

Photographic Observations of XZ Cygni

Plate Number	Date	Julian Day and Gr. H.M.T.	Phase	Pv. Mag.	No. Exposures	Diaphragms	Normal Number
1715....	1914 July 19	2420333.901	$0\overset{d}{.}455$	9.22	5	14, 9, 6	13
1717....		.915	0.002	9.45	5	32, 14, 9, 6	1
1719....		.932	0.019	9.45	5	14, 9, 6	1
1721....		.949	0.036	9.82	5	32, 14, 9	2
1723....		.964	0.051	10.04	5	32, 14, 9	3
1725....		.979	0.066	9.90	5	32, 14, 9	4
1727....		.993	0.080	9.93	5	14	4
1851....	Aug. 26	2420371.656	0.417	10.23	8	14, 9	11
1853....		.674	0.435	9.49	8	14, 9	12
1855....		.693	0.454	9.14	8	14, 9	13
1857....		.712	0.006	9.13	8	14, 9	1
1859....		.732	0.026	9.30	8	14, 9	2
1861....		.751	0.045	9.42	8	14, 9	3
1863....		.769	0.063	9.97	8	14, 9	3
1865....		.787	0.081	10.12	8	14, 9	4
1867....		.805	0.099	10.29	8	14, 9	5
1869....		.825	0.119	10.25	8	14, 9	5
1871....		.849	0.143	10.36	8	14, 9	5
1873....		.867	0.161	10.64	8	14, 9	5
1875....		.885	0.179	10.83	8	14, 9	6
1877....		.906	0.200	10.78	8	14, 9	6
1879....		.924	0.218	10.78	8	14, 9	6
1904*...	Sept. 18	2420394.799	0.230	10.42	8, 2	14, 9	6
1906....		.817	0.248	10.68	8	14, 9	7
1908....		.837	0.268	10.62	8	14, 9	7
1910....		.855	0.286	10.62	8	14, 9	8
1926*....	Sept. 19	2420395.844	0.342	10.58	2, 2	14, 9	9
1939*....	Sept. 20	2420396.737	0.302	10.57	8, 2	14, 9	8
1941....		.758	0.323	10.52	8	14, 9	8
1943....		.775	0.340	10.63	8	14, 9	9
1945....		.793	0.358	10.66	8	14, 9	9
1947....		.813	0.378	10.69	8	14, 9	10
1949....		.836	0.401	10.69	8	14, 9	10
1951....		.853	0.418	10.32	8	14, 9	11
1953....		.871	0.436	9.47	8	14, 9	12
2027....	Sept. 22	2420398.758	0.457	9.12	8	14, 9	13
2029....		.775	0.007	9.12	8	14, 9	1
2031....		.795	0.027	8.95	8	14, 9	2
2033....		.813	0.045	9.70	8	14, 9	2
2035....		.832	0.064	9.72	8	14, 9	3
2037....		.854	0.086	9.93	8	14, 9	4
2043....	Sept. 23	2420399.623	0.388	11.07	4	32, 14	10
2045....		.638	0.403	10.84	4	32, 9	11
2047....		.652	0.417	10.85	4	32, 9	11
2051....		.682	0.447	9.89	4	32, 6	12
2860*....	1915 Nov. 30	2420832.624	0.398	10.68	2, 2	14	10
3214*....	1916 July 7	2421052.703	0.248	10.52	3, 2	14, 9	7
3215*....		.708	0.253	10.60	3, 2	14, 9	7
3232*....	July 8	2421053.704	0.316	10.72	3, 2	14	8
3234*....		.714	0.326	10.72	2, 2	14	9

TABLE II

PHOTO-VISUAL OBSERVATIONS OF XZ CYGNI

Plate Number	Date	Julian Day and Gr. H.M.T.	Phase	Pg. Mag.	No. Exposures	Diaphragms	Normal Number
1716	1914 July 19	2420333.909	$0^{\rm d}.463$	9.28	3	32, 14, 9	12
1718		.924	0.011	9.30	3	32, 14, 9	1
1720		.941	0.028	9.32	4	32, 14, 9, 6	1
1724		.972	0.059	9.52	3	32, 14	3
1726		.987	0.074	9.62	3	40, 32, 14	3
1728		2420334.000	0.087	9.73	3	32	4
1852	Aug. 26	2420371.665	0.426	9.62	8	32, 14	10
1854		.682	0.443	9.32	8	32, 14	11
1856		.703	0.464	9.16	8	32, 14	12
1858		.721	0.016	9.34	8	32, 14	1
1860		.742	0.036	9.11	8	32, 14	2
1862		.760	0.054	9.61	8	32, 14	2
1864		.778	0.072	9.50	8	32, 14	3
1866		.796	0.090	9.62	8	32, 14	4
1868		.814	0.108	9.68	8	32, 14	4
1870		.834	0.128	9.84	8	32, 14	5
1872		.858	0.152	10.04	8	32, 14	5
1874		.876	0.170	9.95	8	32, 14	5
1876		.894	0.188	9.96	8	32, 14	5
1878		.915	0.209	9.99	8	32, 14	6
1905	Sept. 18	2420394.808	0.239	10.05	4	32, 14	6
1907		.826	0.257	10.08	4	32, 14	6
1909		.846	0.277	10.05	4	32, 14	7
1911*		.864	0.295	10.06	4, 2	32, 14	7
1927*	Sept. 19	2420395.857	0.355	10.16	2, 2	32, 14	9
1940	Sept. 20	2420396.745	0.310	10.03	4	32, 14	7
1942		.767	0.332	10.07	4	32, 14	8
1944		.783	0.348	10.08	4	32, 14	8
1948		.826	0.391	10.29	4	32, 14	9
1950		.844	0.409	10.00	4	32, 14	10
1952		.862	0.427	9.78	4	32, 14	11
1954*		.879	0.444	9.32	4, 2	32, 14	11
2028	Sept. 22	2420398.767	0.466	9.04	4	32, 14	12
2030		.786	0.018	9.22	4	32, 14	1
2032		.804	0.036	9.43	4	32, 14	2
2034		.823	0.055	9.54	4	32, 14	2
2036		.844	0.076	9.59	4	32, 14	3
2038		.864	0.096	9.67	4	32, 14	4
2044	Sept. 23	2420399.631	0.396	10.20	4	32, 14	9
2046		.647	0.412	10.06	4	32, 14	10
2861*	1915 Nov. 30	2420832.628	0.402	10.13	2, 1	14	9
3213*	1916 July 7	2421052.699	0.244	10.19	2, 2	14	6
3216*		.712	0.257	10.26	2, 2	14	7
3231*	July 8	2421053.701	0.313	10.28	3, 4	60, 14	8
3233*		.711	0.323	10.17	1, 2	14	8

From Fig. 1 it is apparent at once that the photographic range is much in excess of the photo-visual. At maximum the star is of about the same brightness in blue and in yellow light, indicating a spectrum of perhaps A0. At minimum the difference in brightness reaches nearly 0.6 mag., and at the corresponding point the spectral class is probably F4 or F5. Three spectrograms made by Mr. Adams show an actual range of A0 to A8; but the length of the exposures on his plates (two to two and one-half hours) tends to obscure and lessen the range, though not affecting the type at maximum.

TABLE III

MAGNITUDES OF COMPARISON STARS

Star	B.D. Number	Photographic Magnitude	Photo-visual Magnitude
1*..........	....	11.43±0.03	10.96±0.02
2..........	$+56^\circ2259$	11.88±0.03	10.09±0.07
3..........	$+56^\circ2261$	7.79±0.03	6.98±0.07
4†..........	....	12.16±0.01	10.64±0.03

* Position, 1855: R.A. = $19^h 29^m 46^s$, Dec. = $+56^\circ 4'.5$.
† Position, 1855: R.A. = $19^h 28^m 55^s$, Dec. = $+56^\circ 5'.4$.

TABLE IV

MEAN LIGHT-CURVES

PHOTOGRAPHIC			PHOTO-VISUAL		
No.	Mean Phase	Mean Mag.	No.	Mean Phase	Mean Mag.
1..........	$0^d.008$	9.29	1..........	$0^d.018$	9.30
2..........	.034	9.44	2..........	.045	9.42
3..........	.056	9.79	3..........	.070	9.56
4..........	.078	9.97	4..........	.095	9.68
5..........	.130	10.38	5..........	.160	9.95
6..........	.206	10.70	6..........	.237	10.08
7..........	.254	10.60	7..........	.285	10.10
8..........	.307	10.61	8..........	.329	10.15
9..........	.342	10.65	9..........	.386	10.20
10..........	.391	10.78	10..........	.416	9.89
11..........	.414	10.56	11..........	.438	9.47
12..........	.439	9.62	12..........	0.464	9.16
13..........	0.455	9.16			

The photometric data concerning maximum and minimum light and color of XZ Cygni are as follows:

	Pg. Mag.	Pv. Mag.	C.I.	Color-Class
Maximum....	9.16	9.16	0.00	*a0*
Minimum....	10.78	10.20	0.58	*f4*
Range.......	1.62	1.04	0.58	....

The range and shape of the photographic curve are in fair agreement with the results of Martin and Plummer.[1]

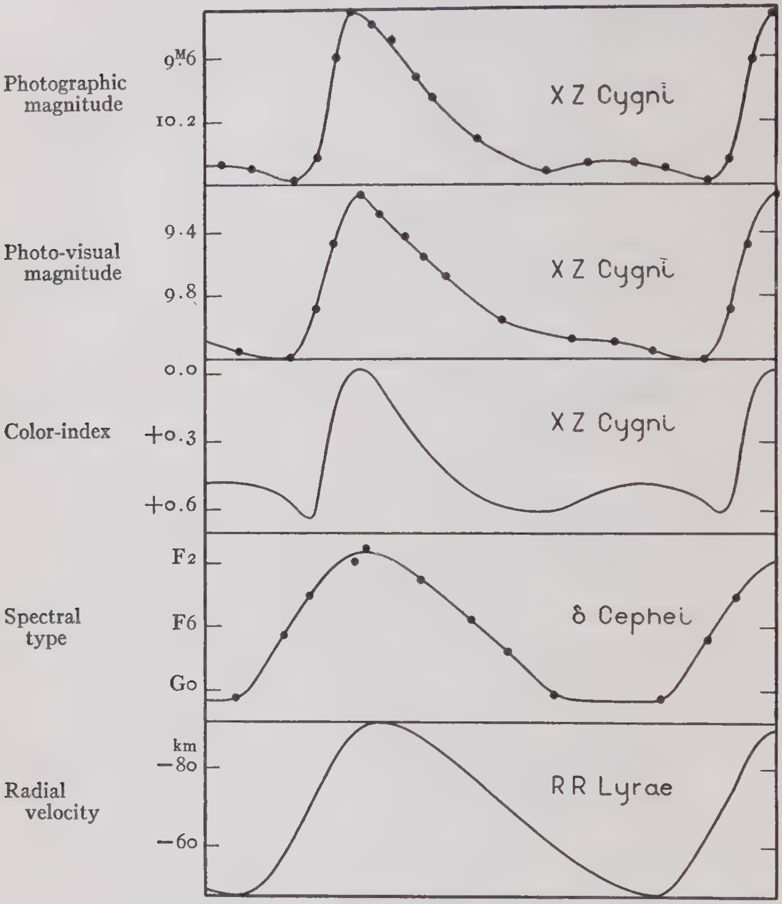

FIG. 2.—Five aspects of Cepheid variation

In conclusion, Fig. 2 is presented as an interesting summary of the various periodic changes which Cepheid variables undergo from one epoch of maximum light to another: (1) variation in photographic light, (2) variation in photo-visual light, (3) variation in color, (4) variation in spectrum,[1] (5) variation in radial velocity.[2] Since data relating to (4) and (5) are not available for XZ Cygni, the curves from other objects of the Cepheid class have been inserted for comparison. There is a striking similarity in the shape and fluctuations of all the curves. It is impossible not to conclude that all these phenomena are due to one underlying cause.

---

[1] *Monthly Notices*, 74, 230, 1914.

MOUNT WILSON SOLAR OBSERVATORY
January 1917

---

[1] *Mt. Wilson Contr.*, No. 124; *Astrophysical Journal*, **44**, 273, 1916.

[2] *Lick Observatory Bulletins*, **7**, 143, 1913.

Contributions from the Mount Wilson Solar Observatory, No. 129
Reprinted from the *Astrophysical Journal*, Vol. XLV, pp. 225–243, 1917

ON THE DISTRIBUTION OF STARS IN TWELVE GLOBULAR CLUSTERS

BY FRANCIS G. PEASE AND HARLOW SHAPLEY

All quantitative studies of the distribution in clusters have been concerned with the relation of the number of stars to distance from the center, and, with the exception of some results for the brighter stars recently published by Bailey,[1] no special attention has been paid to direction from center. It has been remarked in earlier papers that the conclusions relative to cluster structure, which are based on observations of star-density as a function solely of apparent distance, are of limited meaning and application. The brightest stars of each cluster, which are those mainly involved in previous investigations, are not typical in color or luminosity; and, in addition, the possibility of serious systematic error in photographing the highly concentrated interior is so great that little confidence can be placed upon observed distribution laws, except when they are derived from and are supposed to interpret only the outer part of the cluster. The difficulties inherent in stellar concentration are of much less importance, however, when the relative distribution is analyzed on the basis of direction from the center; and this method of study, moreover, is capable of bringing to light a property of clusters that the usual method has failed to reveal.

In the following pages are given the results of star-counts on a series of cluster photographs made with the 60-inch reflector at Mount Wilson. Later, with the accumulation of data bearing on the Eberhard effect and on the various relations of magnitudes and colors, it may be feasible to inquire more closely into the star-density with respect to distance from the center; but for the present it is practicable to discuss the results only as far as they are related to sphericity of cluster-form.

---

[1] *Harvard Annals*, **76**, No. 4, 1915.

The stars were originally counted for a rectangular system of co-ordinates,[1] a reseau on glass being superposed directly upon the original negative and the number of stars being tabulated for each small square, which is 31″.4 on a side. The total area counted on each plate is 675 square minutes of arc, comprising 2464 small squares. In all cases a second count was made with the plate reversed, and frequently several counts were made, particularly at the beginning of the work and for those plates which appeared to give discordant results. Each count was recorded on cross-section paper, and over these records was drawn a system of rings and 30° sectors, as illustrated for one quadrant in Fig. 1. The width of each annular region is four of the small divisions, that is, approximately two minutes of arc; the radius of the central area varies from two to six divisions, depending on the condensation of stars toward the center. Miss Van Deusen and Miss Richmond, of the Computing Division, have made the counts for the rectangular and polar systems, respectively, and have given much service in the statistical discussion of the results.

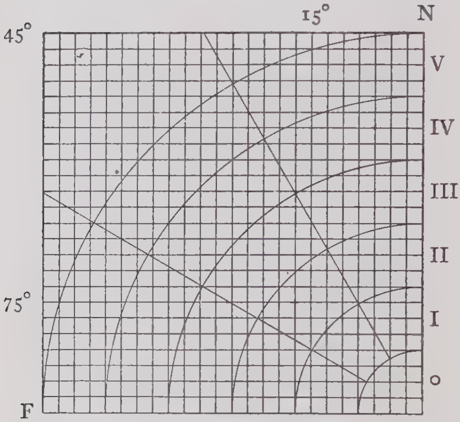

FIG. 1.—Scheme of rectangular and polar divisions (for the first quadrant) used in counting stars in globular clusters.

The photographs for which the counts have been completed are described in Table I. Nos. 64, 65, and 2456P are Seed 27 plates; all others are Seed 23. The total number of stars on each plate, seventh column, includes the count (or, when burned out, the estimate) of stars in the center, and also of those farther from the center than the limiting distance used in Tables II and III. This total number attempts to include all stars on each plate within

---

[1] "Annual Report of the Director of the Mount Wilson Solar Observatory," *Yearbook of the Carnegie Institution of Washington*, 13, 258, 1914.

TABLE I

Description of Plates

Cluster		Plate No.	Date	Exp. Time	No. of Counts	Total No. of Stars	Remarks
N.G.C.	Messier						
5024....	53	102	1912 May 13	180^m	2	10,100	Sky thick
5272....	3	64	Mar. 17	5	2	2,970	
		65	Mar. 17	15	2	6,440	
		89	May 11	20	2	5,230	
		2456P	1915 June 7	60	2	8,000†	
6093....	80	206	1913 July 2	64	2	4,050	Mirror not uniform
6205....	13	213	Sept. 1	1	2	820	
		220	Oct. 27	1	2	1,090	
		212	Sept. 1	3	2	1,700	
		13	1911 July 24	6	2	5,810	High wind
		18*	July 25	6	2	7,870	Troubled by clouds
		211*	1913 Sept. 1	6	2	2,160	
		218*	Oct. 27	6	2	3,140	
		14	1911 July 24	15	4	7,780	
		134*	1912 June 15	15	3	3,830	Very bad seeing
		19	1911 July 25	22	4	14,700	
		15	July 24	37.5	4	18,000	Sky white
		16	July 24	94	2	25,500	Sky white
		133	1912 June 15	300	2	35,000	Strong wind; mirror edge distorted
6218....	12	100	May 12	90	2	6,060	Windy
6229....	......	8	1911 July 23	69	2	1,540	Windy
6254....	10	124	1912 June 12	6	2	1,270	
		123	June 12	20	2	3,260	
		117	June 11	60	3	5,860	High wind
		114	June 10	180	3	12,200	
6341....	2	5	1911 July 2	100	2	6,800	Seeing poor
6402....	14	103	1912 May 13	120	2	4,920	
6779....	56	3	1911 July 2	60	2	6,600	High wind
6934....	......	2	July 1	105	2	3,370	
7078....	15	224*	1913 Oct. 27	1	2	1,100	
		223	Oct. 27	2	2	1,460	
		222	Oct. 27	6	2	2,340	
		21	1911 Aug. 22	6	2	2,030	Good seeing
		22*	Aug. 22	15	2	3,790	
		26	Aug. 25	15	2	3,320	
		225*	1913 Oct. 27	15	2	3,520	
		23	1911 Aug. 22	37.5	2	9,000	
		24	Aug. 22	94	2	21,000	
		25	Aug. 22	312	2	29,000	Plate completed on August 25, 1911

* Detailed counts are not given in Tables II or III.

† The area counted on plate 2456P is only 121 square minutes of arc.

the limits of the reseau, and it shows that conspicuously different totals for a cluster may be obtained from exposures of the same length. Apparently the seeing, transparency, quality of plate, development, and other factors may so influence the outcome that only for the mean of many plates can definite extensions of the magnitude-interval be assumed to result from corresponding increases in the exposure time.

Table II contains the star-counts for the eight clusters for which fairly definite results have been obtained. The clusters are in order of right ascension; the plates for each cluster are in order of increasing exposure time; the rings for each plate are in order of increasing distance from the center, and the sectors are indicated by the position-angle of the line that bisects them.[1] Unless there is a footnote to the contrary, the radius of the central area and the width of the rings are each four divisions (2'.09). The tabulated quantities are mean numbers for two counts. With the aid of plots of the sums of the horizontal and vertical columns in the original rectangular system, independent determinations of the position of the cluster's center were made for each count on every plate, thus giving an origin for the ring and sector system. That the adopted mean center for any cluster may vary slightly from plate to plate should be remembered in discussing the distribution for a given magnitude interval on the basis of differences. For this purpose, however, the combination of results for opposite sectors should largely eliminate the error of centering.

The count of stars in the central region for all but the shortest exposures is uncertain, if not completely impossible. Hence, these results are tabulated for quadrants only, and in general are omitted from the discussion. When the count is incomplete for any sector of the outermost ring, no number is given in the table, and the mean value in the last column refers only to the sectors for which counts are tabulated.

As it will be some years before a systematic continuation of this work can be undertaken, preliminary results are now given in

---

[1] In a communication to the *Proceedings of the National Academy of Sciences*, **3**, 96, 1917, the angles of direction are counted in the opposite sense and from another origin.

PLATE II

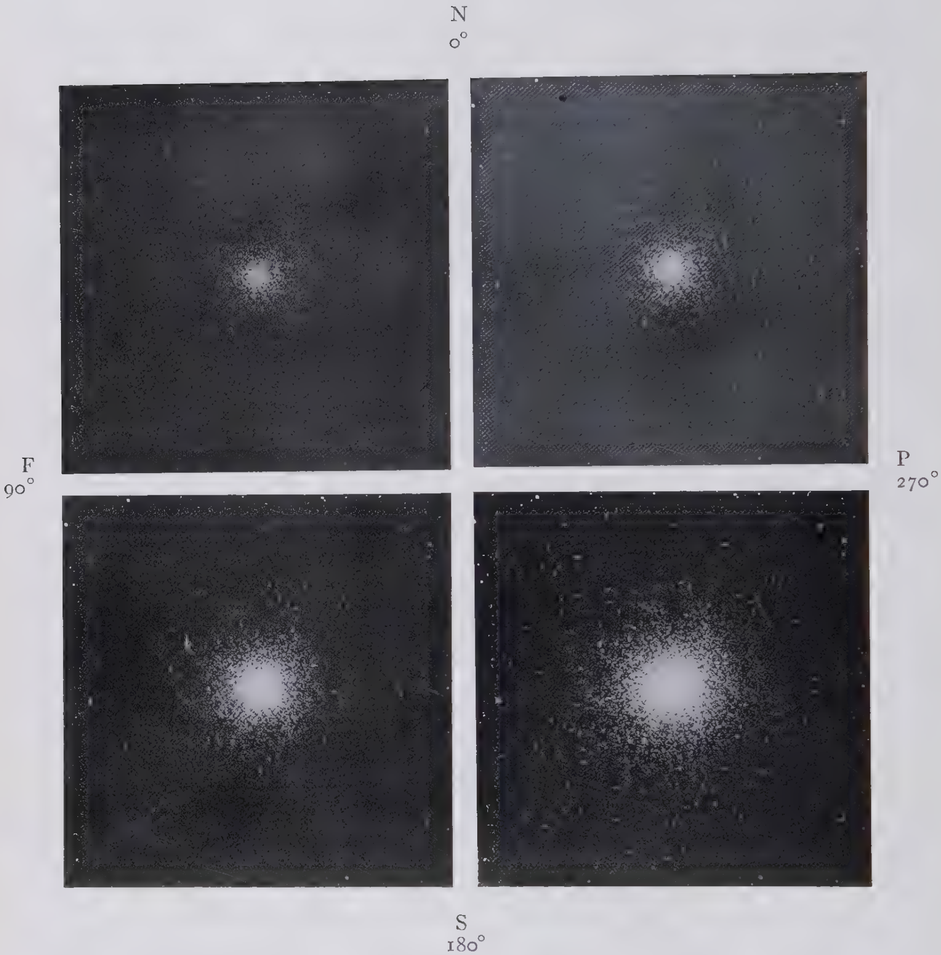

FOUR SUCCESSIVE EXPOSURES ON MESSIER 13

The position-angle of the major axis is 120°. The photographs reproduced are Nos. 13, 14, 15, and 16, described in Table I.

Table III for four clusters that later may be studied definitively. The future work will also include a further investigation of some of the clusters in Table II, in particular Messier 3 and Messier 56.

The following tabular material can be discussed to advantage with the aid of diagrams. The data for Messier 13 are particularly complete and may be closely examined, leaving the results on other clusters for a briefer statement. Fig. 2 shows for several plates of Messier 13 the plot of the number of stars in successive sectors. That the cluster is symmetrically elongated is at once evident. The number of stars in two directions at right angles to each other differs by about 25 per cent. The plates of less than four minutes' exposure, however, dealing as they do with only one or two thousand stars which are peculiar in color and luminosity, do not show definitely this elliptical form. Among these brighter stars the axis of symmetry is not revealed until the distribution is studied on the basis of color-index or variable stars.[1]

At first thought it may be surprising that in a much-studied cluster such a pronounced elliptical distribution could exist and escape earlier detection. The reason must be that to the casual observer the brightest stars are conspicuous to the point of causing prejudice in the estimation of numbers, whereas, to one who actually counts the stars, the eighteenth-magnitude objects are the equal of those five hundred times more luminous. The irregular or sensibly spherical distribution of the giants hides the underlying ellipticity. In spite of the preponderance of the large images, however, the elongation of Messier 13 can be seen on some of the longer exposures, and, to a lesser extent, in the reproductions of the photographs in the accompanying plate.

That the elliptical form of Messier 13 is more or less independent of distance from the center is illustrated in Fig. 3, where, for plate 16, the data appear separately for successive regions, the ordinates, for the sake of intercomparison, being percentage deviations from the mean for each ring. Since in Fig. 2 little asymmetry is apparent that cannot be attributed to accidental groupings and errors of centering, the plots in Fig. 3 and in the following analogous diagrams represent the means for opposite sectors. The relation

---

[1] *Proceedings of the National Academy of Sciences*, **3**, 276, 1917.

TABLE II

DISTRIBUTION OF STARS IN EIGHT CLUSTERS

N.G.C. 5024, MESSIER 53

Plate (Exp.)	Ring	Sectors												Mean
		15°	45°	75°	105°	135°	165°	195°	225°	255°	285°	315°	345°	
102 (180^m)	o*	......	344	......	......	336	......	......	314	......	......	306	......	325
	I	385	384	373	359	402	362	376	362	344	340	378	373	370
	II	200	182	160	187	208	189	200	184	204	204	212	217	196
	III	100	92	85	76	92	94	106	100	98	108	106	102	97
	IV	44	28	37	34	28	34	42	46	40	47	42	38	38
	V	Inc.	14	16	11	16	20	25	24	20	16	24	Inc.	19
	I–II	585	566	533	546	610	551	576	546	548	544	590	590	565
	III–IV	144	120	122	110	120	128	148	146	138	155	148	140	135
	I–IV	729	686	655	656	730	679	724	692	686	699	738	730	700

N.G.C. 5272, MESSIER 3

Plate (Exp.)	Ring	15°	45°	75°	105°	135°	165°	195°	225°	255°	285°	315°	345°	Mean
64 (5^m)	o*	......	459	......	......	514	......	......	474	......	......	418	......	466
	I	48	56	58	50	45	42	60	68	56	56	60	55	54
	II	20	14	20	10	12	16	17	24	16	25	26	16	18
	III	8	10	6	8	6	12	6	10	8	9	10	5	8
	IV	3	10	3	6	3	6	6	4	10	7	10	4	6
	V	Inc.	2	4	3	2	Inc.	Inc.	4	2	2	4	Inc.	3
	I–IV	79	90	87	74	66	76	89	106	90	97	106	80	87
65 (15^m)	o	......	669	......	......	628	......	......	698	......	......	726	......	680
	I	168	153	194	156	150	137	174	196	201	214	192	185	177
	II	70	68	50	54	52	69	54	98	102	121	100	64	75
	III	26	22	21	12	18	29	20	35	50	46	38	40	30
	IV	6	14	8	12	4	16	10	16	26	26	28	14	15
	V	Inc.	8	6	4	6	Inc.	Inc.	8	5	8	12	Inc.	7
	I–II	238	221	244	210	202	206	228	294	303	335	292	249	252
	III–IV	32	36	29	24	22	45	30	51	76	72	66	54	45
	I–IV	270	257	273	234	224	251	258	345	379	407	358	303	297

89 (20^m)....	o	......	632	......	......	628	......	......	644	......	......	635	......	635
	I	150	135	152	138	110	128	115	135	132	152	144	149	137
	II	46	43	42	42	43	68	45	53	42	54	68	48	50
	III	17	17	18	14	15	21	14	21	16	19	20	18	18
	IV	6	16	6	12	4	17	11	9	14	10	16	8	11
	V	Inc.	7	5	4	6	Inc.	Inc.	6	4	4	6	Inc.	5
	I–II	196	178	194	180	153	196	160	188	174	206	212	197	186
	III–IV	23	33	24	26	19	38	25	30	30	29	36	26	28
	I–IV	219	211	218	206	172	234	185	218	204	235	248	223	214
2456P (60^m)	o†	......	233	......	......	320	......	......	259	......	......	156	......	242
	I	233	213	220	208	242	246	240	268	229	248	253	242	237
	II	177	210	197	195	185	195	197	201	197	202	216	174	196
	I–II	410	423	417	403	427	441	437	469	426	450	469	416	432

N.G.C. 6205, MESSIER 13

213 (1^m)....	o	......	124	......	......	140	......	......	140	......	......	114	......	130
	I	9	11	13	8	18	18	12	16	12	18	12	12	13
	II	4	5	4	2	4	8	4	5	3	4	4	2	4
	III	0	2	2	4	2	2	1	2	1	4	1	2	2
	IV	2	2	0	4	0	2	1	2	0	0	0	2	1
	V	1	1	4	2	3	3	1	3	0	0	0	0	2
	I–V	16	21	23	20	27	33	19	28	16	26	17	18	22
220 (1^m)....	o	......	156	......	......	163	......	......	170	......	......	176	......	166
	I–IV‡	......	74	......	......	90	......	......	92	......	......	97	......	88
212 (3^m)....	o	......	237	......	......	257	......	......	236	......	......	258	......	247
	I	32	26	30	22	36	35	30	29	32	32	27	28	30
	II	12	6	12	6	12	16	10	11	10	14	19	8	11
	III	3	4	8	7	2	4	4	6	4	6	6	3	5
	IV	2	6	5	6	0	4	4	7	3	2	2	2	4
	V	Inc.	6	4	2	4	3	2	6	1	4	2	Inc.	3
	I–IV	49	42	55	41	50	59	48	53	49	54	54	41	50

* Radius of central area $1'.05$.

† Intervals of distance from center for successive rings are $0'.0-1'.75$, $1'.75-3'.25$, and $3'.25-4'.75$.

‡ Counted in quadrants only.

TABLE II—*Continued*

N.G.C. 6205, MESSIER 13—*Continued*

Plate (Exp.)	Ring	Sectors 15°	45°	75°	105°	135°	165°	195°	225°	255°	285°	315°	345°	Mean
13 (6^{m})	o	......	792	......	......	858	......	......	786	......	......	840	......	819
	I	100	106	136	162	168	158	104	96	106	170	162	150	135
	II	31	24	46	45	26	29	36	32	38	42	40	23	34
	III	22	11	20	16	14	14	6	16	22	28	20	18	17
	IV	10	8	9	12	6	12	8	10	8	16	13	7	10
	V	Inc.	8	10	7	6	Inc.	Inc.	6	5	9	4	Inc.	7
	I–IV	163	149	211	235	214	213	154	154	174	256	235	198	196
14 (15^{m})	o	......	852	......	......	980	......	......	922	......	......	866	......	905
	I	190	182	249	249	280	222	196	162	190	288	198	196	217
	II	61	50	92	78	84	62	64	36	47	70	71	62	65
	III	26	18	69	51	36	20	14	22	18	24	28	31	30
	IV	19	14	23	18	20	10	10	10	4	19	12	16	15
	V	Inc.	12	8	6	10	Inc.	Inc.	7	6	12	8	Inc.	9
	I–IV	296	264	433	396	420	314	284	230	259	401	309	305	326
19 (22^{m})	o	......	1273	......	......	1231	......	......	1202	......	......	1320	......	1256
	I	414	429	449	483	462	386	341	352	418	474	478	430	426
	II	208	146	182	230	220	144	130	129	164	212	226	186	181
	III	82	65	86	103	92	72	62	64	76	98	111	88	83
	IV	30	32	27	43	40	36	36	38	26	41	37	34	35
	V	Inc.	17	18	12	Inc.	Inc.	Inc.	Inc.	23	16	14	Inc.	17
	I–II	622	575	631	713	682	530	471	481	582	686	704	616	608
	III–IV	112	97	113	146	132	108	98	102	102	139	148	122	118
	I–IV	734	672	744	859	814	638	569	583	684	825	852	738	726
15 ($37^{\mathrm{m}}5$)	o	......	1224	......	......	1223	......	......	1260	......	......	1328	......	1259
	I	404	430	512	554	559	498	462	462	566	568	502	406	494
	II	212	204	254	282	282	204	190	202	260	282	272	208	238
	III	90	88	107	117	133	97	82	90	112	110	139	98	105
	IV	43	48	40	55	52	54	45	50	36	51	50	51	48
	V	Inc.	32	28	22	25	Inc.	Inc.	27	25	25	28	Inc.	22
	I–II	616	634	766	836	841	702	652	664	826	850	774	614	731
	III–IV	133	136	147	172	185	151	127	140	148	161	189	149	153
	I–IV	749	770	913	1008	1026	853	779	804	974	1011	963	763	884

16 (94^m)....	0.........	......	990	......	......	760	......	......	626	......	......	768	......	786
	I.........	623	668	750	762	764	728	712	683	758	778	718	670	718
	II........	358	361	423	464	476	386	330	352	402	438	479	394	405
	III.......	168	207	212	236	226	202	188	194	214	248	249	198	212
	IV........	112	104	90	128	114	115	108	114	112	126	134	99	113
	V.........	Inc.	58	58	50	64	Inc.	Inc.	55	63	70	64	Inc.	60
	I–II......	981	1029	1173	1226	1240	1114	1042	1035	1160	1216	1197	1064	1123
	III–IV....	280	311	302	364	340	317	296	308	326	374	383	297	325
	I–IV......	1261	1340	1475	1590	1580	1431	1338	1343	1486	1590	1580	1361	1448
133 (300^m)..	0*........	......	......	......	......	......	3627	......	......	......	......	......	......	3627
	I.........	560	640	624	684	788	642	586	597	629	658	712	662	648
	II........	362	374	410	471	431	360	302	292	358	396	424	394	381
	III.......	204	220	220	261	244	230	191	196	200	246	232	202	220
	IV........	141	136	116	118	130	Inc.	Inc.	124	130	157	134	100	129
	I–III.....	1126	1234	1254	1416	1463	1232	1079	1085	1187	1300	1368	1258	1250

N.G.C. 6218, MESSIER 12

100 (90^m)...	0.........	......	386	......	......	386	......	......	378	......	......	365	......	379
	I.........	149	168	164	164	178	162	166	174	164	171	176	174	168
	II........	90	100	97	98	108	103	98	106	92	100	93	95	98
	III.......	42	44	48	50	47	39	63	52	40	36	34	50	45
	IV........	22	22	26	24	20	27	30	24	34	30	28	30	26
	V.........	Inc.	23	26	21	22	Inc.	Inc.	22	22	26	15	Inc.	22
	I–IV......	303	334	335	336	353	331	357	356	330	337	331	349	338

N.G.C. 6254, MESSIER 10

124 (6^m)....	0†........	......	68	......	......	85	......	......	92	......	......	81	......	82
	I.........	41	42	34	36	45	50	46	42	42	44	45	37	42
	II........	12	8	10	16	20	14	20	16	15	18	18	8	15
	III.......	4	6	8	8	6	8	7	7	8	6	10	8	7
	IV........	4	4	4	5	2	4	5	3	8	6	4	3	4
	V.........	2	4	7	7	4	5	7	6	6	8	5	4	5
	I–V.......	63	64	63	72	77	81	85	74	79	82	82	60	74

---

* Because of the larger area of the burned-out center, the central region has a radius of 3′.14 instead of the usual 2′.09. The succeeding rings are 2′.09 in width.

† Radius of central area is 1′.05.

TABLE II—*Continued*

N.G.C. 6254, MESSIER 10—*Continued*

Plate (Exp.)	Ring	Sectors												Mean
		15°	45°	75°	105°	135°	165°	195°	225°	255°	285°	315°	345°	
123 (20m)	0*	......	144	......	......	140	......	......	126	......	......	134	......	136
	I	114	131	133	116	110	100	105	108	106	114	126	136	117
	II	42	42	65	62	48	60	48	44	38	42	46	50	49
	III	18	23	22	32	26	20	27	22	19	17	21	24	23
	IV	8	10	8	17	11	14	12	11	12	12	6	9	11
	V	6	6	12	16	11	11	14	14	8	14	6	10	11
	I–V	188	212	240	243	206	205	206	199	183	199	205	229	210
117 (60m)	0	......	432	......	......	454	......	......	424	......	......	439	......	437
	I	156	148	154	176	166	156	170	137	156	154	164	174	159
	II	70	69	86	96	77	70	80	96	66	63	86	84	79
	III	40	29	26	38	42	32	46	24	38	48	44	50	38
	IV	24	15	22	24	12	20	20	18	24	34	30	19	22
	V	Inc.	18	20	18	16	Inc.	Inc.	22	22	14	18	Inc.	18
	I–IV	290	261	288	334	297	278	316	275	284	299	324	327	298
114 (180m)	0*	......	146	......	......	92	......	......	86	......	......	143	......	117
	I	271	304	292	306	314	268	296	290	290	282	293	286	291
	II	274	262	264	270	250	283	268	255	242	276	266	254	264
	III	161	169	150	173	170	162	159	161	164	152	151	154	160
	IV	95	104	104	112	96	103	113	86	102	104	108	83	101
	V	69	62	76	64	48	64	67	54	50	61	68	69	63
	I–III	706	735	706	749	734	713	723	706	696	710	710	694	715
	IV–V	163	166	180	176	144	167	180	140	152	165	176	152	163
	I–V	869	901	886	925	878	880	903	846	842	875	886	846	878

N.G.C. 6341, MESSIER 2

Plate (Exp.)	Ring	15°	45°	75°	105°	135°	165°	195°	225°	255°	285°	315°	345°	Mean
5 (100m)	0*	......	107	......	......	112	......	......	136	......	......	142	......	124
	I	252	226	237	258	303	242	240	228	246	271	268	274	254
	II	154	118	132	148	153	140	124	114	146	171	170	164	144
	III	40	40	38	46	42	52	46	56	49	53	60	43	47
	IV	17	20	14	12	13	24	19	18	17	26	30	27	20
	V	Inc.	10	20	16	18	13	18	14	18	8	15	Inc.	15
	I–II	406	344	369	406	456	382	364	342	392	442	438	438	398
	III–IV	57	60	52	58	55	76	65	74	66	79	90	70	58
	I–IV	463	404	421	464	511	458	429	416	458	521	528	508	465

N.G.C. 6779, MESSIER 56

3 (60^m)	o*	…….	151	…….	…….	158	…….	…….	132	…….	…….	128	…….	142
	I	88	92	94	98	101	82	83	87	90	88	98	94	91
	II	62	54	56	70	68	62	62	62	60	50	54	50	59
	III	84	63	62	67	62	73	74	58	66	66	54	68	66
	IV	84	52	60	70	88	74	79	74	72	66	74	69	72
	V	76	66	82	84	83	84	98	83	90	86	74	81	82
	I–V	394	327	354	389	402	375	396	364	378	356	354	362	371

N.G.C. 7078, MESSIER 15

223 (2^m)	o	…….	256	…….	…….	216	…….	…….	256	…….	…….	268	…….	249
	I	26	18	20	20	13	20	12	17	23	20	18	18	19
	II	2	9	6	6	0	8	6	4	8	5	4	6	5
	III	4	1	6	8	1	5	6	8	4	4	6	2	5
	IV	4	6	2	5	2	4	2	3	2	3	2	3	3
	V	Inc.	2	2	4	2	Inc.	Inc.	4	4	8	4	Inc.	4
	I–IV	36	34	34	39	16	37	26	32	37	32	30	29	32
21 (6^m)	o	…….	394	…….	…….	426	…….	…….	395	…….	…….	392	…….	402
	I	32	31	36	32	24	27	20	29	29	25	26	26	28
	II	8	17	12	10	4	10	11	9	9	8	6	13	10
	III	6	5	8	10	5	6	6	9	4	5	6	9	7
	IV	6	10	6	6	10	4	2	4	3	4	3	7	5
	V	Inc.	4	2	9	4	Inc.	Inc.	6	4	9	4	Inc.	5
	I–IV	52	63	62	58	43	47	39	51	45	42	41	55	50
222 (6^m)	o	…….	433	…….	…….	416	…….	…….	462	…….	…….	463	…….	444
	I	34	34	34	29	26	34	18	33	36	34	30	34	31
	II	14	17	10	12	4	12	12	13	14	10	10	14	12
	III	6	2	8	13	2	5	8	10	6	6	8	8	7
	IV	5	8	6	6	10	4	5	6	4	6	6	8	6
	V	Inc.	3	4	6	3	5	9	12	6	8	4	Inc.	6
	I–IV	59	61	58	60	42	55	43	62	60	56	54	64	56
26 (15^m)	o	…….	488	…….	…….	456	…….	…….	558	…….	…….	556	…….	514
	I	61	51	48	55	46	50	44	64	64	56	47	47	55
	II	18	26	10	16	8	18	24	20	20	20	12	20	16
	III	10	3	11	14	2	8	10	16	12	10	8	9	14
	IV	6	10	6	6	11	8	10	12	5	8	10	10	6
	V	Inc.	4	4	10	8	Inc.	Inc.	12	6	12	11	Inc.	8
	I–IV	95	90	75	91	77	84	88	112	101	94	77	86	89

---

* Radius of central area is 1′.05.

TABLE II—*Continued*

N.G.C. 7078, MESSIER 15—*Continued*

Plate (Exp.)	Ring	Sectors												Mean
		15°	45°	75°	105°	135°	165°	195°	225°	255°	285°	315°	345°	
23 (37^{m}5)	O	......	1028	......	......	965	......	......	1028	......	......	1104	......	1031
	I	242	232	240	210	212	202	248	272	220	213	238	221	229
	II	60	64	54	66	71	58	78	78	76	56	46	62	64
	III	28	30	27	32	18	31	28	39	32	29	30	19	29
	IV	20	18	22	21	19	22	20	21	8	20	24	20	20
	V	Inc.	12	14	18	21	Inc.	Inc.	22	9	18	22	Inc.	17
	I–II	302	296	294	276	283	260	326	350	296	269	284	283	293
	III–IV	48	48	49	53	37	53	48	60	40	49	54	39	48
	I–IV	350	344	343	329	320	313	374	410	336	318	338	322	341
24 (94^{m})	O	......	1499	......	......	1408	......	......	1396	......	......	1499	......	1450
	I	658	620	606	600	570	597	634	638	610	560	614	620	611
	II	264	266	269	250	274	280	320	334	293	262	248	283	279
	III	133	132	112	146	122	128	120	138	146	106	130	114	127
	IV	71	50	70	80	78	72	84	84	54	54	64	53	68
	V	Inc.	35	30	52	40	Inc.	Inc.	60	30	54	39	Inc.	42
	I–II	922	886	875	850	844	877	954	972	903	822	862	903	889
	III–IV	204	182	182	226	200	200	204	222	200	160	194	167	195
	I–IV	1126	1068	1057	1076	1044	1077	1158	1194	1103	982	1056	1070	1084
25 (312^{m})	O	......	......	......	......	......	1972	......	......	......	......	......	......	1972
	I	682	662	624	609	610	593	634	680	635	604	604	674	634
	II	386	372	346	348	385	402	364	414	418	390	412	384	385
	III	218	221	180	200	194	203	174	212	226	192	223	199	204
	IV	144	102	134	121	122	124	134	140	112	130	115	109	124
	V	Inc.	72	62	76	66	Inc.	Inc.	88	68	85	80	Inc.	76
	I–II	1068	1034	970	957	995	995	998	1094	1053	994	1016	1058	1019
	III–IV	362	323	314	321	316	327	308	352	338	322	338	308	327
	I–IV	1430	1357	1284	1278	1311	1322	1306	1446	1391	1316	1354	1366	1347

TABLE III

Preliminary Results for Four Clusters

N.G.C.	Distance from Center	Sectors												Mean
		15°	45°	75°	105°	135°	165°	195°	225°	255°	285°	315°	345°	
6093......	1′.0–11′.5	216	217	222	226	248	246	246	228	221	237	209	185	225
6229......	1.0–11.5	45	46	52	43	47	43	44	42	44	52	49	50	46
6402......	2.1–10.5	198	192	178	188	189	168	193	203	193	182	200	235	193
6934......	1.0–11.5	154	179	170	164	157	180	195	194	195	195	193	188	180

TABLE IV

Percentage Deviations from the Mean for Messier 12 (Plate 100) and Messier 13 (Plate 15)

Cluster	Sectors												Average Deviations
	15°	45°	75°	105°	135°	165°	195°	225°	255°	285°	315°	345°	
Messier 12........	−10	− 1	−1	− 1	+ 4	−2	+ 6	+5	− 2	0	−2	+ 3	± 3
Messier 13........	−15	−13	+3	+14	+16	−4	−12	−9	+10	+14	+9	−14	±11

of ellipticity to magnitude-interval is shown by Fig. 4. The diagram at the top is based on plate 13, the bottom one on plate 16; the values for the second from the top are differences between plates 15 and 13, and the remaining curve represents plate 16 *minus* plate 15. These curves agree in showing ellipticity with approximately the same major axis for all intervals of magnitude; but their differences and irregularities should not be considered too seriously.

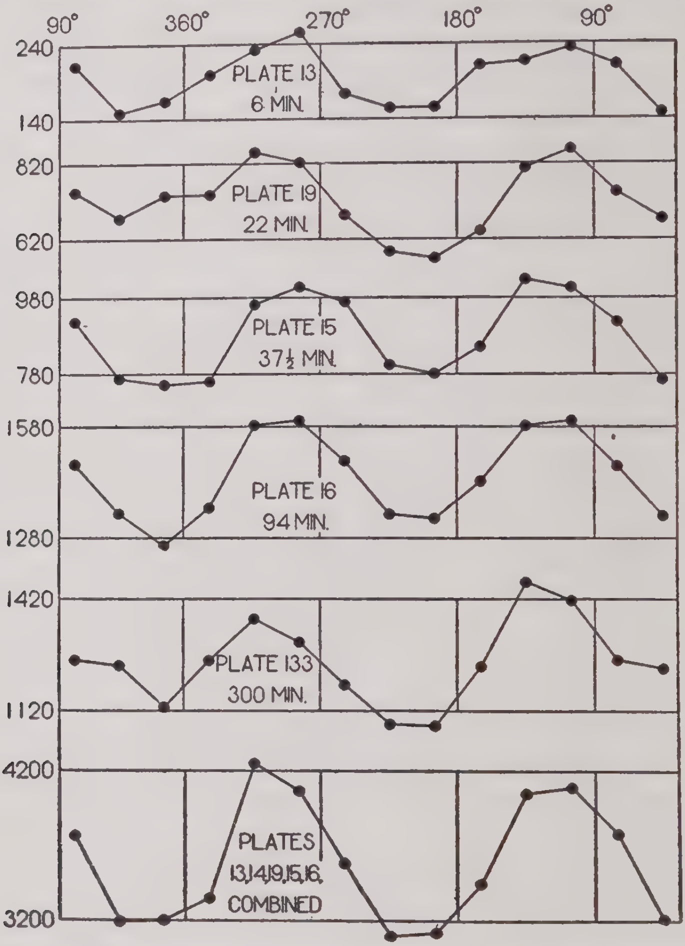

FIG. 2.—The axis of symmetry in Messier 13. Ordinates are numbers of stars. Abscissae are position-angles.

Reverting to the data in Table II, attention should be called to a few points concerning the other clusters.

The tabulated counts show distinctly for Messier 53 two maxima about 180° apart. At position-angle 165°, however, at what should be the highest point of one maximum, the numbers are peculiarly low in Rings I and II, and the resulting depression in the curve persists even when opposite sectors are combined, as in Fig. 5. If, as suggested in earlier communications, the axes of symmetry in these clusters are projections of galactic planes, this phenomenon, which can hardly be attributed to accidental irregularity, would have a close analogue in the great cleft extending south from Cygnus in our Milky Way.

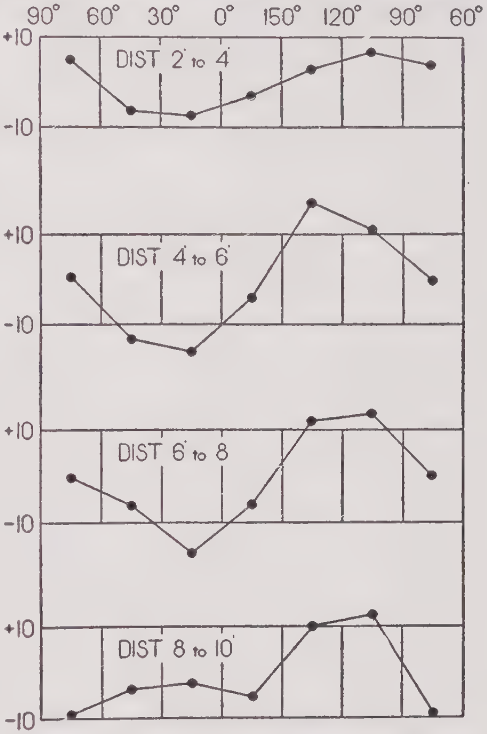

Fig. 3.—Ellipticity of Messier 13 for different distances from the center. Ordinates are percentage deviations. Abscissae are position-angles.

The counts of Messier 3 are not very satisfactory, and data from more plates must be studied. As the results now stand, this cluster is the only one for which the departure from apparent sphericity appears to be non-symmetrical. A pronounced one-sidedness is shown by the results for plate 65; but plate 89, with almost the same number of stars, fails to verify the asymmetry, and the longer exposure, plate 2456P, is not decisive.

Messier 12, Messier 10, and Messier 56 are three clusters for which little or no deviation from apparent sphericity is shown by the counts in Table II, although the exposures for each have been long enough to include many faint stars. This does not mean necessarily that these systems are not flattened. It may indicate that their equatorial planes are inclined at a high angle to the line of sight. A random distribution of galactic planes should make at least one-third of them impossible of direct detection with our present methods; but, as an indirect test, the clusters seen more or less edgewise should show a greater average condensation toward the center than those with high inclinations. This is exactly what we find in the case of each of the three clusters mentioned above, as may be seen from the numbers in Table II, most conspicuously for Messier 56.

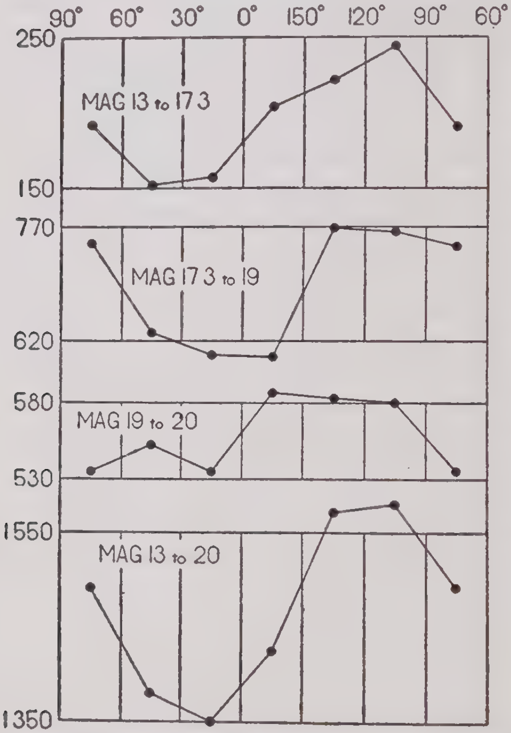

Fig. 4.—Ellipticity of Messier 13 for different intervals of magnitude. Ordinates are numbers of stars. Abscissae are position-angles.

To illustrate these points further, the small, probably accidental, deviation from perfectly circular form for Messier 12 is shown in Table IV, in contrast to the pronounced ellipticity of Messier 13; and the curves in Fig. 6 exhibit the relatively smaller central concentration of the former. The ordinates in this diagram, obtained from the values in the last column of Table II for plates 100 and 15, are made comparable by dividing the mean number for successive rings by the mean for Ring I.[1] It is doubtful, however, if the relative concentration can generally be used as an index of inclination, for uncertainties due to Eberhard effect, to differences in laws of density, and particularly to foreground stars must surely enter to some extent. A curve of the distribution for Messier 10 is shown in Fig. 5.

---

[1] A small correction is made to allow for two squares in the center of plate 15 that are burned out.

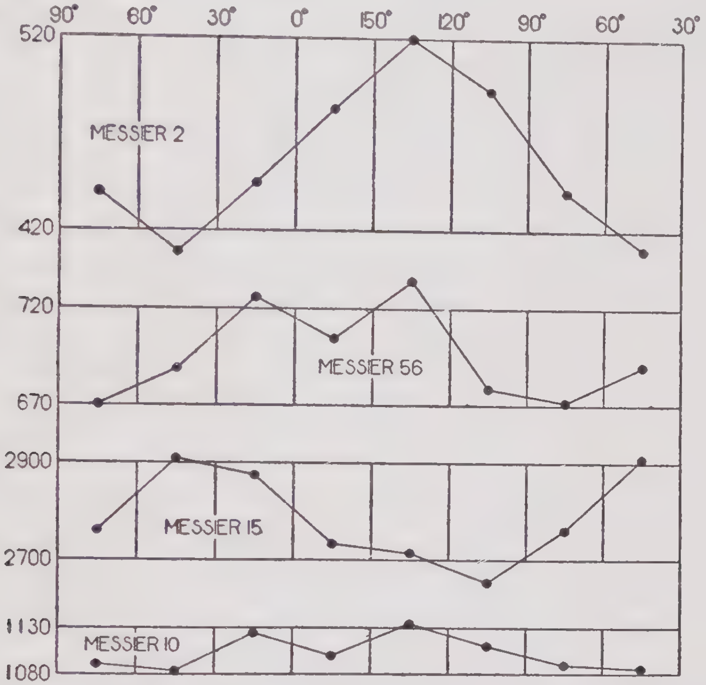

Fig. 5.—Axes of symmetry in globular clusters. Ordinates are numbers of stars. Abscissae are position-angles. Erratum: The second curve is for Messier 53 instead of Messier 56.

Curves are also given in Fig. 5 for Messier 2 and Messier 15. Both show the elongated distribution conspicuously, but for the latter the maxima in the unreflected distribution-curve are not exactly opposite and are of unequal height. This lack of symmetry tends to disappear with increasing exposure and may be only superficial, though the possibility must not be overlooked that the supposed galaxy in this system may be along a small circle of low latitude.

In order to bring together all the available evidence bearing on the forms of globular clusters, Fig. 7 is reproduced here from a communication to the *Proceedings of the National Academy of Sciences.*[1] The concentration of certain types of variables toward the Milky Way is a recognized phenomenon of our galactic system. The diagram shows that in ω Centauri also the ellipticity is much greater for the variables than for the stars in general. This interesting analogy further supports the hypothesis that the globular clusters are flattened systems of stars.

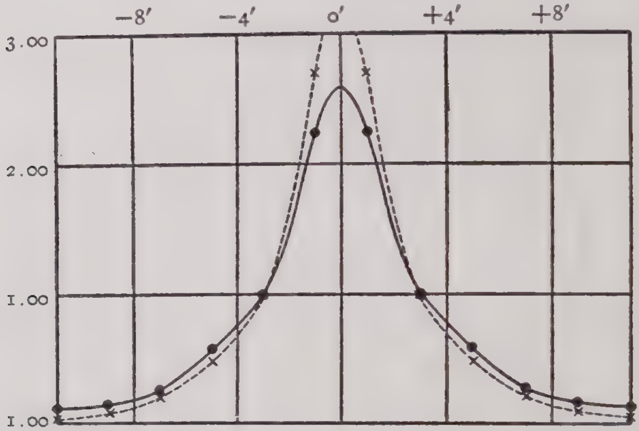

FIG. 6.—Comparison of the central concentration for Messier 12 (full line) and Messier 13, illustrating (with Table IV) the probably great difference in the inclinations of their galactic planes. Ordinates are relative numbers of stars. Abscissae are distances from the center.

SUMMARY

1. The present study of the distribution of stars in globular clusters is based upon counts of more than half a million star images on a series of plates made at the principal focus of the 60-inch reflector at Mount Wilson.

2. The material is used mainly as a test for the presence in these stellar systems of galactic planes, which should reveal themselves through an elliptical distribution of the stars.

3. Of the nine clusters for which fairly definite counts are available, five show elliptical form, three appear sensibly circular, and one may be peculiar. The three clusters with similar density

---

[1] Vol. 3, 276, 1917.

in all directions from the center are noticeably less condensed, a condition that follows naturally if the poles of their galactic planes are assumed to be approximately in the line of sight.

4. The proportion of clusters with measurable elongation here found is about what should be expected on the galactic hypothesis if the inclinations are distributed at random.

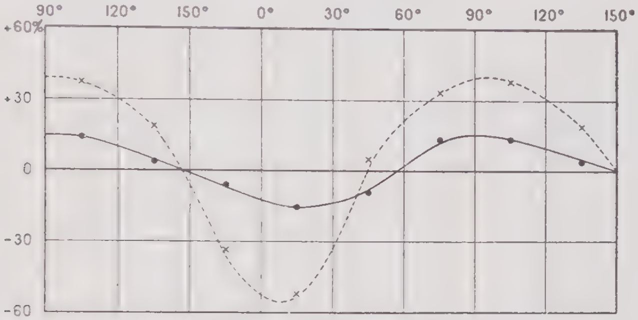

FIG. 7.—Galactic plane in ω Centauri; full line, all stars; dotted line, variables. Ordinates are deviations from mean. Abscissae are position-angles.

5. Axes of symmetry in these clusters do not appear until the arrangement of several thousand stars is analyzed. The failure previously to detect the ellipticity, which in some cases amounts to nearly 30 per cent, must be attributed to an influence of the brighter stars, which, in general, do not show elliptical distribution. The ellipticity appears at all distances from the center, and also for all magnitudes, after the giant red stars have been excluded.

MOUNT WILSON SOLAR OBSERVATORY
March 1917

Contributions from the Mount Wilson Solar Observatory, No. 130
Reprinted from the *Astrophysical Journal*, Vol. XLV, pp. 254–268, 1917

A STUDY WITH THE ELECTRIC FURNACE OF THE ANOMALOUS DISPERSION OF METALLIC VAPORS

By ARTHUR S. KING

The phenomenon of anomalous dispersion consists of a sudden change in the index of refraction of an absorbing medium for wave-lengths in the neighborhood of those which are strongly absorbed. It has been observed for various transparent media which show selective absorption. Metallic vapors, in many cases, show the effect close to their absorption lines when white light is passed through the vapor, and by suitable optical arrangements the change of refractive index may be shown. The principle of crossed prisms used by Kundt is generally employed, a prism of the absorbing vapor being formed with its refracting edge at right angles to the slit of the analyzing spectroscope.

The chief problem in such experiments is the production of a mass of vapor which will act as a prism. Wood,[1] working with sodium, used a cylinder of the vapor inclosed in a horizontal steel tube, heated below by a row of flames and cooled above. For the study of substances of higher melting-points Puccianti,[2] Schön,[3] and Geisler,[4] used an arrangement of the electric arc giving a non-uniform distribution of metallic vapor which acted as a prism. In the case of the arc, the possibilities of varying the state of the absorbing vapor are limited, and it seemed that an adaptation of the electric furnace offered a means of producing vapors of the more refractory elements under conditions which would give anomalous dispersion and, at the same time, permit a control of the temperature and distribution of the vapor by which variations of the phenomena could be studied. The use of mixed vapors in the furnace is a simple matter, so that for a given set of conditions the relative anomalous dispersion shown by the lines of different elements can be observed.

---

[1] *Phil. Mag.*, (6), **3**, 128, 1902; *Physical Optics*, p. 419.

[2] *Memorie della Società degli Spettroscopisti Italiani*, **33**, 133, 1904.

[3] *Zeitschrift für wiss. Photographie*, **5**, 349, 397, 1907.

[4] *Ibid.*, **7**, 89, 1909.

Assuming that the desired non-uniform distribution of vapor is available, a beam of white light, limited by a horizontal slit, is passed through the vapor and, being focused on the slit of the spectrograph, gives a strip of continuous spectrum in which the absorption lines of the vapor appear. The flexure of the continuous spectrum in opposite directions on the two sides of an absorption line registers the amount of anomalous dispersion produced by the vapor for the given line.

Experimental method.—The resistance tubes used in the electric furnace are of Acheson graphite, 30.5 cm long and of 12.5 mm bore, and are heated by the passage of the electric current from end to end. To adapt tubes for the present investigation, a slot about 6 mm wide was filed longitudinally between the end portions, which are held in contact blocks 20 cm apart. When placed in position, with the slot above and fragments of the substance to be examined on the bottom of the tube, a cylinder of vapor was obtained upon heating, having a strong density-gradient in the vapor between the molten mass and the open slot. The water-cooled copper pipe passing about 5 cm above the slot, by which the current was led to one end of the tube, accentuated the temperature difference. The vapor cylinder of varying density was thus equivalent in its dispersive effect to a prism with its refracting edge upward.

Certain features of the arrangement are important in interpreting the results. The most effective condition for producing strong anomalous dispersion of regular type corresponds to a temperature high enough to give broad absorption lines for the element studied, but not too far above the vaporizing-point, since a high density of the vapor in the lower part of the tube is required. If the temperature is such that the substance is fully vaporized, the rapid diffusion upward destroys the density-gradient, the prismatic action is very slight, and wide absorption lines showing little anomalous dispersion are obtained. With a mixture of substances requiring different temperatures for their vaporization, it is obvious that at a given stage one element may form an effective prism, while another has already reached a nearly uniform distribution, the anomalous dispersion being strong for one and weak, or absent, for the other. Also, for a given element, some lines may require a low temperature for their greatest strength, others a much higher temperature, and the same vapor prism will not be effective for both. In fact, a stage may be reached such that the conditions near the bottom of the tube, where high-temperature lines are produced, become positively unfavorable for low-temperature lines, so that the vapor absorbing the latter is denser above than below, and an inverted prism for lines of this character results. It is thus possible for regular and inverted anomalous dispersion to appear simultaneously for lines belonging to two different elements and for lines of different character belonging to the same element. Again, the same spectrum line can be made to show regular anomalous dispersion at low temperature and the inverted effect at higher temperature. All of these differences were observed in the experiments to be described.

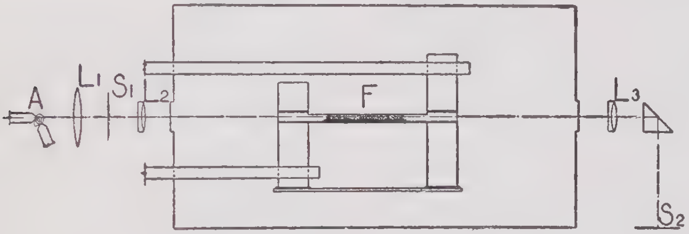

Fig. 1.—Arrangement of furnace and optical train

The arrangement of the optical parts and a vertical section of the furnace interior are shown in Fig. 1. Light from the positive pole of a carbon arc A, operated with 25–30 amperes at 110 volts, was focused on a horizontal slit S_1. The beam, rendered parallel by the lens L_2, passed through the vapor in the furnace tube F, and the image of S_1 was focused sharply on the slit S_2 of the vertical plane-grating spectrograph, the narrow band of white light passing across the slit. Use was made of both the 13- and 30-foot arrangements of the spectrograph, which give dispersions, in the second order, of approximately 2.1 and 0.89 A per mm respectively. Exposures with the 13-foot focus ranged from one-half to one minute.

The longer exposures with the 30-foot focus were used chiefly for large-scale photographs to test for shifts of lines occurring close to strong lines of pronounced anomalous dispersion.

For the production of well-defined anomalous dispersion it was found advantageous to operate the furnace *in vacuo*. At higher pressures the unsteady condition of the gas in the beam of light passing through the chamber is likely to impair the sharpness of the strip of continuous spectrum whose curvature measures the effect.

RESULTS

a) *Conditions for the production of anomalous dispersion.*—When white light from the pole of a carbon arc is passed through the furnace vapor, the absorption lines obtained are those observed in the emission spectrum of the furnace, and their widths in absorption are closely proportional to their emission intensities. The prominent lines of the absorption spectrum are thus the stronger furnace lines, belonging to Classes I and II of the furnace classification, while the faint absorption lines are those of Class III, requiring higher temperature. The furnace lines of higher classes have negligible absorption effect.

In discussions of anomalous dispersion the view that a spectrum line shows large or small dispersion as an inherent characteristic finds frequent expression, much as we say that a line shows large or small pressure displacement. The present experiments give no exception to the rule that the anomalous dispersion corresponds to the absorptive power shown by the line in question, *provided a proper prismatic distribution is present in the absorbing vapor.* This relation is very evident when a stretch of spectrum containing a number of lines of different intensities is examined, for the interval over which the curvature of the continuous spectrum on either side of a line is perceptible increases with the line's strength. The three sections of the titanium spectrum in Plate III illustrate this fact and show clearly the practicability of the furnace method for the study of substances of high melting-point. In the upper strip the emission lines of the furnace spectrum, in most cases reversed, appear as continuations of the absorption lines. It is in harmony with the

PLATE III

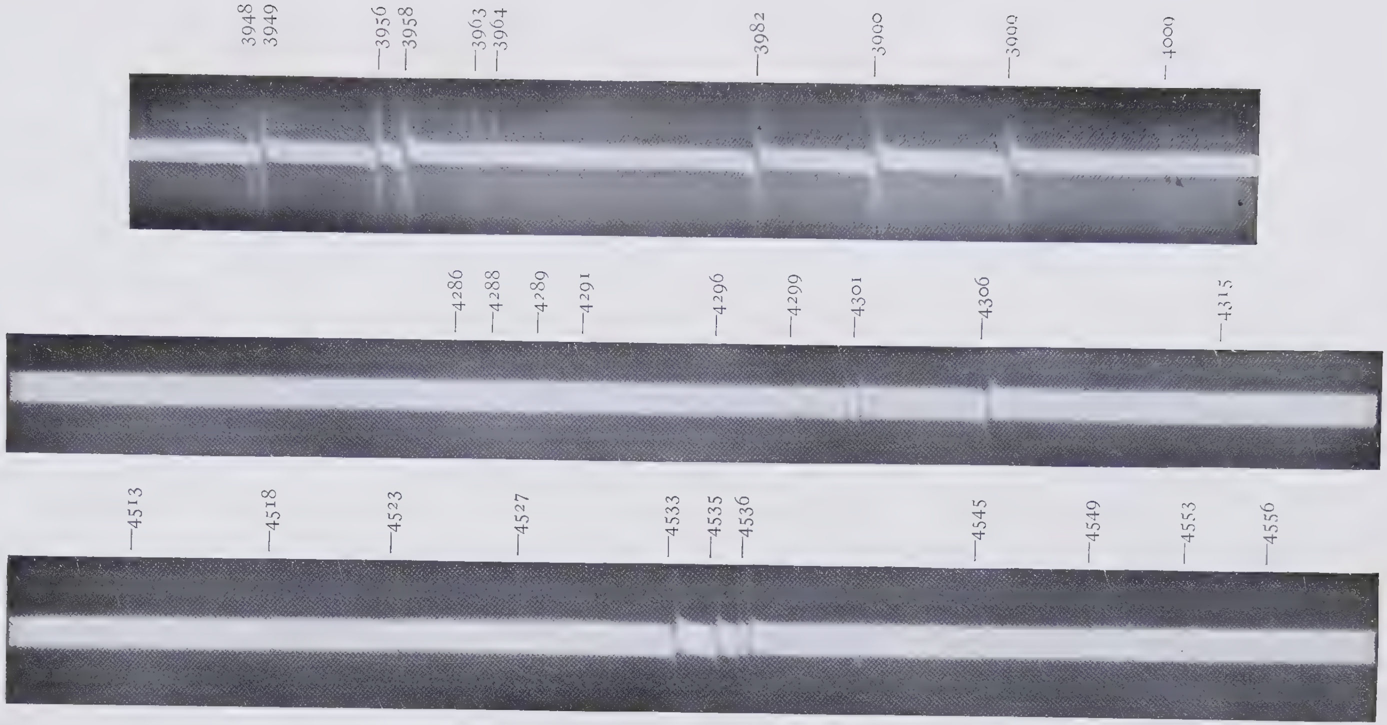

Anomalous Dispersion of Titanium Lines

PLATE IV

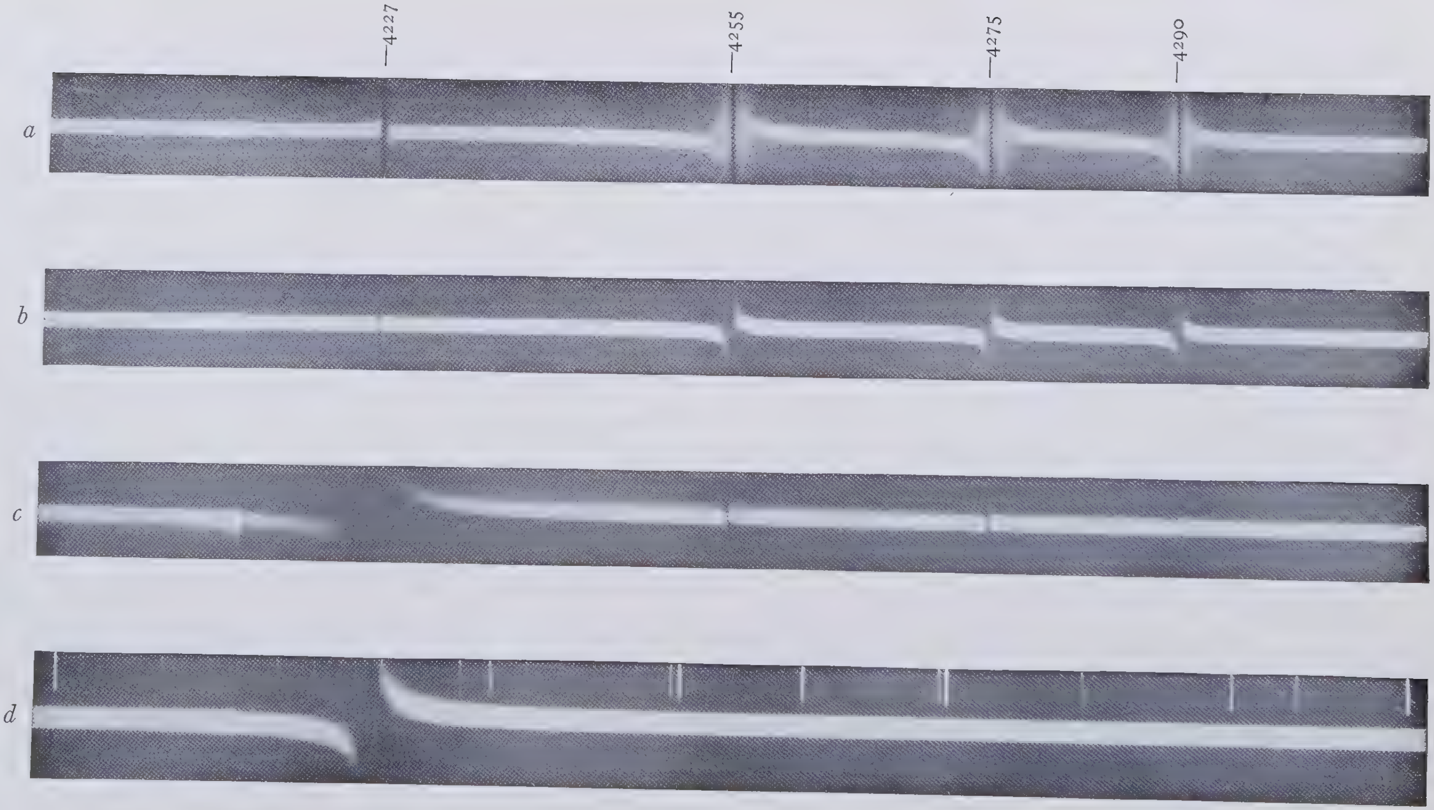

Anomalous Dispersion of λ 4227 of Calcium and of Three Chromium Lines at Four Stages of Decreasing Temperatures, Showing Inverted Effect for λ 4227 at Highest Temperature (*a*)

PLATE V

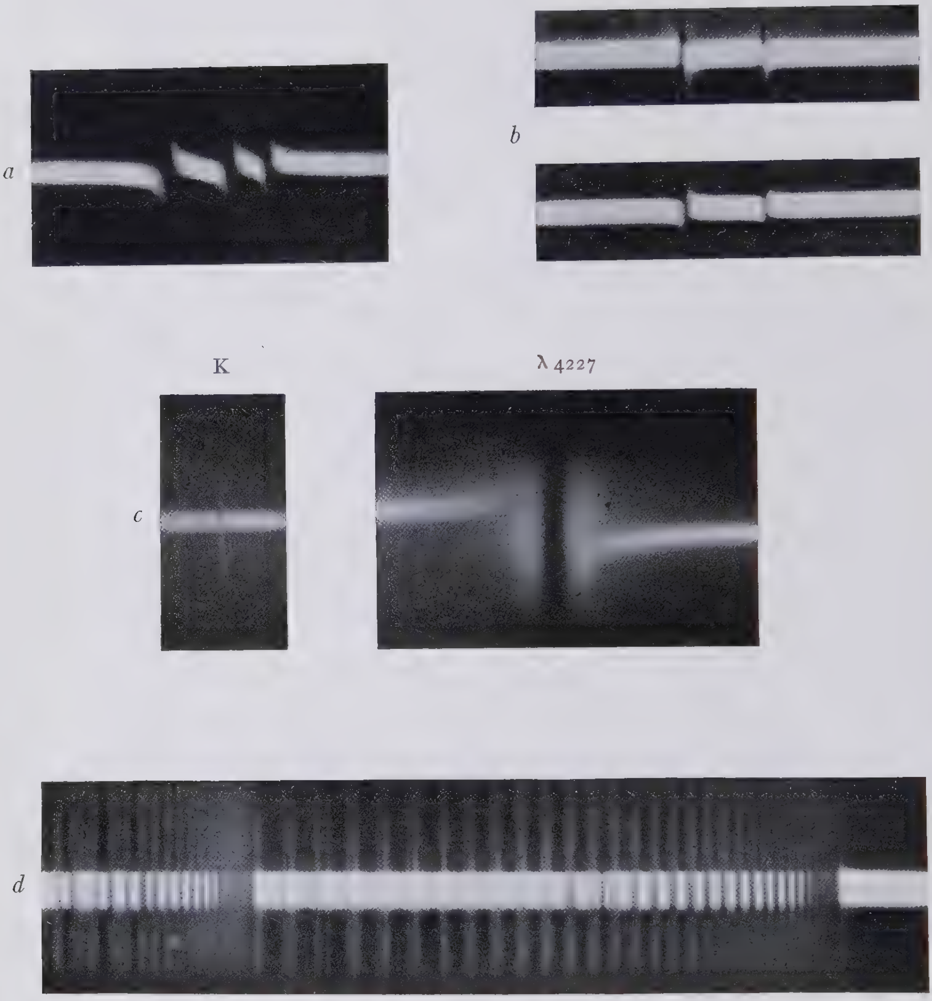

Anomalous Dispersion in Line and Band Spectra

a Manganese lines λλ 4031–35
b D lines (low vapor-density), showing inversion of effect due to higher temperature
c Opposite effects produced simultaneously for calcium lines K and λ 4227
d Anomalous dispersion for "cyanogen" band with principal head at λ 3883

proportionality of anomalous dispersion to the strength of the line that, throughout this investigation, no case was found for which a strong furnace line could not be made to show a correspondingly large anomalous dispersion, though for some lines it was necessary to determine by trial the proper conditions for an effective vapor prism. Of course, it cannot be stated now that this relation is quite general, but the furnace results furnish a high probability that anomalous dispersion is conditioned only by the presence of a vapor prism which strongly absorbs the line in question.

b) *Variability of anomalous dispersion with the condition of the absorbing vapor.*—We may now discuss examples of the condition already noted that, when mixed vapors are used in the furnace tube, a state of the vapor producing anomalous dispersion for one constituent may give a uniform distribution or even invert the prism for the second element, thus causing for this vapor either no curvature of the continuous spectrum or a flexure opposite to that of the first element. Instances in which one element showed strong anomalous dispersion and in which another, at the same time, gave only wide absorption lines occurred constantly during the experiments. Thus the three strong manganese lines λλ 4031, 4033, 4035, though often very wide, gave uniformly no anomalous dispersion at temperatures of the furnace such that neighboring lines of iron, chromium, and titanium showed the effect strongly. At a much lower temperature, however, before the other elements were fully vaporized, they showed very strong anomalous dispersion. The effect is shown in Plate V*a*.

Experiments in which calcium and chromium were vaporized together gave an interesting contrast in the behavior of λ 4227 of the first element to that of λλ 4255, 4275, 4290 of chromium. In Plate IV are reproduced four spectrograms taken at different temperatures; IV*d*, at low temperature (with iron-arc comparison), shows a very large effect for λ 4227, the chromium lines being scarcely visible; IV*c* and IV*b* show flexure in the same direction for both calcium and chromium, though to very different degrees; IV*a*, at the highest temperature of all, gives the maximum effect for the chromium lines, while for λ 4227 the curvature is reversed, thus indicating that the prism of calcium vapor has become inverted, so that the vapor producing λ 4227 is denser above than below, while the chromium prism remains with the denser region below.

Probably the dispersion of all low-temperature flame lines can be inverted in this way by properly chosen temperatures. In addition to the inversion of λ 4227, which occurred on many spectrograms, the effect was obtained for the manganese triplet already mentioned, for the D lines of sodium, for the aluminium pair λλ 3944–62, and for the potassium pair λλ 4044–47. The D lines, made narrow by a small amount of salt in the tube, and showing respectively for low and high temperatures the usual anomalous dispersion (below) and the inverted effect (above), are illustrated in Plate V*b*.

By close adjustment of conditions numerous relative inversions were produced for different elements even of higher melting-points. Thus iron and chromium lines were inverted with respect to titanium when the three were vaporized together, and lines of manganese were inverted with respect to those of iron.

These effects are fully explained on the assumption that each kind of vapor forms an independent absorbing medium which, if conditions are such as to give prismatic distribution, shows its own anomalous dispersion without regard to what may be shown by other vapors in the mixture. By an extension of this principle, lines belonging to the same element, but emitted by different centers, should show simultaneously, under proper conditions, direct and inverted anomalous dispersion; for one set of particles, radiating freely at relatively high temperature, would have the denser part of their prism below, while the other set, emitting lines of lower temperature, would have their prism inverted. To test this possibility, the lines must be in the same region of the spectrum and radically different in their response to temperature; further, both must be radiated by the furnace with sufficient intensity to produce good absorption lines. In the calcium spectrum, λ 4227 and H and K seemed favorable for a comparison. At temperatures high enough to make H and K strong, λ 4227 is uniformly inverted in its anomalous dispersion, so that the main problem was to produce a distinct effect for H and K. This was done by suspending, a few millimeters above the slot in the tube, on insulated supports, a thick rod of graphite, so that when the tube was heated the cold rod increased the temperature-gradient in the calcium vapor. Later a water-cooled copper tube passing 1 cm above the slot was used for the same purpose. A number of spectrograms with these arrangements gave anomalous dispersion for all three lines, the result for H and K being that of a prism with denser vapor below, while λ 4227 showed very large anomalous dispersion in the opposite direction. The effect for the K line and for λ 4227, enlarged from the same negative, is shown in Plate V*c*.

The experiments of Puccianti[1] have shown that this is not an invariable result for these lines, since, with the arc containing calcium as the absorbing source, he obtained anomalous dispersion in the same direction for all three lines, though very different in amount. With the conditions adopted for the furnace it has been possible to make the particles absorbing the H and K lines act as a body of vapor distinct from that absorbing λ 4227.

c) The anomalous dispersion of iron, chromium, and titanium.—The results of observations over an extended range of wave-length on the relative amount of anomalous dispersion shown by different lines and its relation to other spectral characteristics will now be given for iron, chromium, and titanium. For iron and chromium a portion of the range here covered has been studied by Geisler[2] with the interferometer, using the arc to supply the absorbing vapor. Of the effect for titanium no previous investigation is known to the writer.

Tables I, II, and III give the lines of iron, chromium, and titanium, respectively, for which distinct anomalous dispersion has appeared. An estimate of the amount of the effect is given for each line, "1" denoting that the curvature of the continuous spectrum on opposite sides of the line is just perceptible. The wave-lengths for iron are those of Burns[3] on the International System, abbreviated to two decimal places, while the values of Exner and Haschek are used for the chromium and titanium lists.

---

[1] *Memorie della Società degli Spettroscopisti Italiani*, **33**, 133, 1904.

[2] *Zeitschrift für wiss. Photographie*, **7**, 89, 1909.

[3] *Lick Observatory Bulletin*, No. 247, 1913.

TABLE I

IRON

λ	Degree of Anomalous Dispersion	λ	Degree of Anomalous Dispersion	λ	Degree of Anomalous Dispersion
3581.20	8	3795.00	1	3930.30	6
3605.45	5	3798.51	1	4005.25	1
3608.86	2	3799.55	1	4045.82	3
3618.77	2	3812.97	1	4063.60	2
3631.46	2	3815.84	2	4071.75	2
3647.85	2	3820.43	6	4132.06	1
3679.92	3	3824.44	4	4143.87	1
3687.46	2	3825.89	5	4202.03	1
3705.57	3	3827.83	2	4250.79	1
3707.92	1	3834.23	3	4271.76	2
3709.25	1	3840.44	2	4294.13	1
3719.94	20	3841.05	1	4307.91	3
3722.57	4	3856.37	6	4325.77	2
3727.62	2	3859.91	15	4375.93	1*
3733.32	3	3872.51	1	4383.55	4
3734.87	8	3878.58	4	4404.75	2
3737.14	12	3886.29	8	4415.13	1
3745.56	10	3887.05	1	4427.31	1*
3745.90		3895.66	3	5269.54	1
3748.26	6	3899.71	4	5328.04	1
3749.49	5	3902.95	2	5371.50	1
3758.23	4	3906.48	2	5397.14	1
3763.79	3	3920.26	4	5405.78	1
3767.19	2	3922.92	5		
3787.88	1	3927.93	5		

* Subject to inversion of effect at high temperature.

TABLE II

CHROMIUM

λ	Degree of Anomalous Dispersion	λ	Degree of Anomalous Dispersion	λ	Degree of Anomalous Dispersion
3578.81	150	4339.62	4	4626.35	1
3593.64	100	4339.90	2	4646.35	2
3605.49	75	4344.68	4	4651.49	1
3885.36	1	4351.22	1	4652.38	2
3886.92	1	4351.98	5	5204.71	20
3908.91	2	4359.82	2	5206.24	30
3916.41	1	4371.48	2	5208.60	40
3919.32	3	4373.42	1	5247.72	2
3921.21	1	4385.15	2	5264.35	4
3928.82	1	4497.03	2	5265.90	2
3941.67	1	4546.10	2	5296.86	2
3963.85	1	4580.26	1	5298.46	3
4254.51	100	4591.61	1	5345.99	4
4275.00	80	4600.90	1	5348.50	2
4289.90	70	4613.53	1	5410.01	6
4337.74	3	4616.28	1		

TABLE III

Titanium

λ	Degree of Anomalous Dispersion	λ	Degree of Anomalous Dispersion	λ	Degree of Anomalous Dispersion
3635.61	40	4024.76	5	4536.25	3
3642.81	45	4055.17	1	4544.88	2
3653.66	50	4060.42	1	4548.93	3
3654.74	2	4064.39	1	4552.70	3
3658.26	4	4065.24	1	4555.70	2
3660.80	1	4078.62	1	4562.80	1
3669.15	3	4112.87	1	4656.63	5
3671.85	4	4286.19	3	4667.77	6
3690.09	2	4287.59	3	4682.10	6
3717.52	2	4289.26	3	4691.50	1
3722.73	2	4291.19	3	4693.88	1
3729.97	10	4295.93	3	4841.08	2
3741.25	15	4298.89	4	4981.93	6
3753.00	20	4299.40	1	4991.24	6
3753.77	3	4299.81	1	4999.68	5
3771.84	4	4300.73	5	5007.35	4
3901.14	2	4301.24	5	5009.79	1
3904.99	4	4306.09	7	5014.39	6
3914.50	3	4314.96	3	5016.29	1
3921.61	2	4326.54	1	5020.20	1
3924.71	6	4427.28	1	5023.02	1
3930.04	5	4449.35	1	5025.01	1
3947.98	6	4451.13	1	5036.08	1
3948.87	10	4453.52	1	5036.65	1
3956.50	10	4455.50	2	5038.59	1
3958.39	15	4457.61	2	5040.14	5
3963.05	4	4512.90	2	5064.79	4
3964.48	4	4518.19	3	5147.63	1
3981.95	10	4522.98	3	5152.35	1
3982.63	3	4527.47	2	5173.92	4
3989.94	12	4533.40	8	5193.12	4
3998.80	15	4534.95	6	5210.59	5
4009.12	5	4535.71	5	5219.86	1
4009.82	1	4536.12	3	5252.23	1

In comparing the material in Tables I, II, and III with the line-intensities in the emission spectra of iron,[1] chromium,[2] and titanium[3] at various temperatures of the furnace, the degree of anomalous dispersion was found without exception to be roughly proportional to the intensity of the line in question at the temperature (about 2500° C.) to which the vapor was heated in these experiments. All lines of iron and chromium included in Tables I and II have been placed in Class I or Class II of the furnace classification, being strong through a long range of temperatures. The same is true for titanium, except that ten lines of Class III, out of the total of 102, show perceptible anomalous dispersion. The fact that a line is relatively strong at low temperature (Class I) seems to have no bearing, except that pronounced lines of this type, such as λ 4376 of iron, sometimes attain considerable width as absorption lines without showing anomalous dispersion, and in some cases reveal an incipient inversion of the effect when other iron lines show regular anomalous dispersion. It is probably the same effect as was observed distinctly for the calcium lines H, K, and λ 4227.

---

[1] *Mt. Wilson Contr.*, No. 66; *Astrophysical Journal*, **37**, 239, 1913.

[2] *Mt. Wilson Contr.*, No. 94; *Astrophysical Journal*, **41**, 86, 1915.

[3] *Mt. Wilson Contr.*, No. 76; *Astrophysical Journal*, **39**, 139, 1914.

The anomalous dispersion shown by iron lines is much smaller than that for lines of chromium and titanium when the three elements are mixed in the tube. This is especially noticeable in the green and yellow, where the low-temperature iron lines remain narrow and show very small effects. The same relation exists, however, with regard to the widening and reversal of lines in the regular furnace spectra of these elements, and the anomalous dispersion seems to follow closely the ability of a line to reverse.

At the red end of the spectrum the lines of these three elements remain narrow in the furnace, and no anomalous dispersion was obtained. The effect clearly becomes stronger and more general as the wave-length decreases, but this also probably results from the greater absorptive power and the resulting ease of reversal shown by the lines of these elements in the region of shorter wave-length. When strong low-temperature lines, easily reversible in arc and furnace, occur in the region of greater wave-length, they readily show anomalous dispersion. Examples are the D lines, several barium lines in the red, and λ 6708 of lithium. The degree of anomalous dispersion thus appears to have no direct dependence on the wave-length.

d) Anomalous dispersion for a banded spectrum.—It is known that absorption bands may show anomalous dispersion, such effects having been observed by Geisler[1] for the bands of copper, calcium, strontium, barium, and calcium fluoride. On several plates taken in the present experiments a perceptible anomalous dispersion was observed for the "cyanogen" band λ 3883, which the experiments of Grotrian and Runge[1] indicate is due to nitrogen alone. The effect could be increased when the furnace was filled with air at one-half atmosphere, thus giving a larger supply of nitrogen, the appearance under these conditions being shown in Plate V*d*. Not only the dense heads, but the stronger component lines of the band are produced in absorption, with the corresponding parts of the emission band showing faintly above and below. The direction of curvature of the continuous spectrum, forming parallelograms near the head of the band, indicates a greater density in the lower part of the absorbing cylinder. This must result from the presence of more radiating (and absorbing) particles in the region of highest temperature, since, if the band is due to nitrogen alone, the absolute density of the gas should be less in this region where the cylinder absorbs most strongly. The gradation of intensity in the emission lines bears out this conclusion, the portion of the line emitted by the lower layer of gas being strongest.

---

[1] *Zeitschrift für wiss. Photographie*, 7, 89, 1909.

MEASUREMENTS TO DETECT A MUTUAL DISPLACEMENT OF CLOSE LINES DUE TO ANOMALOUS DISPERSION

The theory advanced by Julius,[2] according to which lines very close together in the spectrum should undergo a mutual repulsion when anomalous dispersion is active, has been fully discussed in relation to the lines of the solar spectrum by St. John[3] and Albrecht,[4] and also in a later paper by Julius.[5] An attempt has been made recently by the writer to detect such an effect in the case of electric-furnace lines occurring close together. Lines suitable for this test should be separated by but a few tenths of an angstrom, and, since the theory of the repulsive action is based on a superposition of the changes in refractive index due to the two lines, both should show large anomalous dispersion. As this would require two wide lines, neither of which could be measured with accuracy, cases were looked for in which a narrow absorption line occurred close to a line showing large anomalous dispersion, the wave-length of the narrow line being measured from a neighboring standard line both when anomalous dispersion was active and when it was not. Very few pairs which satisfied these requirements could be found, but they were fulfilled in a fair degree by titanium and calcium lines occurring close to the chromium lines λ 4275 and λ 4290. The dispersion used was 1 mm = 0.89 A.

---

[1] *Physikalische Zeitschrift*, **15**, 545, 1914.

[2] *Astrophysical Journal*, **40**, 1, 1914.

[3] *Mt. Wilson Contr.*, Nos. 93, 123; *Astrophysical Journal*, **41**, 28, 1915; **44**, 311, 1916.

[4] *Astrophysical Journal*, **41**, 333, 1915.

[5] *Ibid.*, **43**, 53, 1916.

Measurements were made on 27 spectrograms which showed varying degrees of anomalous dispersion. The measures for plates in which the titanium or calcium line was superposed on the curved spectrum near the strong chromium line were compared with those for which the anomalous dispersion was very slight and also with those for the emission lines given by the furnace and in the arc. (The test line was known to have the same pressure displacement as the standard line, so that measurements for the arc in air showed no sensible difference from those for the vacuum furnace.)

The following example shows the treatment of this material:

Measurements of λ 4289.237, Ti. (Rowland scale), separated 0.65 A from λ 4289.885, Cr. Standard line: λ 4287.566, Ti.

	Interval when Anomalous Dispersion Is Absent or Negligible	Interval for Large Anomalous Dispersion
	1.670	1.667
	1.674	1.667
	1.665	1.671
	1,670	1.671
	1.669	1.670
	1.668	1.668
	.....	1.670
	.....	1.668
Means...	1.669	1.669

Measures of λ 4289.237 referred to a more distant standard line, λ 4286.168 of titanium, also gave exactly the same result when anomalous dispersion was absent as when present in large degree.

The interval between λ 4289.237 and λ 4291.114 of titanium was also measured, these lines being on opposite sides of the strong chromium line and distant from it 0.65 and 1.23 A, respectively. While not very close to the chromium line, they were within the curved spectrum due to the latter, and any attraction or repulsion exerted on the titanium lines should be additive. The mean measurements with and without anomalous dispersion differed by only 0.001 A.

The calcium line λ 4289.525, distant 0.36 A from λ 4289.885 of chromium, was measured from a neighboring calcium line. A difference with and without anomalous dispersion of 0.002 A was found in the direction indicating an approach to the chromium line, though the difference is probably too small to be significant.

The only difference of appreciable size obtained was for λ 4274.746 of titanium, distant 0.21 A from λ 4274.958 of chromium, the measurements being made from the titanium line λ 4272.590. The difference found was 0.006 A in the direction giving an *approach* to the chromium line. The measurements were very difficult, however, and probably systematically in error, owing to the wide chromium line weakening the continuous spectrum on that side of the titanium line, which would have resulted in a difference of the kind observed. The use of very close pairs, which should be most favorable for the test, thus unavoidably introduces a source of error.

It is thus seen that no evidence whatever of repulsion between close lines is found, so that the effect required by theory must be very small. This conclusion is borne out in a recent deduction by Sir Joseph Larmor,[1] to whom a summary of the foregoing results was submitted, according to which the repulsion to be expected should be too small to be detected by the laboratory methods now available. As long as the effect is small and the lines tested necessarily very close, a serious obstacle arises from the fact that an effort to magnify the effect through stronger anomalous dispersion causes the lines to blend or at least to become unsuitable for measurement.

A further test with these lines was made in the regular furnace to see if a displacement could be found when a line occurs very close to a strong line known to give a high anomalous-dispersion effect.

---

[1] *Astrophysical Journal*, **44**, 265, 1916.

For this it was possible to use a larger scale, a dispersion of 1 mm = 0.6 A being employed. The titanium and calcium lines were photographed with and without the mixture of chromium vapor. Under these conditions the calcium line and one of those of titanium gave differences of 0.002 A, but these were opposite in direction and probably within the errors of measurement, while the other titanium line, closest of the three to a chromium line, agreed within 0.001 A when titanium was used alone and when it was mixed with chromium. For this test the result may therefore be considered negative.

SUMMARY

1. A method has been developed for the study of anomalous dispersion for metallic vapors of substances of high melting-point which allows close control of the conditions of the absorbing vapor.

2. The lines in the spectra of iron, chromium, and titanium, and also lines of special interest in other spectra, have been examined with reference to the degree of anomalous dispersion shown.

3. The rule that the anomalous dispersion shown by a line is in proportion to its strength in absorption was found to hold, provided the vapor absorbing the line in question has a non-uniform distribution equivalent to a prism.

4. Lines showing strong anomalous dispersion at low temperature can often be made, at higher temperature, to show the phenomenon with refraction in the opposite direction, thus indicating that the vapor prism absorbing such lines has been inverted.

5. Under this condition another element, requiring still higher temperature for vaporization, may show anomalous dispersion of regular type, so that for the two elements opposite effects occur simultaneously.

6. The same condition may be brought about for lines belonging to the same element but requiring very different temperatures for their production, λ 4227 of calcium thus showing an effect opposite to that simultaneously given by the H and K lines.

7. The experiments have thus demonstrated the capacity of each element to give its own anomalous dispersion independently of other vapors which may be present, a similar relation holding for

the particles of the same element emitting groups of lines of different character.

8. The greater prevalence of effects of anomalous dispersion in the region of shorter wave-length appears to result from the greater absorptive power generally found for lines in this region. When lines of suitable character occur in the red, correspondingly large effects can be obtained for them.

9. Distinct anomalous dispersion was obtained for the band at λ 3883.

10. Tests for a mutual repulsion between close lines, one of which is in a condition to show large anomalous dispersion, give no evidence of such an effect.

11. No change of wave-length is found when a line in the regular furnace spectrum occurs very close to a strong line known to show large anomalous dispersion.

Mount Wilson Solar Observatory
March 1917

Contributions from the Mount Wilson Solar Observatory, No. 131
Reprinted from the *Astrophysical Journal*, Vol. XLV, pp. 293–305, 1917

THE RELATIONSHIP OF STELLAR MOTIONS TO ABSOLUTE MAGNITUDE

BY WALTER S. ADAMS AND GUSTAF STRÖMBERG

An important product of the radial-velocity observations of recent years is the clear evidence that the stars of large proper motion are characterized by high velocities in space. The fact that large proper motion is to some extent in itself an indication of high velocity must of course enter into consideration, but a computation of space velocities with the aid of mean parallax determinations shows that this cannot account for the results found unless a distribution of velocities is assumed quite other than that of the ordinary law of Maxwell. In a paper published in 1915 Kapteyn and Adams[1] found this result from a discussion of the data for a considerable number of stars, and suggested two alternative hypotheses: (1) that velocity is a function of absolute magnitude; that is, the intrinsically faint stars move more rapidly than the bright stars; (2) that the nearer stars move more rapidly than the distant stars. These conclusions are self-evident, since the stars of large proper motion in general have large parallaxes, and hence are relatively near and intrinsically faint. On the assumption of absolute magnitude as the effective agent, a change of about 1.1 km in radial velocity was found for each unit of magnitude in the case of the K stars.

The results were based wholly upon parallaxes derived from a formula connecting mean parallax with proper motion. The recent development of a method for deriving absolute magnitudes directly from stellar spectra has added greatly to the material available for such an investigation, and we have accordingly taken up the study of the question with a view to discriminating between the suggested explanations. In addition to those stars for which absolute magnitudes have been obtained directly, use has been made of a large number of stars with radial velocities determined at the Lick Observatory. For most of these the parallaxes have been calculated with the aid of a modified formula connecting mean parallax with proper motion. The investigation is based upon about 1300 stars of the F, G, K, and M types of spectrum. In the successive portions of this paper we shall endeavor to indicate, first, the evidence afforded by a direct comparison of the arithmetical mean of the radial velocities with absolute magnitudes; secondly, the effect upon the results of the law of distribution of velocities, of stream-motion, and of errors in the parallax determinations; thirdly, the confirmatory evidence afforded by the linear components of the space-velocities.

---

[1] *Mount Wilson Communications*, No. 1; *Proceedings of the National Academy of Sciences*, 1, 14, 1915,

ARITHMETICAL MEAN OF RADIAL VELOCITIES[1]

As the first and simplest step in the research we have compared radial velocities directly with absolute magnitudes. For this purpose the stars have been divided into groups defined by certain limits of parallax, and within each group the stars have been arranged according to absolute magnitude. The average of the radial velocities freed from the sun's motion is then formed for each mean absolute magnitude within these groups of stars. The results accordingly show the relationship of radial velocity to absolute magnitude among groups of stars located in concentric shells of space around the sun. In this way the effect of magnitude is separated from a possible effect of distance from the sun. In order to secure the large numbers of stars which are necessary for such statistical comparisons, rather wide limits of parallax have been chosen. The results for the F and G stars and for the K and M stars are given separately in Table I. M is the absolute magnitude,[2] and V' the radial velocity corrected for the sun's motion. The number of stars is given in the second column.

A very few stars of quite abnormal velocity have been omitted in the case of the F and G types, but with hardly an exception they are stars of low absolute magnitude, and their inclusion would merely increase the change in V' with absolute magnitude.

[1] In the following pages the arithmetical mean is designated by a bar above the symbol; the geometrical mean, by a bar below.

[2] Absolute magnitude is here defined as apparent magnitude reduced to the distance corresponding to a parallax of $0\overset{''}{.}1$.

The increase in the value of the radial velocity with the absolute magnitude is shown clearly for essentially all of the groups in Table I. It is most marked in the case of the stars of large parallax, since these show the largest range in absolute magnitude, and their parallaxes are most accurately determined. The smallest parallaxes, on the other hand, are subject to much larger percentage errors. The absence of intrinsically faint stars among the groups of small parallax is, of course, due to the fact that such stars are too faint to have been observed for radial velocity with existing instruments. Interpreted directly, therefore, two general conclusions may be drawn from these results: (1) Among stars at the same distance from the sun, as defined by these parallax limits, there is an increase of radial velocity with decrease in absolute brightness. (2) There is little evidence of a variation in radial velocity with distance from the sun.

TABLE I

π	Number	$\overline{M}$	$\overline{V}'$	π	Number	$\overline{M}$	$\overline{V}'$
			F AND G STARS				
			km				km
≧0″.050	42.....	3.0	15.4	0″.024 to 0″.013	105....	0.3	10.8
	57.....	4.8	16.5		79....	1.4	11.7
	29.....	6.8	21.2		41....	3.1	13.5
0.049 to 0.025	56.....	1.2	15.8	≦0.012	83....	0.3	11.6
	87.....	3.0	15.1		58....	1.4	14.0
	27.....	5.6	19.1		19....	2.5	15.4
			K AND M STARS				
≧0.050	29.....	2.4	20.7	0.024 to 0.017	48.....	0.6	14.8
	27.....	6.2	25.1		99.....	1.4	17.5
	38.....	7.7	27.2		18.....	2.7	19.7
	13.....	10.0	30.2	0.016 to 0.013	36.....	0.6	14.5
0.049 to 0.034	36.....	1.3	21.2		41.....	1.3	14.3
	28.....	2.7	24.3		10.....	2.2	17.2
	9.....	6.3	30.7	≦0.012	18.....	0.5	16.3
0.033 to 0.025	23.....	0.3	13.0		33.....	1.4	15.6
	55.....	1.5	14.1		13.....	2.3	13.4
	26.....	2.4	22.0				

If we combine the results for all of the zones according to absolute magnitude we obtain the values given in Table II.

TABLE II

F and G Stars			K and M Stars		
Number	$\overline{M}$	$\overline{V}'$	Number	$\overline{M}$	$\overline{V}'$
		km			km
188	0.3	11.2	125	0.5	14.6
193	1.3	13.6	264	1.4	16.6
189	3.0	14.9	124	2.5	20.6
84	5.1	17.3	74	7.0	26.9
29	6.8	21.2	13	10.0	30.0

A plot of these results in Fig. 1 shows that they are represented with sufficient accuracy by two straight lines nearly, if not quite, parallel to one another. A linear relationship, therefore, is indicated between absolute magnitude and radial velocity, the change in velocity for each unit of magnitude amounting to 1.5 km for the spectral types considered. A value of 1.1 km was found for the stars of type K by Kapteyn and Adams in the paper to which reference has already been made.

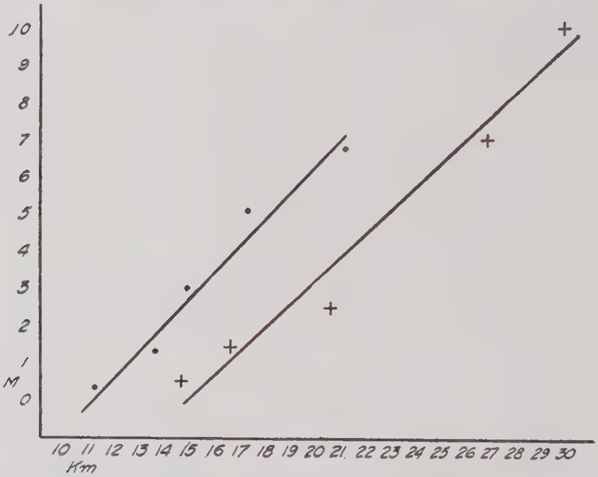

Fig. 1.—Variation of radial velocity with absolute magnitude: points, for F and G stars; crosses, for K and M stars.

DERIVATION OF THE PARALLAXES

The vital importance of accurate parallax determinations for such an investigation is obvious. Since spectroscopic parallaxes were available for only about 700 of the stars used, it became necessary to supplement these values with others derived by aid of a mean parallax formula. A brief description of this formula is therefore essential.

The measurements of van Maanen upon the parallaxes of stars of very small proper motion, together with spectroscopic determinations, have shown that the values for such stars are considerably larger than would be expected from their proper motions. Thus for stars with proper motions less than 0".020 annually the parallaxes appear to be nearly independent of proper motion and dependent only on the magnitude. This is probably due to the fact that a list of stars of very small proper motion, but bright enough to be contained in a catalogue such as that of Boss, involves the selection, not only of distant stars of high intrinsic luminosity, but also of those whose velocity components at right angles to the line of sight are nearly parallel to the sun's velocity component in the same plane and are of the same order of magnitude. Since the intrinsic luminosity of a star cannot be infinitely great, we should expect that the selection of apparently bright stars of very small proper motion would involve a selection of *direction* of space-motion as well as a selection of distant stars. The values given by Kapteyn's mean parallax formula[1] are, therefore, probably too small for stars of very small proper motion.

An additional consideration is that among the distant stars we observe only those of high luminosity. Accordingly, if, as the results of this investigation indicate, the highly luminous stars have small radial velocities and hence small space-velocities, we should expect that the usual mean parallax formula, which is founded on the assumption that the velocity- and the luminosity-curves are independent of distance, would give too small parallaxes for the stars of small proper motion.

For these reasons we have not made use of Kapteyn's equation in its usual form, but have modified it in such a way as to obtain finite parallaxes for zero proper motion by the introduction of an additional constant. The form used is

---

[1] *Publications of the Astronomical Laboratory of Groningen*, No. 8.

$$\pi = A(\mu + c)^b \epsilon^m \text{ or } \log \pi = \log A + b \log (\mu + c) + m \log \epsilon .$$

The spectroscopically observed parallaxes were used in the derivation of the constants in order to render the results homogeneous. Since the value of b was found nearly equal to 1, and it proved most difficult to determine b and c separately, the more simple form

$$\log \pi = \log A + \log (\mu + c) + m \log \epsilon$$

was used for stars with proper motions less than 1″, and gave results in good agreement with observation. Since proper motion is a different measure of parallax in the neighborhood of the sun's apices and apart from them, the constants have been determined separately for the stars near and distant from these points. The formula has been referred to the magnitude scale of the Harvard system.

The mean errors in $\log \pi$ derived from this equation are dependent upon the magnitude and proper motion. They are largest for the stars of types K and M, but are considerably smaller than those given by the formulae of Kapteyn and van Rhijn.[1] Further details of this formula and its use will be given in a future communication.

FREQUENCY DISTRIBUTION OF VELOCITIES

Reference has already been made to the suggestion in the paper by Kapteyn and Adams that the distribution of velocities in space might be quite other than that given by Maxwell's law, and that this fact might be used to explain the smaller radial velocities of the stars of small proper motion. It is evident that, if in any selected group of stars there is an excess of large velocities as compared with that given by Maxwell's law, we are inclined to assign such stars too large parallaxes owing to their large proper motions, and consequently to conclude that the mean intrinsic brightness of the stars in the group is too low. We might, therefore, arrive at false conclusions regarding a relationship between velocity and either distance or absolute magnitude. It is therefore most desirable that the effect of frequency distribution be eliminated so far as possible. The following method was devised by Strömberg for computing the parallaxes in a manner independent of the law of velocity-distribution.

---

[1] *Mt. Wilson Contr.*, No. 110; *Astrophysical Journal*, 43, 36, 1916.

The star's velocity in space is projected upon three axes, one of which corresponds to radial velocity, and the other two to the components of proper motion which are denoted by ν and τ in Kapteyn's notation. The ν axis is directed toward the sun's apex, and the τ axis is at right angles to the ν axis. The three components of the star's velocity in space, corrected for the sun's motion, are as follows:

$$V'=V+V_0\cos d;\qquad V_\nu=\frac{K\nu}{\pi}+V_0\sin d;\qquad V_\tau=\frac{K\tau}{\pi},$$

in which V is the star's radial velocity, V_0 the sun's velocity, d the angle between the star and the sun's apex, K a constant[1] equal to 4.738, and ν and τ the components of the proper motion. If we assume that the frequency function F for these three components is the same, without any assumption as to its nature, we have

$$F(V')=F(V_\tau)\ \text{or}\ F_1(\log V')=F_1(\log V_\tau)\ \text{or}\ \overline{\log V'}=\overline{\log V_\tau}.$$

Denoting mean values by a bar above the symbol, we find

$$\overline{\log\pi}=\log K+\overline{\log\tau}-\overline{\log V'}. \qquad (1)$$

If the *geometrical* means, denoted by a bar below the symbol, are then introduced, we have

$$\log\underline{\pi}=\overline{\log\pi};\qquad \log\underline{\tau}=\overline{\log\tau};\qquad \log\underline{V'}=\overline{\log V'}$$

or, finally,

$$\underline{\pi}=K\frac{\underline{\tau}}{\underline{V'}}. \qquad (2)$$

This equation is of the same form as that derived by Campbell for the arithmetical means and valid for a small range in the parallaxes. Equation (2), however, is correct whatever the variation in π, τ, or V'. In equations (1) and (2) the numerical values of τ and V' are to be considered without regard to sign.

---

[1] W. W. Campbell, *Stellar Motions*, p. 222.

A similar computation using the ν component gives as a final result

$$\underline{\pi}=\frac{K\underline{\nu}}{\underline{(V'-V_0 \sin d)}}. \tag{3}$$

The two equations (2) and (3) have been used to compute the parallaxes for the groups of stars used in Table I. These results are shown in Table III, as well as the geometrical means $\underline{\pi}$ of the parallaxes employed.

TABLE III

Number	π	$\underline{\pi}$	$\underline{\pi}(\tau)$	$\underline{\pi}(\nu)$
	F AND G STARS			
142	$\geqq 0''.050$	$0''.082$	$0''.078$	$0''.086$
95	0.049–0.034	.041	.045	.044
91	.033– .025	.028	.023	.021
122	.024– .017	.020	.017	.013
110	.016– .013	.015	.006	.004
68	0.012– .010	.011	.004	.003
97	$\leqq 0.009$	0.007	0.003	0.003
	K AND M STARS			
108	$\geqq 0''.050$	$0''.094$	$0''.075$	$0''.103$
73	0.049– .034	.039	.021	.030
103	.033– .025	.028	.019	.022
162	.024– .017	.020	.010	.010
86	0.016– .013	.015	.004	.004
63	$\leqq 0.012$	0.009	0.003	0.004

This comparison shows a good degree of accordance for the groups of large parallax between the values of the parallax actually employed and the computed values from the ν and τ components. For the groups of small parallax, however, the values used are appreciably larger than the computed ones. A part of this difference is due to the selection of stars with motions mainly in the line of sight and tangential components parallel and nearly equal to the sun's motion. This is seen from the results of Table IV where the radial velocities for the distant stars are considerably larger than the linear τ components. It is probable, however, that the parallax values employed are subject to a certain amount of systematic

TABLE IV

π	M	$\bar{M}$	$\underline{\pi}$	$\underline{V}'$	$\underline{V}_\tau$	$\frac{1}{2}(\underline{V}'+\underline{V}_\tau)$	No.	$\bar{V}'$	No.
				F AND G STARS					
				km	km	km		km	
≧0″.050	≦3.9..	2.9	0″.076	12.7	8.8	10.8	41	15.3	42
	4.0–4.9..	4.47	.082	13.4	15.2	14.3	35	16.8	34
	5.0–5.9..	5.35	.080	16.9	16.5	16.7	33	16.0	23
	≧6.0..	6.92	.094	19.2	16.9	18.0	33	21.2	29
0.049–0.034	≦1.9..	1.28	.040	9.3	7.9	8.6	19	13.9	19
	2.0–2.9..	2.51	.039	14.6	9.6	12.1	24	15.0	19
	3.0–4.9..	3.73	.042	12.9	21.1	17.0	26	15.4	24
	≧5.0..	5.62	.042	23.2	36.9	30.0	26	20.0	21
0.033–0.025	≦1.9..	1.09	.029	10.5	7.0	8.8	37	16.9	37
	2.0–2.9..	2.32	.028	9.7	7.3	8.5	31	14.6	31
	≧3.0..	4.61	.029	19.0	26.2	22.6	23	15.9	19
0.024–0.017	≦0.9..	0.24	.020	6.2	2.9	4.6	43	8.6	42
	1.0–1.9..	1.44	.020	7.6	8.6	8.1	50	13.6	49
	≧2.0..	3.37	.020	11.5	16.8	14.1	29	11.9	25
0.016–0.013	≦1.9..	0.73	.015	7.6	3.4	5.5	94	12.7	93
	≧2.0..	3.10	.015	11.3	4.6	7.5	16	15.9	16
0.012–0.010	≦0.9..	0.37	.011	7.1	3.4	5.3	36	11.4	35
	≧1.0..	1.52	.011	11.0	4.0	7.5	32	14.1	31
≦0.009	≦0.9..	0.21	.007	7.8	3.4	5.6	49	11.7	48
	≧1.0..	1.73	0.007	14.0	6.7	10.4	48	14.5	46
				K AND M STARS					
≧0″.050	≦2.9..	1.95	0″.066	11.1	8.2	9.6	19	17.2	19
	3.0–6.9..	5.38	.081	14.8	13.2	14.0	38	25.7	37
	7.0–7.9..	7.27	.092	18.8	18.1	18.5	24	27.5	24
	≧8.0..	9.34	.149	22.2	23.1	22.6	27	28.4	27
0.049–0.034	≦1.9..	1.29	.038	16.9	6.2	11.6	36	21.2	36
	2.0–3.9..	2.69	.040	18.1	12.1	15.1	27	24.3	28
	≧4.0..	6.06	.041	24.3	23.1	23.7	9	30.7	9
0.033–0.025	≦0.9..	0.26	.028	6.8	3.1	5.0	23	13.0	23
	1.0–1.9..	1.49	.028	8.2	7.0	7.6	55	14.1	55
	≧2.0..	2.46	.029	17.8	9.4	13.6	25	22.0	26
0.024–0.017	≦0.9..	0.59	.020	9.8	3.3	6.6	46	14.8	48
	1.0–1.9..	1.40	.020	12.2	6.7	9.5	98	17.5	99
	≧2.0..	2.68	.021	14.7	8.3	11.5	18	19.7	18
0.016–0.013	≦0.9..	0.61	.015	10.0	2.5	6.2	35	14.5	36
	≧1.0..	1.48	.015	10.4	2.9	6.7	51	14.8	51
≦0.012	≦0.9..	0.53	.008	9.1	3.4	6.3	18	16.3	18
	1.0–1.9..	1.39	.009	11.8	4.9	8.4	32	15.6	33
	≧2.0..	2.32	0.009	11.3	......	....	13	13.4	13

error, based as they are in the final analysis upon an extremely scanty amount of observational material.

EFFECT OF STREAM-MOTION

The stream-motion of the stars used in this investigation might affect to some extent the means of the radial velocities, although with the relatively large groups employed the influence would certainly be slight. As a means of reducing the effect, we have computed the geometrical means of the radial velocities $\underline{V}'$ and the linear τ components V_τ, and have formed the arithmetical means of these two values. If stream-motion is to be regarded as affecting mainly the direction of the space-velocities, the influence upon the mean of the two components should be greatly diminished. Table IV contains these results. The linear τ component $\underline{V}_\tau$ is calculated from the geometrical mean of the parallaxes of the stars in the group by the aid of the formula

$$\log \underline{V}_\tau = \log K + \overline{\log \tau} - \overline{\log \pi}.$$

For purposes of comparison the arithmetical mean $\overline{V}'$ is added for the different magnitude groups.

The results of Table IV agree with those of Table I in indicating a decided increase in velocity with decreasing absolute brightness among the stars of the several zones. This is true for both of the components used. There seems to be little evidence of a decrease in velocity with distance for a constant absolute magnitude, and it appears certain that the effect if present must be relatively slight.

As a final test of the results, we have used only the stars with parallaxes exceeding 0″.017. For these we have computed the geometrical means of the radial velocities (excluding a few stars with velocities smaller than 0.3 km), and the corresponding τ and ν parallaxes; also the absolute magnitudes and the linear τ components, using the means of $\underline{\pi}(\tau)$ and $\underline{\pi}(\nu)$. The absolute magnitudes and the τ components, therefore, are independent of measured parallaxes and of the frequency-distribution of the velocities. A single exception is found in the last group of the K and M stars for which the observed parallaxes are used. The results are given in Table V.

The increase of velocity with decrease of absolute brightness is shown very clearly in these results. The same result is true for the apparent brightness $\bar{m}$ of Table V. Under this heading are given the arithmetical means of the apparent magnitudes of the stars included within the groups M.

TABLE V

M	No.	$\underline{\pi}(\tau)$	$\underline{\pi}(\nu)$	$\frac{1}{2}(\underline{\pi}(\tau)+\underline{\pi}(\nu))$	$\bar{m}$	$\bar{M}$	$\underline{V}'$	$\underline{V}_\tau$	$\frac{1}{2}(\underline{V}'+\underline{V}_\tau)$
				F AND G STARS					
							km	km	km
≦0.9....	60	0″.012	0″.010	0″.011	3.38	−1.43	6.33	6.69	6.51
1.0–1.9....	94	.023	.018	.020	4.44	+0.99	9.56	10.57	10.06
2.0–2.9....	78	.024	.026	.025	4.84	1.83	10.86	10.59	10.73
3.0–3.9....	52	.094	.073	.084	4.77	4.38	10.31	11.64	10.97
4.0–4.9....	62	.060	.059	.060	5.84	4.71	15.97	16.01	15.99
5.0–5.9....	64	.073	.057	.065	6.69	5.74	19.54	21.97	20.75
≧6.0....	40	0.077	0.095	0.086	7.32	6.99	20.96	18.78	19.98
	450	0.036	0.034	0.035	5.18	2.89	11.89	12.28	12.08
				K AND M STARS					
≦0.9....	77	0.009	0.007	0.008	3.54	−1.89	8.54	9.29	8.92
1.0–1.9....	188	.015	.018	.017	4.44	+0.54	11.65	10.42	11.04
2.0–2.9....	66	.022	.026	.024	4.64	1.57	14.23	13.14	13.69
3.0–5.9....	39	.035	.060	.048	5.55	3.95	20.59	15.20	17.90
6.0–7.9....	48	.081	.124	.102	7.33	7.38	17.97	14.17	16.07
≧8.0....	29	(0.137)	(0.203)	0.147	8.42	9.25	17.88	16.61	17.25
	447	0.022	0.026	0.024	4.98	1.88	12.88	11.64	12.26

RADIAL VELOCITY AND SPECTRAL TYPE

A comparison of the average radial velocity of the F and G stars with that of the K and M stars is complicated by the fact that the former show a much greater velocity-dispersion. Two stars with velocities of over 300 km belong to the F and G group, and there are several others of quite abnormal velocity. These stars have been excluded in the absolute-magnitude discussion, and it is for this reason that Table II cannot be regarded as giving the direct relationship between spectral type and velocity. For these reasons it seems probable to us that the use of the geometrical mean, which is not abnormally influenced by the inclusion of stars of exceptionally high velocity, is preferable for this purpose. Table VI gives the geometrical means of the radial and component velocities together with one-half their sum. The parallaxes have been corrected for systematic errors. All stars with parallaxes exceeding 0ʺ.017 have been included.

TABLE VI

No.	M	$\underline{\pi}(\tau)$	$\underline{\pi}(\nu)$	π	$\bar{M}$	$\underline{V}'$	$\underline{V}_\tau$	$\frac{1}{2}(\underline{V}'+\underline{V}_\tau)$
				F and G Stars				
						km	km	km
154....	$\leqq 1.9$	0ʺ.017	0ʺ.014	0ʺ.016	+0.01	8.14	9.00	8.57
301....	$\geqq 2.0$	0.046	0.044	0.045	+4.03	13.89	14.07	13.98
				K and M Stars				
268....	$\leqq 1.9$	0.013	0.014	0.014	−0.13	10.31	9.91	10.11
184....	$\geqq 2.0$	0.043	0.056	0.050	+4.62	16.17	14.15	15.16

These results indicate that the K and M type stars have a velocity of from 1.0 to 1.5 km higher than the F and G stars of the same absolute magnitude.

CONCLUSIONS AND SUMMARY

1. Radial velocity is a function of absolute magnitude for the 1300 stars used in this investigation. The increase in velocity is about 1.5 km for a decrease in brightness of one magnitude.

a) This effect cannot be ascribed to distance from the sun, since stars at the same distance show the effect strongly.

b) It cannot be due to the law of frequency-distribution of the velocities, since the τ-component velocities calculated under no assumption of the nature of the frequency-law show the effect equally with the radial velocity.

c) It cannot be due to the effect of stream-motion.

2. A modified form of the formula connecting mean parallax with proper motion has been derived and applied to the stars under investigation. This formula gives mean errors considerably below those of the formulae commonly in use.

3. A method has been devised for calculating the geometrical means of the parallaxes of groups of stars, and these values have

been compared with those used in the investigation. The agreement is good for the groups of large parallax; for those of smaller parallax the observed values are somewhat too large.

4. The radial velocity and the τ-component velocity increase with decrease in apparent brightness.

5. The giant and dwarf division among the K and M stars is indicated clearly in the absolute magnitudes (Table V).

6. The use of the geometrical mean of the velocities and the parallaxes possesses some marked advantages for an investigation of this character. In the case of velocities it is unnecessary to exclude abnormally high values, as was done for the arithmetical mean, but only values very near zero. The agreement of the two means in indicating the variation of velocity with absolute magnitude is, therefore, a valuable check on the results. Further, from the geometrical mean of the parallaxes, it is possible to compute directly the mean absolute magnitude by the formula $\overline{M}=\overline{m}+5+5 \log \underline{\pi}$, whatever the range in m and π.

7. The stars of types K and M have mean velocities about 1.0 or 1.5 km higher than the F and G stars of the same absolute magnitude. This conclusion is based upon a discussion of the geometrical means of the radial and component velocities.

Mount Wilson Solar Observatory
April 1917

Contributions from the Mount Wilson Solar Observatory, No. 132
Reprinted from the *Astrophysical Journal*, Vol. XLVI, pp. 24–55, 1917

PHOTOGRAPHS OF NEBULAE WITH THE 60-INCH REFLECTOR 1911–1916

By FRANCIS G. PEASE

The 60-inch reflector with its aperture ratio of F/5 is well adapted for the photography of faint nebulae and all such objects as require great light-gathering power together with considerable scale in order to show their details. For the program of observations, of which some account is given in this paper, the objects selected were in general those whose real nature was unknown or those which possessed curious or questionable characteristics. Many photographs were made under very unfavorable observing conditions, and, in consequence, for these little more than the type is discernible. At times of good seeing, well-known objects were photographed for purposes of measurement. Exposures on several of the bright planetaries were made with the 80- and 100-foot focus, Cassegrain arrangements, with a corresponding increase in scale.

The double-slide plate-holder and its manipulation have been previously described,[1] and but few changes in the instrument or in its usage have been made since that time. Since the actual photographic image is many times the theoretical diameter of the diffraction image, small changes of focus are unimportant in their effect on the images, and intervals of an hour and more were permitted between refocusing. When the image of the guiding star vibrates rapidly, it is found advisable to neglect its excursions to and fro and to follow only the slow drift of its mean center. Both eyes were used alternately for guiding; and on long exposures two guiding stars were used, and correction was made for variation in size and rotation of the field produced by refraction and imperfect adjustment of the instrument. Changes in character of the guiding image during the exposure are responsible for as many plates with elongated images as are irregularities in the driving of the telescope.

---

[1] *Mt. Wilson Contr.*, No. 47; *Astrophysical Journal*, **32**, 26, 1910.

Many objects are so situated as to place the observer in arduous positions for guiding, a difficulty now avoided by using a "gooseneck" microscope—a double-prism device which enables the guiding image to be viewed at a convenient angle.

All negatives were made on Seed 23 plates unless otherwise mentioned. For long exposures and for all those on fields containing bright stars the plates were backed. The usual development was with rodinal, of concentration 1/64 for 30 minutes at 20° C., though in some cases 1/32 for 15 minutes was used. All plates, except a few of early date and those otherwise noted, were taken with the full aperture of 60 inches, with a central stop of 23 inches diameter introduced to cut out the irregularly shaped cell of the Newtonian flat.

The appended list of the nebulae photographed gives (*a*) the approximate position for 1917 (the 1860 position of the *N.G.C.* corrected for precession); (*b*) the constellation; (*c*) the numbers assigned in various catalogues; (*d*) the type (El. = elliptical or elongated, Spl. = spiral, Plan. = planetary, Irr. = irregular, Spe. = spindle); (*e*) the 60-inch plate number, and (*f*), if illustrated, the number of the reproduction.

In the text following Table I is given the *N.G.C.* number of the nebula, its position for 1917, its galactic co-ordinates taken from a chart prepared by Professor Kapteyn, a list of the plates on which the object appears, and a brief description of its principal features. Much of the detail is faint and diffuse, unsuitable for comparator measures, so that the description is based on measures and estimates obtained with a magnifying glass of low power and a photographic reseau giving polar co-ordinates. The orientations have been derived from star trails, but as some of the plates are not provided with trails the results are approximate. Position angle (*p*) is measured from the north toward the east through 360°. The type of spectrum has been added wherever possible, a number of spectrograms, besides those by other observers, having been obtained with the focal-plane spectrograph of the 60-inch reflector.

A left-handed spiral has been defined as one in which an object traveling inward along one of the arms moves in a counter-clockwise direction. Many spirals which are inclined to the line of sight have

PLATE VI

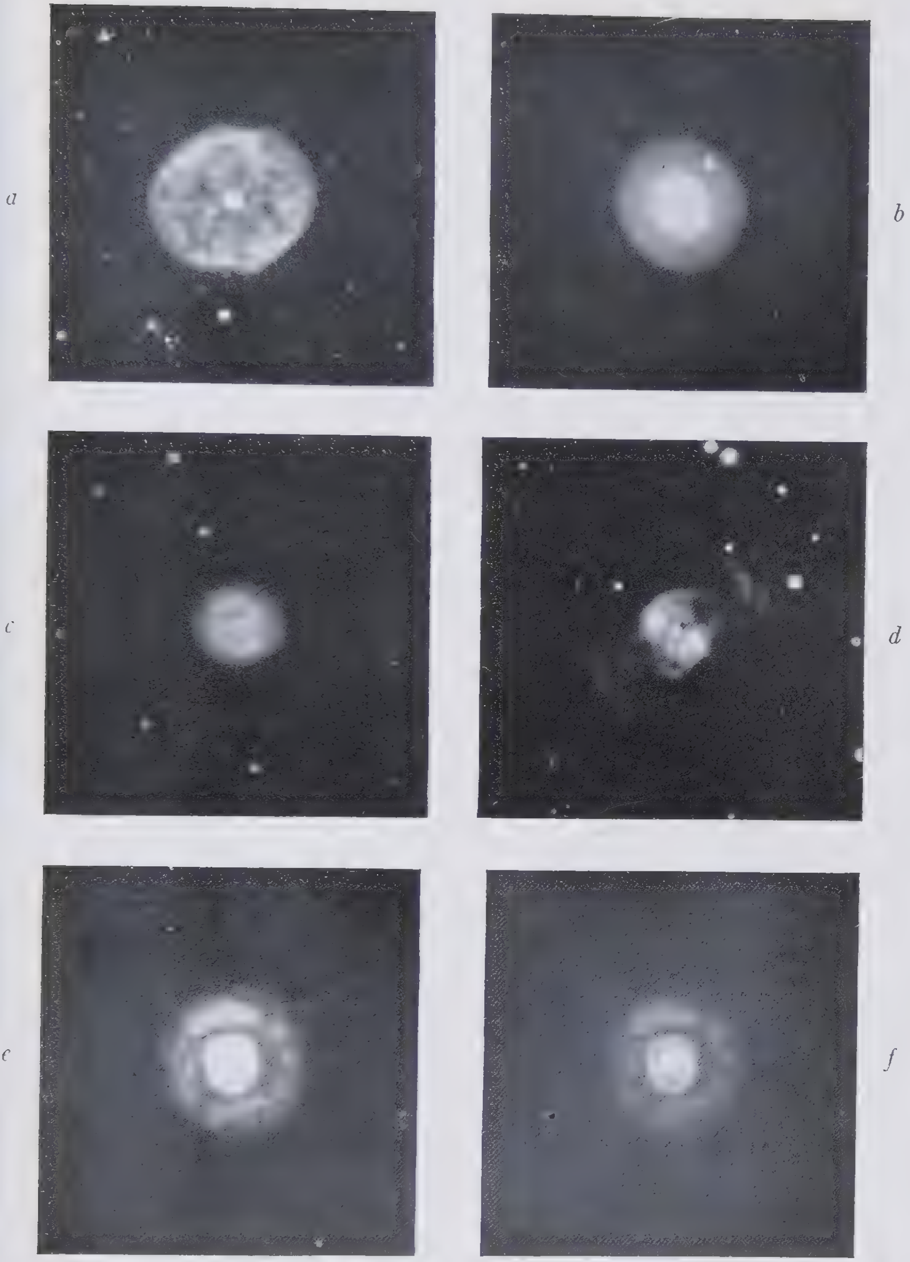

a	N.G.C. 1501	Exposure 120^{m},	Enlargement 10.0,	1 mm = 2″.7	
b	1535	85	11.2	2.4	
c	2022	60	11.1	2.5	
d	2371–2	221	5.2	5.2	
e and *f*	2392	120	4.0	2.1	80-ft. focus

e and *f* are reproduced from the same negative with differences in exposure and development.

PLATE VII

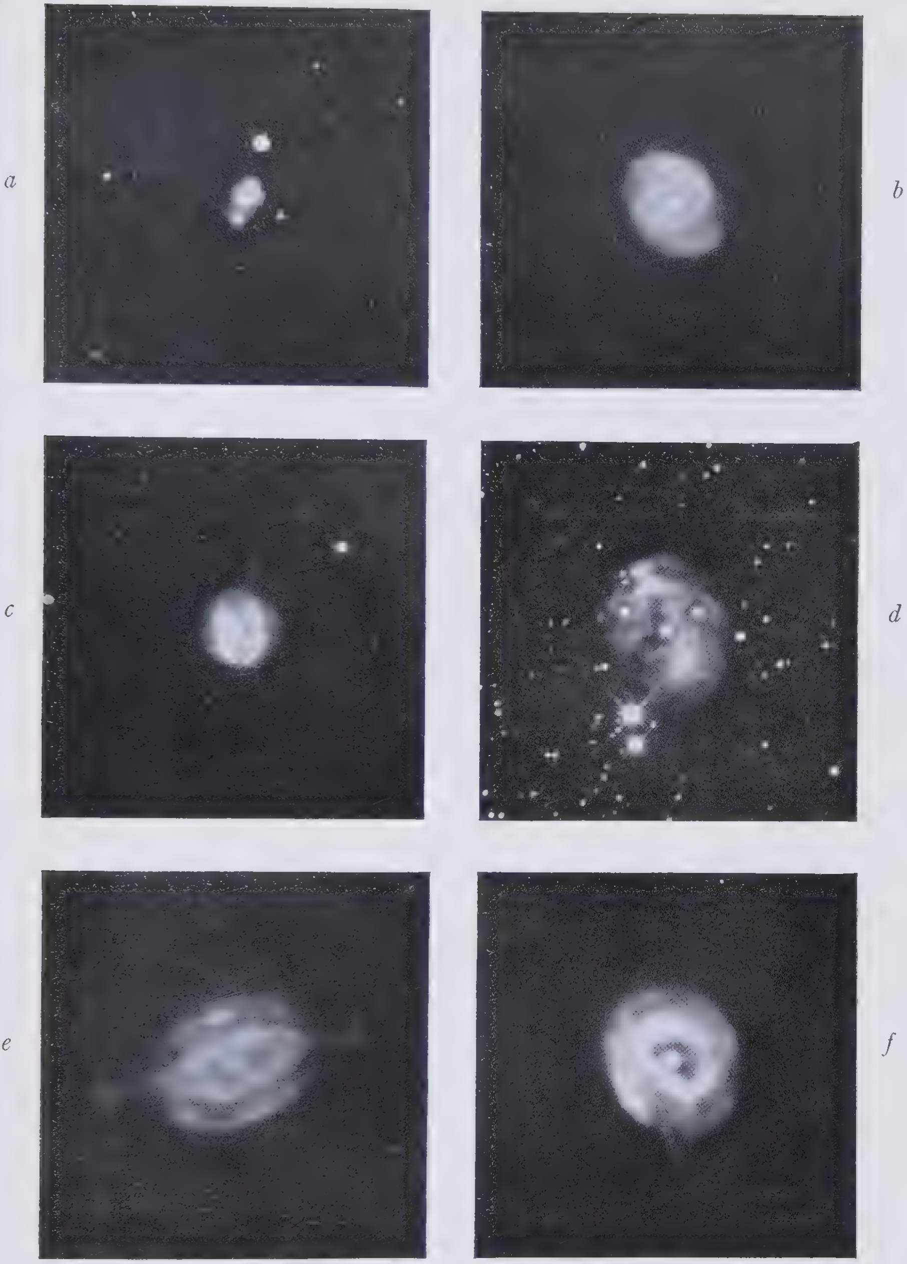

a	N.G.C. 6309	Exposure	90^{m},	Enlargement 9.6,	1 mm = 2″.8	
b	6543		50	4.5	1.5	100-ft. focus
c	6818		75	2.8	2.4	100-ft. focus
d	7008		180	5.9	4.7	
e	7009		210	4.5	1.5	100-ft. focus
f	7662		90	4.5	1.5	100-ft. focus

PLATE VIII

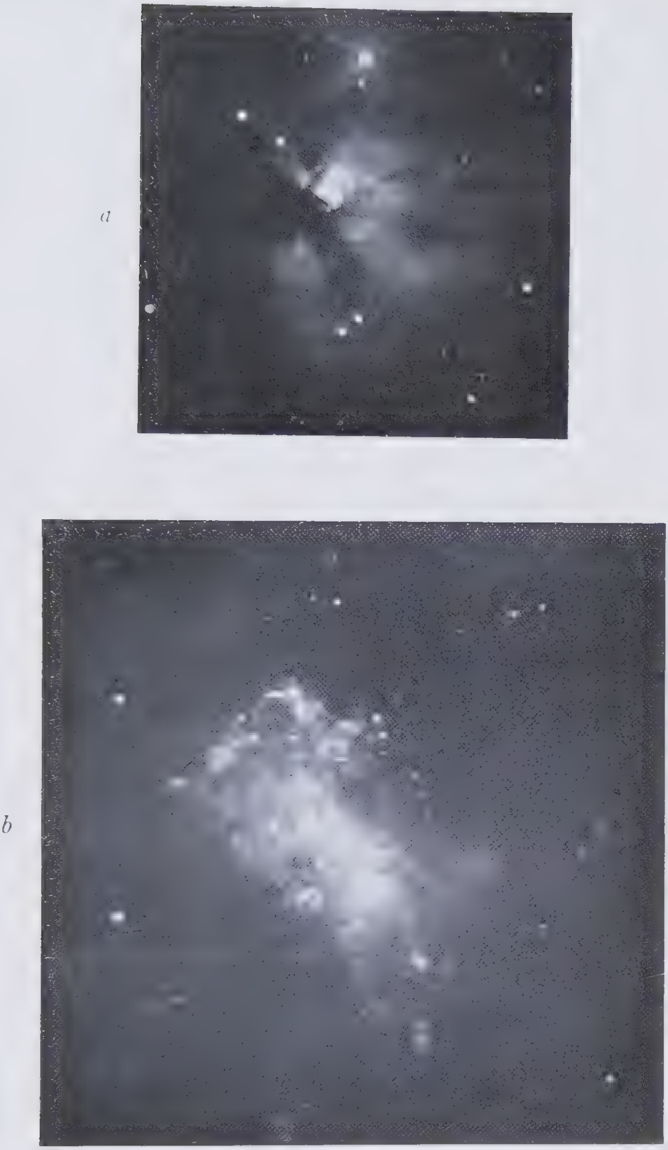

a	N.G.C. 1579	Exposure 420^{m},	Enlargement 3.0,	1 mm = $9\overset{\prime\prime}{.}1$
b	4449	300	5.8	4.7

PLATE IX

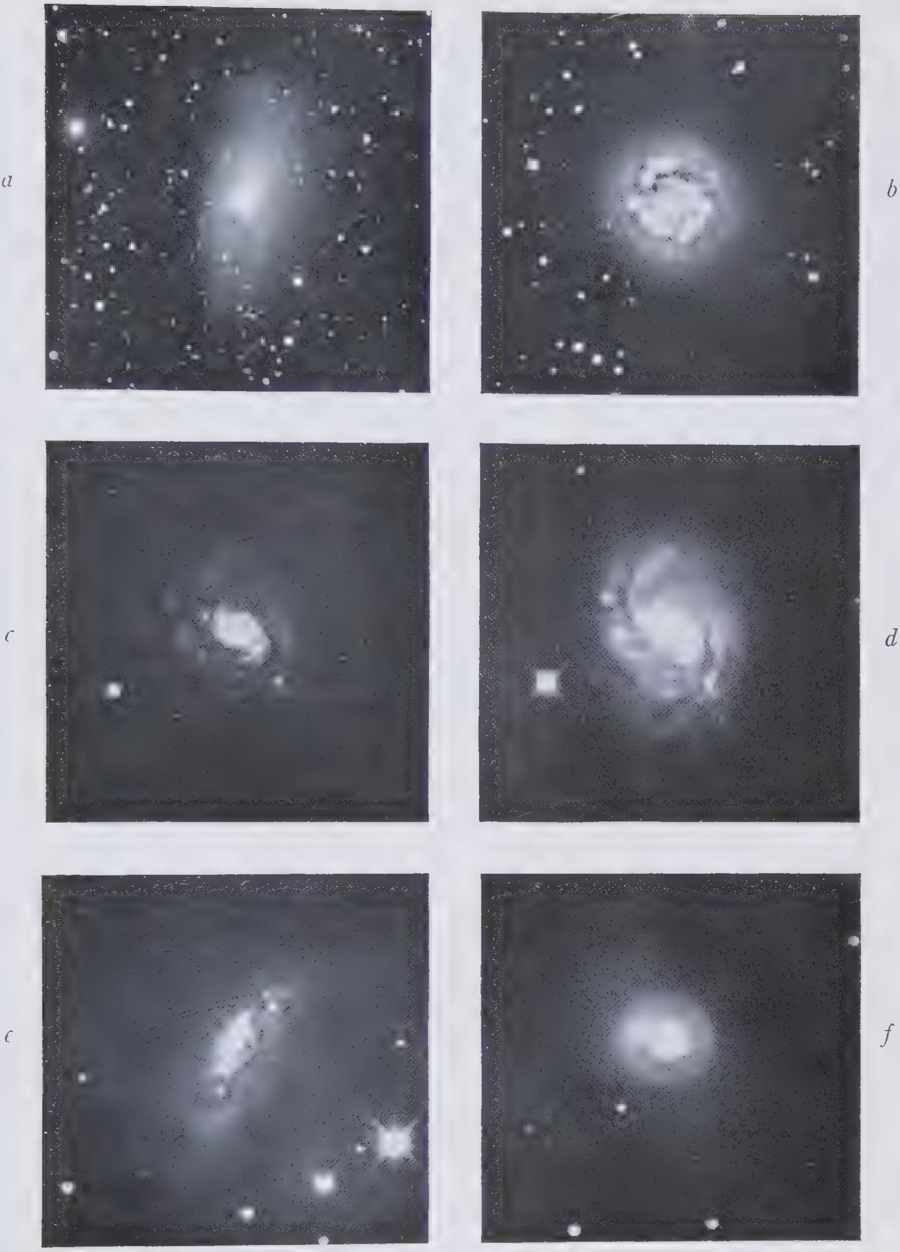

a	N.G.C. 205	Exposure 230^{m},	Enlargement 1.5,	1 mm = $19''.4$
b	278	240	5.8	4.7
c	1068	22	5.5	5.0
d	1068	120	5.5	5.0
e	972	195	6.9	3.9
	2681	190	7.9	3.4

PLATE X

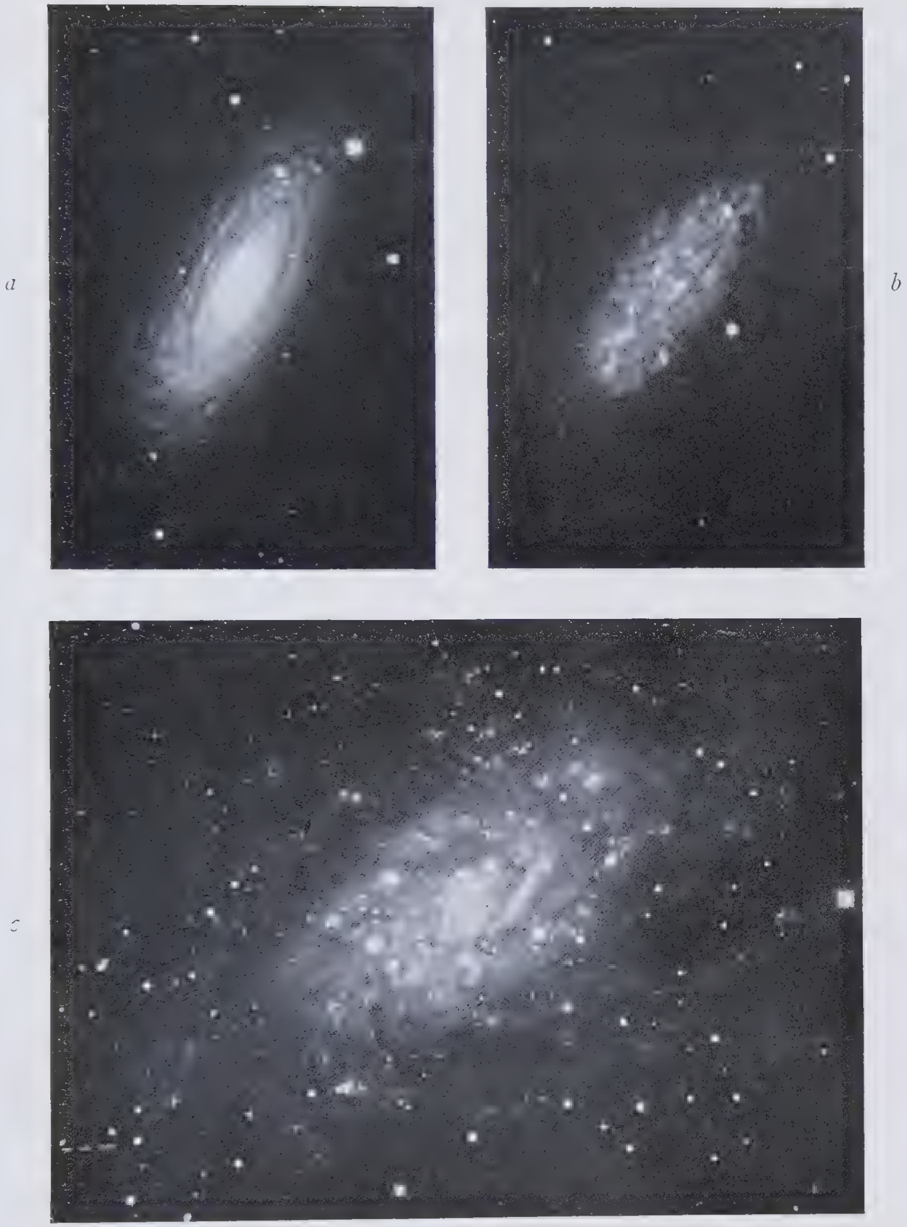

a	N.G.C	2841	Exposure 120^{m},	Enlargement 3.8,	1 mm = 7″2
b		2976	180	4.7	5.7
c		2403	210	2.7	10.0

PLATE XI

a

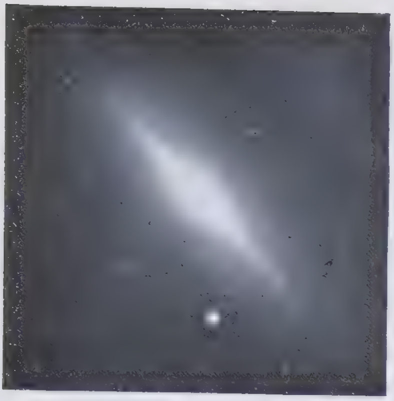

b

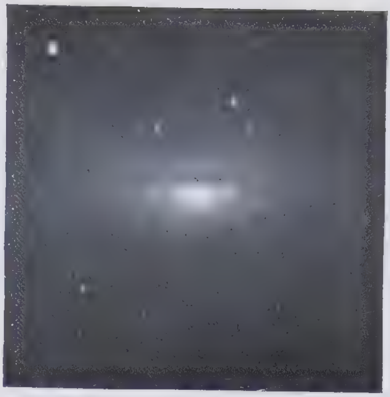

c

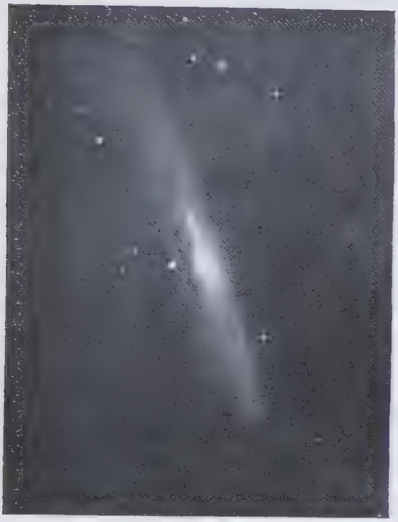

d

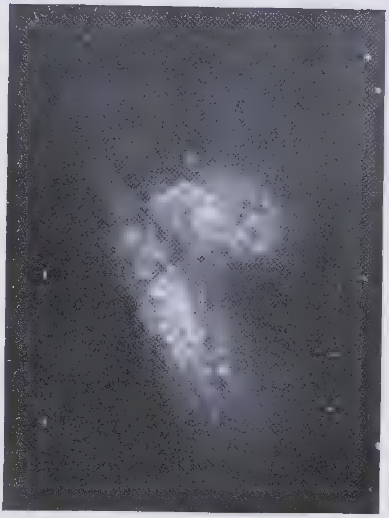

e

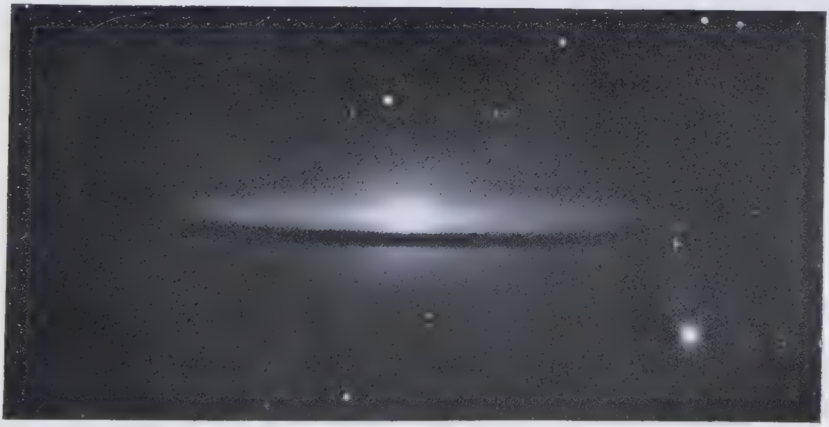

a	N.G.C. 3115	Exposure 100^m,	Enlargement 5·5,	1 mm = 5″.0
b	3593	210	5·5	5·0
c	4216	90	3·0	9·2
d	4567-8	360	4·9	5·6
e	4594	132	4·5	6·0

PLATE XII

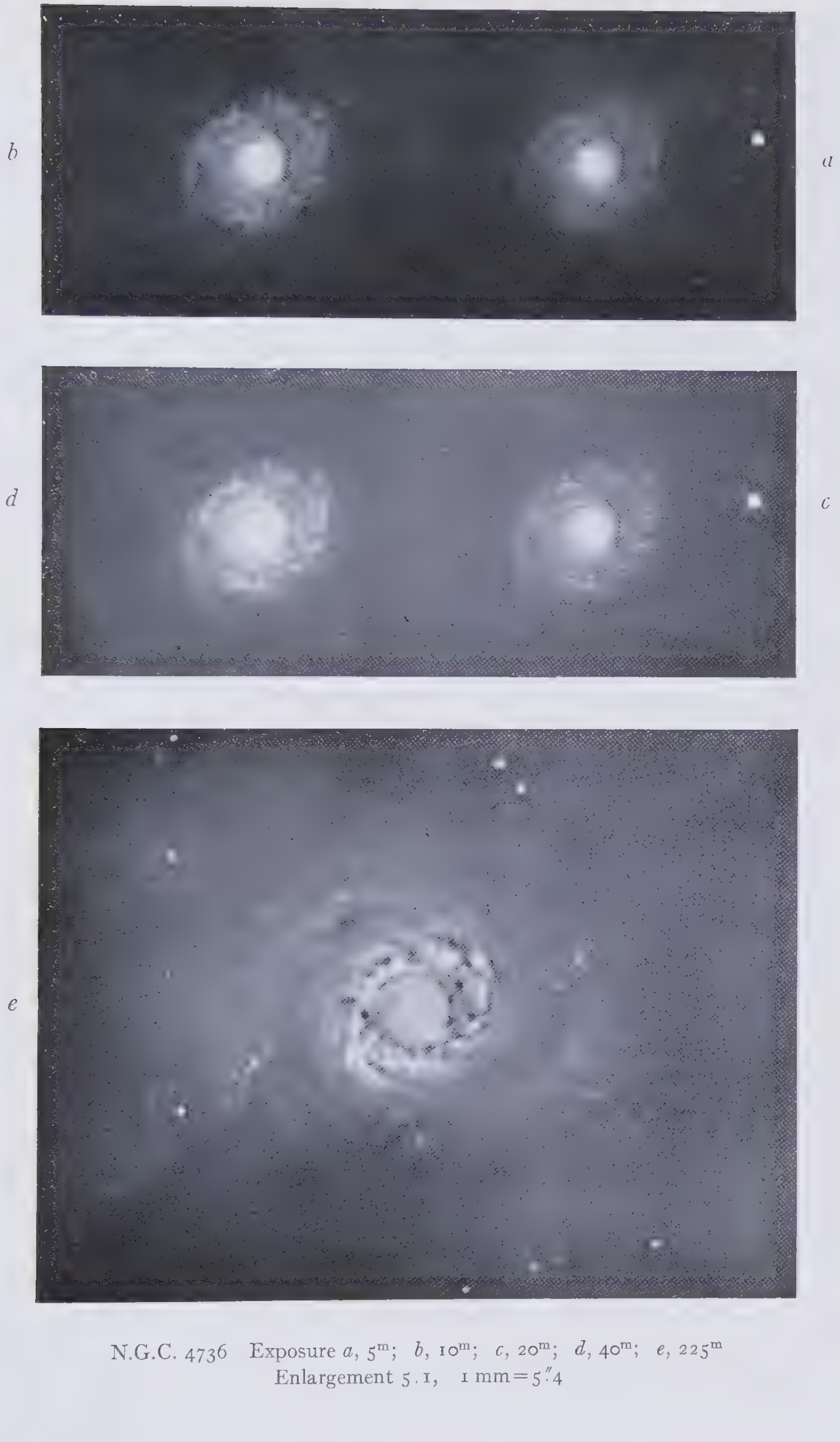

N.G.C. 4736 Exposure *a*, 5^{m}; *b*, 10^{m}; *c*, 20^{m}; *d*, 40^{m}; *e*, 225^{m}
Enlargement 5.1, 1 mm = $5''.4$

PLATE XIII

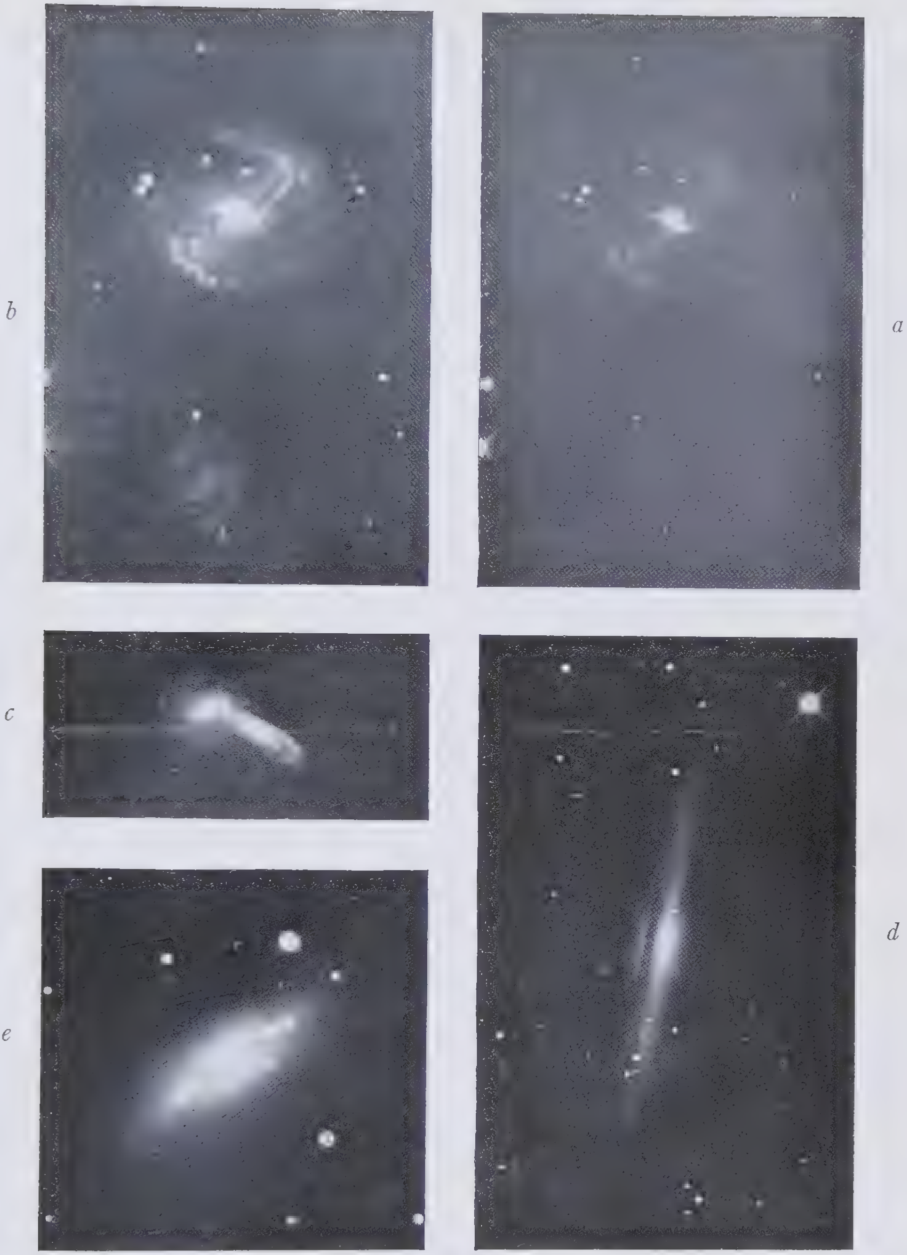

a	N.G.C. 5383	Exposure 180^{m},	Enlargement 5·0,	1 mm = 5″·4
b	5383	360	4·9	5·5
c	5544–5	360	5·5	5·0
d	5746	360	3·4	7·9
e	5866	165	5·0	5·5

PLATE XIV

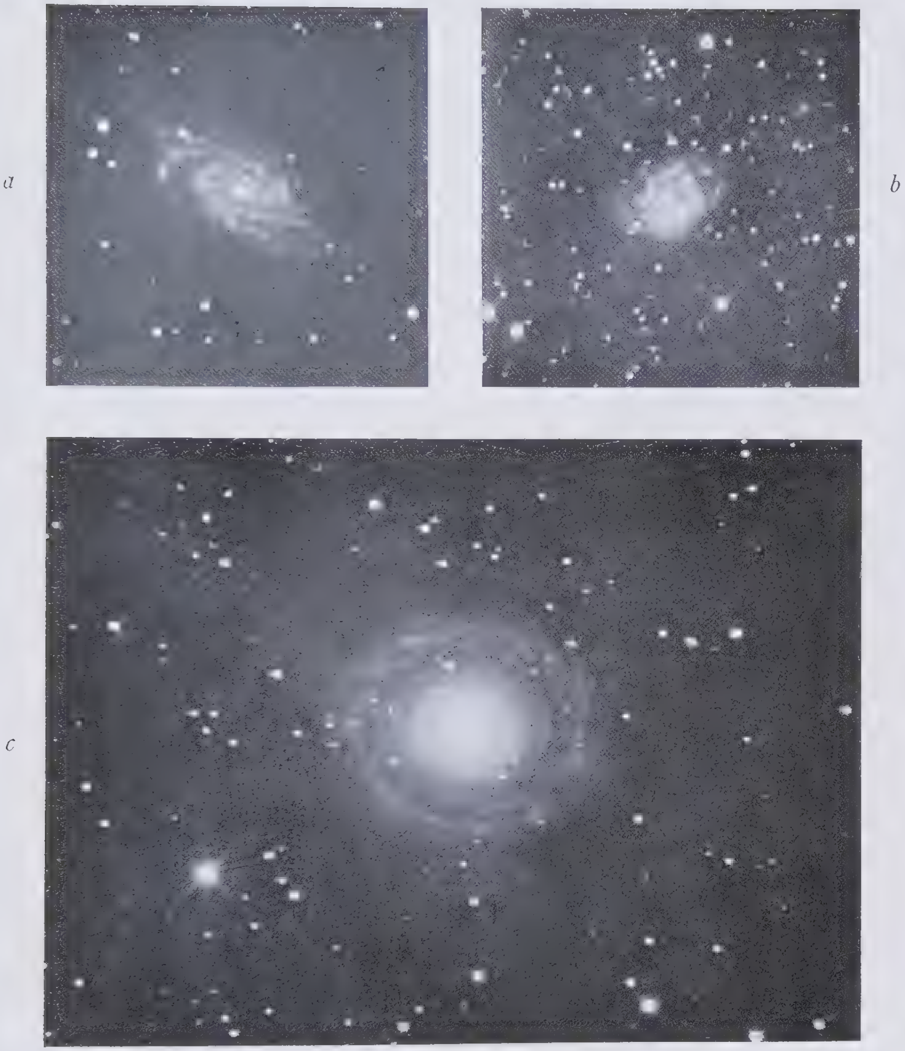

a	N.G C. 6070	Exposure 150^m,	Enlargement 4.2,	1 mm=6″.5
b	6555	360	4.5	6.0
c	7217	330	5.5	5.0

a different shading on one side of the major axis from that on the other, one side being soft while the other is more knotted and of stronger contrast, the latter resembling the effect produced by the sun shining through an irregular bank of clouds. All illustrations are placed with north (N) at the top and west (W, preceding) at the right.

All catalogued nebulae showing on any of the photographs here discussed have been inserted in the list; but those which appear only incidentally are described in the text under the *N.G.C.* number of the object for which the plate was primarily taken (see notes to Table I). A number of uncatalogued nebulae and nebulous stars are also shown. Mention of such is made in the text description of *N.G.C.* 1186, 2681, 2830, 2841, 4406, 5308, 5383, 6555, and 6703.

I am indebted to Mr. Ellerman for the preparation of the positives for the half-tones.

N.G.C. 205 Andromeda

$\alpha=0^h35^m51^s$, $\delta=+41°14'.2$ (1917); $\lambda=89°$, $\beta=-22°$
Plate No. 152, 1912, October 9, 230^m. Images large
Illustrated Plate IX*a*

This is the bright nebula lying on the N*p* side of the great nebula of Andromeda 36'.4 distant. On a diffuse ellipse $10'\times4'$, $p=172°$, gradually fading away at the edge, lies centrally a brighter patch about $1'.5\times1'$. Besides the sharp nucleus there is detail in the bright central part, and dark patches of irregular shape, similar in character to that surrounding the nucleus of the great nebula, lie one on the S end and the other on the N*f* end. The nebula is possibly spiral, but the exposure is not long enough to show detail in the outer nebulosity. Huggins[1] assigns it a continuous spectrum.

N.G.C. 278 Cassiopeia

$\alpha=0^h47^m23^s$, $\delta=+47°6'$ (1917); $\lambda=92°$, $\beta=-16°$
Plate No. 168, 1912, November 8, 240^m. Fine plate.
Illustrated Plate IX*b*

This fine left-handed spiral is seen in plan. Four or five whorls emanating from the nucleus make about a half-revolution before

---

[1] *Philosophical Transactions*, **156**, 388, 1866.

TABLE I

NEGATIVES WITH THE 60-INCH REFLECTOR

N.G.C.	α 1917	δ 1917	Constellation	G.C.	H and Others	h	Type	Plate Nos.	Illustrations
205	$0^{h}\ 35^{m}\ 51^{s}$	$+41^{\circ}\ 14'.2$	Andromeda	105	V 18	44	El.	152	IX*a*
278	0 47 23	+47 6.0	Cassiopeia	158	I 159	71	Spl.	168	IX*b*
650–1	1 37 4	+51 9.2	Perseus	385–6	I 193, M 76	....	Irr.	57, 150, 151, 170	....
895	2 17 29	− 5 54.3	Cetus	529	II 438	219	Spl.	281	....
955	2 26 20	− 1 28.6	Cetus	551	II 278	229	Spe.	229	....
972	2 29 20	+28 56.9	Aries	560	II 211	232	El.	231	IX*e*
1023	2 35 12	+38 42.5	Perseus	575	I 156	242	El.	171	....
1068	2 38 26	− 0 21.9	Cetus	600	M 77	262	Spl.	49, 51, 53	IX*c*, *d*
1186	3 0 4	+42 30.2	Perseus	639	IV 43	281	Spl.	244, 245	....
1501	3 59 50	+60 41.9	Camelopardus	801	IV 53	....	Plan.	174, 178	VI*a*
1535	4 10 23	−12 56.9	Eridanus	826	IV 26	2618	Plan.	163, 182	VI*b*
1579	4 24 46	+35 6.0	Perseus	853	I 217	315	Irr.	227	VIII*a*
1931	5 25 55	+34 11.0	Auriga	1137	I 261	355	Irr.	277, 278	....
2022	5 37 33	+ 9 2.7	Orion	1225	IV 34	365	Plan.	183	VI*c*
2366	7 20 7	+69 11.5	Camelopardus	1515	III 748	....	Irr.	279	....
2371–2	7 20 20	+29 39.1	Gemini	1519–20	II 316–17	444–5	Irr.	257	VI*d*
2392	7 24 16	+21 5.0	Gemini	1532	IV 45	450	Plan.	187, 189, 190, 191, 255	VI*e*, *f*
2403	7 28 49	+65 46.9	Camelopardus	1541	V 44	....	Spl.	169	X*c*
2681	8 47 36	+51 37.7	Ursa Major	1711	I 242	530	Spl.	179	IX*f*
2825	9 14 21	+34 5.1	Lynx	1806	....	581	Spe.	246, 247	....
2826	9 14 22	+33 58.0	Lynx	1807-09	....	....	Spe.	246, 247	....
2827	9 14 23	+34 16.7	Lynx	1808	....	....	El.	246, 247	....
2828	9 14 33	+34 17.2	Lynx	1810	....	....	El.	246, 247	....
2829	9 14 39	+34 0.8	Lynx	1804	....	....	Neb. star	246, 247	....
2830	9 14 44	+34 6.0	Lynx	1811	I 113	582	Spe.	246, 247	....
2831	9 14 45	+34 6.6	Lynx	1812	....	....	Neb. star	246, 247	....
2832	9 14 46	+34 6.9	Lynx	1813	....	....	El.	246, 247	....
2834	9 15 3	+34 3.3	Lynx	1815	....	....	Neb. star	246, 247	....
2839	9 15 36	+33 59.2	Lynx	1821	....	....	Neb. star	246, 247	....
2841	9 16 18	+51 19.7	Ursa Major	1823	I 205	584	Spl.	58	X*a*
2976	9 40 24	+68 17.9	Ursa Major	1905	I 285	625	Spl.	175	X*b*
3115	10 1 6	− 7 18.9	Sextans	2008	I 163	668	Spe.	56	XI*a*
3593	11 10 17	+13 16.0	Leo	2347	I 29	840	Spl.	185	XI*b*
3666	11 20 8	+11 47.9	Leo	2405	I 20	882	Spl.	248	....
3938	11 48 31	+44 35.4	Ursa Major	2597	I 203	1002	Spl.	249	....
4206	12 11 6	+13 30.5	Virgo	2795	II 165	....	Spl.	192	....
4216	12 11 40	+13 36.4	Virgo	2806	I 35	1148	Spl.	192	XI*c*
4222	12 12 10	+13 48.0	Virgo	2841	II 109	....	Spe.	192	....
4236	12 12 48	+69 56.0	Draco	2825	V 51	1163	Irr.	201	....
4374	12 20 52	+13 20.8	Virgo	2930	M 84	1237	Neb. spot	234	....
4387	12 21 30	+13 16.0	Virgo	2955	II 167	1250	El.	234	....

4388	12 21 35	+13 7.2	Virgo	2949-56	II 168	1244	El.	234	
4402	12 21 55	+13 34.8	Virgo	2965			El.	234	
4406	12 21 59	+13 24.3	Virgo	2961	M 86	1253	Neb. spot	234	
4407	12 22 4	+13 6.0	Virgo	2968		1255	El.	234	
4425	12 23 1	+13 11.7	Virgo	2983	II 170	1267	Spe.	234	
4449	12 24 11	+44 33.0	Canes Venatici	3002	I 213	1281	Irr.	198	VIII*b*
4564	12 32 15	+11 53.6	Virgo	3105	II 68	1356	Spe.	235, 237	
4567–8	12 32 20	+11 42.9	Virgo	3108–9	IV 8–9	1358–9	Spl.	235, 237	XI*d*
4594	12 35 40	−11 10.0	Virgo	3132	I 43	1376	Spl.	256, 262	XI*e*
4736	12 46 59	+41 34.3	Canes Venatici	3258	M 94	1456	Spl.	60, 3093P, 3094P	XII*a,b,c,d,e*
4900	12 56 28	+ 2 56.5	Virgo	3356	I 143	1509	Spl ?	188	
5005	13 7 3	+37 30.2	Canes Venatici	3437	I 96	1547	Spl.	59	
5308	13 44 15	+61 23.5	Ursa	3362	I 255	1674	Spe.	196	
5383	13 53 41	+42 14.9	Canes Venatici	3723	I 181	1717	Spl.	195, 199	XIII*a, b*
5544–5	14 13 33	+36 57.3	Boötes	3833–4	II 419	1771	Spl.	127, 261	XIII*c*
5560	14 15 54	+ 4 22.3	Virgo	3845	II 579	1778	Spl.	250	
5566	14 16 10	+ 4 19.8	Virgo	3846	I 144	1779	Spl.	250	
5569	14 16 22	+ 4 20.1	Virgo	3848			Spl.	250	
5740	14 40 21	+ 2 2.0	Virgo	3985	II 538	1872	Spl.	236	
5746	14 40 43	+ 2 18.3	Virgo	3937	I 126	1874	Spl.	236	XIII*d*
5866	15 4 12	+56 5.0	Boötes	4058	I 215	1909	Spe.	129	XIII*e*
5907	15 13 44	+56 38.0	Draco	4087	II 759	1917	Spl.	197	
6070	16 5 45	+ 0 55.7	Serpens	4164	III 553	1947	Spl.	265, 267	XIV*a*
6210	16 41 1	+23 57.2	Hercules	4234	Σ 5	1970	Plan.	139	
6217	16 36 32	+78 22.0	Ursa Minor	4236	I 280		Spl.	200	
6309	17 9 24	−12 48.9	Ophiuchus	5851			Plan.	252, 263	VII*a*
6412	17 32 4	+75 46.6	Draco	4321	VI 41		Spl.	128	
6478	17 46 41	+51 11.6	Draco		SW III		Spl.	135	
6543	17 58 35	+66 38.2	Draco	4373	IV 37		Plan.	9, 10, 11, 20, 34, 238	VII*b*
6555	18 3 28	+17 35.3	Hercules	4383	II 902		Spl.	268	XIV*b*
6702	18 44 33	+45 36.7	Lyra	5931			Neb. spot	269, 270	
6703	18 44 55	+45 27.5	Lyra	5932			Plan. ?	269, 270	
6804	19 27 37	+ 9 2.9	Aquila	4499	VI 38	2043	Plan.	120	
6818	19 39 17	−14 21.1	Sagittarius	4510	VI 51	2047	Plan.	115, 116, 137	VII*c*
6826	19 42 34	+50 19.4	Cygnus	4514	IV 73	2050	Plan.	130, 131, 132	
6894	20 13 3	+30 18.6	Cygnus	4565	IV 13	2072	Plan.	4, 7	
6905	20 18 42	+19 50.3	Delphinus	4572	IV 16	2075	Plan.	145, 147, 149	
7008	20 58 8	+54 13.5	Cepheus	4627	I 192	2099	Irr.	243	VII*d*
7009	20 59 39	−11 41.6	Aquarius	4628	IV 1	2098	Plan.	138, 140	VII*e*
7023	21 0 35	+67 50.3	Draco	4634	IV 74		Irr.	12	
7026	21 3 30	+47 30.8	Cygnus		Burnham		Plan.	156	
7027	21 3 56	+41 54.0	Cygnus		Webb		Plan.	142	
7129	21 41 4	+65 43.3	Cepheus	4702	IV 75	2131	Irr.	273, 274	
7177	21 56 44	+17 20.4	Pegasus	4734	II 247	2139	Spl.	126	
7217	22 4 10	+30 57.2	Pegasus	4760	II 207	2149	Spl.	216	XIV*c*
7662	23 21 54	+42 4.8	Andromeda	4964	IV 18	2241	Plan.	29, 148, 157, 172, 173, 177	VII*f*

NOTES

N.G.C. 2825–2829, 2831, 2832, 2834, 2839, see text description of N.G.C. 2830.
N.G.C. 4206, 4222, see text description of N.G.C. 4216.
N.G.C. 4374, 4387, 4388, 4402, 4407, 4425, see text description of N.G.C. 4406.
N.G.C. 4564, see text description of N.G.C. 4567–8.
N.G.C. 5566, 5569, see text description of N.G.C. 5560.
N.G.C. 5740, see text description of N.G.C. 5746.
N.G.C. 6702, see text description of N.G.C. 6703.

fading suddenly to a very much less intensity, thus forming a bright center irregularly round, $50''$ in diameter. One arm, however, is interrupted, but again continues strong and forms a wing to the bright patch on the northern side. Along these arms lie many bright nebulous knots and condensations. Outside this the arms continue faint, and they fade out at $85''$ diameter. The nucleus is irregular and appears to be a number of knots bunched together, each forming the starting-point of an arm.

N.G.C. 650–651 Persei

$\alpha=1^h37^m4^s$, $\delta=+51°9'$ (1917); $\lambda=99°$, $\beta=-11°$
Plate No. 57, 1912, February 19, 105^m. Poor plate
Plate No. 150, 1912, October 7, 180^m. Poor plate
Plate No. 151, 1912, October 8, 360^m. Poor plate
Plate No. 170, 1912, December 6, 15^m. Poor plate

The shape of this gaseous nebula reminds one of a moth; a strong, irregular, elliptical mass with diaphanous extension on either side. The body is about $1'.6\times 1'$, $p=41°$, with wings extending about $1'$ either side. The whole forms the central zone of a circle of $3'$ diameter, the wing periphery being tangent to the circle. On the E side a faint wisp extends beyond this; at the center of the circle lies a faint star. The brightest spot in the nebula, forming the S*p* portion, is N.G.C. 650; N.G.C. 651 is the N*f* portion. The spectrum of the nebula shows bright lines.[1]

N.G.C. 895 Cetus

$\alpha=2^h17^m29^s$, $\delta=-5°54'.3$ (1917); $\lambda=140°$, $\beta=-58°$
Plate No. 281, 1916, November 28, 75^m. Weak exposure

This is a right-handed spiral $3'.5\times 2'$, $p=120°$. Two prominent arms emerge from the faint nucleus, one of which, as is often the case, is interrupted only to fork out into two branches. This, however, may be merely an effect of contrast caused by an overlapping streamer. Quite away from the nucleus the arms are apparently strings of knotted nebulosity. N.G.C. 894 blends with the spiral.

---

[1] *Astrophysical Journal*, 33, 59, 1911.

N.G.C. 955 Cetus

$\alpha=2^h26^m20^s$, $\delta=-1°28'.6$ (1917); $\lambda=138°$, $\beta=-54°$
Plate No. 229, 1913, November 25, 90^m. Images elongated

This is a spindle nebula, almost certainly spiral, about $80''\times 7''$, $p=20°$, with a stellar nucleus W of the center. At one time it was thought to be variable, but Dreyer has doubted this. The strong part of the nebula forms a rhombus $45''\times 7''$.

N.G.C. 972 Aries

$\alpha=2^h29^m20^s$, $\delta=+28°56'.9$ (1917); $\lambda=116°$, $\beta=-28°$
Plate No. 231, 1913, November 26, 195^m. Good plate
Illustrated Plate IX*e*

This object has the shape of an irregular ellipse of greatly varying intensity, about $2'\times 1'.9$, $p=152°$, almost certainly a left-handed spiral. The strong region E of the major axis is somewhat elliptical in shape, $40''\times 15''$, with its axis parallel to the general figure of the nebula. Its detail is knotted and full of contrast, with a very strong knot at the N end. W of the major axis, except for the knots described below, the nebulosity consists of large softer wisps mingled with dark lanes. At 28″ N*p* the nucleus is a strong triple condensation and at 26″ S*f* the nucleus is a strong knot, both lying on the major axis. There are two more condensations beyond the N one, both surrounded by a dark ring except for a wisp on the rear side as met traveling along the arm from the center and a fine strong thread on the front side.

N.G.C. 1023 Perseus

$\alpha=2^h35^m12^s$, $\delta=+38°42'.5$ (1917); $\lambda=112°$, $\beta=-18°$
Plate No. 171, 1915, December 7, 240^m. Bad seeing

A bright nucleus 15″ in diameter lies on an ellipse $90''\times 45''$, $p=70°$. From this extend faint wings in either direction along the major axis, forming an ellipse $5'\times 1'$, $p=85°$.

Fath[1] found for the nebula a spectrum of the solar type, and Slipher's[2] value of radial velocity is roughly +200 km.

---

[1] *Ibid.*, **37**, 199, 1913.

[2] *Popular Astronomy*, **23**, 36, 1915.

N.G.C. 1068 Cetus

$\alpha=2^h 38^m 26^s$, $\delta=-0°21'.9$ (1917); $\lambda=141°$, $\beta=-51°$
Plate No. 49, 1911, December 22, 120^m. Illustrated Plate IX*d*
Plate No. 53, 1911, December 25, 22^m. Illustrated Plate IX*c*
Good plates

This left-handed spiral is viewed in plan, with three striking gradations of intensity centrally superimposed. Surrounding the bright central nucleus, elongated in $p=40°$, is a strong, distinct spiral forming an ellipse $40''\times 25''$, $p=50°$, consisting mainly of two arms emanating from the ends of the nucleus, which extend a little more than a half-revolution. Distinct nebulous condensations lie along these arms. Outside this strong center is a fainter annulus $130''\times 110''$, $p=10°$, still holding the spiral form. Two of the arms are continuations of the central branches, but there are others besides, all softly mottled in appearance. Beyond this lie two immense and very faint arms, starting at about $p=30°$, and extending to an ellipse $6'\times 5'$, $p=60°$. These are so faint that it is difficult to say more than that they appear mottled. On the plate showing this external faint material the entire central spiral form is so overexposed that no detail shows. The spectrum[1] obtained with the focal-plane slit gives a value for the radial velocity of +765 km, while Slipher's[2] value is +1100 km. Fath[3] found an absorption spectrum with bright lines.

N.G.C. 1186 Perseus

$\alpha=3^h 0^m 4^s$, $\delta=+42°30'.2$ (1917); $\lambda=115°$, $\beta=-13°$
Plate No. 244, 1914, November 13, 75^m. Good plate
Plate No. 245, 1914, November 14, 130^m. Good plate, grain a little coarse

This supposedly variable nebula lies 2° north of Algol. It is a faint left-handed spiral $2'\times 0'.5$, $p=120°$, with faint stellar nucleus. A star several magnitudes brighter than the nucleus lies directly on one of the arms at $p=230°$, $12''$. There is a knot N of the nucleus at $p=330°$, $12''$. There are 15 faint nebulae lying within a radius of $15'$.

---

[1] *Publications of the Astronomical Society of the Pacific*, **27**, 134 and 192, 1915.

[2] *Popular Astronomy*, **23**, 36, 1915.

[3] *Astrophysical Journal*, **33**, 60, 1911.

N.G.C. 1501 Camelopardus

$\alpha=3^h59^m50^s$, $\delta=+60°41'.9$ (1917); $\lambda=112°$, $\beta=+7°$

Plate No. 174, 1912, December 10, 60^m

Plate No. 178, 1913, January 7, 120^m. Illustrated Plate VI*a*

Good plates

This is a fine planetary of regular elliptical shape, $60''\times45''$, $p=120°$, with protuberances at each end of the minor axis, making the total breadth $53''$. The nebula is irregularly mottled, bearing a resemblance to the convolutions of the brain. Its periphery is in general denser than its center, and is twice as dense at the ends of the minor axis as at the extremities of the major axis. There is a bright central stellar nucleus. The spectrum shows bright lines.

N.G.C. 1535 Eridanus

$\alpha=4^h10^m23^s$, $\delta=-12°56'.9$ (1917); $\lambda=174°$, $\beta=-39°$

Plate No. 163, 1912, November 5, 60^m. 100-foot focus

Plate No. 182, 1913, February 4, 85^m. 25-foot focus. Illustrated Plate VI*b*

This is a planetary of almost uniform intensity $46''\times40''$, $p=23°$, on which lie a strong ring, a strong stellar nucleus, and a faint star. The ring is irregularly round, $18''$ in diameter, elongated in the same direction as the disk, quite sharp on the outer edge, but softer on the inner edge, with branches running to the nucleus. The star is at $p=320°$, $17''$. The spectrum shows bright lines; Keeler's[1] value of the radial velocity is -10.4 km.

N.G.C. 1579 Perseus

$\alpha=4^h24^m46^s$, $\delta=+35°6'.0$ (1917); $\lambda=133°$, $\beta=-8°$

Plate No. 227, 1913, October 29, 30, 31, 420^m. Illustrated Plate VIII*a*

This is an irregular nebula of the dispersive type; the dark lanes call to mind the Trifid nebula, and the outer faint nebulosity, that of the Orion nebula. The most prominent bit of nebulosity is a broad arrowhead adjoining the principal dark lane on the N and pointing due E; it is mottled in appearance and full of detail. Directly S of the arrowhead in the dark lane is a very faint star.

---

[1] W. W. Campbell, *Stellar Motions*, p. 210.

The principal part of the nebula lies within a circle of 5′ diameter, while faint patches extend N*p* to a distance of 10′ from the center. There are four stars which form nuclei for patches of nebulosity. Their positions with respect to the faint central star are as follows:

a.....	35° $12'.8$	10	mag. (very rough)
b.....	213° 6.5	11	mag.
c.....	251° 10.0	11	mag.
B.D.+34°883.....	346° 3.1	9.5	mag.

N.G.C. 1931 Auriga

$\alpha=5^h25^m55^s$, $\delta=+34^\circ11'.0$ (1917); $\lambda=143^\circ$, $\beta=+1^\circ$

Plate No. 277, 1916, October 27, 15^m
Plate No. 278, 1916, October 28, 60^m

This group of small stars, one of which is double, is here apparently superimposed upon an irregular, patchy, nebulous mass contained within a circle $1'.5$ in diameter. Several loops appear in the nebulosity, and there are two prominent dark spots. At $3'.7$ S of the nebula lies another star with a nebulous wing to the SW. The region is rich in stars, though the nebula lies in one of the so-called dark lanes, where the stars are much fewer than in the adjacent parts.

N.G.C. 2022 Orion

$\alpha=5^h37^m33^s$, $\delta=+9^\circ2'.7$ (1917); $\lambda=164^\circ$, $\beta=-9^\circ$

Plate No. 183, 1913, February 4, 60^m. Good plate. Illustrated Plate VI*c*

This is a fairly bright planetary with a disk of almost uniform intensity, on which lies a ring and nucleus. The nebula is sharply outlined, and may best be described as the central zone of a circle 30″ in diameter; equator lies in $p=115^\circ$, the distance between the sides being 27″; the S side is a little convex outward. The ring is very much stronger in intensity than the disk. It is elliptical, $20''\times15''$, $p=13^\circ$ (median line), and on the average about 4″ wide. There is a condensation in the ring at each end of the axis in $p=30^\circ$, making the axis 23″ long. There is an interruption in the N side of the ring and a wisp running toward the nucleus from the S knot. The spectrum shows bright lines.

N.G.C. 2366 Camelopardus

$\alpha=7^h20^m7^s$, $\delta=+69°11'.5$ (1917); $\lambda=113°$, $\beta=+29°$

Plate No. 279, 1916, October 30, 60^m. Very weak

This is the same general character as N.G.C. 4449, composed of nebulous knots and soft nebulosity. Very irregular in shape, 3′×1′, $p=30°$, with the brightest star or knot near the S end; 1′ E of this star lies a group irregularly 30″ in diameter.

N.G.C. 2371–2 Gemini

$\alpha=7^h20^m20^s$, $\delta=+29°39'.1$ (1917); $\lambda=157°$, $\beta=+21°$

Plate No. 257, 1916, March 6–7, 221^m. Bad seeing. Images large
Illustrated Plate VI*d*

This gaseous nebula comprises an irregularly round, patchy mass of nebulosity lying within 33″ radius of a stellar nucleus; two wisps on opposite ends of an axis in $p=120°$, each 1′ distant from the nucleus. The striking parts of the nebula are two strong condensations in the central part, diametrically opposite each other on an axis in $p=60°$, each about 15″ in size and 15″ from the nucleus. In the *f* condensation is a faint star, and on the W edge of the *p* one a hazy nucleus. Faint wisps extend from the central mass to points halfway between the nucleus and the outer condensations, the W ones forming a loop, a feature seen also in N.G.C. 7026. Each of the outer wisps is 10″×45″ and lies perpendicular to the line joining them, being slightly convex outward with streamers turned inward.

N.G.C. 2392 Gemini

$\alpha=7^h24^m16^s$, $\delta=+21°5'.0$ (1917); $\lambda=165°$, $\beta=+19°$

Plate No. 187, 1913, March 6, 180^m. 25-foot focus
Plate No. 189, 1913, March 7, 10^m. 25-foot focus
Plate No. 190, 1913, March 7, 30^m. 25-foot focus
Plate No. 191, 1913, March 7, 60^m. 25-foot focus
Plate No. 255, 1915, December 8–9, 120^m. 80-foot focus
Illustrated Plate I*e*, and I*f*
Plate No. 258, 1916, April 1, 30^m. 25-foot focus

This bright planetary can best be described as the pupil of an eye with the surrounding iris. The iris varies only a few seconds from a mean outside diameter of 46″ and consists of a uniform annulus with about 20 bright knots non-uniformly distributed along its median line. The knots are sharply bounded on the side toward the pupil and stringy toward the outside. There are several interruptions in the string of knots, notably at $p=144°$, where two lie diametrically opposite. The brighter knots are on the S side along $p=189°$, where four or five of them form an almost continuous mass. Opposite these is another continuous set, but not so bright. Between the ends of these two series the knots stand more apart. W of the "pupil," between it and the ring of knots, is an elongated condensation lying in a NS position. A 3^h exposure does not extend the disk any, but 3 threads spring from as many knots of the iris on the E side and curve out over the edge of the disk a distance of $5''$. The pupil is stirrup-shaped, $19''\times 17''$, with axis $p=5°$, and has a strong central nucleus. The N periphery is bright; the E has two bright knots, the W two, and the S one that reaches almost to the nucleus, and halfway between the nucleus and the N side is another; between this latter and the N side is a vacant space. The nucleus is listed as B.D. $+21°$ 1609, $9^{\mathrm{M}}\!.1$. A focal-plane spectrum shows a continuous band crossed by projecting bright lines. Campbell and Moore[1] found internal motion in the nebula. Both illustrations are from the same negative, the one to show central detail, the other the external ring.

N.G.C. 2403 Camelopardus

$\alpha=7^h28^m49^s$, $\delta=+65°46'\!.9$ (1917); $\lambda=118°$, $\beta=+30°$

Plate No. 169, 1912, November 8, 210^m. Good plate. Illustrated Plate X*c*

This fine right-handed spiral nebula resembles M 33. The bright part is contained within an ellipse roughly $9'\times 5'$, $p=126°$. Faint knots and arms extend as far as $10'$ from the center. It does not possess the wealth of detail of M 33, but it has the same sharp stellar images, the nebulous stars, the bunching of these into knots, and the dark streaks where one can imagine one looks completely through the nebula to the sky beyond. While M 33 has two strong arms running out from the center, this nebula has but one, which starts from the central mass at the S*p* side, the opposite side being a continuous sheet of nebulosity, not separable into arms. There is no distinct central nucleus.

---

[1] *Publications of the Astronomical Society of the Pacific*, **28**, 119, 1916.

N.G.C. 2681 Ursa Major

$\alpha = 8^h 47^m 36^s$, $\delta = +51^\circ 37'.7$ (1917); $\lambda = 134^\circ$, $\beta = +41^\circ$

Plate No. 179, 1913, January 7, 190^m. Good plate. Illustrated Plate IX*f*

This right-handed spiral is seen in plan. There is a strong central nucleus out of which springs at $p = 35^\circ$ a single arm which wraps itself concentrically around the nucleus at a mean radius of 20″ and stops in the NE quadrant. It is possible that this arm is really continued inward in the ring of nebulosity which entirely surrounds the nucleus at a mean radius of 8″. In the SW quadrant of this ring, however, are two strong condensations, which appear as if they might be very short arms, and a third fine wisp that starts at $p = 185^\circ$ and runs into the outer arm. Traces of the W half of a ring of 40″ radius appear with ends forming elongated knots at $p = 25^\circ$ and 205°, and at a mean radius of $1'.25$ is an almost continuous faint broad ring. A long exposure is necessary to determine whether the two outer rings really form part of the spiral arms. Five small faint nebulae appear on the plate.

N.G.C. 2830 Lynx

$\alpha = 9^h 14^m 44^s$, $\delta = +34^\circ 6'.0$ (1917); $\lambda = 158^\circ$, $\beta = +46^\circ$

Plate No. 246, 1914, November 15, 150^m
Plate No. 247, 1914, November 16, 60^m

This is a spindle nebula 50″×6″, $p = 106^\circ$, with faint stellar nucleus.

The ends of the nebula bend counter-clockwise, giving it a resemblance to the integral sign. The traces of detail show that it is almost certainly a spiral.

On this photograph 36′×36′ are 28 nebulous spots or stars, 6 spindles with nucleus, and 3 without; among them are the following:

N.G.C. 2825—A spindle about 40″×4″, $p = 83^\circ$, of about the same intensity as N.G.C. 2830. It has a stronger nucleus than N.G.C. 2830 and a knot N*f* the nucleus.

N.G.C. 2826—A rhombus about 1′×6″, $p = 143^\circ$, with nucleus and nebulosity much stronger than N.G.C. 2830.

N.G.C. 2827—Faint nucleus in elongated nebulosity in $p=8°$.
N.G.C. 2828—Nebulous star in very faint elongated nebulosity $p=45°$.
N.G.C. 2829—Nebulous star.
N.G.C. 2831—Nebulous star.
N.G.C. 2832—Strong nucleus surrounded by strong nebulosity that fades rapidly to about 14″ diameter, then gradually to 30″ diameter. The whole is elongated, $p=150°$.
N.G.C. 2834—Nebulous star.
N.G.C. 2839—Nebulous star.

N.G.C. 2841 Ursa Major

$\alpha=9^h16^m18^s$, $\delta=+51°19'.7$ (1917); $\lambda=135°$, $\beta=+45°$

Plate No. 58, 1912, February 19, 120^m. Good plate. Illustrated Plate X*a*

This is a fine left-handed spiral nebula $6'.5\times2'.2$, $p=150°$. The strong nucleus lies in an almost uniform glow of nebulosity, but the fine sweeping arms are streamers of nebulous knots. This nebula shows very nicely the difference in the nebulosity on the two sides of the major axis. The W side is softened and permeated with a glow, lacking in the E side, which is of marked contrast. In a field $36'\times36'$, 16 faint nebulae appear.

N.G.C. 2976 Ursa Major

$\alpha=9^h40^m24^s$, $\delta=+68°17'.9$ (1917); $\lambda=111°$, $\beta=+42°$

Plate No. 175, 1912, December 10, 180^m. Good negative
Illustrated Plate X*b*

This bright elliptical nebula $3'.2\times1'$, $p=142°$, is full of condensations and dark lanes, with faint extensions 25″–30″ at each end. The arrangement of some of the patches and dark lanes gives it somewhat the appearance of a spiral, but one cannot be certain. There is no nucleus, but at the center are three bright stellar knots and a fourth elongated knot. There are 11 more of these knots scattered about the nebula, together with many that range from small nebulous spots to areas barely distinguishable from the general nebulosity.

N.G.C. 3115 Sextans

$\alpha=10^h1^m6^s$, $\delta=-7°18'.9$ (1917); $\lambda=216°$, $\beta=+38°$

Plate No. 56, 1911, December 25, 100^m. Good plate. Illustrated Plate XI*a*

This is a bright spindle with an oblate center, which measures about $30''\times25''$. The disk lies in $p=45°$, is about 6″ wide, and strong and continuous for about 45″ either side of the nucleus; then come several interruptions and knots. The whole lies within an elliptical halo of nebulosity 3′×1′. Slipher's[1] value for the radial velocity is roughly +400 km.

N.G.C. 3593 Leo

$\alpha = 11^h 10^m 17^s$, $\delta = +13°16'.0$ (1917); $\lambda = 210°$, $\beta = +64°$

Plate No. 185, 1913, March 5, 210^m. Good plate. Illustrated Plate XI*b*

This nebula has more or less of the spiral characteristics, but it cannot be said for certain that it is a spiral. On a faint patchy elliptical ground of nebulosity 4′.5×1′, $p = 89°$, lies centrally a bright patch 60″×13″. The E 15″ of this ellipse is not much brighter than the fainter nebulosity; the W end is crossed by two straight dark lanes, the one nearest the center running in $p = 39°$ to 219°, the other in $p = 178°$ to 358°, thus forming two isolated bright spots. At the E end of the bright central part are two stellar condensations. At the E end of the faint nebulosity there are a number of dark wisps or tongues curved left-handed. An irregular dark lane runs N of the bright center almost the length of the major axis.

N.G.C. 3666 Leo

$\alpha = 11^h 20^m 8^s$, $\delta = +11°47'.9$ (1917); $\lambda = 215°$, $\beta = +66°$

Plate No. 248, 1915, February 12, 150^m. Weak plate

This is a faint left-handed spiral 3′.5×0′.7, $p = 100°$, the central part 80″×20″ being brighter, and having a number of nebulous knots scattered through it, the brightest of which is the nucleus. At one time it was suspected of variability, but Dreyer's conclusions are opposed to this.

N.G.C. 3938 Ursa Major

$\alpha = 11^h 48^m 31^s$, $\delta = +44°35'.4$ (1917); $\lambda = 118°$, $\beta = +70°$

Plate No. 249, 1915, March 12, 39^m. Poor plate

The photograph is a very weak exposure, but sufficient to show a right-handed open spiral 4′ in diameter, having a small bright nucleus and resembling M 74 or M 101, with most of the material in the well-separated arms.

---

[1] *Popular Astronomy*, **23**, 36, 1915.

N.G.C. 4216 Virgo

$\alpha=12^{h}11^{m}40^{s}$, $\delta=+13^{\circ}36'.4$ (1917); $\lambda=243^{\circ}$, $\beta=+73^{\circ}$
Plate No. 192, 1913, March 7, 90^{m}. Illustrated Plate XI*c*
Good plate, but needs longer exposure

This is a left-handed spiral $6'\times 1'$, $p=21^{\circ}$. The nucleus and the arm starting from it are bright; there is a condensation 1′ N of the nucleus. The *p* side is soft, while the *f* side shows the marked contrast usual in inclined nebulae. There are many nebulous spots scattered over the plate and 10′ *p*, 2′ N of the nucleus of 4216 lies a left-handed nebula about 30″ diameter. The two following nebulae also appear on the plate:

N.G.C. 4206—Faint spiral, $4'\times 30''$, $p=1^{\circ}$.
N.G.C. 4222—Faint spindle, $2'.5\times 10''$, $p=59^{\circ}$.

N.G.C. 4236 Draco

$\alpha=12^{h}12^{m}48^{s}$, $\delta=+69^{\circ}56'.0$ (1917); $\lambda=95^{\circ}$, $\beta=+47^{\circ}$
Plate No. 201, 1913, May 7, 180^{m}. Poor plate

This nebulosity lies S*p* the variable star SW Draconis. It is an irregular cloud of nebulous stars and nebulous haze roughly scattered about a region $15'\times 4'$, $p=160^{\circ}$. The strongest parts are a mixed group in the N*p* corner and a wisp extending from the N end a little to the E of southward for about 7′.

N.G.C. 4406 Virgo

$\alpha=12^{h}21^{m}59^{s}$, $\delta=+13^{\circ}24'.3$ (1917); $\lambda=251^{\circ}$, $\beta=+75^{\circ}$
Plate No. 234, 1914, March 18, 90^{m}

The photograph shows a nebulous spot, having a bright nucleus, gradually decreasing in brightness until it fades away at a mean radius of 35″. It is slightly elongated in $p=130^{\circ}$. Besides a number of faint nebulae and spots the following nebulae appear:

N.G.C. 4374—Practically the same type and size as N.G.C. 4406. The nucleus is possibly a little larger, but the nebula lies near the edge of the plate.

N.G.C. 4387—Of the same type as N.G.C. 4406, $40''\times 15''$. Elongated in $p=140^{\circ}$.

N.G.C. 4388—An elliptical nebula $3'.5\times 30''$, $p=90^{\circ}$, lying near the S edge of the plate. A bright T-shaped knot, base to the N, cuts across the center, with a dark spot on either side. A second bright elongated knot lies just W of the base of the ᴛ. Probably spiral.

N.G.C. 4402—A faint elongated nebula $3' \times 35''$, $p=89°$, dark elongated central space, bright periphery, soft outside and indented inside; probably spiral.

N.G.C. 4407—An elongated nebulous spot lying near the S edge of the plate, $20'' \times 8''$, $p=10°$.

N.G.C. 4425—A spindle consisting of nucleus 8″ diameter in uniform nebulosity about $90'' \times 22''$, $p=30°$.

N.G.C. 4449 Canes Venatici

$\alpha=12^h24^m11^s$, $\delta=+44°33'.0$ (1917); $\lambda=96°$, $\beta=+72°$

Plate No. 198, 1913, April 7, 300^m. Illustrated Plate VIII*b*

This is an irregular nebulous mass in which many nebulous stars are distributed unevenly. The greater part of the nebula is roughly rectangular, about $4'.5 \times 2'.5$, $p=40°$, there being an assemblage of some dozen nebulous stars W of the SW corner. On the original negative there are 230 nebulous stars or patches, about 40 appearing bright and 190 faint, though the gradation is very uniform. Two-thirds of them are in the N half. The nebulosity proper is weak toward the edge, gradually increases inward, and culminates along a central ridge, where it is as strong as the stars themselves. A number of dark irregular rifts appear here and there in it. Wolf[1] found an absorption spectrum similar to that of the Andromeda nebula, with possible bright lines.

N.G.C. 4567–8 Virgo

$\alpha=12^h32^m20^s$, $\delta=+11°42'.9$ (1917); $\lambda=264°$, $\beta=+73°$

Plate No. 235, 1914, March 19–20, 180^m

Plate No. 237, 1914, April 24, May 19, 360^m. Illustrated Plate XI*d*

The plate shows two fine overlapping spirals; one, N.G.C. 4567, seen more nearly in plan than N.G.C. 4568.

N.G.C. 4567 is a right-handed spiral $2' \times 1'.5$, $p=75°$, having a small bright nucleus and two arms consisting chiefly of nebulous stars. The nebulosity is weak and irregular in intensity with a number of dark lanes, notably one following the concave side of the p arm. There is evidence of much disturbance in the nebula, as the W arm is broken off and forked and the E arm offset.

---

[1] *Sitzungsberichte der Heidelberger Akad.*, August 26, 1912.

N.G.C 4568 is a right-handed spiral $4'\times 1'.5$, $p=29^\circ$, having a small nucleus which is fainter than that of N.G.C. 4567. It is hard to trace the arms distinctly about the nucleus, as the nebulous knots are irregularly placed. At their extremities the arms are much broken, especially on the N side, which is crossed with several great rifts; there is no question, however, as to the general trend. The dark rift at the apparent contact line of the two nebulae may really belong to N.G.C. 4568, which apparently lies beyond N.G.C. 4567.

N.G.C. 4564 appears on the plate as a spindle $90''\times 20''$, $p=49^\circ$, with strong nebulous nucleus, $15''$ diameter. There are 6 or more very small faint nebulous spots or spindle nebulae on the plate.

N.G.C. 4594 Virgo

$\alpha=12^h35^m40^s$, $\delta=-11^\circ10'$ (1917); $\lambda=269^\circ$, $\beta=+52^\circ$

Plate No. 256, 1916, February 12, 55^m
Plate No. 259, 1916, April 6, 120^m
Plate No. 262, 1916, May 3, 132^m. Illustrated Plate XI*e*
Plate No. 264, 1916, May 26, 90^m. Seed 27 bathed Wallace 3 dye. Red screen

This fine spiral nebula, $7'\times 1'$, $p=89^\circ$, is seen almost edge-on, the convolutions being so nearly concentric that it is not possible to state whether it is right- or left-handed. It is crossed by a dark streak which lies at the periphery, being possibly an outer ring of cooler material, or perhaps the unilluminated edge of the thin disk of nebulous matter surrounding the brilliant nucleus. The streak is $9''$ wide except near the ends, where it gradually broadens to twice this width. A trace of nebulosity runs almost centrally along the dark streak. A strong halo $2'$ in diameter surrounds the nucleus, and the first ring is much stronger than the surrounding ones. A test for possible differences in temperature, by exposures made on a Seed 23 plate and on a red-sensitive plate with a screen transmitting λ 5650–7600, showed no certain difference.

An 80-hour exposure with the focal-plane spectrograph, the slit parallel to the major axis and across the nucleus, showed that: (*a*) the spectrum is F5; (*b*) the velocity-curve is sensibly linear, $V=-278x+1180$, the radial velocity accordingly being 1180 km and the rotation, at a distance of 2′, 330 km, the W side approaching and the E side receding from the observer.

N.G.C. 4736 Canes Venatici

$\alpha = 12^h46^m59^s$, $\delta = +41^\circ 34'.3$ (1917); $\lambda = 85^\circ$, $\beta = +76^\circ$

Plate No. 60, 1912, February 20, 225^m. Illustrated Plate XII*e*
Plate No. 3093P, 1916, May 8, 5^m. Illustrated Plate XII*b*
Plate No. 3093P, 1916, May 8, 10^m. Illustrated Plate XII*a*
Plate No. 3094P, 1916, May 8, 20^m. Illustrated Plate XII*d*
Plate No. 3094P, 1916, May 8, 40^m. Illustrated Plate XII*c*

This fine right-handed spiral has three regions of very marked difference in brightness. From a very bright, sharp stellar nucleus spring branches of smooth nebulosity, which after a turn about the nucleus break into a series of nebulous knots forming the periphery of an ellipse $2' \times 1'.5$, $p = 126^\circ$. Here the intensity suddenly diminishes while the arms continue in fine sweeping curves of faint smooth nebulosity, devoid of knots save for two or three small patches, to such an extent as to fill an ellipse $5' \times 4'$, $p = 105^\circ$. The nebulosity for a distance of 30″ diameter around the nucleus is very strong. Plates 3093–4 P, taken by Mr. Seares, show the central parts well. The nebula has a solar-type spectrum,[1] with possible Wolf-Rayet bands. Its radial velocity[2] is roughly +200 km.

N.G.C. 4900 Virgo

$\alpha = 12^h50^m28^s$, $\delta = +2^\circ 56'.5$ (1917); $\lambda = 280^\circ$, $\beta = +66^\circ$

Plate No. 188, 1915, March 5, 210^m. Elongated images

The type of this interesting nebula cannot definitely be stated, though the lines are such as are followed by a left-handed spiral. It is irregularly round, 1′.5 in diameter, patchy in appearance, with a number of nebulous stars, a single row around the N rim and a double row on the S side. There is a faint central stellar nucleus crossed by a bright patch of nebulosity $15'' \times 6''$, $p = 145^\circ$. A star much brighter than the nucleus lies on the S*f* point of the rim.

---

[1] *Astrophysical Journal*, **37**, 199–200, 1913.

[2] *Popular Astronomy*, **23**, 36, 1915.

N.G.C. 5005 Canes Venatici

$\alpha=13^h7^m3^s$, $\delta=+37^\circ30'.2$ (1917); $\lambda=64^\circ$, $\beta=+78^\circ$
Plate No. 59, 1912, February 19, 50^m

This left-handed spiral $3'.5\times 1'.3$, $p=69^\circ$, has a stellar nucleus surrounded by strong nebulosity which gradually fades toward the edge. The N half shows contrast, and the S half is smooth.

N.G.C. 5308 Ursa Major

$\alpha=13^h44^m15^s$, $\delta=+61^\circ23'.5$ (1917); $\lambda=76^\circ$, $\beta=+55^\circ$
Plate No. 196, 1913, April 4, 180^m. Good plate

This is a spindle with oblate center $2'\times 0'.25$, $p=60^\circ$, having almost no detail. On either side of the bright nucleus the major axis appears as a bright line, gradually fading toward the rim and apparently interrupted at the nucleus on the *p* side. Several nebulous spots appear on the plate.

N.G.C. 5383 Canes Venatici

$\alpha=13^h53^m41^s$, $\delta=+42^\circ14'.9$ (1917); $\lambda=48^\circ$, $\beta=+69^\circ$
Plate No. 195, 1913, April 3, 180^m. Images elongated. Illustrated Plate XIII*b*
Plate No. 199, 1913, May 5, 6, 360^m. Good plate. Illustrated Plate XIII*a*

This right-handed spiral resembles a pinwheel lying about a very bright multiple nucleus within a circle $2'.25$ diameter. Some disturbance has altered the regularity of distribution of the typical form. On the *f* side much of the nebulosity has been swept into a broad band running in a SE direction to a row of bright nebulous knots lying along the rim at right angles to it; enough nebulosity remains, however, to show the spiral form. In the *p* arm there are no traces of the spiral form, everything being swept into a broad band running in a NW direction from the nucleus for some distance, when it suddenly turns counter-clockwise in a bright ridge diametrically opposite and similar to that of the E arm. A dark streak runs from between the central and S parts of the nucleus and separates the *p* band into two arms; opposite this another dark interrupted streak emanating from between the central and the N members of the nucleus runs E and S, following the line of the spiral. The nucleus consists of 3 almost parallel bright condensations $15''$ to $20''$

long, elongated in *p*=100°, their central lines separated about 6″.5, the northernmost slightly *f*, and the southernmost *p* the central one. A dark streak cuts across the three members of the nucleus, running almost due NS.

S of N.G.C. 5383, 3′.25, lies a faint S-shaped left-handed spiral about 1′ in diameter.

N.G.C. 5544–5 Boötes

$\alpha=14^{h}13^{m}33^{s}$, $\delta=+36°57'.3$ (1917); $\lambda=32°$, $\beta=+68°$

Plate No. 127, 1912, June 13, 180^{m}

Plate No. 261, 1916, May 1, 2, 3, 4, 5, 360^{m}. Illustrated Plate XIII*c*

Good negatives

These are two overlapping spirals, the E one in plan, the W one very much inclined to the line of sight.

N.G.C. 5544 is a left-handed spiral 70″×15″, *p*=60°, its *f* end just tangent to the NW point of the nucleus of N.G.C. 5545. The nucleus is faint and stellar. The arms are about equal in intensity where they start from the nucleus, but that on the E side continues bright for a much greater distance, being interrupted, however, at several points.

N.G.C. 5545 consists of a bright stellar nucleus, a nebulous ring 28″ outside diameter, a fainter diametral streak crossing the nucleus in *p*=130°, and another ring about the same intensity as the inner one, irregularly round, 45″ outside diameter, both being slightly elongated *p*=120°.

In N.G.C. 5545 the nebulosity is entirely soft; in N.G.C. 5544 several knots and condensations appear.

N.G.C. 5560 Virgo

$\alpha=14^{h}15^{m}54^{s}$, $\delta=+4°22'.3$ (1917); $\lambda=318°$, $\beta=+57°$

Plate No. 250, 1915, April 11, 200^{m}

This right-handed spiral is very much inclined to the line of sight. It has a weak nucleus, several knots in nebulosity near the nucleus, and two arms that make a half-revolution, then sweep outward very rapidly and fade away. It is 3′×0′.3, *p*=105°.

N.G.C. 5566 is a right-handed spiral, with a bright nucleus, 18″×8″, *p*=30°. Surrounding the nucleus is faint nebulosity from which the arms emerge. More exposure is needed to bring out the arms well, but they sweep outward so as practically to fill an ellipse $6' \times 1'.5$, $p=32^\circ$. An elliptical ring of nebulosity $90'' \times 45''$, $p=20^\circ$, gives the appearance of overlapping arms.

N.G.C. 5569 is a faint right-handed spiral in plan.

N.G.C. 5746 Virgo

$\alpha=14^h40^m43^s$, $\delta=+2^\circ18'.3$ (1917); $\lambda=323^\circ$, $\beta=+52^\circ$
Plate No. 236, 1914, March 20, 21, 22, 360^m. Good plate
Illustrated Plate XIII*d*

This fine right-handed spiral is seen almost edge-on, having the characteristic oblate center surrounding the bright nucleus. It is crossed by a dark streak parallel to the major axis; nebulosity full of contrast occurs on the W side, the E side being smooth. The spiral form measures $7'.5 \times 0'.75$, $p=170^\circ$, and the oblate halo projects to a semi-minor axis of $30''$.

N.G.C. 5740 lies near the S edge of the plate. It is a left-handed spiral $3' \times 1'.25$, $p=160^\circ$, with bright nucleus, and arms gradually weakening toward the edge. An asteroid trail appears (March 20) $p=234^\circ$, $19'$, S*p* the nucleus, the trail lying in $p=158^\circ$. Through the kindness of Dr. Leuschner, Miss Levy identified this as (304) Olga.

N.G.C. 5866 Boötes

$\alpha=15^h4^m12^s$, $\delta=+56^\circ5'.0$ (1917); $\lambda=58^\circ$, $\beta=+52^\circ$
Plate No. 129, 1912, June 14, 165^m. Illustrated Plate XIII*e*

This nebula is lenticular, $2'.5 \times 0'.75$, $p=126^\circ$, with no apparent nucleus, but with a bright center gradually decreasing in intensity toward the edge. Lying across the center and making an angle of 3° with the major axis is a narrow dark streak, $p=123^\circ$, about $1'$ long. Overlapping this at either end, and extending along the major axis to a distance of $45''$ in either direction from the center, lies a streak as bright as the central nebulosity, which gradually fades out toward the end. Slipher's[1] value for the radial velocity is +600 km.

---

[1] *Popular Astronomy*, **23**, 36, 1915.

N.G.C. 5907 Draco

$\alpha=15^h13^m44^s$, $\delta=+56°38'$ (1917); $\lambda=57°$, $\beta=+51°$

Plate No. 197, 1913, April 4, 90^m. Weak plate

This nebula is a spiral seen edge-on, similar to N.G.C. 5746 in having a longitudinal absorption streak lying just to one side of the nucleus. It measures $11'\times0'.7$, $p=156°$.

N.G.C. 6070 Serpens

$\alpha=16^h5^m45^s$, $\delta=+0°55'.7$ (1917); $\lambda=340°$, $\beta=+35°$

Plate No. 265, 1916, May 26, 75^m
Plate No. 267, 1916, May 27, 150^m. Illustrated Plate XIV*a*

This is a right-handed spiral $3'\times1'.3$, $p=59°$. Several arms dotted with nebulous stars make a full turn or more; those ending on the *f* side are well defined, those on the S*p* side diffused and free of knots. Directly *f* the nucleus two arms of the same curvature appear to overlap. There is a small stellar nucleus in an elongated nebulous knot. In a line a little to E of N of the nucleus the arms are much reduced in intensity.

N.G.C. 6210 Hercules

$\alpha=16^h41^m1^s$, $\delta=+23°57'.2$ (1917); $\lambda=11°$, $\beta=+36°$

Plate No. 139, 1912, July 13, 60^m. 100-foot focus

This is the well-known bright planetary nebula, Struve No. 5. The negative is overexposed, but one can see a bright central nucleus, bright nebulous streaks, fainter short curves bowed outward, some of them fading before returning, and several faint extensions, all of which give the nebula an angular appearance. The focal-plane slit spectrum is continuous for the star and crossed by bright lines projecting on either side. Keeler's[1] value of the radial velocity is −34.3 km and Campbell and Moore[2] have found internal motion.

---

[1] W. W. Campbell, *Stellar Motions*, p. 210.

[2] *Publications of the Astronomical Society of the Pacific*, **28**, 120, 1916.

N.G.C. 6217 Ursa Minor

$\alpha=16^h36^m32^s$, $\delta=+78^\circ22'$ (1917); $\lambda=79^\circ$, $\beta=+33^\circ$
Plate No. 200, 1913, May 6, 60^m. Weak plate

This right-handed spiral has a stellar nucleus. Nebulosity is noticeably absent near nucleus. There are nebulous knots along the arms. It measures $1'.5\times1'$, $p=160^\circ$.

N.G.C. 6309 Ophiuchus

$\alpha=17^h9^m24^s$, $\delta=-12^\circ48'.9$ (1917); $\lambda=337^\circ$, $\beta=+13^\circ$
Plate No. 252, 1915, May 10, 90^m. Illustrated Plate VII*a*
Plate No. 263, 1916, May 5, 10^m

The plate shows a nebulous spot with a well-defined arrowhead at the S end, a blunt arrowhead at the N end, both pointing outward, the two connected by faint nebulosity. A faint stellar nucleus lies at the base of the N head a little N of the center of the nebula. It measures $22''\times12''$, $p=162^\circ$. Keeler's[1] value of the radial velocity is -51.5 km.

N.G.C. 6412 Draco

$\alpha=17^h32^m4^s$, $\delta=+75^\circ6'.6$ (1917); $\lambda=74^\circ$, $\beta=+31^\circ$
Plate No. 128, 1912, June 13, 80^m. Weak plate

This is a faint left-handed spiral $90''\times70''$, $p=160^\circ$, having a faint stellar nucleus, with respect to which there is a knot of about the same brightness, $p=350^\circ$, $36''$.

N.G.C. 6478 Draco

$\alpha=17^h32^m4^s$, $\delta=+51^\circ11'.6$ (1917); $\lambda=46^\circ$, $\beta=+29^\circ$
Plate No. 135, 1912, July 11, 270^m

This is a right-handed spiral, $90''\times30''$, $p=32^\circ$, having a stellar nucleus. A star a little brighter than the nucleus lies at $p=10^\circ$, $14''$. It is surrounded by a dark space $5''$ to $6''$ in diameter, the arms being cut off sharply. Does the star have an absorbing atmosphere? The detail is stronger in contrast on the *p* side. There are over a dozen very small and faint nebulae on this plate.

---

[1] W. W. Campbell, *Stellar Motions*, p. 210.

N.G.C. 6543 Draco

$\alpha=17^h58^m35^s$, $\delta=+66°38'.3$ (1917); $\lambda=63°$, $\beta=+9°$

Plate No. 9, 1911, July 23, 10^m. 25-foot focus
Plate No. 10, 1911, July 23, 20^m. 25-foot focus
Plate No. 11, 1911, July 23, 6^m. 25-foot focus
Plate No. 20, 1911, July 25, 90^s. 25-foot focus
Plate No. 34, 1911, October 18, 50^m. 100-foot focus
Illustrated Plate VII*b*
Plate No. 238, 1914, May 17, 90^m. 80-foot focus

This is the well-known planetary nebula in Draco. The long exposures show a sharply outlined ellipse $24''\times18''$, $p=40°$, without detail, beyond which project ansae $2''$ to $3''$ on an axis in $p=20°$. On the shorter exposures the brighter nebulosity has the appearance of a curved thread which crosses itself several times, the ansae forming the ends. Its continuity is more or less disturbed in several places. Overlapping points are of greater brightness. At two points the thread approaches the bright stellar nucleus, giving almost the appearance of arms starting therefrom, but in neither case do they connect directly with the nucleus. The focal-plane slit spectrum appears as a continuous band corresponding to the nucleus, crossed by bright lines which project on either side. Keeler's[1] value for the radial velocity is -64.7 km, and Campbell and Moore[2] have found internal motion.

N.G.C. 6555 Hercules

$\alpha=18^h3^m28^s$, $\delta=+17°35'.3$ (1917); $\lambda=12°$, $\beta=+16°$

Plate No. 268, 1916, May 28–29, 360^m. Illustrated Plate XIV*b*

This left-handed spiral $1'.5\times1'$, $p=111°$, is in a rich field of stars. There is a star which might be taken for the nucleus, but the real nucleus is a slightly elongated knot a few seconds N. The brightest part of the nebula is a double knot at $p=240°$, $13''$, with respect to star. A number of small faint nebulae appear on the plate.

[1] *Ibid.*

[2] *Lick Observatory Bulletin*, No. 278, 1916.

N.G.C. 6703 Lyra

$\alpha=18^h44^m53^s$, $\delta=+45°27'.5$ (1917); $\lambda=42°$, $\beta=+18°$

Plate No. 269, 1916, July 1, 60^m
Plate No. 270, 1916, July 1, 180^m

A long exposure is necessary to show whether this is a ring nebula of a type very different from that usually met with, or whether a spiral, though indications point toward the former. The central nucleus lies in a bright nebulous spot which gradually fades out at 30″ diameter. The surrounding ring is very faint and narrow and about 80″ diameter.

N.G.C. 6702 appears as a nebulous spot very similar to, but fainter and smaller than, the central part of 6703. It is slightly elongated in $p=60°$.

There are six additional small faint nebulae on the plate, three being nebulous spots and three spindles, the brightest two of the latter with respect to N.G.C. 6703 being at $p=177°$, $8'.9$, elongated in $p=120°$, and $p=132°$, $9'.8$, elongated in 129°.

N.G.C. 6804 Aquila

$\alpha=19^h27^m37^s$, $\delta=+9°2'.9$ (1917); $\lambda=13°$, $\beta=-6°$

Plate No. 120, 1912, June 11, 60^m. Weak

The plate shows the nebula as a faint annulus with an irregularly shaped ring 5″ to 10″ in width and about 32″×25″, $p=60°$. It has the typical central star and another of about the same magnitude lying directly upon the ring at the W end of the major axis. As in many planetaries, the nebulosity is stronger near the ends of the minor axis than near the ends of the major axis. Huggins[1] found that it had a bright-line spectrum.

Plate 294, 1917, June 24–25, 325^m exp., shows a planetary nebula with uniform disk 65″×55″, $p=165°$, on which lies the ring described above. The N*p* and S points of the rim are strengthened while the *f* side is missing.

---

[1] *Philosophical Transactions*, **166**, 386, 1866.

N.G.C. 6818 Sagittarius

$\alpha=19^h39^m17^s$, $\delta=-14°21'.1$ (1917); $\lambda=353°$, $\beta=-19°$

Plate No. 115, 1912, June 10, 5^m. 25-foot focus
Plate No. 116, 1912, June 10, 2^m. 25-foot focus
Plate No. 137, 1912, July 12, 75^m. 100-foot focus. Illustrated Plate VII*c*

This bright planetary nebula is about 25″ in diameter and contains a small faint nucleus and much detail. Upon the faint uniform disk lies a moderately bright elliptical ring $25''\times16''$, $p=9°$, and varying in width and intensity, the N end almost fading into the disk and the other end crossed by a dark streak. From each of two strong knots, about 8″ apart and equidistant from the nucleus in the W limb of the ring, a wisp runs inward to the major axis, the two wisps being parallel. A thread runs from the nucleus NE to the E limb. The spectrum has bright lines; Keeler's[1] value for the radial velocity is -16.7 km.

N.G.C. 6826 Cygnus

$\alpha=19^h42^m34^s$, $\delta=+50°19'.4$ (1917); $\lambda=52°$, $\beta=+12°$

Plate No. 130, 1912, June 14, 10^m
Plate No. 131, 1912, June 14, 5^m
Plate No. 132, 1912, June 14, 25^m
Bathed-process plate and red screen; Pan-Iso developer

This is a bright planetary nebula $30''\times27''$, $p=127°$. The central nucleus is bright, sharply defined, and about 10″ in diameter. A knot appears at each end of the major axis, otherwise the disk is uniform. On the red-sensitive plate the nucleus is about 5″ in diameter and lies in a faint nebulous haze that fades out at about 18″ diameter. The Cassegrain short-focus camera gives a spectrum strongly continuous for the star, crossed by bright lines, some projecting but a slight distance beyond the nucleus, others clear across the disk. Values obtained for the radial velocity are -5.3[2] and -8[3] km.

[1] W. W. Campbell, *Stellar Motions*, p. 210.

[2] *Ibid.*

[3] *Publications of the Astronomical Society of the Pacific*, **27**, 239, 1915.

N.G.C. 6894 Cygnus

$\alpha=20^h13^m3^s$, $\delta=+30°18'.6$ (1917); $\lambda=37°$, $\beta=-3°$

Plate No. 4, 1911, July 2, 60^m
Plate No. 7, 1911, July 3, 14^m

This is a well-defined ring; on the outside there is a haze, particularly on E and W sides; and on the inside, many protrusions toward the center giving an internal-toothed appearance. The strongest thread of the ring measures $42''\times32''$, $p=45°$. The central nucleus is stellar and small. In the N*p* section of the ring is a star with a very faint companion partly surrounded by a dark ring. A. Searle[1] found the spectrum to show bright lines.

N.G.C. 6905 Delphinus

$\alpha=20^h18^m42^s$, $\delta=+19°15'.3$ (1917); $\lambda=29°$, $\beta=-11°$

Plate No. 145, 1912, August 16, 180^m. 100-foot focus
Plate No. 147, 1912, September 5, 175^m. 100-foot focus
Plate No. 149, 1912, September 6, 205^m. 100-foot focus
All plates weak

This is a planetary nebula $47''\times34''$, $p=175°$, containing much detail, strongest on E and W sides and weak along the NS line. Huggins[2] found it to have a bright-line spectrum.

N.G.C. 7008 Cepheus

$\alpha=20^h58^m8^s$, $\delta=+54°13'.5$ (1917); $\lambda=61°$, $\beta=+5°$

Plate No. 243, 1914, July 22, 180^m. Illustrated Plate VII*d*

This planetary nebula is elliptical in shape, $95''\times75''$, $p=5°$, containing much detail. The strongest bits of nebulosity are two condensations just E of the N end of the major axis. On the S*f* side the elliptical form seems eaten away, but traces of nebulosity may be seen connecting with a star which lies $p=156°$, $53''$. A number of stars a magnitude or two fainter than the nucleus appear in the nebula. Except for one, they are surrounded by a dark ring which in turn opens directly on a dark region. As the nucleus itself presents this appearance, it is suggested that these stars lie within the nebula. One of these stars, $p=240°$, $23''$, appears elongated; it may be a double star or a very bright bit of nebulosity. One star at $p=65°$, $29''$, with respect to the nucleus, is but partly surrounded by the dark ring. Huggins[1] found the spectrum to be gaseous.

---

[1] *Harvard Annals*, **33**, 145.

[2] *Philosophical Transactions*, **156**, 385, 1866.

N.G.C. 7009 Aquarius

$\alpha=20^h59^m39^s$, $\delta=-11°41'.6$ (1917); $\lambda=5°$, $\beta=-36°$

Plate No. 138, 1912, July 12, 90^m. 100-foot focus
Plate No. 140, 1912, July 13, 210^m. 100-foot focus. Illustrated Plate VII*e*

This is a most striking planetary, owing to its resemblance to Saturn. The brightest nebulosity is in the form of an elliptical ring, outside diameter $30''\times 13''$, $p=78°$. A second ring, more or less complete in outline, lying across the nucleus and in $p=160°$, almost at right angles to the first, shows as a condensed knot on the N side, broadening out as it approaches the S side. Another feature is the rhomboid-shaped uniform mass with the E and W edges, approximately $18''$ long, lying parallel to a NS line, and with the N and S sides, $23''$ long, slightly convex outward and running parallel to the major axis of the bright ellipse. The faint ansae are about $51''$ apart and connect with the central parts of the nebula through a bar lying in $p=78°$. Other knots and threads besides those described also show. The reproduction has been prepared with a view to detail rather than to relative intensities. The focal-plane slit spectrograph shows a bright-line spectrum. The radial velocity is $+10.1$ km,[2] and Campbell and Moore have found internal motion.[3]

N.G.C. 7023 Draco

$\alpha=21^h0^m35^s$, $\delta=+67°50'.3$ (1917); $\lambda=72°$, $\beta=+14°$

Plate No. 12, 1911, July 23, 149^m

This large nebula contains a great wealth of detail and is intimately connected with a star of the seventh magnitude lying in it.

[1] *Ibid.*, **156**, 387, 1866.

[2] W. W. Campbell, *Stellar Motions*, p. 210.

[3] *Lick Observatory Bulletin*, No. 278.

It occupies one of those dark regions which appear devoid of stars and which have been explained in several ways: the stellar material is at present in the nebula, or the nebula, containing both dark and bright material, lies this side of the stars and cuts off their light. Traces of the nebula extend as far as 9′ from it, but only in those regions that are starless. The nebulosity surrounding the star is strongest and projects on its S*p* side. Several bright filaments run S*p* from the star, and there are two more S of the star running in an EW direction. The spectra of both the star and the nebulosity 13″.6 N of the nucleus photographed with the focal-plane spectrograph are continuous with absorption lines. The velocity of the nucleus is +0.7 km.[1]

N.G.C. 7026 Cygnus

$\alpha = 21^h 3^m 30^s$, $\delta = +47°30'.8$ (1917); $\lambda = 57°$, $\beta = 0°$

Plate No. 156, 1912, October 10, 120^m. 100-foot focus

This bi-nuclear planetary is formed by two nebulous knots of about the same intensity, elongated NS, one lying 6″ almost due E of the other. They are connected by a bar, but there is no central star. There are traces of two loops, one on the N and another on the S, so connecting the knots that the whole forms an ellipse, $27'' \times 11''$, $p = 10°$. The spectrum shows bright lines and Campbell and Moore[2] have found internal motion.

N.G.C. 7027 Cygnus

$\alpha = 21^h 3^m 56^s$, $\delta = +41°54'.0$ (1917); $\lambda = 53°$, $\beta = -5°$

Plate No. 142, 1912, August 15, 30^m. 100-foot focus

This is Webb's bright planetary, a bright starlike patch with faint wings extending 3″ to 4″ to the N and E. A second condensation of about the same intensity as the wing, elongated in $p = 80°$ and of about the same size as the star, lies at $p = 130°, 5''$. The focal-plane spectrum shows very strong bright lines with practically no continuous background. Internal motion has been detected[3] by Campbell and Moore.

---

[1] *Publications of the Astronomical Society of the Pacific*, **27**, 239, 1915.

[2] *Ibid.*, **29**, 55, 1917.

[3] *Ibid.*, **28**, 119, 1916.

N.G.C. 7129 Cepheus

$\alpha=21^h41^m4^s$, $\delta=+65°43'.3$ (1917); $\lambda=73°$, $\beta=+9°$

Plate No. 273, 1916, August 31, 150^m
Plate No. 274, 1916, September 3, 25^m

This nebula lies in one of the vacant Milky Way regions in which one or more bright stars are involved in nebulosity, faint traces of which may be followed over a large part of the dark area. Seven stars are involved in nebulosity, their positions with respect to the brightest, *a*, being as follows:

ab $p=298°$, 58″ *ac* $p=50°$, 62″ *ad* $p=15°$, 60″
ae $p=355°$, $4'.5$ *af* $p=346°$, $4'.9$ *ag* $p=63°$, $5'.9$

The nebulosity about *a* for a distance of 12″ is very strong, completely masking the star; beyond it is fainter and more or less interrupted by dark patches up to a distance of 30″, where the curve begins. From *a* the nebulosity sweeps N*f*, just passes *c* and *d* on the N, and sweeps backward to the W underneath *b*. Fainter clouds appear S*p* as far as $4'.5$ from *a*. Not including *e*, *f*, and *g*, the nebula lies within a circle 6′ in diameter, the center of which is about $1'.5$ S*p* *a*. Two stars lie near this center, but do not seem involved in the nebula; *e*, *f*, and *g* are each centers of nebulosity of medium intensity and irregular form about $1'.5$ to 2′ in diameter. A long exposure will probably show all these stars connected by nebulosity.

N.G.C. 7177 Pegasus

$\alpha=21^h56^m44^s$, $\delta=+17°20'.4$ (1917); $\lambda=43°$, $\beta=-30°$

Plate No. 126, 1912, June 12, 75^m

This nebula is a right-handed spiral with moderately bright nucleus, arms fairly strong over roughly 30″ diameter. Outside of this are traces of arms filling an ellipse $2'.5\times1'.5$, $p=75°$. One arm starts from the nucleus and branches in two, the arm opposite being deformed or missing altogether.

N.G.C. 7217 Pegasus

$\alpha=22^h4^m10^s$, $\delta=+30^\circ57'.2$ (1917); $\lambda=54^\circ$, $\beta=-21^\circ$

Plate No. 216, 1913, September 2, 330^m. Illustrated Plate XIV*c*

This nebula is a fine right-handed spiral seen in plan. It meaures $3'\times2'.5$, $p=80^\circ$. For one turn about the nucleus the nebulosity is quite bright; then it drops in intensity over a space $75''\times60''$, where it fades away to increase again in brightness so as to form a ring, at the periphery $20''$ to $30''$ wide, almost as bright as the second stage. Instead of two separate arms there seem to be many small ones composed of fine, knotted, and stringy nebulosity lying closely parallel. It lies in a region rich in stars. Huggins[1] found the spectrum to be continuous.

N.G.C. 7662 Andromeda

$\alpha=23^h21^m54^s$, $\delta=+42^\circ4'.8$ (1917); $\lambda=74^\circ$, $\beta=-18^\circ$

Plate No. 29, 1911, October 17, 90^m. 100-foot focus, 44-inch aperture
Illustrated Plate VII*f*
Plate No. 148, 1912, September 5, 60^m. 100-foot focus
Plate No. 157, 1912, October 10, 60^m. 100-foot focus. Seed 27 plate
Plate No. 172, 1912, December 10, 1^m, 3^m, 6^m, 10^m
Plate No. 173, 1912, December 10, 7^m, 30^m
Plate No. 177, 1913, January 7, 4^m, 7^m
Plate No. 275, 1916, September 3, 1^m, 4^m, 10^m

This is the well-known planetary in Andromeda with sharp bright nucleus and a mottled disk $31''\times27''$, $p=40^\circ$, on which lies a very bright elliptical ring, $2''$ to $3''$ wide, whose median line is $15''\times9''$, $p=45^\circ$, weakened on the minor axis. The E edge is tipped with a bright line of nebulosity. The longer exposures show a considerable number of knots on the rim, and from two of these, at opposite ends of a diagonal in $p=200^\circ$, threads appear which project over the edges and form ansae. The spectrum with focal-plane slit has bright lines, with practically no continuous background. Keeler's[2] value of the radial velocity is -11.4 km.

MOUNT WILSON SOLAR OBSERVATORY
April 1917

---

[1] *Philosophical Transactions*, **156**, 391, 1866.

[2] W. W. Campbell, *Stellar Motions*, p. 210.

Contributions from the Mount Wilson Solar Observatory, No. 133
Reprinted from the *Astrophysical Journal*, Vol. XLVI, pp. 64–75, 1917

STUDIES BASED ON THE COLORS AND MAGNITUDES IN STELLAR CLUSTERS

FIFTH PAPER: COLOR-INDICES OF STARS IN THE GALACTIC CLOUDS

By HARLOW SHAPLEY

The interpretation of the color results[1] for Messier 11 has involved a more thorough investigation of the general stellar fields of that part of the sky than can be made on the basis of the stars shown on the photographs of the cluster. In this system the presence of faint stars that are conspicuously bluer than those found in Messier 67 and other open clusters of high galactic latitude opens the question of the relation of color to galactic latitude and necessitates an inquiry into the frequency of color-classes in the dense galactic clouds, one of the richest of which surrounds Messier 11. The present paper is concerned with the results for color and magnitude in four fields in the immediate neighborhood of the cluster.

The position of the center of each field is given in Table I. Fields I and II are respectively southwest and northwest of Messier 11, each nearly a degree distant, and in the denser parts of the galactic clouds, as may be seen by referring to Barnard's photographs of the Milky Way.[2] The photographic and photo-

TABLE I

GALACTIC CLOUD FIELDS NEAR MESSIER 11

Field	Central Star	R.A. 1900	Decl. 1900
I........	B.D.-7°4736	$18^h 45^m 6^s$	$-7^\circ\ 8'$
II........	B.D.-6°4913	18 43 18	$-6\ \ 7$
III........	....	18 46 10	$-6\ 28$
IV........	....	18 45 42	$-6\ 17$

---

[1] *Mt. Wilson Contr.*, No. 126; *Astrophysical Journal*, **45**, 164, 1917.

[2] *Publications of the Lick Observatory*, **11**, Plates 62–65, 1915.

visual magnitudes in these two fields were determined by direct comparison with the stars in Messier 11, and those for Field I were also derived through polar comparisons. Table II contains a list and description of the plates used for the first two fields.

TABLE II

Observations on Fields I and II

Plate Number	Date	G.M.T.	Kind of Plate	No. Exp.	Exp. Time	Hour-Angle	Remarks
3201....	1916 July 6	$18^{h}56^{m}$	Iso	3	15, 2^{m}	10° E	I and M 11
3202....	6	19 28	Seed 27	3	3	2° E	I and M 11
3219....	7	18 52	Seed 27	3	3	11° E	I and M 11
3220....	7	19 2	Iso	3	15	8° E	I and M 11
3221....	7	20 10	Seed 27	1	7	9° W	I, for chart
3402....	Aug. 25	16 4	Iso	6	1–10	4° E	II, exp.-ratio
3403....	25	16 34	Iso	5	0.4-4	4° W	II, exp.-ratio
3404....	25	16 52	Seed 27	3	2	8° W	II and M 11
3407....	25	17 59	Iso	6	1–10	25° W	I, exp.-ratio
3431....	Sept. 6	16 4	Iso	3	5	8° W	II and M 11
3463....	24	15 23	Seed 27	3	2	16° W	II and M 11
3464....	24	15 52	Seed 27	3	2	22° W	II and M 11
3465....	24	16 0	Iso	3	10	24° W	II and M 11
3563....	Nov. 22	13 57	Iso	5	3	51° W	I and N.P.
3564....	22	14 3	Seed 27	5	1	53° W	I and N.P.

Field III is about 9′ southeast, and Field IV 7′ north, of the cluster. The magnitudes were determined directly from the plates used for the study of Messier 11, which are described in the first table of the preceding paper of this series. A further partial check of the colors in all fields was obtained by the method of exposure-ratios.[1]

The fifty stars in Field I, for which final results appear in Table III, were selected at random from the several hundred within the measurable limits of the plates. Details concerning the measures and reductions can be omitted. It will suffice to note that the average deviation from the mean of one determination of a photographic magnitude is ±0.10; for a photo-visual magnitude the average deviation is ±0.06. The average probable error of a color-index is about ±0.08. In this field the exposure-ratios for a hundred stars give an independent determination of the colors, and, though the reduction-curve now available is provisional, the

---

[1] F. H. Seares, *Mt. Wilson Communications*, No. 33; *Proceedings of the National Academy of Sciences*, **2**, 521, 1916.

TABLE III

MAGNITUDES AND COLORS IN FIELD I

Star	Δα cos δ	Δδ	Photographic Magnitude	Photo-visual Magnitude	Color-Index
1	−188″	−196″	15.46	13.88	+1$^{\mathrm{M}}$58
2	−177	+448	15.54	14.28	+1.26
3	−154	− 33	14.78	13.65	+1.13
4	−154	+418	14.84	14.59	+0.25
5	−153	− 46	15.42	15.00	+0.42
6	−129	− 56	14.94	13.64	+1.30
7	−128	−149	13.26	12.93	+0.33
8	−119	− 1	15.12	14.62	+0.50
9	−118	+428	15.57	14.61	+0.96
10	−114	+372	14.95	14.53	+0.42
11	−103	−221	14.40	13.77	+0.63
12	− 81	− 20	14.32	14.46	−0.14
13	− 69	+174	15.41	14.43	+0.98
14	− 68	+ 95	15.38	14.86	+0.52
15	− 63	+145	16.24	15.04	+1.20
16	− 55	+330	14.42	13.81	+0.61
17	− 47	− 60	15.49	14.30	+1.19
18	− 44	+319	13.70	12.64	+1.06
19	− 38	+ 72	13.98	13.72	+0.26
20	− 37	+ 12	15.37	13.83	+1.54
21	− 35	+ 18	14.54	13.84	+0.70
22	− 34	− 67	15.31	14.43	+0.88
23	0	+189	15.07	14.64	−0.43
24	+ 25	+146	15.19	14.16	+1.03
25	+ 35	+417	14.45	13.17	+1.28
26	+ 43	+123	15.25	14.58	+0.67
27	+ 44	+196	11.45	11.34	+0.11
28	+ 49	+205	14.99	14.53	+0.46
29	+ 53	+401	14.40	12.64	+1.76
30	+ 59	+231	14.85	14.12	+0.73
31	+ 70	+223	14.77	14.37	+0.40
32	+ 80	+297	15.01	13.05	+1.96
33	+ 83	+ 14	14.96	14.05	+0.91
34	+ 87	+ 66	15.58	14.22	+1.36
35	+ 88	+ 72	13.73	12.57	+1.16
36	+ 93	+234	12.78	12.30	+0.48
37	+106	+119	14.46	14.14	+0.32
38	+116	+ 89	14.36	13.98	+0.38
39	+145	+ 22	14.36	13.83	+0.53
40	+174	+197	13.89	12.93	+0.96
41	+200	+ 79	15.39	14.56	+0.83
42	+220	+138	13.17	13.11	+0.06
43	+229	+109	13.04	12.71	+0.33
44	+244	+188	14.61	13.98	+0.63
45	+351	+216	13.29	11.48	+1.81
46	+253	+154	15.32	14.02	+1.30
47	+358	+133	14.89	13.80	+1.09
48	+361	+126	15.17	14.10	+1.07
49	+363	+169	14.89	14.57	+0.32
50	+367	+113	13.20	12.12	+1.08

results from the different methods are in satisfactory agreement. The positions given in Tables III–VI, which are intended to serve only for identification, were determined, with the aid of a reseau, from enlargements of the original negative, the orientation and scale being derived from catalogue stars.

Table IV contains results for Field II. The average deviation of a magnitude from one plate is ±0.07, giving an average probable error for a color-index of less than ±0.06. This value is independent of the accidental errors in the magnitudes in Messier 11, as thirty or forty of the cluster stars were used in the intercomparison, but it is not free from possible systematic errors in those magnitudes. From the results of the polar comparisons for Field I and from the colors derived by exposure-ratios, this latter source of error is found to be unimportant.

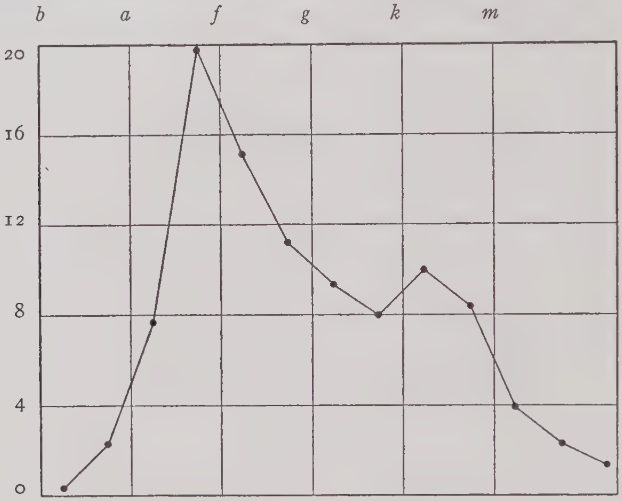

Fig. 1.—Frequency of color-classes in galactic clouds
Abscissae are color-classes; ordinates are percentages

The errors in the magnitudes for Fields III and IV are essentially the same as those given previously for the stars in Messier 11. Stratonoff's catalogue of stars in and near the cluster[1] includes a number of these outlying objects, and, when available, his numbers are given in the second column of Tables V and VI.

---

[1] *Publications de l'Observatoire astronomique et physique de Tachkent*, No. 1, 1899.

TABLE IV

Magnitudes and Colors in Field II

Star	$\Delta\alpha \cos \delta$	$\Delta\delta$	Photographic Magnitude	Photo-visual Magnitude	Color-Index
1	−484″	+ 76″	12.89	12.48	$+0^{\mathrm{M}}.41$
2	−481	+144	15.68	14.50	+1.18
3	−474	+ 1	14.01	13.81	+0.20
4	−468	+ 19	13.99	13.61	+0.38
5	−467	+155	14.82	13.84	+0.98
6	−466	+ 10	16.58	14.35	+2.23
7	−463	−436	12.92	12.75	+0.17
8	−450	+ 42	14.72	14.28	+0.44
9	−449	−431	13.86	13.83	+0.03
10	−445	+ 15	15.12	14.52	+0.60
11	−440	−477	12.64	12.34	+0.30
12	−427	−500	15.84	15.01	+0.83
13	−422	− 25	15.16	13.61	+1.55
14	−411	+147	14.72	14.55	+0.17
15	−389	− 45	14.77	13.48	+1.29
16	−388	− 68	14.24	14.02	+0.22
17	−377	−521	14.47	13.45	+1.02
18	−376	+ 33	15.19	13.28	+1.91
19	−367	−353	15.30	14.97	+0.33
20	−367	−371	16.29	14.83	+1.46
21	−365	−445	14.88	13.28	+1.60
22	−364	+ 90	14.18	12.45	+1.73
23	−356	−316	15.17	14.85	+0.32
24	−354	−327	15.64	15.00	+0.64
25	−353	−526	14.50	14.50	0.00
26	−352	+107	16.69	14.69	+2.00
27	−336	−379	13.99	13.85	+0.14
28	−330	−307	15.40	13.96	+1.44
29	−325	−447	15.05	13.83	+1.22
30	−325	+ 90	16.01	14.61	+1.40
31	−322	+ 60	16.61	14.98	+1.63
32	−318	+256	14.34	14.25	+0.09
33	−315	+198	14.03	12.82	+1.21
34	−315	−373	12.66	11.82	+0.84
35	−314	−366	14.79	14.55	+0.24
36	−314	−323	14.45	14.23	+0.22
37	−303	+239	15.12	14.79	+0.33
38	−302	−208	15.20	14.66	+0.54
39	−299	−317	15.17	14.08	+1.09
40	−294	+127	14.69	14.40	+0.29
41	−292	−350	15.88	15.02	+0.86
42	−292	−199	14.99	13.98	+1.01
43	−289	+280	15.68	14.27	+1.41
44	−288	−330	14.82	14.55	+0.27
45	−283	+ 69	14.41	13.94	+0.47
46	−282	−254	14.21	13.94	+0.27
47	−281	−301	14.79	14.33	+0.46
48	−279	+120	16.64	14.56	+2.08
49	−278	+470	15.63	15.03	+0.60
50	−265	−217	15.13	14.81	+0.32
51	−260	+298	15.57	14.98	+0.59
52	−259	−249	14.74	14.30	+0.44

TABLE IV—*Continued*

Star	Δα cos δ	Δδ	Photographic Magnitude	Photo-visual Magnitude	Color-Index
53	−258″	+330″	15.16	14.63	+0$^{\mathrm{M}}$53
54	−255	+107	14.69	14.35	+0.34
55	−254	+469	13.91	13.83	+0.08
56	−248	+178	14.82	13.28	+1.54
57	−245	+240	15.32	14.81	+0.51
58	−244	+302	16.03	14.56	+1.47
59	−243	+348	16.01	14.87	+1.14
60	−243	+372	13.78	12.03	+1.75
61	−238	+128	13.75	13.55	+0.20
62	−237	+236	14.52	14.18	+0.34
63	−233	−290	14.38	14.16	+0.22
64	−232	+241	14.15	13.85	+0.30
65	−228	−246	15.48	14.30	+1.18
66	−225	+295	14.40	13.34	+1.06
67	−224	−336	13.49	12.83	+0.66
68	−224	+146	14.79	13.94	+0.85
69	−221	+270	14.27	13.85	+0.42
70	−218	+469	15.00	14.74	+0.26
71	−211	+252	14.90	14.43	+0.47
72	−211	+470	13.63	12.39	+1.24
73	−210	+319	14.32	12.50	+1.82
74	−210	+386	14.77	14.55	+0.22
75	−210	+139	16.57	14.52	+2.05
76	−207	−259	16.50	14.57	+1.93
77	−200	−314	14.80	13.51	+1.29
78	−197	−280	15.40	14.23	+1.17
79	−195	+242	16.13	14.66	+1.47
80	−195	−445	12.27	11.43	+0.84
81	−186	+405	15.48	14.52	+0.96
82	−171	−475	15.78	14.48	+1.30
83	−166	−476	15.78	15.04	+0.74
84	−163	−482	16.08	15.09	+0.99
85	−155	−189	15.65	14.51	+1.14
86	−146	+376	16.04	14.79	+1.25
87	−141	−215	15.59	14.92	+0.67
88	−134	+411	14.77	14.90	−0.13
89	−125	+354	15.53	14.23	+1.30
90	−122	−480	14.31	13.96	+0.35
91	−119	−249	15.80	14.55	+1.25
92	−116	+429	15.40	14.80	+0.60
93	− 92	−268	14.87	14.42	+0.45
94	− 86	−514	14.69	13.58	+1.11
95	− 85	+401	15.56	14.15	+1.41
96	− 81	−492	16.08	14.72	+1.36
97	− 79	−479	14.72	14.52	+0.20
98	− 77	+282	14.85	13.96	+0.89
99	− 75	−534	15.49	14.95	+0.54
100	− 67	−282	14.90	14.86	+0.04
101	− 67	−493	15.12	14.85	+0.27
102	− 52	+299	16.18	14.77	+1.41
103	− 49	−482	13.46	13.39	+0.07
104	− 45	+283	15.56	14.35	+1.21
105	− 24	−265	16.26	14.88	+1.38
106	− 10	+315	14.72	14.23	+0.49

TABLE IV—*Continued*

Star	Δα cos δ	Δδ	Photographic Magnitude	Photo-visual Magnitude	Color-Index
107	− 7″	−237″	12.93	12.18	+0$^{\mathrm{M}}$75
108	+ 2	+301	14.54	14.48	+0.06
109	+ 30	+332	14.45	13.05	+1.40
110	+ 31	+291	14.50	14.13	+0.37
111	+ 73	+289	15.20	14.66	+0.54
112	+ 89	−354	15.12	14.61	+0.51
113	+ 94	−349	16.61	14.74	+1.87
114	+100	+339	13.26	12.33	+0.93
115	+100	+150	15.20	14.86	+0.34
116	+100	−165	15.35	14.53	+0.82
117	+101	− 31	13.13	12.36	+0.77
118	+101	+247	15.68	14.37	+1.31
119	+101	− 59	12.36	11.35	+1.01
120	+105	−194	16.11	14.58	+1.53
121	+107	−320	13.91	12.68	+1.23
122	+108	−142	14.80	14.50	+0.30
123	+110	− 69	14.93	13.46	+1.47
124	+118	−424	14.77	14.50	+0.27
125	+121	−218	15.33	14.83	+0.50
126	+127	−350	14.03	13.94	+0.09
127	+130	−353	13.93	13.61	+0.32
128	+144	−177	16.22	14.86	+1.36
129	+150	−347	14.65	14.20	+0.45
130	+154	−424	15.99	14.55	+1.44
131	+155	+281	16.10	14.66	+1.44
132	+163	+ 79	15.94	14.27	+1.67
133	+163	−401	13.56	12.82	+0.74
134	+167	−120	16.07	14.76	+1.31
135	+174	−108	14.99	14.39	+0.60
136	+179	−328	14.90	14.46	+0.44
137	+180	+293	14.86	13.40	+1.46
138	+183	+145	15.17	13.22	+1.95
139	+187	−322	15.83	14.80	+1.03
140	+193	−321	15.50	14.80	+0.70
141	+195	+ 93	15.91	14.48	+1.43
142	+210	−453	15.88	14.50	+1.38
143	+214	−432	12.41	11.93	+0.48
144	+216	−155	15.75	14.27	+1.48
145	+219	−443	14.91	14.97	−0.06
146	+229	−481	13.27	13.32	−0.05
147	+241	−435	14.91	14.25	+0.66
148	+248	−180	14.92	14.02	+0.90
149	+249	−186	13.19	12.19	+1.00
150	+278	−187	16.54	14.86	+1.68
151	+297	−278	15.54	15.01	+0.53
152	+306	−497	12.46	11.50	+0.96
153	+310	−291	15.58	14.20	+1.38
154	+311	−195	16.87	15.25	+1.62
155	+313	−517	12.89	13.06	−0.17
156	+333	−491	13.78	14.20	−0.42
157	+334	−224	13.38	11.99	+1.39

TABLE V

Magnitudes and Colors in Field III

Star	Stratonoff Number	R.A. 1900	Decl. 1900	Photographic Magnitude	Photo-visual Magnitude	Color-Index
1	697	$18^{h}45^{m}55^{s}.8$	−6° 28′ 26″	14.45	14.14	$+0^{M}31$
2	698	56.3	27 37	13.14	11.98	+1.16
3	....	56.7	27 42	16.03	14.83	+1.20
4	710	57.6	28 27	13.23	12.84	+0.39
5	713	58.1	28 43	14.50	14.17	+0.33
6	730	59.9	28 46	14.46	14.21	+0.25
7	....	46 0.2	27 32	15.07	14.74	+0.33
8	....	0.5	28 20	15.38	15.06	+0.32
9	738	0.7	29 2	13.52	11.84	+1.68
10	....	0.9	27 44	15.04	14.58	+0.46
11	740	1.1	28 25	12.02	11.96	+0.06
12	....	2.0	27 56	15.22	14.85	+0.37
13	....	2.1	28 54	15.12	15.18	−0.06
14	....	2.5	28 5	15.04	14.71	+0.33
15	748	2.5	29 20	14.30	14.17	+0.13
16	....	2.7	28 55	14.72	14.24	+0.48
17	....	5.0	28 28	15.02	14.02	+1.00
18	....	5.4	30 35	14.88	13.80	+1.08
19	....	5.4	29 34	14.80	14.74	+0.06
20	769	6.9	27 57	14.21	14.06	+0.15
21	770	6.9	30 18	13.23	12.91	+0.32
22	....	9.1	30 29	15.07	14.95	+0.12
23	....	9.3	30 24	15.27	14.40	+0.87
24	780	9.4	29 10	11.60:	10.67	+0.93
25	....	9.6	27 22	14.84	14.55	+0.29
26	....	9.7	27 35	15.55	14.55	+1.00
27	....	9.8	27 16	14.97	14.55	+0.42
28	782	10.1	30 32	13.76	12.47	+1.29
29	783	10.1	26 28	13.15	11.61	+1.54
30	786	10.3	27 12	13.76	13.64	+0.12
31	....	10.8	25 37	14.76	13.89	+0.87
32	788	10.9	25 54	14.59	13.64	+0.95
33	789	11.2	28 57	14.11	13.84	+0.27
34	....	13.2	28 52	14.93	14.68	+0.25
35	....	13.3	28 42	14.93	14.48	+0.45
36	....	13.6	25 39	15.98	14.55	+1.43
37	795	14.0	25 50	13.93	13.68	+0.25
38	....	14.1	29 43	14.34	12.73	+1.61
39	796	14.2	29 57	13.89	13.49	+0.40
40	....	15.3	27 18	15.55	14.93	+0.62
41	804	15.9	27 16	13.64	13.56	+0.08
42	809	16.6	27 34	13.52	13.36	+0.16
43	811	17.3	28 22	13.80	13.70	+0.10
44	814	17.9	26 13	14.42	14.17	+0.25
45	....	19.0	27 38	14.80	13.84	+0.96
46	823	19.3	27 18	13.19	11.64	+1.55
47	....	20.5	27 47	14.93	14.21	+0.72
48	....	21.5	28 15	15.46	13.98	−1.48
49	....	21.9	28 2	14.88	14.10	+0.78
50	....	22.3	28 49	14.80	14.48	+0.32
51	....	23.1	28 41	14.84	14.21	+0.63
52	831	23.2	28 29	13.56	12.82	+0.74

TABLE VI

MAGNITUDES AND COLORS IN FIELD IV

Star	Stratonoff Number	R.A. 1900	Decl. 1900	Photographic Magnitude	Photo-visual Magnitude	Color-Index
1	177	$18^h45^m26^s.7$	−6° 16′ 38″	13.98	13.68	$+0^M.30$
2	....	27.1	16 24	15.32	15.00	+0.32
3	....	28.4	17 30	15.84	15.16	+0.68
4	....	28.5	17 1	16.56:	14.97	+1.59:
5	195	28.7	18 0	14.74	13.24	+1.50
6	196	28.7	16 29	14.86	14.65	+0.21
7	....	30.6	16 30	16.94:	14.58	+2.36:
8	....	30.8	17 4	15.26	14.83	+0.43
9	....	31.2	17 42	15.50	14.17	+1.33
10	220	31.5	17 37	13.85	12.99	+0.86
11	....	32.3	18 32	14.93	14.52	+0.41
12	241	33.2	15 7	13.37	12.82	+0.55
13	....	33.4	16 29	15.80	14.06	+1.74
14	246	33.5	15 13	13.85	13.33	+0.52
15	255	33.9	18 34	14.89	14.58	+0.31
16	....	34.8	15 22	14.78	14.14	+0.64
17	....	35.0	17 5	16.38	14.71	+1.67
18	....	35.2	17 2	14.86	14.17	+0.69
19	....	35.3	15 12	15.46	14.85	+0.61
20	....	35.6	17 35	15.92	14.58	+1.34
21	304	36.8	15 56	12.67	11.63	+1.04
22	312	37.0	16 30	14.86	14.24	+0.62
23	326	37.7	14 59	14.51	14.17	+0.34
24	339	38.1	18 31	13.30	12.77	+0.53
25*	340	38.1	16 2	12.74	12.04	+0.70
26	367	39.2	16 26	14.03	13.49	+0.54
27	371	39.3	16 38	14.10	13.88	+0.22
28	382	39.8	16 49	13.36	12.64	+0.72
29	....	40.0	16 28	15.35	14.91	+0.44
30	....	40.0	16 35	15.42	14.21	+1.21
31	388	40.1	17 50	14.51	14.21	+0.30
32	....	42.4	16 46	15.92	15.20	+0.72
33	....	42.6	16 16	14.86	13.42	+1.44
34	463	42.8	18 25	14.07	13.76	+0.31
35	....	43.2	16 52	15.01	13.72	+1.29
36	473	43.2	15 34	14.24	13.72	+0.52
37	479	43.3	15 58	13.72	13.42	+0.30
38	....	44.0	15 30	15.39	15.00	+0.39
39	....	45.0	18 41	14.97	14.62	+0.35
40	530	45.4	18 36	13.81	13.08	+0.73
41	549	46.2	18 30	13.02	12.15	+0.87
42	575	47.5	18 26	14.48	14.06	+0.42
43	578	47.5	17 43	14.26	14.02	+0.24
44	587	48.1	17 50	12.45	11.95	+0.50
45	595	48.6	18 18	14.55	14.44	+0.11
46	605	49.1	18 30	14.93	14.62	+0.31
47	626	50.5	18 30	13.18	12.39	+0.79
48	627	50.7	18 3	13.74	13.24	+0.50
49	632	51.0	17 44	14.32	13.49	+0.83
50	641	51.8	16 53	13.02	12.15	+0.87
51	646	52.2	17 26	14.97	14.48	+0.49
52	665	53.3	18 14	13.06	12.39	+0.67
53	673	53.8	18 37	14.44	14.06	+0.38
54	683	54.4	17 26	14.07:	14.10	−0.03:

*This star apparently varies through six-tenths of a magnitude.

The results for the four fields are collected in Tables VII and VIII, the former showing the distribution of the stars among the various color-classes,[1] the latter giving statistical data bearing on the relation of average color-index to luminosity. A wide range in color is immediately apparent; and the plot of the relative frequency of color-classes in Fig. 1 indicates that the distribution of spectral types among the fourteenth-magnitude stars is much the same in this distant galactic region as in the immediate vicinity of the sun.

TABLE VII

PERCENTAGE FREQUENCY OF COLORS IN GALACTIC CLOUDS

Field	Color-Class												Number of Stars
	*b*0	*b*5	*a*0	*a*5	*f*0	*f*5	*g*0	*g*5	*k*0	*k*5	*m*0	*m*5	
I*........	0	2	6	12	18	12	12	16	12	4	2	4	50
II........	1	3	7	17	13	8	8	8	12	12	5	6†	157
III.......	0	2	17	29	10	10	10	8	4	8	4	0	52
IV........	0	0	2	27	24	22	10	0	8	4	4	0	51
All fields..	0.3	2	8	20	15	11	9	8	10	8	4	4‡	310

* The corresponding numbers for Field I from the 100 provisional exposure-ratio color-determinations are 0, 6, 22, 17, 11, 6, 8, 10, 7, 9, 3, 1.

† 2.5 per cent have color-indices greater than +2.00.

‡ 1.3 per cent have color-indices greater than +2.00.

A small but probably real increase of mean color with brightness is suggested by Table VIII. In Messier 11 the corresponding change is very striking,[2] the average color-index decreasing a whole magnitude as the brightness decreases three magnitudes. An examination of the individual values for the fields in the galactic clouds shows that in Table VIII, for all cases, the average deviation of the color-index from the means is large. In other words, stars of all colors are included in each interval of magnitude; and, so far as color is an index of intrinsic luminosity, this may be accepted as an indication of considerable difference in the distances of such stars. Herein the galactic clouds apparently differ from the stellar group comprising the nucleus of Messier 11. There the color-phenomenon is reasonably explained, in the light of results for globular clusters as well as for moving groups of stars, as the characteristic of a relatively condensed physical group whose distances from the sun are sensibly the same.[1] These cluster-stars are probably giants in luminosity, and accordingly the distance of the group must be of the order of 15,000 light-years.

---

[1] Under *b*0 are included stars with color-indices between $-0\overset{\mathrm{M}}{.}40$ and $-0\overset{\mathrm{M}}{.}20$; under *b*5 those between $-0\overset{\mathrm{M}}{.}20$ and $0\overset{\mathrm{M}}{.}00$, etc.

[2] *Mt. Wilson Contr.*, No. 126, Table VIII and Fig. 3.

TABLE VIII

Relation of Color-Index in Galactic Clouds to Photo-visual Magnitude

Field I...	Mean mag....	12.08	13.02	13.81	14.14	14.50	14.80
	Mean color...	+ 1.07	+ 0.91	+ 0.87	+ 0.78	+ 0.59	+ 0.67
	No. stars.....	6	8	10	10	10	6
Field II...	Mean mag....	12.05	13.13	13.82	14.27	14.67	15.01
	Mean color...	+ 0.96	+ 1.07	+ 0.63	+ 0.75	+ 0.93	+ 0.69
	No. stars.....	15	19	21	36	51	15
Field III..	Mean mag....	11.62	13.02	13.78	14.15	14.54	14.89
	Mean color...	+ 1.15	+ 0.62	+ 0.68	+ 0.46	+ 0.61	+ 0.37
	No. stars.....	6	8	9	11	9	9
Field IV..	Mean mag....	12.10	13.01	13.62	14.14	14.56	14.96
	Mean color...	+ 0.78	+ 0.74	+ 0.64	+ 0.72	+ 0.44	+ 0.66
	No. stars.....	7	8	9	11	8	8
All fields..	Mean mag....	11.99	13.07	13.77	14.21	14.62	14.94
	Mean color...	+ 0.98	+ 0.90	+ 0.69	+ 0.70	+ 0.80	+ 0.60
	No. stars.....	34	43	49	68	78	38

The wide dispersion in magnitude of both blue and red stars indicates a similarly great distance for the neighboring galactic clouds. It suggests that the extent of the stellar clouds in the line of sight is relatively very great—in fact, the depth may be as great as, or greater than, the distance to the nearer boundary.

Fainter than the fourteenth photo-visual magnitude the average color-index in Messier 11 begins to increase (see Fig. 3 of the preceding paper). These faint stars might perhaps be considered as at the head of the series of dwarf stars in a stellar system that includes all the grades of luminosity found among the stars at large;

---

[1] The correction of the cluster-results (if it were rigorously possible) for the stars not belonging to the physical group would not affect these conclusions.

but a preferable interpretation is that the physical group in Messier 11, containing chiefly stars of high luminosity, has but a few stars fainter than the fourteenth apparent magnitude. The increasing redness, then, is due to the increasing predominance of the members of the star-clouds, which we now find are of all color-classes with an average index, between the fourteenth and fifteenth magnitudes, of +0.70.

SUMMARY

1. Magnitudes and colors have been determined for three hundred stars in four fields in the vicinity of the open galactic cluster Messier 11. Twenty-three plates have been used in the discussion, and the various errors are satisfactorily small.

2. As in Messier 11, a wide range of color is present; but the change of color with brightness is hardly perceptible. The magnitudes of the blue stars seem to indicate the remoteness of the star-clouds and also their great dimensions. Similar results have been obtained in a number of other galactic fields,[1] all pointing to a diameter of the galactic system considerably greater than generally supposed.

3. The cluster Messier 11 proves to be a physical group in the midst of the star-clouds, which on their own part have the general appearance and some of the properties of an enormous but definitely outlined physical system. There is no certain evidence as yet of the existence of dwarf stars, either in Messier 11 or in the galactic clouds.

Mount Wilson Solar Observatory
April 1917

---

[1] *Mt. Wilson Communications*, No. 44; *Proceedings of the National Academy of Sciences*, **3**, 269, 1917.

Contributions from the Mount Wilson Solar Observatory, No. 134
Reprinted from the *Astrophysical Journal*, Vol. XLVI, pp. 104–116, 1917

A METHOD OF INVESTIGATING THE STARK EFFECT FOR METALS, WITH RESULTS FOR CHROMIUM

By J. A. ANDERSON

The object of the present work was to find a method suitable for the study of the Stark effect for metals having a relatively high melting-point. The spectra of such metals as iron, nickel, chromium, vanadium, and titanium are of special importance in solar work, and if some of their lines show an effect due to an electric field it would at once become possible to determine whether electric fields exist in the solar atmosphere. In previous work on the Stark effect some of the lines of these metals have been observed, but in no case has an electric effect been found for them. Generally the source used has been of feeble intensity as compared to an arc or spark, necessitating the use of low dispersion, and hence the first problem which had to be solved in the present investigation was that of getting a source sufficiently bright to be studied with a spectrograph of moderate dispersion.

APPARATUS

The apparatus shown in Fig. 1 has given general satisfaction; most of the lines of the metals enumerated above can be recorded in exposures of from 10 to 30 minutes to a scale of about 4 A per millimeter, using a spectrograph such as that described in this paper.

A bell-jar, about 15 cm in diameter and about 30 cm high, stands on a glass plate in which there are two openings. The connection to the pump is sealed into one of these, while a larger glass tube, having a platinum electrode at its closed end, is sealed into the other. This larger glass tube is about 2.5 cm in outside diameter for about one-half its length, then tapers to about 1.5 cm in order to form a seat for the ground joint with the long silica tube *D*. *D* is about 20 cm long and 1.2 cm in outside diameter, and carries at its upper end the short silica tube *C*, to which it is fitted by a ground joint. The cathode is in two parts—*B*, made of iron, and *b*, of the metal which is to be studied—and it rests on top of the tube *D*. *C* has a vertical slot, about 1 mm in width, which extends down to the level of the top surface of *b*, the cathode proper. The tube *C* must be ground truly cylindrical inside and must be of a diameter about 0.1 mm larger than the cathode *b*. The necessity for this will be discussed below.

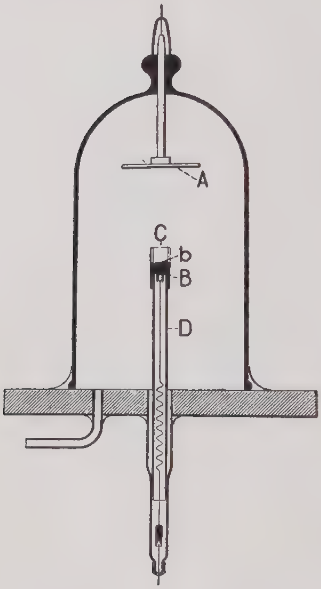

FIG. 1.—Diagram of apparatus. *A*, Anode; *Bb*, Cathode; *C*, Silica tube with slot for observing; *D*, Silica tube.

A fine platinum wire, 33 B. & S. gauge, is attached to *B* by means of a screw and carries at its lower end a short brass cylinder which makes contact with the platinum electrode in the larger glass tube. A mercury contact at this point was tried first, but the mercury vapor gave rise to so much trouble that it became necessary to resort to this form of metallic contact, which has worked admirably.

The anode is a massive disk of aluminium on the end of an aluminium rod. A thick platinum wire, fastened to the rod, is sealed into a glass tube, as indicated at the top of the diagram. The knob at the top of the bell-jar has a hole drilled through it, into which the glass tube is fitted by grinding; it is then sealed in with water-glass.

Direct current to produce the discharge is supplied by a set of high-potential generators connected in series. Each generator gives approximately 800 volts, and for most of the work 8 generators were used. Two spectrograms were obtained with the use of 16 generators, but so much difficulty was experienced in keeping the vessel operating satisfactorily at this high voltage that it was discontinued until some future time, when it will be tried again. A resistance consisting of distilled water with platinum electrodes was always used in series with the tube.

The resistance varied somewhat, but in general it was kept at about 32,000 ohms.

A high-vacuum oil pump is used to exhaust the bell-jar, the pressure employed being such that the Crookes' dark-space has a length of from 4 to 6 mm. At first hydrogen was used as residual gas, but later it was found that spectra of the metals are brighter in air or oxygen, and hence in the major part of the work commercial oxygen was employed. The gas was passed through concentrated sulphuric acid to remove most of the moisture, but, since no drying tube was connected to the vessel directly, there were always traces of water-vapor present. This was found to be a real advantage, as it gave the hydrogen lines with an intensity which was very suitable for determining the field-strength.

PHENOMENA OF THE DISCHARGE

With the use of 8 generators (about 6400 volts), a resistance of about 32,000 ohms in series, and pressure adjusted to give a dark-space of about 4 mm, the initial current, if one of the metals already mentioned is used as a cathode, will be about 100 milliamperes. With manganese the current is usually a little higher, while with magnesium it is about 200 milliamperes, the bell-jar acting as if it had practically no resistance. During the first minute the current usually decreases rapidly, and in about two minutes it becomes steady at approximately 40 milliamperes. In the meantime the cathode *b* has become almost white hot, its temperature being now from 800° to 1000° C. The cathode glow, Crookes' dark-space, and most of the negative glow are confined within the tube *C*, while a soft glow extends with decreasing intensity from the top of *C* up to the anode or even beyond it. On the anode may be a single bright point, or there may be nothing whatever visible. After the current has run about ten minutes, all of the tube *C*, excepting a few millimeters near the top, will be red hot, as will also the cathode *B* and the upper end of the tube *D*. The bell-jar will have warmed up considerably, too, and usually the middle portion of it will be too hot to be touched by hand, while the upper and lower parts will be relatively cool.

In order that the heating of the vessel may be equalized as much as possible, a hollow cylinder made of sheet brass is placed around the cathode. This cylinder, which is about 9 cm in diameter and 18 cm long, rests on the base-plate and reaches to within about 2.5 cm of the anode *A*. A suitable opening opposite the slot in *C* allows the light to pass out to the spectrograph, while the observer can see the cathode by looking obliquely down between *A* and the top of the cylinder. With this arrangement the heating of the bell-jar is much more uniform and also considerably slower, so that an uninterrupted run of from 30 to 60 minutes becomes possible. Since glass expands considerably with a rise in temperature, while silica expands very little, it is obvious that the ground joint between silica and glass must be located where there is little or no change in temperature. Hence this joint is placed well below the base-plate and is so arranged that it can easily be surrounded by a water bath if necessary.

If the cathode does not come in contact with the tube *C*, and if at the same time is not separated from it by too large a space, the discharge takes place only from the upper surface of *b*. If the separation between *b* and *C* is too large, the discharge tends to start from *B*, or even from the wire below *B*, and passing in a thin stream between *b* and *C* produces intense local heating, which soon causes little arcs to form. If, on the other hand, *b* and *C* are in contact, then, when the discharge has passed long enough to heat *C* to redness, *C* itself begins to act as a cathode, and no result can be obtained. Great care is therefore necessary in adjusting the cathode and the tube *C* so there shall be no contact, even after *b* has become white hot.

The only fault the writer has to find with the present design is that after several runs the inner surface of *C* becomes so thickly coated with the metal of the cathode that a contact or short-circuit is unavoidable. The only remedy is to let in air, remove the bell-jar, and clean the tube, which requires only ten minutes of actual manipulation, but really involves two or three days' delay in the experimental work, as will be more fully explained in connection with the results for chromium.

With several days' continued use the upper surface of the cathode *b* becomes hollowed out into a low, nearly flat-bottomed dish, with a rim from 0.5 to 1 mm thick, which is not affected. In order to be able to observe the discharge at the surface of the cathode from the side, it is of course necessary to remove this rim occasionally. In the present work this has been always done when the depth of the dish reached about 0.5 mm.

As is well known, the electric field is by no means uniform in the Crookes' dark-space, but has its greatest intensity at the surface of the cathode, decreasing as the distance from the cathode increases, until it becomes zero at the edge of the negative glow. The rate of decrease of the field with the distance from the cathode—or, better, the rate of increase with the distance measured from the negative glow—is a matter of considerable importance, and it might be expected that this rate would be different for different apparatus.

In the ordinary Lo Surdo type of tube, which has a diameter of from 1 to 2 mm, Takamine and Yoshida[1] have found that the field-strength varies approximately as the square of the distance from the negative glow, so that the components of the hydrogen lines become approximately parabolic curves, the vertices being in the negative glow. In the present apparatus the field-strength varies almost linearly with the distance, as can be seen from Plate XV*a* which shows $H\gamma$, the n-components above, the p-components below. The components are nearly straight lines. This is a very fortunate circumstance, since one can tell at a glance, when examining lines of other elements, whether the displacement varies linearly with the field-strength or not, merely by seeing whether the components are straight lines or curves.

THE SPECTROGRAPH

This is a plane-grating, two-lens type, with the entire mounting constructed of wood in order that changes might easily be made should experience show that the original design could be improved.

The collimator lens is a Voigtländer portrait objective of 38 cm focus and 10 cm aperture; the camera lens is a Cooke astrographic of $F/4.5$ aperture and 45 cm focus. The grating is a 4-inch Rowland, with 14,438 lines per inch, having a rather bright third order. It is mounted in such a manner that its normal always makes an angle of 70° with the axis of the camera lens. The collimator is fixed in the wooden housing of the spectrograph, in order that the discharge vessel and projection system may remain in a fixed position. The camera and grating can rotate through an angle of about 30° around a vertical axis through the center of the grating surface, thus bringing the different portions of the spectrum on the photographic plate.

---

[1] *Memoirs of the College of Science* (Kyoto Imperial University), **11**, No. 2, pp. 137–146, 1917.

As set up, the third order can be covered from about λ 3000 to λ 5000, and the second order from λ 4500 to λ 7500. By giving the collimator another fixed position, of course it would be possible to observe all of the first order or all of the fourth order instead of the regions chosen. An advantage of this form of mounting is that the dispersion at any given point of the photographic plate is always the same, no matter what region of the spectrum happens to fall there. Hence, the dispersion for all points of the plate having been determined, either by a photograph of a known spectrum or by calculation, a scale in angstrom units may be ruled which will fit all plates closely enough for purposes of identification.

The plates used measure about 6×10 cm, and the plate-holder is movable in a vertical direction, so as to allow several exposures on the same plate. In the third order about 400 A are covered with one exposure, the dispersion varying from about 5.2 A per mm at the violet end to about 3.0 A per mm at the red end. In the second order the dispersion is, of course, just two-thirds of that in the third order.

With short exposures pairs of lines having a separation of 0.1 A can as a rule be resolved. With the longer exposures, which are subject to disturbances from temperature-changes and vibration, the practical limit of resolution is about 0.15–0.20 A. The accuracy of wave-length determinations has been found to be easily of the order of 0.01 A.

An image of the slot in *C*, Fig. 1, is projected with a magnification of one-third on the slit by using two achromatic lenses, each of 20 cm focus and 5 cm diameter. Before falling on the projecting lenses the light passes through a double-image prism, so that two images, one immediately above the other, appear on the slit, the vibrations in the upper image being vertical, or parallel to the slot, in the silica tube *C*.

An exposure usually requires from 20 to 30 minutes, but the vessel has then become so hot that from one to one and a half hours are required to cool it before another exposure can be made. (Of course in future work this waste of time will be eliminated by the construction of a vessel which can be cooled artificially, thus making it possible to operate without stopping.)

About one hundred photographs have been taken up to the present time, nearly one-half of which were made with hydrogen as residual gas. These include spectra of iron, chromium, nickel, vanadium, and calcium. Only chromium has been at all carefully studied, however, and the present paper will be limited to a preliminary report on those lines in the spectrum of chromium which show an electric decomposition.

RESULTS FOR CHROMIUM

The chromium spectrum has been photographed from λ 3670 to λ 5410. In the earlier spectrograms very little of interest from the viewpoint of a Stark effect was observed; the normal arc lines were always present, but of the sensitive lines only faint traces of the groups at λλ 4098, 4111, and 4129 could be seen. These showed, however, a suspicion of an electric effect, and hence for some days this region was photographed repeatedly in the hope of bringing out the effect more clearly. One spectrogram happened to show these groups with an intensity something like one hundred times as great as the others, without, however, any marked increase in intensity of the normal arc lines such as λ 4254. Viewed with a small direct-vision pocket spectroscope, the triplet near λ 5200 is always quite intense, but, when the spectrogram just mentioned, No. 55, was made, it was noted that three lines on the red side of the green triplet had an unusually high intensity. These "lines" were later found to be the groups at λλ 5276, 5298, and 5329, and their appearance was always used to indicate the character of the discharge.

Considerable difficulty was encountered in obtaining another spectrogram like No. 55. The record showed that in making this exposure the current was 30 milliamperes; the length of the dark-space, 5 mm; the voltage, approximately 6000; the exposure time, 20 minutes; and the residual gas, air. These conditions were exactly reproduced time after time, and still only mere traces of the sensitive lines were obtained. In these trials the apparatus was as a rule taken down and thoroughly cleaned between exposures. Since this did not lead anywhere, a number of successive runs were made without taking down the apparatus and without letting in any more gas than just necessary to keep the experimental conditions correct. Then it was found that the sensitive condition as a rule developed quite suddenly after about half a dozen successive runs, and, once formed, seemed to persist in successive exposures, until it became necessary to clean the apparatus as a result of a contact between the cathode and the metal deposited in the tube *C*.

Just what this sensitive condition of the cathode is, the writer is not prepared to say; it can be destroyed by letting in air to a pressure of about 1 cm of mercury or more, it seems to form equally well in air and in commercial oxygen, and a small amount of hydrogen or water-vapor does not seem to prevent it; whether it will form in pure hydrogen is not definitely known, but indications are that it will. An exactly analogous condition has been found for iron and nickel, and it would not be surprising if it should turn out to be quite general.

No doubt it is analogous to the condition of the cathode, which is familiar to those who have had experience with the cathode sputtering of such metals as aluminium, chromium, or even nickel. The discharge may be run for a considerable time without any deposition to speak of taking place. Then suddenly the metal begins to come down, and in a short time a good coating is produced. In the present work it has been observed that the deposition on the inner walls of the tube *C* is much more rapid when the sensitive condition exists than without it; also that the upper surface of the cathode is hollowed out quite rapidly under the same circumstances. The appearance of the dark-space and of the cathode itself is also very different. Without the sensitive condition and with a current of, say, 30 milliamperes, the cathode, as seen from above, is of a purplish-red color, and the dark-space is really very dark, while, with the sensitive condition, the cathode appears greenish-white and the dark-space is bright green and really more luminous, at least near the cathode, than the negative glow.

The lines given in the table were all recorded when the cathode was in the sensitive condition, and no doubt many more could have been recorded with longer exposures; those actually used ranged from a few minutes in the ultra-violet up to about 40 minutes in the region λ 4800–λ 5100. Most of the lines are not to be found in published tables for chromium, hence the question naturally arises: Are they really chromium lines or are they due to some impurity? The writer believes them to be due to chromium, for the following reasons:

1. The stronger lines, such as the groups at λλ 4098, 4111, 4129, 5276, 5298, and 5329, appear regularly as hazy lines in the chromium arc in air and as groups of fine lines in the vacuum arc and vacuum furnace.

2. The weaker lines recorded in the table always appear when the stronger lines are present with sufficient intensity, and do not appear when the latter are weak or absent.

3. None of these lines has been observed when any other metal was used as a cathode, although otherwise the conditions were the same.

This does not exclude the possibility that the lines may be due to some compound of chromium and nitrogen or oxygen; if this be so, then, since all come and go together, it follows that the strong lines λ 4129 and λ 5329, which appear regularly in the ordinary arc, as well as a number of other lines, such as λ 4475.50, which show with great intensity on these spectrograms, must also be due to the same compound. Now, the lines of which λ 4475.50 is an example all appear in the chromium arc as regular, though rather weak, lines; in the present investigation they appear unduly strengthened, but they show no electric decomposition.

The spectrum given by the arrangement used is somewhat different from the arc, spark, or furnace spectrum of chromium. A number of arc lines do not appear at all or appear with a relatively very small intensity; others, again, seem to appear with about the intensity to be expected; while still others are stronger than might

TABLE I

AFFECTED CHROMIUM LINES

λ	INT.	*p*-COMPONENT			*n*-COMPONENT		
		Δλ	Int.	Rate of Displacement	Δλ	Int.	Rate of Displacement
3719.12	2	−0.76	....	=	....	....	....
3720.74	5	+0.48	....	=	Complex	....	....
3722.83	2	+1.07	....	+	....	....	....
3730.09	2	−0.96	....	=	....	....	....
3731.85	5	+0.40	....	−	Complex	....	....
3735.13	2	+0.91	....	=	....	....	....
3744.73	1	−0.29	....	=	....	....	....
3747.41	5	+0.32	....	=	−0.13*	....	=
3750.14	1	+0.63	....	=	....	....	....
3862.07	2	−0.42	....	−	−0.42	....	−
3863.11	1	+0.29	....	?	+0.29	....	?
3865.02	4	+0.25	....	=	+0.18	....	=
3870.28	4	+0.11	....	?	+0.04	....	?
3896.14	1	−1.54	....	+	....	....	....
3926.20	1	−0.16	....	=	−0.16	....	=
3929.87	1	+0.06	....	?	+0.06	....	?
4011.96	4	−0.55	....	=	Complex	....	....
4013.26	4	−0.56	....	=	0.00 −0.44	....	.... =
4013.99	3	−0.54	....	=	Complex	....	....
4096.94	1	....	....	....	−0.66	1	=
4097.41	1	....	....	....	+0.21	2	=
4097.80	3	−0.68	8	+	....	....	....
4098.11	4	....	....	....	−0.18† +0.19	7 7	− +
4098.31	4	+0.84	8	=	+0.84	2	−
4103.40	1	+0.06	1	?	+0.06	1	?
4110.75	1	−0.78	10	=	....	....	....
4111.02	5	....	....	....	+0.23	10	=
4111.49	4	+0.59	10	=	−0.69	2	+
4111.82	3	....	....	....	−0.21 +0.11	2 2	= +
4112.18	1	....	....	....	+0.58	2	=
4117.08	2	+0.13	....	?	+0.13	....	?
4128.34	1	−0.47	6	+	−0.51	2	+
4129.36	7	+0.39	8	+	−0.06 +0.06 +0.20 +0.33 +0.46	5 4 4 4 3	= = = = =
4130.13	3	+0.26	6	=	+0.26	2	−
4130.79	1	+0.40	....	?	+0.40	....	?
4136.25	1	+0.08	....	?	+0.08	....	?
4214.89	3	−0.13	....	=	Complex	....	....
4215.20	3	−0.20	....	=	Complex	....	....
4216.14	3	−0.13	....	=	Complex	....	....

* Other weak *n*-components are present.

† This *n*-component is peculiar, as the displacement is constant throughout the entire dark-space.

TABLE I (*Continued*)

λ	Int.	*p*-component			*n*-component		
		Δλ	Int.	Rate of Displacement	Δλ	Int.	Rate of Displacement
4216.45 ..	3	−0.15	....	=	Complex	....	....
4309.05 ..	2	+0.71	....	+	+0.71	....	+
4353.97 ..	3	+0.86	....	=	+0.86	....	=
4389.37 ..	2	−0.11	....	?	−0.11	....	?
4422.68 ..	3	Complex	....	....	Complex	....	....
4423.15 ..	2	Complex	....	....	Complex	....	....
4423.44 ..	1	Complex	....	....	Complex	....	....
4453.96 ..	2h	+0.79	....	=	−0.43‡	....	=
4472.03 ..	2	+0.65	....	=	Complex	....	....
4490.86 ..	1	−0.32	....	=	....	....	....
4494.92 ..	2	+0.54	....	=	−0.25	....	=
4649.59 ..	3	+0.18	....	−	§	....	....
4900.81 ..	1	+0.30	....	=	....	....	....
4948.25 ..	2	+0.34	....	=	Complex	....	....
4983.84 ..	1	+0.54	....	=	Complex‖	....	....
4984.97 ..	1	+0.30	....	=	Complex	....	....
5005.81 ..	2	−1.41	4	=	−0.43	3	=
		+0.53	1	=	+0.31	3	=
		+1.50	3	=	....	....	....
5027.74 ..	2	−1.60	3	=	....	....	....
		+0.06	2	=	+0.21	4	=
		+0.41	2	=	....	....	....
5028.37 ..	1	+0.92	3	=	....	....	....
5055.69 ..	2	−2.19	1	=	+0.03	2	=
		+0.77	2	=	+0.54	2	=
5056.93 ..	1	+0.42	....	=	....	....	....
5275.44 ..	1	−0.12	2	=	−0.20	2	=
5275.92 ..	2	−0.24	6	+	−0.18	3	+
5276.16 ..	2	0.00	3	....	−0.03	6	?
					+0.45	3	=
5280.81 ..	1	+	....	....	....	....	....
5296.88 ..	1	−0.04	2	?	−0.03	4	?
5297.50 ..	3	−0.34	10	=	−0.27	1	?
					+0.17	2	?
5298.18 ..	2	−0.28	1	?	−0.12	8	−
5298.43 ..	2	−0.06	3	?	−0.03	5	?
5298.92 ..	1	+0.49	8	+	....	....	....
5324.19 ..	1	+0.43	3	?	....	....	....
5328.52 ..	4	+0.16	10	+	0.00	5	....
					+0.14	5	+
5329.34 ..	1	+0.11	4	+	−0.32	4	+
5329.94 ..	1	−0.16	2	?	....	....	....
5330.18 ..	1	....	....	....	+0.38	1	=

‡ There is also an *n*-component to the red.

§ This *p*-component is peculiar, as it seems to run without displacement from the negative glow about half-way through the dark-space, where it stops, but a line appears at this point immediately on the red side which continues without further displacement to the surface of the cathode. Breaks of a similar nature have been observed in the *n*-components of λλ 4097.80, 4111.82, and 4128.34, and the *p*-component of λ 4129.36. Some of these may show in the reproductions.

‖ There is also a *p*-component to the violet.

be expected, the group including λ 4475.50 and the stronger lines given in the table being merely those which are strengthened most. A careful study of the general spectrum given with the present arrangement is of course in order, but until a considerable number of elements have been studied in this way, so that conclusions of general validity can be drawn, it would not add materially to our knowledge, and hence a discussion of those lines of chromium which do not show any electric decomposition will not be undertaken in the present communication.

In the table the first column gives the wave-lengths as determined from the photographs, using as standards the unaffected chromium lines which appear with what is considered normal intensity; the second column gives the relative intensities on a scale of 1–10; the third column contains the displacements of the *p*-components reduced to a field-strength of 12,000 volts per centimeter; the fourth column, the intensity of the components in the stronger part of the field; while the fifth column indicates how the displacement varies with the field-strength: a plus sign (+) signifies that the displacement is proportional to a higher power of the field-strength than the first; an equality sign (=), that it is roughly as the first power; while a minus sign (−) indicates that it varies slower than the first power of the electric intensity. In a few cases where the displacement is very small, or the displaced component happens to overlap a neighboring nitrogen band-line, making measurement difficult, a question mark is placed in this column. The sixth, seventh, and eighth columns give similar data for the *n*-components.

Plate XV*c* shows the groups at λλ 4098, 4111, and 4129; XV*a*, the groups at λλ 5005, 5027, and 5055, while the groups λλ 5276, 5298, and 5329 are given in XV*d*. The *n*-components are above, the *p*-components below, in all cases. A drawing made from the results of the measures of the groups reproduced in *c* and *d* appears in the lower half of the plate.

It will be noticed that to the violet of λ 3900 are seven lines showing *p*-components only—in other words, lines which are apparently plane-polarized in the electric field. They are all weak lines, and hence it is possible that, if the *n*-components belonging

PLATE XV

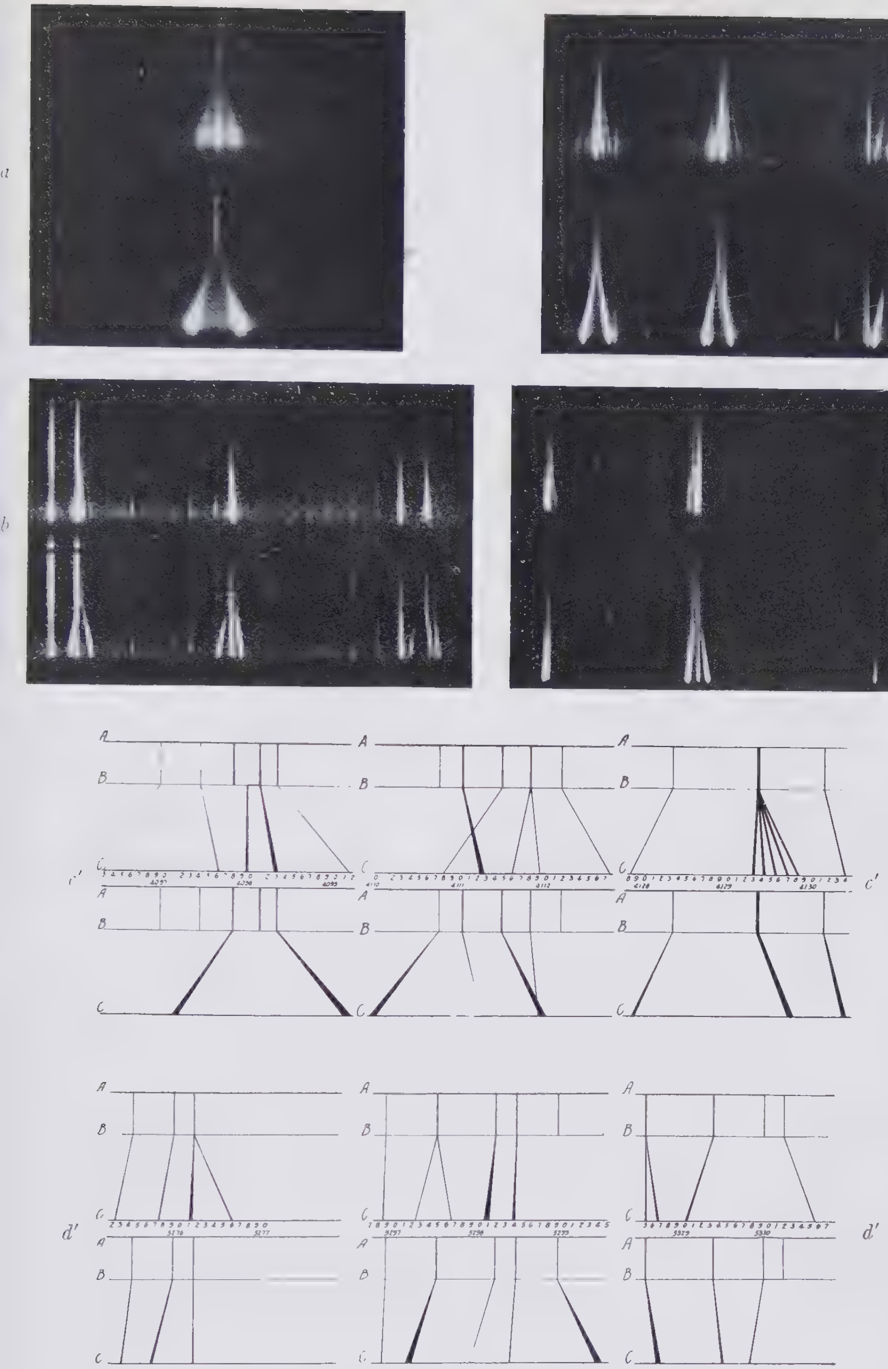

STARK EFFECT

In each illustration the *n*-components are above, the *p*-components below

a, Hγ; *b*, Chromium groups λλ 5005, 5027, 5055;
c, Chromium groups at λλ 4098, 4111, 4129;
d, Chromium groups at λλ 5276, 5298, 5329;
c′, *d′*, drawings representing groups in *c* and *d*,
A–B being the negative glow (field-strength = 0),
C the surface of the cathode (field-strength = 12,000 volts per cm)

to them are complex, they might fail to be registered on account of their very low intensity; and indeed the stronger lines in this region appear to have complex *n*-components. There are, however, several clear cases of lines with only one kind of component—for example, λλ 4097.80 and 4110.75—which have only *p*-components, and λλ 4096.94, 4097.41, 4098.11, 4111.02, 4111.82, and 4112.18, which have only *n*-components.

The lines λλ 4098.11 and 4111.02 are especially interesting; referring to Plate XV we notice that the *p*-component of λ 4098.11 can be traced for only a very small fraction of the distance through the dark-space, while λ 4111.01 can be traced faintly nearly all the way across to the surface of the cathode, although it is clear that the intensity diminishes progressively as we pass down through the dark-space. This shows that in a very weak field both these lines are almost completely unpolarized; as the field increases, they gradually become plane-polarized, λ 4098.11 reaching complete polarization in a much weaker field than λ 4111.02.

A few of the lines belonging to the strong groups near λ 4100 and λ 5300 appear in the solar spectrum, and λ 5297.50 and λ 5329.34 seem well suited for an investigation of possible electric fields in the solar atmosphere.

SUMMARY

1. An apparatus suitable for investigating the Stark effect for metals having a relatively high melting-point is described.

2. With this apparatus the relation between field-intensity and distance from the negative glow is approximately linear.

3. The condition of the cathode is of vital importance.

4. A preliminary survey of the spectrum of chromium from λ 3670 to λ 5410 has been completed and a total of 74 affected lines recorded.

Mount Wilson Solar Observatory
May 1917

Contributions from the Mount Wilson Solar Observatory, No. 135
Reprinted from the *Astrophysical Journal*, Vol. XLVI, pp. 117–137, 1917

A DETERMINATION OF THE GALACTIC CONDENSATION FROM CERTAIN ZONES OF THE *ASTROGRAPHIC CATALOGUE*

BY FREDERICK H. SEARES

In a series of articles recently appearing in the *Monthly Notices*[1] Professor Turner has brought together much valuable material relating to the numbers of stars observed on the photographs for several zones of the *Astrographic Catalogue*. It was his purpose to show that important conclusions may be derived simply by counting the stars within each interval of brightness, even when the scale of luminosity is arbitrary. The result of such counts he has discussed mainly from the standpoint of systematic variations in the distribution of the stars with respect to the Galaxy; but they are perhaps equally important for a determination of the galactic condensation itself, which at present is affected with much uncertainty because of the widely divergent values found by different investigators.

Kapteyn's discussion in 1908[2] of all the material then available led to the conclusion that the concentration toward the Galaxy, which is an easily demonstrated characteristic of the brighter stars, becomes more and more pronounced as increasingly fainter objects are considered. According to his figures the galactic condensation,[3] which for stars of the ninth magnitude is 2.8, rises to 5.7 at the twelfth magnitude; at the fourteenth magnitude its value is 11.5 and at the sixteenth, 27.7. Counts to the limiting magnitude of photographs of 88 Selected Areas made at Mount Wilson with the

---

[1] "A Proposal for the Comparison of the Stellar Magnitude Scales of the Different Observatories Taking Part in the Astrographic Catalogue," *Monthly Notices*, **69**, 392, 1909; **72**, 464, 700, 1912; **75**, 57, 143, 465, 601, 1914–1915; **76**, 2, 149, 1915; **77**, 35, 1916. An article by Pocock in the same journal, **77**, 432, 1917, relates to the same question.

[2] *Groningen Publications*, No. 18.

[3] Ratio of number of stars per unit area at 5° galactic latitude to number at 80°.

60-inch reflector confirm substantially the relatively large value for the faint stars.[1]

The recent investigation by Chapman and Melotte,[2] on the other hand, shows nothing of the rapid increase in the ratio which is so noticeable a feature of Kapteyn's results. From the fifth to the ninth magnitude Chapman and Melotte are in agreement with Kapteyn, but at the sixteenth magnitude their value for the condensation is only 4.2, which is not greatly in excess of that for the brighter stars.

The data collected by Professor Turner contribute directly to the question of this unexplained divergence. In his earlier papers he failed to find any evidence of relatively large numbers of faint stars in the Galaxy,[3] but later the phenomenon was brought to light, and values of the coefficient of condensation were found which are of the same order as that shown by Kapteyn's tables.[4] The matter merits a closer examination, however, for, as will appear later, the Astrographic data afford a striking confirmation of Kapteyn's results as far as the limiting magnitude of the *Catalogue*, which is about 12.5 on the scale of *Groningen Publications*, No. 18.

The numerical data upon which the present discussion is based are given in the upper part of Table I as logarithms of the stellar density N_m—that is, of the total number of stars per square degree to the limiting magnitude m. The limits adopted for Table I are provisionally designated by A, B, C, and D. They are different for the different zones, and later are found to have the values given in the last line of the table. The declination of each zone appears at the head of the table; the hours of right ascension are at the left, while the galactic latitudes corresponding to the middle of each hour are alongside the logarithms of the densities. The quantities below the horizontal line will be explained later.

Comparison with the original tables in the *Monthly Notices* shows that the derivation of the quantities in Table I under the headings A, B, etc., has usually required the formation of the cumulative sums of the numbers of stars for various intervals of brightness within each hour of right ascension. Further, it has been necessary to reduce the results to the square degree as the unit of area. For this purpose the area of an Astrographic plate has been assumed to be 4 degrees. The actual value is 169/144 times this amount,[1] but, as much work had been done before the precise value was discovered, the approximate area was used throughout. The conclusions concerning the galactic condensation are in nowise affected, and, moreover, the totals for the faintest limit in each zone, assuming them to refer to an area of exactly 1 square degree, are probably more nearly correct as they stand, because of the loss of faint stars near the corners of the plates.

---

[1] *Mt. Wilson Communications*, No. 43; *Proceedings of the National Academy of Sciences*, **3**, 217, 1917.

[2] *Memoirs of the Royal Astronomical Society*, **60**, 145, 1914.

[3] *Monthly Notices*, **75**, 607, 608, 1915.

[4] *Groningen Publications*, No. 18, p. 54, 1908.

The mass of material involved is considerable, the real amount being concealed under the summarized form in which it is presented; it represents the results of observations extending over several years at each of nine different observatories. The total area of the zones is nearly 6500 square degrees (that for the Vatican extends from 59° to 65°; the others are 2° wide), or approximately a sixth of the entire sky. The number of stars per zone of course varies with the declination, but ranges from about 30,000 to 80,000 or 90,000; the total is little short of 600,000, although some allowance must be made for the overlap of plates.

The following paragraphs include such details as are necessary for the derivation of the data in Table I from the tabulated counts in the *Monthly Notices.*

Vatican.—Mean counts for zones +64°, +62°, +60°; *M.N.*, **75**, 602, 1915. The original unit is one-tenth of a star per plate of 4 square degrees. Cumulative totals were formed for limiting scale-readings 30 and 0 (A and B in Table I). To reduce to densities (number of stars per square degree), 1.60 must be subtracted from the totals for each hour. Thus, for 0^h the totals are 441 and 9568; their logarithms are 2.64 and 3.98, and the corresponding densities, 1.04 and 2.38, respectively; these appear under the headings A and B in the Vatican section of Table I.

Oxford.—Zone +28°; *M.N.*, **75**, 466, 1915. The original tabular values for 0^h, 1^h, and 2^h are the numbers of stars on 7, 7, and 6 plates, with a repetition of this sequence for the remaining groups

---

[1] *Monthly Notices,* **72**, 466, 1912; **75**, 603, 1915.

TABLE I

Logarithm of Observed Stellar Density, Log N_m

R.A.	Vatican +62°			Oxford +28°				Bordeaux +17°				Toulouse +9°				Algiers −1°		
	Lat.	A	B	Lat.	A	B	C	Lat.	A	B	C	Lat.	A	B	C	Lat.	A	B
0h.....	− 1°	1.04	2.38	−34°	0.49	1.42	1.83	−44°	0.60	1.27	1.58	−52°	0.28	0.99	1.37	−62°	0.88	1.44
1	0	1.19	2.31	−33	0.50	1.34	1.78	−44	0.48	1.30	1.56	−51	0.27	0.95	1.32	−60	0.77	1.36
2	+ 2	1.02	2.13	−28	0.64	1.33	1.78	−38	0.44	1.22	1.49	−45	0.41	0.96	1.40	−53	0.84	1.47
3	+ 6	1.00	2.07	−21	0.67	1.39	1.85	−29	0.55	1.29	1.62	−36	0.33	0.96	1.48	−42	0.92	1.55
4	+10	0.89	1.95	−12	0.37	1.14	1.59	−19	0.47	1.13	1.42	−24	0.58	1.16	1.61	−30	1.14	1.67
5	+16	0.78	2.04	− 1	0.66	1.55	2.12	− 7	0.96	1.75	2.07	−12	0.81	1.42	1.88	−16	1.31	1.80
6	+22	0.74	2.02	+10	0.65	1.80	2.39	+ 6	1.06	1.83	2.20	+ 2	1.34	1.69	2.10	− 3	1.61	2.28
7	+29	0.68	1.92	+22	0.36	1.45	2.15	+18	1.19	1.76	2.08	+15	1.08	1.49	1.96	+10	1.67	2.33
8	+36	0.56	1.69	+35	0.64	1.62	1.94	+32	1.00	1.55	1.81	+28	0.60	1.19	1.70	+24	1.44	2.03
9	+43	0.52	1.59	+48	0.49	1.65	2.02	+44	0.98	1.48	1.69	+42	0.48	1.06	1.58	+36	1.00	1.59
10	+49	0.55	1.64	+61	0.44	1.39	1.78	+58	0.85	1.35	1.52	+54	0.55	0.96	1.35	+48	1.05	1.53
11	+53	0.52	1.53	+75	0.58	1.44	1.76	+71	0.78	1.31	1.59	+64	0.53	0.94	1.35	+56	1.13	1.60
12	+55	0.34	1.54	+87	0.49	1.48	1.87	+79	0.69	1.23	1.62	+70	0.24	0.75	1.22	+60	1.01	1.47
13	+54	0.38	1.54	+79	0.52	1.45	1.75	+75	0.59	1.27	1.58	+68	0.44	0.88	1.31	+58	1.01	1.49
14	+51	0.49	1.57	+66	0.45	1.26	1.69	+62	0.78	1.26	1.50	+58	0.50	0.92	1.30	+51	0.98	1.55
15	+46	0.45	1.63	+53	0.40	1.35	1.72	+50	0.69	1.30	1.70	+46	0.55	1.03	1.52	+40	0.99	1.52
16	+39	0.54	1.72	+40	0.47	1.42	1.82	+36	0.74	1.33	1.73	+34	0.88	1.25	1.63	+28	1.15	1.66
17	+32	0.55	1.69	+28	0.70	1.58	1.92	+24	1.15	1.71	1.97	+20	0.89	1.31	1.79	+16	1.02	1.55
18	+25	0.71	1.87	+15	1.16	1.98	2.41	+10	1.07	1.74	2.05	+ 6	1.30	1.68	2.08	+ 2	1.08	1.51
19	+18	0.68	2.08	+ 3	0.88	1.90	2.45	− 2	1.16	1.84	2.17	− 6	1.12	1.52	1.99	−12	1.24	1.85
20	+12	1.00	2.07	− 8	0.85	1.86	2.31	−14	1.03	1.74	2.09	−19	1.22	1.59	1.95	−24	1.40	1.99
21	+ 7	1.06	2.13	−18	0.58	1.68	2.24	−26	0.73	1.56	1.94	−31	0.75	1.20	1.66	−37	1.26	1.76
22	+ 4	0.96	2.07	−26	0.51	1.60	2.05	−35	0.49	1.41	1.77	−42	0.82	1.20	1.62	−48	0.98	1.48
23	+ 1	1.06	2.22	−32	0.39	1.34	1.82	−42	0.47	1.35	1.71	−49	0.66	1.11	1.46	−58	0.91	1.37
....	0	1.01	2.15	0	0.79	1.81	2.35	0	1.09	1.82	2.18	0	1.27	1.64	2.10	0	1.39	2.02
....	10	0.94	2.10	10	0.75	1.76	2.26	10	1.05	1.77	2.12	10	1.12	1.53	2.00	10	1.37	1.97
....	20	0.76	2.00	20	0.66	1.65	2.12	20	0.92	1.63	1.97	20	0.89	1.36	1.82	20	1.31	1.87
....	30	0.62	1.82	30	0.59	1.51	1.97	30	0.77	1.46	1.78	30	0.72	1.19	1.67	30	1.18	1.74
....	40	0.53	1.67	40	0.54	1.45	1.87	40	0.67	1.33	1.63	40	0.59	1.08	1.54	40	1.05	1.59
....	50	0.49	1.58	50	0.49	1.42	1.82	50	0.62	1.27	1.56	50	0.53	1.00	1.42	50	0.96	1.49
....	60	0.47	1.52	60	0.46	1.38	1.78	.....	.....	.....	.....	60	0.49	0.94	1.32	60	0.95	1.46
....	.....	.....	.....	70	0.45	1.37	1.76	.....	.....	.....	.....	70	0.46	0.89	1.27	.....	.....	.....
Lim. mag.....		9.4	12.0	.....	9.2	11.4	12.5	.....	9.7	11.2	12.0	.....	9.6	10.6	11.6	.....	10.5	11.7

TABLE I—*Continued*

R.A.	Hyderabad −17°				Perth −32°				Cape −41°					Cape −42°			Melbourne −65°		
	Lat.	A	B	C	Lat.	A	B	C	Lat.	A	B	C	D	Lat.	A	B	Lat.	A	B
0h	−77°	0.37	1.36	1.69	−85°	0.61	1.16	1.51	−76°	0.76	1.08	1.48	1.59	−75°	1.21	1.52	−52°	0.81	1.48
1	−75	0.18	1.22	1.61	−78	0.53	1.11	1.45	−73	0.72	1.02	1.41	1.59	−72	1.36	1.59	−51	0.83	1.54
2	−64	0.12	1.26	1.65	−66	0.43	1.10	1.52	−64	0.72	1.02	1.36	1.62	−63	1.27	1.65	−48	0.78	1.42
3	−51	0.17	1.26	1.62	−54	0.52	1.16	1.48	−53	0.83	1.03	1.35	1.61	−53	1.38	1.70	−44	0.89	1.51
4	−38	0.37	1.32	1.76	−40	0.45	1.13	1.58	−42	0.71	1.11	1.50	1.71	−42	1.56	1.85	−38	1.06	1.67
5	−24	0.79	1.66	1.91	−28	0.62	1.26	1.73	−31	0.94	1.47	1.85	2.06	−31	1.75	2.06	−32	1.08	1.76
6	−11	0.77	1.71	2.06	−16	0.86	1.50	1.94	−20	1.07	1.45	1.89	2.05	−20	1.81	2.18	−26	1.20	1.94
7	+ 1	0.61	1.89	2.43	− 4	1.07	1.76	2.16	− 9	1.30	1.78	2.15	2.37	−10	1.94	2.30	−20	1.15	2.05
8	+14	0.49	1.59	2.12	+ 6	1.12	1.88	2.37	0	1.50	1.84	2.24	2.30	0	2.06	2.39	−15	1.22	2.02
9	+25	0.30	1.34	1.84	+15	0.99	1.70	2.12	+ 8	1.34	1.70	2.14	2.33	+ 7	1.88	2.22	−10	1.34	2.17
10	+35	0.11	1.14	1.69	+22	0.94	1.56	1.97	+15	1.00	1.52	2.01	2.23	+14	1.89	2.27	− 6	1.46	2.35
11	+42	0.11	1.16	1.77	+28	0.85	1.52	1.89	+20	0.93	1.43	1.83	2.09	+19	1.55	2.07	− 4	0.93	2.09
12	+45	0.24	1.19	1.70	+30	0.75	1.42	1.81	+22	1.00	1.40	1.88	2.04	+21	1.43	1.90	− 2	1.54	2.40
13	+44	0.40	1.30	1.85	+29	0.76	1.46	1.88	+21	0.93	1.45	1.86	2.13	+20	1.60	2.06	− 3	1.43	2.33
14	+39	0.43	1.47	2.00	+25	0.84	1.58	2.04	+17	0.91	1.39	1.89	2.21	+16	1.60	2.12	− 5	1.48	2.08
15	+31	0.43	1.46	2.03	+18	0.87	1.56	2.01	+11	1.00	1.49	1.98	2.29	+10	1.76	2.30	− 8	1.47	2.41
16	+20	0.48	1.31	1.86	+10	1.02	1.64	2.19	+ 4	1.12	1.51	1.92	2.26	+ 3	1.86	2.33	−12	1.41	2.28
17	+ 8	0.66	1.53	2.17	0	1.32	2.00	2.49	− 6	1.13	1.80	2.25	2.53	− 6	2.07	2.61	−18	0.98	1.93
18	− 4	0.44	1.48	2.19	−12	1.10	1.83	2.36	−16	1.07	1.61	2.20	2.20	−16	2.18	2.71	−24	1.23	2.17
19	−17	0.36	1.42	2.12	−24	0.87	1.48	2.00	−26	0.82	1.31	1.93	1.98	−26	1.73	2.25	−30	0.90	1.72
20	−30	0.35	1.48	2.01	−36	0.63	1.33	1.86	−37	0.79	1.22	1.75	1.84	−37	1.54	1.98	−36	0.84	1.74
21	−43	0.43	1.46	1.82	−48	0.47	1.02	1.55	−49	0.52	1.06	1.43	1.72	−49	1.42	1.87	−42	0.88	1.74
22	−57	0.34	1.31	1.74	−62	0.33	1.00	1.42	−60	0.76	1.12	1.51	1.77	−60	1.37	1.64	−47	0.86	1.65
23	−69	0.21	1.30	1.67	−74	0.69	1.35	1.62	−70	0.84	1.17	1.45	1.66	−70	1.20	1.56	−50	0.60	1.31
....	0	0.60	1.69	2.24	0	1.10	1.82	2.32	0	1.22	1.69	2.19	2.42	0	1.97	2.39	0	1.45	2.28
....	10	0.57	1.61	2.16	10	1.04	1.74	2.22	10	1.12	1.59	2.10	2.33	10	1.87	2.32	10	1.35	2.20
....	20	0.48	1.52	2.01	20	0.90	1.57	2.01	20	0.98	1.45	1.93	2.15	20	1.74	2.15	20	1.17	2.04
....	30	0.39	1.44	1.89	30	0.74	1.38	1.83	30	0.87	1.30	1.77	1.97	30	1.64	2.02	30	1.02	1.82
....	40	0.32	1.38	1.80	40	0.60	1.24	1.69	40	0.81	1.17	1.62	1.82	40	1.53	1.90	40	0.89	1.64
....	50	0.27	1.32	1.73	50	0.55	1.15	1.58	50	0.77	1.10	1.49	1.72	50	1.42	1.77	50	0.82	1.52
....	60	0.24	1.27	1.67	60	0.54	1.11	1.53	60	0.74	1.06	1.44	1.65	60	1.32	1.67	60	0.77	1.46
....	70	0.21	1.24	1.62	70	0.54	1.10	1.51	70	0.73	1.04	1.43	1.62	70	1.27	1.59	.....	.....	.....
....	80	0.20	1.23	1.60	80	0.54	1.10	1.50	80	0.72	1.02	1.42	1.60	80	1.26	1.55	.....	.....	.....
Lim. mag.......	.....	8.8	11.2	12.2	.....	9.6	11.0	12.1	.....	9.9	10.8	11.9	12.4	.....	11.5	12.4	.....	10.2	12.0

of three hours. Cumulative totals were formed for limiting scale-readings 30, 12, and 3 (A, B, and C in Table I), the last also including the values marked "Not measured." The logarithms of the totals were reduced to uniformity by adding log (7/6) = 0.07 to the results for 2^h, 5^h, etc. The constant to be subtracted to reduce the densities is log (4×7) = 1.45. The results for the other Oxford zones included in the discussion in *M.N.*, **75**, 468, cannot be used here, inasmuch as the counts have not been given.

Bordeaux.—Zone +17°; *M.N.*, **72**, 465, 1912. The original numbers are for each half-magnitude interval of the Bordeaux scale. The total number of plates is 180, an average of 7°5 per hour; the actual number is probably 7 and 8 per hour, alternately. There is no statement as to whether the results for the various hours have been reduced to the mean area of 7°5, but, since the correction to the logarithms is only 0.03, alternately positive and negative, the uncertainty is of no consequence and the data can be used as they stand. Cumulative totals were formed for the limits 8.5, 10.0, and 12.0 (A, B, and C in Table I). The constant to be subtracted from the logarithms to reduce to densities is log (4×7.5) = 1.48.

Toulouse.—Zone +9°; *M.N.*, **76**, 150, 1915. The original values are cumulative totals. The limits here adopted are 9.5, 11.0, and 12.3 of the Toulouse scale (A, B, and C in Table I). The totals for 13.3 are not used because of incompleteness. The total number of photographs is 180; the remarks concerning the distribution of the Bordeaux plates also apply here, and the constant is again 1.48.

Algiers.—Zone −1°; *M.N.*, **72**, 700, 1912. In the original tabulation the declination is erroneously given as +1° (*M.N.*, **76**, 155). Cumulative totals were formed for the limits 10.0 and 12.0, inclusive, of the Algiers scale (A and B in Table I). The total number of plates is 180, in groups of 7 and 8, alternately, for the successive hours of right ascension. From the remark under (*b*) *M.N.*, **72**, 702, 1912, it is inferred that the tabulated counts on page 700 have not been referred to the mean area of 7.5 square degrees per hour. To reduce to densities, 1.45 and 1.51 were therefore subtracted alternately from the logarithms of the cumulative totals for the successive hours.

Hyderabad.—Zone −17°; *M.N.*, **77**, 434, 1917. The original tabulation by Pocock gives cumulative totals. Those for N_{50}, N_{20}, and N_8 (A, B, and C in Table I) were adopted. The number of plates is alternately 8 and 7 for the successive hours; but the published totals are for a constant area of 40 square degrees. To reduce to densities, 1.60 has been subtracted from the logarithms.

Perth.—Zone −32°; *M.N.*, **75**, 144, 1915. Cumulative totals have been formed for the limits D, G, and M, inclusive, of the Perth scale (A, B, and C in Table I). The number of plates is alternately 6 and 7, but the tabular values refer to an area of 40 square degrees and the constant is 1.60.

Cape.—Zone −41°; *M.N.*, **75**, 59, 1914. Cumulative totals have been formed for the limits 149, 79, −3, and −5, inclusive, of the Cape scale (A, B, C, and D in Table I). The number of plates is 6 per hour, with a total area of 24 square degrees. To reduce to densities, 1.38 has been subtracted from the logarithms of the totals.

Cape.—Zone −42°; *M.N.*, **76**, 3, 1915. Cumulative totals for "Measured" and "All" stars are given in the original tabulation. Their logarithms, minus the constant 1.38, appear in Table I under the headings A and B. The remaining Cape zones discussed in *M.N.*, **76**, 151, cannot be used for the present purpose.

Melbourne.—Zone −65°; *M.N.*, **77**, 39, 1916. The original tabulation gives cumulative totals. Those adopted are for the limits 15 and "All" (A and B in Table I). The number of plates is 3 per hour, except for hours 1, 4, 7, etc., where the number is 4. The constants for reduction to densities are, respectively, 1.08 and 1.20.

The reliability of the data collected in Table I depends mainly upon two things: first, the constancy of the limiting magnitude for the photographs of any given zone; second, the consistency of the scale of luminosity in which the results for the brightness are expressed. Thus given designations of brightness—for example, scale-readings 30 and 0 for the Vatican zone, which are the limiting values used here—must represent the same degree of brightness wherever they occur in that zone; otherwise the only method which can now be applied to these data for the investigation of the distribution of the stars with respect to the Galaxy will not give dependable results. We have not at present the information necessary for the reduction of the brightness, referred usually to a more or less arbitrary scale, to an absolute scale of magnitudes. Consequently it is vital that the adopted limits should always mean the same thing within any given zone, and that the enumeration of the stars to that limit should be complete.

It is too much to suppose that the conditions thus implied have been rigorously satisfied. Constancy of exposure-time for all the photographs of a zone is of course presupposed, although occasional variations are known to have occurred. But, even with equality in the exposures, absolute uniformity in the limiting magnitude is not to be expected; more or less systematic fluctuations with the seasons are almost certain to occur. The sky is more transparent at one time of year than another, and, even when transparent, the atmosphere, during the winter months, is less tranquil, with a resulting diffuseness of definition in the photographic images that leads to errors of measurement. Seasonal differences in temperature and humidity modify both the sensitiveness and the gradation of the photographic plate, which in turn affect both the limiting magnitude and the consistency of the scale.

It is impossible to specify in advance the extent to which these and other disturbing factors have influenced the data with which we are concerned. Two or three circumstances affecting the completeness of the counts may be mentioned, however: As a rule, photographs for the Oxford zones were rejected unless the number of stars showing two images was at least three times the number recorded by Argelander, but this practice was not followed in the Milky Way. Only three of the plates for the zone at +28° fall below this limit, however.[1] Again, the scale of brightness for the Melbourne zone exhibits a peculiarity caused by the use of different machines for the measurement of the images.[2] A considerable inconsistency affects the results, but apparently only those for the brighter stars. The difficulty has largely been avoided by choosing scale-reading 15, which is beyond the point where the large irregularity begins, as the first limit for the data in Table I. Finally, in the case of the Hyderabad zone, there were large differences in the exposure-times and considerable variations in the sensitiveness of the plates;[1] but apparently an attempt was made to adjust these two factors in such a way as to approximate a constant limiting magnitude. The results at least seem to be as consistent as those of some of the other zones.

---

[1] *Astrographic Catalogue*, Oxford Section, Vol. 4, p. ix, 1908.

[2] *Monthly Notices*, **77**, 36, 1916.

We shall later find evidence of irregularities in all of the zones, but for the present we assume that these exercise upon each other a compensation which reduces to a minimum their influence upon the calculated mean distribution of the stars with respect to the Galaxy.

For the derivation of the mean distribution from the values in Table I we first eliminate as completely as possible the systematic irregularities, whether observational or real in origin, as well as the accidental errors that may have affected the counts. This is accomplished by plotting the numbers in each column with their corresponding galactic latitudes as abscissae. From the smooth curves thus obtained are derived the ordinates for equidistant intervals of galactic latitude which appear below the horizontal line in the lower portion of Table I.

The dispersion of the plotted points with respect to the curves, especially when their sequence in right ascension is borne in mind, reveals at once the more conspicuous irregularities. Thus the Vatican results are closely accordant; we find nearly the same value of the density corresponding to a given galactic latitude, irrespective of the right ascension in which the region is located. The same is true of the Cape zone at −41°, and to a less degree of the C group for Toulouse. On the other hand, the A group in the Toulouse zone and the results for Oxford, Bordeaux, and Algiers show large variations of density with right ascension, which obviously are not directly a function of the galactic latitude. The densities for Melbourne are relatively free from systematic irregularity, but their accidental deviations seem rather large.

Later, when it has become possible to refer the data to an absolute scale of magnitudes, we shall be able to distinguish in advance many of the irregularities that are observational in origin from those which represent real variations in the stellar distribution; and we shall then be in a better position to derive results for the mean distribution. At present we can only assume that the counts for regions in right ascensions differing by twelve hours have been systematically influenced in opposite directions by equal amounts. This at least is a plausible supposition so far as any seasonal effect is concerned. It is on this basis that the curves have been drawn for those zones which show large variations with right ascension.

---

[1] *Ibid.*, 77, 433, 1917.

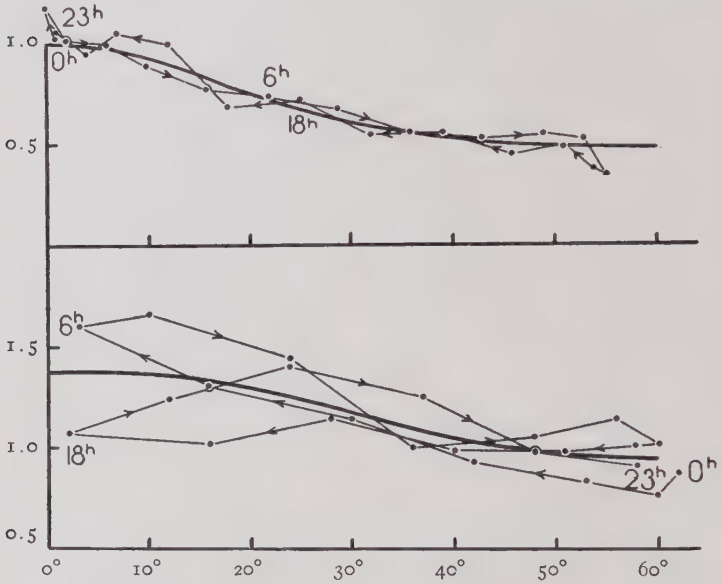

FIG. 1.—Stellar density and galactic latitude. Stars of Group A, Vatican zone, +62° (upper curve), and of Group A, Algiers zone, −1°. Note in lower curve the systematic deviations depending on right ascension.

By way of illustration, two of the curves, those for the A groups of the Vatican and Algiers zones, are reproduced in Fig. 1. The broken line connects the points for adjacent hours of right ascension. For the Vatican curve there are no conspicuous irregularities, but for the Algiers results a different state of affairs exists. Note, for example, the systematic deviation in the plotted densities for 5, 6, and 7 hours from those of 17, 18, and 19 hours, yet the adopted curve probably represents, for the zone, the mean variation of density with latitude with a tolerable degree of precision. The mean densities in the lower part of Table I should therefore be comparatively free from systematic irregularities which depend upon the right ascension.

The material has now to be combined into a final result. It may be remarked parenthetically that the mean data for each zone give directly a clear indication of the relatively high galactic condensation for the faint stars. In every case but one the difference between the values of log N_m standing in adjacent columns opposite 0° is larger than it is for the higher galactic latitudes in the last lines of Table I; in other words, with decreasing brightness the densities increase faster in the Galaxy than they do near the poles of the Milky Way.

The limits of brightness designated by A, B, C, and D were arbitrarily chosen, and thus far their precise relative values have not been determined; but for a combination of the data they must be referred to a numerical scale. We may use either that of Chapman and Melotte or that adopted by Kapteyn in *Groningen Publications*, No. 18. The latter has been chosen, since one of the purposes of the discussion is a detailed comparison of the results from the Astrographic material with the distribution tables of Kapteyn.

The transformation of the limits A, B, etc., into magnitudes depends upon the assumption that, for a given galactic latitude, equal mean densities correspond to the same limiting magnitude, whatever the position of the regions involved. Experience has proved that this supposition is reliable to a high degree, provided the areas compared are not too small; in the present case they are more than ample. With the mean densities (more precisely, the means of the logarithms of the densities) in the lower part of Table I as argument, we have only to interpolate from Kapteyn's tables,[1] for the proper latitude, the corresponding value of the magnitude. The results of this operation appear in the last line of Table I, which contains the mean of the limiting magnitudes thus derived from each of the densities standing immediately above.

---

[1] *Groningen Publications*, No. 18, p. 54, 1908.

In case the observed changes in density with latitude for any limit of brightness—for example, limit A of the Vatican data—were the same as that indicated by Kapteyn's tables, the result of the interpolation would naturally be the same for all the latitudes. The agreement of the individual values of the interpolated magnitudes is shown by Table II. This gives the deviation (individual *minus* mean), in tenths of a magnitude, from the mean limits at the head of the table which have now replaced the provisional designations A, B, etc. Though generally systematic, the residuals are remarkably small and show at a glance that the galactic condensation from the Astrographic data is substantially that found by Kapteyn; the excess of negative signs for 0° denotes a slightly brighter limit for this zone than the average, and consequently a small excess of density in the Galaxy for Kapteyn's results as compared with those from the Astrographic counts.

TABLE II

DEVIATIONS FROM MEAN LIMITING MAGNITUDE
(Unit=0.1 mag.)

Gal. Lat.	+62°		+28°			+17°			+9°			−1°	
	9.4	12.0	9.2	11.4	12.5	9.7	11.2	12.0	9.6	10.6	11.6	10.5	11.7
0°	0	−2	−2	−3	−3	−1	−1	−2	+4	+1	+1	−3	−2
10	+1	−1	−1	−2	−3	0	0	0	+3	+1	+1	−1	−1
20	0	+1	0	0	−1	+1	+1	+1	+1	+1	+1	+1	+2
30	0	+1	+1	0	0	0	+1	0	0	0	+1	+1	+2
40	−1	0	+1	+1	0	−1	0	−1	−1	0	+1	0	+1
50	−1	−1	+1	+1	+1	−1	0	−1	−2	−1	−1	−1	0
60	−1	−1	+1	+1	+1	....	....	....	−2	−2	−2	0	+1
70	....	....	+1	+2	+2	....	....	....	−3	−2	−2	....	....

Gal. Lat.	−17°			−32°			−41°				−42°		−65°	
	8.8	11.2	12.2	9.6	11.0	12.1	9.9	10.8	11.9	12.4	11.5	12.4	10.2	12 0
0°	−2	−4	−2	0	+1	0	0	0	0	−1	−1	−1	+1	0
10	−1	−3	−2	+1	+1	+1	0	0	0	0	−1	0	+1	+1
20	0	−1	0	+1	+2	+1	0	+1	+1	+1	+1	+1	+1	+2
30	+1	0	+1	0	+1	0	0	+1	+1	+1	+2	+2	+1	+1
40	0	+1	+1	−1	0	0	+1	0	0	0	+2	+2	−1	−1
50	0	+1	+1	−2	−1	−2	0	−1	−2	−1	0	0	−1	−2
60	0	+1	+1	−1	−1	−1	0	−1	−2	−1	−1	−1	−2	−2
70	−1	+1	+1	−1	−1	−1	+1	−1	−1	−1	−1	−1	....	....
80	−1	+1	+2	−1	0	0	+1	−1	−1	0	−1	−2	....	....

We are not concerned with these differences for the moment, however; the further combination of the results depends only on the mean limiting magnitude of each zone as a whole. Since these quantities are now referred to the same scale of brightness, the densities to which they correspond are directly comparable and may be united for a further elimination of the errors. Here again a graphical method is convenient. The entire series of mean densities in the lower part of Table I is plotted with the corresponding limiting magnitudes as abscissae. The smooth curve for the points of any given latitude represents the finally adopted variation of density with magnitude for that latitude. The ordinates of these curves have been collected in Table III, which for a limited range in magnitude is the equivalent of Kapteyn's table of densities. The differences between the two tables, in units of the second place of decimals, are given in Table IV. The slightly smaller densities for latitude 0° resulting from the Astrographic material are indicated by the persistent negative sign in the second column of Table IV.

TABLE III

LOG N_m, NUMBER OF STARS PER SQUARE DEGREE BRIGHTER THAN m FOR DIFFERENT GALACTIC LATITUDES

Mag.	0°	10°	20°	30°	40°	50°	60°	70°	80°
8.5	0.50	0.45	0.32	0.24	0.18	0.14	0.12	0.11	0.10
9.0	0.75	0.70	0.56	0.46	0.39	0.34	0.31	0.31	0.30
9.5	1.03	0.96	0.82	0.70	0.61	0.55	0.52	0.51	0.50
10.0	1.29	1.20	1.06	0.94	0.83	0.77	0.73	0.72	0.72
10.5	1.52	1.44	1.30	1.16	1.04	0.98	0.93	0.92	0.92
11.0	1.75	1.67	1.53	1.38	1.25	1.19	1.14	1.12	1.11
11.5	1.99	1.90	1.75	1.60	1.47	1.40	1.35	1.32	1.29
12.0	2.22	2.13	1.97	1.82	1.68	1.60	1.55	1.51	1.46
12.5	2.45	2.36	2.19	2.03	1.90	1.81	1.74	1.69	1.63

A reference to the first series of curves, whose ordinates are summarized in the lower part of Table I, shows that most, if not all, of the systematic differences in Table IV are within the uncertainty of the reduction, and that the curves could be redrawn, without doing any violence to the original data, in such a manner as to remove almost entirely the systematic effect. We may therefore regard the results from the *Astrographic Catalogue* as affording a practically complete confirmation of Kapteyn's values of the galactic condensation for the interval of four magnitudes between 8.5 and 12.5.

TABLE IV

COMPARISON WITH THE DENSITY TABLE OF KAPTEYN
(Table III *minus* Kapteyn, Unit 0.01)

Mag.	0°	10°	20°	30°	40°	50°	60°	70°	80°
8.5	−3	0	0	+2	+2	+1	+1	+1	0
9.0	−3	0	0	+1	0	−2	−2	−1	−2
9.5	−1	+1	+3	+2	0	−3	−3	−3	−1
10.0	0	+1	+3	+3	0	−2	−3	−2	−1
10.5	−1	+1	+4	+3	0	−2	−4	−2	+1
11.0	−3	0	+4	+3	−1	−2	−3	−2	−1
11.5	−3	−1	+4	+4	+1	−1	−1	0	−1
12.0	−4	−1	+3	+4	+1	0	0	+1	−2
12.5	−5	−1	+4	+5	+3	+2	+2	+1	−1

Since the value of the condensation is often expressed as the ratio of the number of stars at latitude 5° to the number at 80°, the results are also given in this form in Table V, alongside the corresponding ratios for Kapteyn and for Chapman and Melotte.

TABLE V

GALACTIC CONDENSATION. RATIO OF NUMBER OF STARS AT 5° TO NUMBER AT 80°

	Magnitude								
	8.5	9.0	9.5	10.0	10.5	11.0	11.5	12.0	12.5
Astrographic Catalogue	2.4	2.7	3.2	3.5	3.8	4.2	4.7	5.4	6.2
Kapteyn	2.6	2.8	3.1	3.4	3.8	4.3	4.9	5.7	6.7
Chapman and Melotte	2.6	2.7	2.8	3.0	3.1	3.2	3.3	3.4	3.5

It is scarcely necessary to remark that the values here found for the condensation are entirely independent of the fact that we have used Kapteyn's tables for the determination of the limiting magnitudes; the result would have been the same had the different zones been reduced to a homogeneous system by the tables of Chapman and Melotte.

It is now of interest to examine the outstanding irregularities in the original data of Table I when compared with the mean densities of Table III. For this purpose the mean densities and latitudes were first formed for 0^h and 1^h, 2^h and 3^h, etc., for the groups of each zone. Since the values in Table I refer to the middle of the hours of right ascension, the results thus derived correspond to the exact hours—1^h, 3^h, etc. The comparison with Table III gives the residuals O.−C. shown in Table VI, in units of the second place of decimals. The means, both with and without regard to sign, are at the bottom, the former being the systematic deviations

TABLE VI

Deviations of Observed Densities from the Mean Distribution
(Unit=0.01 in the logarithm)

R.A.	+62°		+28°			+17°			+9°			−1°	
	9.4	12.0	9.2	11.4	12.5	9.7	11.2	12.0	9.6	10.6	11.6	10.5	11.7
1^h	+15	+12	− 4	−13	−18	−14	− 3	− 8	−30	− 4	− 9	−11	− 3
3	+ 7	− 8	+ 3	−29	−31	−25	−16	−20	−29	−12	− 7	−11	+ 1
5	− 3	− 8	−30	−55	−54	−29	−28	−34	−19	− 9	− 8	− 4	− 6
7	+ 2	+ 9	−22	−15	+ 1	+10	+ 7	+ 4	+19	+ 8	+ 6	+15	+26
9	− 3	− 4	+ 9	+22	+10	+27	+15	+ 4	−16	− 2	+ 6	+ 6	+12
11	+ 4	− 2	+12	+13	+ 7	+22	+12	+ 3	− 2	− 3	− 5	+12	+ 9
13	−13	− 4	+12	+22	+19	+ 5	+ 6	+13	−21	−14	−10	+ 9	+ 4
15	− 4	− 2	+ 3	− 1	− 4	+12	+ 4	+ 3	− 6	− 3	− 2	− 2	+ 3
17	− 6	− 4	+ 5	− 1	−11	+15	+ 5	+ 3	+10	+ 4	+ 3	−19	−21
19	− 5	+ 3	+21	+ 8	+ 6	+ 2	− 2	− 7	+13	+ 3	0	−32	−36
21	+13	− 3	− 4	− 5	− 3	− 3	+ 3	+ 5	+18	+12	+ 8	+17	+19
23	+ 5	− 6	−13	−12	−12	−24	+ 1	+ 3	+12	+12	+ 7	− 2	− 4
Syst. dev.	+ 1	− 1	− 1	− 6	− 8	0	0	− 3	− 4	− 1	− 1	− 2	0
Av. dev.	7	5	12	16	15	16	8	9	16	7	6	12	12

R.A.	−17°			−32°			−41°				−42°		−65°	
	8.8	11.2	12.2	9.6	11.0	12.1	9.9	10.8	11.9	12.4	11.5	12.4	10.2	12.0
1^h	+ 5	+10	+10	+ 3	+ 3	0	+ 7	+ 1	− 2	− 5	− 3	− 8	− 3	− 8
3	−10	+ 3	0	− 8	− 1	− 9	+ 9	− 4	−16	−10	− 4	− 4	− 4	−17
5	+22	+ 3	− 6	−17	−13	−14	− 1	+ 8	− 2	− 3	+14	+ 5	+10	− 3
7	+ 7	0	− 2	− 4	− 4	−12	+ 9	+10	0	− 3	+ 6	+ 2	+ 6	+ 8
9	− 6	−16	− 7	+ 6	+12	+ 7	+22	+14	+ 6	− 4	+ 2	− 6	+ 1	0
11	−20	−22	− 7	+10	+ 8	− 1	− 8	0	− 4	− 1	− 9	− 4	−14	+ 4
13	+ 4	− 7	+ 5	+ 2	+ 6	− 2	− 2	+ 1	− 3	− 3	−23	−16	+12	+16
15	+ 9	+ 6	+18	+ 2	+ 7	+ 4	−13	− 8	− 9	+ 1	−18	− 5	+15	+ 7
17	+ 3	−28	−13	+13	+11	+12	−11	0	− 8	+ 1	− 1	+ 9	− 3	+ 5
19	−20	−31	− 6	+ 9	+10	+14	− 6	+ 4	+16	− 3	+22	+36	− 1	+ 8
21	+ 6	+ 8	+ 9	−10	− 6	− 1	−11	0	− 3	− 5	+ 3	+ 9	− 6	+ 5
23	+ 5	+ 9	+ 8	− 4	+ 6	− 4	+12	+10	− 2	+ 4	− 6	− 8	−14	−14
Syst. dev.	0	− 5	+ 1	0	+ 3	0	+ 1	+ 3	− 2	− 3	− 1	+ 1	0	+ 1
Av. dev.	10	12	8	7	7	7	9	5	6	4	9	9	7	8

of the groups, the latter the average deviation of the mean of a pair of densities, from the adopted values in Table III.

The systematic differences are unimportant and attract attention only in those cases (mainly in the Oxford zone at $+28^\circ$) in which two or three abnormally low values were more or less ignored in drawing the original curves. Had the corresponding residuals likewise been disregarded in forming the means for Table VI, the systematic deviations would have been small throughout. The small average deviations for the Vatican zone at $+62^\circ$ and the Cape zone at -41° recall the remark of an earlier paragraph concerning the internal consistency of the results for these zones.

Examining the individual residuals, we find numerous instances of persistence of sign, which show clearly a more or less regular variation in the observed densities with right ascension. Moreover, the similarity in the sequence of signs for the different limiting magnitudes within a given zone suggests that the variations in the observed density have the same general character for stars of all degrees of brightness.

To exhibit more clearly the nature of the irregularities, the left-hand set of curves shown in Fig. 2 has been prepared. Their ordinates are the means, for each zone, of the deviations shown in Table VI for each hour of right ascension; the abscissae are right ascensions. To avoid confusion, the results for the two Cape zones at -41° and -42°, which are much alike, have been combined. There are occasional similarities in the curves which are suggestive—for example, the first 12 hours for the zones at $+28^\circ$, $+17^\circ$, $+9^\circ$, and -1°; but, so far as the present data alone are concerned, it is impossible to say whether the irregularities represent real variations in the distribution of the stars or nothing more than a seasonal influence upon the limiting magnitude and gradation of the photographic plates, superposed upon accidental errors of observation.

If now we examine the relation of the results thus derived to the spiral[1] found by Turner to characterize the distribution of the stars of these same zones of the *Astrographic Catalogue*, we must consider the deviations in Table VI from a different standpoint. The curve in question, whose equation is

$$\alpha+3.66\,\delta=247^\circ,$$

---

[1] *Monthly Notices*, **76**, 7, 152, 1915.

represents the median line of a region of "obscuration" in which the ratio of the density of the faint stars to that of the bright stars is relatively small. Within any given zone—that is, for a constant declination—Turner has found the value of this ratio to vary with

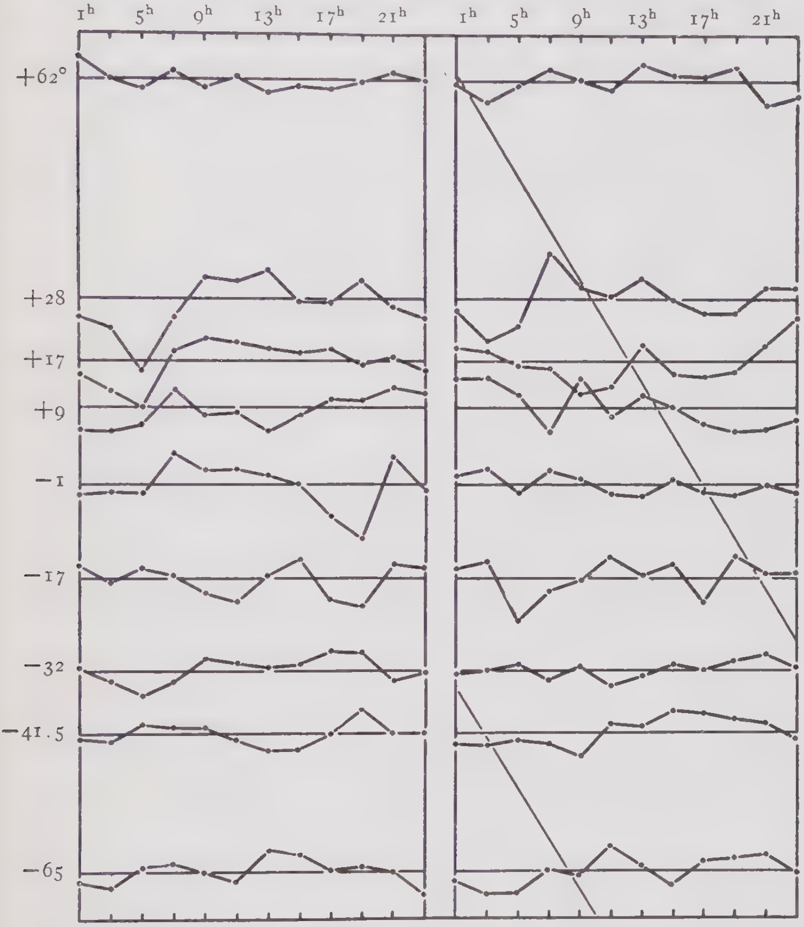

FIG. 2.—Irregularities in observed densities for various Astrographic zones. Vertical spacing of curves proportional to declination of zones given at the left; abscissae are right ascensions.

Left: Deviations from mean distribution shown in Table III. Ordinates are the means, for each hour, of the quantities in Table VI.

Right: Deviations in ratio of faint stars to bright. Ordinates are differences, last group *minus* first group, of quantities in Table VI. The median line of Turner's spiral of obscuration is indicated by the inclined lines.

right ascension between limits which depend upon the limiting magnitudes.

For a comparison with this result we may begin by forming the differences of the logarithms of the densities in Table I for the extremes of limiting magnitude there shown. It is simpler, however, to form the differences, for the extreme magnitudes in each zone, of the residuals given in Table VI. Since the deviations themselves have the form O.−C., the difference of any pair, for the limiting magnitudes F and B, may be written

$$\delta=(\log D_{\mathrm{F}}-\log N_{\mathrm{F}})-(\log D_{\mathrm{B}}-\log N_{\mathrm{B}}) \tag{1}$$

or

$$\delta=\log\frac{D_{\mathrm{F}}\,N_{\mathrm{B}}}{D_{\mathrm{B}}\,N_{\mathrm{F}}} \tag{2}$$

in which the values of D and N are the observed and the mean tabular densities, respectively (Tables I and III), for the two limits.

It is the variation of δ with right ascension in which we are interested; $D_{\mathrm{F}}/D_{\mathrm{B}}$ is the ratio of the density of the faint stars to that of the bright stars, and $N_{\mathrm{B}}/N_{\mathrm{F}}$ a factor, varying with galactic latitude but not longitude, which neutralizes the influence of the relatively high galactic concentration of the faint stars toward the Galaxy. In other words, as is evident at once from Table VI, the difference in the deviations for a faint and a bright limit is the logarithm of the ratio of the number of faint to bright stars in excess of the normal ratio corresponding to the mean distribution shown in Table III.

The variation of δ with right ascension is shown by the right-hand set of curves in Fig. 2, whose ordinates were obtained by subtracting the first column for each zone in Table VI from the last, after correction for the systematic deviations at the bottom. The fluctuations are of the same order of magnitude as those shown in the other part of the figure; some similarities of form are vaguely suggested, although there is nothing that cannot be accounted for on the basis of inherent uncertainties in the data; but, whether the fluctuations are real or not, there is obviously no relation between them and Turner's spiral, which is represented by the inclined lines crossing the figure. An agreement with his results would require a well-defined minimum in each of the curves at the point of intersection with the spiral. Moreover, the amplitude of the variations shown in Fig. 2 is much less than that required, for his difference between the "unobscured" and "obscured" regions amounts to about 0.4 in the logarithm of the ratio of faint stars to bright.[1]

In seeking an explanation for this divergence, we may consider equation (2). Unless I have misunderstood his method of reduction, Professor Turner has treated the variations in the quantity log D_F/D_B as though they were independent of the galactic condensation; this indeed could be done, were the condensation not dependent upon brightness. Thus in *M.N.*, **76,** 3, 1915, Table I, zone −42°, he has given the deviations of log A/M (another notation for log D_F/D_B) from its mean value; and on the following page he discusses the sequence of signs for these deviations, and for a similar series for zone −41°, from the standpoint of the "obscured" region. Later, these same deviations, modified by a constant, reappear in Table IV, *M.N.*, **76,** 153, 1915, where they are subjected to the analysis which leads to the spiral whose equation is given above. Again, the deviations given in *M.N.*, **75,** 468, 1915, Table III, for the differences of the logarithms of the densities corresponding to two limiting magnitudes enter unchanged into Table VI, p. 156 of Vol. **76.**[2] In neither case has there been any allowance, apparently, for the galactic phenomenon in deriving the spiral; and, similarly, in the preliminary description of the obscured patches shown in *M.N.*, **75,** 480, 1915, the discussion seems always to be based upon the unmodified ratio of the number of faint stars to the number of bright stars. In fact, only traces of the relatively high condensation of the faint stars had been detected in the Astrographic counts when the first account of the obscured areas was prepared.[3]

The quantity whose variations have been studied by Professor Turner, and upon which he has based his conclusions, is, therefore, by equation (1),

$$\delta' = \log D_F - \log D_B = \delta + \log N_F - \log N_B \qquad (3)$$

---

[1] *Monthly Notices*, **75,** 480, 1915.

[2] Here, as in Table IV of the same article, the first difference is for the hour of right ascension which stands at the head of the column.

[3] *Monthly Notices*, **75,** 481, 1915.

which differs from the quantity δ whose values are shown graphically in Fig. 2 by the amount $\log N_F/N_B$. But this latter quantity is not independent of the galactic latitude. Its variation is a consequence of the relatively high galactic concentration of the faint stars. Were the condensation the same for stars of all magnitudes, its value would be a constant for any pair of limits F and B; but, as we approach the Galaxy, the faint stars increase in numbers more rapidly than the bright ones, with a resulting increase in $\log N_F/N_B$.

There is a wide range in the galactic latitudes of the Astrographic zones, and the changes in the factor $\log N_F/N_B$ accounts for a large part of the variation in $\log D_F/D_B$ studied by Professor Turner. When their influence is removed, there remain only the differences δ illustrated in Fig. 2. It is thus evident that high latitudes will contribute toward the formation of an "obscured" region; a reference to the diagram in *M.N.*, **75**, 480, 1915, shows that in general the centers of these regions are remote from the Galaxy. Again, the sequence of numbers in the last column of Table IV, *M.N.*, **76**, 153, 1915, which represent the amount of the obscuration phenomenon per magnitude, is approximately duplicated by the variations in the values of $\log N_F/N_B$ interpolated from Table III for the appropriate latitudes and for limiting magnitudes differing by $1^{M}_{.}0$; for example, 12.5 and 11.5. Since the curves in Fig. 2 reveal no trace of the spiral of obscuration, it seems necessary to attribute the origin of that phenomenon to the influence of the relatively high concentration of the faint stars in the galactic regions.

The question under consideration is really that of the uniformity of the stellar distribution in galactic longitude. The evidence presented here suggests that the irregularities cannot be large, at least for the fainter stars, and this conclusion is strengthened by an examination of the densities derived from the photographs of the Selected Areas made with the 60-inch reflector.[1] The limiting magnitude for these plates is about 17.5; a noticeable variation of density with right ascension is present, but it is of the character to be expected from seasonal influences. The counts on the

---

[1] *Mt. Wilson Communications*, No. 42; *Proceedings National Academy of Sciences*, **3**, 188, 1917.

Franklin-Adams plates,[1] limiting magnitude about 17, show even smaller systematic irregularities than those affecting the Mount Wilson photographs. Neither the Mervel Hill nor the Johannesburg series of plates reveals any variation in right ascension or galactic longitude that cannot reasonably be attributed to accidental errors.

SUMMARY

Counts collected by Professor Turner of nearly 600,000 stars on the photographs for 10 zones of the *Astrographic Catalogue*, extending from declination +62° to −65°, have been discussed from the standpoint of stellar distribution with respect to the Galaxy. The galactic condensation found is very nearly that derived by Kapteyn (Tables III, IV, and V). The deviations of the observed densities (Table VI) from the mean distribution show systematic variations in right ascension which are definite, but not larger than the uncertainties affecting the results. They are not in agreement with the spiral of obscuration derived by Turner from the same data; the origin of this latter phenomenon is to be found in the failure to allow for the high galactic concentration for the faint stars.

Mount Wilson Solar Observatory
June 1917

---

[1] *Memoirs of the Astronomical Society*, 60, 171, 1914.

Contributions from the Mount Wilson Solar Observatory, No. 136

THE PHOTOGRAPHIC DETERMINATION OF STELLAR PARALLAXES WITH THE 60-INCH REFLECTOR

SECOND SERIES

By ADRIAAN VAN MAANEN

Since the publication of the detailed results for the parallaxes of twenty fields,[1] thirty more regions have been completed, besides the determination of the parallax of the planetary nebula N.G.C. 7662, an account of which was published in *Proceedings of the National Academy of Sciences*, **3**, 133, 1917.[2] The work for the present series of parallaxes was carried on in practically the same way as that described in the previous paper; it will therefore be necessary to mention only the few changes made in the program of observations and reductions.

A more accurate determination of the scale of the plates taken at the 80-foot focus of the 60-inch reflector was made from photographs of the region of the double cluster in Perseus; the result is 1 mm=8".227 instead of 1 mm=8".245, as given in the earlier paper. Since further measures show that 1 mm on the plates equals 5050 instead of 5000 parts of the micrometer screw of the stereocomparator, the factor 0.001629 instead of 0.001649 should be used to convert into seconds of arc the parallaxes and proper motions expressed in 1/2000 of a revolution of the micrometer screw. This new value affects the parallaxes of only two stars in the first series, viz., those of Boss 2921 and Boss 3650; in both cases the corrected parallaxes are 0".001 smaller than those previously given.

As in the case of the first series, the two exposures to be compared were always made at nearly the same hour-angle; the largest difference is 10°, while in only 9 of the 237 cases is the difference larger than 5°. In all cases, therefore, the influence of differential refraction is less than 0".001, which is well within the limits of the errors.

---

[1] *Mt. Wilson Contr.*, No. 111.

[2] *Mt. Wilson Communications*, No. 40.

In June 1916 the supply of rodinal used for developing the photographs gave out, and it became necessary to substitute another developer; plates numbered 963 to 1005 have been developed with Wallace's contrasty developer.[1]

In the measuring machine only one change has been made, viz., a slow motion which moves both plates horizontally; this additional motion is very convenient, as it permits the use of the same part of the micrometer screw for the different stars on the plates.

To investigate the measures for systematic errors due to a possible tilt of the plate-carriers of the stereocomparator, care was taken in all but 6 of the fields that about as many pairs of plates were measured with the morning exposures in the left as in the right plate-carrier. The algebraic mean of the residuals v for these pairs was found to be less than 1 part of the micrometer screw, showing that no appreciable systematic error is due to this cause.

In the fields of Boss 2881, 3078, 3398, and 3736, which are in high galactic latitudes, the scarcity of stars made it necessary to use one or two comparison stars whose distances from the central star are greater than 8′, the limit adopted in the first paper; the distances did not, however, exceed 10′.

As before, the zero point of the co-ordinates was made to coincide with the parallax star, except in the case of the double stars Boss 178, 2285–6, 4892–3, 5433–4, and 5682–3; here the zero point was taken half-way between the two components.

The detailed results for each star are collected in the tables, which are arranged in the same way as in the previous paper.

SUMMARY OF RESULTS

The results are summarized in Table I, which is analogous to that of the first series with the following exceptions:

In the case of Boss 5683 the difference in magnitude between 5682 and 5683, as given by Boss, was added to the Harvard magnitude of 5682.

At the bottom of the table are results for three objects not contained in Boss's *Catalogue.* The magnitudes for the two B.D. stars were taken from the *Bonner Durchmusterung*.

---

[1] *Astrophysical Journal*, **20**, 118, 1904.

The mean number of exposures is 16; the mean probable error is 0″0055, a result slightly better than the mean of 0″0060 for the first series; this may be due to the slightly larger number of exposures used or to the better quality of the plates, as in general a smaller number of poor plates has been used in this series.

TABLE I

Number in Boss *P.G.C.*	Mag. Harvard	Spectrum	P.M. Boss	Relative Parallax	P.E.	No. of Exp.	μ_α Boss	μ_αvM	Boss—vM
106	6.38	G6	0″014	+0″003	0″007	14	+0″013	+0″032	−0″019
178_1	6.29	F*	0.092	+0.009	0.004	16	+0.092	+0.102	−0.010
178_2	6.29	F*	0.092	+0.007	0.003	16	+0.092	+0.081	+0.011
637	6.23	F3	0.016	+0.008	0.003	18	+0.015	−0.014	+0.029
933	5.67	F4p	0.022	+0.012	0.004	14	−0.004	−0.024	+0.020
1014	6.11	Ma(G6)	0.011	−0.001	0.007	16	+0.010	+0.006	+0.004
1971	5.64	K0	0.089	−0.002	0.007	18	+0.037	+0.104	−0.067
2285	6.04	F5*	0.195	+0.020	0.005	16	−0.125	−0.109	−0.016
2286	7.15	F5*	0.201	+0.024	0.008	16	−0.135	−0.122	−0.013
2338	6.14	G4	0.020	+0.005	0.003	12	+0.003	−0.004	+0.007
2528	6.27	G8	0.079	+0.013	0.003	18	−0.076	−0.065	−0.011
2603	6.43	K*	0.049	+0.010	0.005	16	−0.012	−0.015	+0.003
2881	6.29	G9	0.103	+0.034	0.002	12	−0.088	−0.082	−0.006
3078	5.74	F3	0.347	+0.040	0.008	16	−0.346	−0.331	−0.015
3398	5.90	Mc(G8)	0.065	+0.041	0.009	12	+0.032	+0.104	−0.072
3736	5.98	K0	0.096	+0.055	0.005	16	−0.029	−0.065	+0.036
3816	5.71	G5*	0.068	+0.042	0.006	14	+0.061	+0.075	−0.014
3867	5.98	Mb(G6)	0.004	+0.003	0.006	20	−0.004	−0.002	−0.002
4130	5.64	K1	0.046	+0.006	0.006	16	+0.045	+0.074	−0.029
4262	5.78	Mb	0.054	+0.020	0.004	16	+0.036	+0.051	−0.015
4307	5.48	G6	0.059	−0.001	0.005	16	+0.059	+0.077	−0.018
4480	6.46	K1	0.052	+0.018	0.003	16	−0.018	−0.014	−0.004
4629	5.49	K1	0.016	0.000	0.004	16	+0.016	+0.037	−0.021
4647	6.25	K1	0.062	+0.034	0.008	14	−0.033	−0.042	+0.009
4892	6.84	G2	0.630	+0.044	0.003	16	−0.174	−0.158	−0.016
4893	6.62	G2	0.655	+0.042	0.004	16	−0.190	−0.155	−0.035
5433	5.57	K8	5.278	+0.325	0.011	18	+4.161	+4.169	−0.008
5434	6.28	K8	5.155	+0.320	0.008	12	+4.132	+4.107	+0.025
5682	6.49	F7	0.143	+0.003	0.008	16	−0.139	−0.122	−0.017
5683	6.89	G2	0.144	+0.005	0.007	16	−0.141	−0.108	−0.033
5691	5.78	F0	0.127	+0.011	0.008	16	+0.119	+0.141	−0.022
5772	6.13	F5	0.337	+0.058	0.007	16	+0.336	+0.324	+0.012
5989	5.65	F9	0.270	+0.047	0.004	20	+0.116	+0.113	+0.003
B.D. +35°4001	8.5	O	....	+0.011	0.005	16	....	+0.010	....
B.D. +35°4013	8.0	O	....	+0.002	0.003	14	....	+0.051	....
N.G.C. 7662 ..	......	Pl. Neb.	....	+0.021	0.004	16	....	−0.003	....

As the mean magnitude of the comparison stars is 12.4,[1] the relative parallaxes require a correction of about +0″002 in order to reduce them to absolute parallaxes.

---

[1] On the scale of *Publications of the Astron. Lab. at Groningen*, No. 18.

Boss 106 $\alpha = 0^h 27^m 33^s$ $\delta = +27°44'$

Pl. No.	Date			t	Obs.	Qy	p	m	Remarks
648_1..	1915	Aug.	2	−1°5	vM	gg	+0.789	+0.59	
648_2..			2	+2.5	vM	g	+0.789	+0.59	
665 ..			31	−5.5	vM	g	+0.462	+0.67	Clouds 20^m exp.
666 ..			31	+0.7	H	g	+0.461	+0.67	Clouds 20^m exp.
751_1..		Nov.	2	−3.5	vM	fg	−0.483	+0.84	Hazy 20^m exp.
751_2..			2	+2.5	H	fg	−0.483	+0.84	Hazy 20^m exp.
752 ..			2	+9.5	vM	fg	−0.483	+0.84	Hazy 20^m exp. Trail
760_1..			4	−8.0	H	g	−0.506	+0.85	Hazy 20^m exp.
760_2..			4	−2.0	vM	g	−0.506	+0.85	Hazy 25^m exp.
765_1..		Dec.	2	−16.0	vM	g	−0.801	+0.92	Hazy 20^m exp.
765_2..			2	−10.7	H	fg	−0.801	+0.92	Clouds 17^m exp.
1051_1..	1916	July	23	−13.2	vM	g	+0.857	+1.56	
1051_2..			23	−9.5	H	g	+0.857	+1.56	
1065 ..		Aug.	3	+5.0	vM	fg	+0.773	+1.59	

Mor.–Ev.	Δp	Δm	M	v	Δt
1051_1–765_1...	+1.66	+0.64	+25	+9	+2°8
1051_2–765_2...	+1.66	+0.64	+28	+12	+1.2
665 –760_1...	+0.97	−0.18	−10	−8	+2.5
648_1–751_1...	+1.27	−0.25	−13	−10	+2.0
666 –760_2...	+0.97	−0.18	+25	+27	+2.7
648_2–751_2...	+1.27	−0.25	−14	−11	0.0
1065 –752 ...	+1.26	+0.75	−5	−22	−4.5

$$+1.56\,\mu_\alpha + 2.09\,\pi = +34 \qquad \pi = +1.6 = +0''.003 \pm 0''.007$$
$$+2.09\,\mu_\alpha + 12.21\,\pi = +61 \qquad \mu_\alpha = +19.7 = +0''.032 \pm 0''.019$$

Comp. Star	Br.	x	y	π	P.E.
1........	f	+1'.0	+0'.1	−0''.002	±0''.007
2........	bf	+6.3	+2.5	0.000	0.009
3........	f	+3.3	−1.6	+0.021	0.007
4........	f	−0.4	−3.0	−0.026	0.008
5........	ff	−6.5	−1.1	+0.018	0.015
6........	f	−4.0	+2.2	−0.010	±0.012

Boss 178 = Bu 439 $\alpha = 0^h44^m31^s$ $\delta = +27^\circ10'$

Pl. No.	Date			t	Obs.	Qy	p	m	Remarks
400_1..	1914	Dec.	8	−9°.2	vM	fg	−0.812	−0.06	Clouds 20^m exp.
400_2..			8	−5.0	vM	fas	−0.812	−0.06	Clouds 7^m exp.
407_1..			9	+4.0	vM	g	−0.821	−0.06	
407_2..			9	+8.5	H	g	−0.821	−0.06	
618 ..	1915	July	31	−2.0	vM	g	+0.842	+0.58	
632 ..		Aug.	1	−12.2	vM	fg	+0.834	+0.59	
633 ..			1	−7.0	H	g	+0.834	+0.59	
634 ..			1	−2.0	vM	fg	+0.834	+0.59	
694_1..		Sept.	2	−7.7	H	fg	+0.500	+0.67	
694_2..			2	−3.5	vM	fg	+0.499	+0.67	
695_1..			2	+2.0	H	fg	+0.499	+0.67	
695_2..			2	+7.0	vM	fg	+0.499	+0.67	Trail
766 ..		Dec.	2	−6.0	vM	g	−0.765	+0.92	Clouds 25^m exp.
1144_1..	1916	Nov.	16	−7.0	H	fg	−0.609	+1.88	Clouds 20^m exp.
1144_2..			16	−1.5	vM	fg	−0.609	+1.88	Clouds 20^m exp.
1165 ..			17	−10.7	H	g	−0.622	+1.89	

Mor.–Ev.	Δp	Δm	M (178_1)	M (178_2)	v (178_1)	v (178_2)	Δt
632 − 1165	+1.46	−1.30	−90	−65	−16	−7	−1°.5
694_1 − 400_1......	+1.31	+0.73	+37	+32	−16	−10	+1.5
633 − 1144_1......	+1.44	−1.29	−78	−49	−5	+9	0.0
694_2 − 766	+1.26	−0.25	+1	−18	+10	−11	+2.5
618 − 400_2......	+1.65	+0.64	+60	+53	+11	+14	+3.0
634 − 1144_2......	+1.44	−1.29	−56	−55	+17	+3	−0.5
695_1 − 407_1......	+1.32	+0.73	+48	+46	−5	+4	−2.0
695_2 − 407_2......	+1.32	+0.73	+57	+36	+4	−6	−1.5

$$\left.\begin{array}{l} +7.07\,\mu_a - 2.00\,\pi = +432 \\ -2.00\,\mu_a + 15.78\,\pi = -\ \ 38 \end{array}\right\}(178_1)\quad \left.\begin{array}{r} +341 \\ -\ \ 30 \end{array}\right\}(178_2)$$

$$(178_1)\left\{\begin{array}{l} \pi = +\ \ 5.5 = +0''.009 \pm 0''.004 \\ \mu_a = +62.7 = +0''.102 \pm 0''.006 \end{array}\right. \qquad (178_2)\left\{\begin{array}{l} \pi = +\ \ 4.3 = +0''.007 \pm 0''.003 \\ \mu_a = +49.4 = +0''.081 \pm 0''.004 \end{array}\right.$$

Comp. Star	Br.	x	y	π	P.E.
1........	f	−0′.1	+5′.8	−0″.002	±0″.014
2........	bf	+5.9	+4.7	+0.005	0.005
3........	b	+6.5	−1.8	+0.005	0.004
4........	f	+2.1	−5.5	−0.015	0.008
5........	f	−2.2	−3.8	+0.008	0.005
6........	f	−4.1	−5.9	+0.003	0.005
7........	bf	−5.1	+1.4	+0.004	0.007
8........	f	−4.0	+5.1	−0.007	±0.009

Boss 637 $\alpha=2^h43^m3^s$ $\delta=+68°28'$

Pl. No.	Date	t	Obs.	Qy	p	m	Remarks
709_1..	1915 Sept. 29	− 8°0	vM	g	+0.585	+0.75	
709_2..	29	− 4.0	vM	g	+0.585	+0.75	
726_1..	30	− 6.0	vM	g	+0.572	+0.75	
726_2..	30	− 2.0	vM	g	+0.572	+0.75	
786 ..	1916 Jan. 3	−15.0	H	f	−0.802	+1.01	
787 ..	3	− 3.5	vM	f	−0.802	+1.01	Hazy 20^m exp.
789 ..	11	−11.5	vM	f	−0.861	+1.03	Plates frosted during drying
790 ..	11	− 5.7	vM	f	−0.864	+1.03	
791 ..	11	+ 5.5	vM	f	−0.864	+1.03	
800 ..	12	− 9.2	vM	fg	−0.869	+1.04	
801 ..	12	− 5.0	vM	fg	−0.869	+1.04	
802 ..	12	+ 2.5	vM	fg	−0.869	+1.04	
803 ..	12	+ 6.5	vM	f	−0.871	+1.04	
1093_1..	Sept. 19	−17.0	H	g	+0.695	+1.72	
1093_2..	19	−12.0	vM	g	+0.695	+1.72	
1113_1..	20	+ 1.0	vM	g	+0.683	+1.73	
1113_2..	20	+ 5.2	H	g	+0.683	+1.73	
1114 ..	20	+11.0	vM	fg	+0.683	+1.73	Trail

Mor.–Ev.	Δp	Δm	M	v	Δt
1093_1–786....	+1.50	+0.71	+ 7	+ 5	−2°0
1093_2–789 ...	+1.56	+0.69	− 1	− 3	−0.5
709_1–800 ...	+1.45	−0.29	+12	+ 2	+1.2
726_1–790....	+1.44	−0.28	− 7	−16	−0.3
709_2–801 ...	+1.45	−0.29	+28	+18	+1.0
726_2–787_1...	+1.37	−0.26	+ 5	− 4	+1.5
1113_1–802 ...	+1.55	+0.69	− 8	− 9	−1.5
1113_2–791 ...	+1.55	+0.70	− 1	− 3	−0.3
1114 –803 ...	+1.55	+0.69	+12	+10	+4.5

$$+2.74\,\mu_a+3.78\,\pi=-5 \qquad \pi=+5.1=+0\overset{\prime\prime}{.}008\pm0\overset{\prime\prime}{.}003$$
$$+3.78\,\mu_a+20.03\,\pi=+69 \qquad \mu_a=-8.8=-0\overset{\prime\prime}{.}014\pm0\overset{\prime\prime}{.}008$$

Comp. Star	Br.	x	y	π	P.E.
1........	f	+2′3	+4′0	+0″012	±0″010
2........	f	+6.2	−0.1	−0.005	0.008
3........	f	+0.3	−2.6	−0.017	0.005
4........	bf	+0.4	−4.9	+0.005	0.010
5........	f	−3.7	−1.2	+0.019	0.005
6........	bf	−1.0	−0.4	−0.004	0.017
7........	f	−5.5	+4.7	−0.011	±0.005

Boss 933 $\alpha = 3^h 58^m 23^s$ $\delta = +23°50'$

Pl. No.	Date	t	Obs.	Qy	p	m	Remarks
69_1 ..	1913 Dec. 22	−4°.0	vM	f	−0.466	−1.02	
69_2 ..	22	+0.5	H	f	−0.466	−1.02	Hazy
81 ..	1914 Jan. 20	−1.5	vM	fg	−0.821	−0.94	Thick
295 ..	Oct. 11	−3.0	vM	g	+0.674	−0.22	
296 ..	11	+3.5	H	g	+0.674	−0.22	
1096 ..	1916 Sept. 19	−10.7	H	fg	+0.891	+1.72	
1097 ..	19	−6.0	vM	f	+0.891	+1.72	
1098 ..	19	−0.2	H	g	+0.889	+1.72	
1115_1 ..	20	+0.2	H	g	+0.884	+1.73	
1115_2 ..	20	+4.2	vM	g	+0.884	+1.73	Sector-belt broken after 10^m exp.
1239 ..	1917 Jan. 29	−11.0	vM	fg	−0.895	+2.08	
1240 ..	29	−6.7	vM	fg	−0.895	+2.08	
1241 ..	29	0.0	vM	fg	−0.895	+2.08	
1242 ..	29	+4.2	vM	fg	−0.895	+2.08	Trail

Mor.–Ev.	Δp	Δm	M	v	Δt
1096 −1239...	+1.79	−0.36	+39	+21	+0°.3
1097 −1240...	+1.79	−0.36	+ 6	−12	+0.7
295 − 69_1...	+1.14	+0.80	0	+ 4	+1.0
1098 − 81...	+1.71	+2.66	−35	− 8	+1.3
1115_1−1241...	+1.78	−0.35	+18	0	+0.2
296 − 69_2...	+1.14	+0.80	+17	+21	+3.0
1115_2−1242...	+1.78	−0.35	+ 3	−15	0.0

$$+8.86\,\mu_a + 3.85\,\pi = -102 \qquad \pi = +7.3 = +0''.012 \pm 0''.004$$
$$+3.85\,\mu_a + 18.26\,\pi = +77 \qquad \mu_a = -14.7 = -0''.024 \pm 0''.006$$

Comp. Star	Br.	x	y	π	P.E.
1........	f	+3'.2	+6'.0	+0''.006	±0''.003
2........	ff	+4.1	+1.9	−0.010	0.006
3........	f	+6.7	−1.2	+0.005	0.005
4........	f	+0.5	−3.3	−0.002	0.011
5........	ff	+1.2	−6.0	0.000	0.012
6........	f	−3.7	−0.8	+0.008	0.008
7........	f	−7.0	+1.1	+0.006	0.007
8........	bf	−4.0	+1.6	−0.013	±0.010

Boss 1014 = Bu 2149 $\alpha=4^h16^m30^s$ $\delta=+20^\circ35'$

Pl. No.	Date			t	Obs.	Qy	p	m	Remarks
313 ...	1914	Oct.	12	$-\ 9^\circ.7$	H	g	$+0.717$	$+0.78$	
330_1 ...			13	-11.0	vM	g	$+0.707$	$+0.79$	
330_2 ...			13	$-\ 6.0$	H	g	$+0.707$	$+0.79$	
331 ...			13	$+\ 1.5$	vM	g	$+0.706$	$+0.79$	Trail
437_1 ...	1915	Jan.	10	$-\ 3.7$	H	f	-0.665	$+1.03$	
437_2 ...			10	$+\ 0.2$	vM	fas	-0.665	$+1.03$	
438 ...			10	$+\ 6.0$	H	fg	-0.665	$+1.03$	
451 ...		Feb.	6	$-\ 1.2$	vM	g	-0.918	$+1.10$	
452 ...			6	$+\ 5.2$	H	g	-0.918	$+1.10$	
471_1 ...			7	$-\ 6.2$	vM	g	-0.925	$+1.11$	
471_2 ...			7	$-\ 2.2$	vM	g	-0.925	$+1.11$	
472 ...			7	$+\ 3.5$	H	fg	-0.925	$+1.11$	
713 ...		Sept.	29	$-\ 1.2$	vM	fg	$+0.855$	$+1.75$	
729 ...			30	$+\ 0.7$	vM	fg	$+0.843$	$+1.75$	
730 ...			30	$+\ 6.2$	vM	fg	$+0.843$	$+1.75$	
746 ...		Oct.	1	$+\ 4.0$	H	fg	$+0.835$	$+1.75$	

Mor.–Ev.	Δp	Δm	M (1014)	M (Comp.)	v (1014)	v (Comp.)	Δt
330_1–471_1	$+1.63$	-0.32	$+27$	$+26$	$+29$	$+31$	$-4^\circ.8$
313 –437_1	$+1.38$	-0.25	$-\ 9$	-11	$-\ 7$	$-\ 6$	-6.0
330_2–471_2	$+1.63$	-0.32	$+\ 4$	$-\ 2$	$+\ 6$	$+\ 3$	-3.8
713 –451	$+1.77$	$+0.65$	-36	-18	-37	-23	0.0
729 –437_2	$+1.51$	$+0.72$	$+23$	$+29$	$+21$	$+23$	$+0.5$
331 –472	$+1.63$	-0.32	-29	-31	-27	-26	-2.0
746 –452	$+1.75$	$+0.65$	$+29$	$+17$	$+28$	$+12$	-1.2
730 –438	$+1.51$	$+0.72$	-10	$-\ 7$	-12	-13	$+0.2$

$$\left.\begin{aligned}+2.24\,\mu_a+\ \ 2.56\,\pi&=+7\\+2.56\,\mu_a+20.63\,\pi&=-1\end{aligned}\right\}\ (1014)\quad\left.\begin{matrix}+21\\+\ \ 4\end{matrix}\right\}(\text{Comp.})$$

$$(1014)\left\{\begin{aligned}\pi&=-0.5=-0''.001\pm0''.007\\\mu_a&=+3.7=+0''.006\pm0''.021\end{aligned}\right.\qquad(\text{Comp.})\left\{\begin{aligned}\pi&=-\ \ 1.1=-0''.002\pm0''.006\\\mu_a&=+10.6=+0''.017\pm0''.018\end{aligned}\right.$$

Comp. Star	Br.	x	y	π	P.E.
1	bf	$+7'.4$	$+0'.8$	$+0''.025$	$\pm0''.010$
2	f	$+2.1$	$+4.4$	-0.035	0.012
3	f	-0.3	$+4.9$	$+0.003$	0.008
4	ff	-2.2	$+0.3$	-0.005	0.013
5	bf	-7.3	-0.8	$+0.017$	0.010
6	f	0.0	-4.0	$+0.003$	0.009
7	b	$+1.0$	-6.0	-0.007	±0.006

Boss 1971 $\alpha=7^h26^m2^s$ $\delta=+17^\circ18'$

Pl. No.	Date	t	Obs.	Qy	p	m	Remarks
768_1..	1915 Dec. 6	$-7^\circ.0$	vM	g	+0.569	+0.93	Some astigmatism of 60-in. mirror
768_2..	6	−3.5	vM	fg	+0.569	+0.93	
769 ..	6	+2.0	H	fas	+0.569	+0.93	
775_1..	7	−6.2	vM	g	+0.555	+0.94	
775_2..	7	−2.0	vM	g	+0.555	+0.94	
813_1..	1916 Feb. 24	−15.7	H	fg	−0.695	+1.15	Hazy 20^m exp.
813_2..	24	−10.5	vM	g	−0.695	+1.15	Hazy 20^m exp.
814_1..	24	−2.7	H	g	−0.695	+1.15	Hazy 20^m exp.
814_2..	24	+2.5	vM	g	−0.695	+1.15	Hazy 20^m exp.
820 ..	Mar. 11	−5.5	vM	g	−0.862	+1.20	
821 ..	11	−0.5	H	g	−0.862	+1.20	
822 ..	11	+5.0	vM	g	−0.862	+1.20	
848 ..	25	−0.2	vM	fg	−0.954	−1.24	Some astigmatism of 60-in. mirror
849 ..	25	+5.5	H	g	−0.954	+1.24	Trail
1154 ..	Nov. 16	−16.0	H	fg	+0.803	+1.88	
1157 ..	16	+1.0	vM	fg	+0.803	+1.88	
1158 ..	16	+6.5	H	fg	+0.803	+1.88	
1184 ..	18	+3.2	vM	fg	+0.783	+1.89	

Mor.–Ev.	Δp	Δm	M	v	Δt
1154 −813_1...	+1.50	+0.73	+37	−8	$-0^\circ.3$
768_1−813_2...	+1.26	−0.22	−44	−29	+3.5
775_1−820 ...	+1.42	−0.26	+1	+20	−0.7
768_2−814_1...	+1.26	−0.22	+3	+18	−0.8
775_2−821 ...	+1.42	−0.26	+6	+25	−1.5
1157 −848 ...	+1.76	+0.64	+22	−17	+1.2
769 −814_2...	+1.26	−0.22	−56	−41	−0.5
1184 −822 ...	+1.65	+0.69	+62	+20	−1.8
1158 −849 ...	+1.76	+0.64	+45	+6	+1.0

$$+2.12\,\mu_a+\ 2.92\,\pi=+132 \qquad \pi\ =-\ 1.1=-0''.002\pm0''.007$$

$$+2.92\,\mu_a+19.98\,\pi=+164 \qquad \mu_a=+63.8=+0''.104\pm0''.022$$

Comp. Star	Br.	x	y	π	P.E.
1.......	bf	$+1'.1$	$+2'.7$	$+0''.004$	$\pm0''.005$
2.......	bf	+1.9	+4.7	+0.002	0.009
3.......	f	+6.7	−1.4	+0.017	0.004
4.......	f	+3.6	−5.5	−0.013	0.004
5.......	f	+1.1	−3.6	+0.001	0.009
6.......	bf	−0.4	−3.3	−0.013	0.016
7.......	bf	−5.4	−2.1	+0.013	0.012
8.......	f	−6.6	+2.1	+0.008	0.006
9.......	f	−0.8	+1.4	+0.003	0.009
10.......	b	−1.9	+4.4	−0.023	±0.013

Boss 2285, 2286 = Bu 4677 $\alpha = 8^h 30^m 32^s$ $\delta = +6°58'$

Pl. No.	Date			t	Obs.	Qy	p	m	Remarks
776_1 . .	1915	Dec.	7	−10°7	vM	g	+0.733	+0.94	
776_2 . .			7	− 6.5	vM	g	+0.733	+0.94	
777_1 . .			7	+ 0.5	vM	fg	+0.733	+0.94	
777_2 . .			7	+ 4.5	vM	gas	+0.731	+0.94	
823 . .	1916	Mar.	11	+ 1.7	H	g	−0.693	+1.20	
824 . .			11	+ 6.5	vM	g	−0.693	+1.20	
825 . .			11	+12.2	H	g	−0.693	+1.20	
850_1 . .			25	− 3.2	vM	g	−0.835	+1.24	
850_2 . .			25	+ 1.0	H	g	−0.835	+1.24	
865 . .			26	−14.5	vM	fg	−0.844	+1.24	Some astigmatism
866_1 . .			26	− 9.2	H	g	−0.844	+1.24	of 60-in. mirror
866_2 . .			26	− 5.0	vM	gas	−0.844	+1.24	Trail
1185 . .		Nov.	18	− 4.7	vM	f	+0.893	+1.89	20^m exp.
1186 . .			18	+ 1.2	vM	f	+0.893	+1.89	20^m exp.
1197 . .		Dec.	16	−16.0	vM	fg	+0.612	+1.96	
1200 . .			16	+10.5	H	fg	+0.614	+1.96	

Mor.–Ev.	Δp	Δm	M (2285)	M (2286)	v (2285)	v (2286)	Δt
1197 −865	+1.46	+0.72	−40	−76	−10	−44	−1°5
776_1–866_1	+1.58	−0.30	+19	+23	−20	−24	−1.5
776_2–866_2	+1.58	−0.30	+21	+44	−18	− 3	−1.5
1185 −850_1	+1.73	+0.65	−20	− 9	+ 2	+14	−1.5
777_1–850_2	+1.57	−0.30	+67	+86	+28	+39	−0.5
1186 −823	+1.59	+0.69	− 8	−21	+19	+ 7	−0.5
772_2–824	+1.42	−0.26	+44	+23	+10	−18	−2.0
1200 −825	+1.31	+0.76	−46	−14	−11	+23	−1.7

$$\left.\begin{aligned} +2.34\,\mu_\alpha + 2.49\,\pi &= -126 \\ +2.49\,\mu_\alpha + 18.85\,\pi &= +64 \end{aligned}\right\}(2285)\left.\begin{matrix} -138 \\ +96 \end{matrix}\right\}(2286)$$

$$(2285)\left\{\begin{aligned} \pi &= +12.2 = +0.''020 \pm 0.''005 \\ \mu_\alpha &= -66.8 = -0.''109 \pm 0.''015 \end{aligned}\right. \qquad (2286)\left\{\begin{aligned} \pi &= +15.0 = +0.''024 \pm 0.''008 \\ \mu_\alpha &= -75.0 = -0.''122 \pm 0.''023 \end{aligned}\right.$$

Comp. Star	Br.	x	y	π	P.E.
1.	bf	+3'.2	+3'.4	+0''.005	±0''.009
2.	bf	+6.9	+0.8	−0.008	0.010
3.	b	+1.4	−0.8	−0.006	0.012
4.	bf	+3.2	−4.1	+0.008	0.005
5.	bf	−0.8	−5.6	−0.008	0.006
6.	f	−2.6	−2.3	−0.002	0.007
7.	bf	−1.9	+0.4	+0.027	0.010
8.	f	−6.5	+2.1	−0.008	0.009
9.	f	−2.2	+4.9	−0.005	±0.011

Boss 2338 $\alpha=8^h39^m13^s$ $\delta=+31°4'$

Pl. No.	Date			t	Obs.	Qy	p	m	Remarks
59 . . .	1913	Nov.	22	+ 0°.7	vM	pf	+0.881	−0.10	
73_1 . . .		Dec.	22	− 1.5	vM	fas	+0.568	−0.02	
73_2 . . .			22	+ 3.0	H	pf	+0.568	−0.02	
92_1 . . .	1914	Feb.	26	− 6.0	vM	pf	−0.482	+0.16	
92_2 . . .			26	− 1.5	vM	pf	−0.482	+0.16	
96_1 . . .			27	− 8.5	vM	f	−0.497	+0.16	Some astigmatism of 60-in. mirror
96_2 . . .			27	− 4.2	vM	f	−0.497	+0.16	
494_1 . . .	1915	Mar.	8	+ 2.5	vM	fg	−0.617	+1.19	20^m exp.
494_2 . . .			8	+ 8.2	vM	fg	−0.617	+1.19	20^m exp. Trail
770_1 . . .		Dec.	6	−10.0	vM	g	+0.762	+1.93	
770_2 . . .			6	− 5.5	H	fg	+0.762	+1.93	
772 . .			6	+12.0	vM	fg	+0.762	+1.93	

Mor.–Ev.	Δp	Δm	M	v	Δt
770_1 − 96_1	+1.26	+1.77	+ 6	+ 6	−1°.5
770_2 − 92_1	+1.24	+1.77	− 5	− 5	+0.5
73_1 − 96_2	+1.07	−0.18	+14	+11	+2.7
59 − 92_2	+1.36	−0.26	+ 5	0	+2.2
73_2 − 494_1	+1.19	−1.21	+ 3	− 4	+0.5
772 − 494_2	+1.38	+0.74	− 6	− 8	+3.8

$$+8.37\,\mu_\alpha+3.46\,\pi=-10 \qquad \pi=+3.0=+0''.005+0''.003$$

$$+3.46\,\mu_\alpha+9.44\,\pi=+20 \qquad \mu_\alpha=-2.4=-0''.004\pm0''.003$$

Comp. Star	Br.	x	y	π	P.E.
1	f	−0′.1	+0′.7	−0″.006	±0″.012
2	f	+2.9	+6.6	+0.013	0.006
3	f	−5.1	−0.3	−0.008	0.004
4	f	+0.5	−6.2	+0.019	0.006
5	bf	+5.2	−2.2	−0.017	±0.004

Boss 2528 $\alpha=9^h20^m0^s$ $\delta=+17°1'$

Pl. No.	Date			t	Obs.	Qy	p	m	Remarks
104 ...	1914	April	17	− 2°2	vM	pf	−0.896	+0.30	
113_1...			18	0.0	vM	gas	−0.901	+0.30	Some astigmatism of 60-in. mirror
113_2...			18	+ 4.2	vM	gas	−0.901	+0.30	
122 ...			19	+ 1.5	vM	gas	−0.907	+0.30	
418 ...		Dec.	9	−10.7	H	fg	+0.811	+0.94	
419 ...			9	− 3.5	vM	fg	+0.811	+0.94	Clouds 20^m exp.
426_1...	1915	Jan.	9	− 3.5	vM	fg	+0.448	+1.03	
426_2...			9	+ 0.5	vM	f	+0.448	+1.03	
427 ...			9	+ 6.0	H	f	+0.448	+1.03	
445_1...			10	− 1.0	vM	g	+0.433	+1.03	
445_2...			10	+ 3.5	H	g	+0.433	+1.03	
446 ...			10	+ 9.7	vM	g	+0.432	+1.03	Trail
796 ...	1916	Jan.	11	− 1.0	vM	g	+0.420	+2.03	
851_1...		Mar.	25	− 5.0	vM	vg	−0.700	+2.24	
851_2...			25	− 0.7	H	g	−0.700	+2.24	
852_1...			25	+ 4.5	vM	vg	−0.700	+2.24	
852_2...			25	+ 9.7	H	g	−0.700	+2.24	
867 ...			26	−10.7	H	g	−0.711	+2.24	

Mor.-Ev.	Δp	Δm	M	v	Δt
418 −867	+1.52	−1.30	+55	− 9	0°0
419 −851_1....	+1.51	−1.30	+73	+ 9	+1.5
426_1−104	+1.34	+0.73	−35	−17	−1.3
445_1−851_2....	+1.13	−1.21	+58	+ 1	−0.3
796 −113_1....	+1.32	+1.73	−48	+10	−1.0
426_2−122	+1.36	+0.73	−10	+ 8	−1.0
445_2−113_2....	+1.33	+0.73	−23	− 5	−0.7
427 −852_1....	+1.15	−1.21	+55	− 2	+1.5
446 −852_2....	+1.13	−1.21	+64	+ 7	0.0

$$+12.34\,\mu_\alpha - 2.85\,\pi = -514 \qquad \pi = +8.1 = +0''013 \pm 0''003$$

$$-2.85\,\mu_\alpha + 15.63\,\pi = +240 \qquad \mu_\alpha = -39.8 = -0''065 \pm 0''003$$

Comp. Star	Br.	x	y	π	P.E.
1........	ff	+1′6	+1′0	+0″022	±0″012
2........	f	+1.8	+3.0	+0.002	0.010
3........	f	+2.9	+5.8	−0.015	0.007
4........	bf	−4.8	+2.3	+0.001	0.003
5........	b	−5.1	−1.1	+0.011	0.007
6........	f	−3.6	−4.1	−0.017	0.009
7........	f	+3.4	−3.6	+0.023	0.009
8........	bf	+3.5	−3.7	−0.024	±0.008

Boss 2603 $\alpha = 9^h 35^m 53^s$ $\delta = +26^\circ 22'$

Pl. No.	Date	t	Obs.	Qy	p	m	Remarks
771_1..	1915 Dec. 6	−13°0	vM	fg	+0.860	+0.93	
771_2..	6	− 8.7	H	fg	+0.860	+0.93	
778 ..	7	− 0.5	vM	g	+0.853	+0.94	
797 ..	1916 Jan. 11	+ 2.0	vM	fg	+0.477	+1.03	
868_1..	Mar. 26	− 9.0	vM	g	−0.661	+1.24	
868_2..	26	− 4.0	H	fg	−0.661	+1.24	
869_1..	26	+ 1.5	vM	g	−0.661	+1.24	
869_2..	26	+ 5.7	H	fg	−0.661	+1.24	Trail
896 ..	April 23	+ 2.0	vM	f	−0.905	+1.32	
897_1..	23	+ 6.5	H	fg	−0.905	+1.32	
897_2..	23	+11.0	vM	g	−0.905	+1.32	
911 ..	24	+ 3.0	vM	fg	−0.910	+1.32	
1201_1..	Dec. 16	+ 1.0	vM	fg	+0.796	+1.96	
1201_2..	16	+ 5.5	H	fg	+0.796	+1.96	
1202 ..	16	+10.0	vM	fg	+0.796	+1.96	
1221 ..	17	+ 2.0	vM	fg	+0.767	+1.97	

Mor.–Ev.	Δp	Δm	M	v	Δt
771_1–868_1...	+1.52	−0.31	−15	−28	−4°0
771_2–868_2...	+1.52	−0.31	+ 4	− 9	−4.7
778 –869_1...	+1.51	−0.30	+30	+17	−2.0
1201_1–896 ...	+1.70	+0.64	+ 9	+ 4	−1.0
797 –911 ...	+1.39	−0.29	+26	+14	−1.0
1221 –869_2...	+1.43	+0.73	−19	−22	−3.7
1201_2–897_1...	+1.70	+0.64	+13	+ 8	−1.0
1202 –897_2...	+1.70	+0.64	+16	+11	−1.0

$$+2.13\,\mu_a + 2.52\,\pi = -3 \qquad \pi = +6.3 = +0''010 \pm 0''005$$

$$+2.52\,\mu_a + 19.54\,\pi = +101 \qquad \mu_a = -8.9 = -0''015 \pm 0''015$$

Comp. Star	Br.	x	y	π	P.E.
1........	bf	+1′1	+4′0	−0″010	±0″009
2........	f	+3.6	−3.8	+0.017	0.008
3........	f	+3.7	−4.0	−0.007	0.009
4........	f	−2.2	−2.7	−0.007	0.004
5........	bf	−4.9	−1.8	+0.012	0.004
6........	f	−1.4	+0.8	−0.020	0.006
7........	f	−0.5	+6.9	+0.015	±0.007

Boss 2881 $\alpha=10^h43^m26^s$ $\delta=+29^\circ57'$

Pl. No.	Date			t	Obs.	Qy	p	m	Remarks
507_1...	1915	April	6	− 2°5	vM	fg	−0.555	+0.27	
507_2...			6	+ 2.0	vM	fg	−0.556	+0.27	
508 ...			6	+ 8.2	vM	fg	−0.556	+0.27	Trail
773 ...		Dec.	6	− 8.0	vM	fg	+0.907	+0.93	
774 ...			6	− 2.5	H	fg	+0.907	+0.93	
779_1...			7	−10.7	vM	g	+0.907	+0.94	
779_2...			7	− 6.7	vM	g	+0.907	+0.94	
798_1...	1916	Jan.	11	− 5.2	vM	g	+0.685	+1.03	
798_2...			11	− 0.7	vM	fg	+0.685	+1.03	
912_1...		April	24	− 8.0	H	fg	−0.765	+1.32	
912_2...			24	− 3.5	vM	g	−0.765	+1.32	
913 ...			24	+ 0.7	H	g	−0.765	+1.32	

Mor.–Ev.	Δp	Δm	M	v	Δt
779_1–912_1....	+1.67	−0.38	+56	+ 2	−2°7
773 –912_2....	+1.67	−0.39	+53	− 2	−4.5
779_2–507_1....	+1.46	+0.67	+ 7	+11	−4.2
798_1–913	+1.45	−0.29	+41	− 4	−5.9
774 –507_2....	+1.46	+0.66	− 4	− 1	−4.5
798_2–508	+1.24	+0.76	−21	− 9	−8.9

$$+1.84\,\mu_a+\ 1.18\,\pi=-\ 68 \qquad \pi\ =+20.8=+0''.034\pm0''.002$$
$$+1.18\,\mu_a+13.48\,\pi=+220 \qquad \mu_a=-50.3=-0''.082\pm0''.006$$

Comp. Star	Br.	x	y	π	P.E.
1........	f	+3'.8	+3'.4	+0''.021	±0''.007
2........	f	+7.8	−1.6	−0.010	0.010
3........	b	+1.4	−5.4	−0.012	0.009
4........	f	−5.5	−4.4	+0.005	0.007
5........	bf	−1.6	−1.4	+0.022	0.005
6........	f	−4.1	+3.6	−0.016	0.005
7........	f	−3.0	+4.1	−0.010	±0.004

Boss 3078 $\alpha = 11^h 36^m 22^s$ $\delta = +32^\circ 18'$

Pl. No.	Date			t	Obs.	Qy	p	m	Remarks
463_1..	1915	Feb.	6	−8°5	vM	gas	+0.535	+0.10	
463_2..			6	−2.5	H	g	+0.535	+0.10	
464 ..			6	+4.0	vM	g	+0.534	+0.10	
465 ..			6	+9.5	H	fg	+0.534	+0.10	
899_1..	1916	April	23	−3.0	H	fg	−0.595	+1.31	Some astigmatism of 60-in. mirror
899_2..			23	+3.2	vM	fg	−0.595	+1.31	
900_1..			23	+8.5	H	g	−0.595	+1.31	
900_2..			23	+13.0	vM	g	−0.595	+1.31	Trail
914_1..			24	−5.2	vM	g	−0.605	+1.32	
914_2..			24	−1.0	H	g	−0.605	+1.32	
951 ..		May	25	+9.2	vM	f	−0.880	+1.40	
952 ..			25	+14.0	H	f	−0.880	+1.40	
1265 ..	1917	Feb.	12	−2.5	vM	fg	+0.449	+2.12	
1267 ..			12	+9.5	vM	fg	+0.447	+2.12	
1278 ..			13	+4.7	vM	fg	+0.434	+2.12	
1279 ..			13	+11.0	H	f	+0.433	+2.12	

Mor.–Ev.	Δp	Δm	M	v	Δt
463_1–914_1...	+1.14	−1.22	+301	+25	−3°3
1265 –899_1...	+1.04	+0.81	−158	−19	+0.5
463_2–914_2...	+1.14	−1.22	+235	−41	−1.5
464 –899_2...	+1.13	−1.21	+267	−9	+0.8
1278 –900_1...	+1.03	+0.81	−134	+6	−3.8
465 –951 ...	+1.41	−1.30	+320	+21	+0.3
1267 –900_2...	+1.04	+0.81	−134	+5	−3.5
1279 –952 ...	+1.31	+0.72	−109	+5	−3.0

$$+8.63\,\mu_\alpha - 2.53\,\pi = -1817 \qquad \pi = +24.6 = +0''.040 \pm 0''.008$$

$$-2.53\,\mu_\alpha + 10.81\,\pi = +780 \qquad \mu_\alpha = -203.3 = -0''.331 \pm 0''.009$$

Comp. Star	Br.	x	y	π	P.E.
1........	f	+3′7	+6′5	−0″001	±0″007
2........	ff	+5.9	−2.3	+0.019	0.019
3........	f	+4.8	−5.6	−0.014	0.015
4........	b	−1.2	+0.7	−0.012	0.010
5........	bf	−6.9	−3.3	+0.007	0.007
6........	f	−6.7	+4.3	0.000	±0.009

Boss 3398 $\alpha = 13^h 1^m 31^s$ $\delta = +23^{\circ} 9'$

Pl. No.	Date			t	Obs.	Qy	p	m	Remarks
100 . . .	1914	Feb.	27	$+0^{s}.5$	vM	fg	+0.562	+0.16	
131_1 . . .		May	17	+ 8.0	P	f	−0.596	+0.38	
131_2 . . .			17	+15.2	P	fg	−0.596	+0.38	
134_1 . . .			18	+ 3.0	P	fg	−0.608	+0.38	
134_2 . . .			18	+ 8.0	P	g	−0.608	+0.38	
467 . . .	1915	Feb.	6	+ 4.2	H	f	+0.782	+1.10	
468 . . .			6	+ 9.7	vM	f	+0.782	+1.10	Trail
483 . . .			7	+ 1.0	vM	fg	+0.771	+1.11	
501 . . .		Mar.	8	+ 6.0	vM	g	+0.445	+1.19	
502 . . .			8	+11.2	C	f	+0.445	+1.19	
538 . . .		June	3	+ 3.2	vM	pf	−0.773	+1.42	
553 . . .			4	+ 2.2	vM	g	−0.783	+1.43	

Mor.-Ev.	Δp	Δm	M	v	Δt
$100-134_1$	+1.17	−0.22	+ 20	+ 5	$-2^{s}.5$
483–553	+1.55	−0.32	+ 43	+24	−1.2
467–538	+1.56	−0.32	− 5	−24	+1.0
$501-131_1$	+1.04	+0.81	+ 67	−11	−2.0
$468-134_2$	+1.39	+0.72	+ 59	−22	+1.7
$502-131_2$	+1.04	+0.81	+110	+32	−4.0

$$+2.09\,\mu_{\alpha} + 1.42\,\pi = +169 \qquad \pi = +25.0 = +0''.041 \pm 0''.009$$

$$+1.42\,\mu_{\alpha} + 10.29\,\pi = +348 \qquad \mu_{\alpha} = +63.9 = +0''.104 \pm 0''.021$$

Comp. Star	Br.	x	y	π	P.E.
1	f	+5′.4	+5′.1	−0″.027	±0″.007
2	bf	−4.5	+7.5	+0.034	0.012
3	ff	−5.2	+0.1	−0.052	0.019
4	f	+1.1	−6.3	−0.011	0.014
5	f	+4.5	−4.5	+0.037	±0.010

Boss 3736 $\alpha = 14^h 33^m 35^s$ $\delta = +18°44'$

Pl. No.	Date	t	Obs.	Qy	p	m	Remarks
567 ...	1915 July 2	+ 6°7	vM	fg	−0.830	+0.50	Aperture 60 in.
581 ...	3	+ 7.5	vM	fg	−0.837	+0.51	
582 ...	3	+12.0	H	fg	−0.837	+0.51	
597 ...	4	+10.5	vM	pf	−0.846	+0.51	Seeing poor 20^m exp. Trail
833 ...	1916 Mar. 11	− 5.0	H	g	+0.716	+1.19	
841 ...	24	−13.0	H	f	+0.557	+1.23	
842 ...	24	− 7.5	vM	fg	+0.557	+1.23	
843 ...	24	− 2.5	H	fg	+0.557	+1.23	
861_1...	25	+ 6.5	vM	g	+0.541	+1.24	
861_2...	25	+11.2	H	g	+0.541	+1.24	
877_1...	26	+ 6.7	vM	g	+0.526	+1.24	
877_2...	26	+11.5	H	g	+0.526	+1.24	
963 ...	June 22	− 3.0	vM	g	−0.743	+1.48	Some astigmatism of 60-in. mirror
964 ...	22	+ 1.7	H	g	−0.743	+1.48	
978 ...	23	− 2.0	vM	g	−0.754	+1.48	
992 ...	24	− 0.5	vM	g	−0.764	+1.49	

Mor.–Ev.	Δp	Δm	M	v	Δt
841 –963.....	+1.30	−0.25	+46	− 8	−10°0
842 –978.....	+1.31	−0.25	+70	+15	− 5.5
833 –992.....	+1.48	−0.30	+46	−16	− 4.5
843 –964.....	+1.30	−0.25	+64	+10	− 4.2
861_1–567.....	+1.37	+0.74	+30	+13	− 0.2
877_1–581.....	+1.36	+0.73	− 5	−22	− 0.8
861_2–597.....	+1.39	+0.73	+31	+13	+ 0.7
877_2–582.....	+1.36	+0.73	+14	− 3	− 0.5

$$+2.41\,\mu_a + 2.58\,\pi = -9 \qquad \pi = +34.0 = +0''.055 \pm 0''.005$$
$$+2.58\,\mu_a + 14.80\,\pi = +399 \qquad \mu_a = -40.1 = -0''.065 \pm 0''.012$$

Comp. Star	Br.	x	y	π	P.E.
1........	f	+7′6	+5′2	+0″009	±0″004
2........	ff	+4.0	−6.7	−0.002	0.002
3........	f	−1.5	−1.4	+0.008	0.007
4........	f	−8.6	−0.1	+0.009	0.007
5........	f	−2.5	+2.2	−0.024	±0.011

Boss 3816 $\alpha=14^h52^m26^s$ $\delta=+0°14'$

Pl. No.	Date	t	Obs.	Qy	p	m	Remarks
860_1..	1916 Mar. 25	−9°0	vM	fg	+0.617	+0.24	
860_2..	25	−4.5	H	fg	+0.617	+0.24	
876_1..	26	−9.0	vM	g	+0.604	+0.24	
876_2..	26	−4.5	H	g	+0.604	+0.24	
965_1..	June 22	+3.0	vM	g	−0.698	+0.48	
965_2..	22	+7.5	H	gas	−0.698	+0.48	
979_1..	23	−0.7	H	g	−0.708	+0.48	
979_2..	23	+3.5	vM	g	−0.708	+0.48	
980 ..	23	+8.5	H	g	−0.708	+0.48	
993_1..	24	+0.2	H	gas	−0.719	+0.48	
993_2..	24	+4.5	vM	g	−0.719	+0.48	
1301 ..	1917 Mar. 15	+5.5	vM	g	+0.735	+1.21	
1316_1..	16	+2.7	H	fg	+0.724	+1.21	
1316_2..	16	+8.0	vM	fg	+0.724	+1.21	Trail

Mor.-Ev.	Δp	Δm	M	v	Δt
860_1–979_1...	+1.33	−0.24	+40	+17	−8°3
876_1–993_1...	+1.32	−0.24	−4	−27	−9.2
860_2–965_1...	+1.32	−0.24	+28	+5	−7.5
876_2–979_2...	+1.31	−0.24	+27	+5	−8.0
1316_1–993_2...	+1.44	+0.73	+68	−3	−1.8
1301 –965_2...	+1.43	+0.73	+55	−15	−2.0
1316_2–980 ...	+1.43	+0.73	+87	+17	−0.5

$$+1.83\,\mu_\alpha+1.86\,\pi=+132 \qquad \pi=+25.5=+0''042\pm0''006$$
$$+1.86\,\mu_\alpha+13.12\,\pi=+421 \qquad \mu_\alpha=+46.2=+0''075\pm0''016$$

Comp. Star	Br.	x	y	π	P.E.
1........	f	+4′0	+5′8	−0″011	±0″003
2........	f	+3.2	−3.8	+0.028	0.009
3........	b	+0.5	−4.4	−0.018	0.004
4........	b	−1.0	−1.1	−0.040	0.020
5........	f	−1.2	+1.4	+0.035	0.013
6........	bf	−6.0	+1.6	+0.007	±0.007

Boss 3867 $\alpha=15^h7^m31^s$ $\delta=+19^\circ21'$

Pl. No.	Date			t	Obs.	Qy	p	m	Remarks
102_1...	1914	Feb.	27	$-5^\circ.0$	vM	g	+0.898	+0.16	
102_2...			27	-1.0	C	fg	+0.898	+0.16	
141_1...		June	16	-2.0	Sh	g	−0.569	+0.46	
141_2...			16	$+3.5$	H	fg	−0.571	+0.46	
504 ...	1915	Mar.	8	$+3.2$	vM	fg	+0.848	+1.19	Two exp. superposed
505 ...			8	$+11.0$	vM	f	+0.848	+1.19	
516_1...		April	6	$+4.7$	vM	fg	+0.525	+1.27	
516_2...			6	$+9.5$	vM	fg	+0.525	+1.27	Trail
541_1...		June	3	-2.5	H	f	−0.376	+1.42	
541_2...			3	$+2.0$	vM	f	−0.376	+1.42	
542 ...			3	$+7.2$	H	pf	−0.376	+1.42	
556_1...			4	-5.0	vM	g	−0.391	+1.43	
556_2...			4	-0.7	H	fg	−0.391	+1.43	
557 ...			4	$+3.5$	vM	fg	−0.391	+1.43	
568_1...		July	2	$+5.2$	H	fg	−0.758	+1.50	
568_2...			2	$+10.2$	vM	g	−0.758	+1.50	
834_1...	1916	Mar.	11	-7.5	vM	g	+0.810	+2.20	
834_2...			11	-2.7	H	g	+0.810	+2.20	
835_1...			11	$+2.5$	vM	fg	+0.810	+2.20	
835_2...			11	$+7.0$	H	g	+0.810	+2.20	

Mor.–Ev.	Δp	Δm	M	v	Δt
834_1–556_1....	+1.20	+0.77	+21	+20	$-2^\circ.5$
102_1–541_1....	+1.27	−1.26	−11	−15	−2.5
834_2–141_1....	+1.38	+1.74	+27	+26	−0.7
102_2–556_2....	+1.29	−1.27	+21	+17	−0.3
835_1–541_2....	+1.19	+0.78	−36	−37	+0.5
504 –557	+1.24	−0.24	−10	−12	−0.3
516_1–141_2....	+1.10	+0.81	−25	−26	+1.2
835_2–568_1....	+1.57	+0.70	− 3	− 5	+1.8
516_2–542	+0.90	−0.15	+19	+17	+2.3
505 –568_2....	+1.61	−0.31	+17	+14	+0.8

$$+8.76\,\mu_\alpha+\ 2.06\,\pi=-\ 6 \qquad \pi\ =+2.0=+0''.003+0''.006$$
$$+2.06\,\mu_\alpha+16.64\,\pi=+31 \qquad \mu_\alpha=-1.2=-0''.002\pm0''.009$$

Comp. Star	Br.	x	y	π	P.E.
1........	ff	$-1'.4$	$+2'.5$	$-0''.012$	$\pm0''.009$
2........	f	−3.6	−0.4	+0.007	0.005
3........	f	−2.6	−2.5	0.000	0.004
4........	bf	+1.1	−2.9	+0.001	0.006
5........	f	+4.5	−1.9	−0.001	0.005
6........	bf	+3.4	+6.0	+0.005	±0.005

Boss 4130 $\alpha=16^h8^m19^s$ $\delta=+5°17'$

Pl. No.	Date	t	Obs.	Qy	p	m	Remarks
583_1...	1915 July 3	− 5°5	vM	fg	−0.603	+0.51	
583_2...	3	− 1.0	H	fg	−0.603	+0.51	
584_1...	3	+ 4.2	vM	g	−0.603	+0.51	
584_2...	3	+ 8.5	H	g	−0.603	+0.51	Trail
836_1...	1916 Mar. 11	− 1.7	vM	g	+0.933	+1.20	
836_2...	11	+ 2.5	H	g	+0.933	+1.20	
862_1...	25	− 6.0	vM	g	+0.840	+1.24	
862_2...	25	− 1.7	H	g	+0.838	+1.24	
863_1...	25	+ 4.0	vM	g	+0.838	+1.24	
863_2...	25	+ 8.5	H	g	+0.838	+1.24	
864 ...	25	+13.5	vM	g	+0.838	+1.24	
889 ...	April 22	− 7.7	H	g	+0.514	+1.31	
966_1...	June 22	− 6.0	vM	g	−0.457	+1.48	
966_2...	22	− 2.0	H	g	−0.457	+1.48	
967 ...	22	+ 3.0	vM	g	−0.457	+1.48	
982 ...	23	+ 9.0	vM	g	−0.471	+1.48	

Mor.–Ev.	Δp	Δm	M	v	Δt
889 −966_1....	+0.97	−0.17	−34	−30	−1°7
862_1−583_1....	+1.44	+0.73	+47	+ 8	−0.5
836_1−966_2....	+1.39	−0.28	− 8	0	+0.3
862_2−583_2....	+1.44	+0.73	+36	− 3	−0.7
836_2−967	+1.39	−0.28	− 4	+ 4	−0.5
863_1−584_1....	+1.44	+0.73	+15	−24	−0.2
863_2−584_2....	+1.44	+0.73	+58	+20	0.0
864 −982	+1.31	−0.24	+10	+16	+4.5

$+2.37\,\mu_\alpha+\ \ 2.95\,\pi=+120$ $\qquad\pi\ =+\ 3.7=+0''006\pm0''006$

$+2.95\,\mu_\alpha+14.80\,\pi=+189$ $\qquad\mu_\alpha=+45.6=+0''074\pm0''016$

Comp. Star	Br.	x	y	π	P.E.
1........	bf	+0'7	+3'0	−0''004	±0''004
2........	f	+2.9	+4.8	+0.007	0.010
3........	bf	+5.6	+3.6	+0.005	0.007
4........	f	+0.7	−6.3	−0.004	0.006
5........	f	−0.4	−3.4	+0.001	0.010
6........	f	−0.3	−2.2	+0.003	0.009
7........	ff	−4.4	−4.1	+0.008	0.009
8........	bf	−4.5	+4.7	−0.014	±0.006

Boss 4262 $\alpha=16^h40^m51^s$ $\delta=+15°56'$

Pl. No.	Date	t	Obs.	Qy	p	m	Remarks
605_1..	1915 July 31	$-0°.5$	vM	g	-0.833	$+0.58$	
605_2..	31	$+4.0$	vM	g	-0.833	$+0.58$	
606 ..	31	$+10.0$	H	g	-0.833	$+0.58$	Trail
619 ..	Aug. 1	$+2.0$	vM	fg	-0.841	$+0.59$	Some astigmatism of 60-in. mirror
878_1..	1916 Mar. 26	-13.5	vM	g	$+0.898$	$+1.24$	
878_2..	26	-9.5	H	g	$+0.898$	$+1.24$	
879_1..	26	-4.0	vM	vg	$+0.898$	$+1.24$	
879_2..	26	$+0.7$	H	vg	$+0.898$	$+1.24$	
906_1..	April 23	-6.5	vM	g	$+0.614$	$+1.31$	
906_2..	23	-2.0	H	vg	$+0.614$	$+1.31$	
907 ..	23	$+4.0$	vM	vg	$+0.614$	$+1.31$	Clouds 20^m exp.
908 ..	23	$+10.2$	H	gas	$+0.614$	$+1.31$	Clouds 20^m exp.
1006 ..	July 21	-9.0	vM	g	-0.738	$+1.56$	Some astigmatism of 60-in. mirror
1007 ..	21	-3.7	H	g	-0.738	$+1.56$	
1023 ..	22	-7.0	vM	fg	-0.749	$+1.56$	
1039 ..	23	-0.7	H	gas	-0.761	$+1.56$	

Mor.–Ev.	Δp	Δm	M	v	Δt	Remarks
878_1–1006	$+1.64$	-0.32	$+6$	-4	$-4°.5$	
878_2–1023	$+1.65$	-0.32	-1	-11	-2.5	
906_1–1007	$+1.35$	-0.25	-5	-13	-2.8	
879_1–1039	$+1.66$	-0.32	$+34$	$+24$	-3.3	
906_2– 605_1....	$+1.45$	$+0.73$	$+30$	-10	-1.5	
879_2– 619	$+1.74$	$+0.65$	$+50$	$+9$	-1.3	
907 – 605_2....	$+1.45$	$+0.73$	$+35$	-5	0.0	
908 – 606	$+1.45$	$+0.73$	$+46$	$+6$	$+0.2$	Defect on plate 908, Star 1

$$+2.37\,\mu_a+2.39\,\pi=+103 \qquad \pi=+12.0=+0''.020\pm0''.004$$
$$+2.39\,\mu_a+19.32\,\pi=+306 \qquad \mu_a=+31.4=+0''.051\pm0''.010$$

Comp. Star	Br.	x	y	π	P.E.
1........	f	$+0'.3$	$+1'.2$	$-0''.011$	$\pm0''.013$
2........	f	$+0.7$	$+4.9$	$+0.002$	0.005
3........	f	$+7.1$	-1.2	$+0.007$	0.006
4........	f	$+0.8$	-2.1	-0.006	0.010
5........	bf	-0.7	-4.9	-0.005	0.003
6........	bf	-3.0	$+1.1$	$+0.007$	0.007
7........	bf	-4.3	$+0.7$	$+0.004$	±0.008

Boss 4307 $\alpha=16^h50^m37^s$ $\delta=+21°7'$

Pl. No.	Date			t	Obs.	Qy	p	m	Remarks
569_1 . .	1915	July	2	$-\ 8°5$	H	fg	-0.443	$+0.50$	
569_2 . .			2	$-\ 4.0$	vM	fg	-0.444	$+0.50$	
570_1 . .			2	$+\ 2.0$	H	g	-0.444	$+0.50$	
570_2 . .			2	$+\ 6.5$	vM	g	-0.444	$+0.50$	Trail
845 . .	1916	Mar.	24	-13.0	vM	f	$+0.929$	$+1.23$	
846 . .			24	$-\ 5.7$	H	fg	$+0.929$	$+1.23$	20^m exp.
847 . .			24	$+\ 1.5$	vM	fg	$+0.929$	$+1.23$	20^m exp.
890_1 . .		April	22	-11.2	vM	fg	$+0.659$	$+1.31$	
890_2 . .			22	$-\ 7.2$	H	f	$+0.659$	$+1.31$	
891_1 . .			22	$-\ 0.7$	vM	g	$+0.659$	$+1.31$	
891_2 . .			22	$+\ 4.0$	H	fg	$+0.659$	$+1.31$	
892 . .			22	$+\ 8.5$	vM	fg	$+0.659$	$+1.31$	
1008_1 . .		July	21	$-\ 0.5$	Duncan	g	-0.714	$+1.56$	
1008_2 . .			21	$+\ 4.0$	vM	g	-0.714	$+1.56$	
1024 . .			22	$-\ 4.2$	H	gas	-0.724	$+1.56$	Some astigmatism
1038 . .			23	$-\ 8.5$	vM	fg	-0.736	$+1.56$	of 60-in. mirror

Mor.–Ev.	Δp	Δm	M	v	Δt
$845-569_1$ . . .	$+1.37$	$+0.73$	$+16$	-17	$-4°5$
890_1-1038 . . .	$+1.40$	-0.25	-14	$-\ 1$	-2.7
890_2-1024 . . .	$+1.38$	-0.25	-12	$+\ 1$	-3.0
$846-569_2$ . . .	$+1.37$	$+0.73$	$+56$	$+23$	-1.7
891_1-1008_1 . . .	$+1.37$	-0.25	-14	$-\ 1$	-0.2
$847-570_1$ . . .	$+1.37$	$+0.73$	$+15$	-18	-0.5
891_2-1008_2 . . .	$+1.37$	-0.25	$-\ 6$	$+\ 7$	0.0
$892-570_2$ . . .	$+1.10$	$+0.81$	$+50$	$+13$	$+2.0$

$$+2.49\,\mu_\alpha+\ 2.51\,\pi=+116 \qquad \pi\ =-\ 0.5=-0''.001\pm0''.005$$
$$+2.51\,\mu_\alpha+14.47\,\pi=+111 \qquad \mu_\alpha=+47.1=+0''.077\pm0''.012$$

Comp. Star	Br.	x	y	π	P.E.
1.	f	$+0'.4$	$+2'.7$	$-0''.031$	$\pm0''.009$
2.	f	$+1.4$	$+2.1$	$+0.001$	0.010
3.	f	$+1.9$	$+2.1$	$+0.013$	0.012
4.	f	$+5.1$	$+1.1$	$+0.010$	0.004
5.	f	$+1.9$	-3.0	$+0.008$	0.003
6.	bf	-0.1	-4.1	-0.016	0.005
7.	bf	-4.0	-0.5	$+0.014$	0.004
8.	f	-6.0	$+0.5$	-0.002	±0.003

Boss 4480 = Bu 8114 $\alpha = 17^h 36^m 59^s$ $\delta = +24°34'$

Pl. No.	Date			t	Obs.	Qy	p	m	Remarks
635_1..	1915	Aug.	2	−11°0	vM	fg	−0.714	+0.59	
635_2..			2	− 7.2	vM	g	−0.714	+0.59	
636_1..			2	− 2.0	H	g	−0.714	+0.59	
636_2..			2	+ 2.2	vM	g	−0.714	+0.59	Trail
909 ..	1916	April	23	+ 3.7	vM	gas	+0.780	+1.31	Clouds 20^m exp.
910 ..			23	+10.0	H	g	+0.780	+1.31	Clouds 20^m exp.
922_1..			24	−12.0	vM	g	+0.771	+1.32	
922_2..			24	− 7.7	H	g	+0.771	+1.32	
923_1..			24	− 2.5	vM	fg	+0.771	+1.32	
923_2..			24	+ 2.0	H	fg	+0.771	+1.32	
924_1..			24	+ 7.0	vM	g	+0.771	+1.32	
924_2..			24	+11.2	H	g	+0.771	+1.32	
1009_1..		July	21	− 1.7	H	g	−0.570	+1.56	
1009_2..			21	+ 2.5	vM	g	−0.571	+1.56	
1010_1..			21	+ 7.2	H	fg	−0.571	+1.56	
1010_2..			21	+12.0	vM	g	−0.571	+1.56	

Mor.–Ev.	Δp	Δm	M	v	Δt
922_1– 635_1...	+1.49	+0.73	+ 7	− 3	−1°0
922_2– 635_2...	+1.49	+0.73	+18	+ 8	−0.5
923_1– 636_1...	+1.49	+0.73	+18	+ 8	−0.5
923_2–1009_1...	+1.34	−0.24	+19	+ 3	+3.7
909 – 636_2...	+1.49	+0.72	− 3	−13	+1.5
924_1–1009_2...	+1.34	−0.24	+23	+ 7	+4.5
910 –1010_1...	+1.35	−0.25	+22	+ 5	+2.8
924_2–1010_2...	+1.34	−0.24	+ 2	−14	−0.8

$$+2.35\,\mu_a + 3.04\,\pi = +13 \qquad \pi = +10.8 = +0''.018 \pm 0''.003$$
$$+3.04\,\mu_a + 16.10\,\pi = +149 \qquad \mu_a = -8.4 = -0''.014 \pm 0''.008$$

The 8^M5 companion, not being covered by the sector, shows large images on the plates. The result of the measures is

$$\pi = +0''.022 \pm 0''.008$$
$$\mu_a = -0''.031 \pm 0''.020.$$

According to Burnham, the stars have the same proper motion.

Comp. Star	Br.	x	y	π	P.E.
1........	bf	+0′5	+3′7	+0″011	±0″008
2........	bf	+3.3	+4.7	−0.001	0.004
3........	f	+2.3	−1.1	0.000	0.005
4........	f	+2.5	−5.8	+0.005	0.006
5........	f	−0.1	−3.4	+0.002	0.010
6........	f	−1.6	−2.6	−0.026	0.007
7........	bf	−2.1	−0.1	+0.008	0.006
8........	f	−4.0	+0.5	+0.019	0.009
9........	bf	−1.5	+4.5	−0.017	±0.004

Boss 4629 $\alpha = 18^h15^m4^s$ $\delta = +24°24'$

Pl. No.	Date	t	Obs.	Qy	p	m	Remarks
637_1..	1915 Aug. 2	−0°2	H	g	−0.599	+0.59	
637^2..	2	+4.0	vM	g	−0.599	+0.59	
652^1..	3	−4.0	vM	g	−0.613	+0.59	
652_2..	3	+1.2	H	g	−0.613	+0.59	
893 ..	1916 April 22	−5.7	H	fg	+0.875	+1.31	
894 ..	22	−1.5	vM	f	+0.875	+1.31	
895 ..	22	+3.5	H	f	+0.875	+1.31	
929_1..	May 9	−8.0	H	g	+0.703	+1.36	
929_2..	9	−4.0	vM	g	+0.701	+1.36	
930_1..	9	+1.5	H	fg	+0.701	+1.36	
930_2..	9	+6.0	vM	fg	+0.701	+1.36	
938 ..	22	−2.0	vM	g	+0.531	+1.39	
1054_1..	Aug. 3	−4.0	vM	g	−0.622	+1.59	
1054_2..	3	+0.5	H	g	−0.622	+1.59	
1068 ..	4	+1.0	vM	fg	−0.636	+1.60	Thick 25^m exp. Trail
1070 ..	5	−6.5	H	fg	−0.648	+1.60	Hazy 25^m exp.

Mor.–Ev.	Δp	Δm	M	v	Δt
929_1–1070 ...	+1.35	−0.24	− 4	+ 2	−1°5
893 − 652_1...	+1.49	+0.72	+29	+12	−1.7
929_2–1054_1...	+1.32	−0.23	− 4	+ 1	0.0
938 − 637_1...	+1.13	+0.80	+27	+ 9	−1.8
894 −1054_2...	+1.50	−0.28	+ 8	+14	−2.0
930_1–1068 ...	+1.34	−0.24	−23	−17	+0.5
895 − 652_2...	+1.49	+0.72	+ 7	−10	+2.3
930_2− 637_2...	+1.30	+0.77	+ 5	−13	+2.0

$$+2.52\,\mu_a + 2.68\,\pi = +58 \qquad \pi = 0.0 = 0''.000 \pm 0''.004$$
$$+2.68\,\mu_a + 15.02\,\pi = +62 \qquad \mu_a = +23.0 = +0''.037 \pm 0''.010$$

Comp. Star	Br.	x	y	π	P.E.
1.......	f	+0′1	+3′7	+0″023	±0″004
2.......	f	+4.7	+2.6	−0.027	0.006
3.......	b	+3.3	+0.3	+0.010	0.010
4.......	f	+4.7	−3.4	+0.018	0.012
5.......	f	−1.1	−4.3	+0.004	0.012
6.......	f	−1.9	−3.8	−0.014	0.010
7.......	f	−2.5	+0.4	−0.003	0.016
8.......	f	−2.5	+1.8	−0.041	0.014
9.......	f	−3.8	+2.5	+0.033	0.006
10.......	ff	−0.7	+0.5	0.000	±0.015

Boss 4647 $\alpha=18^h17^m36^s$ $\delta=+51^\circ18'$

Pl. No.	Date	t	Obs.	Qy	p	m	Remarks
622_1..	1915 Aug. 1	$+5^\circ.0$	yM	g	-0.578	$+0.59$	
622_2..	1	$+9.5$	H	fg	-0.578	$+0.59$	Trail
653_1..	3	$+6.7$	vM	g	-0.603	$+0.59$	
653_2..	3	$+11.5$	H	g	-0.603	$+0.59$	
939_1..	1916 May 22	$+4.0$	vM	fg	$+0.541$	$+1.39$	
939_2..	22	$+8.0$	vM	g	$+0.539$	$+1.39$	
949 ..	24	$+1.0$	vM	f	$+0.510$	$+1.40$	20^m exp.
950_1..	24	$+7.0$	H	fg	$+0.510$	$+1.40$	20^m exp. 5^m without sector running
950_2..	24	$+15.0$	vM	fg	$+0.510$	$+1.40$	25^m exp.
959_1..	25	-15.0	vM	g	$+0.496$	$+1.40$	
959_2..	25	-10.5	H	g	$+0.496$	$+1.40$	
1055 ..	Aug. 3	$+6.0$	vM	g	-0.616	$+1.59$	
1066 ..	4	-16.5	vM	g	-0.627	$+1.60$	Thick 25^m exp.
1067 ..	4	-9.0	H	g	-0.629	$+1.60$	Thick 25^m exp.

Mor.–Ev.	Δp	Δm	M	v	Δt
959_1–1066 ...	$+1.12$	-0.20	$+25$	-4	$+1^\circ.5$
959_2–1067 ...	$+1.13$	-0.20	$+33$	$+4$	-1.5
949 – 622_1...	$+1.09$	$+0.81$	$+33$	$+31$	-4.0
939_1–1055 ...	$+1.16$	-0.20	$+30$	$+1$	-2.0
950_1– 653_1...	$+1.11$	$+0.81$	-17	-19	$+0.3$
939_2– 622_2...	$+1.12$	$+0.80$	$+7$	$+4$	-1.5
950_2– 653_2...	$+1.11$	$+0.81$	-14	-16	$+3.5$

$+2.74\,\mu_a+2.90\,\pi=-10$ $\pi=+21.0=+0''.034\pm0''.008$

$+2.90\,\mu_a+8.78\,\pi=+109$ $\mu_a=-25.9=-0''.042\pm0''.015$

Comp. Star	Br.	x	y	π	P.E.
1........	bf	$+0'.3$	$+2'.6$	$+0''.005$	$\pm0''.006$
2........	f	$+4.4$	$+1.4$	-0.020	0.017
3........	bf	$+4.4$	-1.0	$+0.018$	0.017
4........	f	-1.0	-1.9	$+0.007$	0.017
5........	ff	-1.6	-3.8	$+0.001$	0.007
6........	f	-2.6	-0.1	-0.020	0.023
7........	b	-4.0	$+3.0$	$+0.010$	±0.012

Boss 4892, 4893 = Bu 9137 $\alpha = 19^h 9^m 30^s$ $\delta = +49°40'$

Pl. No.	Date			t	Obs.	Qy	p	m	Remarks
673 . .	1915	Sept.	1	−15°0	vM	f	−0.794	+0.67	
674_1 . .			1	−10.2	H	fg	−0.794	+0.67	
674_2 . .			1	− 6.0	vM	fg	−0.794	+0.67	
675 . .			1	− 1.0	H	fg	−0.794	+0.67	
940_1 . .	1916	May	22	+ 2.7	vM	fg	+0.701	+1.39	
940_2 . .			22	+ 6.7	vM	fg	+0.701	+1.39	
960_1 . .			25	−17.0	vM	fg	+0.664	+1.40	
960_2 . .			25	−12.2	H	fg	+0.664	+1.40	
961_1 . .			25	− 7.0	vM	g	+0.664	+1.40	
961_2 . .			25	− 2.2	H	g	+0.664	+1.40	
962_1 . .			25	+ 3.0	vM	g	+0.664	+1.40	
962_2 . .			25	+ 7.5	H	g	+0.664	+1.40	
1100_1 . .		Sept.	20	0.0	vM	fg	−0.945	+1.73	
1100_2 . .			20	+ 4.0	vM	fg	−0.945	+1.73	
1101 . .			20	+ 9.2	H	gas	−0.945	+1.73	Trail
1117 . .			21	+ 0.2	vM	fg	−0.948	+1.73	

Mor.–Ev.	Δp	Δm	M (4892)	M (4893)	v (4892)	v (4893)	Δt
960_1– 673	+1.46	+0.73	−11	− 3	+20	+28	−2°0
960_2– 674_1	+1.46	+0.73	−50	−49	−19	−18	−2.0
961_1– 674_2	+1.46	+0.73	−36	−35	− 5	− 4	−1.0
961_2– 675	+1.46	+0.73	−27	−38	+ 4	− 7	−1.2
940_1–1100_1	+1.65	−0.34	+72	+70	− 6	− 5	+2.7
962_1–1117	+1.61	−0.33	+81	+81	+ 5	+ 8	+2.8
940_2–1100_2	+1.65	−0.34	+78	+69	0	− 6	+2.7
962_2–1101	+1.61	−0.33	+74	+75	+ 2	+ 2	−1.7

$$\left.\begin{aligned}+2.58\,\mu_a+\ \ 2.10\,\pi&=-193\\+2.10\,\mu_a+19.14\,\pi&=+316\end{aligned}\right\}(4892)\left.\begin{matrix}-191\\+299\end{matrix}\right\}(4893)$$

$$(4892)\begin{cases}\pi\ \ =+27.1=+0''.044\pm0''.003\\\mu_a=-96.8=-0''.158\pm0''.009\end{cases}\qquad(4893)\begin{cases}\pi\ \ =+26.0=+0''.042\pm0''.004\\\mu_a=-95.2=-0''.155\pm0''.011\end{cases}$$

Comp. Star	Br.	x	y	π	P.E.
1.	f	+0′.1	+1′.0	−0″.009	±0″.006
2.	f	+0.8	+3.7	−0.001	0.007
3.	b	+2.9	+0.3	+0.011	0.006
4.	f	0.0	−2.9	−0.011	0.008
5.	f	−1.1	−5.9	−0.001	0.007
6.	bf	−3.0	+1.5	+0.020	0.007
7.	bf	−2.7	+4.3	−0.012	±0.008

B.D.+35° 4001 $\alpha = 20^h 6^m 29^s$ $\delta = +35^\circ 53'$

Pl. No.	Date	t	Obs.	Qy	p	m	Remarks
699_1..	1915 Sept. 29	− 9°5	vM	g	−0.898	+0.75	Some astigmatism of 60-in. mirror
699_2..	29	− 4.2	vM	fg	−0.898	+0.75	
716_1..	30	−10.0	vM	fg	−0.903	+0.75	
716_2..	30	− 6.0	vM	fg	−0.903	+0.75	
973_1..	1916 June 22	− 8.0	vM	g	+0.469	+1.48	
973_2..	22	− 4.0	H	g	+0.468	+1.48	
974_1..	22	+ 2.0	vM	vg	+0.468	+1.48	
974_2..	22	+ 6.0	H	g	+0.468	+1.48	
975 ..	22	+11.0	vM	g	+0.468	+1.48	Trail of Boss 5210
987_1..	23	−11.0	vM	g	+0.453	+1.48	
987_2..	23	− 6.7	H	g	+0.453	+1.48	
988 ..	23	− 1.5	vM	g	+0.453	+1.48	
1084 ..	Sept. 19	+ 4.0	vM	fg	−0.827	+1.72	Clouds 20^m exp.
1085 ..	19	+10.5	H	g	−0.827	+1.72	Hazy 20^m exp.
1102_1..	20	+ 2.0	vM	vg	−0.836	+1.73	
1102_2..	20	+ 6.5	H	g	−0.836	+1.73	

Mor.–Ev.	Δp	Δm	M	v	Δt
987_1− 716_1...	+1.36	+0.73	+24	+ 9	−1°0
973_1− 699_1...	+1.37	+0.73	+20	+ 5	+1.5
987_2− 716_2...	+1.36	+0.73	+18	+ 3	−0.7
973_2− 699_2...	+1.37	+0.73	− 5	−20	+0.2
988 −1102_1...	+1.29	−0.25	+20	+13	−3.5
974_1−1084 ...	+1.30	−0.24	+23	+16	−2.0
974_2−1102_2...	+1.30	−0.25	−15	−22	−0.5
975 −1085 ...	+1.30	−0.24	+ 3	− 4	+0.5

$$+2.36\,\mu_\alpha + 2.71\,\pi = +34 \qquad \pi = +7.0 = +0''.011 \pm 0''.005$$

$$+2.71\,\mu_\alpha + 14.19\,\pi = +117 \qquad \pi_\alpha = +6.4 = +0''.010 \pm 0''.013$$

Comp. Star	Br.	x	y	π	P.E.
1........	bf	+1′.2	+1′.8	−0″.018	±0″.013
2........	f	+4.5	+0.4	−0.011	0.007
3........	f	+2.9	−1.1	+0.009	0.008
4........	bf	+0.7	−2.1	+0.011	0.007
5........	bf	−1.6	−0.1	+0.003	0.009
6........	f	−2.2	−1.2	+0.002	0.012
7........	f	−4.0	−1.1	−0.014	0.014
8........	f	−0.4	+3.4	+0.019	±0.009

B.D.+35° 4013 $\alpha=20^h8^m8^s$ $\delta=+35°54'$

Pl. No.	Date	t	Obs.	Qy	p	m	Remarks
661 . .	1915 Aug. 31	+11°.7	H	g	−0.602	+0.67	Hazy 20^m exp.
678_1. .	Sept. 1	+ 8.2	H	fg	−0.616	+0.67	
678_2. .	1	+13.0	vM	fg	−0.616	+0.67	
688 . .	2	+12.5	vM	f	−0.629	+0.67	
989_1. .	1916 June 23	+ 4.7	H	g	+0.458	+1.48	
989_2. .	23	+ 9.0	vM	g	+0.458	+1.48	
990 . .	23	+13.5	H	g	+0.458	+1.48	
1001 . .	24	− 2.5	H	vg	+0.444	+1.49	
1002_1. .	24	+ 2.5	H	g	+0.444	+1.49	
1002_2. .	24	+ 6.0	vM	vg	+0.444	+1.49	
1003 . .	24	+11.0	H	g	+0.444	+1.49	
1119_1. .	Sept. 21	− 0.5	vM	fg	−0.838	+1.73	
1119_2. .	21	+ 3.5	H	fg	−0.838	+1.73	
1120 . .	21	+ 7.5	vM	fg	−0.838	+1.73	Clouds 10^m exp.

Mor.-Ev.	Δp	Δm	M	v	Δt
1001 −1119_1. . .	+1.28	−0.24	−18	−13	−2°.0
1002_1−1119_2. . .	+1.28	−0.24	+ 2	+ 7	−1.0
989_1−1120 . . .	+1.30	−0.25	− 2	+ 4	−2.8
1002_2− 678_1 . .	+1.06	+0.82	+23	− 5	−2.2
989_2− 661 . . .	+1.06	+0.81	+25	− 2	−2.7
1003 − 688 . . .	+1.07	+0.82	+32	+ 4	−1.5
990 − 678_2. . .	+1.07	+0.81	+29	+ 2	+0.5

$$+2.84\,\mu_\alpha+2.53\,\pi=+92 \qquad \pi=+\ 1.5=+0''.002\pm0''.003$$
$$+2.53\,\mu_\alpha+9.49\,\pi=+93 \qquad \mu_\alpha=+31.1=+0''.051\pm0''.006$$

Comp. Star	Br.	x	y	π	P.E.
1.	f	+0′.1	+2′.1	−0″.020	±0″.004
2.	bf	+2.5	+2.1	+0.009	0.006
3.	bf	+1.6	−0.7	+0.007	0.010
4.	f	+2.6	−1.0	+0.003	0.014
5.	f	+0.7	−3.4	−0.009	0.009
6.	bf	−2.5	−1.8	+0.007	0.009
7.	bf	−2.6	−0.5	+0.001	0.005
8.	bf	−2.7	+3.2	+0.002	±0.006

Boss 5433, 5434 = Bu 10732 $\alpha = 21^h2^m25^s$ and $21^h2^m26^s$ $\delta = +38°15'$

Pl. No.	Date			t	Obs.	Qy	p	m	Remarks
336 ...	1914	Oct.	14	+ 8°7	vM	f	−0.885	+0.789	
337 ...			14	+14.5	H	f	−0.885	+0.789	Trail
351_1...			15	− 1.0	vM	fg	−0.890	+0.792	
351_2...			15	+ 4.0	vM	fg	−0.890	+0.792	5434 not measured on account of defect in plate
576_1...	1915	July	2	− 6.0	vM	g	+0.531	+1.504	
576_2...			2	− 1.5	H	g	+0.531	+1.504	
577 ...			2	+ 3.7	vM	g	+0.531	+1.504	
578 ...			2	+ 9.0	H	fg	+0.529	+1.504	
579 ...			2	+13.5	vM	fg	+0.529	+1.504	5434 behind sector support
595_1...			3	+12.0	H	g	+0.516	+1.507	
595_2...			3	+16.2	vM	fg	+0.516	+1.507	5434 behind sector-support
601_1...			4	− 6.5	H	f	+0.504	+1.510	
601_2...			4	− 2.0	vM	f	+0.504	+1.510	
700 ...		Sept.	29	−11.0	vM	gas	−0.763	+1.748	
719_1...			30	+ 5.0	vM	fas	−0.773	+1.751	
719_2...			30	+ 9.0	vM	fas	−0.773	+1.751	
735_1...		Oct.	1	− 7.5	vM	fg	−0.781	+1.754	
735_2...			1	− 3.5	H	fg	−0.781	+1.754	

Mor.–Ev.	Δp	Δm	M (5433)	M (5434)	v (5433)	v (5434)	Δt
601_1–700	+1.267	−0.238	− 377	− 357	−21	− 5	+4°5
576_1–735_1.......	+1.312	−0.250	− 399	− 382	−21	− 9	+1.5
601_2–735_2.......	+1.285	−0.244	− 406	− 382	−39	−19	+1.5
576_2–351_1.......	+1.421	+0.712	+2132	+2094	+26	+20	−0.5
577 –351_2.......	+1.421	+0.712	+2140	....	+34	....	−0.3
578 –719_1.......	+1.302	−0.247	− 364	− 339	+ 8	+28	+4.0
595_1–336	+1.401	+0.718	+2084	+2068	−34	−17	+3.3
579 –719_2.......	+1.302	−0.247	− 311	....	+61	....	+4.5
595_2–337	+1.401	+0.718	+2095	....	−23	....	+1.7

$$\left.\begin{array}{l} +2.348\,\mu_a + 2.448\,\pi = +6498 \\ +2.448\,\mu_a + 16.331\,\pi = +9524 \end{array}\right\}(5433) \qquad \left.\begin{array}{l} +1.264\,\mu_a + 0.752\,\pi = +3334 \\ +0.752\,\mu_a + 10.654\,\pi = +3988 \end{array}\right\}(5434)$$

$$(5433)\left\{\begin{array}{l} \pi = +199.5 = +0''.325 \pm 0''.011 \\ \mu_a = +2559.4 = +4''.169 \pm 0''.028 \end{array}\right. \qquad (5434)\left\{\begin{array}{l} \pi = +196.3 = +0''.320 \pm 0''.008 \\ \mu_a = +2520.9 = +4''.107 \pm 0''.023 \end{array}\right.$$

Comp. Star	Br.	x	y	π	P.E.
1........	f	+1'.2	+0'.4	+0''.018	±0''.008
2........	f	+6.2	+1.2	−0.002	0.008
3........	bf	+1.5	+2.6	+0.006	0.007
4........	f	−3.0	+4.3	−0.009	0.006
5........	bf	−5.2	+0.7	+0.004	0.004
6........	f	−2.1	−0.5	−0.009	0.010
7........	b	−2.1	−5.2	+0.010	0.005
8........	f	+3.6	−3.8	−0.015	±0.011

Boss 5682, 5683 = Bu 11514 $\alpha = 22^h1^m49^s$ and $22^h1^m56^s$ $\delta = +82°23'$

Pl. No.	Date			t	Obs.	Qy	p	m	Remarks
303_1..	1914	Oct.	12	− 8°0	vM	f	−0.725	−0.22	
303_2..			12	− 3.0	H	fg	−0.725	−0.22	
304_1..			12	+ 4.0	vM	fg	−0.727	−0.22	
304_2..			12	+ 9.7	H	fg	−0.727	−0.22	
1017_1..	1916	July	21	− 5.0	vM	f	+0.462	+1.56	
1017_2..			21	− 0.5	H	fg	+0.462	+1.56	
1018_1..			21	+ 4.0	vM	f	+0.462	+1.56	
1018_2..			21	+ 8.7	H	f	+0.462	+1.56	
1033 ..			22	−10.0	vM	fg	+0.450	+1.56	
1034_1..			22	− 0.5	vM	g	+0.449	+1.56	
1034_2..			22	+ 3.7	H	vg	+0.449	+1.56	
1048 ..			23	− 5.0	vM	g	+0.436	+1.56	
1104_1..		Sept.	20	− 4.0	vM	fg	−0.467	+1.73	
1104_2..			20	0.0	H	fg	−0.467	+1.73	Trail
1162 ..		Nov.	17	+ 4.0	vM	g	−0.925	+1.88	Hazy 20^m exp.
1171 ..			18	+ 3.0	vM	fg	−0.924	+1.89	

Mor.–Ev.	Δp	Δm	M (5682)	M (5683)	v (5682)	v (5683)	Δt
1033 − 303_1.....	+1.18	+1.78	−149	−118	−18	− 4	−2°0
1017_1−1104_1.....	+0.93	−0.17	+ 27	+ 25	+12	+11	−1.0
1048 − 303_2.....	+1.16	+1.78	−145	−115	−14	− 1	−2.0
1017_2−1104_2.....	+0.93	−0.17	− 3	+ 21	−18	+ 7	−0.5
1034_1−1171	+1.37	−0.33	+ 22	− 4	− 5	−30	−3.5
1034_2−1162	+1.37	−0.32	+ 36	+ 44	+10	+19	−0.3
1018_1− 304_1.....	+1.19	+1.78	−132	−122	− 1	− 8	0.0
1018_2− 304_2.....	+1.19	+1.78	− 98	−103	+33	+11	−1.0

$$\left.\begin{aligned}+12.95\,\mu_\alpha+\ 7.19\,\pi&=-955\\+\ 7.19\,\mu_\alpha+11.06\,\pi&=-517\end{aligned}\right\}(5682)\left.\begin{aligned}-836\\-442\end{aligned}\right\}(5683)$$

$$(5682)\left\{\begin{aligned}\pi&=+\ 1.8=+0''.003\pm0''.008\\\mu_\alpha&=-74.7=-0''.122\pm0''.007\end{aligned}\right.\qquad(5683)\left\{\begin{aligned}\pi&=+\ 3.1=+0''.005\pm0''.007\\\mu_\alpha&=-66.3=-0''.108\pm0''.006\end{aligned}\right.$$

Comp. Star	Br.	x	y	π	P.E.
1........	f	+0'.8	+5'.6	−0''.031	±0''.010
2........	f	+2.5	+1.4	+0.012	0.012
3........	f	+5.8	+0.5	+0.017	0.013
4........	bf	+1.6	−7.3	−0.012	0.008
5........	bf	−5.6	−1.4	−0.018	0.014
6........	f	−5.8	+1.4	+0.031	±0.011

Boss 5691 $\alpha = 22^h 2^m 43^s$ $\delta = +18°59'$

Pl. No.	Date	t	Obs.	Qy	p	m	Remarks
338_1..	1914 Oct. 14	+7°5	vM	fg	−0.741	−0.21	
338_2..	14	+12.5	H	fg	−0.741	−0.21	
352_1..	15	−3.5	C	fg	−0.750	−0.21	
352_2..	15	+1.0	vM	fg	−0.750	−0.21	
976 ..	1916 June 22	−9.5	H	fg	+0.801	+1.48	
977 ..	22	−5.0	vM	g	+0.801	+1.48	
991_1..	23	−9.5	vM	g	+0.794	+1.48	
991_2..	23	−5.5	H	g	+0.794	+1.48	
1035_1..	July 22	+9.2	vM	fg	+0.457	+1.56	
1035_2..	22	+13.5	H	fg	+0.456	+1.56	
1049_1..	23	+1.0	H	g	+0.443	+1.56	
1049_2..	23	+5.0	vM	g	+0.443	+1.56	
1086_1..	Sept. 19	−11.0	vM	fg	−0.445	+1.72	
1086_2..	19	−6.7	H	g	−0.446	+1.72	
1087 ..	19	−1.0	vM	g	−0.446	+1.72	Trail
1141 ..	Nov. 16	+5.5	vM	g	−0.923	+1.88	Clouds 20^m exp.

Mor.–Ev.	Δp	Δm	M	v	Δt
976 −1086_1...	+1.25	−0.24	−3	+9	+1°5
991_1−1086_2...	+1.24	−0.24	+24	+36	−2.8
991_2− 352_1...	+1.54	+1.69	+146	−11	−2.0
977 −1087 ...	+1.25	−0.24	−40	−28	−4.0
1049_1− 352_2...	+1.19	+1.77	+151	−10	0.0
1049_2−1141 ...	+1.37	−0.32	−32	−13	−0.5
1035_1− 338_1...	+1.20	+1.77	+159	−2	+1.7
1035_2− 338_2...	+1.20	+1.77	+183	+22	+1.0

$$+12.53\,\mu_\alpha + 7.61\,\pi = +1134 \qquad \pi = +6.9 = +0''.011 \pm 0''.008$$
$$+7.61\,\mu_\alpha + 13.21\,\pi = +748 \qquad \mu_\alpha = +86.3 = +0''.141 \pm 0''.009$$

Comp. Star	Br.	x	y	π	P.E.
1........	bf	+0′.7	+3′.3	−0″.001	±0″.011
2........	bf	+5.6	+2.5	−0.004	0.007
3........	f	+4.8	−0.8	+0.006	0.005
4........	bf	+0.8	−4.9	−0.005	0.007
5........	bf	−1.6	−5.1	+0.008	0.009
6........	f	−3.4	0.0	−0.010	0.008
7........	f	−2.7	+0.8	−0.006	0.007
8........	bf	−3.7	+4.7	+0.010	±0.007

Boss 5772 $\alpha=22^h18^m51^s$ $\delta=+20°21'$

Pl. No.	Date		t	Obs.	Qy	p	m	Remarks
366 . . .	1914	Nov. 10	+ 5°7	vM	g	−0.893	−0.14	
382$_1$. . .		11	− 6.2	vM	fg	−0.895	−0.13	
282$_2$. . .		11	− 1.7	vM	fg	−0.895	−0.13	
383 . . .		11	+ 4.5	H	fg	−0.895	−0.13	Trail
613$_1$. . .	1915	July 31	− 8.0	vM	g	+0.397	+0.58	
613$_2$. . .		31	− 3.0	vM	g	+0.397	+0.58	
614$_1$. . .		31	+ 2.7	H	g	+0.396	+0.58	
614$_2$. . .		31	+ 7.5	vM	g	+0.396	+0.58	
629 . . .		Aug. 1	0.0	vM	g	+0.382	+0.59	
645$_1$. . .		2	+ 1.7	H	g	+0.368	+0.59	
645$_2$. . .		2	+ 6.0	vM	g	+0.368	+0.59	
646 . . .		2	+11.2	H	g	+0.368	+0.59	
703$_1$. . .		Sept. 29	− 1.0	vM	g	−0.512	+0.75	
703$_2$. . .		29	+ 3.5	vM	g	−0.512	+0.75	
704 . . .		29	+ 8.0	vM	g	−0.512	+0.75	
721 . . .		30	+10.5	vM	g	−0.523	+0.75	

Mor.–Ev.	Δp	Δm	M	v	Δt	Remarks
613$_1$–382$_1$.	+1.29	+0.71	+186	− 1	−1°8	
613$_2$–382$_2$.	+1.29	+0.71	+164	−23	−1.3	
629 –703$_1$.	+0.89	−0.16	+ 9	+ 9	+1.0	
645$_1$–703$_2$.	+0.88	−0.16	+ 7	+ 8	−1.8	Star 1 not measured
614$_1$–383	+1.29	+0.71	+190	+ 3	−1.8	
645$_2$–366	+1.26	+0.73	+212	+22	+0.3	Star 1 not measured
614$_2$–704	+0.91	−0.17	− 12	−10	−0.5	
646 –721	+0.89	−0.16	− 2	− 2	+0.7	

$$+2.15\,\mu_\alpha+3.11\,\pi=+538 \qquad \pi=+35.6=+0''.058\pm0''.007$$

$$+3.11\,\mu_\alpha+9.75\,\pi=+965 \qquad \mu_\alpha=+198.7=+0''.324\pm0''.015$$

Comp. Star	Br.	x	y	π	P.E.
1.	f	+2′7	+1′5	0″000	±0″013
2.	f	+3.3	+3.3	−0.010	0.008
3.	f	−4.9	+5.8	0.000	0.010
4.	bf	−3.7	+1.6	+0.013	0.016
5.	f	−1.6	−3.7	−0.026	0.013
6.	f	−0.3	−2.6	+0.020	0.010
7.	bf	+2.9	−4.8	0.000	±0.009

Boss 5989 $\alpha=23^h12^m9^s$ $\delta=+52°40'$

Pl. No.	Date	*t*	Obs.	Qy	*p*	*m*	Remarks
353_1	1914 Oct. 15	− 8°5	vM	fg	−0.526	−0.21	
353_2	15	− 4.0	vM	fg	−0.526	−0.21	
354	15	+ 1.5	vM	fg	−0.526	−0.21	Trail
405	Dec. 9	+ 8.7	vM	g	−0.905	−0.06	
647_1	1915 Aug. 2	+ 6.5	vM	g	+0.566	+0.59	
647_2	2	+11.2	H	g	+0.566	+0.59	
656_1	3	− 8.5	vM	g	+0.554	+0.59	Clouds 20^m exp.
656_2	3	− 3.0	H	g	+0.554	+0.59	Clouds 20^m exp.
763_1	Dec. 1	+ 1.0	vM	gas	−0.898	+0.92	Some astigmatism of 60-in. mirror
763_2	1	+ 6.0	vM	gas	−0.898	+0.92	
764	1	+13.0	H	fg	−0.898	+0.92	Clouds 20^m exp.
1019	1916 July 21	− 3.0	vM	g	+0.696	+1.56	
1020	21	+ 1.7	H	g	+0.696	+1.56	
1021	21	+ 6.0	vM	g	+0.696	+1.56	
1022	21	+10.7	H	fg	+0.696	+1.56	
1036	22	+ 2.0	vM	g	+0.685	+1.56	
1037	22	+ 7.0	H	g	+0.685	+1.56	
1125	Oct. 21	− 5.2	H	f	−0.616	+1.81	
1142	Nov. 16	− 2.0	H	fg	−0.840	+1.88	Clouds 20^m exp.
1164	17	+ 5.5	vM	g	−0.845	+1.88	Trail

Mor.-Ev.	Δ*p*	Δ*m*	*M*	*v*	Δ*t*
656_1 − 353_1	+1.08	+0.80	+ 88	+ 1	0°0
656_2 − 353_2	+1.08	+0.80	+ 85	− 2	+1.0
1019 − 1125	+1.31	−0.25	+ 39	+19	+2.2
1020 − 763_1	+1.59	+0.64	+ 94	+ 5	+0.7
1036 − 1142	+1.53	−0.32	+ 31	+ 9	+4.0
1021 − 354	+1.22	+1.77	+160	+ 2	+4.5
647_1 − 763_2	+1.46	−0.33	+ 29	+10	+0.5
1037 − 1164	+1.53	−0.32	− 17	−39	+1.5
1022 − 405	+1.60	+1.62	+155	− 4	+2.0
647_2 − 764	+1.46	−0.33	+ 20	+ 1	−1.8

$$+7.92\,\mu_\alpha+5.22\,\pi=+700 \qquad \pi=+28.6=+0''.047\pm0''.004$$
$$+5.22\,\mu_\alpha+19.58\,\pi=+922 \qquad \mu_\alpha=+69.5=+0''.113\pm0''.007$$

Comp. Star	Br.	*x*	*y*	*π*	P.E.
1	bf	+1′5	+3′3	+0″008	±0″006
2	bf	+4.9	+4.9	−0.009	0.007
3	f	+5.2	+1.5	0.000	0.008
4	bb	+3.0	−4.4	+0.010	0.007
5	f	+1.4	−2.9	−0.007	0.007
6	bf	0.0	−4.1	+0.006	0.004
7	f	−3.8	−4.5	−0.004	0.010
8	f	−7.5	−0.4	−0.003	0.005
9	f	−1.4	+1.6	−0.016	0.007
10	bf	−2.9	+5.2	+0.014	±0.006

DISCUSSION OF SYSTEMATIC ERRORS

The material now available seems to warrant a more thorough search for systematic errors than was possible when the first series was published. Such an investigation is the more necessary because we are dealing here with stars of generally small parallaxes. With few exceptions the data are for stars of magnitude 5.00 to 7.00, of type F, G, K, and M and of proper motion <0.″500 annually. The influence of any systematic error will therefore be more disturbing in conclusions derived from this material than it would in the case of nearer stars.

The discussion of systematic errors can be divided into two parts, which may be classed as internal and external systematic errors: the first are to be derived from the materials *inter se;* the second from a comparison with other sources.

TABLE II

	bb	b	bf	f	ff	All
Mean π.....	+0.″010	−0.″005	+0.″003	−0.″001	0.″000	0.″000
Mean P.E...	0.007	0.009	0.008	0.008	0.011	0.008
n..........	1	13	69	133	13	229

Internal systematic errors.—Two known sources of possible error belong to this class:

a) A magnitude error, due to the fact that the comparison stars are not all of the same magnitude and that the reduced parallax star is not equal to the weighted mean magnitude of the comparison stars. If such a systematic error exists, the parallaxes of the comparison stars should show a progressive change with their magnitudes.

Table II gives the mean parallaxes, their probable errors, and the numbers of the comparison stars of different magnitudes used in the present paper. No systematic error is revealed by these values. The approximate values of these magnitudes are (on the scale of *Publications of the Astron. Lab. at Groningen,* No. 18) bb=11.2−11.6; b=11.7−12.1; bf=12.2−12.5; f=12.6−13.2; ff=13.3−13.7. While for the brighter stars the probable error of a parallax is the same as that found in the first series, that of the faintest stars has decreased from 0.″014 to 0.″011; probably this is due to the entire avoidance of the very faintest images on the plates. That no magnitude error is present in this second series can also be seen from a comparison of the parallaxes of the components of the double stars measured. Table III gives the values found in the seven cases. For each of these pairs, Burnham, in his *General Catalogue of Double Stars*, states that the two components are either relatively fixed or have a common proper motion; for all cases we may therefore expect the same parallax for the two components. The companion of Boss 4480 was not behind the sector; the difference in magnitude of the components is therefore 6.46+5.00−8.76=+2.70, where 5.00 represents the value of the reduction in the magnitude of the parallax star due to the use of a sector with opening of 3°.6. It is evident that the values of $\Delta\pi$ bear no relation to those of Δm; in fact, the differences in the parallaxes of the components are well within the uncertainty of the determination.

TABLE III

Number in Boss *P.G.C.*	Number in Bu.	Mag.	Relative Parallax	Δm	$\Delta\pi$
178_1 178_2	439	6.29 6.29	+0.009 +0.007	0.00	+0.002
1904 Comp	2149	6.11 9.21	−0.001 −0.002	−3.10	+0.001
2285 2286	4677	6.04 7.15	+0.020 +0.024	−1.11	−0.004
4480 Comp	8114	6.46+5.00 8.76	+0.018 +0.022	+2.70	−0.004
4892 4893	9137	6.84 6.62	+0.044 +0.042	+0.22	+0.002
5433 5434	10732	5.57 6.28	+0.325 +0.320	−0.71	+0.005
5682 5683	11514	6.49 6.89	+0.003 +0.005	−0.40	−0.002

Since in the first series a small magnitude error was found to exist, the final correction to the mean parallax for both series due to this cause may be estimated to be −0″.001.

b) Error due to the neglect of the quadratic terms of x and y. An investigation of the existence of such an error was made in the same way as in the first paper. The comparison stars were divided into 49 groups, according to their positions on the plates, each group containing from 1 to 14 stars. The weighted mean of each group was then used as the second member of an equation of condition of the form:

$$+a+bx+cy+dx^2+exy+fy^2=\text{mean }\pi$$

These equations, solved by least squares, gave as a resulting correction to the parallaxes of the central stars +0″0001±0″0005. The analogous correction for the first series was +0″0008±0″0020; for the mean of all parallaxes it is therefore +0″0004.

External systematic errors.—*a*) A comparison of the parallaxes for those stars which have also been investigated by other observers affords as yet little material. Six fields only have been measured in common with other observers, viz., Boss 592–3, the results of which were kindly communicated to me by Mr. Pitman, of the Sproul Observatory; Boss 4892–3, for which the parallax has been determined by Flint, Chase, Kostinsky, Russell, Mitchell, and Jewdokimow; B.D.+35°4001 and B.D. +35°4013, results for which have been published by Kapteyn; Boss 5433–4, the well-known double star 61 Cygni, for which, besides the results given by Kapteyn in *Publications of the Astronomical Laboratory at Groningen*, No. 24, determinations are available from the Yerkes and Sproul Observatories as well as others by Abetti, Struve, and Jewdokimow; finally, N.G.C. 7662; neither the measures of this field by Wilsing nor the rediscussion of them by Huss are of value for the present purpose, however, and it has therefore been omitted. Using for the two B.D. stars the mean of the values given by Kapteyn and those corrected for a magnitude error,[1] and for the other stars, the weighted means of the observations mentioned, we have material as collected in Table IV. For this comparison corrections were added to the observed parallaxes in order to reduce the published values to absolute parallaxes. The agreement is satisfactory, the mean difference being −0″0006. It is to be noted, however, that this comparison is based on five objects only and is therefore rather uncertain.

---

[1] *Publications of the Astronomical Society of the Pacific*, **28**, 280, 1916.

b) A comparison of the values $\mu_{a\mathrm{Boss}}$ and $\mu_{a\mathrm{vM}}$ shows a large majority of negative values in the differences $\mu_{a\mathrm{Boss}}-\mu_{a\mathrm{vM}}$ given in Table I. The mean difference is $-0''.009$, while in the former paper the analogous value was $+0''.001$. It may be remarked here that the differences $\Delta\mu_a$ seem to be independent of μ and of μ_a; reference to this point will be made under (*c*).

With a perfectly symmetrical distribution of plates during the interval a star was under observation, a difference in μ_a would not be reflected in the parallax. Since, however, for practical reasons parallax observations cannot be made under ideal conditions in this respect, it becomes necessary to see what the influence on the mean final parallaxes of a difference in μ_a will be. For this purpose we may take the mean of the equations of condition,

TABLE IV

Designation	Other Obs.	P.E.	vM	P.E.	Others—vM
Boss 592–3	+0″.031	0″.012	+0″.021	0″.014	+0″.010
Boss 4892–3	+0.049	0.006	+0.045	0.003	+0.004
B.D. +35°4001	+0.001	0.025	+0.013	0.005	−0.012
B.D. +35°4013	+0.024	0.020	+0.004	0.003	+0.020
Boss 5433–4	+0.299	0.003	+0.324	0.008	−0.025

$$\Delta p\pi+\Delta m\mu_a=M,$$

used in this paper; we find this to be approximately

$$+1.38\,\pi+0.23\,\mu_a=\overline{M}.$$

From this it appears that we shall have the difference in μ_a reflected in the final mean parallax as a systematic error amounting to $-\frac{0.23}{1.38}\Delta\mu_a$, or in our case to $-0''.0018$. The parallaxes would therefore require the correction $+0''.0018$.

To check this result I also derived the parallaxes of each individual star by using Boss's values of μ_a in the equations of condition.

The differences found for the parallaxes are very small, except for the cases in which the distribution of the plates with regard to the time is far from symmetrical, as, for instance, with Boss 5682–3 and Boss 5691. The mean correction for all fields in this series derived in this way was found to be +0″.0016; for the old series the analogous correction was −0″.0009, while for all the parallaxes it is in the mean +0″.0006.

c) Comparing the parallaxes of both series with those which can be derived for the same stars from the tables published by van Rhijn,[1] we find the mean difference for 47 stars (excluding those of type O and M) to be −0″.0071. In order to see whether this difference is a function of proper motion, the results have been derived separately for stars of different μ. The differences are given in Table V; Boss 5210 was excluded, as this was the only B-type star whose parallax was determined by me. All stars included are therefore of type F, G, or K.

TABLE V

Limits of μ	0″.000–0″.049	0″.050–0″.099	0″.100–0″.199	0″.200–0″.499	0″.500–0″.999	>1″.000
Mean μ	0″.027	0″.076	0″.144	0″.284	0″.642	5″.216
Mean π_{vR}	+0.006	+0.014	+0.020	+0.035	+0.056	+0.266
Mean π_{vM}	+0.009	+0.021	+0.021	+0.055	+0.045	+0.324
$\pi_{vR}-\pi_{vM}$	−0.003	−0.007	−0.001	−0.020	+0.011	−0.058
n	15	13	9	5	2	2

Each of the last two columns contains the results for one double star, viz., Boss 4892–3 and Boss 5433–4; little weight therefore can be attached to them; excluding also these four stars the mean difference $\pi_{vR}-\pi_{vM}$ becomes −0″.0056. The table presents no evidence that the difference $\Delta\pi$ is a function of the proper motion; such a relation, had it existed, could hardly have been attributed to the Mount Wilson values, as it would have been accompanied by a relation between $\Delta\mu_a$ and μ, which, as was stated under (*b*), does not occur.

d) The difference found under (*c*) is considerable; it therefore seemed advisable to compare the values of van Rhijn's tables with the directly determined parallaxes of other observers. The material available for stars with proper motions less than 0.″100 is extremely scarce; collecting all the results for stars of type F, G, and K having magnitudes between 5.00 and 6.99 and proper motions less than 0.″500, there are only 68 stars with 86 observations. Table VI shows the results of the comparison for different observers.

---

[1] *Derivation of the Change of Color with Distance and Apparent Magnitude.* Dissertation. Groningen: Hoitsema, 1915; *Astrophysical Journal*, **43**, 36, 1916,

TABLE VI

Observer	$\pi_{vR}-\pi$ Obs.	n
Abetti	+0.″008	11
Flint	−0.001	18
Greenwich	+0.010	7
Jewdokimow	+0.007	3
Jost	−0.059	7
Miller	−0.031	11
Mitchell	−0.034	6
Russell	+0.001	1
Yale	+0.020	14
Yerkes	+0.002	8

The mean of all 86 differences is −0.″0064. If we compare this result with the mean difference of −0.″0056, derived from my own observations of stars of the same type, magnitude, and proper motion, we find a discrepancy of only 0.″0008. We can scarcely avoid the conclusion that the mean of all directly observed parallaxes for stars of the kind specified is appreciably larger than that derived from van Rhijn's tables.

TABLE VII

Limits of μ	0.″000–0.″049	0.″050–0.″099	0.″100–0.″199	0.″200–0.″499	0.″500–0.″999	>1.″000
Mean μ	0.″024	0.″072	0.″135	0.″305	0.″642	5.″216
Mean π_{Adams}	+0.010	+0.018	+0.023	+0.052	+0.047	+0.322
Mean π_{vM}	+0.008	+0.028	+0.026	+0.062	+0.045	+0.324
$\pi_{Adams}-\pi_{vM}$	+0.002	−0.010	−0.003	−0.010	+0.002	−0.002
n	19	14	6	4	2	2

e) Mr. Adams kindly allows me to compare the parallaxes derived by his ingenious spectroscopic method with those given here. Forty-six stars have been observed in common. The results of the comparison are collected in Table VII. It should be stated, however, that this comparison is not an independent one, since in deriving his reduction-curves for the smaller proper-motion stars Adams used about ten parallaxes derived by me, while he has also made use of part of the material mentioned under (*d*). The mean difference $\pi_{\text{Adams}}-\pi_{\text{vM}}$ for 46 stars is −0″.0033.

SUMMARY

Collecting all the material which points to systematic error in the Mount Wilson parallaxes, we have the corrections shown in Table VIII.

TABLE VIII

Internal methods	*a* correction for magnitude	−0″.001
	b correction for neglect of x^2, xy, y^2	0.000
External methods	*a* correction from 5 fields in common with others	−0.001
	b correction from comparison of μ_α Boss and vM	+0.001
	c correction from comparison with van Rhijn	−0.007
	d correction from comparison with other obs. through van Rhijn	+0.001
	e correction from comparison with Adams	−0.003

From these data it seems safe to conclude that the Mount Wilson parallaxes can be affected only by very small systematic errors.

The difference $\pi_{\text{vR}}-\pi_{\text{vM}}$ alone is so large as to attract special attention. In seeking an explanation for the origin of this difference, we should note that there are two causes which tend to make van Rhijn's tables give parallaxes for stars of small proper motion that are too small: First, the formula on which the tables are based gives zero parallaxes for stars of zero proper motion. Second, the tabular values for stars of the class in question have been based, to some extent at least, upon parallactic motions. Because of their small relative motion, stars accompanying the sun in its motion through space will thus be grouped among the distant objects, while actually their parallaxes may be considerable. The following points are also to be noted:

First, a systematic correction of −0″.0071 would make 16 of the total of 56 absolute parallaxes negative, while 10 of the 20 stars of proper motion less than 0″.050 would have negative absolute parallaxes; both numbers are highly improbable, if we keep in mind the smallness of the probable errors.

Second, a systematic correction in π would be reflected in μ_α increased by about six times its amount, as was pointed out on page 37. We should therefore expect a systematic difference of about $+0\overset{''}{.}040$ in μ_α; unless Boss's proper motions have been vitiated by the same amount, we should find a much larger difference between $\mu_{\alpha\mathrm{Boss}}$ and $\mu_{\alpha\mathrm{vM}}$ than actually appears.

Third, the close agreement of the observed mean difference $\pi_{\mathrm{vR}}-\pi_{\mathrm{vM}}$ with that of $\pi_{\mathrm{vR}}-$ all other directly observed parallaxes makes it probable that this difference is not attributable to the Mount Wilson parallaxes.

Finally, the values found for the absolute magnitudes and for the τ-components of the proper motions expressed in km per second, when derived with the help of these parallaxes, are in close agreement with our present knowledge of these quantities,[1] and this agreement is lacking when we use our parallaxes after applying a correction of $-0\overset{''}{.}0071$.

To show this last point, the mean absolute magnitudes, $\overline{M}$, and the mean τ-components of the proper motions expressed in km per second, $\overline{V}$, were derived for groups of stars of specified proper motions. The F-, G-, and K-type stars were divided into four groups; those of the M-type, into two groups, according to their proper motions. For each group the mean M and V were derived by the formulae

$$\overline{M}=\overline{m}+5+5\,(\log)\,\overline{\pi} \quad \text{and} \quad \overline{V}=4.74\,\frac{\overline{\tau}}{\pi}$$

The same was done after correcting the mean parallaxes by $-0\overset{''}{.}003$ and $-0\overset{''}{.}0071$, respectively. The results are collected in Table IX.

Doubt may be expressed as to the propriety of using the mean values of m, π, and τ in the derivation of $\overline{M}$ and $\overline{V}$. This, to be sure, tends to decrease the values of $\overline{M}$ and $\overline{V}$. Our parallaxes, however, are vitiated by probable errors, and these, on the other hand, tend to increase the mean values of $\overline{M}$ and $\overline{V}$. The result cannot be far from the truth.

---

[1] Cf., for instance, W. S. Adams and G. Strömberg, *Astrophysical Journal*, **45**, 296, 1917.

A glance at Table IX, which gives data for various intervals of proper motion, shows that in general the values of $\overline{M}$ and $\overline{V}$ derived from the uncorrected parallaxes and from those corrected by −0″003 are about equally probable. Only the small group of the M-type stars with very small proper motions give, in the second case, improbable values for $\overline{M}$ and $\overline{V}$, namely, −3.95 and 52, respectively.

A correction of −0″0071, which would be necessary in order to make our parallaxes agree with van Rhijn's tables, gives, on the other hand, very improbable values of $\overline{M}$ and $\overline{V}$ for the large group of F, G, and K stars with proper motions less than 0″050, while for the small proper-motion stars of the M-type the mean absolute parallax becomes negative, and the values of $\overline{M}$ and $\overline{V}$ become illusory. It may therefore be concluded that there is no reason to suppose that the systematic error in the Mount Wilson parallaxes surpasses 0″003.

TABLE IX

	Stars of Type F, G, and K								Stars of Type M			
	0″000–0″049		0″050–0″099		0″100–0″199		0″200–0″499		0″000–0″049		0″050–0″099	
	$\overline{M}$	$\overline{V}$	$\overline{M}$	$\overline{V}$	$\overline{M}$	$\overline{V}$	$\overline{M}$	$\overline{V}$	$\overline{M}$	$\overline{V}$	$\overline{M}$	$\overline{V}$
$\pi=\pi$ abs.......	+0.66	9	+2.58	11	+2.85	12	+4.74	7	−0.91	13	+4.38	7
$\pi_1=\pi-0''003$...	−0.26	13	+2.25	13	+2.50	14	+4.61	8	−3.95	52	+4.24	7
$\pi_2=\pi-0''0071$..	−3.02	47	+1.63	17	+1.81	19	+4.44	9	......	....	+4.04	8
n.............	15		13		9		5		4		3	

I wish to express my thanks to Miss Helen N. Davis and Miss Coral Wolfe, of the Computing Division, for much assistance in the computations. I am greatly indebted to Mr. W. P. Hoge, who has helped most efficiently in securing the exposures.

Mount Wilson Solar Observatory
May 1917

Contributions from the Mount Wilson Solar Observatory, No. 137
Reprinted from the *Astrophysical Journal*, Vol. XLVI, pp. 138–166, 1917

THE ELIMINATION OF POLE-EFFECT FROM THE SOURCE FOR SECONDARY STANDARDS OF WAVE-LENGTH

By CHARLES E. ST. JOHN and HAROLD D. BABCOCK

I. INTRODUCTION

Since the publication of the list of secondary standards of wave-length by the International Committee,[1] the attention of several spectroscopists has been devoted to the problem of adding to the number of such spectral lines. It has been sought to extend the range of wave-length covered and also to provide standards at more frequent intervals than was at first thought necessary. Determinations of wave-lengths by interference methods have been published by Burns, Meggers, and Merrill,[2] Meissner,[3] Burns and Meggers,[4] Eversheim,[5] Burns,[6] Werner,[7] and still other investigations are in progress. During the past year preliminary work in this field has been carried on at this observatory, and it is the purpose of the present paper to contribute some of the results which are now at hand.

A primary requisite which a spectral line must have in order to serve as a standard of wave-length is reproducibility. In practice this quantity depends upon two factors which determine the errors involved in locating the line in the spectrum, namely, the absolute constancy of the wave-length under the range of working conditions permitted, and the characteristics of the curve defining the intensity distribution in the line. But quite aside from the question of reproducibility, it is equally important from a practical point of view that the adopted value of a standard should be its fundamental wave-length, that is, the wave-length free from displacements due to disturbing conditions in the arc itself that are associated primarily with proximity to the poles but are extended in range by increased current strength. It is not the purpose by this term to distinguish between a possible effect due to changes in the relative intensities of the components of a complex vibrating system and that of perturbing influences acting upon the emitting centers, or to suggest an explanation of pole-effect. When, as will appear later in the paper, arc conditions are such that sensitive lines yield their fundamental wave-lengths, these lines then behave like normally stable lines. The absolute measure of pole-effect in any source is obtained by comparing the wave-lengths given by it with the corresponding fundamental values as defined above.

---

[1] *Astrophysical Journal*, **32**, 215, 1910, and **39**, 93, 1914.

[2] *Scientific Papers of Bureau of Standards*, No. 274, 1916.

[3] *Annalen der Physik*, **51**, 95, 1916.

[4] *Scientific Papers of Bureau of Standards*, No. 251, 1915.

[5] *Annalen der Physik*, **45**, 454, 1914.

[6] *Journal de Physique* (5), **3**, 457, 1913.

[7] *Annalen der Physik*, **44**, 289, 1914.

The introduction of the pressure-effect into the values of the secondary standards, by operating the iron arc at atmospheric pressure, is undesirable from this point of view. But while for special purposes, we do, indeed, employ the arc *in vacuo* as a source of reference lines, it can hardly be recommended as a general source of secondary standards on account of its greatly diminished brightness and of the inconvenience attending its use. Moreover, the revisions of the values of the pressure-effect which are now in progress will soon supply precise data for the elimination of this factor when necessary, and the correction, being dependent in amount only upon the barometer reading, can be applied with certainty. Pole-effect, on the other hand, does not lend itself readily to such simple treatment, chiefly on account of its rapid variation from point to point in the arc and its sensitiveness to change in arc conditions. These practical considerations permit a distinction to be drawn between pole-effect and pressure-effect in regard to their bearing upon the establishment of a system of standard wave-lengths.

The phenomena of pole-effect have been studied by Goos,[1] Gale and Whitney,[2] Royds,[3] Whitney,[4] and St. John and Babcock[5] under a variety of conditions, but hitherto none of the suggested explanations has met with general acceptance. While it is possible that some of the relations between pole-effect, arc-length, and current-strength, which are now quantitatively measured, may throw light upon the nature of the effect, it is not our purpose to discuss here the theories that have been proposed to account for it.

---

[1] *Astrophysical Journal*, **38**, 141, 1913.

[2] *Ibid.*, **43**, 161, 1916.

[3] *Kodaikanal Bulletins*, Nos. 38 and 40, 1914.

[4] *Astrophysical Journal*, **44**, 65, 1916.

[5] *Mt. Wilson Contr.*, No. 106; *Astrophysical Journal*, **42**, 231, 1915.

The present paper consists in an examination for pole-effect of an iron arc operated according to the specifications of the International Committee, and an experimental study of the conditions under which the error introduced by polar influence may be avoided in another form of arc.

2. APPARATUS AND METHODS

The observations discussed here were made both with the plane-grating spectrograph and with interference apparatus. The former instrument is the same as that used in a previous investigation on the pole-effect.[1] When employed in conjunction with the totally reflecting prisms and rotating sector over the slit, it has proved a powerful means of measuring minute changes in wave-length. Interference methods are also especially applicable to problems of this character; certain distinct advantages are made available by this means—namely, the possibility of obtaining a great extent of spectrum upon each photograph under strictly uniform observing conditions, the integrating action over a specified portion of a source, and the comparative insensibility to instrumental displacements. The errors inherent in this method and those which affect results derived from gratings enter in different ways, and accordance in the values reached by the two methods, used independently, is a strong indication that both are free from systematic inaccuracy.

The interference apparatus which has recently been installed in this laboratory is in general similar to that described by Fabry and Buisson.[2] The auxiliary dispersion is provided by a Rowland concave grating of 635 cm radius of curvature, which receives parallel light from a collimating mirror of nearly the same focal length, thus giving a spectrum free from astigmatism. The

[1] *Loc. cit.* [2] *Journal de Physique*, **9**, 929, 1910.

grating has approximately 87,500 lines, each 50 mm long, spaced 590 to the millimeter, and provides a scale of 5 A per millimeter in the first order. Flat plates 25 cm long are used in the camera, covering 1200 A in excellent focus in the first-order spectrum, which can be observed into the infra-red as far as λ 9000. The etalon consists of fused quartz plates 40 mm in diameter, held parallel and at a fixed distance by invar separators. Silver films cathodically deposited are used for the portion of the spectrum thus far studied. The etalon is contained in a small, double-walled wooden box, and this, with the mirrors which project the rings upon the slit, is protected by an outer wooden case. The whole system stands upon the large cement pier which supports the slit and grating of the spectrograph.

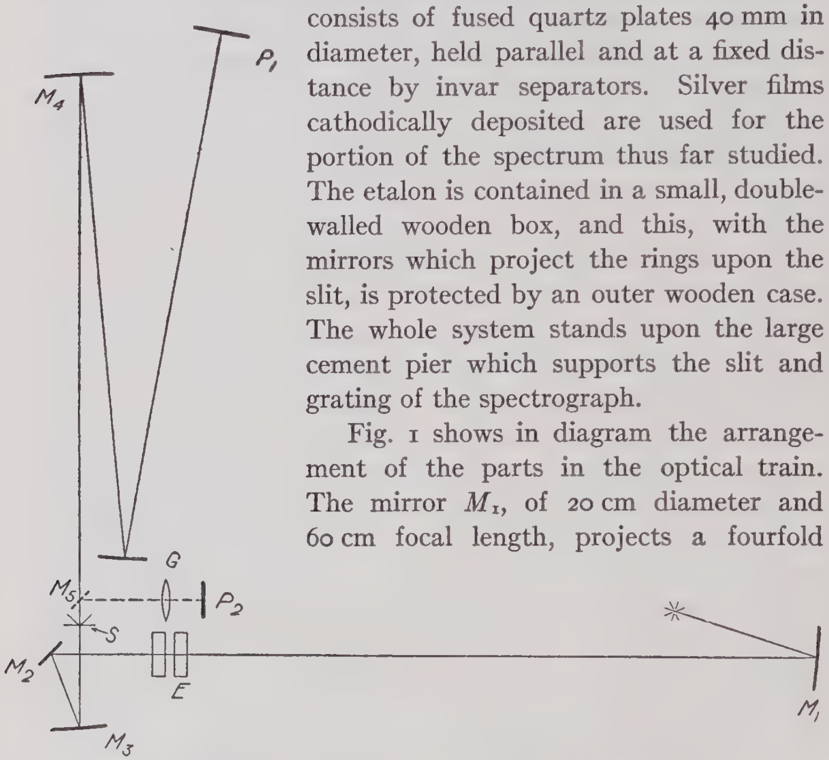

FIG. 1.—Optical system and arrangement of interference apparatus

Fig. 1 shows in diagram the arrangement of the parts in the optical train. The mirror M_1, of 20 cm diameter and 60 cm focal length, projects a fourfold enlarged image of the source upon the diaphragm in front of the quartz plates E. The rings are projected upon the slit S by means of the plane mirror M_2 and the concave mirror M_3. The latter has a diameter of 10 cm and a focal length of 63.3 cm. Behind the slit a plane mirror M_5 can be moved on vertical ways into or out of the beam of light which ordinarily passes to the collimator M_4, the grating G, and the plate P_1. If it is desired to photograph the red cadmium rings when the camera is in a position which does not include that wave-length, the mirror M_5 is brought into position behind the slit so that the rings can be received in the auxiliary camera as shown. Important advantages are found in the precise achromatism of the system, in the fact that no essential part of the apparatus has to be touched between successive exposures, and in the comparative freedom from temperature disturbances. The gain in accuracy to be expected with the use of large-scale interference rings and increased auxiliary dispersion, pointed out by Pfund,[1] is realized in this apparatus, and it is doubtful whether further increase in the focal length of the projecting mirror M_3 is desirable. The focal length adopted permits the use of low magnification in the measuring microscope, with the consequent advantages in regard to the grain of the plate.

It is of interest to calculate the plate factor in angstroms per millimeter at any point in the interference system for a given set of conditions, in order to compare what one sees on photographs taken with this apparatus with the images of spectral lines formed by gratings or other instruments. It can easily be shown from the elementary theory of the interferometer that

$$\frac{pr^2}{2F^2}-E-(n-1)=0 \qquad (1)$$

where

p = order of interference at center of ring system.
F = effective focal length of lens or mirror which projects the rings on the slit, as actually affected by any magnification in the spectrograph.
E = fractional order of interference.
n = number of ring, counting innermost ring as the first.
r = radius of n^{th} ring.

Now, if wave-length λ is measured from the center of the ring system in units of spectral range, we have at the n^{th} ring

$$\lambda=n-1+E.$$

But from equation (1) we find

$$r^2=\frac{n-1+E}{4K},$$

---

[1] *Astrophysical Journal*, **28**, 211, 1908.

where K is written for $p/8F^2$, so that we may write

$$\lambda = 4Kr^2 .$$

Accordingly

$$\frac{d\lambda}{dr} = 8Kr ,$$

and in order to express this quantity in angstroms per millimeter it must be multiplied by the value of the spectral range, which is λ/p. This gives

$$\frac{d\lambda}{dr} = \frac{8K\lambda r}{p} = \frac{\lambda}{F^2} r .$$

For the first ring, with the aid of equation (1), this is readily transformed into

$$\frac{d\lambda}{dr} = \frac{\lambda}{F}\sqrt{\frac{2E}{p}} .$$

If we assume

$\lambda = 5000$ A, $F = 633$ mm, $p = 40{,}000$ (10 mm etalon), $E = 0.5$,

we obtain

$$\frac{d\lambda}{dr} = 0.040 \text{ A per mm.}$$

For comparison it may be added that for λ 5000 in the fourth order of a grating having 590 lines to the millimeter, used at 9.1 meters focus, the plate factor is 0.370 A per mm, i.e., the dispersion is about one-tenth of that calculated above for the interference method.

Attention may be called to the necessity for accurate focusing of the enlarged image of the source upon the diaphragm in front of the etalon when it is desired to select any specified portion of it for study. A large relative aperture of the projecting mirror makes it possible to focus with precision, especially when the following method is used: On looking through the arc toward the projecting mirror it is easy to locate the image of the diaphragm, since the light normally incident upon the first silver film is largely returned over the path which it traversed and greatly augments the illumination. The image of the diaphragm appears, then, to float in the arc and is so much brighter than its surroundings as to be easily

PLATE XVI

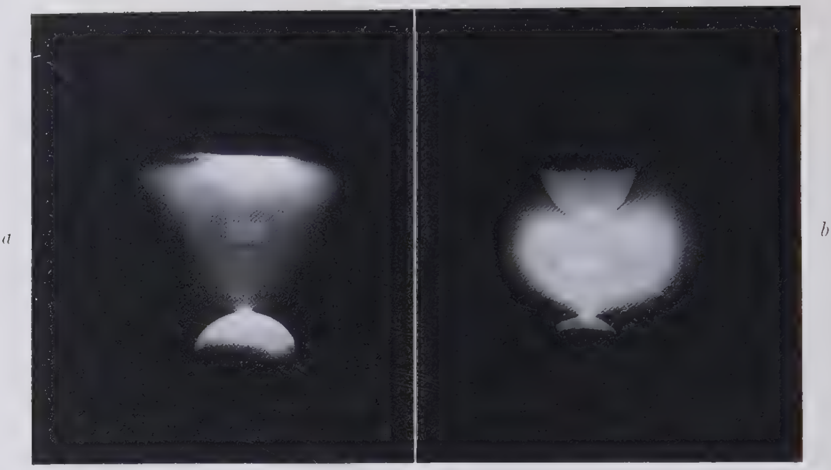

Distribution of Luminosity in 12-mm, 5-amp Pfund Arc (*a*) and in International Arc (*b*) with Superposed Images of Defining Diaphragm

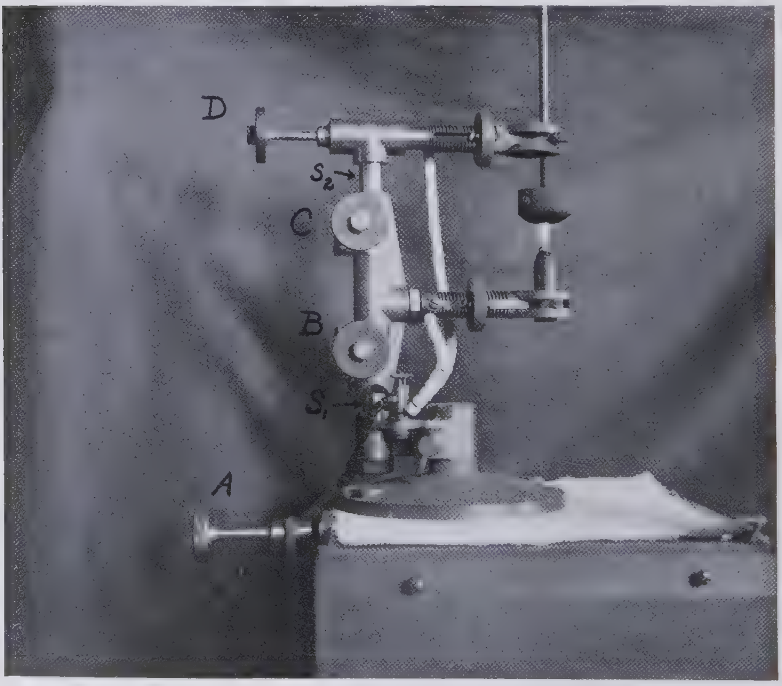

Arc Lamp for Precision Observations

observed. It can also be seen when the arc is not burning, provided the general illumination in the room is sufficient, and its position can be very satisfactorily located by means of a hand magnifier. The electrodes of the arc, with the current cut off, can be observed simultaneously, and freedom from parallax insures a precise focus. In Plate XVI are shown images of the arc, to which reference will be made later, with the diaphragm placed as in use. Owing to the fact that the arc and its image are somewhat off the axis of the projecting mirror, a small amount of astigmatism is introduced. By taking care to make the focus perfect for horizontal lines, we find that this feature becomes of advantage rather than otherwise, since it tends to smooth out the variations in intensity which exist in a horizontal section of the arc and to make the illumination of the diaphragm more uniform while leaving the extent of the arc-axis in use sharply defined.

The observations to be described were obtained for the most part with a diaphragm measuring 5×12 mm, but for special purposes others of circular shape are employed, having diameters of 5, 9, and 12 mm. The rectangular diaphragm is especially useful when it is necessary to economize light while using only a limited extent of the axis of the arc.

To test the auxiliary spectrograph for distortion of the field of view in a direction parallel to the spectral lines, a plate was placed over the slit, having a series of ten narrow openings arranged to simulate the relative positions of the sections of interference rings formed by the slit. With the etalon removed an exposure was made to the spectrum which reproduced each line broken into ten dots, with much the same appearance as though produced by interference. An examination of the distances separating these dots for lines in different portions of the negative and a comparison with the distances of the slots in the occulting plate showed constant magnification and freedom from distortion in all parts of the field.

The method of observation is essentially that of Fabry and Buisson. The etalon is usually adjusted with the aid of the green mercury line by observing the rings in a telescope while a very small exploring diaphragm is moved about in the beam of light. When the adjustment for parallelism is complete with large aperture, the diaphragm is inserted very close to the first plate without touching any sensitive part of the instrument, and the protecting cover is put in place. The exposures are so distributed as to provide a check upon the constancy of the etalon.

The use of standard distance-gauges over the slit for the purpose of reducing linear diameters to angular measure is avoided, the observed diameters themselves furnishing all the necessary data as follows: The diameters are measured upon a machine provided with two precision screws whose axes are at right angles, from two to five rings being observed, according to the nature of the problem at hand. When four or five diameters are observed, the fractional order may be most accurately found from a least-squares solution of the observational equations, which are written in the form of equation (1) above. For differential observations upon the wave-length of the same line under slightly different conditions two rings are generally observed, and a plate-constant, $K\lambda$, is determined. It is the average of all the values obtained by dividing each approximate wave-length by the difference in the squares of the diameters corresponding to it. The value of K for any line is then taken by redivision, and the fractional order is quickly obtained from each diameter.

The integral order of interference and the correction for change of phase are readily found by well-known methods, a convenient arrangement of which is described by Meggers.[1]

The arc lamp is supported upon a small wooden platform, which is provided with a coarse screw for moving it at right angles to the line of sight. This permits easy correction of position without disturbing the setting for focus. Details of the mounting are shown in the lower half of Plate XVI. The guiding screw referred to is marked A. The base of the lamp is heavy enough to give sufficient stability, and the moving parts are well defined in position. Screw B provides a vertical motion of the entire upper part of the lamp, read on a millimeter scale S_1. The upper electrode is moved up and down relatively to the lower by screw C, the scale S_2 serving to show

[1] *Scientific Papers of Bureau of Standards*, No. 251, 1915.

the arc-length. For centering the electrodes screw *D* provides a separate horizontal motion for the upper terminal. Current for the arc is supplied by direct-current generators at a maximum of 300 volts. The voltages commonly used are 110 and 220, with lamp resistance in series with the arc for control. An ammeter is kept in circuit and the current is read to 1/5 ampere.

3. OBSERVATIONS

a) *Provisional standard source.*—In order to examine a given source for the presence and amount of pole-effect contained in it, a reference source practically free from this disturbing influence is essential. Our former conclusion, that the center of a 6-mm, 6-ampere Pfund arc is free from pole-effect,[1] is incorrect, as will be shown below, and a substitute was sought in the Pfund arc having the negative pole of carbon. Such an arc has been tested for pole-effect and found suitable for the purpose. The length of arc was maintained between 6 and 8 mm, and the current was 6 amperes on the average. The measurements summarized in Table I were made on plates obtained with the 30-foot plane-grating spectrograph, using sector and prisms over the slit. The

TABLE I

POLE-EFFECT IN PFUND ARC WITH CARBON NEGATIVE POLE
IRON LINES OF GROUP *d*

PLATE	NEGATIVE POLE *minus* CENTER		PLATE	POSITIVE POLE *minus* CENTER	
	Number Lines	Mean Shift		Number Lines	Mean Shift
		A			A
1	29	+0.003	1	38	+0.007*
2	31	.000	2	38	.008*
3	29	+ .001	3	37	.002
4	32	.000	4	36	.003
5	32	− .001	5	38	.003
6	36	.000	6	37	.002
7	36	− .001	7	37	+0.003
8	36	0.000			
Mean		0.000	Mean		+0.004

* No sector used.

---

[1] *Astrophysical Journal*, **27**, 298, 1906.

lines observed all belong to group *d*. For these lines no difference is found between wave-length at negative pole and at center, while a comparatively small displacement appears at the positive pole. A narrow central zone of this arc was accordingly adopted provisionally as a standard source, assumed to be free from pole-effect.

b) *Pole-effect in center of international arc.*—In accordance with the specifications of the International Committee on Wave-Lengths,[1] an arc 6 mm long between iron rods 7 mm in diameter, fed by a current of 6 amperes, under a pressure of 220 volts, having its positive pole above, will be referred to in this paper as the international arc. Light is taken from a central zone not exceeding 2 mm in width.

TABLE II

CENTER INTERNATIONAL ARC *minus* CENTER PFUND CARBON-POLE ARC
IRON LINES OF GROUP *d*

Plate	Number Lines	Mean Shift	Plate	Number Lines	Mean Shift
		A			A
1	21	+0.004	7	34	+0.005
2	19	.006	8	33	.006
3	14	.010	9	34	.006
4	33	.007	10	32	+0.004
5	23	.008			
6	38	+0.006	Mean...	....	+0.006

Mean pole-effect in 6-mm, 6-ampere Pfund arc for the same lines is +0.010 A.

The slit of the 30-foot spectrograph was placed at right angles to the axis of this arc at its middle point, as recommended for finest definition in the specifications of the committee, and by means of a small totally reflecting prism simultaneous exposures were made upon this source and upon the corresponding part of the provisional standard source. A rotating sector equalized the effective intensity upon all parts of the slit, and special care was taken to see that each light-source completely illuminated the grating. As shown in Table II, ten exposures give for some thirty sensitive lines in the region λ 3840–λ 4200 a mean value of +0.006 A for the difference, international *minus* Pfund carbon-pole arc. The conclusion indicated is that the international arc has pole-effect, even in its central section, at least 0.006 A in amount.

---

[1] *Trans. International Union for Co-operation in Solar Research*, 4, 59, 1914.

c) *Distribution of pole-effect in international arc.*—Spectra from near the negative pole of the international arc and from its center were compared by means of the 30-foot spectrograph, using the method of simultaneous exposures already referred to. The difference in brightness of the two parts of the arc was compensated by a rotating sector; control measurements made upon stable lines showed freedom from instrumental displacement; the distinguishing feature of the pole-effect appeared in the opposite displacements given by lines of groups *d* and *e*. From 35 to 40 sensitive lines between λ 3800 and λ 4200 were observed upon each of seven plates, the mean values obtained being shown in the left-hand part of Table III. The polarity of the international arc was then reversed, making the upper pole negative, as it is in the Pfund arc, and the difference negative pole *minus* center was again observed in the same manner. The results of these measurements are collected in the right-hand part of Table III, which is self-explanatory. The mean pole-effect measured in the Pfund arc for the same list of lines is added at the bottom of the table for comparison. These

TABLE III

INTERNATIONAL ARC, NEGATIVE POLE *minus* CENTER

PLATE	NORMAL POLARITY, POS. POLE ABOVE			
	Group *d*		Group *e*	
	Number Lines	Mean Shift	Number Lines	Mean Shift
		A		A
1......	34	+0.021	3	−0.012
2......	40	.019	3	.012
3......	40	.018	3	.013
4......	37	.014	3	.009
5......	34	.018	3	.012
6......	33	.019	3	.011
7......	33	+0.017	3	−0.010
Means	......	+0.018	......	−0.011

Pole-effect in 6-mm, 6-ampere Pfund arc for the the same lines: Group *d*, +0.011 A; Group *e*, −0.009 A.

PLATE	INVERTED POLARITY, NEG. POLE ABOVE			
	Group *d*		Group *e*	
	Number Lines	Mean Shift	Number Lines	Mean Shift
		A		A
1......	19	+0.018	1	−0.004
2......	21	.013	2	.004
3......	39	.010	3	.001
4......	38	.008	2	.004
5......	39	.013	3	.008
6......	41	.010	3	.009
7......	41	.011	3	.012
8......	41	.013	3	.010
9......	40	.013	3	.009
10......	40	.010	3	.007
11......	40	+0.013	3	−0.005
Means	......	+0.012	......	−0.007

observations leave no doubt as to the existence of pole-effect in the international arc in somewhat greater amount than in the 6-mm, 6-ampere Pfund arc. The amount of material discussed in the case of the *d* lines is thought sufficient to give real meaning to the difference in the two mean values in Table III; the investigations bearing upon this point are still in progress.

The interference method was next employed for comparing integrated wave-lengths over the central half of the international arc with the corresponding values from the provisional standard source described above. A suitable diaphragm, placed in front of the etalon, selects the desired portion of the source, and since with proper precautions the instrument integrates all the light falling upon the diaphragm it is well suited to such a purpose. Under these conditions it was found that the central half of the international arc gave wave-lengths for 30 sensitive lines greater on the average by 0.005 A than the corresponding portion of the Pfund arc having the negative pole of carbon, although 59 stable lines showed no change in wave-length between the two sources. Furthermore, a comparison of the central half of the international arc with the central third of the same arc was made by a suitable exchange of diaphragms. In this case a list of 35 lines known to be free from pole-effect showed no variation, but 35 sensitive lines of group *d* showed a mean decrease of 0.003 A when the smaller portion of the arc was used. These facts are most readily explicable on the assumption that the central half of the international arc exhibits pole-effect, and a comparison of the two mean differences given above indicates that even the recommended central third of the international arc is somewhat affected by the polar influence. Although these data are not sufficient to afford a reliable measure of the amount of pole-effect in the central third of the arc, they tend to confirm the more exact quantitative measures presented above in section *b*.

Tests made toward the close of the investigation by the method described in the following section show that when the international arc is lengthened to 12 mm a central zone 1¼ mm wide still contains measurable pole-effect. The lines of a well-known list belonging to group *e* are, on the average, displaced toward the violet 0.004 A from the positions which they have when free from pole-effect. The lines of group *d* which were tested show less displacement, but, on the whole, a tendency to shift toward the red.

d) *Development of the Pfund arc for standard purposes.*—The source described above as a provisional standard, the Pfund arc with carbon negative pole, is for many purposes all that could be desired. It is especially useful in the ultra-violet, where it yields most of the strong iron lines unreversed and very narrow. No difficulty is experienced from the so-called carbon bands when only the central region of the arc is used, and, as Pfund says, it yields iron lines "rivaling in homogeneity and sharpness the red and green lines of cadmium produced in a vacuum arc."[1] But its intensity, especially in the region of longer wave-lengths, is relatively feeble. The international arc, on the other hand, has been found characterized by a troublesome amount of pole-effect, which necessitates the introduction of uncertain correction terms before it can be safely employed as a reference source in many kinds of spectroscopic problems. A study has been made of the Pfund arc, accordingly, in order to develop its possibilities as a source suitable for a standard.

The interference method is so well suited to such a problem that extensive use has been made of it. For the most part a 5-mm etalon was used, this rather short length being chosen in order that the widest lines, which are in some cases most sensitive to pole-effect, might give measurable interference fringes. A diaphragm in front of the etalon selected a horizontal section through the center of the arc $1\frac{1}{4}$ mm wide.

The method usually employed for differential interference observations was abandoned, partly on account of the prolonged exposures sometimes necessary, and also because of the saving of labor and greater accuracy made possible by the plan adopted. The procedure followed consisted in determining the wave-lengths of the sensitive lines of groups *d* and *e* from each source in terms of selected stable lines occurring upon the same plate. Three sharp *a* lines in the green, which by comparison with the green mercury line have been found to be constant in wave-length under varying arc conditions, were adopted as reference standards.

---

[1] *Astrophysical Journal*, **27**, 298, 1906.

It should be noted that the existence of pole-effect in small or moderate amounts is not necessarily accompanied by any suggestive appearance of the spectral lines, such as unsymmetrical widening. The only certain test for the effect is the actual measurement of the wave-length. The differences shown in the accompanying tables cannot be attributed to unsymmetrical widening dependent upon increase of intensity, or to an "intensity equation" directly, since the individual lines exhibit a much greater range of intensity upon each plate than a given line shows from one plate to another, while the differences of wave-length are substantially the same for all lines of a given group. Burns, Meggers, and Merrill conclude[1] that "interferometer wave-lengths are comparatively unaffected by any intensity equation," and, so far as the present data bear upon this question, they seem to confirm that conclusion.

While the method employed eliminates systematic instrumental errors from these measurements, the objection may be raised that the observer tends to set the cross-wire of his microscope in a systematically different way upon lines belonging to different groups. All of the photographs at present under discussion, however, resemble one another very closely; they were taken with the same etalon, had approximately equivalent exposures, and were measured by the same observer, so that if such a source of error is present at all it is constant upon this series of plates. The differences that are shown in the behavior of these sensitive lines appear to arise, therefore, from actual changes in the wave-lengths of the lines.

Reference has already been made on page 9 to a former paper in which the pole-effect was studied under certain conditions of arc-length and current-strength for this type of arc. In that investigation the center of the arc was used for the working standards, but the tests made to ascertain whether it was itself entirely free from polar influence are now seen to be inadequate. In Table IV are given the results of a comparison of the center of such a 6-mm,

---

[1] *Scientific Papers of Bureau of Standards*, No. 274, 1916.

6-ampere Pfund arc with the same region of the Pfund arc having the negative pole of carbon. A small amount of pole-effect is clearly indicated for lines belonging to both groups *d* and *e*.

A visual examination of the Pfund arc through a dense neutral screen shows a clearly defined structure consisting of the outer layer, which owes its luminosity principally to the band spectrum of iron oxide, a darker space within, which emits very little of the red end of the spectrum, and two brilliant streams of vapor in the axis of the dark space, of which the one proceeding from the negative pole is by far the brighter. Traces of this structure are shown in Plate XVI*a*. This photograph of the Pfund arc was made with light from the spectral region λλ 5800–7000, and the original contrasts have been considerably reduced by means of ammonium persulphate. Plate XVI*a*, on the other hand, shows the international arc photographed in the same way with no reduction of the scale of contrast. The original exposure in this case was very much less than for the Pfund arc. If such photographs are taken with blue and violet light, the outer mantle is found much reduced, and the inner "dark" space, referred to above, is very much increased in relative intensity. Our observations upon pole-effect have led us to associate it with the bright streams of vapor which issue from the poles, and it was therefore natural

TABLE IV

POLE-EFFECT IN CENTER OF 6-MM, 6-AMPERE PFUND ARC

GROUP *d*			GROUP *e*		
Carbon Neg. Pole	Pfund	Shift	Carbon Neg. Pole	Pfund	Shift
5232.950	.952	+0.002	5383.377	.371	−0.006
5266.568	.570	.002	5404.146	.140	.006
5324.190	.192	.002	5410.918	.912	.006
5569.628	.631	.003	5415.204	.196	.008
5572.852	.855	.003	5424.073	.065	−0.008
5586.766	.767	.001			
5615.653	.656	.003			
5624.552	.557	+0.005			
Mean	....	+0.003	Mean	....	−0.007

to choose the comparatively dark region between the adjacent ends of these vapor streams as a source presumably free from pole-effect. In the 6-mm, 6-ampere Pfund arc, however, as was shown above, this procedure is not permissible, but the observations next to be described show that simple modifications of the arc attain the desired result.

A normal Pfund arc 12 mm long was operated at varying current-strengths under a pressure of 220 volts. It was found that with currents of from 4 amperes to 7 amperes the arc was remarkably steady, and any desired portion of it could be selected with considerable accuracy; exposures of an hour's duration could be made without restriking the arc. With further increase of current, intervals of unsteadiness appeared, but satisfactory plates could be taken up to 8.5 amperes. For each current-strength employed the wave-lengths of a series of *d* lines and of certain *e* lines were determined in terms of the same three standard *a* lines according to the method described above. The results are displayed in Table V and in the diagram, Fig. 2. The wave-lengths have had applied to them the necessary small corrections for phase-change.

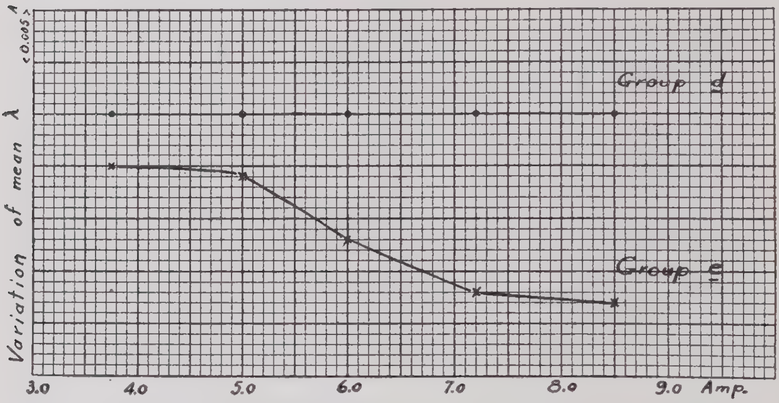

FIG. 2.—Relation between wave-length and current-strength for sensitive lines

A comparison of the means at the bottom of the columns shows striking uniformity for the *d* lines, but for currents above 5 amperes very definite displacements for the lines of group *e*. Special attention should be called to the fact that, for currents of 5 amperes or less, even the sensitive *e* lines show practically constant values. The obvious interpretation of these results is that for the arc specified a central zone at least 1¼ mm wide is free from pole-effect when the current is less than 5 amperes, and wave-lengths derived from it have their fundamental values.

TABLE V

RELATION OF WAVE-LENGTH AT CENTER OF 12-MM PFUND ARC TO CURRENT-STRENGTH
STANDARDS λλ5397.132, 5405.781, 5434.528

λ	CURRENT IN AMPERES					MEANS
	3.75	5.00	6.00	7.20	8.50	
			GROUP *d*			
5232	.950	.950	.951	.950	.952	.951
5266	.568	.567	.565	.567	.563	.566
5324	.190	.188	.189	.188	.186	.188
5569	.629	.628	.629	.627	.627	.628
5572	.852	.851	.851	.852	.851	.851
5586	.767	.765	.765	.767	.766	.766
5602	.954	.955	.953	.954	.954	.954
5615	.652	.653	.655	.655	.655	.654
5624	.552	.556	.549	.552	.553	.552
5488	.457	.457	.457	.457	.457	.457
			GROUP *e*			
5383	.379	.377	.372	.370	.371	....
5404	.148	.146	.138	.135	.132	....
5410	.918	.920	.912	.910	.908	....
5415	.205	.205	.198	.188	.190	....
5424	.075	.073	.070	.062	.059	....
5407	.545	.544	.538	.533	.532	....

Confirmation of this conclusion is afforded in Table VI, in which the second column presents for group *d* means taken from all the measures in Table V, and for group *e* the means from the two lowest currents given in that table; the third column gives the results for the same lines in the carbon-pole Pfund arc, in terms of the same standards. The succeeding columns add corresponding data from Pfund arcs having negative poles of copper, brass, and chromium steel, respectively. The arc-length was nearly 12 mm, and the current was approximately 5 amperes in each case. The variations in the means are undoubtedly within the errors of measurement, as it must be remembered that the lines concerned are among the most difficult of all iron lines to measure. Since the pole-effect is found to have its greatest value in the vicinity of the negative pole, it seems improbable that such accordance would be found if the values in the second column obtained with the iron pole were affected by it, as this hypothesis would require exactly equal amounts to appear in the other arcs considered.

TABLE VI

SENSITIVE LINES INDEPENDENT OF CONSTITUTION OF NEGATIVE POLE
CENTER OF 12-MM, 5-AMPERE PFUND ARC

λ	NEGATIVE POLE					WTD. MEAN
	Iron	Carbon	Copper	Brass	Cr. Steel	
			GROUP *d*			
5232........	.951	.950	.950	.949	.950	.950
5266........	.566	.568	.566	.566	.565	.566
5324........	.188	.190	.190	.190	.189	.189
5569........	.628	.628	.628	.630	.627	.628
5572........	.851	.852	.852	.851	.852	.851
5586........	.766	.766	.765	.764	.768	.765
5615........	.654	.653	.653	.655	.652	.654
5624........	.552	.552	.554	.552	.552	.552
5474........	.144	.145	.145	.145	.144	....
			GROUP *e*			
5383........	.378	.377	.377	.378	.378	.378
5404........	.147	.146	.145	.144	.143	.145
5410........	.919	.918	.917	.917	.920	.918
5415........	.205	.204	.206	.205	.206	.205
5424........	.074	.073	.073	.074	.074	.074
5407........	.545	.544	.544	.544	.544	....

It is found by examining monochromatic images of the Pfund arc, formed by various spectral lines, that the distribution of luminosity in the iron vapor is practically independent of the constitution of the negative pole, as far as such observations have been made. Under these conditions there is a slight increase in the brightness of the iron vapor close to the pole in question, but it is not conspicuous. The brilliant stream issuing from this electrode, on the other hand, shows in general the same characteristic distribution for the various substances which we have used for cathodes in our mixed arcs. In each case there is great increase of intensity close to the negative pole. Since it has been shown above that, in the case of the Pfund arc having the negative pole of carbon, the pole-effect disappears in the vicinity of the cathode, we have evidence here which suggests that it is not mere proximity to the negative pole which produces the effect, but that an essential condition is that the emitting centers originate with this stream. Our experience in obtaining photographs for measurement on pole-effect amply confirms this idea, for when the prism selecting the light at the pole is given a slight lateral displacement out of this narrow stream, the observed pole-effect is greatly diminished.

Furthermore, in a former investigation already referred to, it was found that when the Pfund arc is operated *in vacuo* the pole-effect disappears and that the brilliant vapor stream which issues from the negative pole at atmospheric pressure is lacking, the arc appearing as a soft nebulous glow, brighter, indeed, near the negative pole, but without definite structure. In the light of these observations it is difficult to see how pole-effect can be directly dependent upon anything in the nature of electronic bombardment of the metal vapor by particles from the negative pole.

The gradual appearance of pole-effect in the center of an arc as its length is decreased may be seen in Table VII. The current was kept constant at 5 amperes, and arc-lengths of 12, 10, 8, and 6 mm were employed, the method of observation being the same as that referred to in the preceding paragraphs. The lines of group *d* are shown to remain practically constant in wave-length under these conditions, but the *e* lines, which offer a more sensitive test for the presence of pole-effect, show it definitely for lengths less than 8 mm. By a combination of the data presented in Tables V and VII it is found that, in order to be free from pole-effect in the center of the Pfund arc, the length must be at least 8 mm and the current not over 5 amperes. Under these conditions a horizontal zone at least 1¼ mm wide may be used with safety, even for observations upon the most sensitive lines of group *e*. For *d* lines, on the other hand, the arc-length may be as short as 6 mm for a current of 5 amperes, or the current may be as much as 8.5 amperes for a length of 12 mm without introducing an appreciable amount of pole-effect.

TABLE VII

Relation of Pole-Effect to Arc-Length for 5-ampere Pfund Arc
Center of Arc Used

λ	Arc-Length in Millimeters			
	6	8	10	12
	Iron Lines of Group *d*			
5232.......	.951	.950	.949	.950
5266.......	.566	.569	.566	.567
5324.......	.189	.191	.189	.188
5569.......	.626	.628	.629	.628
5572.......	.850	.852	.852	.851
5586.......	.763	.765	.765	.765
5615.......	.652	.653	.654	.653
5624.......	.552	.552	.552	.556
5474.......	.144	.145	.144	.145
	Iron Lines of Group *e*			
5383.......	.372	.375	.376	.377
5404.......	.141	.144	.144	.146
5410.......	.912	.916	.916	.920
5415.......	.197	.205	.204	.205
5424.......	.063	.071	.072	.073
5407.......	.537	.542	.542	.544

A set of conditions under which the Pfund arc may be used without introducing pole-effect having been developed, it is of interest to examine the wave-lengths of lines in the adopted list of international secondary standards known to exhibit pole-effect. In Table VIII, the first column gives the value published by the International Committee, the second shows the fundamental value obtained under these conditions, and the third contains the differences. The Mount Wilson values are not final, but represent our best knowledge of these lines at present. Definitive wave-lengths covering a wide range of spectrum will appear in a later paper. The mean difference shown in Table VIII is practically coincident with the mean difference obtained above in Table II, although the observations involved in the two cases are entirely independent.

TABLE VIII

POLE-EFFECT IN INTERNATIONAL SECONDARY STANDARDS

I.A.	Mt. Wilson	I.A. *minus* Mt. Wilson	I.A.	Mt. Wilson	I.A. *minus* Mt. Wilson
4707.288....	.282	+0.006	5232.957...	.949	+0.008
4736.786....	.782	.004	5266.569...	.566	.003
4859.758....	.752	.006	5302.315...	.309	.006
4878.225....	.219	.006	5324.196...	.188	.008
4903.325....	.318	.007	5569.633...	.627	.006
4919.007....	.001	.006	5586.772...	.765	.007
4966.104....	.096	.008	5615.661...	.653	+0.008
5001.881....	.873	.008			
5192.363....	.356	+0.007	Mean...	....	+0.0065

In Table IX we compare our values with the determinations by Burns, Meggers, and Merrill[1] for lines of group *d*. The mean indicated makes it clear that pole-effect played a part in their investigation, and that its amount was substantially the same as that existing in the international secondary standards. This latter fact is sufficient to account for the failure of these observers to find evidence of it in their results, as they made no comparisons with a source free from this influence. They say in their paper:[2]

TABLE IX

POLE-EFFECT IN RECENT INTERFEROMETER OBSERVATIONS—GROUP *d*

Mean λ free from Pole-Effect	Burns, Meggers, Merrill	Difference	Mean λ free from Pole-Effect	Burns, Meggers, Merrill	Difference
5232.949....	.957	+0.008	5586.765...	.772	+0.007
5266.566....	.572	.006	5615.653...	.661	.008
5302.309....	.315	.006	5624.552...	.559	+0.007
5324.188....	.195	.007			
5569.627....	.633	.006	Mean...	....	+0.007
5572.851....	.859	+0.008			

---

[1] *Scientific Papers of Bureau of Standards*, No. 274, 1916.

[2] *Ibid.*

"Thus it seems probable that the measurement of additional lines on the plates from which the I.A. standards were obtained would lead to the same values of the wave-lengths as though the plates had been taken under normal conditions." This conclusion is confirmed by the observations presented above, but it must be sharply distinguished from the statement in the summary at the end of their paper to the effect that "interferometer observations under the conditions described were found to be reasonably free from the effects of pole shifts." No evidence was adduced by them in support of this statement, and in the light of the present data it is seen to be unwarranted.

e) Comparative sharpness of iron lines in different arcs.—An apparent superiority of the international arc over the Pfund type lies in its increased intensity for unreversed lines, but this increase of intensity is accompanied by a corresponding increase in width of the lines themselves, as quantitatively measured by Nutting,[1] so that the advantage gained in exposure time is offset by the disadvantage of lower reproducibility in the international arc. The relative sharpness of certain lines in the region λλ 5167–5455 in the international arc and in the Pfund arc when free from pole-effect is shown in Plate XVII, in which *a* is taken from the center of the international arc and *b* from the Pfund arc. The etalon used was 15 mm long, i.e., the order of interference is about 55,000. The diaphragm admitted from the center of the arc an equatorial section $1\frac{1}{4}$ mm wide, while the specifications permit the use of 2 mm in the case of the international arc. If this larger amount had been used, the difference between the two arcs would have been still further increased. The prominent lines of group *a* are shown reversed in the international arc, and there is practically no material suitable for measurement upon the plate from which this illustration was made. Upon a plate from the Pfund arc free from pole-effect, however, we are able to measure all lines of sufficient intensity, and a still higher order of interference could be used. The number of lines which reverse in the international arc, but are unreversed and suitable for measurement in the Pfund arc, is still greater in the region of shorter wave-lengths.

[1] *Bulletin of Bureau of Standards*, **2**, 439, 1906.

PLATE XVII

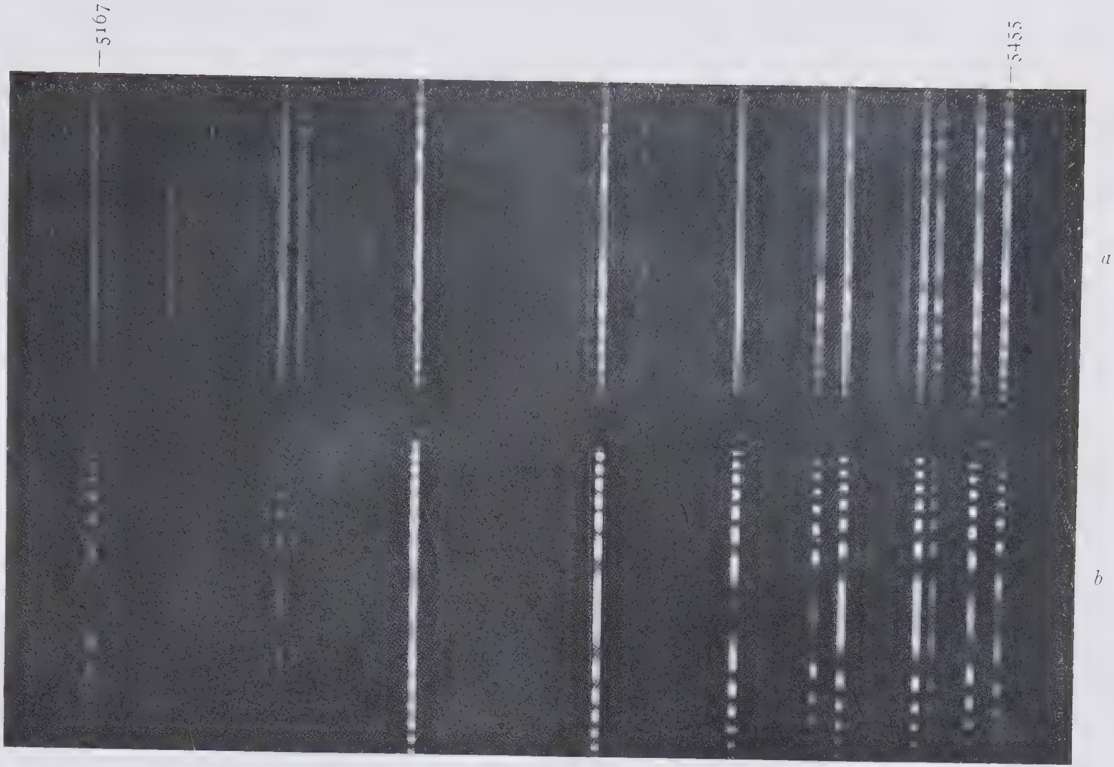

Comparative Sharpness of Lines from International Arc (*a*) and Proposed Arc (*b*); 15-mm Etalon

4. THE IMPORTANCE OF FUNDAMENTAL WAVE-LENGTHS

The main purpose of the new determinations is to obtain extensive lists of wave-lengths that may be used for deriving the constants and testing the accuracy of series formulae, for comparing wave-lengths in terrestrial and cosmic sources, and for studying the changes in wave-length due to varying experimental conditions. For most purposes it is not a sufficient criterion that a wave-length be reproducible; it should also represent the fundamental vibration under standard conditions. Evidence that this end may be attained has been furnished by three lines of investigation: change of current-strength, of arc-length, and of constituents of negative pole. The basal assumption is that when no further variation in wave-length accompanies a change of any one of the three variables, the other two being held constant, the fundamental condition has been reached.

An entirely independent demonstration of pole-effect in the measures of Burns, Meggers, and Merrill and of the misleading interpretations that may follow from their use in statistical investigations is shown in Table X. The first column contains their wave-lengths; the second and third, our determinations in the center of a 6-mm Pfund arc and in the sun made from high-dispersion spectrograms taken with a plane-grating spectrograph.

TABLE X

Pole-Effect Shown by Fictitious Sun-Arc Displacements

Burns, Meggers, Merrill	Mt. Wilson		B, M & M *minus* Mt. Wilson Arc	Mt. Wilson Sun *minus* B, M & M	Mt. Wilson Sun *minus* Mt. Wilson Arc
	Arc	Sun			
5192.362	.356	.359	+0.006	−0.003	+0.003
5205.609	.606	.613	.003	+ .004	.007
5232.957	.950	.954	.007	− .003	.004
5281.807	.798	.802	.009	− .005	.004
5324.195	.189	.193	.006	− .002	.004
5379.579	.576	.578	.003	− .001	.002
5393.183	.177	.182	+0.006	−0.001	+0.005
Means			+0.006	−0.002	+0.004

For 17 flame lines, group *a*, mean difference Burns, Meggers, and Merrill *minus* Mount Wilson is −0.0004 A.

The wave-lengths of these sensitive lines were referred to well-established standards belonging to group *a*. It is obvious from the last two columns of Table X that opposite conclusions may be drawn from such comparisons, depending upon whether the arc wave-lengths used are contaminated with pole-effect, as in the Burns, Meggers, and Merrill measures, or whether they represent the more nearly fundamental values of the Mount Wilson data. In early work at Mount Wilson upon sun-arc comparisons the iron lines in the solar spectrum of groups *c* and *d* were displaced to the violet, and the lines of group *e*, abnormally to the red. It is now recognized that this arose from residual pole-effect in the center of the arc. Recent determinations with the 12-mm arc yield results of the same sign and magnitude for lines of the sensitive groups as for stable lines on the same plates as shown in Table XI. The disappearance of the abnormal behavior of such lines furnishes confirmatory evidence that pole-effect has been eliminated from the iron arc and indicates that the solar lines are produced under conditions in which pole-effect plays no part.

TABLE XI

SUN-ARC DISPLACEMENTS FOR UNSTABLE LINES BECOME NORMAL WHEN POLE-EFFECT IS ELIMINATED

λ	FE LINES, GROUP *d*		λ	FE LINES, GROUP *e*	
	Old Obsus. Pole-Effect	New Obsus. No Pole-Effcet		Old Obsus. Pole-Effect	New Obsus. No Pole-Effect
5393........	−0.006	+0.001	5364.......	+0.021	+0.011
5476........	.004	.008	5367.......	.020	.008
5569........	.002	.005	5364.......	.012	.008
5572........	.002	.007	5383.......	.018	.006
5586........	.006	.006	5404.......	.015	.006
5615........	.000	.006	5410.......	.016	.012
5624........	.008	.006	5415.......	.026	.005
5638........	−0.008	+0.016	5424.......	+0.028	+0.008
Means..	−0.004	+0.007	Means..	+0.019	+0.008
9 stable lines, group *a*				+0.008	+0.008

Not only is there evidence of pole-effect in the international iron wave-lengths, but it appears also in the determinations for other elements. In any given spectral region a "Standard R−I," Rowland *minus* international, for lines whose wave-lengths in sun and arc are equal, may be obtained from stable iron lines by taking account of their sun-arc displacements. In Table XII are shown some results obtained by applying this criterion. The apparent displacement of the solar lines to the violet for lines showing positive pole-effect, indicated by negative values in the last column, and the abnormally large displacement to the red for lines with negative pole-effect are so similar to the results found for iron before the elimination of this disturbing influence that the abnormal sun-arc displacement shown in Table XII must be referred to errors in the arc wave-lengths rather than to conditions in the sun.

TABLE XII

Pole-Effect in the Published Wave-Lengths of Other Elements

	Rowland λ	Pole-Effect	R−F	Standard R−I	Sun-Arc
Manganese...	4783.613	+0.012	0.181	0.187	−0.006
Fuchs*......	4823.694	+0.011	0.175		−0.012
			R−Holtz		
Calcium.....	6102.937	+0.017‡	0.201	0.204	−0.003
Holtz†......	6122.434		0.202		−0.002
	6162.390		0.194		−0.010
	3624.410	−0.037‡	0.152	0.136	+0.016
	3647.707		0.152		+0.016

* *Zeitschrift für Wissenschaftliche Photographie*, **14**, 263, 1914.

† *Ibid.*, **12**, 101, 1913.

‡ Whitney, *Astrophysical Journal* **44**, 65, 1916.

A similar conclusion relative to the errors in the calcium wave-lengths of Holtz is reached when they are compared with the measurements *in vacuo* made by Crew and McCauley,[1] as in Table XIII. In this case the difference, Holtz *minus* Crew and McCauley, should be the pressure-displacement per atmosphere. Here again abnormal values are found bearing a relation to pole-effect similar to that observed for iron before its elimination from the iron data. As pole-effect practically disappears for iron *in vacuo*, it may be assumed with a high degree of probability that the abnormal pressure-shifts indicated are due to errors in the wave-lengths of Holtz at atmospheric pressure rather than in those of Crew and McCauley *in vacuo.*

---

[1] *Astrophysical Journal*, **39**, 29, 1914.

Data are not at hand for testing other published determinations. The tests here applied are simply illustrations of statistical comparisons already undertaken that have misled the investigator and of the uses to which such data may properly be applied. If the great labor expended upon the redetermination of wave-lengths is to be justified by results, due consideration should be given to the elimination of pole-effect, a necessary preliminary to wave-length determinations. It is not too much to hope that the new data will be valuable for a generation at least, as the Rowland measures have been in the past, but, as the matter now stands, it is a question whether any of the published determinations of wave-lengths or of pressure-displacements for the more sensitive lines are sufficiently free from pole-effect to comply with the more and more exacting demands that will be made upon such fundamental data.

TABLE XIII

FICTITIOUS PRESSURE-DISPLACEMENTS FOR CALCIUM DUE TO POLE-EFFECT

Series	Holtz	Crew and McCauley	Holtz *minus* C. and McC.	Pos. Pole *minus* Center Whitney
t..........	4092.690	.649	+0.041	+0.055
t..........	4094.983	.944	+0.039	
t..........	4098.575	.552	+0.023	
			+0.034	
T_2.........	6102.736	.716	+0.020	+0.017
T_2.	6122.232	.216	+0.016	
T_2	6162.196	.177	+0.019	
			+0.018	
T_1.........	3624.106	.107	−0.001	−0.037
T_1.........	3630.739	.749	−0.010	
T_1.........	3630.958	.973	−0.015	
T_1.........	3644.757	.760	−0.003	
			−0.007	

5. CONCLUSIONS

From the data presented above, the superiority of the Pfund arc 12 mm long, carrying a current of 5 amperes, as a source of standard spectrum lines appears to be established. Whether viewed from the standpoint of higher reproducibility, owing to increased sharpness of lines, or from that of attaining the fundamental wave-length, owing to the freedom from pole-effect, the advantage lies with this type of arc in preference to the arc specified by the International Committee. It is true that from λ 5650 to the red the decrease in brightness in the Pfund arc is sufficient to require rather long exposures when this source is used with high-dispersion apparatus; but from that point in the spectrum to the ultra-violet no difficulty is experienced. The international arc, on the other hand, is lacking in stable lines in the region λλ 5600–6000. To the red of λ 6027 there is a sufficient number of lines belonging to group *b*, which, being free from pole-effect, may be used as standards when observed in any form of arc.

The uniformity in the wave-lengths of the stable lines under varying conditions of arc is especially to be noted, along with the fact that even the most sensitive lines are unaffected in position by change of constitution of the negative electrode, while, under the set of working conditions developed, their wave-lengths exhibit remarkable constancy.

Attention should be directed also to the advantage of using the Pfund arc, under conditions similar to those described in this paper, as a source for working standards of intensity. The same conditions that favor constancy of wave-length also make for uniformity in the system of relative intensities, and the comparatively large range of working conditions permitted with this form of arc makes it much better suited to the purpose than an arc in which the intensity-gradient of a given line from center to pole is much steeper, as it is in the international arc. Obviously, if the intensity of a sensitive line is 5 or 10 times as great at the negative pole as it is at the center of an arc, it is highly important to reproduce with the greatest care the conditions under which the line is observed, if it is to be used as a reference standard of intensity. A slight change in the position of a slit which is at right angles to the axis of the arc introduces an entirely new system of relative intensities in the case of a short arc, and a comparatively small error in focusing the image upon the slit will produce a similar result. Ample enlargement of the image, an achromatic projecting system accurately focused on the slit at a definite position and azimuth, preferably 90° to the axis of the arc at its midpoint, and a source in which the intensity-gradients from center to pole of even the sensitive lines are low, are some of the conditions which should be observed if the systems of relative intensity for spectrum lines in terms of the "arc" intensities used by different investigators are to have definite meaning.

It is a pleasure to acknowledge our indebtedness to the careful measurements and reductions carried out for us by Miss M. O. Burns, of the computing staff.

6. SUMMARY

1. The interference apparatus now in use at this observatory is described, and the methods of observation and reduction are explained.

2. By means of this instrument and a powerful plane-grating spectrograph quantitative data have been collected relating to the relative merits of three forms of iron arc when used as sources for standards of wave-length and of intensity.

3. The international arc has been shown to exhibit large pole-effects, not only at the negative pole, but in the central one-half, central one-third, and even in the central plane section.

4. The displacements at the negative pole as compared with the center are greater in this arc when the negative pole is below than when it is above.

5. In the Pfund arc with a carbon negative pole the wave-lengths of sensitive lines are the same at the negative pole and at the center.

6. The ordinary Pfund arc 6 mm long, carrying 6 amperes, has measurable pole-effect in its central region.

7. The Pfund arc operated with 5 amperes or less, at a length of 12 mm, is free from pole-effect in a central zone at least $1\frac{1}{4}$ mm wide.

8. The poorest lines in the iron spectrum, those of group *e*, when free from pole-effect, can be measured with high precision.

9. When pole-effect is eliminated, the wave-lengths of iron lines are found to be independent of the nature of the negative pole, whether this be of iron, carbon, copper, brass, or chromium steel.

10. The adopted wave-lengths of international standards belonging to groups *c* and *d* are shown to be influenced by pole-effect.

11. This influence enters to about the same extent into the values of wave-length recently published by other observers.

12. In the green part of the iron spectrum the pole-effect in Nos. 10 and 11 amounts to +0.006 A for lines of group *d*.

13. The sharpness of both stable and sensitive lines, when observed in a source free from pole-effect, is shown to be much greater than it is in the international arc.

14. The importance of eliminating pole-effect is shown by the misleading results obtained by using published data contaminated by this influence.

15. The abnormal sun-arc displacements formerly obtained for lines of groups *d* and *e* become of the same sign and order as for stable lines when pole-effect is eliminated.

16. Attention is directed to the importance of certain precautions to be observed when iron-arc lines are to be used for comparisons of intensity.

MOUNT WILSON SOLAR OBSERVATORY
June 1917

Contributions from the Mount Wilson Solar Observatory, No. 138
Reprinted from the *Astrophysical Journal*, Vol. XLVI, pp. 249–265, 1917

THE PRINCIPLE OF GENERALIZED RELATIVITY AND THE DISPLACEMENT OF FRAUNHOFER LINES TOWARD THE RED

By CHARLES E. ST. JOHN

According to Einstein's equivalence principle of generalized relativity, the lines in solar and stellar spectra should be displaced to the red when referred to the corresponding terrestrial lines. For any given frequency the magnitude of the effect depends upon the difference in gravitational potential between the gravitational field in which the emitting center is located and the terrestrial field where the radiation is received and measured. Einstein[1] deduces an approximate relation between the frequencies in the solar and terrestrial fields, namely,

$$(n_0-n)/n_0=2\times 10^{-6}\,,$$

or, postulating the constant space-velocity of light,

$$\lambda-\lambda_0=2\times 10^{-6}\lambda.$$

The calculated displacement of two parts in a million is well within the possibilities of observation, being 0.010 A for λ 5000. A less approximate and perhaps more objective statement is, "at the surface of the sun the displacement is equivalent to the Doppler displacement produced by a radial velocity of 0.634 km per sec."[2]

As the occurrence or non-occurrence of such displacements is of fundamental importance in the theory of relativity and in the interpretation of observations of solar and stellar spectra, definite results from an investigation carried on with powerful instruments at command would have a double significance. The present contribution presents the details of such an investigation in which the primary object has been to determine what consideration must be given to this deduction from the equivalence principle of generalized relativity in the discussion of observations of solar spectra.

---

[1] *Annalen der Physik*, **35**, 905, 1911.

[2] A. S. Eddington, *Monthly Notices*, **77**, 380, 1917.

INSTRUMENTS AND METHODS

The 30-foot Littrow spectrograph and the 60-foot tower telescope on Mount Wilson were used in obtaining the main portion of the data. A grating of high resolving power and excellent definition was at our disposal through the kindness of the Physical Laboratory of Johns Hopkins University, the ruled surface being 114×160 mm and the number of lines 95,000. The third and fourth orders with scales of 0.56 A and 0.36 A per mm were used.

A common defect in narrow comparison spectra obtained by the usual occulting arrangement at the slit is the unsymmetrical ends of the arc lines and the irregular edges of the solar spectra. This disturbing element was eliminated, and the ease and accuracy of the measurements were increased by stretching a violin string on each side of the central strip of spectrum and close to the photographic film. This also removed the effect of a slight astigmatism without involving the movement of an occulting shutter. Other possible instrumental displacements were avoided by making all comparison exposures simultaneous, the relative intensities being controlled by a rotating sector.[1] The data in particularly important cases are the means of the closely agreeing measures made by three observers, and in all instances depend upon at least two.

SELECTION OF OBSERVATIONAL MATERIAL

Besides the principle of relativity, three other causes have been suggested which might account for a displacement of the Fraunhofer lines in the direction of longer wave-lengths—namely, differences of pressure, motion in the line of sight, and anomalous refraction. While anomalous refraction may produce sporadic effects under occasionally favorable density-gradients in the solar atmosphere, the conclusion from investigations and observations at this observatory is that, within the present limit of precision of measurement, the positions of the Fraunhofer lines in the spectrum of the solar disk are not systematically affected by anomalous refraction.[1] Any effect due to the difference in gravitational potential between the solar and terrestrial fields may be freed from that due to pressure by using lines whose pressure-shifts are negligible, such as those in the bands of the carbon arc at λ 3883 variously assigned to carbon, cyanogen, and nitrogen;[2] it may be freed from the influence of motion in the line of sight by observations upon the same lines at the sun's polar limb.

---

[1] St. John and Babcock, *Mt. Wilson Contr.*, No. 106; *Astrophysical Journal*, **42**, 231, 1915.

The richness of the ultra-violet Fraunhofer spectrum and the multiplicity of lines in the carbon-arc spectrum make the selection of suitable lines a matter of grave consideration from the point of view both of precision in measurement and of contamination by blends with lines sensitive to pressure changes. From an examination of high-dispersion spectrograms of excellent definition lines were selected whose separation from neighboring lines was sufficient to assure that the measurements would be free from systematic errors. A previous investigation had revealed such errors and shown that their magnitude depends upon the degree of proximity and the character and intensity of the adjacent lines; it also furnished data for determining for spectrographs of the dispersion and resolving power used in this investigation the limiting separation from neighboring lines within which measurements become unreliable.[3]

The lines finally selected were those of the nitrogen (cyanogen) bands listed in Tables I and II. Since they show wide variations in character and surroundings, an estimate was made of the weight to be assigned to results for individual lines. This estimate, based upon the appearance of the lines in both solar and arc spectra, is the observer's a priori judgment whether the measurements would have high, medium, or low weight. These estimated weights are entered in the appropriate tables.

---

[1] St. John, *Mt. Wilson Contr.*, Nos. 93 and 123; *Astrophysical Journal*, **41**, 28, 1915, and **44**, 311, 1916.

[2] The observations of Grotrian and Runge show that these bands are produced under experimental conditions that apparently preclude the presence of carbon, and that the essential condition is the presence of nitrogen in the absence of oxygen (*Physikalische Zeitschrift*, **15**, 545, 1914).

[3] St. John and Ware, *Mt. Wilson Contr.*, No. 120; *Astrophysical Journal*, **44**, 15, 1916.

THE OBSERVATIONS

A. The arc wave-lengths.—The wave-lengths of the lines under investigation were determined in the arc in terms of the same international iron standards and under the same instrumental conditions as were later used for their solar wave-lengths. The agreement with the wave-lengths of Uhler and Patterson was so close that the mean was taken as the probable value. For a few difficult cases, in which evidently neighboring lines might have affected the measures, appeal was made to the difference, Rowland *minus* International, to decide which was the more probable wave-length of the arc-line. Uhler and Patterson[1] consider their wave-lengths for sharp lines on a clear background to be correct in absolute value to ±0.005 A. This appears to be an underestimate of the accuracy, as the mean difference, Uhler and Patterson *minus* Mount Wilson, taken without regard to sign, is only 0.003 A even when difficult lines are included in the comparison. The decimals of the adopted values of the wave-lengths are in the fourth column of Table I.

B. Sun—arc displacements.—The critical questions are the behavior of the investigated lines at the center of the solar disk and the relation between center and limb displacements. Owing to the importance of the possible results and the limited observational material available, the questions have been approached from several directions:

1. At the center: (*a*) The center—arc displacements were directly determined from simultaneous exposures on the sun and the equatorial sections of a carbon arc 6–7 mm long, fed by a current of 6–7 amperes. These and all other comparisons between solar and terrestrial sources have been corrected for the earth's motion. The results are in the first column of Table I.

(*b*) The absolute wave-lengths of the solar lines were obtained from simultaneous exposures on the sun and on the iron arc, in terms of the same iron standards as were used for the arc wave-lengths. The differences between the solar and arc wave-lengths in the third and fourth columns of Table I furnish an independent determination of the center—arc displacements given in the fifth column.

---

[1] *Astrophysical Journal*, **42**, 438, 1915.

(*c*) The stable iron lines are displaced to the red in the solar spectrum. The positive differences, Rowland wave-length *minus* International wave-length, for such lines when decreased by the corresponding displacements center *minus* arc give the difference R−I that would be shown by lines whose solar and arc wave-lengths are equal. For the spectral region under consideration the mean value of this difference is 0.137A, which will be referred to as the "standard" R−I. Lines for which R−I is greater than 0.137A are displaced to the red in the sun; those for which it is less are displaced to the violet, the excess and deficit being the measures of the corresponding center−arc displacements. Hence a

TABLE I

RELATIVE DISPLACEMENTS OF SOLAR AND ARC LINES OF THE NITROGEN (CYANOGEN) BANDS AT CENTER OF SUN

SECTION A. LINES OF SOLAR INTENSITY 00–1

(*a*) SUN−ARC	λ CENTER OF SUN		λ ARC I.U.	(*b*) λ SUN *minus* λ ARC	(*c*) ROWLAND *minus* λ ARC	INTENSITY ROWLAND	SERIES	WEIGHT
	R-System	I.U.						
+0.002..	3819.200	.061	.062	−0.001	0.138	1 Nd	B_1	High
+ .002..	3825.260	.126	.125	+ .001	.135	00	C_1	High
− .002..	3833.744	.610	.610	.000	.134	0	C_1	Medium
.000..	3842.780	.644	.648	− .004	.132	0	......	High
+ .001..	3845.152	.021	.019	+ .002	.133	1	B_1	High
.000..	3846.667	.534	.536	− .002	.131	00	......	High
.000..	3848.981	.848	.848	.000	.133	1 N	B_1	High
+ .002..	3850.784	.652	.648	+ .004	.136	0	B_1	Low
.000..	3854.192	.062	.063	− .001	.129	0	B_1	High
+ .002..	3854.988	.855	.854	+ .001	.134	1	B_1	Low
.000..	3857.058	.926	.922	+ .004	.136	0	......	High
+ .002..	3857.288	.156	.158	− .002	.130	1	B_1	High
+ .002..	3858.723	.591	.592	− .001	.131	0	B_1	Medium
− .002..	3867.116	.980	.983	− .003	.133	0	A_2	High
+ .002..	3867.200	.064	.061	+ .003	.139	0	A_2	High
− .003..	3867.908	.776	.779	− .003	.129	1	A_2	High
.000..	3868.542	.410	.410	.000	.132	1	A_2	Low
+ .004..	3868.624	.489	.486	+ .003	.138	00	B_2	Low
.000..	3868.702	.570	.572	− .002	.130	0	A_2	High
+ .003..	3868.782	.648	.644	+ .004	.138	00	A_2	Low
− .002..	3872.312	.178	.181	− .003	.131	0	A_2	High
− .001..	3876.448	.312	.315	− .003	.133	0	A_1	High
− .001..	3877.482	.346	.351	− .005	.131	1	A_1	High
+ .001..	3879.716	.580	.579	+ .001	.137	1	A_1	Medium
+0.003..	3880.102	.966	.964	+0.002	0.138	1	A_1	Low
+0.0006.	....	....	....	−0.0002	0.134	....	......	....

Average number of measures per line, 13. Average mean deviation per line, 0.002 A.

TABLE I—*Continued*

SECTION B. LINES OF SOLAR INTENSITY 2–4 AND PARTIALLY RESOLVED PAIRS

(a) Sun−Arc	λ Center of Sun		λ Arc I.U.	(b) λ Sun *minus* λ Arc	(c) Rowland *minus* λ Arc	Intensity Rowland	Series	Weight
	R-System	I.U.						
	R.346					1	A_1	
+0.001..	3819.384	.241	.244	−0.003	0.140			Low
	R.412					1	A_1	
	R.406					0	A_1	
+ .001..	3822.435	.290	.290	.000	.145			Low
	R.470					0	A_1	
	R.745					0	B_1	
.000..	3830.774	.630	.637	− .007	.137			Low
	R.801					0	B_1	
+ .004..	3831.174	.038	.034	+ .004	.140	3	A_1d	Low
	R.639					1	A_1	
+ .005..	3836.660	.520	.516	+ .004	.144			Low
	R.689					1	A_1	
+ .005..	3844.377	.238	.235	+ .003	.142	4	A_1d	Low
− .002..	3846.131	.993	.999	− .006	.132	2	B_1	High
	R.777					1	A_1	
.000..	3846.796	.657	.656	+ .001	.140			Low
	R.814					1	A_1	
+ .004..	3851.426	.292	.286	+ .006	.140	2 N	A_1d	Medium
+ .006..	3852.541	.408	.402	+ .006	.139	2 N	A_1d	Low
− .003..	3853.621	.487	.491	− .004	.130	2 N	A_1d	Low
+ .006..	3856.800	.667	.665	+ .002	.135	2 N	A_1d	Low
+ .004..	3858.822	.692	.684	+ .008	.138	2 N	A_1d	Medium
+ .002..	3862.626	.493	.489	+ .004	.137	2	A_1b	Low
+ .004..	3863.534	.402	.399	+ .003	.135	3 N	A_1b	Low
+ .004..	3864.438	.308	.303	+ .005	.135	3	A_1	High
+ .003..	3865.284	.150	.150	.000	.134	3	A_1sB_1	Low
0.000..	3866.125	.989	.993	−0.004	0.132	3 N	A_1sB_2	Low
+0.0024	....	....	....	+0.0012	0.138	....	......	....

Average number of measures per line, 22. Average mean deviation per line, 0.003 A.

comparison of this "standard" value with R−I for the carbon-arc or nitrogen bands furnishes a method independent of the direct center−arc determinations.

A preliminary examination indicated that as a class the carbon-arc lines were not appreciably displaced to the red in the solar spectrum. A possible explanation of this systematic difference in the behavior of the iron and the band lines was that the Rowland wave-lengths for the two classes of lines did not form a homogeneous system. It is known that Rowland made an intensive investigation of these band lines, but it is not clear how their wave-lengths were connected with his standards. The solar wave-lengths of the lines under investigation have therefore been redetermined in the Rowland system, the Rowland values for the neighboring iron lines being used as standards. There are no systematic differences between the Rowland and Mount Wilson measurements, the sums of the positive and negative differences for 57 lines being +0.086 and −0.094 A. The means of the two measurements have been taken as the wave-lengths in the Rowland system and are entered in the second column of Table I. In the sixth column are given the differences, Rowland *minus* International. For the lines of solar intensity 00–1 a mean displacement of 0.003 A to the violet is indicated, and for those of intensity 2–4 a displacement of 0.001 A to the red.

(*d*) A fourth independent method of determining the center−arc shifts is based upon the observations detailed below, which refer to the limb and its relation to the center, as the displacements, limb−arc, decreased by the corresponding limb−center values, are another measure of the center−arc shifts.

2. At the sun's limb: (*a*) The absolute wave-lengths of the investigated solar lines were measured at the limb in terms of the iron standards used for the arc wave-lengths. The results are in the second column of Table II. Simultaneous exposures were made on the center of the iron arc and the sun's limb in latitude 90° at a point distant from the edge one-eightieth of the diameter of the solar image. The displacements at the limb are then λ limb−λ arc as given in the third column.

(*b*) A check is furnished by increasing the center−arc displacements by the limb−center shifts independently obtained. The latter were found by the method used by Adams,[1] and also from simultaneous exposures on the center and on a point on the limb in latitude 90°. The means of the closely agreeing results given by these two methods are entered in the fifth column of Table II under the heading "Limb *minus* Center."

It is to be remarked that the Rowland intensities given in Tables I and II should in many cases be modified. It is especially difficult to estimate the intensities of the components of close pairs. In general, the values assigned are too low. For example, the double lines $\left\{\begin{matrix}3836.639, 1\\ 3836.689, 1\end{matrix}\right\}$ and $\left\{\begin{matrix}3846.777, 1\\ 3846.814, 1\end{matrix}\right\}$ are like 3844.378, 4*d*, in appearance and intensity in both arc and solar spectra. Though quite differently estimated by Rowland, they are placed in the same section of these tables, and, similarly, all partially resolved doublets measured as single lines are classed with nominally stronger lines, which in reality are more or less close pairs of similar lines.

---

[1] *Mt. Wilson Contr.*, No. 43; *Astrophysical Journal*, **31**, 30, 1910.

The lines under investigation are within a region of 60 A, in which Rowland catalogues about 250 lines belonging to the bands. In equal regions to the red and violet of the bands there are 400 and 450 metallic lines, respectively. If the region λ 3819–λ 3880 is equally rich in such lines, the probability of blends among the 250 band lines is high. It is highest for broad lines formed by the coalescing of the components of doublets, higher even than for narrower lines of greater inherent intensity; moreover, the errors of measurement may be systematic, as frequently the compound lines are unsymmetrical. As the probable occurrence of blends is least for the

TABLE II

BEHAVIOR OF THE LINES OF THE NITROGEN (CYANOGEN) BANDS AT THE SUN'S LIMB

SECTION A. LINES OF INTENSITY 00–1

Lines	(*a*) λ Limb	λ Limb *minus* λ Arc	λ Limb *minus* λ Center	λ Limb *minus* λ Center	Intensity	Series	Weight
3819.197 ...	.064	+0.002	+0.003	+0.003	1 N	B_1	High
3825.256 ...	.126	+ .001	.000	+ .003	00	C_1	Low
3833.744 ...	.611	+ .001	+ .001	+ .004	0	C_1	Medium
3842.779 ...	.646	− .002	+ .002	+ .005	0	......	High
3845.149 ...	.023	+ .004	+ .002	+ .002	1	B_1	Medium
3846.666 ...	.536	.000	+ .002	.000	00	......	Medium
3848.979 ...	.846	− .002	− .002	− .002	1 N	B_1	High
3854.191 ...	.065	+ .002	+ .003	+ .004	0	B_1	High
3854.989 ...	.855	+ .001	.000	+ .001	1	B_1	Low
3857.063 ...	.927	+ .005	+ .001	+ .002	0	......	Medium
3857.288 ...	.156	− .002	.000	+ .008	1	B_1	Medium
3867.118 ...	.982	− .001	+ .002	+ .001	0	A_2	Low
3867.906 ...	.779	.000	+ .003	+ .002	1	A_2	High
3876.448 ...	.310	− .005	− .002	.000	0	A_1	High
3877.481 ...	.346	− .005	.000	− .002	1	A_1	High
3879.716 ...	.579	.000	− .001	− .002	1	A_1	Medium
3880.105 ...	.964	0.000	−0.002	−0.004	1	A_1	Medium
....	....	0.0000	+0.0007	+0.0015	....	......	....

TABLE II—*Continued*

SECTION B. LINES OF INTENSITY 2–4 AND PARTIALLY RESOLVED PAIRS

Lines	(a) λ Limb	λ Limb *minus* λ Arc	λ Limb *minus* λ Center	λ Limb *minus* λ Center	Intensity	Series	Weight
3819.346 3819.412 . .	.247	+0.003	+0.006	+0.004	1 1	A_1 A_1	Low
3822.406 3822.470 . .	.291	+ .001	+ .001	+ .002	0 0	A_1 A_1	Low
3830.745 3830.801 . .	.636	− .001	+ .006	− .002	0 0	B_1 B_1	Low
3831.174 . . .	.039	+ .005	+ .001	+ .002	3 d	A_1d	Low
3836.639 3836.689 . .	.523	+ .007	+ .003	+ .002	1 1	A_1 A_1	Low
3844.378 . . .	.239	+ .004	+ .001	+ .004	4 d	A_1d	Low
3846.131 . . .	.997	− .002	+ .004	.000	2	B_1	High
3846.777 3846.814 . .	.660	+ .004	+ .003	.000	1 1	A_1 A_1	Low
3851.427 . . .	.295	+ .009	+ .003	+ .005	2 N	A_1d	Low
3852.541 . . .	.406	+ .004	− .002	+ .002	2 N	A_1d	Low
3853.620 . . .	.492	+ .001	+ .005	+ .004	2 N	A_1d	Low
3856.802 . . .	.671	+ .006	+ .004	+ .007	2 N	A_1d	Low
3858.822 . . .	.692	+ .008	.000	+ .002	2 N	A_1d	Low
3862.626 . . .	.494	+ .005	+ .001	+ .001	2	A_1b	Low
3863.533 . . .	.401	+ .002	− .001	.000	3 N	A_1b	Low
3864.438 . . .	.308	+ .005	.000	+ .003	3	A_1	High
3865.282 . . .	.154	+ .004	+ .004	+ .002	3	A_1sB_1	Low
3866.122 . . .	.995	+0.002	+0.006	+0.004	3 N	A_1sB_2	Low
. . . .	. . . .	+0.0037	+0.0025	+0.0023	. . . .	. . . . . .	. . . .

narrowest lines, the division between Sections A and B of Tables I and II has been based upon line-intensity. For this reason, and because of the relatively high precision of measurement, greater weight is to be attributed to the data of Sections A.

The series classification in the column next to the last in Tables I and II is from the work of Uhler and Patterson.[1] A_1 is the nominally "singlet" series from the first head, but in all probability it is a series of doublets. Its ultimate doublet character, according to Uhler and Patterson, appears at λ 3860.626, line 47 of the series, though preliminary widening is evident in line 44 at λ 3863.390. They say:

---

[1] *Astrophysical Journal*, **42**, 434, 1915.

> On leaving the head and going toward shorter wave-lengths one acquires the impression that the A_2 series (doublets from the first head) gradually grows out of and away from A_1. The first component of A_2 appears as a close companion of the eighth line of A_1. The second component of A_2 appears as a close component of line 13 of A_1 [λ 3881.587].

The number of lines suitable for measurement in the series A_1 is limited by the conditions that they be free from the A_2 lines and the disturbing influences of their own doublet character. In the shorter B_1 and C_1 series—singlets from the second and third heads—duplicity is not a disturbing factor, and the components of the A_2 and B_2 doublets are probably by nature single. The conditions that the corresponding solar lines, inherently more difficult to measure, should be measurable with fair accuracy, further limits the available material. Sections A of Tables I and II contain nearly all the lines under investigation that fulfil the conditions necessary for measurements of high weight.

DISCUSSION

The mean results from the data in Tables I and II are exhibited in Table III and may be briefly summarized as follows: The magnitude of the displacement to the red required by Einstein's deduction is approximately 0.008 A for the spectral region considered. Compared with this the observations at the center of the sun show a mean displacement of approximately 0.001 A to the violet for the 25 lines of greater weight, and of 0.001 A to the red for the 18 lines of lesser weight, or a zero displacement for the 43 lines. As a displacement due to relativity would be independent of the character of the radiating centers, this discrepancy between the calculated and observed values for the center of the solar disk requires some influence producing displacements of solar lines to the violet of just the magnitude to balance the predicted effect. Anomalous refraction, if active, would tend to displace the lines to the red; the wave-lengths of the lines employed are not appreciably affected by pressure; there is no evidence that wave-length depends upon the temperature of the source; of known causes there is left only the possibility of an outward radial movement of the solar vapors with a velocity at this level of 0.634 km per second, which masks the assumed gravitational effect. At the sun's limb the radial movement would be across the line of sight, the Doppler effect would vanish, and the gravitational displacement of 0.008 A to the red should appear. For the lines whose measurement at the limb is most dependable, the 17 lines of Section A in Table II, the mean shift between the sun's limb and the arc is zero. There are three reasons for assigning a high weight to this mean, namely: under the highest resolving power used the lines show no sign of duplicity; the narrowness of the lines reduces the chances for blends and in so far increases the probability that we are working with uncontaminated lines; and their isolation from adjacent lines is sufficient for measures of precision.

TABLE III

Comparative Solar and Terrestrial Wave-Lengths of Lines in the Nitrogen (Cyanogen) Bands

	Section A	Section B
At Center of Sun	25 Lines	18 Lines
Intensity	00–1	2–4
a) Direct comparison of solar and arc spectra	+0.0006	+0.0024
b) λ in center spectrum *minus* λ in arc spectrum	− .0002	+ .0012
c) (R−I) for band-lines *minus* "Standard" (R−I)	− .0030	+ .0010
d) (λ limb−λ arc) *minus* (λ limb−λ center)	− .0011	+ .0008
Mean (center−arc)	−0.0009	+0.0013
At Limb of Sun	17 Lines	18 Lines
Intensity	00–1	2–4
a) λ in limb spectrum *minus* λ in arc spectrum	0.0000	+0.0037
b) (λ center−λ arc)+(λ limb−λ center)	+0.0001	+0.0035
Mean (limb−arc)	0.0000	+0.0036

If the results of lower weight for the 18 compound and broader lines in Section B are included, the displacement to the red at the limb is 0.0018 A, or one-fourth of the calculated amount. The displacement shown by the broader lines may, however, be due to blends with lines of other elements. Adams found that, at the limb, displacement of the metallic lines to the red is the general rule. In passing from the center to the limb the mean for 120 lines is 0.007 A. Undetected blends with such lines tend to introduce systematic displacement to the red at the limb for lines not sensitive to edge-effect and normally undisplaced.

Adams found for 14 lines of the ultra-violet fluting a shift, relative to the center, of 0.002 A to the red, with which the mean for the 35 lines in Table II is in agreement. He attributes this displacement between center and limb to rising convection currents. The 25 lines in Section A, Table I, lines of lowest level, indicate a rise of the vapors from the sun's interior of 0.08 km per second. This compares well with 0.12 km per second suggested by Adams. The displacement to the red in passing from the center to the limb for these low-level lines appears to be due to the disappearance at the limb of the Doppler-Fizeau effect in the ascending currents at the level where these weak lines originate. For the strong lines in Section B, the small displacement to the red at the sun's center may be accounted for by a downward drift at the higher level of origin, in which all high-level lines appear to be involved. For both the weak and the strong lines the displacement is, however, of the order of the errors in measurement, and great weight cannot be given to their distinctive behavior.

OTHER OBSERVATIONS

In an investigation bearing upon the behavior of the high-level calcium vapor in the solar atmosphere[1] the wave-lengths of the H and K lines were determined in the arc and at the solar limb, with results as follows:

	H_3	K_3
1 mm from the limb....	3968.478	3933.667
At the limb..........	3968.476	3933.665
In the arc............	3968.476	3933.667

Though the close agreement between the solar and arc wavelengths may in part be fortuitous and the evidence for equality should not be unduly stressed, the observations indicate with a high degree of probability that the difference is not of the order of 0.008 A, as required by the principle of relativity.

---

[1] St. John, *Mt. Wilson Contr.*, No. 48; *Astrophysical Journal*, **32**, 36, 1910.

As the gravitational effect is proportional to wave-length, the displacement due to it should be more evident for lines of great wave-length. The Mount Wilson data on the comparative wave-lengths of the iron lines in the sun and arc give for 25 lines of the stable *b* group, mean λ 6300, a mean displacement to the red at the sun's center of 0.004 A instead of 0.013 A, required by the relativity theory, a discrepancy between calculated and observed values too large to be attributed to errors of observation.

A complete report of an investigation by Schwarzschild, "Über die Verschiebungen der Bande bei 3883 Å.E. im Sonnenspektrum,"[1] has not yet reached America. According to the abstract in the *Beiblätter*, he finds that at the center of the sun there is a displacement indicating a downward velocity of 0.2 km per second and that, if this downward movement is taken into account, there remain only slight displacements, which cannot be considered favorable to the Einstein theory.

For lack of fuller data a satisfactory comparison cannot be made between Schwarzschild's results and those in this paper. If the lines used by him are similar in character and intensity to those in Section B of Table I, as seems probable, there is good agreement between his displacement to the red interpreted as a downward movement of 0.2 km per second and the mean of 0.0014 A for the lines in Section B corresponding to a downward velocity of 0.1 km per second.

In *Bulletin* No. 39 of the Kodaikanal Observatory Evershed and Royds give the results of their measurement of 12 lines in the band at λ 3883 and their rather startling deduction of the receding of the solar atmosphere at the sun's center and all around the circumference where it is supposed to attain a velocity of recession of about 1 km per second. This suggested flow of the solar vapors from the hemisphere turned earthward at all points of the sun's limb is assumed to be due to a repulsion of the solar gases by the earth. They base this hypothesis upon a displacement to the red, indicated by their measurement of lines in the band at λ 3883. They appreciate the difficulties involved in the idea, but consider that there is no alternative. The crucial point is the behavior of such lines at the sun's limb. As is evident from the summation in Table III, the Mount Wilson observations, based upon a larger number of lines, fail to confirm the results found at Kodaikanal. For the lines of highest weight there is no displacement to the red either at the center or at the limb. The measurements are inherently difficult, and results may be more or less influenced by the choice of lines and by the resolving power, definition, and dispersion of the spectrographs used.

---

[1] *Beiblätter*, **39**, 480, 1915.

The displacements between center and arc observed at Kodaikanal and at Mount Wilson, the appearance upon the Mount Wilson plates, and the estimated weights of the Mount Wilson measures are given in Table IV. The unresolved triplet groups (A_1, A_2, A_2), near the head of the band, where the A_2 doublets begin to appear and to separate from A_1, are unsymmetrical in the sun and arc. After the triplet character becomes discernible, the components vary progressively in intensity and spacing so that settings upon the complexes are difficult and liable to systematic errors until the separation is sufficient to free a line completely. The weights of the Mount Wilson measures are based largely upon the degree of isolation of the lines.

Evershed and Royds are of the opinion that the negative shifts for λ 3876 and λ 3877 are due to arc conditions and that the general shift to the red of 0.005 A observed by them is too small for the same reason. They state that the general effect of arc conditions is to reduce sun—arc shifts. When light is taken from near the poles of an iron arc or when a short arc with strong current is used, the sun—arc displacements for a large group of iron lines are negative, but this has not been observed for the lines of all elements. An examination of the carbon arc for pole-effect shows that the wave-lengths of these band lines are free from this disturbing influence. Simultaneous exposures were made upon the pole and center of the carbon arc with the 30-foot spectrograph in the fifth order of a Michelson grating of 66,000 lines. The scale of the spectrograms is 3 mm to an angstrom. The results for lines of the series A_1, B_1,

C_1, A_2, and B_2 are given in Table V. There is no evidence of such instability as the iron lines of groups *d* and *e* show.

TABLE IV

THE APPEARANCE ON THE MOUNT WILSON PLATES OF THE LINES USED AT KODAIKANAL

LINES	INTENSITY	CENTER *minus* ARC		IN THE ARC	IN THE SUN
		Kodaikanal	Mt. Wilson		
3863.533....	3 N	+0.010	+0.002	A_1, broad, confused with B_2	Trace of line on red edge: weight very low in sun and arc
3864.438....	3	+ .008	+ .003	A_1	Free: weight high
3876.448....	0	− .002	− .003	A_1	Free: weight high
3876.556.... 3876.622....	0 0	+ .005	+ .003	A_2 A_2	Incomplete resolution: weight low
3877.481....	1	− .001	− .003	A_1	Free: weight high
3877.587.... 3877.646....	0 0	+ .006	+ .002	A_2 A_2	Red component > violet, weight low
3879.331 .... 3879.394 .... 3879.458	1 0 0	+ .005	....	A_1 A_2 A_2	Not measurable as single line. A_2 blended with another line
3879.796 .... 3879.851	0 0	+ .003	+ .003	A_2 A_2	Partial resolution: weight low
3880.465 .... 3880.532 .... 3880.596	1 2 1	+ .007	+ .003	A_1 A_2 A_2	Resolved triplet, middle component a blend, weight very low
3880.815 .... 3880.931	1 1	+ .004	+ .003	A_1 A_2 A_2	Resolved triplet, middle component weak, weight low
3881.729 .... 3881.825	1 1	+ .008	+ .002	A_1 first appearance of 2d component of A_2 A_2 series A_2	Apparent doublet, violet component of triplet blends with middle component, weight low
3882.828 .... 3882.893	1 0	+0.008	+0.002	A_1 first appearance of 1st component of A_2 A_2 series	Unsymmetrical in arc and sun, weight low
Mean ...	....	+0.005	+0.0015	....	....

In the case of λ 3876 and λ 3877 an observed displacement to the violet might arise from the proximity of the lines on the red, if dispersion and resolution are insufficient, as there is then a tendency on the part of the measurer to displace the violet and red components of close pairs to the violet and red, respectively.[1] On the Mount Wilson spectrograms the resolution is complete, and the separation from the adjacent lines is sufficient to show an equally intense background on both sides of the lines—conditions that experience has shown are necessary and sufficient for measures of precision. Two similar lines, λ 3879 and λ 3880, nearer the head and less separated from the adjacent lines on the red, whose measurement is presumably more liable to errors of this type, give 0.000 and +0.002 A, the mean of the four being −0.001 A. As a score of other lines of like intensity yield a similar result, it seems probable that small displacements are characteristic of these low-level lines and that within the limits of error displacements to the violet are not, on that ground alone, to be discarded. These observations remove the necessity felt by Evershed and Royds of assuming an effect of the earth driving the solar vapors from the sun's earthward-turned hemisphere and leave the question of limb-effect for further investigation, with pressure, level, and line-intensity as probable contributing factors.

TABLE V

NEGATIVE POLE *minus* CENTER OF THE CARBON ARC

λ	Series	Pole-Center	λ	Series	Pole-Center
3819.197.......	B_1	0.000	3867.906......	A_2	0.000
3825.256.......	C_1	− .001	3868.539......	A_1	.000
3833.744.......	C_1	.000	3868.625......	B_2	.000
3845.149.......	B_1	.000	3868.700......	A_2	.000
3846.131.......	B_1	− .001	3868.785......	A_2	.000
3864.438.......	A_1	.000	3872.312......	A_2	+ .001
3867.118.......	A_2	.000	3876.448......	A_1	.000
3867.205.......	A_2	−0.001	3877.481......	A_1	0.000
			Mean.....	....	0.000

I wish to express my appreciation of the assistance given in this difficult investigation by Miss Miller, who has had a large share in the measurements of each type, and to Miss Ware, who has checked the results of Miss Miller and myself in the most critical cases.

---

[1] St. John and Ware, *Mt. Wilson Contr.*, No. 120; *Astrophysical Journal*, 44, 15, 1916.

SUMMARY AND CONCLUSIONS

1. The wave-lengths of a group of lines in the band spectrum of nitrogen (cyanogen) have been measured at the center and at the limb of the sun and in the carbon arc, in terms of identical iron standards, and their solar wave-lengths have been redetermined in the Rowland system.

2. Emphasis was put upon the selection of lines, with a view to precision of measurement and freedom from blends, which is particularly important for observations of the limb, where measurements are inherently difficult and blends with metallic lines introduce systematic errors of the sign required by the relativity theory.

3. Sun—arc displacements have been determined at the center directly and by three indirect methods.

4. Limb—center and limb—arc displacements have each been determined by two methods.

5. The sun—arc displacements for iron lines in the region were measured, and from these a standard value for Rowland *minus* International was found for lines showing no displacement at the sun's center. With this the corresponding R—I for the selected band lines was compared.

6. The mean sun—arc displacement at the sun's center for 25 band lines of intensity 00–1 is −0.001 A, and for 18 lines of intensity 2–4 it is +0.0014 A, with a mean of zero for the 43 lines.

7. The mean sun—arc displacement at the limb for 17 band lines of intensity 00–1 is 0.000 A, and for 18 lines of intensity 2–4 it is +0.0036 A, with a mean of +0.0018 A for 35 lines.

8. The conclusion is that within the limits of error there is no evidence in these observations of a displacement to longer wave-length, either at the center or at the limb of the sun, of the order of 0.008 A, as required by the principle of relativity.

9. There is a limb-effect not due to motion, in which pressure, level, and line-intensity appear to be involved in varying degrees for different elements.

Mount Wilson Solar Observatory
June 1917

Contributions from the Mount Wilson Solar Observatory, No. 139
Reprinted from the *Astrophysical Journal*, Vol. XLVI, pp. 232–237, 1917

THE SPIRAL OF OBSCURATION

COMMENTS ON PROFESSOR TURNER'S REPLY

By FREDERICK H. SEARES

Professor Turner discusses[1] numerically the data in Table VI of *Mount Wilson Contribution* No. 135[2] and concludes that they give very good evidence in support of the spiral of obscuration. He demonstrates the substantial agreement of the progressive change in the sums of quantities derived from this table, when appropriately rearranged,[3] with the varying ratio of faint stars to bright stars defined by the spiral. But is not something more than accordance in the sums required for the substantiation of the spiral? Such an agreement might appear when the differences in each line but one of Professor Turner's table were all zero, although the evidence obviously would not then support the spiral, but indicate instead a local phenomenon affecting only a single zone of declination. Evidently the number of zones agreeing with the spiral must also be considered, and unless these are numerous the support of individual favorable cases will be accepted with caution.

Examining Professor Turner's table, we find that the clustering of signs is to be traced mainly to the similar variations affecting the zones at +17°, −41°, and −42°, although part of it is attributable to the circumstance that the algebraic sums of the quantities in each line are not zero. Adding a constant to each line to make the sums zero and transferring the results for +17° to the bottom, we have Table I, whose sums display the same progressive change as was found by Professor Turner.

For the first six zones the clustering is no longer conspicuous. It is pronounced, however, for the last three, whose minima agree satisfactorily with the obscured region of the spiral. Two zones (+62°, −1°) among the first six are also in agreement, although the amplitude is not much larger than the accidental errors. The sequence of signs for +9° suggests an agreement, but the beginning of the series corresponds to a nodal point rather than a minimum. The remaining three cases (+28°, −17°, −32°) are unfavorable. The zone at −65° is not included, as it has already been rejected by Professor Turner as discordant. Noting that the two Cape zones have essentially the same declination and count, therefore, as one, we find no excess of favorable cases, even when the last three zones are included.

---

[1] *Astrophysical Journal*, **46**, 226, 1917. [2] *Ibid.*, **46**, 117, 1917.

[3] See last line of his table on p. 227 and the related discussion.

TABLE I

(Unit=0.01 in Logarithm)

Zone	First Hour	(1)	(3)	(5)	(7)	(9)	(11)	(13)	(15)	(17)	(19)	(21)	(23)
+62°........	1	− 1	−13	− 3	+ 9	+ 1	− 4	+11	+ 4	+ 4	+10	−14	− 9
+28........	9	+ 8	+ 2	+14	0	− 9	− 8	+ 8	+ 8	− 7	−27	−17	+30
+ 9........	15	+ 1	−10	−16	−13	− 8	+18	+19	+ 8	−16	+19	− 6	+ 8
− 1........	17	− 4	− 6	0	− 4	+ 6	+10	− 4	+ 9	+ 4	− 5	− 7	+ 3
−17........	21	+ 3	+ 3	+ 5	+10	−28	− 9	− 1	+13	+ 1	+ 9	−16	+14
−32........	1	− 2	0	+ 4	− 7	+ 2	−10	− 3	+ 3	0	+ 6	+10	+ 1
−41........	3	−16	+ 1	− 9	−23	+10	+ 2	+17	+15	+ 6	+ 9	− 5	− 9
−42........	3	− 2	−11	− 6	−10	+ 3	+ 5	+11	+ 8	+12	+ 4	− 4	− 7
+17........	13	+10	− 7	−10	− 7	+10	+29	+ 8	+ 7	− 3	− 4	−21	−17
Sum first six..........		+ 5	−24	+ 4	− 5	−36	− 3	+30	+45	−14	+12	−50	+47
Sum last three........		− 8	−17	−25	−40	+23	+36	+36	+30	+15	+ 9	−30	−33
Sum all zones.........		− 3	−41	−21	−45	−13	+33	+66	+75	+ 1	+21	−80	+14
Mean lat., first six.....		39°	38°	39°	39°	37°	32°	30°	26°	26°	31°	32°	35°
Mean lat., last three...		64	43	20	4	18	27	24	12	18	33	56	71

A certain amount of progressive fluctuation is to be expected, however. Seasonal factors, for example, are almost certain to influence the results; and even when their phases are distributed at random from zone to zone, the number of cases agreeing with an assigned distribution closely enough to be accepted as favorable to that distribution will be considerable. In the present instance it does not appear that this number is large enough to establish a relation between the observed distribution and the spiral of obscuration. These details may be verified by an inspection of the curves in the right half of Fig. 2 of *Mount Wilson Contribution* No. 135.

Examining now the question quantitatively, we form the sums for each column of the first six zones and find an oscillation of sign that appears to be wholly fortuitous, whence we conclude that the fluctuation noted by Professor Turner is caused by the pronounced variation affecting the zones at $-41°$, $-42°$, and $+17°$. In other words, the irregular distribution in these two regions affects appreciably the mean for all the data, and it is this dominating influence of the Cape and Bordeaux results that appears in Professor Turner's figures; but, since the total number of cases of agreement is not greater than might have been expected because of inherent uncertainties, I see no reason for modifying the judgment previously expressed.

Irregularities in the stellar distribution undoubtedly exist, and eventually it may appear that those remaining after eliminating the effect of the galactic condensation possess a systematic character; but I should hesitate to believe that at present we have any reliable indication of such a phenomenon. As far as the data under discussion are concerned, the spiral

$$\alpha - 2.24\,\delta = 206°$$

seems to represent them much better than the one proposed by Professor Turner. The matter is immediately tested by drawing a line across the right half of Fig. 2 of my original paper in such a way as to intersect the $+62°$ axis at $\alpha = 23^h$, and the $-65°$ axis at $\alpha = 4^h$. This will then represent the line of greatest obscuration, and inspection shows that in no case will the agreement with the minima of the individual curves be less satisfactory than before, while for $+28°$, $-32°$, and $-65°$ there will be an appreciable improvement. But at the present moment, in view of the undoubted presence of seasonal influence and other systematic errors in the Astrographic counts, I should attach no significance to this circumstance.

Finally, it is important to note that an appropriate modification of the galactic condensation adopted for the faint stars will remove entirely the progressive variation which arises from the preponderating influence of the zones at $-41°$, $-42°$, and $+17°$. Let us examine the mean latitudes in the last two lines of the table. For the first six zones these are sensibly the same for all the columns, but for the last three zones they show a marked variation. Now the quantities in the body of the table are differences of the form[1]

$$\delta = \log \frac{D_F}{D_B} - \log \frac{N_F}{N_B},$$

the first term involving the observed value of the ratio of faint stars to bright, while the second includes the value of this ratio calculated from the mean densities in Table III, *Mount Wilson Contribution* No. 135. A change in the adopted galactic condensation of faint stars relative to bright stars will modify the second term, but for a specified galactic latitude the change will be constant and the *relative* values of δ for a series of equal latitudes will remain unchanged. Since the mean latitudes for the first six zones are nearly equal, the sequence of the sums of the tabular quantities for these zones will not be appreciably affected by a change in the condensation.

On the other hand, the three zones which show a marked fluctuation in δ also show a wide range in the mean latitudes. Positive values of δ in these zones correspond in general to small galactic latitudes, and negative values to large latitudes. Now suppose the tabulated mean density for the faint stars to be slightly increased in the lower latitudes. This will increase N_F and reduce the positive values of δ to zero. A similar but opposite change in N_F for the higher latitudes will neutralize the negative values of δ.

I have previously mentioned[2] the uncertainty affecting the determination of the galactic condensation from the Astrographic data, and a reference to the lower curve in Fig. 1 of *Mount Wilson Contribution* No. 135, which illustrates the difficulty experienced in drawing some of the curves, will indicate whence this uncertainty arises. The modification necessary to eliminate entirely the progressive variation in the sums of δ for all the zones is well within this uncertainty, and for this reason the mean densities derived in *Mount Wilson Contribution* No. 135 may be accepted for the present.

These conclusions are also in harmony with other circumstances. For example, it is a contention of this discussion that the spiral of obscuration, for the most part, is only the increasing galactic condensation which appears with increasing limiting magnitude exhibited under another form, and that the spiral disappears when the data are freed from the effects of the condensation. Treated by themselves, the Cape results for −41° indicate a very high relative value of the condensation, much higher than the mean for all the data. When corrected with the aid of tables of mean distribution, traces of the galactic concentration (or of the spiral) will remain, and this is just what we find for the zone in question.

---

[1] See equation (1) of *Mt. Wilson Contr.*, No. 135.

[2] *Mt. Wilson Contr.*, No. 135, p. 13; *Astrophysical Journal*, **46**, 129, 1917.

Professor Turner has commented on the magnitude of the condensation for this zone,[1] and it is of interest to note that, with the exception of the zone at +62°, the other values of the condensation coefficients given by him[2] are all similarly related to the systematic variations shown in the right half of Fig. 2, *Mount Wilson Contribution* No. 135. Thus the Bordeaux and Algiers coefficients (+17°, −1°) are also large, and the corresponding curves, like that for the Cape, have been counted as cases favorable to the spiral, while the small values for Oxford and Perth (+28°, −32°) correspond to unfavorable cases.

The remaining comments to be made on Professor Turner's reply are altogether minor in character. He refers to my use of only a part of the material collected by him. To avoid misunderstanding it may be well to repeat that some of his published data are not in a form suitable for the investigation undertaken in *Mount Wilson Contribution* No. 135. All that could be used were included in the discussion.

I think that we are entirely in agreement as to the importance of the counts he has collected. They undoubtedly admit of a close co-ordination of the scales of the various Astrographic zones, as Professor Turner himself has shown by the comparisons that he has made with the scale of Chapman and Melotte. The regularity of increase in stellar density with decreasing galactic latitude, which appears even when the counts are restricted to comparatively small areas, is an impressive phenomenon and an excellent indication of the value of density as a measure of stellar brightness.

[1] *Monthly Notices*, **75**, 608, 1915.

[2] *Ibid.*

The meaning of the sentence from my article quoted by Professor Turner in the last paragraph of his reply would have been clearer had the wording been different. The implication was that we wish information as to the uniformity of distribution after the galactic condensation has been removed. By looking for irregularities along parallels of latitude, the effect of the condensation will not enter, and we may feel certain that any irregularities thus discovered will not be the consequence of residual errors in the adopted values of the condensation. But to trace the course of any irregularity, galactic latitude, the second co-ordinate, naturally requires consideration, as Professor Turner suggests.

Mount Wilson Solar Observatory
August 22, 1917

Contributions from the Mount Wilson Solar Observatory, No. 140
Reprinted from the *Astrophysical Journal*, Vol. XLVI, pp. 281–290, 1917

NOTES ON THE COLOR-CURVE AND LIGHT-ELEMENTS OF W URSAE MAJORIS

By HARLOW SHAPLEY and J. VAN DER BILT

The variable W Ursae Majoris[1] is of particular interest because of its exceptionally short period (four hours between minima) and because when interpreted as an eclipsing binary its mean density is more than twice that of the sun. Discussions of the orbit have been published by H. N. Russell[2] and H. Shapley.[3] A further study of the light-variations and orbit, on the basis of simultaneous photographic and photo-visual observations, was begun with the 60-inch reflector in 1916. The work was discontinued, however, upon learning that a similar investigation, based on Potsdam visual observations and unpublished photographic measures from Harvard, was already under way at Princeton.[4] The following pages contain a brief discussion of the color-curve obtained from the preliminary Mount Wilson observations, and an investigation of the light-elements based upon a considerable number of published and unpublished observations of minima during the last thirteen years.

OBSERVATIONS AT MOUNT WILSON AND UTRECHT

The magnitudes of the comparison stars used on the photographs with the 60-inch reflector were determined in the usual manner from ten polar-comparison plates (Table I). Magnitudes of the variable, derived from a series of Seed 27 and Cramer isochromatic plates made on April 26, 1916, are given in Table II. Six, seven, or eight exposures were made on each plate with exposure-times of one-half, one, or two minutes. The phases were computed with the formula given below. A plot of these results shows that the color-index on the Mount Wilson system is about +0.85, with little evidence of change during the cycle of light-variation.[1]

---

[1] W Ursae Majoris = B.D. $+56^\circ 1400$; $\alpha = 9^h 36^m 43^s$, $\delta = +56^\circ 24'.5$ (1900.0); spectrum G.

[2] *Astrophysical Journal*, **36**, 139, 1912.

[3] *Contributions from the Princeton University Observatory*, No. 3, p. 82, 1915.

[4] Since this paper was written the Princeton results have appeared in *Astrophysical Journal*, **45**, 306, 1917.

TABLE I

MAGNITUDES OF COMPARISON STARS

STAR	B.D.	*H.A.*, 63 VISUAL	MOUNT WILSON		COLOR-INDEX
			Photo-visual	Photographic	
a.	+56°1397	. . . .	6.64	7.65	+1.01
b.	+56 1399	8.74	8.76	9.90	+1.14
c.	+56 1398	8.73	8.80	10.08	+1.28

TABLE II

MOUNT WILSON OBSERVATIONS OF W URSAE MAJORIS
April 26, 1916; J.D. 2420980

PHOTOGRAPHIC					PHOTO-VISUAL				
Plate	Gr. H.M.T.	Apertures	Phase	Mag.	Plate	Gr. H.M.T.	Apertures	Phase	Mag.
3034P .	${}^{d}672$	14, 9, 6	$-0^{d}142$	8.76	3035P	${}^{d}676$	14, 9, 6	$-0^{d}138$	7.91
3036. . .	.702	14, 9	− .112	8.70	3037. .	.706	14	− .108	. . . . . .
3038. . .	.720	14, 9	− .094	8.64	3039. .	.724	14, 9	− .090	7.88
3040. . .	.737	14, 9	− .077	8.81	3041. .	.740	14, 9	− .074	7.96
3042. . .	.754	14, 6	− .060	8.84	3043. .	.758	14, 9	− .056	8.07
3044. . .	.771	14, 9	− .043	8.96	3045. .	.774	14, 9	− .040	8.03
3046. . .	.789	14	− .025	9.06	3047. .	.792	14, 9	− .022	8.18
3048. . .	.802	14, 9, 6	− .012	9.20	3049. .	.805	14, 9	− .009	8.41
3050. . .	.814	14, 9	.000	9.27	3051. .	.817	14, 9	+ .003	8.29
3052. . .	.829	14, 9, 6	+ .015	8.79	3053. .	.832	14, 9	+ .018	8.15
3054. . .	.841	14, 9	+ .027	8.67	3055. .	.844	14, 9	+ .030	7.98
3056. . .	.856	14, 9, 6	+0.042	8.52	3057. .	.860	14, 9, 6	+0.046	7.81

Though the light-curves of this variable often show an asymmetry which, if real, could not be accounted for completely by the simple eclipse theory, the star evidently is not a Cepheid variable, as is sometimes supposed, since no conspicuous change of color is found. Moreover, Russell has no difficulty in interpreting the light-curve, or in explaining the differences between visual and photographic curves through differences in darkening at the limb.[2]

[1] The last two plates are uncertain because of the low altitude of the field.

[2] *Popular Astronomy*, **25**, 30, 1917.

At the Utrecht Observatory 105 observations of W Ursae Majoris were obtained with the polarizing photometer attached to the $4\frac{1}{2}$-inch refractor.[1] At maximum the variable is a little too bright for this instrument, but the minima can be determined very sharply. The following comparison stars were used:

$a =$ B.D. $+54^\circ 1329 =$ Potsdam Gen. Cat. 5731; Mag. $= 7.73$
$b = \quad +56^\circ 1412 = a + 0^{\mathrm{M}}.33 \quad 8.06$
$c = \quad +56^\circ 1399 = a + 1.38 \quad 9.11$

The brightness of both *b* and *c* was derived from the measured differences with *a*.

The method of observation differed somewhat from the usual one inasmuch as more settings were made on the rapidly changing variable than on the comparison stars. In the interval covered by the observations on each evening three to five measures of each of the comparison stars were secured, and these were plotted against the time on squared paper. After allowance for extinction, the settings were usually remarkably constant and could be read accurately for the times corresponding to the measures on the variable. In this way the latter could be closely followed through the steep ascents and descents of its light-curve.

The Utrecht observations are given in detail in Table III, the fifth column containing the differences in hundredths of a magnitude between the adopted value and that given by each of the comparison stars.

THE LIGHT-ELEMENTS

Since about 6000 epochs have elapsed since the latest discussion, a revision of the light-elements can now be made. In view of the possibility that the light-curve may be changeable in form, as many individual minima are included in the computation as can be derived with sufficient accuracy from the published series of observations.

The list in Table IV contains 67 minima, extending over an interval of 29,273 epochs. That numbered 61 has not been used in the derivation of elements. Nos. 59 and 60 were received from Professor Jordan after the completion of the solution and have been

---

[1] The instrument has been described in *Recherches astronomique de l'Observatoire d'Utrecht*, **6**, 10, 1916.

TABLE III

Utrecht Observations of W Ursae Majoris

Date	J.D. and Gr.M.T. 2420000+	Phase	Mag.	Residuals*		
				a	*b*	*c*
1916 April 28	0982.461	0^{d}071	8.42	+ 5	....	− 5
	.505	.116	8.16	− 2	....	+ 3
	.548	.158	7.72	+ 1	....	0
April 29	0983.408	.018	8.07	− 9	....	+ 9
	.420	.029	8.11	− 7	....	+ 7
	.429	.039	8.06	− 5	....	+ 5
	.440	.049	8.14	− 1	....	+ 2
	.452	.062	8.24	0	....	0
	.503	.113	8.30	+ 1	....	0
	.515	.125	8.23	+ 2	....	− 2
	.524	.134	7.97	+ 3	....	− 2
	.535	.144	7.90	+ 4	....	− 3
	.544	.153	7.87	+ 5	....	− 5
May 11	0995.408	.008	7.80	−11	....	+12
	.421	.021	7.94	− 9	....	+10
	.428	.028	7.87	− 8	....	+ 8
	.433	.033	7.92	− 7	....	+ 7
	.438	.038	8.02	− 6	....	+ 7
	.444	.044	8.06	− 5	....	+ 6
	.450	.050	8.15	− 5	....	+ 5
	.459	.059	8.24	− 4	....	+ 5
	.468	.068	8.48	− 4	....	+ 5
	.473	.073	8.43	− 4	....	+ 4
	.480	.080	8.65	− 4	....	+ 5
	.489	.089	9.09	− 3	....	+ 3
	.495	.095	8.71	− 1	....	+ 2
	.501	.101	8.76	0	....	+ 1
	.508	.108	8.54	+ 1	....	0
	.514	.114	8.30	+ 1	....	0
	.525	.125	8.16	+ 1	....	0
	.547	.147	7.99	+ 2	....	− 1
	.556	.156	7.99	+ 1	....	0
May 17	1001.410	.005	7.92	....	+ 1	− 1
	.423	.018	7.92	....	+ 1	0
	.428	.023	7.88	....	0	0
	.434	.029	7.97	....	0	0
	.438	.033	7.99	....	0	0
	.448	.043	7.97	....	− 2	+ 3
	.461	.056	8.14	....	− 3	+ 3
	.465	.060	8.19	....	− 3	+ 3
	.469	.065	8.28	....	− 3	+ 4
	.474	.069	8.39	....	− 4	+ 5
	.483	.078	8.48	....	− 5	+ 5
	.486	.082	8.60	....	− 5	+ 5
	.491	.086	8.69	....	− 5	+ 5
	.495	.090	8.70	....	− 5	+ 5
	.500	.095	8.55	....	− 5	+ 6
	.505	.101	8.44	....	− 5	+ 5
	.517	.112	8.32	....	− 5	+ 6
	.527	.122	8.02	....	− 6	+ 6
	.536	0.131	7.89	....	− 5	+ 6

---

* A positive residual means that the adopted magnitude is brighter than that derived from the comparison star.

TABLE III—*Continued*

Date	J.D. and Gr.M.T. 2420000+	Phase	Mag.	Residuals		
				a	*b*	*c*
1916 May 19	1003.408	$0^{d}001$	7.95	+8	−4	−3
	.415	.009	7.88	+5	−3	−3
	.424	.019	7.98	+3	−2	−2
	.429	.024	7.96	+1	−1	−1
	.434	.027	8.00	0	+1	−1
	.439	.034	7.99	−2	+2	0
	.448	.043	8.01	−4	+3	0
	.456	.051	7.99	−4	+4	+1
	.465	.060	8.18	−4	+3	+2
	.469	.064	8.26	−4	+3	+2
	.473	.068	8.50	−4	+2	+3
	.478	.072	8.53	−4	+2	+3
	.482	.076	8.41	−5	+1	+3
	.487	.081	8.47	−5	0	+4
	.496	.090	8.70	−3	−1	+4
	.500	.094	8.71	−3	−1	+3
	.505	.098	8.65	−2	−1	+3
	.510	.104	8.41	−2	−1	+2
	.520	.113	8.26	0	0	+1
	.530	.123	8.05	−1	+2	−2
	.541	.135	7.93	−3	+4	0
	.554	.148	7.89	−6	+5	+1
May 21	1005.415	.007	8.18	....	+2	−2
	.421	.013	8.03	....	+3	−3
	.433	.025	8.10	....	+6	−6
	.443	.035	7.90	+9	+1	−10
	.451	.043	8.01	+7	+3	−9
	.459	.051	7.97	+6	+2	−7
	.466	.058	8.14	+5	0	−6
	.472	.064	8.30	+4	0	−5
	.475	.067	8.35	+5	0	−5
	.479	.071	8.44	+5	−1	−4
	.483	.075	8.60	+5	−1	−4
	.487	.079	8.63	+5	−2	−3
	.490	.082	8.54	+5	−2	−2
	.496	.088	8.84	+5	−2	−4
	.500	.092	8.86	+6	−1	−5
	.505	.097	8.70	+7	0	−6
	.509	.101	8.62	+8	0	−8
	.516	.108	8.51	+10	+1	−11
	.526	.118	8.28	+10	+2	−13
	.533	.125	8.09	+11	+2	−14
May 28	1012.420	.007	8.08	....	+3	−2
	.432	.018	8.01	....	0	0
	.437	.023	7.96	....	−1	+2
	.442	.028	7.93	....	−3	+3
	.450	.036	8.07	....	−6	+6
	.459	.045	8.26	....	−6	+6
	.480	.067	8.52	....	−2	+2
	.486	.073	8.44	....	0	0
	.499	.085	8.74	....	0	+1
	.509	.095	8.57	....	−2	+2
	.517	.104	8.54	....	−1	+2
	.525	0.112	8.34	....	+1	0

TABLE IV

LIST OF MINIMA

No.	Observed Minima Date	Gr.M.T.	Red. to Sun	Epoch	Obsd. J.D. (Helioc.)	O−C Days	O−C Min.	Observer	Remarks	Reference
1	1903 Jan. 14	4h 34m	+6m	0	6129.194	−0.006	8.0	MK	....	*Ap. J.*, **17**, 205
2	17	4 40	+6	18	6132.199	− 4	5.2	“	....	
3	17	8 31	+6	19	6132.359	− 11	15.3	“	....	
4	18	8 34	+6	25	6133.361	− 10	13.8	“	....	
5	Feb. 20	5 25	+6	222	6166.230	− 4	5.2	“	....	*A.N.*, 4005
6	Apr. 24	10 51	0	601	6229.452	− 7	9.5	“	....	
7	1904 Jan. 10	8 50	+6	2165	6490.372	+ 7	10.7	F	....	*A.N.*, 3963
8	17	8 59	+6	2207	6497.378	+ 7	10.7	“	....	
9	27	5 17	+6	2266	6507.224	+ 11	16.4	“	Uncertain	
10	27	9 12	+6	2267	6507.387	+ 7	10.7	“	Good	
11	Feb. 13	5 14	+6	2368	6524.222	− 7	9.5	MK	....	*A.N.*, 4005
12	17	9 40	+6	2393	6528.407	+ 8	12.1	F	Fair	*A.N.*, 3963
13	19	5 43	+6	2404	6530.242	+ 8	12.1	“	Fair	
14	Mar. 14	6 30	+4	2548	6554.274:	+ 18:	26.5	“	Uncertain	
15	1905 Jan. 17	8 43	+6	4401	6863.367	− 6	8.0	MK	....	*A.N.*, 4005
16	Nov. 9	19 15	+1	6178	7159.803	− 8	11.8	PJ	Fair	*Ap.J.*, **23**, 84
17	Dec. 7	20 7	+4	6346	7187.841	+ 4	5.9	“	Poor	
18	1906 July 26	9 7	−6	7728	7418.376	− 6	8.0	MK	Good	*A.N.*, 4128
19	1907 Mar. 4	5 59	+5	9052	7639.253	+ 2	3.3	T	Orange filter*	*Pulkowa Mitt.*, **2**, No. 21
20	5	10 0	+5	9059	7640.419	+ 1	0.9	“	Green-blue†	
21	7	9 55	+5	9071	7642.417	− 3	4.9	“	Orange‡	
22	24	6 24	+3	9172	7659.269	− 0	0.1	“	Orange*	
23	29	6 36	+3	9202	7664.277	+ 3	4.9	“	Ultra-violet*	
24	30	6 40	+3	9208	7665.280	+ 3	4.9	“	Ultra-violet*	
25	Apr. 1	6 42	+2	9220	7667.281	+ 5	6.6	“	Ultra-violet‡	
26	10	6 54	+2	9274	7676.289	+ 4	6.2	“	Ultra-violet*	
27	12	6 54	+1	9286	7678.288	+ 2	2.2	“	Orange§	
28	13	6 59	+1	9292	7679.292	+ 5	6.6	“	Green-blue‡	
29	15	7 1	+1	9304	7681.293	+ 4	5.5	“	Green-blue†	
30	29	11 11	0	9389	7695.466	− 3	4.2	“	Orange*	
31	May 1	11 23	0	9401	7697.474	+0.003	4.8	“	Ultra-violet*	

32	1907	June	8	8	9	−4	9628	7735.337	−0.002	2.3	Ba	Fair	*M.N.*, **69**, 86
33			9	8	14	−4	9634	7736.340	+0	0.6	“	Good	
34			19	8	24	−5	9694	7746.347	−2	2.3	“	Fair	
35		July	18	9	7	−6	9868	7775.376	+0	0.6	“	Good	
36			22	9	7	−6	9892	7779.376	−4	5.2	“	Good	
37			25	9	10	−6	9910	7782.378	−4	5.2	“	Good	
38		Aug.	6	9	23	−6	9982	7794.387	−6	8.0	“	Fair	
39			11	9	38	−6	10012	7799.397	−1	0.9	“	Uncertain	
40	1908	Jan.	2	8	45	+6	10875	7943.369	+6	9.2	“	Good	
41			14	8	56	+6	10947	7955.376	+2	3.5	“	Fair	
42		Mar.	25	10	28	+3	11373	8026.438	−1	0.9	“	Fair	
43		Apr.	15	10	56	+2	11499	8047.457	−2	2.3	“	Fair	
44			26	11	18	0	11565	8058.471	+2	3.5	“	Good	
45		May	3	11	28	−1	11607	8065.477	+2	3.5	“	Good	
46			14	11	44	−2	11673	8076.487	+2	3.5	“	Good	
47	1910	Apr.	4	6	44	+2	15808	8766.282	−2	2.3	H	Good	*Riv. di Astr.*, **4**, 310
48			6	6	43	+2	15820	8768.281	−5	6.6	“	Good	
49			7	6	58	+2	15826	8769.292	+5	7.8	“	Fair	
50	1911	July	9	9	2	−6	18572	9227.372	−2	2.3	L	Good	*A.N.*, 4542
51	1913	June	25	9	11	−5	22870	9944.379	+15	21.6	P	Uncertain	*Mem. Sp. It.*, **2**, 193
52		July	1	9	21	−6	22906	9950.385	+15	22.4	“	Fair	
53			3	8	53	−6	22918	9952.366	−6	8.0	“	Fair	
54			4	9	2	−6	22924	9953.372	−1	0.9	“	Good	
55			5	9	2	−6	22930	9954.372	−1	0.9	“	Fair	
56			6	8	40	−6	22936	9955.357	−17	22.5	“	Uncertain	
57			7	8	54	−6	22942	9956.366	−9	12.4	“	Uncertain	
58			8	9	15	−6	22948	9957.381	+5	7.8	“	Uncertain	
59	1915	Jan.	28	17	19	+6	26361	0526.726	−5	7.5	J	....	Letter
60			29	17	22	+6	26367	0527.728	−4	5.9	“	....	
61	1916	Apr.	26	19	25	0	29083	0980.809	−5	7.3	Sh	Good	This paper
62			29	11	28	0	29099	0983.478	−6	8.0	Bi	Fair	
63		May	11	11	48	−2	29171	0995.490	−5	6.6	“	Good	
64			17	11	53	−2	29207	1001.494	−6	8.0	“	Good	
65			19	11	54	−2	29219	1003.494	−8	11.0	“	Good	
66			21	11	59	−3	29231	1005.497	−7	9.5	“	Good	
67			28	12	14	−3	29273	1012.508	−0.002	2.3	“	Fair	

* Good. † Uncertain; minimum phase very flat. ‡ Uncertain. § Uncertain; light-curve discordant.

used only to indicate the representation in 1915 by the adopted elements.[1]

For the designation of the observers the following abbreviations are used, the method of observation being indicated in parentheses: MK = Müller and Kempf (photometric); F = Fauth (estimates); PJ = Parkhurst and Jordan (photographic); T = Tikhoff (photographic); Ba = Baldwin (photometric); H = Horn (photographic); L = Lazzarino (photometric); P = Padova (photometric); J = Jordan (photographic); Sh = Shapley (photographic); Bi = Van der Bilt (photometric).

The following points are to be noted:

1. The minima published by Müller and Kempf and those by Parkhurst and Jordan have been taken as they stand. There are two misprints in the latter's comparison with Müller and Kempf's data;[2] the calculated time of the minimum of December 7 should be $19^{h}55^{m}$, and the residual minus instead of plus.

2. The detailed observations of Fauth, made by Argelander's method, are not accessible. Though the results are probably less accurate than those obtained by photometric methods, we have not thought ourselves justified in rejecting them on account of this a priori assumption.

3. All the observations made by Tikhoff have been plotted and several minima derived which had not been discussed previously.

Color Screen	Residuals (Unit is $0\overset{\mathrm{d}}{.}0001$)	Mean Residual
Orange.	+23, −33, − 1, +15, −29	− 5
Green-blue.	+ 6, +46, +38	+30
Ultra-violet.	+34, +34, +46, +43, +33	+38

Though the various filters seem to give systematic differences in the time of minimum, the accompanying tabulation, based on data

---

[1] For the sake of completeness, times of minima have also been computed for the new Harvard photographic observations from the data given by Russell, Fowler, and Borton in Table IX, *Astrophysical Journal*, **45**, 321, 1917. The representation of these times by our adopted light-elements is as follows:

Mean Epoch.	1,120	7,380	16,000	24,600
O−C.	$+0\overset{\mathrm{d}}{.}0015$	$+0\overset{\mathrm{d}}{.}0008$	$+0\overset{\mathrm{d}}{.}0016$	$-0\overset{\mathrm{d}}{.}0004$

[2] *Astrophysical Journal*, **23**, 84, 1906.

in Table IV, shows that these differences hardly exceed the observational uncertainty.[1] The individual measures have a considerable accidental error, and as only one of the color-filters was used at each minimum systematic errors may be involved if the period is not strictly uniform.

4. All the observations by Baldwin have also been plotted, and with the aid of the mean light-curve given by him several new minima were derived from incomplete light-curves and are available for the discussion.

5. Horn, working with photographic trails, gives the times of three maxima. Since it is uncertain whether the minima occur exactly half-way between the maxima, and since the latter can usually not be determined with the same accuracy as the minima, we have made a new grouping of Horn's observations for an independent derivation of the minima. A striking feature of his mean light-curve, entirely differing from the results of other observers, is that the horizontal line through the points of median magnitude is divided by the light-curve into approximately equal parts. The curves obtained by other observers all indicate that the part of this line below the maximum is nearly three times as long as that above the minimum. The actual figures are:

Müller and Kempf..........	$0^{\mathrm{d}}.125$	and	$0^{\mathrm{d}}.042$
Baldwin...................	0.121	"	0.046
Van der Bilt..............	0.125	"	0.042
Horn......................	0.097	"	0.070

Further, one (and probably two) of Horn's observed curves shows a constant minimum of more than 25 minutes. The explanation of both phenomena may be that the photographic trails at minimum were so faint that they could not be measured accurately.

6. The mean light-curve published by Padova was derived from a very non-homogeneous grouping. A new mean curve has been constructed and the separate minima determined as accurately as the observations allow.

---

[1] For a note on the interpretation of Tikhoff's results see Kron, *Potsdam Publications*, **22**, Pt. 3, p. 56, 1912.

The 64 minima used in the computation yield the following new light-elements:

$$\text{Heliocentric Minimum} = \text{J.D. } 2418075.8176 + 0\overset{d}{.}1668196E, \text{ Gr.M.T.},$$

the period of revolution being double the interval between minima.

The residuals to which the foregoing formula leads are given, both in fractions of a day and in minutes of time, in the sixth and seventh columns. The mean residual is $0\overset{d}{.}0050$. The algebraic sum of the residuals is $-0\overset{d}{.}0014$. There are 30 positive and 34 negative residuals, 37 recurrences of sign, and only 26 changes, which points to some systematic change in the period. The evidence for this is strengthened by the fact that the first and the last six residuals are all negative, with practically the same mean value, viz.:

Mean epoch = 148, Mean residual = $-0\overset{d}{.}0066$
" " = 29,200, " " = -0.0053.

Were the time of normal minimum displaced by this amount, all but four of the intermediate residuals would become positive.

There is, however, no indication of a systematic difference between the odd and even minima. We derive:

Mean residual of 39 even minima = $+0\overset{d}{.}0005$
Mean residual of 25 odd minima = -0.0009,

a difference wholly covered by the observational errors.

From the present study a perturbation of some character appears certain, but the data are as yet insufficient to determine the law of variation.

SUMMARY

1. Mount Wilson photographic observations of W Ursae Majoris, the star of highest known density, give a color-index in agreement with its spectral type (G), and show no conspicuous change of color between minimum and maximum light.

2. From a series of photometric measures made at the Utrecht Observatory (Table III) the times of six minima have been derived.

3. A study of 64 minima, distributed throughout an interval that includes 29,000 recurrences of minimum light, reveals a small but distinct perturbation of the period (Table IV).

Mount Wilson Solar Observatory
June 1917

Contributions from the Mount Wilson Solar Observatory, No. 141
Reprinted from the *Astrophysical Journal*, Vol. XLVI, pp. 298–300, 1917

SOLAR HYDROGEN "BOMBS"

By FERDINAND ELLERMAN

Visual and photographic observations of a solar phenomenon which had previously escaped our attention have been carried on at this observatory during the past two years.

On September 21, 1915, while the writer was observing the Hα line for reversals and distortions in an active spot-group, there suddenly appeared a very brilliant and very narrow band extending four or five angstroms on either side of the line, but not crossing it. In a couple of minutes it faded away and was not seen again. A month later, on October 21, more observations were recorded and a spectrogram was secured.

On the first occasion the appearance was so extraordinary that it seemed hardly real; after the second observation, however, the existence of such phenomena as part of the solar activity seemed established, and a search has been made for them whenever conditions of seeing and other work have permitted.

There are two conditions essential for observation—good seeing and a large solar image—as the area of the phenomenon, even with the 16-inch image of the sun at the 150-foot tower telescope, is so small that only with difficulty is the point of disturbance kept on the slit.

The appearance of the phenomenon indicates something in the nature of an explosion, in which hydrogen seems to be the only element playing a part. The duration is only a few minutes—from one to three on the average, and from five to ten minutes rarely. This sudden performance suggested the name of hydrogen "bomb," which we have adopted to designate it.

In the *Astrophysical Journal*, **30**, 78, 1909, Dr. Walter M. Mitchell gives an account of solar observations made at Haverford College Observatory, together with a drawing which illustrates the appearance of Hα in the spectrum of a "bomb," and from his description there seems to be no doubt of its being such. This is the only recorded observation of the kind that has come to our notice, and it must have been an unusually large one to have been seen with the instrument used by Dr. Mitchell. Furthermore, he mentions D_3 as showing the band, while our observations have failed to detect it.

While the average width of the Hα band is about 8 A, in an exceptional and probably an extreme case it was as wide as 30 A. In general the band appears symmetrical on each side of the line, but in a few measured cases the extension was greater on the violet side than on the red. In none have we found greater extension on the red side.

The regions where the "bombs" are likely to appear are around and among active spot-groups, especially groups which are developing and composed of many members. In such groups they appear at the outer edge of the penumbra, or at points between the spots, and also at small distances to one side. When a "bomb" appears and fades away, the point of disturbance should be kept under observation, as it is very probable that others will appear in the same place. At times they seem to follow one another like the balls of a Roman candle at intervals varying from ten to twenty minutes or more.

They frequently appear in the faculae so that their spectra are superposed on those of the faculae, thus giving the appearance of great extension to the bright "bomb" band. On rarer occasions they are superposed on bright reversals of Hα over eruptive regions, but this is an uncommon occurrence, and the distinction is easily made between the two phenomena by the flickering of the "bomb" band compared to the Hα reversal, due to the effect of seeing.

The observations have been confined mainly to Hα, although D_1, D_2, D_3; b_1, b_2, b_4; Hβ and Hγ have been examined. None but the hydrogen lines have shown the band. Hβ has been photographed and shows the band fairly well, but not as well as Hα nor of as great width. Hγ also shows the band, but less clearly than Hβ.

The level at which the "bombs" occur must lie well below the reversing layer, as the hydrogen absorption line is not affected by them, nor do they seem to affect the other Fraunhofer lines.

PLATE XVIII

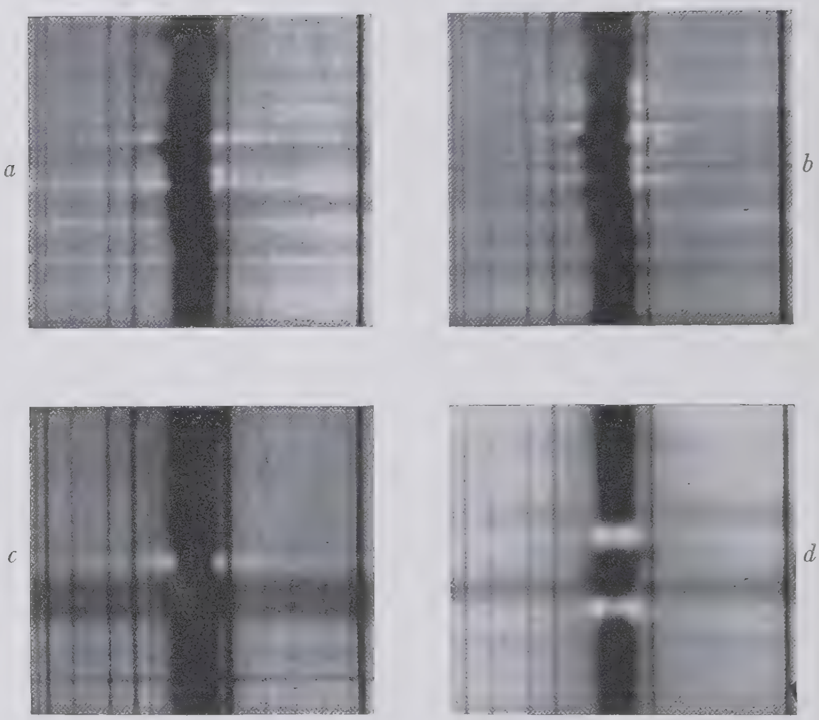

a and *b*. Appearance of the Hα line in an active sun-spot region, showing the bands of "bombs" and the distortions of the line.

c. Spectrum of a "bomb" (close to the dark Hα line) superposed on the spectrum of a facula.

d. Appearance of reversals in an active region.

In Plate XVIII, *a* and *b*, are shown spectra of "bombs" which appeared in regions where the Hα line shows considerable distortion due to radial velocities of the hydrogen flocculi. It will be noted that the "bomb" bands do not extend as far on each side of Hα as mentioned above, but this is to be expected, as it is impossible to guide and keep the image of the "bomb" on the slit perfectly during the entire exposure, and the fainter extensions which are easily observed visually are lost in the photograph. Plate XVIII, *c*, shows the "bomb" band superposed on the spectrum of a facula, and in *d* are shown two bright reversals of Hα near a small spot, to illustrate the difference in appearance between ordinary eruptive reversals of Hα and the bright band due to "bombs."

MOUNT WILSON SOLAR OBSERVATORY
October 1917

Contributions from the Mount Wilson Solar Observatory, No. 142
Reprinted from the *Astrophysical Journal*, Vol. XLVI, pp. 313–339, 1917

THE LUMINOSITIES AND PARALLAXES OF FIVE HUNDRED STARS

FIRST LIST

By WALTER S. ADAMS and A. H. JOY

The determination by means of a study of their spectra of the luminosities and parallaxes of the stars under investigation for radial velocity at the Mount Wilson Observatory has been continued as a regular part of the stellar spectroscopic work. The methods employed are essentially those described by one of us in a series of papers[1] published somewhat more than a year ago. So far as these methods have been modified or extended in the course of the present investigation, reference will be made accordingly.

Although the observational material and the number of parallax determinations have accumulated rapidly, it has seemed preferable to us to delay the publication of the results until enough were available to make possible a detailed comparison with the trigonometrical parallaxes. Moreover, we have found that the accuracy of the estimation of relative line-intensities depends to a considerable extent upon the number of photographs. A single spectrogram, owing to under- or over-exposure or peculiarities in the plate-grain, will sometimes give an inaccurate value which subsequent plates will correct. Accordingly we have attempted as far as possible to secure at least three photographs of the spectrum of each star.

Another important consideration is the fact that measured parallaxes[2] of a high degree of accuracy are being published at frequent intervals. Since the spectroscopic determinations depend upon empirical curves connecting line-intensity with absolute magnitude, and since this absolute magnitude is calculated from the measured parallax, it is desirable from time to time to readjust the curves with the aid of such new material as is available.

---

[1] Adams, *Mount Wilson Communications*, Nos. 23–26; *Proceedings of the National Academy of Sciences*, 2, 143, 1916.

[2] The term "measured parallaxes" is used in this article to designate those determined trigonometrically. In the absence of a better term "spectroscopic parallax" is also employed. This should not be confused with the radial-velocity method used for parallax determinations in double-star systems, and employed, for example, by Wright in the case of α Centauri.

In the list of results for 500 stars which is given in this communication the attempt has been made to include as many stars as possible with measured parallaxes. Since many of the recent values by Mitchell and Miller are for relatively bright stars, we have added to our observing list the stars of the *American Ephemeris* with types between F0 and M. In addition there are included many stars of small proper motion observed by van Maanen. The measured parallaxes of a number of these have been used in the establishment of the relationships between line-intensity and absolute magnitude and have proved of great value. For the most part they are stars of high luminosity and so are particularly useful in fixing the lower portions of the magnitude-curves. A number of the results of Mitchell have been equally valuable in this respect. About 80 stars in all have been used in determining the reduction formulae for the various types.

There are three classes of stars in the list for which modifications have been made of the methods of reduction used previously. These are the early F-type stars and the giants and dwarfs of type M. It was soon found in the case of the F0 to F5 stars that the line λ 4455 of calcium showed but little variation with absolute magnitude. On the other hand, the strontium line at λ 4215 still remained available, and a search was made for additional lines to supplement it. Such lines were found in the similar strontium line at λ 4077, and the line at λ 4290, which probably is due, at least mainly, to enhanced titanium. All three of these lines increase in intensity with increase of luminosity. They are compared in intensity with three neighboring iron lines, λ 4072, λ 4250, and λ 4271, respectively, and the reduction-curves have been formed in the usual way by determining these differences for stars of measured parallax. This method gives satisfactory results for stars with spectra between A8 and F5. For stars later than F5 the usual lines λ 4215 and λ 4455 are employed.

The giant M-type stars have proved most difficult of treatment. The plan finally adopted in their case has been to compare the spectrum of each star with that of α Orionis, which probably is the most highly luminous star of this type of which we have any certain knowledge, and to estimate the differences in intensity of certain selected lines in their spectra. The lines chosen are λ 4077 of strontium, a line of uncertain origin at λ 4207, λ 4215 of strontium, and the two hydrogen lines Hδ and Hγ. All of these lines increase in intensity with the luminosity of the star. They are nearly as strong in the spectrum of α Scorpii as in that of α Orionis, and this star has served as one of the fundamental points for the reduction curves. Its parallax as determined from group-motion has been furnished to us by the kindness of Professor Russell. Additional points for the reduction-curves are provided by the parallaxes of M-type stars of van Maanen and Mitchell. This method of reduction, though not entirely satisfactory, is the best which we have as yet been able to devise.

The recent determinations of the parallax of the star of large proper motion discovered by Barnard indicate that its absolute magnitude is about 13.3. The reduction-curves previously used for stars of this type depended upon extreme values of about 11.0, and were nearly asymptotic to the magnitude axis at this point. Accordingly it became essential to extend the curves to include fainter stars of this type. The calcium line at λ 4455 reaches so great an intensity in all dwarf M-type stars that it becomes difficult to make use of it for the determination of relatively small differences. An examination, however, of the low-temperature line of strontium at λ 4607 showed a marked increase of intensity in the spectrum of Barnard's star as compared with other stars of this class, and the character of the line is such as to make estimates of its intensity comparatively simple. We have therefore used this line in determining the relative absolute magnitudes of the various dwarf M stars. It is worthy of note that in the case of both classes of M-type stars the modifications introduced into the reduction method have been for the purpose of securing more accurate determinations of magnitude within each class. They may therefore be regarded as an attempt at a second approximation, with the separation into the two classes as the first.

The results of our determinations are given in Table I. The values for spectral types and absolute magnitude are the means of

TABLE I

No.	Name	Harv. Visual Mag.	Harv. Spec.	α 1900	δ 1900	μ	No. Pl.	Spectrum		Abs. Visual Mag.	Lum.	π	Trig. π	Auth.
								Est.	Meas.					
1	Lal. 47231r	8.9	K2	$0^{h}\ 0^{m}.4$	+45° 16′	0″.90	4	K7	K7	+9.3	0.019	0″.120	+0″.096	Y, S, Fox
2	Σ 3062 Br	6.9	F	0 1.0	+57 53	0.266	3	G4	G2	+5.2	0.832	0.046	+0.036	Mil.
3	Σ 3062 Ft	8.0	....	0 1.0	+57 53	0.266	2	G9	G8	+5.3	0.759	0.029		
4	12 Ceti	6.0	K	0 24.9	− 4 31	0.011	3	K5	K2	+1.7	20.9	0.014	....	....
5	Boss 96	5.7	G5	0 26.2	+52 17	0.056	3	K0	K0	+0.3	75.9	0.008	+0.008	vM
6	Boss 106	6.4	G5	0 27.5	+27 44	0.014	3	G6	G7	+0.4	69.2	0.006	+0.005	vM
7	Pi. 0h130	5.7	K	0 32.2	−25 19	1.39	3	G8	G6	+4.8	1.20	0.066	....	....
8	ε Androm	4.5	G5	0 33.3	+28 46	0.336	3	G3	G4	+1.3	30.2	0.023	+0.075	S and M, Mil.
9	δ Androm	3.5	K0	0 34.0	+30 19	0.162	2	K3	K3	+1.4	27.5	0.038	....	....
10	Lal. 999	7.4	G	0 34.0	+ 2 35	0.79	3	G3	G1	+5.2	0.832	0.036	+0.033	Y, Jw.
11	α Cassiop	2.2 2.8–	K0	0 34.8	+55 59	0.060	2	G8	G8	−0.9	229.	0.018– 0.024	+0.023	F, M
12	Lal. 1045	7.5	K	0 35.3	+39 39	0.81	3	K3	K3	+5.8	0.479	0.046	+0.017	Y
13	η Cassiop. Br	3.6	F8	0 43.0	+57 17	1.242	3	F9	G0	+5.0	1.00	0.190	+0.191	5
14	η Cassiop. Ft	7.6	....	0 43.0	+57 17	1.242	1	K4	K0	+8.7	0.033	0.166	....	....
15	Groom. 145	8.0	K	0 43.3	+69 54	0.54	3	K2	K2	+6.2	0.331	0.044	+0.028	Y
16	A. G. Hels 914	8.7	....	1 0.3	+63 24	1.62	2	K7	K6	+8.6	0.036	0.096	....	....
17	Lal. 1966	7.9	F5	1 3.3	+61 1	0.69	3	F5	F5	+5.1	0.912	0.028	+0.022	Y, S and M
18	β Androm	2.4	Ma	1 4.1	+35 5	0.216	2	Ma	G8	+1.6	22.9	0.069	+0.058	F, M
19	W.B. 1h161	8.0	K	1 13.5	− 1 23	0.54	5	K0	G9	+6.1	0.363	0.042	−0.011	Y
20	Lal. 2387	8.5	G	1 14.0	− 9 27	0.57	2	G1	G1	+4.7	1.32	0.017	+0.026	Y
21	Lal. 2450	8.1	F8	1 16.9	+18 10	0.57	3	G0	G1	+5.7	0.525	0.033	+0.017	Y
22	ω Androm	5.0	F5	1 21.7	+44 53	0.356	1	F0	F1	+3.4	4.37	0.048	+0.037	F, Jw., M
23	α Urs. Min	2.1	F8	1 22.6	+88 46	0.044	8	F8	F8	+0.6	57.5	0.050	+0.041	10
24	Lal. 2682	7.8	G5	1 23.6	+21 13	0.53	6	K3	K2	+6.5	0.251	0.055	+0.009	Y
25	η Piscium	3.7	G5	1 26.1	+14 50	0.031	2	G5	G5	+0.3	75.9	0.021	+0.056	M
26	40 Cassiop	5.5	K	1 30.5	+72 32	0.008	3	G6	G5	+0.2	83.2	0.009	....	....
27	υ Androm	4.2	G0	1 30.9	+40 54	0.418	2	F9	F9	+4.0	2.51	0.091	+0.057	M
28	Lal. 2966	7.6	G5	1 34.2	+66 25	0.76	3	G4	G2	+6.2	0.331	0.052	+0.036	Y
29	Lal. 3128	5.3	G8	1 37.1	+19 47	0.718	4	K1	K1	+5.5	0.631	0.110	+0.129	Y
30	τ Ceti	3.6	K0	1 39.4	−16 28	1.922	3	G7	G5	+6.2	0.331	0.331	+0.317	4
31	Boss 405	5.8	F	1 43.0	+32 11	0.354	3	F6	F8	+3.9	2.75	0.042	....	....
32	Boss 420	5.6	K	1 47.3	+40 14	0.009	3	K2	K1	+0.6	57.5	0.010	+0.006	vM
33	Lal. 3922	7.5	G	2 2.5	− 1 5	0.50	3	F9	G0	+3.8	3.02	0.018	−0.042	Y
34	55 Cassiop	6.2	F5	2 6.6	+66 3	0.003	3	F5	F7	+1.9	17.4	0.014	....	....
35	6 Persei	5.4	K0	2 7.0	+50 36	0.386	1	G6	G3	−0.3	132.	0.008	−0.001	L and J
36	Lal. 3987	7.8	K	2 7.5	+67 13	0.56	3	K2	K2	+6.0	0.398	0.044	+0.097	Y
37	W.B. 2h95	8.3	G	2 9.5	− 1 40	0.97	5	F8	F9	+4.4	1.74	0.017	+0.014	Y
38	Lal. 4141	6.9	G	2 9.7	+23 49	0.60	4	G7	G4	+4.5	1.58	0.033	+0.029	Y
39	Lal. 4268	5.8	F5	2 12.8	+ 1 17	0.527	3	F7	F8	+4.0	2.51	0.044	....	....

40	Boss 556	6.5	G	2 22.1	+ 9 45	0.355	4	F5	F6	+4.5	1.58	0.040	......	......
41	Boss 592	7.4	F	2 31.2	+24 13	0.152	3	F5	F7	+3.7	3.31	0.018	+0.010	vM
42	Boss 593	6.6	F5	2 31.2	+24 13	0.140	6	F3	F5	+3.9	2.75	0.028	+0.030	vM
43	Lal. 4855	7.2	G	2 32.6	+30 24	0.60	3	F8	F8	+4.7	1.32	0.032	+0.026	Y, F
44	θ Persei	4.2	G0	2 37.4	+48 48	0.351	3	F7	F7	+4.2	2.09	0.100	+0.088	S
45	SU Cassiop	5.9– 6.3	F	2 43.0	+68 28	0.016	7	F5	F5	+1.0	39.8	0.010	+0.010	vM
46	η Persei	3.9	K0	2 43.4	+55 29	0.030	2	K3	G4	+0.5	63.1	0.021	......	......
47	τ Persei	4.1	G0p	2 47.2	+52 21	0.008	2	G1	G1	+1.5	25.1	0.030	......	......
48	20 Persei	5.3	F	2 47.4	+37 56	0.099	4	F0	F2	+3.3	4.79	0.040	+0.013	S and M, Mil.
49	Boss 672	5.6	G5p	2 53.0	+46 49	0.035	3	G3	G3	+1.5	25.1	0.015	−0.007	vM
50	α Ceti	2.8	Ma	2 57.1	+ 3 42	0.078	2	Ma	G8	+0.5	63.1	0.035	+0.022	M
51	ρ Persei	3.4– 4.2	Mb	2 58.9	+38 27	0.173	2	Mb	G7	−0.5	158.	0.011– 0.017	+0.047	R, M
52	ι Persei	4.2	G	3 1.8	+49 14	1.269	3	G0	G0	+4.1	2.29	0.096	+0.126	4
53	δ Arietis	4.5	K0	3 5.9	+19 21	0.152	2	K0	G9	+1.0	39.8	0.020	......	......
54	α Persei	1.9	F5	3 17.2	+49 30	0.039	3	F5	F7	+0.3	75.9	0.048	+0.016	F, S and M
55	Lal. 6320	7.9	K5	3 20.1	− 5 42	0.86	3	K5	K5	+7.1	0.145	0.069	+0.062	Y, M, Jw.
56	ε Eridani	3.8	K	3 28.2	− 9 48	0.972	4	K2	K1	+6.1	0.363	0.288	+0.317	Y, F, M
57	10 Tauri	4.4	G5	3 31.8	+ 0 5	0.536	4	F8	F9	+3.8	3.02	0.076	+0.074	Y, Jw.
58	Boss 831	5.9	A	3 34.1	− 5 57	0.204	2	K0	K0	+3.2	5.25	0.029	......	......
59	W.B. 3ʰ617	7.2	F8	3 35.3	− 3 32	0.79	3	F6	F7	+4.6	1.45	0.030	−0.073	Y
60	ν Persei	3.9	F5	3 38.4	+42 16	0.009	2	F5	F6	+0.7	52.5	0.023	......	......
61	δ Eridani	3.7	K	3 38.4	−10 6	0.749	3	G9	G9	+2.9	6.92	0.069	+0.147	Y, F, M
62	B.D. +23°535	7.9	......	3 41.4	+23 25	......	3	F5	F5	+3.9	2.75	0.016	+0.007	Y
63	γ Eridani	3.2	K5	3 53.4	−13 48	0.130	2	K6	K0	+1.5	25.1	0.046	......	......
64	Lal. 7443	8.6	G	3 56.5	+35 2	2.19	3	K0	G8	+6.7	0.209	0.042	+0.040	6
65	Boss 933	5.7	Comp.	3 58.4	+23 50	0.022	3	F5p	F7	+1.4	27.5	0.014	+0.014	vM
66	A Tauri	4.5	K0	3 58.8	+21 49	0.113	2	K0	G9	+1.1	36.3	0.021	......	......
67	43 Tauri	5.7	G	4 3.3	+19 21	0.114	2	K1	K0	+1.8	19.1	0.017	+0.024	M
68	o² Eridani	4.5	G2	4 10.7	− 7 49	4.085	4	K1	K0	+6.0	0.398	0.200	+0.182	4
69	γ Tauri	3.9	K0	4 14.1	+15 23	0.120	3	G7	G8	+0.1	91.2	0.017	......	......
70	Boss 1014	6.1	K	4 16.4	+20 35	0.011	3	Ma	G5	+0.5	63.1	0.008	+0.001	vM
71	δ Tauri	3.9	K0	4 17.1	+17 18	0.115	2	G8	G9	+0.8	47.9	0.024	......	......
72	ε Tauri	3.6	K0	4 22.8	+18 58	0.120	4	G9	G9	0.0	100.	0.019	......	......
73	θ¹ Tauri	4.0	K0	4 22.9	+15 44	0.108	3	G9	G8	+0.9	43.7	0.024	......	......
74	A. Oe. 4961	8.5	......	4 29.9	+52 42	0.48	4	K6	K5	+8.6	0.036	0.105	+0.099	S and M
75	α Tauri	1.1	K5	4 30.2	+16 18	0.201	6	K5	K2	+0.9	43.7	0.091	+0.070	5
76	Groom. 864	7.3	G	4 34.5	+41 56	0.73	2	G2	G1	+6.1	0.363	0.058	+0.028	Y, F
77	Boss 1128	5.8	Mb	4 42.7	+63 20	0.111	4	Mb	K0	+2.2	13.2	0.019	......	......
78	Boss 1131	6.8	G5	4 42.8	+18 33	0.440	6	F9	G0	+4.9	1.10	0.042	......	......
79	π³ Orionis	3.3	F8	4 44.4	+ 6 47	0.471	2	F5	F6	+4.4	1.74	0.166	+0.156	M
80	Lal. 9091	7.0	F5	4 45.7	+10 54	0.10	3	F9	F8	+4.6	1.45	0.033	+0.007	F, Mil.
81	Lal. 9109	6.7	F5	4 46.2	+13 29	0.13	3	F7	F6	+3.9	2.75	0.027	+0.007	F
82	ι Aurigae	2.9	K2	4 50.5	+33 0	0.028	2	K3	K0	−0.1	110.	0.025	−0.011	F
83	A. G. Leid. 1812	8.0	......	4 51.3	+34 7	0.76	3	G9	G7	+7.7	0.083	0.087	......	......
84	β Camelop	4.2	G0	4 54.5	+60 18	0.013	2	F7p	F8	−0.9	229.	0.010	......	......

TABLE I—*Continued*

No.	Name	Harv. Visual Mag.	Harv. Spec.	α 1900	δ 1900	μ	No. Pl.	Spectrum		Abs. Visual Mag.	Lum.	π	Trig. π	Auth.
								Est.	Meas.					
85.....	ε Aurigae..............	3.0– 4.5	F5p	$4^h54^m.8$	+43° 41′	0″.014	2	F5p	F7	−0.3	132.	0″.011– 0.022	+0″.060	Jw.
86.....	ζ Aurigae..............	3.9	K0p	4 55.5	+40 56	0.032	2	G8	G1	+1.1	36.3	0.027	−0.028	Ab.
87.....	ε Leporis..............	3.3	K5	5 1.2	−22 30	0.072	2	K4	K1	+1.6	22.9	0.046	....	....
88.....	Boss 1217..............	6.3	G	5 2.3	+ 9 21	0.381	3	G0	G0	+5.0	1.00	0.055	....	....
89.....	α Aurigae..............	0.2	G0	5 9.3	+45 54	0.437	4	G1	G0	+0.3	75.9	0.105	+0.075	F, Y, Jw.
90.....	λ Aurigae..............	4.8	G0	5 12.1	+40 1	0.846	2	G3	G2	+4.8	1.20	0.100	+0.089	5
91.....	Lal. 9960..............	8.5	K	5 14.1	− 3 11	0.73	3	K5	K4	+6.8	0.191	0.046	+0.074	Y
92.....	17 Camelop..............	5.8	Ma	5 20.7	+62 59	0.005	3	Ma	G8	+1.3	30.2	0.013	....	....
93.....	β Leporis..............	3.0	G0	5 24.0	−20 50	0.094	2	G1	G1	+1.1	36.3	0.042	....	....
94.....	Groom. 966..............	6.4	K5	5 26.3	+74 59	0.019	3	Ma	G8	+1.7	20.9	0.012	....	....
95.....	W.B. 5^h592..............	8.9	Ma	5 26.4	− 3 42	2.23	5	Ma	Ma	+9.9	0.011	0.158	+0.176	F, Sc., Jw.
96.....	α Leporis..............	2.7	F0	5 28.3	−17 54	0.003	2	F4p	F5	+0.4	69.2	0.035	+0.014	M
97.....	Groom. 990..............	8.1	K	5 30.4	+51 23	0.56	3	K2	K0	+6.0	0.398	0.038	+0.028	Y
98.....	ϕ^2 Orionis..............	4.4	K	5 31.4	+ 9 14	0.321	3	G7	G6	+1.3	30.2	0.024	+0.024	S and M, Mil.
99.....	γ Leporis Ft..............	6.4	K	5 40.3	−22 27	0.461	1	K5	K3	+7.5	0.100	0.166	+0.145	M
100.....	γ Leporis Br..............	3.8	F8	5 40.3	−22 29	0.468	2	F7	F7	+4.7	1.32	0.151	+0.108	M
101.....	δ Leporis..............	3.9	K0	5 47.0	−20 53	0.696	2	G7	G6	+1.1	36.3	0.027	....	....
102.....	δ Aurigae..............	3.9	K0	5 51.3	+54 17	0.153	3	G7	G8	+0.7	52.5	0.023	+0.025	Ab., M
103.....	η Leporis..............	3.8	F5	5 51.9	−14 11	0.138	2	F3	F3	+2.1	14.5	0.046	....	....
104.....	A.G. Ber. 1866..............	9.0	....	5 57.2	+19 23	0.76	3	F9	G0	+5.2	0.832	0.017	....	....
105.....	1 Gemin..............	4.3	G5	5 58.0	+23 16	0.108	2	G3	G3	+2.9	6.92	0.052	....	....
106.....	Boss 1549..............	6.1	K	6 6.3	+22 56	0.027	4	Ma	G4	+0.7	52.5	0.008	+0.003	vM
107.....	η Gemin..............	3.2– 4.2	Ma	6 8.8	+22 32	0.065	2	Ma	G6	+1.7	20.9	0.032– 0.050	+0.005	R, M
108.....	W.B. 6^h128..............	8.4	G	6 9.5	+44 45	0.413	3	G8	G8	+8.0	0.063	0.083	+0.102	Ram.
109.....	ψ^1 Aurigae..............	5.1	K2	6 17.2	+49 20	0.014	2	K3	G5p	+1.1	36.3	0.016	....	....
110.....	Boss 1627..............	6.0	G	6 22.1	+58 14	0.33	5	G9	G7	+1.6	22.9	0.013	−0.006	Ab.
111.....	23 Hev. Cam..............	5.6	F8	6 29.2	+79 40	0.637	3	F8	F7	+4.6	1.45	0.063	+0.037	Y
112.....	ε Gemin..............	3.2	G5	6 37.8	+25 14	0.020	2	G8	G2	−1.0	251.	0.014	....	....
113.....	ψ^5 Aurigae..............	5.3	G0	6 39.5	+43 41	0.158	2	F8	F8	+4.0	2.51	0.055	+0.078	Jo.
114.....	ξ Gemin..............	3.4	F5	6 39.7	+13 0	0.231	2	F4	F4	+1.0	39.8	0.033	+0.042	M
115.....	Lal. 13284..............	6.9	K	6 47.4	− 5 3	0.57	5	K5	K4	+7.2	0.132	0.115	+0.121	Y
116.....	A.G. Bonn 5621..............	8.3	....	6 49.5	+40 13	0.57	3	K4	K3	+7.1	0.145	0.058	....	....
117.....	θ Can. Maj..............	4.2	K2	6 49.5	−11 55	0.138	2	K4	K1	+1.5	25.1	0.029	+0.017	L and J
118.....	W.B. 6^h1500..............	7.7	G	6 51.4	+ 1 18	0.57	3	G6	G3	+6.0	0.398	0.046	+0.006	Y
119.....	ζ Gemin..............	3.7– 4.3	G0	6 58.2	+20 43	0.009	2	F8p	G0	+0.5	63.1	0.017– 0.023	+0.025	Ab., Mil.
120.....	Lal. 13849..............	6.5	G5	7 4.2	+21 25	0.52	3	K0	G7	+4.0	2.51	0.032	+0.052	Y, Mil.
121.....	Boss 1868..............	5.9	K	7 9.7	+28 4	0.020	3	Ma	K2	+0.8	47.9	0.010	+0.008	vM

122	Lal. 14146	7.3	G	7 11.3	−12 53	0.55	3	F8	F9	+5.9	0.437	0.052	+0.080	Y
123	ι Gemin	3.9	K0	7 19.5	+28 0	0.145	2	G9	G8	+0.8	47.9	0.024	+0.013	M
124	Boss 1971	5.6	G5	7 26.0	+17 18	0.089	3	K1	K1	+0.6	57.5	0.010	0.000	vM
125	Comp. α Gemin	9.0	....	7 28.2	+32 6	....	3	K9p	....	+9.0	0.025	0.100	....	....
126	α Can. Min	0.5	F5	7 34.1	+ 5 29	1.242	6	F3	F4	+3.1	5.75	0.331	+0.309	5
127	Boss 2020	5.8	Ma	7 36.4	+14 27	0.015	3	Mb	G5	+0.4	69.2	0.008	+0.006	vM
128	γ Monoc	4.1	K	7 36.5	− 9 19	0.079	2	G9	G9	+0.7	52.5	0.021	+0.005	M
129	σ Gemin	4.3	K	7 37.1	+29 8	0.247	1	G9	G7	+1.1	36.3	0.023	+0.030	Jo., L and J
130	W.B. 7ʰ1029	6.8	....	7 38.2	+39 49	0.52	3	F6	F7	+4.6	1.45	0.036	....	....
131	β Gemin	1.2	K0	7 39.2	+28 16	0.623	4	G9	G8	+0.8	47.9	0.083	+0.064	Y
132	28 Hev. Cam	6.5	G5	7 39.8	+80 31	0.50	3	K0	G5	+4.2	2.09	0.035	+0.049	Y, Gr.
133	Lal. 15290	8.2	G	7 47.2	+30 55	1.97	3	F7	F8	+5.9	0.437	0.035	+0.045	4
134	Lal. 15394	8.2	....	7 49.1	+19 31	0.50	4	K3	K3	+6.4	0.275	0.044	....	....
135	Boss 2098	6.0	K	7 51.3	+16 3	0.056	3	K3	K2	+1.4	27.5	0.012	....	....
136	Lal. 15547	8.6	F8	7 53.7	+21 8	0.59	3	G9	K0	+5.9	0.437	0.029	+0.089	Y
137	ω Cancri	5.9	K	7 54.9	+25 40	0.014	3	G9	G7	−0.2	120.	0.006	....	....
138	Boss 2148	6.4	K5	8 2.5	+42 43	0.073	4	K4	K2	+1.3	30.20	0.009	−0.030	Ab.
139	3 H. Urs. Maj	5.5	G5	8 2.9	+68 46	0.006	3	G5	G4	+0.2	83.2	0.009	....	....
140	ζ Cancri Br	5.2	G0	8 6.5	+17 57	0.155	2	F8	F9	+3.4	4.37	0.044	+0.031	Mil., F
141	ζ Cancri Ft	6.0	....	8 6.5	+17 57	0.155	2	G0	G0	+4.1	2.29	0.042	+0.035	Mil., F
142	β Cancri	3.8	K2	8 11.1	+ 9 30	0.075	2	K3	K1	+1.1	36.3	0.029	0.000	M
143	W.B. 8ʰ181	8.6	K	8 12.0	+30 56	0.90	3	K6	K6	+7.0	0.158	0.048	+0.014	Y, F
144	Boss 2236	6.3	F5	8 20.6	+45 59	0.362	3	G4	G0	+4.3	1.91	0.040	....	....
145	Groom. 1450	6.0	K0	8 26.4	+38 22	0.204	2	K2	K1	+1.3	30.2	0.011	....	....
146	32 Lyncis	6.1	F	8 26.9	+36 47	0.139	3	F3	F4	+4.5	1.58	0.048	+0.088	Jo.
147	Boss 2275	6.4	G	8 27.1	+24 25	0.091	3	G9	G7	+0.3	75.9	0.006	....	....
148	A.G. Cam. 3181	8.6	....	8 28.2	+54 4	0.93	3	G7	G7	+2.1	14.5	0.005	....	....
149	W.B. 8ʰ596	8.6	....	8 28.8	+42 6	0.76	3	K4	K2	+6.7	0.209	0.042	+0.023	S and M
150	Lal. 16904	8.1	G5	8 33.1	+56 2	0.44	3	G3	G2	+6.4	0.275	0.046	−0.042	Y
151	Lal. 17161	8.4	G	8 38.6	+42 3	0.69	3	K3	K3	+7.2	0.132	0.058	−0.073	Y
152	δ Cancri	4.2	K0	8 39.0	+18 31	0.240	2	K0	G9	+1.0	39.8	0.023	+0.053	M
153	Boss 2338	6.1	G	8 39.2	+31 4	0.020	3	G3	G3	+0.8	47.9	0.008	+0.007	vM
154	ε Hydrae Br	3.5	F8	8 41.5	+ 6 47	0.196	5	F9	G0	+2.5	10.0	0.063	+0.004	Mil.
155	ε Hydrae Ft	7.5	....	8 41.5	+ 6 47	0.196	3	F4	F6	+3.6	3.63	0.016		
156	Fed. 1384¹	9.2	K2	8 46.0	+71 11	1.40	3	K8	K6	+9.7	0.013	0.126	+0.086	F, Gr.
157	Fed. 1384²	9.2	....	8 46.0	+71 11	1.38	1	K7	K5	+9.2	0.021	0.100	+0.086	F, Gr.
158	Boss 2410	6.6	Ma	8 53.5	+18 31	0.089	3	Mc	G8	+1.6	22.9	0.010	....	....
159	10 Urs. Maj	4.1	F	8 54.2	+42 11	0.504	4	F4	F5	+4.4	1.74	0.115	+0.062	F, Y, Mil.
160	81 π¹ Cancri	6.4	G	9 6.8	+15 24	0.576	4	G8	G6	+4.9	1.10	0.050	−0.008	Y
161	Lal. 18115¹	7.9	K5	9 7.6	+53 7	1.69	3	K8	K7	+8.6	0.036	0.138	+0.152	5
162	Lal. 18115²	7.9	....	9 7.6	+53 7	1.69	3	K8	K5	+9.2	0.021	0.182	+0.152	5
163	Lal. 18286	7.3	K5	9 12.0	+29 0	0.52	3	K3	K4	+6.9	0.174	0.083	+0.067	Y, F, Mil.
164	83 Cancri	6.6	F5	9 13.4	+18 8	0.180	2	F6	F7	+4.9	1.10	0.046	....	....
165	Boss 2528	6.3	G5	9 20.0	+17 1	0.079	3	K0	G9	+1.1	36.3	0.009	+0.015	vM
166	Lal. 18672	7.7	....	9 24.7	+ 6 5	0.54	3	K4	K3	+5.9	0.437	0.044	....	....
167	d Urs. Maj	4.6	G0	9 25.6	+70 16	0.090	1	G3	G2	+2.7	8.32	0.042	+0.048	Y
168	θ Urs. Maj	3.3	F8	9 26.2	+52 8	1.092	3	F5	F5	+3.5	3.98	0.110	+0.098	4

TABLE I—*Continued*

No.	Name	Harv. Visual Mag.	Harv. Spec.	α 1900	δ 1900	μ	No. Pl.	Spectrum		Abs. Visual Mag.	Lum.	π	Trig. π	Auth.
								Est.	Meas.					
169.....	11 Leo. Min..........	5.5	K	$9^{h}29^{m}.7$	+36° 16′	0″.745	3	K1	G6	+ 4.4	1.74	0″.060	+0″.179	Y, Jo., Mi
170.....	o Leonis............	3.8	F5p	9 35.8	+10 21	0.150	2	F4p	F5	+ 1.3	30.2	0.032	+0.034	M
171.....	Boss 2603...........	6.4	K	9 35.9	+26 22	0.049	2	K1	G8	+ 0.6	57.5	0.007	+0.012	vM
172.....	W.B. $9^{h}954$..........	9.3	....	9 46.2	−11 49	1.95	1	K8	....	+ 9.7	0.013	0.120	....	....
173.....	Groom. 1596.........	8.2	G5	9 54.9	+56 5	0.49	3	G5	G5	+ 5.6	0.575	0.030	+0.069	Y
174.....	Comp. α Leonis......	7.6	G	10 3.0	+12 27	0.247	3	K2	K0	+ 6.0	0.398	0.048	....	....
175.....	Lal. 19780..........	7.5	G	10 3.3	−19 15	0.38	3	G2	G0	+ 5.3	0.759	0.036	+0.057	F
176.....	Lal. 19821..........	8.5	G5	10 6.3	+24 15	0.42	3	G2	G1	+ 5.0	1.00	0.020	+0.049	Y
177.....	A.Oe. 10640.........	9.2	....	10 7.5	+53 1	0.70	1	K5	K4	+ 8.1	0.057	0.060	+0.074	L and J
178.....	Lal. 19896..........	7.7	G5	10 8.9	+ 3 39	0.47	3	G0	G0	+ 5.4	0.692	0.035	−0.048	Y
179.....	39 Leonis...........	5.8	F5	10 11.7	+23 36	0.44	4	F5	F6	+ 4.6	1.45	0.057	+0.092	Y
180.....	Munich II 5178......	8.8	....	10 15.7	− 0 58	0.70	2	K5	K4	+ 7.8	0.076	0.063	....	....
181.....	Brad. 1433..........	5.9	G	10 16.2	+41 44	0.194	3	F7	F8	+ 3.6	3.63	0.035	+0.090	Jo., Mil.
182.....	μ Urs. Maj..........	3.2	K5	10 16.4	+42 0	0.084	2	K5	G8	+ 1.8	19.1	0.052	+0.051	Y
183.....	Groom. 1646.........	6.5	F8	10 21.9	+49 19	0.898	4	G1	G1	+ 6.1	0.363	0.083	+0.078	K, R, F
184.....	Pi. $10^{h}96$............	7.6	F8	10 27.7	+49 42	0.30	3	F6	F6	+ 5.4	0.692	0.036	+0.045	K
185.....	W.B. $10^{h}520$.........	5.7	F	10 31.6	−11 42	0.734	3	F6	F6	+ 4.4	1.74	0.055	+0.001	Y, F
186.....	38 Leo. Min.........	5.8	K	10 33.4	+38 26	0.227	7	F9	F8	+ 2.8	7.59	0.025	+0.029	Ab.
187.....	B.D. +47°1806.......	(9.0)	....	10 38.1	+46 49	....	2	F8	F8	+ 4.1	2.29	0.010	....	....
188.....	Lal. 20670..........	7.7	G5	10 38.1	+46 44	0.280	7	F9	G0	+ 4.6	1.45	0.024	−0.004	K
189.....	Boss 2881...........	6.3	K	10 43.4	+29 57	0.103	3	K0	G9	+ 1.1	36.3	0.009	+0.036	vM
190.....	Groom. 1697.........	6.1	K	10 46.7	+70 23	0.403	3	K1	K1	+ 2.9	6.92	0.023	−0.011	Y
191.....	46 Leo. Min.........	3.7	K0	10 47.7	+34 45	0.304	4	K1	G9	+ 1.1	36.3	0.030	+0.092	Ab.
192.....	Boss 2910...........	5.9	K	10 50.2	+34 2	0.113	3	K0	G9	+ 0.5	63.1	0.008	+0.014	Ab.
193.....	Lal. 21008..........	8.5	G	10 50.9	+28 17	0.50	3	G5	G5	+ 5.2	0.832	0.022	+0.050	Y
194.....	Boss 2921...........	6.2	Ma	10 54.0	+36 38	0.095	3	Ma	G9	+ 3.6	3.63	0.030	+0.079	vM
195.....	Lal. 21185..........	7.6	Ma	10 57.9	+36 38	4.77	3	Ma	K8	+10.8	0.005	0.437	+0.422	7
196.....	χ Leonis............	4.7	F0	10 59.9	+ 7 53	0.350	2	F4	F5	+ 0.1	91.2	0.012	+0.015	M
197.....	51 Leo. Min.........	7.5	G	10 59.9	+25 45	0.409	3	F5	F6	+ 4.6	1.45	0.026	+0.039	Y
198.....	Lal. 21258..........	8.9	Ma	11 0.5	+44 2	4.47	3	Ma	Ma	+11.2	0.003	0.288	+0.203	5
199.....	ψ Urs. Maj..........	3.2	K0	11 4.0	+45 2	0.069	2	G9	G9	+ 1.6	22.9	0.048	....	....
200.....	Lal. 21368..........	8.9	K5	11 5.6	+31 0	0.58	3	K6	K4	+ 8.2	0.052	0.072	+0.048	Y
201.....	Fed. 1831 Br........	7.7	K5	11 8.7	+74 1	0.45	3	K5	K5	+ 7.0	0.158	0.072	+0.088	Bg., F
202.....	Groom. 1757.........	6.0	K	11 11.1	+50 1	0.092	4	K0	G9	+ 1.6	22.9	0.013	−0.081	Y
203.....	Boss 2983...........	5.4	Mb	11 12.1	+ 2 34	0.159	3	Ma	K2	+ 2.8	7.59	0.030	....	....
204.....	ξ Urs. Maj. Br.......	4.0	G	11 12.9	+32 6	0.732	3	F9	F9	+ 5.0	1.00	0.158	+0.158	Y, Ab., F
205.....	ξ Urs. Maj. Ft.......	4.9	....	11 12.9	+32 6	0.732	2	G1	G1	+ 5.6	0.575	0.138		
206.....	Lal. 21565..........	7.2	K	11 13.2	− 4 31	0.79	5	G8	G5	+ 6.1	0.363	0.060	+0.006	Y
207.....	δ Crateris..........	3.8	K0	11 14.3	−14 14	0.230	2	G8	G7	+ 0.3	75.9	0.020	....	....
208.....	A.Oe. 11677.........	9.2	....	11 14.8	+66 23	3.03	3	Ma	K8	+10.9	0.004	0.219	+0.198	Bg.

209.....	83 Leonis Br.	6.5	K	11 21.7	+ 3 33	0.743	3	G9	G7	+ 4.9	1.10	0.048	+0.023	Y, R
210.....	83 Leonis Ft.	7.6	....	11 21.7	+ 3 33	0.736	3	K4	K5	+ 6.3	0.302	0.055	+0.023	Y, R
211.....	Boss 3025	6.0	K	11 24.5	+15 58	0.066	3	K3	K2	+ 1.5	25.1	0.013	....	....
212.....	Boss 3030	5.7	K	11 25.3	+18 58	0.078	3	K0	G8	+ 0.7	52.5	0.010	+0.024	vM
213.....	Boss 3032	6.2	G	11 26.6	+14 55	0.387	4	F9	F9	+ 4.9	1.10	0.055	....	....
214.....	Groom. 1812	6.3	F	11 33.5	+45 40	0.583	2	F9	F9	+ 3.7	3.31	0.030	+0.038	K
215.....	Boss 3078	5.7	F	11 36.4	+32 18	0.347	3	F2	F3	+ 3.9	2.75	0.044	+0.042	vM
216.....	Groom. 1822	7.9	G	11 40.3	+48 14	0.66	3	F9	F9	+ 4.4	1.74	0.020	+0.024	K
217.....	Boss 3089	4.2	Ma	11 40.7	+ 7 5	0.188	3	Ma	G6	+ 1.9	17.4	0.035	....	....
218.....	93 Leonis	4.5	F8	11 42.8	+20 46	0.155	2	F5p	F7	+ 2.9	6.92	0.048	+0.024	M
219.....	β Virginis	3.8	F8	11 45.5	+ 2 20	0.793	2	F8	F8	+ 3.8	3.02	0.100	+0.116	Y, M
220.....	Groom. 1830	6.5	G5	11 47.2	+38 26	7.037	4	G9	G5	+ 6.0	0.398	0.079	+0.102	6
221.....	Lal. 22585	5.6	G	11 55.6	− 9 53	0.491	5	G9	G7	+ 4.2	2.09	0.052	+0.118	Y
222.....	Pi. $11^{h}218$	6.8	K	11 57.4	+43 39	0.67	3	G9	G6	+ 3.5	3.98	0.022	+0.017	K, F
223.....	Lal. 22701	8.4	G	12 0.2	− 0 57	0.51	3	G9	G6	+ 8.1	0.057	0.087	+0.110	Y
224.....	Boss 3169	6.1	K	12 4.6	+ 2 28	0.190	4	K2	K1	+ 1.8	19.1	0.014	....	....
225.....	W.B. $12^{h}69$	7.3	G	12 7.4	− 2 32	0.73	3	G4	G2	+ 4.4	1.74	0.026	+0.011	Y, F
226.....	Lal. 22954	6.1	F5	12 10.0	− 9 44	1.03	3	F3	F4	+ 4.7	1.32	0.052	+0.026	Y, F
227.....	Boss 3233	6.1	K	12 20.2	+24 29	0.072	3	G9	G9	+ 0.5	63.1	0.008	+0.005	vM
228.....	Lal. 23361	8.5	G	12 24.6	− 2 46	0.69	4	G2	G3	+ 7.0	0.158	0.050	+0.095	Y
229.....	Boss 3274	6.5	K	12 28.0	+10 51	0.063	3	G8	G8	+ 0.3	75.9	0.006	....	....
230.....	β Can. Ven	4.3	G0	12 29.0	+41 54	0.758	3	G0	G0	+ 4.4	1.74	0.105	+0.096	Y, F
231.....	Boss 3294	6.0	Ma	12 33.3	+ 2 24	0.090	3	Mb	G9	+ 2.3	12.0	0.018	....	....
232.....	γ Virginis N	3.7	F0	12 36.6	− 0 54	0.564	3	F0	A8	+ 3.1	5.75	0.076	+0.068	Bel, R, F
233.....	γ Virginis S	3.7	F0	12 36.6	− 0 54	0.564	3	F0	A8	+ 3.2	5.25	0.079	....	....
234.....	Boss 3321	6.0	F	12 40.3	+39 49	0.375	3	F6	F7	+ 4.9	1.10	0.060	....	....
235.....	33 Virginis	5.9	K	12 41.3	+10 6	0.531	3	K2	G9	+ 3.3	4.79	0.030	+0.002	Y, Mil.
236.....	Lal. 23917	8.3	F8	12 44.6	+ 1 45	0.68	3	G7	G4	+ 6.5	0.251	0.044	+0.029	Y, Sc.
237.....	δ Virginis	3.7	Ma	12 50.6	+ 3 56	0.479	3	Mb	G7	+ 1.3	30.2	0.033	−0.030	Y
238.....	Lal. 24168	7.7	G	12 53.9	− 9 18	0.82	3	K1	G9	+ 7.0	0.158	0.072	−0.015	Y
239.....	ε Virginis	3.0	K0	12 57.2	+11 30	0.273	2	G6	G6	+ 0.4	69.2	0.030	+0.034	F
240.....	Boss 3398	5.9	Mbp	13 1.5	+23 9	0.066	4	Mc	G9	+ 1.8	19.1	0.015	+0.043	vM
241.....	Lal. 24414	6.9	G	13 3.8	+ 5 46	0.72	3	G4	G2	+ 3.4	4.37	0.020	+0.008	Y
242.....	Lal. 24504	8.5	G	13 6.4	+10 9	0.54	3	F8	G2	+ 4.4	1.74	0.015	+0.028	Y
243.....	β Comae	4.3	G0	13 7.2	+28 23	1.184	3	G1	G0	+ 4.6	1.45	0.115	+0.116	P, F, Y
244.....	A.G. Ber. 4855	7.8	....	13 7.5	+18 3	0.60	3	F6	F8	+ 5.3	0.759	0.032	....	....
245.....	Lal. 24652	7.0	....	13 11.9	+17 35	0.70	3	K3	K1	+ 6.7	0.209	0.087	....	....
246.....	W.B. $13^{h}216$	8.8	G5	13 15.7	+ 4 39	0.58	5	K4	K3	+ 6.0	0.398	0.028	−0.021	Y
247.....	Lal. 24774	8.3	K	13 16.1	+43 38	0.45	3	K0	K0	+ 5.7	0.525	0.030	+0.179	Y
248.....	70 Virginis	5.2	G5	13 23.5	+14 19	0.634	2	G4	G4	+ 3.1	5.75	0.038	+0.149	Y
249.....	Lal. 25012	7.5	G	13 26.6	− 1 49	0.91	3	G9	G7	+ 7.5	0.100	0.100	+0.053	Y
250.....	Boss 3500	6.2	K	13 26.9	+42 37	0.094	3	K0	K0	+ 1.6	22.9	0.012	....	....
251.....	Boss 3534	5.2	Ma	13 36.4	− 8 12	0.108	3	Ma	G9	+ 1.0	39.8	0.014	....	....
252.....	A.G. Ber. A. 4999	9.6	....	13 40.2	+18 21	1.92	1	K9	Ma	+10.2	0.008	0.132	+0.094	Sc., R
253.....	Lal. 25372	8.7	K	13 40.7	+15 26	2.32	3	Ma	Ma	+10.4	0.007	0.219	+0.176	4
254.....	Boss 3554	6.3	F5	13 42.0	+ 6 51	0.499	4	F9	G0	+ 4.7	1.32	0.048	....	....
255.....	τ Boötis	4.5	F5	13 42.5	+17 57	0.487	2	F6	F6	+ 3.1	5.75	0.052	+0.040	Y

TABLE I—*Continued*

No.	Name	Harv. Visual Mag.	Harv. Spec.	α 1900	δ 1900	μ	No. Pl.	Spectrum		Abs. Visual Mag.	Lum.	π	Trig. π	Auth.
								Est.	Meas.					
256	Boss 3605	6.0	K	$13^{h}53^{m}.8$	+15° 8′	0″.087	3	K4	K2	+ 1.1	36.3	0″.010	....	....
257	*d* Boötis	4.8	F5	14 5.8	+25 34	0.076	2	F7	F8	+ 2.6	9.12	0.036	....	....
258	κ Virginis	4.3	K0	14 7.6	− 9 48	0.130	2	K2	G9	+ 1.6	22.9	0.029	....	....
259	Boss 3647	6.3	F5	14 9.1	− 5 29	0.317	3	F8	F8	+ 4.1	2.29	0.036	....	....
260	Boss 3650	5.5	F	14 9.3	+13 26	0.267	3	F7	F7	+ 4.1	2.29	0.052	+0″.097	vM
261	α Boötis	0.2	K0	14 11.1	+19 42	2.282	6	K0	G9	+ 0.9	43.7	0.138	+0.075	F, Y
262	Lal. 26294	8.3	....	14 17.7	+30 6	0.56	3	K5	K4	+ 8.7	0.033	0.120	....	....
263	Ber. B. 5072	9.5	....	14 21.1	+24 6	1.38	1	K8	K6	+ 9.0	0.025	0.079	+0.072	R, L and J
264	θ Boötis	4.1	F8	14 21.8	+52 19	0.471	2	F6	F6	+ 3.4	4.37	0.072	....	....
265	ρ Boötis	3.8	K0	14 27.5	+30 49	0.149	2	K3	K1	+ 0.9	43.7	0.026	....	....
266	σ Boötis	4.5	F0	14 30.3	+30 11	0.228	2	F0	F2	+ 3.5	3.98	0.063	....	....
267	Lal. 26630	6.2	G	14 31.7	−11 53	0.946	3	F5	F5	+ 4.3	1.91	0.042	+0.049	Y
268	Boss 3736	6.0	K	14 33.6	+18 44	0.096	3	K0	K0	+ 1.1	36.3	0.011	+0.057	vM
269	μ Virginis	4.0	F5	14 37.8	− 5 13	0.339	2	F1	F2	+ 2.9	6.92	0.060	....	....
270	ε Boötis Br	2.7	K0p	14 40.6	+27 30	0.049	3	G8	G8	− 0.7	191.	0.021	+0.050	F
271	Lal. 27026	7.7	G5	14 46.0	−23 53	1.02	3	K5	K4	+ 6.6	0.229	0.060	+0.041	F
272	ξ Boötis Br	4.7	G5	14 46.8	+19 31	0.168	3	G6	G6	+ 5.5	0.631	0.145	+0.230	M
273	ξ Boötis Ft	6.6	....	14 46.8	+19 31	0.168	2	K3	K3	+ 7.6	0.091	0.158		
274	Lal. 27137	6.3	....	14 48.8	+19 33	0.53	3	G9	K0	+ 5.8	0.479	0.079	....	....
275	β Urs. Min	2.2	K5	14 51.0	+74 34	0.030	2	K4	K1	+ 0.6	57.5	0.048	+0.014	F
276	Boss 3810	5.6	K	14 51.3	−11 0	0.002	5	K3	K0	+ 2.2	13.2	0.021	....	....
277	Pi. $14^{h}212$ Br	5.8	K	14 51.6	−20 58	2.039	3	K5	K6	+ 6.8	0.191	0.158	+0.174	Sitter, F, M
278	Pi. $14^{h}212$ Ft	8.7	....	14 51.6	−20 58	2.07	1	Ma	....	+10.1	0.009	0.190	+0.212	M
279	Boss 3816	5.7	G5	14 52.4	+ 0 14	0.069	3	K1	K1	+ 1.4	27.5	0.014	+0.044	vM
280	β Boötis	3.6	G5	14 58.2	+40 47	0.063	2	G5	G4	+ 0.4	69.2	0.023	....	....
281	Lal. 27558	8.7	....	15 3.0	+ 9 16	0.54	3	F6	F7	+ 4.7	1.32	0.016	....	....
282	A.Oe. 14318	9.6	K5	15 4.7	−15 59	3.76	1	K0	G8	+ 6.2	0.331	0.021	+0.035	R, L and J
283	A.Oe. 14320	9.2	G	15 4.7	−15 54	3.75	2	G8	G5	+ 6.0	0.398	0.023	+0.054	R, L and J
284	Boss 3867	6.0	Mb	15 7.5	+19 21	0.004	3	Mb	G6	+ 0.4	69.2	0.008	+0.005	vM
285	Lal. 27742	6.8	G	15 8.2	+19 39	0.68	3	G6	G3	+ 3.9	2.75	0.026	+0.018	R, Y
286	Lal. 27743	7.6		15 8.2	+19 40	0.62	4	G9	G5	+ 4.9	1.10	0.029	−0.071	R
287	3 Serpentis	5.2	K0	15 10.2	+ 5 19	0.023	2	G9	G6	+ 0.2	83.2	0.009	....	....
288	δ Boötis	3.5	K0	15 11.4	+33 41	0.155	2	G5	G4	+ 0.2	83.2	0.022	....	....
289	5 Serpentis	5.2	G	15 14.2	+ 2 9	0.644	2	F7	F7	+ 4.2	2.09	0.063	+0.094	Y
290	Lal. 27958	8.0	G	15 14.8	+26 4	0.51	3	G8	G6	+ 4.3	1.91	0.018	+0.031	Y
291	Boss 3900	6.2	G	15 15.2	−17 48	0.069	4	G9	G6	+ 0.6	57.5	0.008	....	....
292	6 Serpentis	5.5	K	15 15.9	+ 1 5	0.125	3	K5	K2	+ 2.5	10.0	0.025	+0.133	F
293	W.B.$15^{h}268$	8.7	K5	15 17.7	+ 1 47	0.52	3	K4	K4	+ 6.3	0.302	0.033	+0.118	Y
294	η Coronae	5.6	G	15 19.1	+30 39	0.237	3	G0	G0	+ 4.8	1.20	0.069	+0.078	S
295	μ^1 Boötis	4.5	F0	15 20.7	+37 44	0.169	3	F0	....	+ 3.1	5.75	0.052	+0.039	Mil.

296.....	μ^2 Boötis............	6.7	K	15 20.7	+37 44	0.169	3	G0	G0	+ 5.3	0.759	0.052	+0.055	F, Mil.
297.....	τ^1 Serpentis..........	5.5	Ma	15 21.2	+15 47	0.033	2	K6	K1	+ 1.1	36.3	0.013	....	....
298.....	β Cor. Bor...........	3.7	Fp	15 23.7	+29 27	0.190	3	F2p	F2	+ 1.2	33.1	0.032	....	....
299.....	Lal. 28358...........	6.9	F8	15 26.6	+57 47	0.29	3	F5	F5	+ 4.2	2.09	0.029	+0.029	F
300.....	Boss 3952...........	4.8	K	15 28.7	− 9 43	0.389	3	K2	G9	+ 1.5	25.1	0.022	....	....
301.....	γ Librae............	4.0	K0	15 29.9	−14 27	0.065	2	G9	G8	+ 0.4	69.2	0.019	....	....
302.....	Boss 3963...........	6.1	K	15 31.0	+17 59	0.081	5	G7	G6	+ 0.8	47.9	0.009	....	....
303.....	α Serpentis..........	2.8	K0	15 39.3	+ 6 44	0.130	3	K1	K1	+ 0.2	83.2	0.030	+0.151	F
304.....	κ Serpentis..........	4.3	K5	15 44.2	+18 27	0.110	2	K7	K0	+ 0.9	43.7	0.021	....	....
305.....	39 Serpentis.........	6.2	G	15 48.5	+13 31	0.586	4	G1	G1	+ 5.5	0.631	0.072	+0.040	Y
306.....	Boss 4048...........	5.8	K5	15 50.2	+20 36	0.083	3	K4	G8	+ 0.9	43.7	0.011	+0.040	vM
307.....	γ Serpentis..........	3.9	F8	15 51.8	+15 59	0.133	2	F4	F5	+ 3.9	2.75	0.100	+0.066	4
308.....	W.B. 15^h1323........	8.0	....	15 54.5	+28 1	0.85	3	G8	G9	+ 6.4	0.275	0.048	....	....
309.....	Lal. 29085...........	5.5	F	15 54.7	−16 14	0.75	6	F5	F5	+ 4.2	2.09	0.055	....	....
310.....	ρ Cor. Bor...........	5.4	F	15 57.2	+33 36	0.81	3	F8	F9	+ 3.9	2.75	0.050	+0.031	Y
311.....	Lal. 29307...........	7.5	....	15 59.9	+25 31	0.87	3	K0	G8	+ 5.4	0.692	0.038	+0.058	S
312.....	θ Draconis...........	4.1	F8	16 0.0	+58 50	0.459	2	F7	F8	+ 3.6	3.63	0.079	+0.066	Kostinsky
313.....	Lal. 29330...........	8.5	....	16 1.2	+10 57	0.50	7	K0	G9	+ 7.4	0.110	0.060	....	....
314.....	Lal. 29381...........	6.8	G5	16 1.5	+39 26	0.55	3	G8	G6	+ 6.7	0.209	0.096	+0.069	Y
315.....	Boss 4096...........	5.6	Ma	16 2.0	−26 4	0.122	3	Ma	G8	+ 2.0	15.8	0.019	....	....
316.....	Lal. 29439...........	9.2	G5	16 2.9	+38 55	0.60	3	K4	K2	+ 7.1	0.145	0.038	+0.014	Y, K
317.....	κ Herculis...........	5.3	G5	16 3.6	+17 19	0.046	2	G6	G4	+ 0.1	91.2	0.009	−0.004	L and J
318.....	τ Cor. Bor...........	4.9	K	16 5.3	+36 45	0.325	4	K0	K0	+ 2.0	15.8	0.026	+0.102	F
319.....	Boss 4130...........	5.6	G5	16 8.3	+ 5 17	0.046	3	K4	K2	+ 1.1	36.3	0.012	+0.008	vM
320.....	δ Ophiuchi..........	3.0	Ma	16 9.1	− 3 26	0.161	3	Ma	G8	+ 2.2	13.2	0.069	....	....
321.....	Lal. 29617...........	5.6	F	16 10.2	− 8 6	0.563	5	F9	G1	+ 4.4	1.74	0.058	+0.039	Y
322.....	σ Coronae Ft........	6.8	....	16 10.9	+34 7	0.302	4	F9	F9	+ 5.1	0.912	0.046	+0.031	F
323.....	σ Coronae Br........	5.8	G0	16 10.9	+34 7		4	F8p	G1	+ 4.4	1.74	0.052		
324.....	Lal. 29917...........	8.6	K2	16 16.5	+67 29	0.50	3	K7	K5	+ 8.0	0.063	0.076	+0.151	Y
325.....	ν^1 Cor. Bor...........	5.4	Ma	16 18.6	+34 2	0.049	2	Ma	G9	+ 0.9	43.7	0.013	....	....
326.....	ν^2 Cor. Bor...........	5.3	K5	16 18.7	+33 56	0.055	2	K6	K2	+ 1.6	22.9	0.018	....	....
327.....	η Draconis...........	2.9	G5	16 22.6	+61 44	0.062	3	G6	G5	+ 0.9	43.7	0.040	+0.019	F, M
328.....	α Scorpii............	1.2	Map	16 23.3	−26 13	0.034	2	Ma	G2	− 3.0	1584.	0.014	+0.030	Finlay
329.....	Lal. 30024...........	7.0	G5	16 24.5	+18 37	0.53	3	K2	K2	+ 7.2	0.132	0.110	+0.088	Y
330.....	Lal. 30044...........	7.3	G	16 25.6	+ 4 26	1.46	3	F6	F6	+ 5.5	0.631	0.044	+0.011	F, Y
331.....	β Herculis...........	2.8	K0	16 25.9	+21 42	0.107	2	G6	G7	− 0.1	110.	0.026	+0.020	F
332.....	Boss 4222...........	5.9	F	16 31.1	− 2 7	0.546	3	G9	G9	+ 5.4	0.692	0.079	....	....
333.....	Lal. 30271...........	7.2	G	16 32.6	+31 9	0.49	3	F6	F6	+ 5.2	0.832	0.040	+0.012	Y
334.....	Gro. 19 Area VII 308.	8.6	....	16 34.1	+51 45	0.115	3	G2	G2	+ 4.5	1.58	0.015	+0.017	K
335.....	ζ Herculis...........	3.0	G0	16 37.5	+31 47	0.608	3	G1	G1	+ 2.1	14.5	0.066	+0.118	4
336.....	Boss 4262...........	5.8	Ma	16 40.8	+15 56	0.054	3	Mb	G9	+ 1.8	19.1	0.016	+0.022	vM
337.....	W.B. 16^h906.........	8.8	K	16 50.1	− 8 9	1.27	4	Md	....	+10.0	0.010	0.174	+0.150	Y, L and J
338.....	Boss 4303...........	6.5	G	16 50.2	−16 39	0.089	3	K0	K0	+ 3.0	6.31	0.020	....	....
339.....	Boss 4307...........	5.5	F	16 50.6	+21 7	0.059	3	G7	G6	+ 0.9	43.7	0.012	+0.001	vM
340.....	Boss 4326...........	6.4	K	16 56.0	−18 44	0.052	3	G9	G8	+ 0.9	43.7	0.008	....	....
341.....	Boss 4371...........	5.2	K	17 9.2	−26 27	1.224	3	K2	K1	+ 6.3	0.302	0.166	+0.152	F
342.....	α Herculis...........	{3.1– 3.9}	Mb	17 10.1	+14 30	0.030	2	Mc	G5	− 0.7	191.	{0.012– 0.017}	....	....

TABLE I—*Continued*

No.	Name	Harv. Visual Mag.	Harv. Spec.	α 1900	δ 1900	μ	No. Pl.	Spectrum		Abs. Visual Mag.	Lum.	π	Trig. π	Auth.
								Est.	Meas.					
343	Boss 4393	5.8	K	$17^h14^m.9$	+28° 56′	0″.045	4	G8	G8	+ 0.6	57.5	0″.009	+0″.015	vM
344	72 Herculis	5.4	G	17 16.9	+32 36	1.06	4	F8	G1	+ 5.8	0.479	0.120	+0.123	F, Y
345	Lal. 32047	6.3	K	17 25.3	+67 23	0.52	3	G9	G8	+ 5.9	0.437	0.083	+0.062	Y, Gr
346	B.D. +1°3450	7.2	K2	17 26.5	+ 1 45	....	3	K3	K4	+ 1.8	19.1	0.008	+0.039	Y
347	λ Herculis	4.5	K0	17 26.7	+26 11	0.021	3	K2	K1	+ 0.5	63.1	0.016	....	....
348	W.B. 17^h514	8.6	G	17 29.9	+ 6 4	0.58	4	F5	F6	+ 4.4	1.74	0.014	−0.004	Y
349	Anon	9.1	....	17 33.5	+18 37	1.29	1	K8	K6	+10.0	0.010	0.151	+0.128	S and M, L and J
350	26 Draconis	5.3	F	17 34.0	+61 57	0.563	2	G0	G0	+ 4.7	1.32	0.076	+0.087	Y, Mil.
351	B.D. +18°3424	9.2	....	17 34.3	+18 37	0.09	1	K1	K0	+ 6.5	0.251	0.029	+0.008	S and M
352	Lal. 32322	8.4	....	17 36.3	+37 16	0.88	3	F7	F9	+ 5.0	1.00	0.021	....	....
353	A.Oe. 17415	9.1	K	17 37.0	+68 26	1.30	5	Mb	Mb	+10.6	0.006	0.200	+0.254	4
354	Boss 4480	6.5	F8	17 37.0	+24 34	0.052	3	K1	K1	+ 0.6	57.5	0.007	+0.020	vM
355	Lal. 32390	7.5	....	17 39.0	+21 40	0.61	3	G8	G6	+ 5.9	0.437	0.048	....	....
356	μ Herculis	3.5	G5	17 42.5	+27 47	0.817	3	G5	G4	+ 3.2	5.25	0.087	+0.095	4
357	Comp. μ Herculis	9.7	....	17 42.5	+27 47	0.817	1	Mb	....	+ 9.6	0.014	0.096	+0.056	R
358	Barnard's P.M. Star	9.7	....	17 52.9	+ 4 25	10.3	3	Mb	....	+13.3	0.0005	0.50	+0.50	Sc. (Allegheny)
359	γ Draconis	2.4	K5	17 54.3	+51 30	0.027	3	K5	K1	+ 1.4	27.5	0.063	+0.015	4
360	Boss 4555	5.9	K	17 57.1	+45 30	0.044	3	K6	K3	+ 1.5	25.1	0.013	+0.026	vM
361	B.D. +26°3151	7.3	....	17 58.4	+26 20	0.66	3	K0	K0	+ 6.1	0.363	0.058	....	....
362	70 Ophiuchi Br	4.1	K0	18 0.4	+ 2 31	1.131	3	K0	G9	+ 5.6	0.575	0.200	+0.187	6
363	70 Ophiuchi Ft	6.0	....	18 0.4	+ 2 31	1.131	3	K5	K7	+ 7.6	0.091	0.209	+0.170	M
364	99 Herculis Br	5.2	F8	18 3.2	+30 33	0.113	3	F4	F6	+ 5.3	0.759	0.105	+0.074	F
365	Lal. 33439	6.7	G5	18 6.3	+38 27	0.62	3	K2	K2	+ 6.4	0.275	0.087	+0.045	Y
366	Boss 4629	5.5	K	18 15.1	+24 24	0.016	3	K2	K0	+ 0.4	69.2	0.010	+0.002	vM
367	η Serpentis	3.4	K0	18 16.1	− 2 55	0.898	3	G8	G7	+ 1.8	19.1	0.048	+0.057	Y, Jw.
368	Boss 4647	6.2	K	18 17.6	+51 18	0.062	3	K1	K0	+ 0.5	63.1	0.008	+0.036	vM
369	109 Herculis	3.9	K0	18 19.4	+21 43	0.324	2	K2	K1	+ 1.0	39.8	0.026	+0.029	Jo.
370	Gro. 19, Area II 66	7.7	G5	18 21.4	+ 8 44	0.498	3	G5	G4	+ 6.3	0.302	0.052	+0.037	K
371	Gro. 19, Area II 75	8.1	G5	18 21.6	+ 8 34	0.498	3	G8	G8	+ 4.3	1.91	0.018	....	....
372	λ Sagittarii	2.9	K0	18 21.8	−25 29	0.197	2	K0	G9	+ 2.3	12.0	0.076	+0.069	F
373	Gro. 19, Area II 90	8.6	G5	18 22.0	+ 8 3	0.157	3	G1	G0	+ 5.3	0.759	0.022	+0.015	K
374	χ Draconis	3.7	F8	18 22.9	+72 41	0.638	4	F5	F6	+ 5.0	1.00	0.182	+0.105	Y, Gr., M
375	1 Aquilae	4.1	K0	18 29.8	− 8 19	0.318	2	K4	K2	+ 1.1	36.3	0.025	....	....
376	A.G. Leid. 6797	8.7	....	18 37.1	+31 28	0.82	3	K3	K2	+ 7.3	0.120	0.052	....	....
377	110 Herculis	4.3	F5	18 41.4	+20 27	0.345	3	F4	F4	+ 3.5	3.98	0.069	+0.080	M, Jo.
378	Pos. Med. 2164^1	8.9	K	18 41.7	+59 29	2.28	2	Mb	Mb	+10.7	0.005	0.229	+0.290	R, Sc.
379	o Draconis	4.8	K0	18 49.7	+59 16	0.086	3	G8	G4	− 0.2	120.	0.010	....	....
380	R Lyrae	4.0– 4.7	Mb	18 52.3	+43 49	0.077	3	Mc	G8	+ 0.8	47.9	0.016– 0.023	+0.028	Ab.
381	Munich 18180	9.4	Ma	18 53.1	+ 5 48	1.24	3	K7	K6	+ 9.2	0.021	0.091	+0.069	R, Sc.

382	Brad. 2388	5.2	G	18 53.3	+32 46	0.23	3	F7	F9	+ 4.7	1.32	0.079	+0.116	F, Jw., Mil.
383	Boss 4860	5.8	K	19 1.2	+31 36	0.085	3	K5	K1	+ 1.4	27.5	0.013	+0.026	vM
384	Munich 18816	9.3	K	19 2.2	+ 7 29	0.80	3	K5	K3	+ 8.0	0.063	0.055	+0.040	Sc.
385	Boss 4892	6.8	K	19 9.5	+49 40	0.63	4	G4	G3	+ 5.5	0.631	0.055	+0.038	R, M, vM
386	Boss 4893	6.6	K	19 9.5	+49 40	0.654	4	G6	G2	+ 5.5	0.631	0.060	+0.052	R, M, vM
387	δ Draconis	3.2	K0	19 12.5	+67 29	0.133	2	G9	G7	+ 0.5	63.1	0.029	....	....
388	θ Lyrae	4.5	K	19 12.9	+37 57	0.012	5	G9	G7	− 0.8	209.	0.009	....	....
389	Boss 4915	6.3	A	19 13.3	−15 43	0.285	4	K2	G9	+ 1.7	20.9	0.011	....	....
390	Boss 4920	6.0	F	19 14.0	+46 49	0.285	3	F4	F5	+ 3.2	5.25	0.027	....	....
391	κ Cygni	4.0	K0	19 14.8	+53 11	0.133	3	G7	G7	+ 0.9	43.7	0.024	+0.062	Ab.
392	3 Cygni	6.2	K	19 21.3	+24 44	0.658	2	F6	F4	+ 4.1	2.29	0.038	+0.060	Y, Jo., F
393	Boss 4976	4.6	Ma	19 24.5	+24 28	0.170	4	Ma	K1	+ 1.6	22.9	0.025	....	....
394	Groom. 2875	6.7	G5	19 29.5	+58 23	0.66	3	K3	K2	+ 6.1	0.363	0.076	−0.055	Y
395	Lal. 37120	6.6	G	19 29.7	+32 59	0.52	4	F9	F9	+ 4.6	1.45	0.040	+0.058	Y
396	σ Draconis	4.8	K	19 32.6	+69 29	1.840	3	G8	G7	+ 5.4	0.692	0.132	+0.198	4
397	θ Cygni	4.6	F5	19 33.8	+49 59	0.249	3	F3	F4	+ 3.7	3.31	0.066	+0.073	Y, F, M, Ab.
398	54 Sagittarii	5.4	K0	19 35.0	−16 31	0.085	2	K1	K0	+ 0.8	47.9	0.012	....	....
399	Boss 5037	6.3	F	19 39.2	+50 18	0.217	3	G1	G1	+ 5.3	0.759	0.063	+0.048	S and M
400	Boss 5038	6.4	F5	19 39.2	+50 17	0.220	4	G4	G3	+ 4.4	1.74	0.040	+0.033	S and M
401	Boss 5043	6.0	K	19 40.4	+41 32	0.017	3	K6	K1	+ 0.9	43.7	0.009	+0.006	vM
402	Boss 5044	5.1	K	19 40.5	−20 0	0.165	3	K0	G9	+ 0.1	91.2	0.010	....	....
403	γ Aquilae	2.8	K2	19 41.5	+10 22	0.014	2	K3	G9	+ 0.3	75.9	0.032	−0.009	F
404	δ Sagittae	3.8	Map	19 42.9	+18 17	0.009	3	Ma	G1	+ 1.8	19.1	0.040	....	....
405	η Aquilae	{3.7– 4.4}	G0	19 47.4	+ 0 45	0.012	3	(F9)	(G0)	+ 0.5	63.1	{0.016– 0.023}	+0.006	M
406	β Aquilae	3.9	K0	19 50.4	+ 6 9	0.484	4	G8	G7	+ 3.2	5.25	0.072	+0.071	M
407	Lal. 38100	6.3	F8	19 54.4	−10 13	0.488	3	F9	F8	+ 4.6	1.45	0.046	−0.004	Y
408	Lal. 38139	7.3	....	19 55.5	−12 31	0.50	3	F4	F5	+ 4.9	1.10	0.033	....	....
409	Lal. 38287	7.2	G	19 58.0	+15 20	0.60	3	G8	G5	+ 6.6	0.229	0.076	+0.088	Y
410	Lal. 38380	5.7	G5	19 59.5	+29 38	0.86	3	G9	G7	+ 4.0	2.51	0.046	+0.050	Y, F
411	Boss 5146	5.9	G	19 59.6	+16 48	0.557	3	F9	G0	+ 5.2	0.832	0.072	+0.104	Y, Jo.
412	Lal. 38383	7.2	G	19 59.7	+23 5	1.39	3	K2	K0	+ 7.6	0.091	0.120	+0.099	Jw., Y, F
413	Boss 5157	5.5	K	20 2.6	+35 42	0.496	3	G9	G6	+ 3.0	6.31	0.032	....	....
414	Groom. 3042	5.7	A	20 3.6	+52 52	0.334	4	F4	F4	+ 4.5	1.58	0.057	+0.066	Y, Ab.
415	Lal. 38683	7.3	G5	20 6.6	+15 53	0.55	3	K1	K1	+ 6.7	0.209	0.076	+0.077	Y
416	Lal. 38711	5.7	G2	20 9.0	−27 20	1.256	3	K3	K2	+ 4.9	1.10	0.069	....	....
417	Boss 5184	5.7	F	20 9.9	+61 47	0.155	3	F6	F4	+ 2.5	10.0	0.023	+0.037	vM
418	o² Cygni	4.0	K0p	20 10.5	+46 26	0.002	3	G9p	G1	+ 1.2	33.1	0.028	+0.003	M
419	24 Vulpeculae	5.4	K0	20 12.5	+24 22	0.027	3	G7	G5	+ 0.7	52.5	0.012	....	....
420	A.G. Cam. 6486	7.4	....	20 15.9	+55 5	0.81	4	F3	F4	+ 3.7	3.31	0.018	....	....
421	Groom. 3150	6.1	G	20 16.5	+66 32	0.557	3	F7	G0	+ 6.1	0.363	0.100	+0.120	Y, Jw.
422	A.Oe. 20452	8.1	F8	20 17.7	−21 40	1.22	4	F6	F7	+ 4.8	1.20	0.022	....	....
423	γ Cygni	2.3	F8p	20 18.6	+39 56	0.003	3	F9p	G0	+ 1.3	30.2	0.063	+0.072	F, Y
424	Boss 5263	5.8	G	20 26.9	−10 12	0.317	6	G4	G2	+ 4.3	1.91	0.050	+0.035	F
425	Lal. 39704	7.0	G5	20 29.3	+41 33	0.50	3	K0	G7	+ 6.4	0.275	0.076	+0.007	Y, Jo.
426	β Delphini	3.7	F5	20 32.9	+14 15	0.113	3	F3	F3	+ 1.6	22.9	0.038	+0.017	F, M, Mil.
427	Lal. 39866	8.4	K	20 34.6	+ 4 37	0.85	6	K5	K3	+ 8.0	0.063	0.083	+0.068	Y, Sc.

TABLE I—*Continued*

No.	Name	Harv. Visual Mag.	Harv. Spec.	α 1900	δ 1900	μ	No. Pl.	Spectrum		Abs. Visual Mag.	Lum.	π	Trig. π	Auth.
								Est.	Meas.					
428	Groom. 3263	6.0	F	$20^{\mathrm{h}}38^{\mathrm{m}}2$	+60° 9′	0″186	3	F5	F6	+ 4.4	1.74	0″048	+0″049	Y, Ab.
429	γ Delphini Br.	4.5	G5	20 42.0	+15 46	0.207	3	K1	K1	+ 1.2	33.1	0.022	+0.076	M
430	ϵ Cygni	2.6	K0	20 42.2	+33 36	0.483	2	G8	G7	+ 0.8	47.9	0.044	+0.016	4
431	η Cephei	3.6	K0	20 43.3	+61 27	0.826	3	G9	G8	+ 2.4	11.0	0.058	+0.116	Y, Ab., S and M
432	Fed. 3638	7.8	G5	20 52.4	+74 23	0.70	3	G6	G4	+ 5.2	0.832	0.030	−0.020	Y, F
433	ϵ Equulei	5.3	F5	20 54.1	+ 3 55	0.191	4	F2	F3	+ 3.2	5.25	0.038	+0.048	M
434	Groom. 3357	6.6	G	20 56.1	+39 51	0.33	3	F7	F8	+ 4.6	1.45	0.040	+0.077	Jo.
435	W.B. $20^{\mathrm{h}}1454$	8.0	F8	20 59.1	+ 2 36	0.55	3	F6	F6	+ 5.0	1.00	0.025	−0.066	Y
436	Lal. 40844	8.8	K	21 0.4	+ 6 41	0.57	4	K6	K4	+ 8.7	0.033	0.096	+0.167	Y
437	61^{1} Cygni	5.6	K5	21 2.4	+38 15	5.271	6	K7	K7	+ 7.9	0.069	0.288	+0.313	16
438	61^{2} Cygni	6.3	K5	21 2.4	+38 15	5.157	6	K8	K7	+ 8.7	0.033	0.302	+0.309	16
439	B.D. +38°4362	7.9	K2	21 5.2	+38 19	....	3	K2	G9	+ 1.2	33.1	0.005	−0.031	R
440	W.B. $21^{\mathrm{h}}97$	7.3	F8	21 7.4	+17 21	0.91	3	F3	F2	+ 5.8	0.479	0.050	+0.018	Y, F, Jw.
441	ζ Cygni	3.4	K0	21 8.7	+29 49	0.059	3	G6	G7	− 0.4	145.	0.017	+0.048	M
442	δ Equulei	5.0	F5	21 9.6	+ 9 36	0.306	4	F4	F5	+ 4.0	2.51	0.063	+0.067	F, Hus.
443	τ Cygni	3.8	F0	21 10.8	+37 37	0.455	3	F1	F1	+ 1.9	17.4	0.042	+0.031	4
444	Lal. 41363	6.5	G	21 14.0	−26 46	0.67	2	G9	G5	+ 5.1	0.912	0.052	....	....
445	Boss 5519	5.7	F	21 23.9	+31 47	0.134	3	F0	F1	+ 3.7	3.31	0.040	+0.032	vM
446	W.B. $21^{\mathrm{h}}502$	9.1	....	21 24.5	−12 56	1.06	2	K5	K6	+ 8.6	0.036	0.079	....	....
447	g Cygni	5.3	K0	21 25.8	+46 6	0.114	3	G9	G8	+ 1.0	39.8	0.014	+0.042	Ab., Mil.
448	ρ Cygni	4.2	K	21 30.2	+45 9	0.095	2	G6	G4	+ 2.1	14.5	0.038	+0.042	Y, Ab.
449	Boss 5559	6.8	F5	21 34.4	− 0 30	0.236	4	F6	F6	+ 5.2	0.832	0.048	+0.017	F, Jw.
450	ϵ Pegasi	2.5	K0	21 39.3	+ 9 25	0.025	3	K0	G4	− 0.3	132.	0.028	+0.041	F
451	A.G. Ber. 8366	8.8	....	21 39.7	+24 53	0.68	3	K1	G7	+ 6.3	0.302	0.032	....	....
452	κ Pegasi	4.3	F5	21 40.1	+25 11	0.033	3	F2	F3	+ 3.4	4.37	0.066	+0.040	5
453	Boss 5602	6.5	K	21 41.8	+25 6	0.148	4	K3	K2	+ 1.5	25.1	0.010	....	....
454	Lal. 42883	6.8	F5	21 54.2	+29 21	0.54	4	F6	F4	+ 5.9	0.437	0.066	+0.041	Y, F, Jw.
455	α Aquarii	3.2	G0	22 0.6	− 0 48	0.015	2	G0p	F8	+ 0.2	83.2	0.025	+0.010	M
456	Boss 5682	(7.1)	F8	22 1.8	+82 23	0.142	3	F6	F7	+ 3.8	3.02	0.022	+0.007	vM
457	ι Pegasi	4.0	F5	22 2.4	+24 51	0.299	3	F3	F4	+ 4.0	2.51	0.100	+0.097	M, Mil.
458	Boss 5691	5.8	F	22 2.7	+18 59	0.126	3	F1	F3	+ 3.3	4.79	0.032	+0.013	vM
459	Lal. 43205	8.0	G5	22 3.1	+52 39	0.61	3	K0	G7	+ 3.6	3.63	0.013	+0.051	4
460	Lal. 43492	6.9	G	22 12.2	+12 24	0.84	3	G1	G0	+ 5.8	0.479	0.060	+0.015	4
461	Boss 5772	6.1	G	22 18.8	+20 21	0.338	6	F5	F5	+ 4.5	1.58	0.048	+0.060	vM
462	Boss 5786	5.8	G	22 21.5	+ 3 53	0.295	4	F5	F6	+ 4.1	2.29	0.046	+0.067	F, Jw.
463	Boss 5790	4.9	K	22 22.8	+ 4 12	0.325	4	G9	G9	+ 1.3	30.2	0.019	....	....
464	Krüger 60	9.2	K5	22 24.5	+57 12	0.94	4	Mb	Mb	+11.2	0.003	0.251	+0.256	Sc., R, Bar.
465	η Pegasi	3.1	G0	22 38.3	+29 42	0.036	2	G2	G3	+ 1.2	33.1	0.042	−0.028	F
466	Boss 5868	6.1	K	22 39.6	+38 56	0.016	3	K4	K3	+ 0.9	43.7	0.009	+0.011	vM
467	Pi. $22^{\mathrm{h}}214$	6.5	G5	22 40.9	+29 55	0.47	4	K0	G8	+ 4.4	1.74	0.038	+0.015	Y, L and J

468	λ Pegasi	4.1	K0	22 41.7	+23 2	0.060	2	G7	G6	− 0.5	158.	0.012	....	....
469	ι Cephei	3.7	K0	22 46.1	+65 40	0.139	2	K0	G9	+ 1.1	36.3	0.030	+0.036	M
470	σ Pegasi	5.3	F	22 47.3	+ 9 18	0.516	3	F4	F5	+ 3.9	2.75	0.052	+0.033	Y, F
471	Boss 5920	6.5	F5	22 53.5	+ 8 50	0.420	3	G0	F9	+ 4.4	1.74	0.038	....	....
472	Lal. 45028	7.8	K	22 56.6	− 4 23	0.54	4	K2	K3	+ 5.8	0.479	0.040	+0.053	Y, M
473	β Pegasi	2.6	Ma	22 58.9	+27 32	0.234	3	Mb	G7	+ 1.3	30.2	0.055	....	....
474	Fed. 4371	7.5	G	23 1.2	+67 52	0.60	3	G5	G1	+ 7.0	0.158	0.079	+0.056	Y
475	Lal. 45292	8.2	K	23 4.0	− 2 48	0.59	3	K5	K3	+ 6.6	0.229	0.048	+0.035	Y
476	Boss 5972	5.8	A	23 5.8	+43 0	0.275	3	F5	F4	+ 4.1	2.29	0.046	....	....
477	Boss 5976	5.6	K	23 8.5	+56 37	2.105	3	K5	K6	+ 6.6	0.229	0.158	+0.172	4
478	Lal. 45455	8.6	....	23 8.9	− 9 28	0.56	4	F4	F6	+ 5.1	0.912	0.020	....	....
479	Lal. 45456	9.0	F5	23 8.9	− 9 29	0.55	4	G0	G2	+ 5.8	0.479	0.023	+0.019	Y
480	ψ¹ Aquarii	4.5	K0	23 10.6	− 9 38	0.367	4	K0	G9	+ 1.1	36.3	0.021	....	....
481	γ Piscium	3.8	K0	23 12.0	+ 2 44	0.753	3	G5	G4	+ 1.2	33.1	0.030	−0.041	Y
482	Boss 5989	5.6	F	23 12.1	+52 40	0.270	3	F9	F8	+ 4.1	2.29	0.050	+0.049	vM
483	Lal. 45638	8.2	G5	23 13.8	+ 4 52	0.52	3	K2	G9	+ 6.6	0.229	0.048	+0.016	Y, Jw., M
484	W.B. 23^h257	8.5	....	23 15.0	+28 19	0.57	3	K1	K1	+ 6.8	0.191	0.046	+0.060	S
485	Lal. 45755	7.6	F8	23 16.8	+43 33	0.67	3	K0	G7	+ 6.3	0.302	0.055	+0.039	Y, R
486	υ Pegasi	4.6	G0	23 20.4	+22 51	0.191	3	F6	F6	+ 2.5	10.0	0.038	....	....
487	A.Oe. 25685	7.5	....	23 26.5	+58 37	1.08	3	K0	K0	+ 5.8	0.479	0.046	+0.075	Y
488	B.D. +62°2244	7.3	G5	23 28.2	+62 36	0.44	3	G5	G3	+ 4.3	1.91	0.025	−0.012	Y
489	ι Piscium	4.3	G0	23 34.8	+ 5 5	0.574	3	F5	F7	+ 4.3	1.91	0.100	+0.142	Y, Jw.
490	γ Cephei	3.4	K0	23 35.2	+77 4	0.169	2	K1	K1	+ 2.4	11.0	0.063	+0.071	S and M
491	Lal. 46495	7.0	G	23 38.5	+57 31	0.62	3	G0	F9	+ 4.9	1.10	0.038	−0.062	Y, F
492	Boss 6097	6.6	G	23 39.9	+55 15	0.029	3	G6	G6	+ 0.7	52.5	0.007	+0.008	vM
493	W.B. 23^h819	8.6	....	23 40.0	+29 0	0.85	2	K1	K1	+ 7.4	0.110	0.058	....	....
494	τ Cassiop	5.1	K	23 42.2	+58 6	0.087	4	K0	G9	+ 0.6	57.5	0.013	....	....
495	Lal. 46650	8.9	Ma	23 44.0	+ 1 52	1.39	4	Ma	Ma	+10.3	0.008	0.190	+0.182	5
496	Boss 6129	6.6	K	23 47.5	+74 59	0.332	7	K3p	K3	+ 7.2	0.132	0.132	....	....
497	ρ Cassiop	5.0	F8p	23 49.4	+56 57	0.007	5	G4p	G3	− 0.4	145.	0.008	....	....
498	B.D. +26°4721	7.8	....	23 54.2	+26 43	....	3	K2	G6	+ 0.1	91.2	0.003	....	....
499	85 Pegasi	5.9	G	23 56.9	+26 33	1.291	5	G1	G1	+ 5.8	0.479	0.096	+0.099	5
500	Lal. 47207	6.2	G	23 59.6	+34 6	0.78	3	G0	G0	+ 4.4	1.74	0.044	+0.008	Y

the results obtained by three observers, Adams, Joy, and Miss Burwell. The successive columns of the table contain the following data: (1) number of the star; (2) name of star; (3) visual magnitude as given by the Harvard observers wherever possible; (4) spectral type from Harvard determinations; for the fainter stars many of the values are taken from the recent list of measured parallaxes compiled by Walkey;[1] (5) right ascension; (6) declination; (7) total proper motion; (8) number of photographs of spectrum; (9) spectrum as determined from estimates of the general characteristics of the lines; (10) spectrum as determined from the intensities of the hydrogen lines; (11) absolute visual magnitude; (12) luminosity in terms of the sun as unity, the value 5.0 being taken as the sun's absolute magnitude; (13) parallax as computed from the absolute magnitude by the formula $5 \log \pi = M - m - 5$; (14) measured or trigonometric parallax; (15) authorities for the measured parallax; when these exceed three a figure is given in this column to indicate the number of determinations. The following abbreviations are used:

Ab.	Abetti	M	Mitchell (McCormick)
Bar.	Barnard	Mil.	Miller
Bel.	Belopolsky	Ram.	Rambaut
Bg.	Bergstrand	R	Russell
F	Flint	S	Slocum (Yerkes)
Gr.	Greenwich	Sc.	Schlesinger (Yerkes)
Hus.	Hussey	S. and M.	Slocum and Mitchell (Yerkes)
Jw.	Jewdokimow		
Jo.	Jost	vM	van Maanen
K	Kapteyn	Y	Yale
L and J	Lee and Joy (Yerkes)		

It is with considerable hesitation that we have decided to give values of the parallax resulting from the absolute magnitudes to three decimal places. From the relation connecting parallax and magnitude it follows that

$$\frac{d\pi}{\pi} = \frac{dM - dm}{2.2}$$

The percentage uncertainty in a calculated parallax is therefore proportional to the uncertainty in the magnitudes; but the absolute error depends upon the parallax itself. For many stars, particularly those of large parallax upon which even moderate errors in the magnitudes have a marked influence, the third decimal is probably undesirable. On the other hand, because of uniformity and the universal practice in the case of measured parallaxes, it has seemed preferable to retain it. An additional reason is the great number of stars of very small parallax. Attention should be called to the influence of uncertainties in the apparent magnitudes upon the parallaxes. In the case of some of the fainter stars and the components of close pairs this may be very appreciable.

---

[1] *Journal of British Astronomical Association*, **27**, Appendix, 1917.

NOTES ON INDIVIDUAL STARS

No. 45. This star is Boss 637. The mean spectral type is given and the mean magnitude is used for the computation of the parallax.

Nos. 69, 71, 72, 73. These are the brightest stars of the Hyades and form part of the moving cluster in Taurus. The parallax of this cluster as computed by Kapteyn is +0.″023.

No. 125. The spectrum contains bright hydrogen lines, but the bands are not sufficiently strong for classification as Md.

No. 248. An unpublished parallax kindly communicated by Professor Mitchell is +0.″050.

No. 303. An unpublished parallax by Mitchell is +0.″043.

No. 357. The apparent magnitude is uncertain.

No. 358. This star is used as a standard for reduction of absolute magnitudes. Hence the parallax agreement is necessary.

No. 405. The mean spectral type is given.

No. 456. The apparent magnitude is uncertain.

No. 496. This star has a composite spectrum and is a spectroscopic binary. The absolute magnitudes show a considerable range on different photographs.

COMPARISON WITH THE MEASURED PARALLAXES

There are in the list 360 stars with measured parallaxes. If we divide these stars according to spectral type and absolute magnitude we obtain the comparison given in Table II. The differences Δ are spectroscopic *minus* measured values. The mean difference, accordingly, for the 360 stars is +0.″0037, the spectroscopic values being the larger. The very large discordance in the case of the K3–K9 stars under M = +2.0 to 4.9 is due to No. 292 of the list with but a single measured parallax. The average difference taken regardless of sign between the spectroscopic and the measured values for all the stars is 0.″026.

TABLE II

TYPE	M = −3.0 to +1.9		+2.0 to +4.9		+5.0 to +7.9		+8.0 to +13.3		Total	
	No.	Δ	No.	Δ	No.	Δ	No.	Δ	No.	Δ
F0–F8...	12	+0.″003	62	+0.″004	14	+0.″018	.....	....	88	+0.″006
F9–G7...	22	+0.005	35	+0.007	34	+0.007	.....	....	91	+0.007
G8–K2...	38	−0.004	21	−0.011	35	+0.002	2	−0.021	96	−0.004
K3–K9...	16	+0.011	1	−0.108	23	+0.014	17	+0.005	57	+0.008
Ma–Md..	14	+0.004	1	−0.049	.....	....	13	+0.008	28	+0.004
All....	102	+0.002	120	+0.001	106	+0.008	32	+0.004	360	+0.0037

If the comparison is limited to the stars with several parallax measurements the systematic difference nearly disappears. Thus there are 59 stars in the list with parallaxes measured by three or more observers. The mean difference, spectroscopic *minus* measured values, for these stars is +0.″001.

TABLE III

Observer	No.	Δ
Miller..........................	34	−0.″008
Mitchell.........................	53	+0.003
Schlesinger......................	15	+0.005
Slocum, Slocum and Mitchell, and Lee and Joy..................	36	+0.013
van Maanen.....................	48	−0.006
Yale...........................	148	+0.008

A comparison with the measured parallaxes of various observers may also prove of interest. The results are given in Table III. Most of the Yerkes determinations are combined in one group.

COMPARISON OF SPECTRAL TYPES

Of the 500 stars in the list, 441 have spectral determinations by the Harvard observers. For the faintest of these stars only the even spectral class is given without subdivisions, or at most with divisions of five units such as G5 or K5. Accordingly the comparison is not altogether a fair one. The results are as follows, the unit being one-tenth of a spectral division, the interval, for example, from K0 to K1:

	Δ	Average Difference
Harvard–Mount Wilson estimates ..	−1.6	3.4
Harvard–Mount Wilson measures...	−0.7	3.2

These results are influenced greatly by a small number of large discrepancies, such as classifications of A and K for the same star in the two sets of observations.

A more valuable comparison is that of the brighter stars in the list. For these higher dispersion has been employed by the Harvard observers and the spectral division is given more closely. Using the values of the *American Ephemeris* we have in the case of 164 stars:

	Δ	Average Difference
Harvard–Mount Wilson estimates..	+0.5	1.6
Harvard–Mount Wilson measures...	+1.2	2.2

Although the number of stars used is much smaller in this case, the agreement is better than in the previous one. It is, of course, clear from the definition of the estimated and measured determinations of the Mount Wilson values that the estimates should be the more closely comparable with the Harvard results.

INTENSITY OF THE HYDROGEN LINES

The intensity of the hydrogen lines in stars of the same general type of spectrum must be recognized as furnishing valuable evidence as to the position of these stars in the system of stellar development.

The fact that the hydrogen lines are remarkably intense in the giant M stars and weak in the dwarf M stars was found some years ago in the course of classification work at this Observatory,[1] and a tendency in the same direction was recognized for some stars of the K type. Accordingly, in all recent classification work we have made two determinations of type. The first is based upon the general characteristics of the spectrum, such as the high-temperature and low-temperature lines, the intensity of the blue calcium line at λ 4227, the prominence of the bands, and many other features. For this purpose photographs of the spectra of stars typical of each type have been selected, and the spectrum to be classified is compared with these in turn. The second method of classification is based directly upon the intensities of the hydrogen lines and has been described fully elsewhere.[2] If therefore we compare the spectral types as derived by these two methods we obtain a measure of the intensities of the hydrogen lines. When the two determinations of type agree, the hydrogen lines are normal; when the measured value gives an earlier type, the hydrogen lines are exceptionally strong.

The comparison of the estimated spectral types of the stars in Table I with those derived from the hydrogen lines gives results of considerable interest. If we employ as the unit the same spectral subdivision as before, that is, the interval from K0 to K1, for example, and divide the stars into groups arranged according to spectral type and absolute magnitude we obtain Table IV. Under "Abs. Visual Mag." is given the arithmetical mean of the absolute magnitudes, and under "Est.−Meas." the difference in spectral type in the units referred to. Thus a value of +3.7 in this column means that the type from the hydrogen lines is 3.7 units earlier than the estimated value. If, for example, the estimated value were K8 the measured value would be K4.3.

It is probable that a difference of at least one unit in the two values for spectral type is due to accidental error or to a systematic deviation in the classification curves. The stars of low luminosity therefore show but little difference between the estimated and the measured values throughout all the spectral types, and the same is true for the high-luminosity stars of the earlier types. The hydrogen lines, accordingly, are normal for all of these stars. In the case of the high-luminosity stars, however, the intensity of the hydrogen lines is quite abnormal for the later K and more especially the M stars. There seems to be little doubt that this behavior is related to the well-recognized giant and dwarf division of these stars, and that great intensity of the hydrogen lines is to be associated with high luminosity. They have accordingly been used as criteria for absolute magnitude in the case of the giant M stars.

---

[1] *Mt. Wilson Contr.*, No. 89; *Astrophysical Journal*, **40**, 385, 1914.

[2] *Mount Wilson Communications*, Nos. 23–26; *Proceedings of the National Academy of Sciences*, **2**, 143, 1916.

TABLE IV

	No.	$M \leqq 3.9$		No.	$M \geqq 4.0$	
		Abs. Visual Mag.	Est. − Meas.		Abs. Visual Mag.	Est. − Meas.
F0–F4	28	2.8	− 0.7	10	4.7	−0.9
F5–F9	33	2.5	− 0.8	66	4.7	−0.6
G0–G4	14	1.6	+ 0.4	37	5.1	+0.7
G5–G9	63	0.8	+ 1.2	38	5.5	+1.7
K0–K3	58	1.2	+ 1.6	45	6.2	+1.2
K4–K9	21	1.3	+ 3.7	41	7.9	+1.0
M	30	1.2	+12.5	9	10.8	+0.4

THE GIANT AND DWARF DIVISIONS

The direct evidence bearing on the division into two classes afforded by the stars in this list may be most clearly indicated by a tabulation of the numbers of stars of the various absolute magnitudes. For this purpose narrow limits of magnitude should be selected. In Table V the results are given for an interval of 0.5 magnitude.

A graphical representation of these results is shown in Fig. 1. The clearly marked separation in the case of the M- and later K-type stars is seen persisting in the form of two strong maxima as far as those of the G type. The crests of these maxima draw more closely together in the successive types. There seem to be the rudiments of the first maximum among even the F stars, though this is perhaps uncertain. The extraordinary grouping of the F stars around the magnitudes 3.0 to 5.5 is their most characteristic feature. The absolute magnitudes of the maxima of frequency for the various types may be summarized as follows:

TABLE V

Absolute Magnitudes	Ma–Md	K9–K4	K3–K0	G9–G0	F9–F0
− 3.0 to − 2.6	1	....	....	....	....
− 2.5 − 2.1	....	....	....	....	....
− 2.0 − 1.6	....	....	....	....	....
− 1.5 − 1.1	....	....	....	....	....
− 1.0 − 0.6	1	....	....	4	1
− 0.5 − 0.1	1	....	2	7	1
0.0 + 0.4	2	....	6	17	3
+ 0.5 + 0.9	6	6	13	19	4
+ 1.0 + 1.4	5	7	18	11	6
+ 1.5 + 1.9	8	7	10	5	3
+ 2.0 + 2.4	4	....	4	4	1
+ 2.5 + 2.9	1	1	1	3	7
+ 3.0 + 3.4	....	....	3	5	13
+ 3.5 + 3.9	1	....	1	2	23
+ 4.0 + 4.4	....	....	4	14	28
+ 4.5 + 4.9	....	....	1	12	26
+ 5.0 + 5.4	....	....	1	15	15
+ 5.5 + 5.9	....	1	6	15	6
+ 6.0 + 6.4	....	3	16	10	1
+ 6.5 + 6.9	....	6	8	3	....
+ 7.0 + 7.4	....	6	7	2	....
+ 7.5 + 7.9	....	4	2	1	....
+ 8.0 + 8.4	....	5	....	2	....
+ 8.5 + 8.9	....	8	....	1	....
+ 9.0 + 9.4	....	6	....	....	....
+ 9.5 + 9.9	2	2	....	....	....
+10.0 +10.4	3	2	....	....	....
+10.5 +10.9	4	....	....	....	....
+11.0 +11.4	2	....	....	....	....
+11.5 +11.9	....	....	....	....	....
+12.0 +12.4	....	....	....	....	....
+12.5 +12.9	....	....	....	....	....
+13.0 +13.4	1	....	....	....	....

	Ma–Md	K9–K4	K3–K0	G9–G0	F9–F0
Giant....	+ 1.6	+1.4	+1.3	+0.6	(+1.1)
Dwarf....	+10.8	+7.8	+6.3	+5.3	+4.1

The question whether the selection of the stars observed may be accountable for the absence of stars of magnitude intermediate between those of the two groups in the case of the M and K types should perhaps be discussed briefly. For the M stars it does

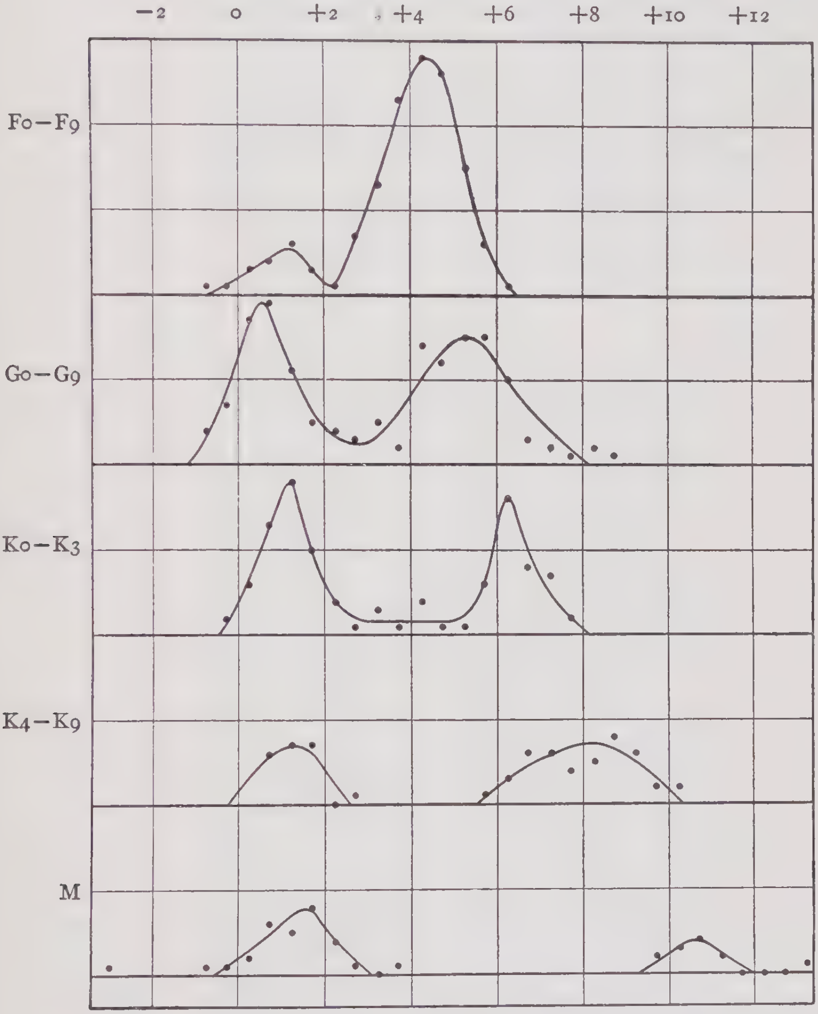

Fig. 1.—Frequency-curves of absolute magnitudes for different spectral types

not seem possible that this can be the case. Our observations have included all of the known faint stars of this type with large proper motions; about 15 stars with small proper motions and apparent magnitudes between 7.5 and 8.5; and over one-third of the stars of this type listed in the catalogue of Boss with various proper motions. Throughout this list of about 110 stars the spectral differences between the two classes persist clearly, and there is no evidence whatsoever of an intermediate type of spectrum. The interval of over six magnitudes remains without representation.

The same argument applies, but in less degree, to the K-type stars. Among the great number of K stars given in Table I there is a wide variety in proper motion and apparent magnitude. It is difficult to see why this list, which contains representatives of both the giant and the dwarf classes, should not contain a full share of stars of intermediate absolute magnitudes, if such exist.

In the case of the G-type stars it is possible that the basis of selection of the material has affected the results somewhat. The fact that stars of very large proper motion and of very small proper motion have formed a considerable portion of the observing list would tend to give an excess of very bright and very faint stars. This may account in part, but probably not wholly, for the two maxima of the G-type stars shown in Fig. 1. The stars of the *American Ephemeris*, which have not been selected on the basis of proper motion, should tend to smooth out these maxima.

THE BEHAVIOR IN LABORATORY SOURCES OF THE LINES USED FOR ABSOLUTE MAGNITUDE

Three of the most important lines used in the determinations of magnitude are the strontium lines λ 4077, λ 4215, and λ 4607. The first two of these are well-known enhanced lines, being very strong in the spectrum of the electric spark, and, as Mr. King has shown, weak in low-temperature sources such as the electric furnace. The line λ 4607 is of the opposite type and is very strong in the furnace spectrum. A reproduction of photographs of these lines made by Mr. King is given in Plate XIX. The two lines λ 4077 and λ 4215 are identical in behavior in laboratory sources, and it is of interest to note that both are very prominent lines in the spectrum of the solar chromosphere.

The calcium line at λ 4455 is a well-known low-temperature line analogous in behavior to λ 4607 of strontium. The line at λ 4290

PLATE XIX

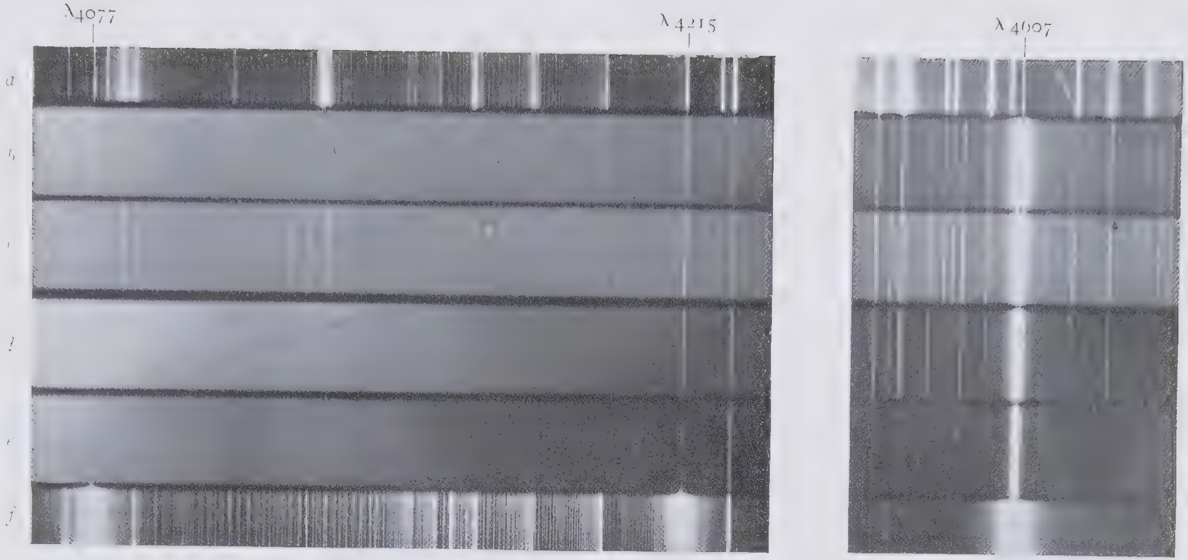

Variation with Temperature of Lines in Furnace Spectrum of Strontium

a, Barium arc

b–e, Furnace spectra of strontium: *b*, 2350° C., high vapor-density; *c*, 2350° C., low vapor-density;
d, 2000° C.; *e*, 1650° C.

f, Strontium arc

is a strongly enhanced titanium line and appears at an early stage in stellar spectra of type A.

Summarizing these results for all of the lines used we have the comparison given in Table VI.

It is probable that the line at λ 4207, like so many of the unidentified lines of Rowland's table, is enhanced. The hydrogen lines Hγ and Hδ cannot well be classified according to laboratory behavior, although they certainly are not low-temperature lines. The intensity of the hydrogen lines in stellar spectra of types A and B points rather to the opposite conclusion.

TABLE VI

Line	El.	Spectral Types	High-Lumin. Stars	Low-Lumin. Stars	Spark	Furnace
4077..........	Sr	A8–F5	Strong	Weak	Strong	Weak
4215..........	Sr	A8–M	Strong	Weak	Strong	Weak
4290..........	Ti	A8–F5	Strong	Weak	Strong	Weak
4455..........	Ca	F6–M	Weak	Strong	Weak	Strong
4607..........	Sr	M	Weak	Strong	Weak	Strong
4207..........	....	M	Strong	Weak	Unknown	Unknown
Hδ, Hγ.......	H	M	Strong	Weak	....	....

The conclusion is obvious that the enhanced lines are relatively strong in the high-luminosity stars and the low-temperature lines strong in the fainter stars. That this is purely a temperature effect, however, is doubtful. The investigations of King with the electric furnace have shown the importance of the influence of vapor-density upon line-intensities, and we should expect wide variations in this respect in the atmospheres of different stars. The observed behavior may well be due to a combination of effects of both temperature and vapor-density in stellar atmospheres. The main consideration, however, is the direct evidence that the use of the absolute-magnitude lines has a definite physical basis and that the lines employed as criteria are as clearly distinguished by their behavior in laboratory sources as in stellar spectra.

GENERAL CRITERIA FOR ABSOLUTE MAGNITUDE

A study of the characteristics of the spectra of stars of very high and very low luminosity makes it clear that the variation of the lines used as magnitude criteria forms but a portion of a much more general difference. This is most marked in the case of the M-type stars, but it is evident in other types as well. For stars of the same spectral type, the enhanced lines and the hydrogen lines are relatively strong in those of high luminosity and weak in those of low luminosity, while the low-temperature lines are relatively weak in the brighter stars and strong in the fainter stars. To illustrate we may take the case of two stars representing the giant and dwarf classes of M stars:

	α Orionis	Lal. 21185
Hydrogen lines	Very strong (G2)	Weak
Enhanced lines	Strong	Weak
λ 4227 of Ca	Weak	Very strong
Low-temperature lines of Ca, Sr, Fe, Ti, etc.	Weak	Very strong

A very similar result, though somewhat less in degree, is found from a comparison of K-type stars of high and low luminosity. There is little question that λ 4227 of calcium is strongly dependent upon absolute magnitude, being very intense in the low-luminosity stars. We have as yet been unable to employ it satisfactorily, however, because of its great intensity and its rapid change with spectral type.

SUMMARY

1. The absolute magnitudes, luminosities, spectral types, and parallaxes of 500 stars have been determined from investigations of their spectra.

2. A comparison with the directly measured parallaxes of 360 of these stars shows the spectroscopic values to be about +0.″004 larger in the mean. The average difference is 0.″026, if all parallaxes are included. A comparison with the 59 parallax values determined by three or more observers gives a difference of +0.″001 in the mean.

3. A method of determining the absolute magnitudes of stars of types A8 to F5 has been derived, and improvements have been made in the methods used for the two classes of M-type stars.

4. A comparison of the determinations of spectral type with those made by the Harvard observers gives a difference of −1.6 spectral divisions in the mean, the Mount Wilson estimates being the later. A comparison for 164 stars listed in the *American Ephemeris* gives a difference of +0.5 division.

5. Abnormal intensity of the hydrogen lines is a characteristic of the highly luminous stars of the later types. This is almost certainly related to the giant and dwarf division among these stars.

6. A comparison of the number of stars of each absolute magnitude shows very clearly the giant and dwarf divisions for the M, K, and probably G types of spectrum, with a slight indication even in the case of the F stars. It is almost certain, in the case of the first two of these types at least, that these results cannot be ascribed to the selection of the stars.

7. The lines used for determinations of absolute magnitude are lines which in laboratory sources show marked variations with vapor-density and temperature. The lines which are strong in the highly luminous stars are strong in the electric spark; those strong in the fainter stars are strong in the electric furnace. The correspondence is complete.

8. The high-luminosity stars are characterized by spectra in which both the hydrogen lines and the enhanced lines are abnormally strong. In the spectra of the fainter stars all of the low-temperature lines are strong, including the blue line λ 4227 of calcium. The lines used for determinations of magnitude form but a part of this more general spectral distinction.

Mount Wilson Solar Observatory
September 1917

Contributions from the Mount Wilson Solar Observatory, No. 143
Reprinted from the *Astrophysical Journal*, Vol. XLVI, pp. 291–295, 1917

BAXANDALL'S EXPLANATION OF AN "ABNORMAL" SOLAR SPECTRUM

By GEORGE E. HALE

The following letter from Mr. Baxandall gives a simple and adequate explanation of two "abnormal" photographs of the solar spectrum in the neighborhood of a sun-spot, taken at the Kenwood Observatory in 1894, and described in this *Journal* in 1902.[1] The photographs in question were among several made in parallel strips on a single photographic plate, for the purpose of ascertaining the exposure times required for spectra of different orders. The slit of the spectrograph happened to lie across a sun-spot in the 2-inch solar image given by the Kenwood refractor, and most of the photographs on the plate show the usual bright reversals of H and K over the spot region. In two of them, however, these reversals were absent, and the spectra were so changed in appearance as to be unrecognizable. The idea that their peculiarities might be due to the chance superposition of two spectra of different orders was entertained at the time, but the absence of the bright H and K reversals where they should have appeared, together with other causes, unfortunately led us to dismiss this explanation. Finally, after much hesitation because of the improbable character of the spectrum, and after copies of the photographs had been sent to a number of spectroscopists in the hope that an explanation could be found, I published the photographs, together with measures of the lines and estimate of their intensities by Mr. Adams. These showed that most of the lines of the "abnormal" spectra were solar lines in Rowland's table, greatly changed in relative intensity. One of the "abnormal" spectra was intermediate in character between the solar spectrum and the other "abnormal" spectrum, and both showed two unknown bright lines, which, with other features mentioned by Mr. Baxandall, should have furnished us the clue so effectively recognized and applied by him. The fact that the apparent wave-lengths of these bright lines changed appreciably between the two exposures helped to mislead me, but I shall not attempt to offer any excuse for being so easily deceived.

---

[1] "Solar Research at the Yerkes Observatory," *Astrophysical Journal*, **16**, 220, 1902.

Mr. Baxandall's letter is as follows:

SOLAR PHYSICS OBSERVATORY
Cambridge, June 4, 1916

DEAR PROFESSOR HALE:

It is only after considerable hesitation that I have decided to send you the present communication. It relates to your paper of 1902, containing an account of an apparently anomalous solar spectrum which has been considered to be due to a fleeting upheaval in the solar atmosphere. Doubtless, in common with many others engaged in spectroscopic investigations, I have always felt somewhat sceptical as to the reality of the phenomenon to which the abnormality of the spectrum was supposed to be due, although I have never been able to explain the strange spectra from any other point of view. My unbelief was based mainly on the following heads:

1. The isolated nature of the type of abnormality shown.
2. The restricted part of the spectrum in which it revealed itself.
3. The fact that there was no kind of lead given by the type of line or chemical elements involved.

I have on many occasions referred to your plates in the hope of getting some light on the real origin of the peculiar spectra, but with no success, until on Friday last, while examining the spectra again, I became conscious of the fact that the grouping of many of the most outstandingly strong lines in the abnormal spectrum had a familiar aspect, and the aspect was that of some of the chief landmarks in the solar spectrum itself. Thus the three strong lines 3921.87, 3927.77, and 3930.45 of the abnormal spectrum and the weaker bunch of lines 3916.84–3918.50 to the left, struck me as being uncommonly like the Fe triplet 4045, 4063, 4072, and the manganese bunch 4030–4036 of the normal solar spectrum. Then it dawned on me that probably by some chance circumstance, a small-dispersion solar spectrum had been superposed on your third-order spectra. Measuring on your reproduction the range of the three strong lines mentioned, I found it was exactly one-third the space occupied by the three Fe lines 4046–4072 on your third-order spectra. This suggests that the superposed spectrum was one of the first order of the grating used in your research. Employing this measured interval between your abnormal lines 3921.87, 3930.45 as a unit, and working backward on your spectra, I found that the two strange narrow bright lines 3884.64, 3896.21 agree in position with the H and K lines of the superposed spectrum. As these bright lines apparently extend equal distances on each side of the spot band, they are probably reversals of H and K in the added spectrum.

Working in the same way to the right, and taking the most outstanding line λ 3981 of your list, this revealed itself as the 4226.9 (Ca) line of the superposed spectrum. As the same proportion of one to three held in every case where intervals between solar landmarks were considered, it seems to me that the evidence is very conclusive that the strengthened lines in the abnormal spectrum are really due to the strong and outstanding lines of the small-scale superposed spectrum. The fact that it is only over a restricted region of your large-scale spectra where the abnormalities occur is also in favor of the contention that a small-scale superposed spectrum is involved.

As the intermediate spectrum shows a far closer resemblance to the normal solar spectrum, I have not thought it worth while to investigate in a similar manner to the above the irregularities in that spectrum, especially as, if it is satisfactorily established that any superposition of spectra has taken place, the whole argument for an upheaval in the solar photosphere must of necessity fall to the ground.

I feel sure that if a solar spectrum is prepared of such a scale that the lines 4071.9 Fe, 4226.9 Ca, on it are the same interval apart as the abnormal lines 3930.45, 3981.98 of your reproduction, and the strips so adjusted that these two pairs fit, the counterparts of the outstanding groups and lines of the normal spectrum will be apparent in your reproduced abnormal spectra along the whole range of the superposed spectrum. A few of the normal groups and lines will doubtless be modified in intensity where an outstandingly strong line of your "real" third-order spectrum blends with a line or group in the superposed spectrum.

I append a short list of lines which I consider, from rough measurements on the reproductions, to be identical: that is, the apparently abnormal lines of the reproduction, which I think are the real lines of the superimposed spectrum.

After I had come to the conclusion expressed above, I noticed that you mention in your paper having a suspicion at the time of the investigation that superposed spectra might be the cause of the apparent anomaly, but that after consideration you had come to the conclusion that that view was untenable. There is now little or no doubt in my mind that this is the real explanation. At the same time, I concede that, if you still have the original plates, you have the best opportunity of testing the points I raise.

I may mention just one other point. If the two bright narrow lines are not H and K reversals of the added spectrum, what are the chances against your measured wave-length interval between the two (when assumed to be real lines in the third-order spectra) being exactly one-third of the real wave-length interval between H and K? Thus your mean interval between the lines is 11.635 $\mu\mu$. One-third the interval between H and K is 11.600 $\mu\mu$. The difference between these two is probably within the errors of measurement.

Yours very truly,

F. E. Baxandall

All the lines in the first column are well-strengthened lines in the abnormal spectrum, and all those in the second column are conspicuous lines in the normal solar spectrum. If any two of the former be taken it will be found that the interval between them is approximately one-third the interval between the corresponding two of the latter. The chance against this being a fortuitous result seems to me to be "beyond arithmetic."

Strengthened Lines in "Abnormal Spectrum"	Corresponding Lines in Superposed Spectrum	
3884.67 (bright)	3933.83 K (Ca) reversal	
3896.21 "	3968.63 H (Ca) "	
3908.41	4005.41 Fe	
3908.90	4007.	Narrow solar group
3916.84 to 3918.50	4030.9 to 4035.9	Mn group
3921.87	4045.98 Fe	Well-known triplet
3927.77	4063.76 Fe	
3930.45	4071.91 Fe	
3972.61	4198.40 to 4199.27	Narrow solar group
3973.74	4202.20 Fe	
3981.98	4226.90 Ca	
3989.91	4250.29 Fe 4250.95	
3993.05	4260.15 Fe 4260.64	
3996.80	4271.33 Fe 4271.93	
4005.41 to 4011.03 wide hazy group	4299. to 4315.	Fraunhofer's "g" group
4013.95	4324.	Narrow solar group
4014.70	4325.94 Fe	
4033.81	4383.72 Fe	Well-known triplet
4040.80	4404.93 Fe	
4044.19	4415.29 Fe	

As a further check we may compute the approximate wave-lengths of the solar lines corresponding to lines of the "abnormal" spectrum, on the assumption that a first-order spectrum is superposed on the third order, λ 3921.87 of the third order being coincident with λ 4045.98 of the first order.

Abnormal	Calculated First Order	O−C
3884.5 bright......	3933.3 (K)	+0.5
3896.1 "	3968.3 (H)	+0.3
3927.8............	4063.8	0.0
3930.4............	4071.9	0.0
3940.3............	4101.6	+0.3
3950.5............	4132.3	−0.1
3954.4............	4144.0	0.0
3982.0............	4227.2	−0.3
4014.7............	4325.9	0.0
4033.8............	4383.5	+0.2
4040.8............	4404.6	+0.3
4044.2............	4414.8	+0.5

Evidently no further evidence is needed to establish the truth of Mr. Baxandall's conclusions.[1]

Mount Wilson Solar Observatory
October 8, 1917

---

[1] Absence from the Observatory and the pressure of other duties have unduly delayed the re-examination of the original photographs and the publication of this note, which has experienced the fate of several other astronomical manuscripts, essentially completed many months ago, but still unpublished.

Contributions from the Mount Wilson Solar Observatory, No. 144
Reprinted from the *Astrophysical Journal*, Vol. XLVII, pp. 7–37, 1918

A DETERMINATION OF THE SOLAR MOTION AND THE STREAM-MOTION FROM RADIAL VELOCITIES AND ABSOLUTE MAGNITUDES OF STARS OF LATE SPECTRAL TYPES

By GUSTAF STRÖMBERG

In a recent memoir[1] by Adams and myself the results of an investigation concerning the relationship of average radial velocity to absolute magnitude have been published and we have shown that the intrinsically faint stars have a higher velocity than those that are intrinsically brighter. The stars were grouped in different shells according to distance from the sun, and no decided variation of velocity with distance could be found. Continuing this investigation, I have confirmed these results, and have further studied the solar motion and stream-motion as functions of absolute magnitude. This study, as well as the preceding, is based wholly on stars of the spectral types F, G, K, and M. For about 700 of these stars Adams has determined spectroscopically the absolute magnitudes and parallaxes.

When I commenced this work a number of the spectroscopic parallaxes were not definitely determined, and for this reason the absolute motions of the stars in space have not been computed, the radial velocities alone having been used. Hence the absolute magnitude has been employed only for the grouping of the stars. In order to increase the material, use has been made of about 600 determinations of radial velocity from the Lick and Mills Observatories. For these stars mean parallaxes have been computed from their proper motions and apparent magnitudes.

MEAN PARALLAXES

As mentioned in the paper cited, the recent determinations of stellar parallaxes by van Maanen, and of absolute magnitudes by Adams, indicate that stars of very small proper motion have parallaxes considerably larger than would be expected from their proper motions, were the mean parallactic formula of Kapteyn employed. This is perhaps due to the fact that a list of apparently bright stars of late types, chosen on account of small proper motion, involves the selection, not only of distant stars of high intrinsic luminosity, but also of nearer stars whose velocity at right angles to the line of sight is nearly equal in direction and magnitude to the component of the sun's velocity in the same plane. Such a selection of stars of very small proper motion had actually been made in forming the list of stars to be observed for absolute luminosity and radial velocity at the Mount Wilson Observatory.

---

[1] *Mt. Wilson Contr.*, No. 131; *Astrophysical Journal*, 45, 5, 1917.

Kapteyn's formula for computing mean parallaxes from proper motion and apparent magnitude is[1]

$$\pi = A\mu^b \epsilon^m, \tag{1}$$

where μ is the proper motion and m the apparent magnitude, A, b, and ϵ being constants determined from measured parallaxes and from the parallactic motions of the stars. To render the material homogeneous, new constants were determined from 700 spectroscopically determined parallaxes. It was then found that the equation (1) gave a quite unsatisfactory representation of the smaller parallax. It is to be observed that hitherto the constants for the stars of later type have been based mainly on stars of large parallax, the formula for stars of small parallax being merely an extrapolation. Kapteyn's formula, however, is given a theoretical basis by Schwarzschild[2] on the assumption of a constant luminosity-curve and velocity-curve for all stars at all distances. Now if the velocity is a function of absolute magnitude, the velocity-curves and luminosity-curves are dependent on one another; and since among the distant stars we observe only those of high luminosity, both curves are dependent on the distance. There is further a strong tendency, especially among the K and M stars, to a separation of the absolute magnitudes into two groups, one of very high luminosity, the "giants," and one of very low luminosity, the "dwarfs."

---

[1] *Groningen Publications*, No. 8. Constants redetermined by van Rhijn, *Mt. Wilson Contr.*, No. 110; *Astrophysical Journal*, **43**, 36, 1916.

[2] *Astronomische Nachrichten*, **190**, 361, 1912.

We should also note that the small parallaxes determined spectroscopically can be measured with the same percentage of error as the large parallaxes, provided there are no large systematic errors. In using spectroscopic parallaxes we have the great advantage of securing logarithmic error-distribution within the different groups, as well as in their combination, while in the case of the directly measured parallaxes we have a normal distribution of error in the parallaxes themselves, assuming that we are dealing with a group of stars at the same distance. In Fig. 1 are plotted the values of $\log \pi$ as a function of $\log \mu$ for the spectral types F and G, K and M. The stars are treated separately according as they are near or distant from the sun's apices, and all have been reduced to the apparent magnitude 6.0 on the Harvard system. The points are the means of the logarithms of the parallaxes for different groups of stars of different proper motions. From the figure we see that the straight line

$$\log \pi = \log A + b \log \mu$$

gives a poor representation of the parallaxes of stars of small proper motion. Introducing the constants given by van Rhijn, which differ but slightly from those of Kapteyn, we have

$$\log \pi = -1.078 + 0.695 \log \mu - 0.0482\,(m-6). \qquad (2)$$

The equation

$$\log \pi = \log A + b \log (\mu + c) \qquad (3)$$

gives a decidedly better representation of the observations. The constant b, which gives the direction of the asymptote for large proper motion, is very difficult of determination, the stars of large motion being too few in number for the purpose. Without affecting the accuracy appreciably, however, we may put $b=1$, an error in b affecting only the parallaxes of stars of very large proper motion.

Table I gives the values of the constants in the equation

$$\log \pi = \log A' + \log (\mu + c) + (m-6) \log \epsilon \qquad (4)$$

together with their mean errors. The mean error of $\log \pi$ is denoted by r, and the angular distance from the sun's apex by d.

From the comparison with the observations in Fig. 1 we see that there is a break in the continuity for the stars of types K and M between parallaxes 0″.3 and 0″.08 ($\log \pi = -1.6$ and -1.1), corresponding to the division of the stars into giants and dwarfs.

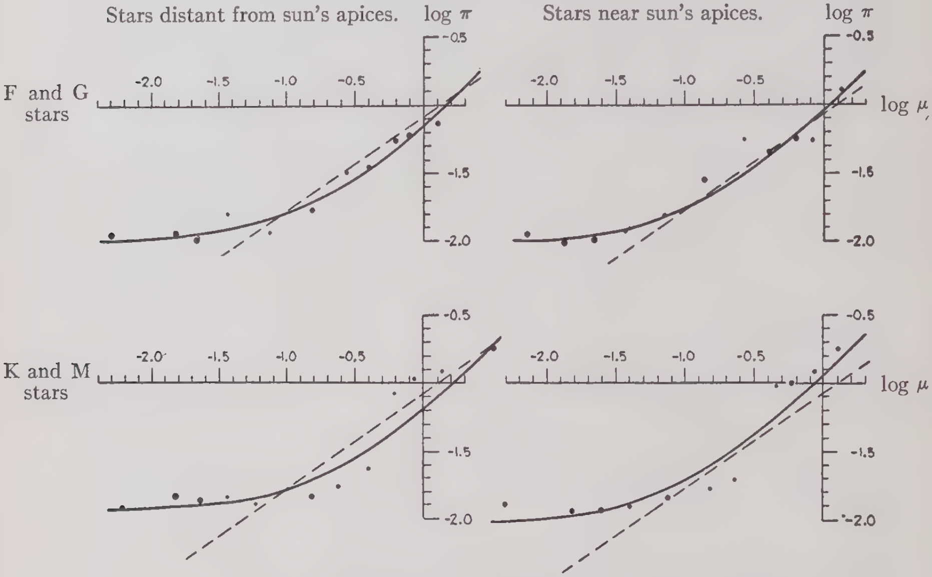

FIG. 1.—Relation between log π and log μ. The points represent means of log π, spectroscopically determined, for groups of stars, all parallaxes having been reduced to the sixth magnitude. The continuous curves represent

$$\log \pi = \log A + \log (\mu + c);$$

the broken lines represent

$$\log \pi = \log A + b \log \mu.$$

TABLE I

CONSTANTS FOR MEAN PARALLAX FORMULA

d	log A'	c	log ϵ	r	No.
	F and G Stars				
60°–120°	-1.208 ± 0.049	$+0''.157 \pm 0''.027$	-0.110 ± 0.015	± 0.073	244
0°–60°, 120°–180°	-1.081 ± 0.065	$+0.109 \pm 0.024$	-0.087 ± 0.040	± 0.093	202
	K and M Stars				
60°–120°	-1.253 ± 0.101	$+0''.200 \pm 0''.049$	-0.101 ± 0.020	± 0.15	117
0°–60°, 120°–180°	-0.965 ± 0.086	$+0.084 \pm 0.033$	-0.115 ± 0.018	± 0.15	135

Since there are scarcely any intermediate stars, I have not thought it necessary to compute separate constants for the stars of these two classes.

The difference in size of the points in Fig. 1 represents the difference in weights, which is based directly upon the number of stars in the different groups.

The values of log ϵ are probably not representative of all stars, since the faint stars are selected mainly on account of large proper motion and thus have parallaxes that are too large.

For values of μ smaller than about 0".03, the parallax is almost independent of proper motion, and we find

$$\log \pi = \log A' + \log c + (m-6) \log \epsilon . \tag{5}$$

or

$$\log \pi = -1.400 - 0.102\, m$$

SYSTEMATIC ERRORS OF THE PARALLAXES

In a paper by Kapteyn and Adams[1] it was suggested that in case the frequency function of the velocities were different from that given by Maxwell's law, its character would affect seriously the interpretation of the relationship found between proper motion and radial velocity. In order to eliminate this effect, Adams and I have used a formula for mean parallax which is independent of the nature of the frequency function of the velocity components, and based only on the assumption that for a group of stars scattered over the whole sky this function is the same in all directions. A brief account of the derivation of the formula and of the final equations used was included in our paper. A more detailed and complete statement is given here.

The star's velocity in space corrected for the sun's motion is projected on three axes, one coinciding with the radial velocity; of the other two, at right angles to the line of sight, one is directed toward the sun's apex and the other is at right angles thereto. The three components of the star's velocity in space, corrected for the sun's motion, are therefore

$$V' = V + V_0 \cos d ; \quad V_\nu = \frac{k\nu}{\pi} + V_0 \sin d ; \quad V_\tau = \frac{k\tau}{\pi} , \tag{6}$$

---

[1] *Mount Wilson Communications*, No. 1; *Proceedings of the National Academy of Sciences*, **1**, 14, 1915.

in which V is the star's radial velocity, V_0 the sun's velocity, d the angle between the star and the sun's apex, ν and τ the components of the proper motion in the directions mentioned, and k a constant equal to 4.738 km/sec. Assuming the frequency function F to be the same in these three directions, we have

$$F(V')=F(V_\nu)=F(V_\tau).$$

In a group of stars the logarithms of the parallaxes are distributed more nearly in accordance with a normal frequency-curve than are the parallaxes themselves. In forming the mean parallax we therefore deal with the logarithms and use the geometrical instead of the arithmetical mean, and write accordingly,

$$\text{Geometrical Mean Parallax}=\underline{\pi}=\sqrt[n]{\Pi(\pi)}\,,$$

whence

$$\log \underline{\pi}=\frac{1}{n}\Sigma \log \pi=\overline{\log \pi},$$

in which n is the number of individual parallaxes. A further advantage of this method of procedure is that the ratios in equation (6) are thus transformed into differences from which we can form directly $\overline{\log \pi}$ or $\log \underline{\pi}$, whatever the range in the parallax.

We have, therefore,

$$F_1\,(\log V')=F_1\,(\log V_\tau) \text{ or } \overline{\log V'}=\overline{\log V_\tau}$$

where V' is to be taken regardless of sign. We then find

$$\overline{\log \pi}=\log k+\overline{\log \tau}-\overline{\log V'}$$

or

$$\underline{\pi}=\frac{k\tau}{\underline{V'}}\,, \tag{7}$$

a bar above the symbol denoting the arithmetical mean, a bar below the symbol the geometrical mean.

For the ν component we have

$$F(V')=F(V_\nu)=F\left(\frac{k\nu}{\pi}+V_0 \sin d\right).$$

Hence,

$$F_1(V'-V_0 \sin d)=F_1\left(\frac{k\nu}{\pi}\right)$$

and

$$F_2[\log (V'-V_0 \sin d)]=F_2\left(\log \frac{k\nu}{\pi}\right)$$

or, finally,

$$\overline{\log \pi}=\log k+\overline{\log \nu}-\overline{\log (V'-V_0 \sin d)} \tag{8}$$

or

$$\pi=\frac{k\nu}{V'-V_0 \sin d}.$$

Since $F(V')$ can be assumed to be equal to $F(-V')$ we also find

$$F(-V')=F\left(\frac{k\nu}{\pi}+V_0 \sin d\right)$$

or

$$F_1 [\log (-V'-V_0 \sin d)]=F_1[\log (V'+V_0 \sin d)]=F_1\left(\log\frac{k\nu}{\pi}\right).$$

Hence,

$$\overline{\log \pi}=\log k+\overline{\log \nu}-\overline{\log (V'+V_0 \sin d)} \tag{8a}$$

or

$$\pi=\frac{k\nu}{V'+V_0 \sin d}.$$

Taking the mean of (8) and (8*a*) we find

$$\overline{\log \pi}=\log k+\overline{\log \nu}-\tfrac{1}{2}[\overline{\log (V'+V_0 \sin d)}+\overline{\log (V'-V_0 \sin d)}]. \tag{9}$$

For a large group of stars scattered over the whole sky there can be only a small effect of preferential motion, and the assumption of the equality of the frequency function in the three components probably is nearly fulfilled. Furthermore, among the stars of later type the *K*-term, which can be interpreted either as a systematic error in the determination of radial velocity or as a general dilatation or contraction of the stellar system, appears to be very small. In the paper by Adams and myself already cited, we found for parallaxes larger than 0.″017 a good agreement between the values computed from the formulae (7) and (8) and the parallaxes actually employed, the latter being in part spectroscopic determinations and in part computed from formula (5). For smaller parallaxes, however, equations (7) and (8) gave smaller values than those actually employed.

Formulae (7) and (9) have now been applied to a large number of parallaxes determined spectroscopically by Adams in order to find the systematic errors in his values. Stars of proper motion smaller than 0."020 annually have been excluded. Table II contains the result of the comparison. $\overline{M}_A$ is the mean absolute magnitude as determined by Adams, $\overline{m}$ the mean apparent magnitude, and $\underline{\pi}_A = 10^{0.2(\overline{M}-\overline{m})-1}$ the geometrical mean of the spectroscopic parallaxes; $\underline{\pi}_\tau$ and $\underline{\pi}_\nu$ have been computed by equations (7) and (9). $\underline{V'}$ is the geometrical mean of the radial velocities and $\overline{M}_1$ the absolute magnitude computed from

TABLE II

SYSTEMATIC ERROR OF SPECTROSCOPIC PARALLAXES

M	No.	$\overline{m}$	$\overline{M}_A$	$\underline{\pi}_A$	$\underline{\pi}_\tau$	$\underline{\pi}_\nu$	$\frac{1}{2}(\underline{\pi}_\tau+\underline{\pi}_\nu)$	$\underline{V'}$	$\overline{M}_1$	$O-C$ $\overline{M}_A-\overline{M}_1$
					A8–F7 Stars					
≦3.9	32	4.81	+2.54	0."035	0."034	0."043	0."038	km 10.3	+2.71	−0.17
≧4.0	33	5.89	+4.78	0.060	0.041	0.057	0.049	17.8	+4.34	+0.44
					F8–G7 Stars					
≦3.9	81	5.07	+1.49	0.019	0.024	0.020	0.022	11.0	+1.79	−0.30
≧4.0	104	6.61	+5.34	0.056	0.049	0.079	0.064	23.9	+5.64	−0.30
					G8–K4 Stars					
≦1.9	89	5.04	+1.00	0.0156	0.0161	0.0176	0.0168	10.3	+1.16	−0.16
≧2.0	91	6.87	+5.26	0.0477	0.0421	0.0460	0.0441	18.9	+5.09	+0.17

$$\overline{M}_1 = \overline{m}+5+5\log\pi , \qquad (10)$$

where

$$\pi = \tfrac{1}{2}(\underline{\pi}_\nu+\underline{\pi}_\tau) .$$

Formulae (7) and (9) for the mean parallax appear to possess some advantages over those commonly used when the range in proper motion is large. It is not necessary that the variation in π be very small, which is an essential condition both in Campbell's formula $\overline{\pi} = k\overline{\tau}/\overline{V'}$ and in the formula for computing mean parallaxes from the parallactic motion, namely,

$$\Sigma V_\nu = 0 ,$$

or

$$\pi = -\frac{kv\,\overline{\sin d}}{V_0\,\overline{\sin^2 d}}\,.$$

In order to secure this result, the stars usually are divided into groups of the same proper motion and apparent magnitude, but we then often obtain groups which are too small to furnish values of π accurate enough for deriving absolute magnitudes. Further if the geometrical mean of π is used, we can compute directly from the mean apparent magnitude the mean absolute magnitude, whatever the range in π.

The largest difference in absolute magnitude in Table II is only 0.4, corresponding to an error in the parallax of $\frac{1}{5}$ of its value. We may therefore assume that the systematic errors in the spectroscopic parallaxes are comparatively small.

AVERAGE RADIAL VELOCITY AND ABSOLUTE MAGNITUDE

In the paper by Adams and myself it was stated that a very pronounced correlation exists between absolute magnitude and average radial velocity. In that investigation types F and G were combined as well as types K and M. I have now treated types F, G, and K separately and have found as before that no appreciable effect of distance can be detected by studying separately stars at nearly the same distance. In addition, I have computed the so-called *K*-term, i.e., the algebraic mean of the radial velocities corrected for the sun's motion. With reversed sign this term can be regarded as the systematic correction to the measured radial velocities, on the assumption that the algebraic sum of the radial velocities corrected for the sun's motion is equal to zero.

The results are in Table III. $\overline{M}$ is the mean absolute magnitude, $\overline{m}$ the mean apparent magnitude, $\underline{\pi}$ the geometrical mean of the parallaxes, $\underline{V'}$ the geometrical mean of the radial velocities corrected for the sun's motion, θ the average radial velocity regardless of sign, and K the algebraic mean of the radial velocities. The radial velocities are here corrected for the sun's motion, the constants

$$A = 270^\circ, \qquad D = +30^\circ, \qquad V = 20.0\ \text{km}$$

being assumed. The ratio of the number of stars within galactic latitudes +30° and −30° to the whole number of stars in the group is denoted by c, which is, accordingly, a measure of the galactic condensation. Were the stars uniformly distributed over the sky the value of c would be 0.5.

TABLE III

RADIAL VELOCITY AND ABSOLUTE MAGNITUDE

M	No.	$\overline{M}$	$\overline{m}$	$\underline{\pi}$	$\underline{V'}$	c	No.	θ	K
	F Stars								
					km			km	km
≦0.9	56	0.24	4.16	0″.016	7.0	0.86	56	10.8	+0.8
1.0–1.9	73	1.54	4.83	.022	9.7	.55	73	14.4	+0.8
2.0–2.9	66	2.42	5.32	.026	8.6	.64	65	12.9	−1.5
≧3.0	104	4.28	5.70	.052	15.3	.45	92	16.3	−1.0
	299	2.44	5.12	0.029	10.4	0.59	286	14.0	−0.3
	G Stars								
≦0.9	152	0.31	4.91	.012	7.8	.66	149	11.3	+1.3
1.0–1.9	112	1.38	5.76	.013	10.0	.50	108	13.1	+0.2
2.0–3.9	58	2.74	5.60	.027	14.5	.50	51	17.2	−2.7
4.0–5.9	73	4.97	6.49	.050	15.3	.42	59	15.7	−2.3
≧6.0	36	6.90	7.36	.081	20.2	.39	30	21.2	−4.9
	431	2.25	5.70	0.020	11.0	0.53	397	14.1	−0.5
	K Stars								
≦0.9	124	0.52	4.18	.018	8.5	.72	124	13.5	+1.6
1.0–1.9	251	1.42	4.84	.021	11.6	.54	251	16.5	+1.8
2.0–4.9	108	2.59	5.08	.032	14.7	.53	107	21.0	+6.1
≧5.0	78	7.10	7.45	.085	17.4	.46	78	27.6	−7.9
	561	2.23	5.11	0.027	12.0	0.56	560	18.3	+1.2

Both the geometrical means, $\underline{V'}$, and the arithmetical means, θ, of the radial velocities show a decided increase with decreasing brightness. There is, however, for all three types an apparent deviation from a linear relationship between radial velocity and absolute magnitude. If we plot the numbers, we find a break in the straight line at absolute magnitude 2 for F stars, at 3 or 4 for G stars, and between 4 and 6 for K stars. The same break occurs in the K-term, the absolutely bright stars having a positive K-term and the absolutely faint a negative *K*-term. This break in the continuity is probably related to the division of stars into the giant and dwarf classes.

If we assume the mean velocity to be a function of the mass rather than of the absolute brightness, the more massive stars having smaller velocity than the less massive, we find that the ratio of luminosity to mass is larger for the giants than for the dwarfs. This is in harmony with Adams' results that the low-temperature lines are strengthened in the spectra of the dwarf stars.

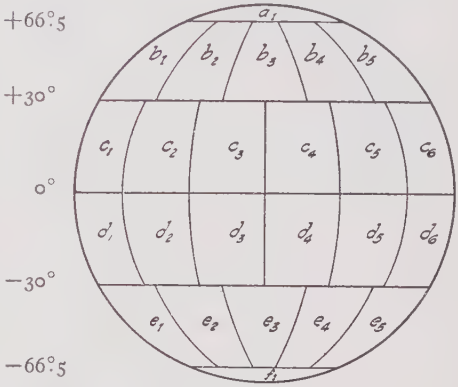

FIG. 2.—Distribution of forty-eight standard regions in the sky.

From Table III we find further that the very luminous stars show a much larger galactic concentration than the absolutely faint stars, the latter seeming rather to avoid the galaxy.

SOLAR MOTION AND ABSOLUTE MAGNITUDE

In order to find whether any decided relationship exists between the solar motion and the absolute magnitude, I have grouped the stars according to absolute magnitude, taking types F and G together. Only the radial velocities have been used in this investigation. Adopting a method of Charlier,[1] I divided the sky into 48 regions of equal area; but instead of using the equator as a plane of symmetry, I have grouped the stars in areas symmetrical to the galactic plane. This was done mainly to simplify the study of the stream-motion. Fig. 2 shows the location and designation of the areas.

Regions c_1 to c_{12} and d_1 to d_{12} are situated along the galactic equator between latitudes +30° and −30°, the origin of longitude being the intersection of the galactic and celestial equators. The regions b_1 to b_{10} and e_1 to e_{10} are situated between latitudes ±31° and ±66°. Regions *a* and *f* are in latitudes higher than ±67°.

---

[1] *Meddelanden från Lunds Observatorium*, Ser. II, No. 8, 1912.

The centers of gravity of regions a_1 to c_{12} are given in Table IV. The centers for areas *d*, *e*, and *f* have the same longitudes, but galactic latitudes −14°48, −45°1, and −80°, respectively.

TABLE IV

CENTERS OF GRAVITY OF STANDARD REGIONS

Region	Gal. Long.	Gal. Lat.	Region	Gal. Long.	Gal. Lat.
a_1..........	90°	+80°	c_1..........	15°	+14°48
a_2..........	270	+80	c_2..........	45	+14.48
b_1..........	18	+45.1	c_3..........	75	+14.48
b_2..........	54	+45.1	c_4..........	105	+14.48
b_3..........	90	+45.1	c_5..........	135	+14.48
b_4..........	126	+45.1	c_6..........	165	+14.48
b_5..........	162	+45.1	c_7..........	195	+14.48
b_6..........	198	+45.1	c_8..........	225	+14.48
b_7..........	234	+45.1	c_9..........	255	+14.48
b_8..........	270	+45.1	c_{10}..........	285	+14.48
b_9..........	306	+45.1	c_{11}..........	315	+14.48
b_{10}..........	342	+45.1	c_{12}..........	345	+14.48

The pole of the galactic plane is assumed to have the co-ordinates[1] $\alpha=190°6$, $\delta=+27°2$ (1900).

The equations for finding equatorial from galactic co-ordinates are then

$$\left.\begin{aligned}\cos\alpha\cos\delta&=+0.1846x+0.4494y-0.8740z\\ \sin\alpha\cos\delta&=-0.9828x+0.0844y-0.1642z\\ \sin\delta&=+0.8893y+0.4573z\end{aligned}\right\}\qquad(11)$$

where

$$x=\cos l\cos b,\qquad y=\sin l\cos b,\qquad z=\sin b.\qquad(12)$$

The use of the galactic co-ordinates instead of equatorial is of no advantage in the computation of the solar apex, but is very convenient in the study of the stream-motion.

The equation of condition for the determination of the sun's motion from radial velocities is

$$\gamma_1X_0+\gamma_2Y_0+\gamma_3Z_0+K=\overline{V},\qquad(13)$$

---

[1] *Groningen Publications*, No. 18, 1908.

which is to be computed for each region separately, γ_1, γ_2, and γ_3 being the direction-cosines of the center of gravity of the regions, $\overline{V}$ the algebraic mean of the observed radial velocities, K the K-term, and X_0, Y_0, and Z_0 the components of the motion of the centroid of the group of stars relative to the sun. Further,

$$X_0 = -V_0 \cos B_0 \cos L_0, \quad Y_0 = -V_0 \cos B_0 \sin L_0, \quad Z_0 = -V_0 \sin B_0 \quad (14)$$

where L_0 and B_0 are the galactic co-ordinates of the sun's apex and V_0 the sun's velocity.

The different regions have been given weights proportional to the number of stars in each. The results, with mean errors appended, are in Table V; θ is the average radial velocity.

TABLE V

SUN'S APEX AND VELOCITY

M	No.	$\overline{M}$	$\overline{m}$	A	D	V_0	K	θ
					F and G Stars			
						km	km	km
≦0.9	211	0.31	4.68	251°.6 ± 6°.6	+22°.7 ± 6°.1	19.4 ± 1.8	+ 0.2 ± 1.8	11.4
1.0–1.9	177	1.44	5.42	267.5 ± 11.0	+36.3 ± 12.4	16.6 ± 2.4	+ 0.0 ± 1.5	14.6
2.0–3.9	167	2.76	5.27	271.6 ± 9.0	+34.6 ± 10.0	22.0 ± 2.8	− 2.1 ± 1.7	16.2
≧4.0	170	5.29	6.41	279.7 ± 9.5	(+ 7.4 ± 9.9)	(26.5 ± 4.1)	− 1.9 ± 2.7	23.9
	725	2.32	5.40	268.1 ± 4.1	+25.2 ± 4.9	19.94 ± 1.38	− 0.69 ± 0.85	17.15
					K Stars			
≦0.9	122	0.54	4.22	282°.4 ± 9°.2	+32.8 ± 8.8	23.6 ± 2.6	+ 2.0 ± 1.6	13.6
1.0–1.9	245	1.41	4.86	268.6 ± 8.3	+36.5 ± 9.2	20.5 ± 2.4	+ 1.1 ± 1.4	16.6
2.0–4.9	99	2.58	5.12	282.1 ± 9.9	+16.1 ± 9.4	26.4 ± 4.6	+ 5.8 ± 2.4	18.1
≧5.0	79	7.07	7.41	(285.9 ± 28.9)	(−13.0 ± 34.4)	(15.3 ± 6.6)	(−11.1 ± 4.9	26.5
	545	2.25	5.13	277.5 ± 5.5	+32.2 ± 5.8	22.23 ± 1.73	+ 1.05 ± 1.00	18.46
					Giant M Stars			
Bright	135	1.5	4.98	264°.8 ± 7°.4	+26.3 ± 8.2	27.0 ± 3.3	+ 1.25 ± 1.86	16.9

There is an indication that the absolutely faint stars give a smaller declination of the sun's apex than the brighter stars, which is in harmony with the result that stars of large proper motion give a smaller declination of the apex than stars of small motion. This is usually explained on the two-drift theory: Drift I having the greater velocity relative to the sun, the stars belonging to it have on an average greater proper motions than those of Drift II. The relation to absolutely faint stars is partly the result of a selection of stars of large proper motion. The results for the faint stars, however, are very uncertain, as these have been observed mainly in the northern sky only (Mount Wilson Observatory).

Putting $K = 0$, the discrepancy in the declination of the sun's apex is much diminished. The results corresponding to this assumption are in Table V*a*.

TABLE V*a*

SUN'S APEX AND VELOCITY—*K*-TERM = 0

$\overline{M}$	A	D	V_0	θ
		F and G Stars		
			km	km
0.31	251°.4	+22.5	19.4	11.3
1.44	267.5	+36.3	16.6	14.6
2.76	272.1	+36.4	22.8	16.3
5.29	279.6	+10.9	27.1	23.9
2.32	268.3	+26.1	20.13	17.15
		K Stars		
0.54	279.6	+33.8	24.0	13.7
1.41	268.1	+37.2	20.4	16.6
2.58	284.5	+20.1	26.0	18.6
7.07	289.0	+26.5	22.1	26.2
2.25	277.0	+32.5	22.16	18.5
		Giant M Stars		
1.5	264.2	+26.1	26.8	16.9

From all later-type stars (excluding dwarf M stars) we find for the solar motion

$A_0 = 270°.9 \pm 3°.28$
$D_0 = +29.2 \pm 3.45$
$V_0 = 21.48 \pm 1.02$ km/sec
$\theta = 17.71$ km/sec
$K = +0.36 \pm 0.60$ km/sec

$K = 0$ (assumed)
$A_0 = 270°.7$
$D_0 = +29.0$
$V_0 = 21.42$ km/sec
$\theta = 17.71$ km/sec

No. of stars 1405

The values of θ are found a posteriori from the least-squares solution. Their increase with the decreasing brightness is well shown. There is no pronounced relationship between absolute magnitude and solar motion, except the decrease of declination for the intrinsically faint stars, which probably is partly an effect of different proportions of stars belonging to the two drifts. It is to be observed that these faint stars cannot be compared with apparently faint stars, which according to Dyson and others give a high declination for the sun's apex. The latter are mainly very distant stars, while the dwarfs are stars at very small distances.

PREFERENTIAL MOTIONS

The preferential motion of the stars used in this investigation has been determined from the radial velocities alone. Instead of using the dispersion—that is, the square root of the sum of the squares of radial velocities corrected for the solar motion divided by the number of stars—I have used the average radial velocity as a measure of the mobility in the line of sight. Squaring the velocities exaggerates the effect of a few high velocities, and even if we exclude velocities larger than a certain limit, there is often too great a number of high velocities near this limit. (Cf. Eddington, *Stellar Movements*, p. 147.)

The grouping of stars according to absolute brightness is very useful for the study of preferential motion, since the different groups are then more homogeneous as regards their mean velocities and only a very few stars of high velocity have to be excluded. Since the reductions for each star were computed before the solar motion was determined, I assumed for the latter $A=270°$, $D=+30°$, and $V_0=20.0$ km. These differ slightly from the values just found for the later-type stars, but the effect of the difference is quite inappreciable. No systematic correction has been applied to the measured radial velocities (K-term) since the values found in Table V have rather large errors, and are themselves probably too small to affect the result appreciably. The average velocity corrected for the sun's motion was computed for each region, the corrections for the sun's motion being determined separately for each star, and the co-ordinates of the center of the region were used for computing the velocity surface.

I have made use neither of the ellipsoidal theory nor of the method for computing the two drifts, but have employed a more general method, which enables me to take into account the difference in mean velocity at opposite points of the sky. We know that the sun is somewhat north of the real galactic plane, and, further, that the B-type stars and the apparently faint stars in general are not uniformly distributed in galactic longitude. If in accordance with Turner's suggestion we assume the stream-motion to be a gravitational effect, we cannot expect a priori the velocity surface to be symmetrical with respect to the sun, but may anticipate it to be related in some way to the eccentric position of the sun in the stellar system. Since the mean distance of the late-type stars is of the same order of magnitude as the distance to the center of the stellar system, we may expect asymmetrical (odd) terms in the analytical expression of the velocity surface. Such asymmetrical terms would also exist if the velocity of the stream-motion were different in different regions of space, which has been suggested by Kapteyn (*Mount Wilson Annual Report*, 1916, p. 255).

We desire to express the average radial velocity as a continuous function of the longitude and latitude of the different regions. We start from the following rational integral function of the direction-cosines:[1]

$$\begin{aligned} r=a_0+b_1x+b_2y+b_3z+c_1x^2+c_2y^2+c_3z^2+c_4xy+c_5xz \\ +c_6yz+d_1x^3+d_2y^3+d_3z^3+d_4x^2y+d_5xy^2+d_6x^2z \\ +d_7xz^2+d_8y^2z+d_9yz^2+d_{10}xyz+\ \ldots\ . \end{aligned} \tag{15}$$

in which r is the radius vector and equal to the average radial velocity θ, and x, y, and z are the direction-cosines of a point on the surface as defined by equation (12). We then have

$$x^2+y^2+z^2=1. \tag{16}$$

The intersection of this surface with the XY-plane has the equation

$$r=a_0+b_1x+b_2y+c_1x^2+c_2y^2+c_4xy+d_1x^3+d_2y^3+d_4x_2y+d_5xy^2+\ \ldots\ . \tag{17}$$

---

[1] Such a surface including terms of second order only was used by Eddington, *Monthly Notices*, 75, 521, 1915, as representing approximately an ellipsoidal velocity-distribution.

Introducing the longitudes we find

$$r=a_0+\beta_1 \cos l+\beta_2 \sin l+\gamma_1 \cos 2l+ \gamma_2 \sin 2l+ \ldots \quad (18)$$

whence we see that (17) can be represented by harmonic terms of the same order as the degree of equation (15). This property holds for every intersection of the surface with a plane through the origin, for the form of equation (15) is unaltered if we change the direction of the axes of the system of co-ordinates. The arguments of the harmonic terms are thus multiples of longitudes reckoned in the intersection plane. Taking into account this property, we find that the number of independent coefficients in the equation of the surface is $(n+1)^2$ where n is the degree of the equation. In equation (15) some of the coefficients are thus superfluous, a fact depending on the circumstance that x, y, and z are connected by equation (16). These we shall eliminate as follows.

It is convenient to define the coefficients in the expression for the surface in such a way that the terms in x, y, and z represent deviations from the mean radius vector. We therefore introduce the condition $\bar{r}=a_0$, $\bar{r}$ being the mean of all the radii vectores to the surface. The integral over the sphere for all other terms must be equal to zero. This is the case for each of the terms as they stand, except those involving x^2, y^2, and z^2. The condition that the integrals for the sum of these terms may also be zero is found as follows: Since x, y, and z are direction-cosines, the definite integrals of x^2, y^2, and z^2 over the sphere are equal. Denoting the value of these integrals by σ, the required condition is

$$(c_1+c_2+c_3)\sigma=0,$$

whence

$$c_3=-c_1-c_2.$$

To eliminate the remaining superfluous coefficients we write the identities

$$\left.\begin{aligned} \alpha x^3+\alpha xy^2+\alpha xz^2-\alpha x=0 \\ \beta x^2y+\beta y^3+\beta yz^2-\beta y=0 \\ \gamma x^2z+\gamma y^2z+\gamma z^3-\gamma z=0 \end{aligned}\right\} \quad (19)$$

where α, β, and γ are quite arbitrary. Assuming

$$d_7+\alpha=d_8+\gamma=d_9+\beta=0$$

and adding equations (15) and (19) and simplifying, we find

$$\begin{aligned} r=\bar{r}&+B_1x+B_2y+B_3z+C_1x^2+C_2y^2-(C_1+C_2)z^2+C_3xy+C_4xz \\ &+C_5yz+D_1x^3+D_2y^3+D_3z^3+D_4x^2y+D_5xy^2+D_6x^2z+D_7xyz, \end{aligned} \tag{20}$$

which contains no superfluous coefficients.

Introducing now longitudes and latitudes defined by equation (12), we find the following trigonometrical expression for the surface:

$$\begin{aligned} r=\bar{r}&+\beta_1 \cos b \cos l+\beta_2 \cos b \sin l+\beta_3 \sin b+\gamma_1 \cos^2 b \cos 2l \\ &+\gamma_2 \cos^2 b \sin 2l+\gamma_3(2/3-\cos^2 b)+\gamma_4 \sin 2b \cos l \\ &+\gamma_5 \sin 2b \sin l+\delta_1, \cos^3 b \cos 3l+\delta_2 \cos^3 b \sin 3l \\ &+\delta_3 \cos^3 b \cos l+\delta_4 \cos^3 b \sin l+\delta_5 \sin^3 b \\ &+\delta_6 \cos^2 b \sin b \cos 2l+\delta_7 \cos^2 b \sin b \sin 2l. \end{aligned} \tag{21}$$

Equation (21) is the expression for the surface to terms of the third order inclusive. For application I have changed the form of (21) somewhat in order to separate the terms more easily and to secure nearly the same variation in the different trigonometrical combinations, so that the coefficients may indicate nearly the real effect of the different terms.

The form used is:

$$\begin{aligned} \theta=a_0&+a_1 \cos b \cos l+a_2 \cos b \sin l+a_3 \sin b+a_4 \cos^2 b \cos 2l \\ &+a_5 \cos^2 b \sin 2l+a_6 (2-3 \cos^2 b)+a_7 \sin 2b \cos l \\ &+a_8 \sin 2b \sin l+a_9 \cos^3 b \cos 3l+a_{10} \cos^3 b \sin 3l \\ &+a_{11} \cos 3b \cos l+a_{12} \cos 3b \sin l+a_{13} \sin 3b \\ &+a_{14}\, 8/3 \cos^2 b \sin b \cos 2l+a_{15}\, 8/3 \cos^2 b \sin b \sin 2l. \end{aligned} \tag{22}$$

The terms with coefficients a_1 to a_3 are of the first order, a_4 to a_8 of the second order, and a_9 to a_{15} of the third order: i.e., they have 1, 2, and 3 maxima and minima, respectively. Each term represents a deviation from the sphere $\theta=\bar{\theta}=a_0$ but does not affect the mean value of $\bar{\theta}=a_0$ for the whole sphere.

Turning to Tables III and V, we find that average velocity is more closely related to absolute luminosity than to spectral type. For this reason and in order to obtain groups large enough for studying the variation in average velocity for different regions in the sky, the stars were divided into three groups having different radial velocities, each including stars of types F, G, and K. The first group contains the stars intrinsically brightest with absolute magnitudes equal to or less than 1.9 for F and G stars, and equal to or less than 0.9 for the K stars. The average radial velocity for this group varies from 11.4 to 14.6 km (see Table V). In the second group of stars, of absolute magnitudes 2.0–3.9 for F and G stars and 1.0–4.9 for the K stars, the average radial velocity ranges from 16.2 to 18.1 km. In the last group all stars fainter than these limits were taken together, with average velocity ranging from 23.9 to 26.5 km. This group also includes 11 dwarf M stars with an average radial velocity of about 30 km. These groups are more homogeneous with regard to velocity and probably even to mass than groups based solely on spectral types. Further data are given in Table VI.

TABLE VI

GROUPS FOR STUDY OF PREFERENTIAL MOTION

Group	No.	$\bar{M}$	$\bar{m}$	$\underline{\pi}$	θ
					km
I Very bright.......	509	0.76	4.83	0″.015	13.11
II Bright...........	513	2.08	5.09	0.025	17.13
III Faint............	260	6.05	6.82	0.070	25.88

The average velocity for the stars of these groups in each of the standard regions, corrected for the sun's motion, is given in Table VII. The problem is the representation of these data by the surface defined by equation (22).

TERMS OF EVEN DEGREE

Since the terms of odd degree are equal and opposite in sign for opposite points in the sky, we may eliminate them by using the means for opposite regions. We can thus derive independently the terms of even degree. The corresponding equation,[1] representing radial velocities, is

$$\theta = a_0 + a_4 \cos^2 b \cos 2l + a_5 \cos^2 b \sin 2l + a_6 (2 - 3 \cos^2 b) \\ + a_7 \sin 2b \cos l + a_8 \sin 2b \sin l .$$

In combining opposite regions the average radial velocity was computed by giving weights proportional to the number of stars; but for the determination of the constants of the surface, the 24 means

---

[1] This expression was used by Hough and Halm for computing the solar motion on the assumption of two opposite streams (*Monthly Notices*, **70**, 94, 1909).

TABLE VII

Velocities for Standard Regions

Region	I		II		III		Region	I		II		III	
	θ	No.	θ	No.	θ	No.		θ	No.	θ	No.	θ	No.
	km		km		km			km		km		km	
a_1....	.....	0	8.3	7	35.3	11	f_1....	11.5	10	8.4	6	15.2	3
a_2....	5.9	4	18.2	13	25.8	3	f_2....	16.0	7	23.6	9	5.4	2
	5.9	4	14.7	20	33.3	14		13.3	17	17.5	15	11.3	5
b_1.....	11.8	12	18.4	17	31.4	14	e_1....	12.2	14	11.2	9	39.7	4
b_2.....	8.2	5	17.6	10	16.2	8	e_2....	12.2	6	15.3	12	27.9	9
b_3.....	13.0	12	20.3	6	(20.3)	1	e_3....	13.0	16	15.7	11	25.2	13
b_4.....	11.6	12	16.9	9	32.2	13	e_4....	13.9	9	21.3	7	21.9	9
b_5.....	14.8	17	16.2	10	26.4	13	e_5....	15.8	4	23.6	8	23.7	3
b_6.....	16.1	6	16.3	10	(34.5)	2	e_6....	14.0	4	8.8	15	(36.6)	1
b_7.....	11.6	5	21.9	8	8.6	5	e_7....	9.4	7	19.6	14	25.2	3
b_8.....	5.9	5	13.6	5	4.1	7	e_8....	8.6	5	18.1	16	(18.1)	1
b_9.....	8.0	4	17.7	11	31.0	8	e_9....	11.1	8	21.4	8	(30.8)	5
b_{10}....	14.0	3	17.0	14	35.8	8	e_{10}...	12.5	9	17.6	9	(36.3)	1
	12.20	81	17.63	100	25.7	79		12.25	82	16.68	109	27.1	49
c_1.....	10.8	15	22.1	12	20.2	9	d_1....	12.9	10	9.2	8	30.3	11
c_2.....	11.4	24	14.5	11	18.2	8	d_2....	14.3	26	19.1	18	23.8	8
c_3.....	14.8	12	15.3	21	22.9	7	d_3....	14.0	18	14.0	12	19.0	11
c_4.....	5.0	9	9.6	12	14.5	6	d_4....	16.0	18	19.9	21	26.7	6
c_5.....	10.4	13	16.2	8	39.0	9	d_5....	11.7	16	18.9	7	36.9	3
c_6.....	17.2	18	14.8	8	19.0	6	d_6....	18.0	12	20.2	8	32.0	8
c_7.....	18.2	11	20.0	7	27.5	4	d_7....	18.9	12	35.9	7	......	0
c_8.....	14.4	8	15.4	9	(0.8)	1	d_8....	11.2	14	14.3	10	(4.7)	1
c_9.....	9.2	12	9.7	10	......	0	d_9....	13.3	19	11.6	12	(0.7)	1
c_{10}....	9.1	4	16.3	14	(68.0)	1	d_{10}...	8.3	10	16.3	13	(25.7)	1
c_{11}....	18.6	9	15.7	12	(6.0)	2	d_{11}...	16.6	12	26.3	13	......	0
c_{12}....	16.6	8	17.6	8	29.7	8	d_{12}...	13.7	15	27.8	8	43.0	2
	13.07	143	15.47	132	24.1	61		14.09	182	19.03	137	26.5	52

thus obtained were given equal weight. The following values of the coefficients and their mean errors were found from a least-squares solution.

	Coefficient	I	II	III
		km	km	km
	a_0	12.97±0.42	17.29±0.58	25.46±1.33
$\cos^2 b \cos 2l$......	a_4	+ 2.54±0.75	+ 2.62±1.04	+ 5.13±2.37
$\cos^2 b \sin 2l$.......	a_5	− 0.51±0.75	− 1.81±1.04	− 5.68±2.37
$2-3 \cos^2 b$.......	a_6	− 0.58±0.46	− 0.42±0.63	+ 0.80±1.44
$\sin 2b \cos l$......	a_7	− 0.09±0.76	+ 0.90±1.05	− 1.76±2.39
$\sin 2b \sin l$.......	a_8	− 0.86±0.75	+ 0.77±1.03	− 0.30±2.35

The last three coefficients have rather large errors as compared with the coefficients themselves, and hence they might be excluded in computing the axes. Since all the terms, however, are of equal geometrical significance, we can secure a little more accuracy by taking all into account. The very small term $-0.09 \sin 2b \cos l$, however, has been omitted.

Introducing direction-cosines, we find

$$\begin{array}{rl}
\text{I} & \theta=12.97+3.12x^2-1.96y^2-1.16z^2-1.02xy-0.18xz-1.72yz \\
\text{II} & \theta=17.29+3.04x^2-2.20y^2-0.85z^3-3.62xy+1.80xz+1.54yz \\
\text{III} & \theta=25.46+4.33x^2-5.93y^2+1.60z^2-11.36xy-3.52xz-0.60yz
\end{array}$$

In forming the maxima and minima of these expressions for the determination of the position of the axes of the surfaces, we must take into account the condition (16). We therefore write equal to zero the partial derivatives of the function

$$\theta-\lambda\,(x^2+y^2+z^2-1),$$

in which λ is an arbitrary coefficient.

The direction-cosines x, y, and z of the axes of the surface are therefore given by the equations

$$\text{Group I..}\left\{\begin{array}{llll}
(+3.12-\lambda)x-0.51y & & -0.09z & =0 \\
-0.51x & +(-1.96-\lambda)y-0.86z & & =0 \\
-0.09x & -0.86y & +(-1.16-\lambda)z & =0
\end{array}\right.$$

$$\text{Group II..}\left\{\begin{array}{llll}
(+3.04-\lambda)x-1.81y & & +0.90z & =0 \\
-1.81x & +(-2.20-\lambda)y+0.77z & & =0 \\
+0.90x & +0.77y & +(-0.85-\lambda)z & =0
\end{array}\right.$$

$$\text{Group III..}\left\{\begin{array}{llll}
(+4.33-\lambda)x-11.36y & & -3.52z & =0 \\
-11.36x & +(-5.93-\lambda)y-0.60z & & =0 \\
-3.52x & -0.60y & +(1.60-\lambda)z & =0
\end{array}\right.$$

The discriminating cubics of these equations are

$$\begin{array}{rl}
\text{I} & \lambda^3-8.469\lambda-5.025=0 \\
\text{II} & \lambda^3-12.081\lambda-5.940=0 \\
\text{III} & \lambda^3-170.04\lambda+223.64=0
\end{array}$$

The roots of the cubics are

	λ_1	λ_2	λ_3
I	+ 3.17	−0.62	− 2.55
II	+ 3.70	−0.50	− 3.20
III	+12.32	+1.33	−13.65

The axes of the surfaces thus computed are in Table VIII.

The maximum axis, which can be assumed to be identical with the axis of preferential motion in the ellipsoidal and the two-drift theory, lies in all cases near the galactic equator. The intermediate axis lies in all cases nearest to the galactic pole.

TABLE VIII

VERTICES OF MOTION. TERMS OF EVEN DEGREE

Group	Axis	θ	l	b	α	δ
		km				
I	Maximum	16.14	174°3	+ 0°1	98°0	+ 5°1
	Minimum	10.42	84.3	+31.9	236.0	+83.2
	Third direction	12.35	264.4	+58.1	187.7	− 4.5
II	Maximum	20.98	164.0	− 8.0	85.9	+10.3
	Minimum	14.09	70.4	−23.6	348.4	+35.7
	Third direction	16.79	91.8	+64.9	189.4	+52.3
III	Maximum	32.38	148.5	+14.1	99.6	+34.1
	Minimum	17.32	56.2	+ 9.1	303.7	+53.4
	Third direction	25.58	294.2	+73.1	197.6	+11.7

For comparison I give here a list of other determinations of the principal vertex mainly from Eddington, *Stellar Movements*, p. 124:

		α	δ
Distant stars:	Kapteyn	91°	+13°
	Rudolph	96	+ 7
	Hough and Halm	90	+ 8
	Eddington	95	+ 3
	Schwarzschild	93	+ 6
	Eddington	94	+12
	*Hough and Halm	88	+27
	*Gyllenberg[1]	84	+ 5
	Raymond[2]	92	+ 4
	*Present Paper (I and II)	92	+ 8
Nearer stars:	Charlier	103	+19
	Dyson	88	+21
	Beljawsky	86	+24
	Raymond[2]	92	+35
	*Present Paper (III)	100	+34

(The asterisk indicates that the determination is based on radial velocities.)

---

[1] *Meddelanden från Lunds Observatorium*, Ser. II, No. 13, 1915.

[2] *Astronomical Journal*, **30**, 191, 1917.

There is here some indication that the nearer stars yield a higher declination for the principal vertex. The same result is found in the present investigation, the declination of the vertex having values +5°1, +10°3, and +34°1; and it is even more marked in the galactic longitudes 174°3, 164°0, 148°5.

ASYMMETRICAL TERMS

In order to find if there are systematic differences in the average radial velocities in opposite regions, I have computed the terms of the first and third orders in the expression for the surface given by equation (22). One-half of the difference of the average velocities for opposite regions represents their effect. The number of stars in some regions of the third groups being too small, I have discussed in this way only stars of the first and second groups.

The expression used for the asymmetrical terms is

$$\begin{aligned}\Delta\theta = {} & a_1 \cos b \cos l + a_2 \cos b \sin l + a_9 \cos^3 b \cos 3l + a_{10} \cos^3 b \sin 3l \\ & + a_{11} \cos 3b \cos l + a_{12} \cos 3b \sin l + a_{13} \sin 3b \\ & + a_{14}\, 8/3 \cos^2 b \sin b \cos 2l + a_{15}\, 8/3 \cos^2 b \sin b \sin 2l .\end{aligned}$$

The term $a_3 \sin b$ is omitted, the stars near the pole of the galaxy being too few to yield a good determination. In the second group I have replaced the term $a_{13} \sin 3b$ by the fifth-order term $a_{16} \sin 4b \cos b$, which proved to be very large.

Assigning equal weights to the different regions, a least-squares solution gave the following values for the coefficients:

		I	II
		km	km
$\cos b \cos l$	a_1	-1.21 ± 0.45	-0.47 ± 0.91
$\cos b \sin l$	a_2	$+0.84 \pm 0.45$	-0.35 ± 0.91
$\cos^3 b \cos 3l$	a_9	-1.94 ± 0.52	-1.87 ± 1.07
$\cos^3 b \sin 3l$	a_{10}	-2.15 ± 0.52	-2.47 ± 1.07
$\cos 3b \cos l$	a_{11}	$+0.74 \pm 0.53$	$+0.25 \pm 1.09$
$\cos 3b \sin l$	a_{12}	-1.34 ± 0.53	-0.29 ± 1.09
$\sin 3b$	a_{13}	-0.66 ± 0.38	....
$8/3 \cos^2 b \sin b \cos 2l$	a_{14}	$+0.98 \pm 0.47$	$+0.14 \pm 0.97$
$8/3 \cos^2 b \sin b \sin 2l$	a_{15}	$+0.32 \pm 0.47$	$+2.73 \pm 0.97$
$\sin 4b \cos b$	a_{16}	....	-2.35 ± 0.89

For the second group a new solution was made putting $a_1 = a_2 = a_{11} = a_{12} = a_{14} = 0$. The values were not changed, but the mean errors of the four remaining terms were reduced to ±0.94, 0.94, 0.85, and 0.78, respectively.

The complete expressions for the surfaces used in computing the maxima and minima are thus

$$\text{I}\quad \theta=12.97-1.21\cos b\cos l+0.84\cos b\sin l+2.54\cos^2 b\cos 2l$$
$$-0.51\cos^2 b\sin 2l-0.86\sin 2b\sin l-1.94\cos^3 b\cos 3l$$
$$-2.15\cos^3 b\sin 3l+0.74\cos 3b\cos l-1.34\cos 3b\sin l$$
$$+0.98\times 8/3\cos^2 b\sin b\cos 2l+0.32\times 8/3\cos^2 b\sin b\sin 2l$$
$$-0.58\,(2-3\cos^2 b)-0.66\sin 3b.$$

$$\text{II}\quad \theta=17.29+2.62\cos^2 b\cos 2l-1.81\cos^2 b\sin 2l+0.90\sin 2b\cos l$$
$$+0.77\sin 2b\sin l-1.87\cos^3 b\cos 3l-2.47\cos^3 b\sin 3l$$
$$+2.73\times 8/3\cos^2 b\sin b\sin 2l-0.42\,(2-3\cos^2 b)$$
$$-2.35\sin 4b\cos b.$$

In Figs. 3 and 4 are shown the intersections of these surfaces with the galactic equator. The radii vectores of the dots represent the average radial velocity for the squares along the galaxy, i.e., c_1+d_1, c_2+d_2, etc., whose values are in Table IX. The dotted curves are the intersections with the galactic equator of the surfaces containing only terms of second order.

TABLE IX

INTERSECTIONS OF VELOCITY SURFACE WITH GALACTIC EQUATOR

REGION	GAL. LONG.	I				II			
		No.	$\theta_{\text{obs.}}$	$\theta_{\text{comp.}}$	O−C	No.	$\theta_{\text{obs.}}$	$\theta_{\text{comp.}}$	O−C
			km	km	km		km	km	km
c_1+d_1........	15°	25	11.6	12.0	−0.4	20	16.9	16.0	+0.9
c_2+d_2........	45	50	12.9	12.2	+0.7	29	17.3	15.5	+1.8
c_3+d_3........	75	30	14.3	13.4	+0.9	33	14.8	17.6	−2.8
c_4+d_4........	105	27	12.3	11.4	+0.9	33	16.1	16.8	−0.7
c_5+d_5........	135	29	11.1	11.1	0.0	15	17.5	16.5	+1.0
c_6+d_6........	165	30	17.5	16.2	+1.3	16	17.5	20.4	−2.9
c_7+d_7........	195	23	18.6	19.0	−0.4	14	28.0	22.1	+5.9
c_8+d_8........	225	22	12.3	13.9	−1.6	19	14.8	16.3	−1.5
c_9+d_9........	255	31	11.7	8.8	+2.9	22	10.7	11.5	−0.8
$c_{10}+d_{10}$.......	285	14	8.5	11.8	−3.3	27	16.3	15.9	+0.4
$c_{11}+d_{11}$.......	315	21	17.4	17.0	+0.4	25	21.2	22.6	−1.4
$c_{12}+d_{12}$.......	345	23	14.8	15.8	−1.0	16	22.7	21.3	+1.4
		325				269			

For both groups of stars we find a very marked three-lobed curve of nearly the same general appearance and position in the galactic equator. The three maxima are produced by the large third-order terms $a_9 \cos^3 b \cos 3l$ and $a_{10} \cos^3 b \sin 3l$. The sums of these terms for the two groups are

$$\text{I}\quad 2.90 \cos^3 b \cos 3(l-76^\circ\!.0) \qquad \text{II}\quad 3.10 \cos^3 b \cos 3(l-77^\circ\!.6)$$

with mean errors in the coefficients of ±0.74 and ±1.33, respectively. They are of the same magnitude as the second-order terms which determine the stream-motion, namely,

$$\text{I}\quad 2.59 \cos^2 b \cos 2(l-174^\circ\!.3) \qquad \text{II}\quad 3.18 \cos^2 b \cos 2(l-162^\circ\!.7)$$

the mean errors here being ±1.06 and ±1.47. The evidence for these third-order terms has therefore much the same definiteness as that for the existence of the stream-motion.

The maxima of the surfaces were obtained by assuming approximate values of the longitudes and latitudes of the axes and computing corrections to their co-ordinates with the aid of the formulae

$$\Delta b\frac{\partial^2\theta}{\partial b^2}+\Delta l\frac{\partial^2\theta}{\partial b\partial l}+\frac{\partial\theta}{\partial b}=0$$

$$\Delta b\frac{\partial^2\theta}{\partial b\partial l}+\Delta l\frac{\partial^2\theta}{\partial l^2}+\frac{\partial\theta}{\partial l}=0$$

the derivatives being calculated with approximate value of b and l. The two principal maxima of the radius vector for each surface are given in Table X.

TABLE X

CO-ORDINATES OF MAXIMUM RADIAL VELOCITIES

Group	Maximum θ	l	b	α	δ
	km				
I.........	19.60	190°	+4°	109°	−7°
	17.50	324	−2	264	−33
II........	24.23	179	−18	84	−7
	26.33	322	−19	283	−41

An approximately symmetrical plane perpendicular to the galactic equator was found for the two surfaces in longitudes

$$\text{I}\quad L=258^\circ\!.6\pm5^\circ\!.9 \qquad \text{II}\quad L=256^\circ\!.6\pm3^\circ\!.0$$

Each of these directions nearly bisects the angle between the two maximal axes of the surfaces. In Figs. 3 and 4 the directions of the planes of symmetry are indicated by arrows.

VELOCITY SURFACE OF THE DWARF STARS

In order to find the longitudes of the maxima of the average radial velocities, a harmonic analysis was made taking together all stars between galactic latitudes $-66°$ and $+66°$. The values of θ for the different regions are found in Table XI.

TABLE XI

AVERAGE VELOCITIES—DWARF STARS

Region	Gal. Long.	No.	$\theta_{\text{obs.}}$	$\theta_{\text{comp.}}$	O−C
			km	km	km
$b_1+e_1+c_1+d_1$..........	16°.5	38	29.3	29.6	−0.3
$b_2+e_2+c_2+d_2$..........	49.5	33	21.7	21.6	+0.1
$b_3+e_3+c_3+d_3+c_4+d_4$....	90.0	44	21.9	23.2	−1.3
$b_4+e_4+c_5+d_5$..........	130.5	34	31.7	28.6	+3.1
$b_5+e_5+c_6+d_6$..........	163.5	30	26.2	29.7	−3.5
$b_6+e_6+c_7+d_7$..........	196.5	7	30.8	27.3	+3.5
$b_7+e_7+c_8+d_8$..........	229.5	10	12.4	15.3	−2.9
$b_8+e_8+c_9+d_9+c_{10}+d_{10}$...	270.0	11	12.8	11.7	+1.1
$b_9+e_9+c_{11}+d_{11}$..........	310.5	15	27.6	27.6	0.0
$b_{10}+e_{10}+c_{12}+d_{12}$........	343.5	19	34.0	33.9	+0.1

The computed average velocities were derived from the expression

$$\theta = 24.35 + 1.78 \cos l + 3.76 \sin l + 6.88 \cos 2l - 4.88 \sin 2l \\ - 0.17 \cos 3l - 2.01 \sin 3l,$$

which is the result of the analysis.

The maximum values of θ are in longitudes 157° and 340°, and there is further a pronounced minimum in longitude 252°. The longitude of the symmetrical plane is 254°, in close agreement with that found for the more distant stars. The curve is given in Fig. 5.

TENTATIVE EXPLANATION OF THE PROPERTIES OF THE VELOCITY SURFACE

It is possible that the asymmetrical form of the surface representing the average radial velocities $\theta = f(b, l)$ depends upon the eccentric position of the sun in the galactic system of stars. This suggestion is supported by the fact, derived by a consideration of

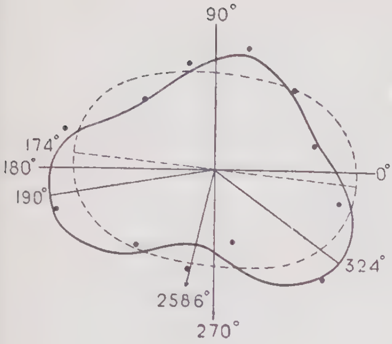

Fig. 3

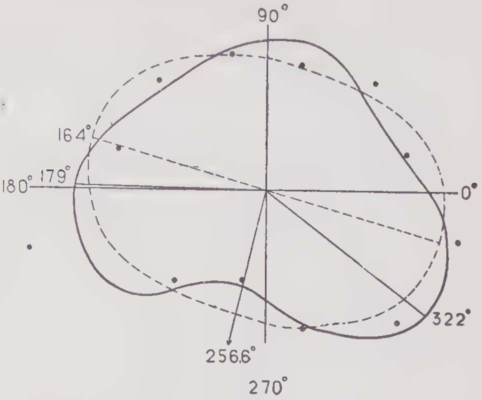

Fig. 4

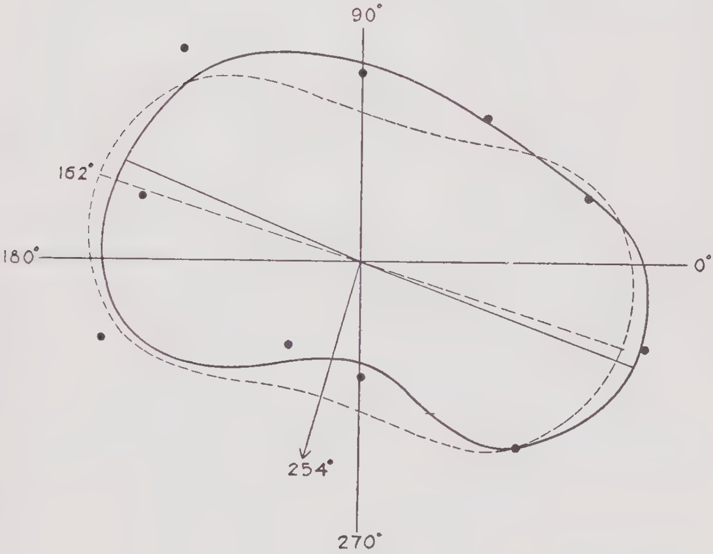

Fig. 5

Figs. 3, 4, 5.—Intersections between the average radial-velocity surfaces and the galactic equator for the three groups of stars—Fig. 3 for the stars intrinsically brightest and most distant, Fig. 5 for those intrinsically faintest and nearest, and Fig. 4 for the stars intermediate in luminosity and distance. The radii vectores of the points represent the average radial velocity (1 cm = 9 km/sec.) in regions adjacent to the galactic equator. The full curves are the intersections when terms to the third order inclusive are taken into account; the dotted curves, when terms of the second order only are used. The projections of the maximal axes of the surfaces are indicated by straight lines; the arrows indicate the longitudes of approximately symmetrical planes perpendicular to the galactic equator.

the terms depending on galactic latitude alone, that in all groups the average radial velocity is a maximum somewhat south of the galactic equator.

We thus find the following expressions for the variation in latitude alone:

$$\begin{array}{rl} \text{I} & \theta=12.97-0.58\,(2-3\cos^2 b)-0.66\sin 3b \\ \text{II} & \theta=17.29-0.42\,(2-3\cos^2 b)-2.35\sin 4b\cos b \\ \text{III} & \theta=25.46-0.37\,(2-3\cos^2 b)+4.95\sin b-4.94\sin 3b \end{array}$$

the last being derived from a separate analysis of the average velocities in the six different zones. The curve corresponding to Group II is given in Fig. 6.

All these functions have maximum values of θ for negative values of the latitude. Thus,

$$\begin{array}{rll} \text{I} & \theta_{\text{max.}}=13.9\text{ km} & b=-19^\circ\!.1 \\ \text{II} & \theta_{\text{max.}}=19.7\text{ km} & b=-19.9 \\ \text{III} & \theta_{\text{max.}}=28.4\text{ km} & b=-22.8^{1} \end{array}$$

Since the sun is situated north of the real galactic plane at a distance of about 20 parsecs, the result may possibly indicate a maximum of space velocity in this plane.

The position of the center of the galactic system has recently been determined by Charlier[2] and by Walkey.[3] Charlier gives for the co-ordinates of the center of 800 B-type stars

$$\alpha=115^\circ\!.5,\quad \delta=-55^\circ\!.6;\qquad l=236^\circ,\quad b=-14^\circ$$

$$\text{Distance}=18.21\text{ siriometers}=88.3\text{ parsecs.}$$

Walkey finds for 30,736 stars of all types $l=246^\circ$, and for the B and A stars separately

834 B stars, $l=239^\circ$
10,337 A stars, $l=250^\circ$

The last value agrees well with the longitude of the planes symmetrical to the velocity surfaces ($258^\circ\!.6$, $256^\circ\!.6$, 254°).[4]

---

[1] This, however, is not the principal maximum which lies at the galactic north pole.

[2] *Meddelanden från Lunds Observatorium*, Ser. II, No. 14, 1916.

[3] *Monthly Notices*, **74**, 649, 1914.

[4] A new determination by H. Nort of the star-densities as a function of galactic longitude has recently appeared. He finds from the Harvard Map of stars down to eleventh magnitude a largest concentration at longitude 275° (*Recherches Astronomiques de l'observatoire d'Utrecht*, **7**, 1917).

We may assume that the maximum of average radial velocity occurs when the angle between the line of sight and the direction of preferential motion in space is a minimum. The fact that the two maximal axes of the surface are inclined to each other might therefore be interpreted as a result of a preferential motion around the center in both directions. The plane of symmetry of the surface would then contain the center around which the stars are moving. The agreement between the longitudes of the symmetrical planes and the longitude of the center of the galaxy as determined by Charlier and Walkey supports this hypothesis. The increase in the values of the difference in the longitudes of the axes of maximum radial velocity (134°, 143°, and 183°), as we pass from the distant stars to the nearer, is also in harmony with such a suggestion. Further, if the stars are moving around the center of the stellar system, we may expect a minimum of orbital velocity near the center.[1] Such a minimum is perhaps indicated by the exceptionally small values of the radial velocity near longitude 257°.

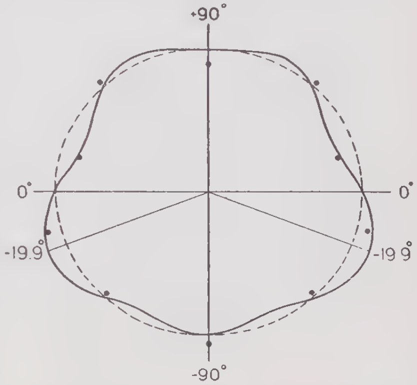

FIG. 6.—Intersection of a plane through the axis of the galaxy with the surface of revolution representing the average radial velocities for stars of Group II when terms depending on galactic latitude alone are included. Dotted curve corresponds to terms of even orders.

That the stream-motion possibly is a motion around the center of the galaxy is further indicated by the fact that the axis of preferential motion is in the galactic plane and nearly perpendicular to the direction toward the center of the stellar system.

The increase in average radial velocity with decreasing brightness is well shown in Figs. 3–5, which are drawn to the same scale. For almost every region when separately considered the radius vector increases with decreasing brightness in passing from Group I to Group III.

---

[1] Strömgren, "Über Bewegungsformen in Globular Clusters," *Astronomische Nachrichten*, **203**, 17, 1916.

SUMMARY OF RESULTS

The radial velocities of stars of spectral types F, G, and K have been studied, the stars being grouped according to absolute luminosity with the aid of Adams' spectroscopic parallaxes. The relationship of proper motion to parallax has been determined, and the systematic errors in these parallaxes have been calculated by assuming the same frequency-distribution of the velocity-components in the line of sight as at right angles to it. The variation with absolute brightness of average radial velocity, of the K-term, of galactic concentration, of the solar motion, and of the stream-motion has been studied. The following are the main results.

1. In the formula of Kapteyn for computing mean parallax from proper motion and apparent magnitude it is necessary to add a term c to the proper motion in order to secure satisfactory agreement with the measured parallaxes of the very distant stars. The parallaxes of these stars appear to be almost independent of proper motion.

2. The systematic errors in Adams' spectroscopically determined parallaxes are small, the maximum error being one-fifth of the parallaxes.

3. For stars of types F, G, and K there seems to be a steady increase of average radial velocity with decreasing brightness. For all three types there seems to be a break in the linear relationship, corresponding to the division into giants and dwarfs. If we suppose the relation between velocity and luminosity to be an effect of mass, the giants probably have a higher ratio of luminosity to mass than the dwarfs.

4. The intrinsically bright stars have a higher galactic concentration than the fainter stars.

5. The K-term seems to be positive for the brightest stars and negative for the fainter stars.

6. No decided relationship between the constants of the solar motion and absolute brightness could be found. The intrinsically faint stars show, however, a somewhat lower declination for the

sun's apex than the brighter ones. Since the fainter stars have been observed mainly in the Northern Hemisphere, the declination of the apex is somewhat uncertain.

7. The preferential motions of three different groups of stars have been studied, the groups including stars of different luminosities and distances. A general expression for a surface representing a continuous variation of the radius vector (=average radial velocity) with direction has been used. This takes into account not only symmetrical terms affecting opposite points in the sky equally, but also asymmetrical terms with opposite effects at opposite points. The major axis of this surface agrees well with the axis of preferential motion usually adopted, if only terms of even order are used. Adding terms of odd order (asymmetrical terms), we find that the two axes of maximum radial velocity are not in a straight line, but are directed toward points near the galactic equator, and differing in galactic longitude by 134°, 143°, and 183°, respectively, for the three groups. The best approximation for a symmetrical plane perpendicular to the galaxy has for the three groups galactic longitudes 259°, 257°, and 254°, which agree well with the longitude of the center of the stellar system as determined by Charlier and by Walkey. This perhaps indicates that the stars studied are mainly moving around the center of the galactic system, with a preferential motion in the galactic plane.

Mount Wilson Solar Observatory
October 1917

Contributions from the Mount Wilson Solar Observatory, No. 145
Reprinted from the *Astrophysical Journal*, Vol. XLVII, pp. 46–50, 1918

NOTE ON THE CEPHEID VARIABLE SU CASSIOPEIAE

BY WALTER S. ADAMS AND HARLOW SHAPLEY

A variation in the radial velocity of Boss 637, SU Cassiopeiae,[1] was found by Adams in the course of the regular spectroscopic work with the 60-inch reflector. The observations and measures were made without knowledge of the variations in light, as the star is not listed as variable in the *Preliminary General Catalogue*. The spectrograms on hand permit an inquiry into spectroscopic parallax, variation of velocity, and changes in spectral type, and the last may be compared with the analogous variations previously found from objective-prism plates. The material is discussed in the present note, which also includes some remarks on the variation in light.

The variability in brightness was detected in 1906 by Müller and Kempf[2] from the discordances in measures for the *Potsdam Photometric Durchmusterung*. A special photometric study indicated a variation between magnitudes 5.93 and 6.26, with a period defined by the formula,

$$\text{Max.} = \text{J.D. } 2417287.30 + 1.9498 . E, \quad \text{G.M.T.}$$

The visual light-curve was found to differ from that of typical Cepheids in its small amplitude and symmetrical form.

In 1906–1908 the star was observed photographically by J. A. Parkhurst,[3] who also found the variation peculiarly small and nearly symmetrical with respect to maximum light. The elements by Müller and Kempf being unsatisfactory, the period $1^{d}.9490$ was substituted for the value above. From the photographic magnitudes at maximum and minimum, 6.52 and 6.99, respectively, Parkhurst derived a variation in color-index from 0.59 to 0.73. An objective-prism plate at phase $1^{d}.28$ gave a spectrum of F3, in fair agreement with the color-index. Because of the star's faintness, the attempt to find a variation in radial velocity with the Bruce spectrograph and the 40-inch refractor was considered inconclusive, although the observed range was from −1 km to −16 km.

---

[1] $\alpha = 2^{h}43^{m}2^{s}.9$, $\delta = +68^{\circ}28'27''$ (1900.0).

[2] *Astronomische Nachrichten*, **173**, 307, 1907.

[3] *Astrophysical Journal*, **28**, 279, 1908.

An examination of the light-curve by Shapley[1] has shown that the variation cannot be interpreted as the result of the rotation of a simple ellipsoidal body. The conclusion that the star is a Cepheid, notwithstanding the form and amplitude of its light-curve, is verified by the spectroscopic work described below.

Variations in spectral type from A8 to F5 were recorded in 1916 on plates made with the 10-inch photographic telescope at Mount Wilson.[2] The type of spectrum and the brightness of the spectral images (compared with those of neighboring stars) indicated that neither the formula by Müller and Kempf nor its modification by Parkhurst then represented the variation in light; but the epoch given by Müller and Kempf with an intermediate value of the period, $1^{d}.94935$, was found sufficiently accurate for the work on spectral variation.

A new investigation of the period has now been made, employing (1) the observations made at the Potsdam and Yerkes observatories; (2) a redetermination of the magnitudes on the objective-prism plates of 1915 and 1916; and (3) a series of visual estimates on four nights in August, 1917. The result has been checked with the observations of spectral type mentioned in the preceding paragraph, as well as those derived from the slit spectrograms, and with the observations of radial velocity given below. The variations in light, velocity, and spectrum are all relatively small and gradual, making high accuracy for the elements impossible. The following formula, however, gives satisfactory phases for all variations:

$$\text{Max.} = \text{J.D. } 2417287.10 + 1.9495 \cdot \text{E}, \quad \text{G.M.T.}$$

There is some evidence that the period is not constant.

The spectroscopic observations with the 60-inch telescope are given in Table I. The phases have been computed from the preceding maximum of the light-curve. Describing the velocity-variations in terms of the orbital elements of a spectroscopic binary, the following results are obtained from a graphical solution:

---

[1] *Astronomische Nachrichten*, **194**, 357, 1913.

[2] *Mt. Wilson Contr.*, No. 124; *Astrophysical Journal*, **44**, 273, 1916.

$$
\begin{aligned}
\text{Epoch of Max. Vel. of Approach} &= \text{J.D. } 2420197.65,\ \text{G.M.T.}\\
\text{Period} &= 1^{d}9495\\
e &= 0.0\\
K &= 11.0\ \text{km/sec.}\\
V_0 &= -7.0\ \text{km/sec.}\\
a \sin i &= 295{,}000\ \text{km}\\
\frac{m^3 \sin^3 i}{(m+m_1)^2} &= 0.0003\,.
\end{aligned}
$$

The epoch of maximum negative velocity precedes the maximum of light by $0^{d}05$. The elements are entirely typical of Cepheid variables that have small ranges of velocity and nearly symmetrical velocity-curves. In Fig. 1 the observations are plotted along the computed velocity-curves. The average deviation is ± 1.5 km.

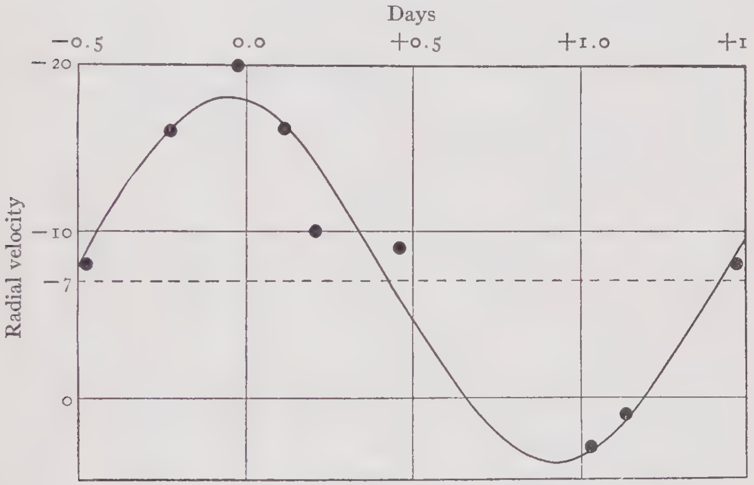

FIG 1.—Velocity-curve of SU Cassiopeiae

The spectral types determined by Adams from the spectrograms made with the 60-inch reflector are given in the last column of

Table I. The types derived by Shapley from the plates made with the 10-inch refractor are in Table II,[1] with phases based on the new elements. The variation of spectrum with magnitude is illustrated in Fig. 2.

TABLE I

Observations with 60-Inch Reflector

Plate	Date	J.D. and G.M.T.	Epoch	Phase	Velocity	Spectrum
					km	
γ 2897....	1913 Nov. 16	2420088.745	1437	$0^{\mathrm{d}}21$	−10	F2
3072....	1914 Feb. 1	0165.692	1476	1.13	+ 1	F5
3171....	Mar. 5	0197.675	1492	1.93	−20	F0
3898....	Nov. 24	0461.915	1628	1.04	+ 3	F6
5116....	1916 Oct. 7	1144.943	1978	1.73	−16	F0
5239....	Nov. 9	1177.821	1995	1.47	− 8:	F3
5311....	Dec. 7	1205.706	2010	0.12	−16	F2
6200....	1917 Sept. 6	1478.986	2150	0.47	− 9	F4

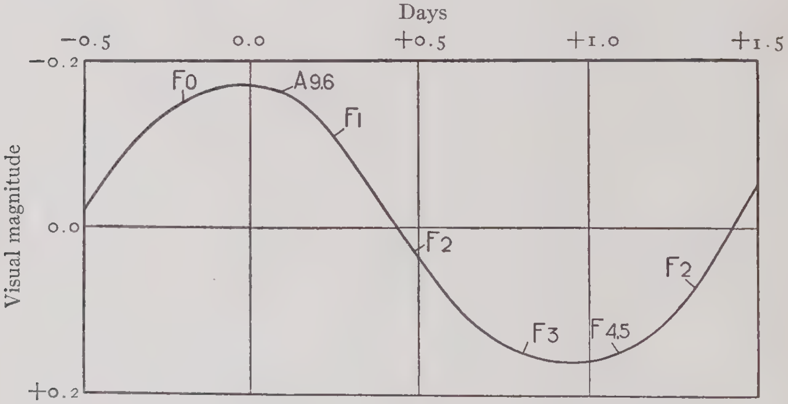

Fig. 2.—Variation of the spectral type of SU Cassiopeiae

The proper motion of SU Cassiopeiae is mainly parallactic, being 0″016 in position-angle 108°. The parallax, according to a recent determination by van Maanen,[1] is $+0\overset{''}{.}010 \pm 0.003$; the spectroscopic parallax is in exact agreement if the visual magnitude is taken to be 6.23, as given in the *Preliminary General Catalogue.* With the corresponding value of the distance, the total velocity in space with respect to the sun is 10 kilometers a second.

---

[1] *Mt. Wilson Contr.*, No. 124; *Astrophysical Journal*, 44, 273, 1916. Types marked as uncertain in the earlier paper are now omitted, and a typographical error is corrected. A new classification of all plates yielded but one correction; for the plate on Julian Day 2420841 the spectrum is F3 instead of F1.

TABLE II

OBSERVATIONS WITH 10-INCH REFRACTOR

J.D. and G.M.T.	Epoch	Phase	Spectrum	J.D. and G.M.T.	Epoch	Phase	Spectrum
2420841.836...	1823	$0\overset{\mathrm{d}}{.}80$	F3	2420900.727...	1853	$1\overset{\mathrm{d}}{.}21$	F2
0894.775...	1850	1.11	F3	0900.731...	"	1.21	F1
0894.782...	"	1.11	F4	0901.685...	1854	0.21	A9
0896.711...	1851	1.09	F5	0901.694...	"	0.22	F0
0899.622...	1853	0.10	A9	0901.702...	"	0.23	F2
0899.631...	"	0.11	A8	0901.714...	"	0.24	F1
0899.820...	"	0.30	F2	0901.725...	"	0.25	F0
0899.832...	"	0.31	F0	0901.737...	"	0.27	F0
0900.722...	"	1.20	F2				

MOUNT WILSON SOLAR OBSERVATORY
November 1917

[1] *Mt. Wilson Contr.*, No. 136, 1917.

Contributions from the Mount Wilson Solar Observatory, No. 146
Reprinted from the *Astrophysical Journal*, Vol. XLVII, pp. 189–192, 1918

RADIAL VELOCITY AND ABSOLUTE MAGNITUDE

COMMENTS ON PROFESSOR PERRINE'S ARTICLE[1]

BY WALTER S. ADAMS AND GUSTAF STRÖMBERG

Professor Perrine has been so kind as to send us the manuscript of his article in advance of publication, and it will perhaps aid the reader to form a clearer idea of the points at issue if we comment briefly upon certain matters involved. The question is primarily one of the interpretation of the increase of radial velocity with proper motion. Perrine considers this as mainly an effect of distance from the sun, while we regard it as dependent principally upon the absolute magnitudes of the stars considered.

In Tables I and II of his article Perrine has divided the stars into two groups defined by proper motions less than 0."1 and greater than 0."1, respectively. Within these groups he arranges the stars according to apparent magnitude and gives the radial velocities along the axes of the ellipsoid. Of the stars in Tables I and II he says: "In the stars of small μ (Table I) the average μ is not given for the different groups of magnitudes, but it will probably not differ very greatly, as the same superior limit was adopted for all. . . . . In Table II the range of values of μ is considerable and is taken into account." As a result of this argument Perrine concludes that the grouping by apparent magnitude becomes a grouping according to relative absolute magnitude as well.

To this mode of treatment of the stars in Table I we are obliged to object seriously. The dispersion in distance among these stars is enormous, much greater than that for the stars in Table II, if we assume, as Perrine does, that distance is inversely proportional to proper motion. Since B stars are included by him in Table I, we may have a range of from 0."001 to 0."100 in the proper motion, or a range in distance of 100 to 1 on this basis. It would be more correct, in studying the relation of velocity to distance, to assume that the stars within the zone of proper motions larger than 0.″1 are all at the same distance than to assume this for the more distant stars without proof. It is therefore not possible to conclude that the grouping of stars according to apparent magnitude in Table I corresponds to a grouping according to absolute magnitude.

---

[1] *Astrophysical Journal*, **47**, 189, 1918.

A second very natural objection to Perrine's method of applying to the radial velocities of the stars in Table II factors which will reduce all the stars to the same proper motion (and distance) is the nature of the consequences involved. If a group of stars with an average proper motion of 0.″3 has one-half the average radial velocity of a group with a proper motion of 0.″6, the velocity of a group with proper motion of 0.″005 will be far less than any average observed radial velocity. It would be necessary to assume that the change of velocity with distance is greatest near the sun. This involves the remarkable assumption that the sun is a singular point in space (at the present time), and also it is opposed to Perrine's hypothesis that cosmical matter acts as a resisting medium, since he supposes this matter to lie in relatively distant galactic regions.

In a discussion of our results Perrine concludes that in the two groups of stars of types F and G, and K and M, which have the largest parallaxes, there is a "small but well-defined progression in the mean parallaxes of the groups in the same direction as the progression in velocity." This is quite true, but this progression corresponds to an exceedingly small range in distance when compared with that of the more distant stars. The two groups to which he refers have parallaxes larger than 0.″05. If velocity is inversely proportional to distance within this comparatively narrow zone, as Perrine assumes when reducing to the same proper motion, we should have a velocity approaching zero at a relatively small distance, a conclusion which is contradicted by observation.

Perrine selects from our results only two groups of stars from a total of thirteen, since the parallaxes are most reliable in the case of the larger values. No doubt the distances of the nearer stars are known more accurately, but it is quite inadmissible to neglect the evidence afforded by the stars of small parallax. One of the principal advantages of the spectroscopic method of deriving parallaxes is that it is independent of their absolute values. Accordingly the relative determinations of distance, even among the stars of smallest parallax, should be entitled to considerable weight. We find, however, that the average radial velocity for a group of over 200 stars with an average parallax of about 0."010 is practically the same as that for a similar group with a parallax of 0."050 of the same absolute magnitude.

Two other statements by Professor Perrine require a word of comment. His reference to Tables V and VI of our previous article as indicating increase of radial velocity with increase of parallax is due to a misconception of their purpose. Among the very distant stars we cannot observe stars of very low absolute magnitude, since such stars are apparently too faint. Accordingly Tables V and VI naturally show a progression of magnitude with increase of parallax and radial velocity. The attempt to separate the effect of distance from that of absolute magnitude is confined to the previous discussion, and the results are contained in Table IV.

As regards the effect of stream-motion upon our velocities, no attempt was made to eliminate it completely from our earlier results. There can, however, be no doubt that its influence was reduced greatly by our inclusion of velocities at right angles to the line of sight, and the confirmatory evidence obtained from these values is of considerable importance. An extended investigation of stream-motion as related to absolute magnitude has since been made by Strömberg.[1] Its results are in agreement with our previous conclusions.

In general, it may be said that the principal cause of difference between Professor Perrine and ourselves is one of point of view. We have attempted in our discussion of stellar motions to find a fundamental relationship which would apply over the entire range of distance and absolute magnitude which has been investigated. For the reasons already given it does not seem possible to conclude that a law making radial velocity inversely proportional to distance from the sun can hold over more than a very limited range.

---

[1] *Mt. Wilson Contr.*, No. 144; *Astrophysical Journal*, **47**, 7, 1918.

Outside of a comparatively narrow limit it would give values of the radial velocity much too high or too low, unless the law were modified greatly. Moreover, such a relationship would assign to the sun an extraordinary position in the stellar system, which we have no reason for believing that it holds. It is a star of very moderate size and mass, and is known to lie at a comparatively great distance from the center of the galaxy. It would seem far more probable that any relationship between velocity and distance would be one in which the latter was measured from some much more fundamental reference point than our sun.

Mount Wilson Solar Observatory
February 1918

ON THE PARALLAXES AND MOTION OF THE BRIGHTER GALACTIC HELIUM STARS BETWEEN GALACTIC LONGITUDES 150° AND 216°

By J. C. KAPTEYN

CONTENTS

PAGE
1. INTRODUCTION 3
2. THE MATERIALS 4
3. THE NEBULA-GROUP 5
4. SYSTEMATIC ERROR IN BOSS'S μ_{α} AND μ_{δ} 6
5. FIRST DETERMINATION OF THE ELEMENTS 11
6. COMMUNITY OF MOTION OF THE FOUR GROUPS 13
7. COMMUNITY OF MOTION (*Continued*) 15
8. INFLUENCE OF SYSTEMATIC ERROR AND SUMMARY OF DEFINITIVE ELEMENTS 19
9. OBSERVED DISTRIBUTION OF THE VALUES OF v 20
10. OBSERVED DISTRIBUTION OF THE VALUES OF τ 22
11. PROBABLE VALUE OF r_u AND DISTRIBUTION OF THE COMPONENTS OF THE PECULIAR MOTION 24
12. REMARKS 30
13. RANGE IN DISTANCE OR PARALLAX AS A FUNCTION OF λ AND v . . 32
14. CASE $r_u = 0.0$ 41
15. PROBABLE ERRORS OF THE PARALLAXES 44
16. APPLICATION OF THE METHOD TO THE VALUES OF τ 46
17. ADDITIONAL EVIDENCE AS TO THE VALUES OF THE PARALLAXES . . 49
18. THE NEBULA-GROUP. ITS PARALLAX 56
19. TESTS FOR THE PARALLAX OF THE NEBULA-GROUP 63
20. MOTION OF THE NEBULA-GROUP 63
21. LUMINOSITY-CURVE OF THE B0–B5 STARS 65
22. LUMINOSITY-CURVE OF THE B8–B9 STARS 68
23. LUMINOSITY-CURVE OF THE B3 STARS 69
24. LUMINOSITY-CURVE OF THE B5 STARS 70
25. FURTHER LUMINOSITY-CURVES AND SUMMARY OF RESULTS . . . 71
26. LUMINOSITY-CURVE OF THE A STARS 73
27. REMARKS ON THE GEOMETRICAL FORM OF THE LUMINOSITY-CURVES 79
28. SUMMARY 86
29. NOTATION 92

Contributions from the Mount Wilson Solar Observatory, No. 147
Reprinted from the *Astrophysical Journal*, Vol. XLVII, 1918

ON THE PARALLAXES AND MOTION OF THE BRIGHTER GALACTIC HELIUM STARS BETWEEN GALACTIC LONGITUDES 150° AND 216°

By J. C. KAPTEYN[1]

I. INTRODUCTION

In *Mount Wilson Contribution* No. 82 an attempt was made to derive the individual parallaxes and motions of practically all the known helium stars between galactic latitudes ±30° and galactic longitudes 216°–360°. The present paper aims at a similar determination for stars within the same limits of latitude and between longitudes 150°–216°.[2]

As in the earlier publication, the limits in latitude were thus chosen in order that the overwhelming majority of the B stars should be included in such a way that a tolerable idea of their distribution in space could be obtained by projection on a single plane, namely, that of the galaxy. The limit at $l=216°$ forms the boundary between the stars of *Mount Wilson Contribution* No. 82 and those now under consideration; that at $l=150°$ has been chosen rather arbitrarily. There is at this point some indication of a natural limit in the arrangement of the bright helium stars of small proper motion ($\mu=0.''016$) shown by Plate IX in *Mount Wilson Contribution* No. 82. Whether later studies confirm this indication or not does not matter much, because it is my intention later to extend the study of the distribution of the helium stars to the remaining galactic longitudes, at least as far as possible. Down to longitude 110° provisional investigations already indicate that, here too, useful results may be expected.

The region now to be considered offers far greater difficulties than that treated in *Mount Wilson Contribution* No. 82. These are a consequence of the proper motions which, in general, are exceptionally small and, superficially, show scarcely any recognizable regularity in their directions. Under the circumstances it may seem a bold undertaking to subject these stars to a treatment which in general is applicable only to motions approximately parallel and equal. One circumstance, however, proves that below the apparent irregularity there must be hidden a real similarity: the radial velocities of the stars throughout the region vary relatively little. Hence (*a*) the stars must lie near the antivertex[1] and (*b*) the range of real velocity must be small.

---

[1] Research Associate of the Carnegie Institution of Washington, Mount Wilson Solar Observatory.

[2] A small supplementary group of 8 stars between $b=-30°$ to $-42°$, $l=156°$ to 178°, was added for a particular purpose (see Sec. 8).

Circumstance (*a*) explains why the proper motions are so small and makes large differences in the position angles of the motions appear as a necessity; (*b*) makes it all but certain that the seeming irregularities in the proper motions are not greater than might be expected among stars moving along approximately parallel lines with approximately equal velocities. As a matter of fact, investigation shows that the proper motions, instead of contradicting the conclusions as to the approximate equality of motion derived from the radial velocities, prove that the spectroscopic velocities give a very inadequate idea as to the degree of this equality. The seeming irregularity of the motions is due to the fact that the systematic part (stream-motion) is to a great extent obliterated by foreshortening, while the irregular part (peculiar motion) shows as strongly as anywhere else.

As the present investigation furnishes the parallaxes of practically all the B stars within the region considered, a map showing the positions of the stars in space might have been given, as was done for longitudes 216°–360° in *Mount Wilson Contribution* No. 82. I have not done so, in the hope that further investigation will furnish data for extending this map to include all of the B stars between $-30°$ and $+30°$ of galactic latitude.

2. THE MATERIALS

In the main I have used (as in *Mount Wilson Contribution* No. 82) all the B stars in Boss's catalogue, 168 in all. The spectra and the magnitudes have been taken from *Harvard Annals*, **50**, the proper motions from Boss. Besides these bright stars I had the good fortune to be able to include all the faint B and A stars within the limits

---

[1] The name "antivertex," in analogy with the name "antiapex," is used for the point around which the motions *converge*, whereas the name "vertex" is reserved for the divergent.

$$\text{R.A. } 5^{h}0^{m} \text{ to } 6^{h}0^{m} \quad \text{Dec. } -10° \text{ to } +20° \tag{1}$$

for which Miss Cannon has recently determined the spectra. This list contains 412 B and 760 A stars, many of them fainter than magnitude 9.0, some even fainter than 9.5.

It is a pleasure to me to extend my warmest thanks both to Professor Pickering and to Miss Cannon for their generous help and courtesy. In using their results I have had a foretaste of the vast possibilities that will be afforded by the completion of the undertaking known as the *Revised Draper Catalogue.*

3. THE NEBULA-GROUP

A glance at the lower map of Plate IX in *Mount Wilson Contribution* No. 82 shows that the bright B stars between $5^{h}20^{m}$ and $5^{h}40^{m}$, on both sides of the equator, are particularly crowded. This crowding, however, is shown with perfect distinctness only by the Pickering-Cannon stars. Defining the position of the group by hour- and parallel-circles we have the limits at

$$\text{R.A. } 5^{h}13^{m} \text{ and } 5^{h}40^{m} \quad \text{Dec. } -9° \text{ and } +5° \text{ (1900)}. \tag{2}$$

With a more complicated boundary-line we might diminish the area by about 20 per cent.

Within this boundary the B0–B5 stars are about 12 times and the B8–B9 stars about 5.7 times more numerous than in the surrounding regions. This alone proves, incontestably in my opinion, that we have to do with a local group which probably does not extend in depth much farther than it does laterally.

We have still further proof. The bright B stars, the stars of our list in Boss's catalogue within the limits (2), are almost exclusively of spectral types B0–B3, whereas outside the group they include a considerable number of B5–B9 stars. Omitting one star marked B whose subclass is unknown, I find the following numbers of stars:

	Oe5–B3	B5	B8–B9	
Within limits (2)................	23	1	1	(P)
Outside limits (2)................	80	21	41	

Add to this the facts that, as will presently appear, the radial velocities of the Oe5–B3 stars are very nearly equal, and consequently that the component u[1] of the peculiar motion is exceptionally small; that the component τ of the proper motion, as already explained, is not greater than the observational errors—all of which proves that the real motions of these stars are very nearly parallel and equal, much more so than is the case with the stars outside the limits (2); and there can be no doubt that we have to deal with a local group, somewhat of the nature of the Pleiades or the Hyades. As this local group surrounds the famous Orion Nebula, which very probably, though we cannot yet say certainly, forms part of the group, I will call it the Nebula-group.

4. SYSTEMATIC ERROR IN BOSS'S μ_α AND μ_δ

I will begin by studying the stars outside the Nebula-group. But such a study must of necessity be preceded by an investigation of the systematic errors in the proper motions of Boss's catalogue. In the case of proper motions so exceptionally small (a total motion as great as 0″.04 is found for only 6 per cent of our stars), such errors are of very considerable importance. It will be our aim not only to find plausible values for them, but to arrange all our calculations in such a way that the residual uncertainty has a minimum effect.

The determination of these errors will be based on the hypothesis that the direction of motion of the stars of small proper motion is not systematically different from that of the stars whose motions are somewhat more considerable. If the systematic motion of the B stars is wholly a parallactic displacement, as is generally assumed, the hypothesis will be justified. The same will be true if all the stars considered have the same stream-motion; only in the case of different stream-motions will it fail. To diminish the probability of such a state of affairs, and to increase the number of objects on which we can base our conclusions, stars in neighboring parts of the sky and of different spectra were included in the investigation.

The method itself I have explained in several places, for example, *Mount Wilson Contribution* No. 82, p. 48. Let p_1 represent the average position angle of the motions of stars of small proper motion, p_2 the same quantity for the stars of large proper motion, and suppose the two reduced to the same point of the sky. If then p_1 and p_2 differ, the difference will be attributed to systematic errors in μ_α and μ_δ. The equation of condition given in *Mount Wilson Contribution* No. 82 supposes that the corrections $\delta\mu_\alpha$ and $\delta\mu_\delta$ are small as compared with the motions μ_α and μ_δ themselves. In the present case, where the proper motions are as a rule so exceedingly small, the validity of such a supposition seems doubtful, and it will be preferable to use the equation in its rigorous form:

---

[1] For the meaning of our notation see *Mt. Wilson Contr.* No. 82, p. 76.

$$\frac{\mu_2 \cos p_2 - \mu_1 \cos p_1}{\mu_1 \mu_2}\delta\mu_\alpha - \frac{\mu_2 \sin p_2 - \mu_1 \sin p_1}{\mu_1 \mu_2}\delta\mu_\delta = \sin (p_2 - p_1) \qquad (3)$$

I began with the four regions (A) including most of the stars contained in the present paper, with the exception of the Nebula-group and its nearest surroundings.

$$\left.\begin{array}{llllllll}
\text{Group } 1 & l^{*}\ 150^\circ & \text{to} & 165^\circ & b\ -12^\circ & \text{to} & +\ 4^\circ \\
\text{“} \quad 2 & \text{“} \quad 200 & \text{“} & 216 & \text{“} \ -10 & \text{“} & +\ 3 \\
\text{“} \quad 3 & \alpha \quad 3^h30^m & \text{“} & 5^h12^m & \delta\ -17 & \text{“} & +\ 3 \\
\text{“} \quad 4 & \text{“} \quad 6\ 10 & \text{“} & 8\ 10 & \text{“} \ -16 & \text{“} & +10
\end{array}\right\} \qquad (A)$$

In order to increase the weight of the determination somewhat, I included not only the B stars, but also the A0–A3 stars with total proper motion below 0″.100. The spectra B0–B8 and B8–A3 were treated separately at first, but as no real difference seemed to exist the results were combined. The mean right ascensions and declinations of the stars of large and small proper motion were of course found to be slightly different. The reduction to the same point was made by adopting for the vertex the provisional position 17^h48^m, $+9^\circ$. The results obtained are given in Table I.

Substituting in (3) we find

$$\left.\begin{array}{rrrrrr}
 & & & \text{Average } \delta & \text{No. Stars} & \text{Adopted Weight} \\
-48.1\,\delta\mu_\alpha & -\ 8.6\,\delta\mu_\delta & =+0.078 & +17^\circ & 38 & 9 \\
+29.9 & +50.2 & =+0.485 & -27 & 31 & 6 \\
-70.7 & -14.9 & =-0.309 & -\ 3 & 17 & 2 \\
-39.1 & +44.2 & =+0.156 & -\ 4 & 38 & 4
\end{array}\right\} \qquad (4)$$

---

* The inconsistency in giving the limits of part of the regions in galactic longitude and latitude and of the other part in right ascension and declination is due to the later introduction of the third and fourth regions, which at first were left out of consideration.

A solution by least squares leads to

$$\left.\begin{aligned}\delta\mu_\alpha &= +0''.0004 \pm 0''.0019\\ \delta\mu_\delta &= +0.0072 \pm 0.0024\end{aligned}\right\} \qquad (5)$$

With respect to the probable errors (last column of Table I), this solution represents the observations satisfactorily. We thus find a vanishing correction for the proper motion in right ascension, but a considerable one for that in declination. Reasons will be found for assuming that the error is greatest between declinations -15° and -35°. For these we have, exclusively by the second group, putting $\delta\mu_\alpha = 0''.000$,

TABLE I

AVERAGE POSITION ANGLE OF μ

Group	α	δ	$100\,\mu$	p	r	No. Stars	p_2-p_1 obs.	p_2-p_1 comp.	O−C	P.E.
1.........	5^h43^m	$+17^\circ$	$1''.20$ 2.89	$162^\circ.0$ 166.5	$7^\circ.5$ 2.0	11 27	$+4^\circ.5$	$-3^\circ.5$	$+8^\circ.0$	$\pm 7^\circ.7$
2.........	7 21	−27	1.18 3.05	256.0 285.0	8.0 4.0	14 17	+29	+21.5	+ 7.5	9.0
3.........	4 43	− 3	0.98 3.28	182.0 164.0	20.0 13.0	7 10	−18	− 6.5	−11.5	23.8
4.........	6 53	− 4	1.19 3.92	215.5 224.5	15.0 6.0	15 23	+ 9	+18.5	− 9.5	±16.2
					Total	124				

$$\delta\mu_\delta = +0''.0097 \qquad (\text{Dec. } -27^\circ) \qquad (6)$$

This result, if well established, would be so important that I have sought for further evidence. For reasons already given, there will be advantages in including stars of neighboring regions and of different spectra. The following represents what I have been able to find.

a) *Astronomische Nachrichten*, **160**, 338, 1903.—From Table IV of this article we find the results in Table II. The values $\delta\mu_\delta$ Kapt. were obtained on the hypothesis adopted above. There is a very serious difference in Zone -18° to -36° between the proper motions from Boss and those obtained by adopting our hypothesis. For the present purpose we derive from Table II: Correction to Boss's μ_δ, between the limits $\alpha = 0^h$ to 24^h, $\delta = -18^\circ$ to -36°,

$$\delta\mu_\delta = \frac{+0''.42 - (-1''.17)}{100} = +0''.016. \tag{7}$$

It is worth remarking that for Auwers' proper motions the correction is small; in fact, does not exceed the limits of its uncertainty.

TABLE II

Zone	$100\ \delta\mu_\delta$		
	Kapt.−Cape	Boss−Cape	Auw.−Cape
0° to -18° ..	....	$+0''.11$	....
-18 " -36 ..	$+0''.42 \pm 0''.24$	-1.17	$+0''.12 \pm 0''.17$ (133)
-36 " -54 ..	-0.22 ± 0.19	-0.27	$+0.30 \pm 0.19$ (100)
-54 " -72 ..	$+0.37 \pm 0.22$	$+0.83$	$+0.91 \pm 0.26$ (57)

b) *Groningen Publications*, No. 21, p. 40 (34).—Weersma finds, by the principle here used, for Zone $\delta = -20^\circ$ to -40°

$$\mu_\delta \text{ Kapt.} - \mu_\delta \text{ Newcomb} = +0''.0087 \tag{8}$$

where μ_δ Kapt. again stands for the proper motion in δ corrected by the foregoing hypothesis. By a direct comparison of Newcomb's and Boss's catalogues between $\alpha = 4^h.5$ to $8^h.5$, $\delta = -5^\circ$ to -35° I find

$$\mu_\delta \text{ Newcomb} - \mu_\delta \text{ Boss} = +0''.0033 \text{ (34 stars).} \tag{9}$$

From (8) and (9)

$$\delta\mu_\delta = \mu_\delta \text{ Kapt.} - \mu_\delta \text{ Boss} = +0''.0120. \tag{10}$$

c) *G, K, M stars with proper motions* $\geqq 0''.017$.—The correction (5) depends on a comparison of stars of proper motions $\leqq 0''.016$ with those having greater motion. If the correction is confirmed by stars with proper motions $\geqq 0''.017$, the probability that we have to deal, not with systematic proper motion, but with systematic catalogue error, will be enormously increased, especially if we use stars of quite different spectra. It is desirable that the investigation cover the regions (A); but it is important, first, to increase the number of stars by extending these limits, and, second, to avoid the neighborhood of the antiapex (6^h, -34°). I therefore selected the region R.A. 7^h to 12^h, Dec. $-15°$ to $-40°$ and considered two classes of stars,

$$a)\ 0''.017 \leqq \mu \leqq 0''.050, \qquad b)\ \mu \geqq 0''.070.$$

All the Boss stars of spectrum G, K, M, and, further, those of unknown spectrum were used. I was thus led to the enormous difference:

$$\delta\mu_\delta = +0''.026 \quad (69 \text{ stars}) \tag{11}$$

No great weight can be attributed to this result, because the values of p vary so much that in a few cases there is uncertainty whether they ought not to be increased by 360°.

d) *Finally by a direct comparison* of Boss's catalogue with the fundamental catalogues of Auwers and Newcomb for the region R.A. 4^h30^m to 8^h30^m, Dec. $-5°$ to $-35°$ I find

$$\left.\begin{aligned} \delta\mu_\delta &= +0''.0015 \quad (33 \text{ stars) by Auwers} \\ &= \underline{+\ \ .003} \quad (34 \text{ stars) by Newcomb} \end{aligned}\right\} \tag{12}$$
$$\delta\mu_\delta = +0''.002$$

Summarizing, we have

TABLE III

	Equation	Limits		$\delta\mu_\delta$
B–A3 (second group)......	(6)	$7^h.0$ to $8^h.0$	$-24°$ to $-36°$	$+0''.010$
All spectra................	(7)	0.0 " 24.0	-18 " -36	$+\ .016$
All spectra................	(10)	0.0 " 24.0	-20 " -40	$+\ .012$
G, K, M, and unknown....	(11)	8.0 " 12.0	-17 " -40	$(+\ .026)$
Auwers, Newcomb.........	(12)	4.5 " 8.5	-5 " -35	$+\ .002$
Boss....................	....	....	....	0.000

For stars in the positive declinations of the region under consideration the position angles p are little affected by a correction of μ_δ. Moreover, there is every reason to believe that the correction is small. For the declinations 0° to $-20°$, the last two equations of (4), putting $\delta\mu_\alpha = 0.000$, give $\delta\mu_\delta = +0''.0050$. Considering everything, I finally resolved to adopt the following values:

$$\left.\begin{array}{cc} \delta & \delta\mu_\delta \\ -20° \text{ to } -40° & +0''.008 \\ 0 \ \text{"} \ -20 & +0.004 \\ 0 \ \text{"} \ +20 & 0.000 \end{array}\right\} \tag{13}$$

Boss's proper motions in declination, thus corrected, are given in Table XXXIX and have been used in all the discussions. His proper motions in right ascension were adopted uncorrected.

5. FIRST DETERMINATION OF THE ELEMENTS

For all the B stars in each of the regions (A) averages were found for α, δ, μ_α, μ_δ, with the results shown in Table IV. A second summary including only stars with proper motions $\geqq 0''.017$ is given in Table V.

TABLE IV

AVERAGES FOR ALL B STARS

GROUP	α	δ	No.	μ_α (Great Circle)	μ_δ	v Vert. (14)	p OBS.	p COMP.		λ Vert. (24)
								Vert. (14)	Vert. (24)	
1.......	5^h46^m	+17°.0	23	+0″.0031	−0″.0186	0″.0189	170°.5	172°.5	180°	152°.0
2.......	7 18	−27.6	25	−0.0129	+0.0094	0.0160	306.0	310.5	305	152.4
3.......	4 20	− 4.7	12	+0.0081	−0.0017	0.0083	102.0	103.0	108	158.3
4.......	6 47	− 5.8	18	−0.0132	−0.0063	0.0146	244.0	251.0	253	163.5

TABLE V

AVERAGES FOR B STARS HAVING $\mu \geqq 0''.017$

GROUP	α	δ	No.	p OBS.	p COMP.	
					Vert. (14)	Vert. (24)
1...........	5^h52^m	+17°.2	15	172°.6	176°.0	184°
2...........	7 19	−27.3	15	303.4	309.0	302
3...........	4 17	− 3.1	9	104.3	106.5	111
4...........	6 49	− 3.7	9	249.0	242.0	245

If the stars in these regions have the same motion in space, the directions defined by the values of p must intersect in a single point. This is indeed the case with extreme approximation, the position of the antivertex being:

$$\left.\begin{array}{ll}\text{From Table IV} & 6^h\ 0^m,\ -10^\circ.5\\ \text{From Table V} & 5\ 57\ ,\ -10\end{array}\right\}\ \text{Adopted } 6^h0^m,\ -10^\circ \qquad (14)$$

All the directions of Table IV pass this point within a distance of about 2°; those of Table V within 2°.5.

This close convergence to a single point makes the community of motion in the four regions highly probable. Assuming this coincidence of motion for the moment, I determined the stream-velocity from the radial velocities. On account of the scarcity of data I extended the regions a little, using the limits:

$$\left.\begin{array}{llllllll} \text{Group } 1 & \text{R.A.} & 5^{h}12^{m} & \text{to } 6^{h}30^{m}, & \text{Dec.} & +10^{\circ} & \text{to} & +30^{\circ} \\ \text{"} \quad 2 & \text{"} & 5\ 45 & \text{"} \quad 7\ 45 & \text{"} & -36 & \text{"} & -20 \\ \text{"} \quad 3 & \text{"} & 4\ \ 0 & \text{"} \quad 5\ 12 & \text{"} & -16 & \text{"} & +15 \\ \text{"} \quad 4 & \text{"} & 5\ 43 & \text{"} \quad 8\ 10 & \text{"} & -19 & \text{"} & +10 \end{array}\right\} \qquad (15)$$

For the average radial velocities, first applying the constant correction −4.3 km (see *Mount Wilson Contribution* No. 82, p. 28), we find the results in Table VI.

TABLE VI

RADIAL VELOCITIES

Group	α	δ	λ Vert. (24)	No.	$\rho-4.3$	ρ comp. Vert. (24)	O−C	P.E.
					km	km	km	km
1........	$5^{h}44^{m}$	$+18^{\circ}.8$	150°	9	+16.1	+17.3	−1.2	±1.8
2........	6 39	−29.4	157	9	+23.3	+18.4	+4.9	±1.5
3........	4 39	− 1.3	161	9	+14.7	+18.9	−4.2	±0.8
4........	6 42	−10.5	166	11	+21.9	+19.4	+2.5	±1.9

From this we compute the stream-velocity V by

$$V \cos \lambda = \rho, \qquad (16)$$

in which λ represents the angular distance from the antivertex

$$5^{h}44^{m}, \qquad -11^{\circ} \qquad (17)$$

which differs only slightly from (14) and will later be accepted as the definitive position. A least-squares solution leads to

$$V = 20.55 \text{ km} \quad \text{(38 stars)}. \qquad (18)$$

Outside the limits (15) there are three stars in our list with known radial velocities. Including these,

$$V = 20.0 \pm 1.5 \text{ km} \quad \text{(41 stars)}. \qquad (19)$$

Finally we compute the average parallax by (see *Mount Wilson Contribution* No. 82, p. 35)

$$\bar{\pi}=\frac{\bar{v}}{0.212\ V\sin\lambda}\,. \tag{20}$$

Adopting (17) and (19) we obtain from the data of Table IV

$$\bar{\pi}=0''.0083\pm0''.0008 \quad (78\text{ stars}). \tag{21}$$

6. COMMUNITY OF MOTION OF THE FOUR GROUPS

It was remarked that the intersection of the four lines defined by the values of p in Tables IV and V is a strong argument in favor of the supposition that the four groups have the same motion. There are, however, other criteria. If there is community of motion, and if we may assume that the values of the mean parallax are about the same for the four groups, the values of v in Table IV must be proportional to sin λ. With vertex (14) the proportionality, as indicated by Table VII, is not close. It can be greatly improved by diminishing the right ascension of the antivertex, and would be quite satisfactory (see Table VII) if we adopted

TABLE VII

GROUP	*v* OBS.	0″.0351 SIN λ VERT. (14)	O−C		
			Vert. (14)	Vert. (22)	Vert. (24)
1.	0″.0189	0″.0164	+0″.0025	+0″.0027	+0″.0026
2.	0.0160	0.0148	+0.0012	−0.0026	−0.0014
3.	0.0083	0.0154	−0.0071	−0.0006	−0.0046
4.	0.0146	0.0079	+0.0067	+0.0005	+0.0035

$$5^{h}12^{m}, \qquad -10^{\circ} \tag{22}$$

instead of (14). This, however, would not satisfy the directions of Tables IV and V, and we must accept a compromise between the two positions.

Adopting for each of the four regions the values

$$V=20.0\text{ km}, \qquad \bar{\pi}=0''.0081, \tag{23}$$

the latter of which slightly diverges from (21) but agrees with the definitive value adopted later, we can compute for each of the four regions a separate vertex. Table IV furnishes for the centers of each of the regions the direction of the antivertex, whereas its distance λ can be found from v by (20) and (23). I thus find for the antivertices:

Group	α	δ	No.	Deviation
1..........	$6^h\ 6^m$	$-15^\circ.8$	23	$8^\circ.0$
2..........	5 50	$-$ 9.3	25	4.3
3..........	5 18	$-$ 7.3	12	6.9
4..........	5 12	-16.0	18	7.3
Mean...	5 37	-12.2	....	....

The last column shows the distance of the individual antivertices from the mean of all. Taking into account the small number of stars from which these antivertices were obtained, and considering that the supposed absolute equality of $\bar{\pi}$ for the four groups is highly improbable, the deviations are not greater than might reasonably have been expected. Certainly they afford no sufficient reason for doubting the community of motion.

As the position (14), which rests on the directions in Table IV and is thus independent of any supposition as to the equality of the values of π, whereas this supposition is involved in the result obtained just now, I will adopt as *final* the intermediate position of the antivertex

$$5^h 44^m, \qquad -11^\circ. \tag{24}$$

The values of p computed with the aid of (24) have been inserted in Tables IV and V. To my regret the computed values of p and λ given in Table XXXIX have been derived with a slightly different antivertex, viz.,

$$5^h 48^m, \qquad -9^\circ. \tag{25}$$

I have not judged it worth while to repeat the computations because the two positions probably agree within the uncertainty of (24).[1]

---

[1] Further, (24) is probably also to be considered as only provisional. A preliminary investigation seems to show that the community of motion extends much beyond the limits adopted in the present paper. If this proves to be true, it will be necessary later to treat all the stars with common motion as a whole, which will probably change the definitive elements a little.

7. COMMUNITY OF MOTION, CONTINUED

A more serious objection to the assumption of community of motion is furnished by the radial velocities. If from the data in Table VI we compute the stream-velocity V separately for the four regions we obtain

$$\left.\begin{array}{llll}\text{Group } 1 & l=157^\circ, & V=-18.6\pm 2.1\ \text{km} & \text{No.} = 9 \\ \text{“} \quad 2 & 205 & -25.3\pm 1.6 & 9 \\ \text{“} \quad 3 & 164 & -15.6\pm 0.85 & 9 \\ \text{“} \quad 4 & 186 & -22.6\pm 2.0 & 11 \end{array}\right\} \quad (26)$$

Comparing the results of the second and third groups we find a difference of

$$9.7\pm 1.8\ \text{km}, \qquad (27)$$

which seems real enough. At all events it becomes necessary to examine the matter more closely.

I first made a brief preliminary investigation for the region adjoining those of the present paper on the side of the small galactic longitudes (120° to 150°). It turned out that the direction of motion here passes very near the point (24), which satisfies the directions of all four regions under consideration. For the radial velocity there is a decidedly closer approach to the first and third regions than to the other two, which lie on the side of greater longitudes—see (26)—the part of the sky investigated in *Mount Wilson Contribution* No. 82. It would therefore excite no particular surprise if we found the velocity, or even all the elements of motion, to diverge somewhat from those of the other regions toward those of the region treated in *Mount Wilson Contribution* No. 82. As a matter of fact, we really find the reverse. Indeed, the observations in the second and fourth regions, badly as they are represented in radial velocity by the elements (19) and (24), are still much better represented by these elements than by those for the higher galactic longitudes, namely,

$$\text{Vertex, } 18^h 24^m, \quad +39^\circ; \quad V=-18.0. \qquad (28)$$

The results of the comparison are

GROUP	p OBS.	ρ OBS. -4.3	COMPUTATION BY				O−C			
			(19) and (24)		(28)		(19) and (24)		(28)	
			p	ρ	p	ρ	p	ρ	p	ρ
2.........	306°	+23.3	305°	+18.4	221°	+17.7	+1°	+4.9	+85°	+5.6
4.........	244	+21.9	253	+19.4	188	+15.7	−9	+2.5	+56	+6.2

The position angles are therefore not at all represented by (28), and the radial velocities markedly worse than by (19). The case therefore stands thus: If we accept the reality of the divergence of the radial velocity of Group 2, this group can be considered as local only, for it stands apart from the stars, both in lower and in higher galactic longitudes. If we do this, there is every reason for also including the fourth region in the local group, which thus becomes extensive enough for a determination of all its elements.

The directions furnished by Table IV for Groups 2 and 4 cut each other at an angle of 65°; those for Groups 1 and 3, at an angle slightly greater. If therefore we take the points of intersection as the antivertices, they must in both cases be considered well determined. Both agree almost perfectly with position (14) obtained from the four regions together. Accepting these vertices, the stream-velocity is obtained by the data of Table VI. I find

$$\left.\begin{array}{lll} \text{Groups 2 and 4} & V=23.5\pm1.2 & \text{(20 stars)} \\ \text{\ \ \ ``\ \ \ \ 1 \ ``\ \ 3} & \underline{V=17.2\pm1.2} & \text{(18 stars)} \\ \text{\ \ \ \ \ \ Difference} & \ \ \ \ 6.3\pm1.7 & \end{array}\right\} \qquad (29)$$

The result thus would be that the second and fourth regions form a local group whose direction of motion coincides absolutely with that of the others but whose velocity is 37 per cent greater.

Some further criteria may be considered:

1. A local group can usually be seen as such on an ordinary star map. If on the map in *Mount Wilson Contribution* No. 82

($\mu \leqq 0''.016$) we exclude the Nebula-group (2) there seems to be indicated a group within the limits, approximately,

$$l = 180° \text{ to } 216°; \quad b = -30° \text{ to } +4°, \tag{30}$$

which covers Group 2 and the richer part of Group 4.

2. In a local group we expect the proper motions to be nearly equal. The proximity of the antivertex and the minuteness of the proper motions, which result in their being strongly influenced by observational errors, and finally the fact that, if the group is not very condensed, many extraneous stars will be seen projected on it, make the criterion less effective in the present case than ordinarily. If we call proper motions $\leqq 0''.016$ small, then, within the limits (30), 61 per cent of the motions are small; outside these limits, only 39 per cent.

3. In local groups we expect to find a distribution of spectra differing from that in the rest of the sky. Thus, in the Nebula-group we found a strong predominance of the Oe5–B3 stars (see Section 3). Within the limits (30) we find that 77 per cent of all the stars are Oe5–B5; outside these limits there are 59 per cent.

4. For the mean parallax of the stars within the limits (30) we find, as above, $\bar{\pi} = 0''.0076$, which scarcely differs from (21) and (23).

5. For the Nebula-group we shall find further on $\bar{\pi} = 0''.0054$. Its stream-velocity can scarcely differ from the value in (19). If at all different, it seems to be rather smaller. The elements for Groups 2 and 4 do not approach those of the Nebula-group more than they do those of Groups 1 and 3.

In conclusion, we cannot deny the possibility of a local group; still, in my opinion, the similarity in the direction of the motions outweighs all other arguments, so that the probability is not in favor of such a group. The difference (29) of 6.3 km between the stream-velocities of Groups 2+4 and 1+3, which is the main argument in favor, is indeed almost four times the probable error. But such a result is perhaps not so surprising for radial velocities as it would be for other quantities, because there must still be numerous cases of undiscovered orbital motion.

In what follows we shall assume that the stream-motions of all four groups are the same. The question can probably be settled without difficulty by the fainter stars as soon as the *Revised Draper Catalogue* is published. Even if it should then be proved that there really is a local group, our results will be little altered. The parallaxes, and consequently the absolute magnitudes, M, in the main will not be altered, and the same, of course, holds for the luminosity-curve. The computed values of p also will not change. Only the values of the radial velocities will be somewhat different, for instead of computing these with (19) we shall have to use (29).

The average values of the parallax finally adopted are in some cases slightly different from the mean in (23), because, first, our four groups do not include all the available material, and, secondly, it does not seem reasonable to adopt exactly the same value for all the partial groups. From the new computation Boss 1401, 1517, and 1994 were excluded—the first and the last because they do not seem to belong to the same system as the rest of the stars (as proved by the values of p), and No. 1517 because it has so exceptionally large a proper motion. The values thus obtained for the groups of different λ are given in Table VIII. For certain purposes they have been further contracted into the considerably overlapping groups in Table IX.

TABLE VIII

λ	Mean λ	$\bar{\pi}$	No. of Stars	Weight
145° to 149°...	147°	0″.0081	26	138
150 " 154 ...	152	0.0075	40	160
155 " 159 ...	157	0.0107	28	77
160 " 164 ...	162	0.0066	17	29

TABLE IX

λ	Mean λ	$\bar{\pi}$	No. of Stars	Weight
145° to 154°...	150°	0″.0077	66	11
150 " 159 ...	154	0.0087	68	9
152 " 167 ...	157.5	0.0083	75½	4

From Table VIII, I find, in good agreement with (23), for the general average:

$$\bar{\pi} = +0''.0081 \pm 0''.0007 \quad \text{(111 stars).} \tag{31}$$

8. INFLUENCE OF SYSTEMATIC ERROR AND SUMMARY OF DEFINITIVE ELEMENTS

On account of the excessive smallness of the proper motions and the consequently strong influence of observational errors, it will not be deemed superfluous if we try to find the effect of any remaining traces of systematic error. For this purpose I made new solutions with the data in Tables IV and VI on the supposition: (*a*) that Boss's values of μ_α require a constant correction $\delta\mu_\alpha = +0''.0030$; (*b*) that the values of μ_δ in Table XXXIX, that is, of Boss's μ_δ corrected by (13), require a further correction $\delta\mu_\delta = +0''.0030$; (*c*) that the correction (13) for μ_δ is wholly false, our new solution thus, in this case, starting with the uncorrected μ_α and μ_δ of Boss.

For this special investigation I have disregarded the values of the *v* in the derivation of the vertex and adopted as antivertex the point toward which all the directions converge with the greatest approximation. I thus found

Case		Antivertex		$\bar{\pi}$	V
(1)	No correction	$6^{h}\ 0^{m}$	$-10^{\circ}.5$	$0''.0082$	20.8
(2)	Correction (*a*)	6 12	− 8	0.0080	21.3
(3)	" (*b*)	5 55	− 4	0.0082	20.8
(4)	" (*c*)	5 52	−18	0.0076	20.55

(32)

In every case the four directions of Table IV intersect nearly at a single point. This is most perfectly realized in the cases (1) and (2), where none of the directions deviate from the adopted antivertex more than 2°. In cases (3) and (4) the greatest distance is 4° or 4°.5.

In view of these results I think we may conclude that, as a consequence of the remaining systematic errors and the consideration of the values of *v* in Section 6, it is not impossible that there may still be an error of 3° or 4° in the position of the antivertex, but that the resulting uncertainties in V and π must be negligible.

This freedom of V from systematic error is due to the fact that the region as a whole is so near the antivertex, and to the further fact that the four separate regions lie fairly symmetrically around the antivertex. As for π, its freedom from systematic error is wholly attributable to this last circumstance. It was this consideration which in great part led to our choice of the four regions and compelled us to introduce a supplementary group outside the limit at galactic latitude −30°.

The danger from the systematic errors being thus in great measure avoided, there is every reason to accept the probable errors as a measure of the accuracy obtained. Collecting results, we have as *definitive elements:*

$$\left.\begin{array}{ll}\text{Vertex} & 17^h44^m,\quad +11^\circ\quad (\text{uncertainty } \pm 3^\circ \text{ or } \pm 4^\circ)\\ & V = -20.0 \pm 1.5 \text{ km (P.E.)}\\ & \bar{\pi} = 0''.0081 \pm 0''.0007 \text{ (P.E.)}\end{array}\right\} \quad (33)$$

This will not prevent the adoption for π of the separate values of Table IX. It is a very significant fact, to which I hope to revert in a later publication, that this vertex coincides so nearly with that of the first stream of all the non-helium stars, for which Eddington in *Monthly Notices*, **71**, 42, 1910, finds 18^h3^m, $+14^\circ.6$.

9. OBSERVED DISTRIBUTION OF THE VALUES OF υ

Now that a good estimate of the average π has been obtained, we have to find the range in distance. It would be most desirable to determine the individual parallax of each star, but as this is not feasible, we will try to derive mean parallaxes for stars having given values of λ and υ and, further, the probable deviation of the individual parallaxes from this mean. The amount of this deviation as a fraction of the parallax will determine the confidence with which we may use the mean parallax as a substitute for the individual parallaxes.

I will begin with the consideration of certain necessary data: first of all, with an examination of the distribution of the values of υ for different values of λ. By countings in Table XXXIX, omitting stars within 15° of the antivertex and excluding Boss 1517, I find the data in Table X.

The number of stars being so small, pains have been taken to smooth thoroughly the results. We first contract the data into three partially overlapping zones:

λ	$\bar{\lambda}$	$\bar{\upsilon}$	No.	
145° to 154°	150	$0''.0164$	66	
150 " 159	154	0.0161	68	(34)
152 " 167	157.5	0.0135	$75\frac{1}{2}$	

Even so, it is not easy to arrive at an entirely satisfactory result. The difficulty would be greatly reduced if we knew the form of the frequency curve for the v. If there were no observational errors, such a form could be assigned, at least if we assumed—on grounds presently to be given—that the values of u (component of *linear* peculiar motion) are distributed according to an error-curve. For it follows from formula (20) that, for any definite value of π,

TABLE X

DISTRIBUTION OF THE VALUES OF v

100 v	λ						Totals
	145°–149°	150°–151°	152°–154°	155°–159°	160°–164°	165°–167°	
6″.0 to 7″.0..	....	1	....	....	....	....	1
5.0 “ 6.0..	....	....	....	....	....	....	....
4.0 “ 5.0..	1	....	1	....	....	1	3
3.0 “ 4.0..	5½	2	1	7	1	....	16½
2.0 “ 3.0..	6½	5	4	8½	1	....	25
1.0 “ 2.0..	6	3½	9	1½	4	2	26
0.0 “ 1.0..	5	2½	7	9	7	½	31
0.0 “ −1.0..	2	1½	1½	1	4	2½	12½
−1.0 “ −2.0..	....	....	....	½	....	....	½
<−2.0....	....	....	1	½	....	....	1½
Totals......	26	15½	24½	28	17	6	117

$$\pi = 0.212\, v\, V \sin \lambda \tag{35}$$

with individual deviations following an error-curve having the probable error

$$r_v = \pm 0.212\, \pi r_u,$$

where r_u is a constant for which later will be found the value 1.67 km. The deviations of v are thus seen to be proportional to v. From the theory developed elsewhere[1] it follows that the values of v, for the same value of λ, will be distributed according to the formula

$$\text{Prob.}\ {}_{v}^{v+\delta v} = \frac{h}{\sqrt{\pi}} \cdot \frac{\text{Mod.}}{v} e^{-h^2[\log v - M]^2} \delta v, \tag{a}$$

that is, the values log v will be distributed according to an error-curve.

---

[1] *Skew Frequency Curves in Biology and Statistics*, Noordhoff (Groningen), 1903, p. 21.

This, however, holds only in the absence of observational errors. Since these follow an error-curve, the distribution of the observed values of v will be something between (a) and an ordinary error-curve. In particular the real curve, unlike (a), will yield certain frequencies for negative values of v.

Now we obtain an intermediate curve if in (a) we substitute $v+K$ (K being a constant) for v. The formula then becomes

$$\text{Prob.}\,{}_{v}^{v+\delta v}=\frac{h}{\sqrt{\pi}}\cdot\frac{\text{Mod.}}{v+K}e^{-h^2[\log(v+K)-M]^2}\delta v, \tag{b}$$

which implies that the distribution of log ($v+K$) follows an error-curve.

Led by these considerations I have tried to learn whether it is possible to determine the three constants in (b) in such a way that the observed frequencies are well represented. This being really the case, I have considered the best representation by (b) as that to be adopted. The derivation of the best-fitting values of h, K, M is very easy.[1] It is to be recommended that this be made in such a way that the arithmetical mean values $\bar{v}$ in (34) are perfectly represented. This gives as a first condition between the constants

$$\log(\bar{v}+K)=M+\frac{1}{4h^2\cdot\text{Mod.}}. \tag{36}$$

The values obtained are as follows:

λ	150°	154°	157°.5	
h	9.347	15.274	6.280	
K	0.0608	0.1095	0.0451	(37)
M	−1.1190	−0.9033	−1.2464	

These being substituted in (b), we find by integration (which offers no difficulty) the values in the second, fifth, and eighth columns of Table XI. Those in the other columns will be explained in Section 13.

10. OBSERVED DISTRIBUTION OF THE VALUES OF τ

In order to increase the reliability of the conclusions, I have confined myself to the stars for which the probable error of τ does not exceed 0ʺ.0069. The number of stars is thus somewhat diminished, but this is not so material here, because stars at arbitrarily different distances from the vertex can be combined. Boss in his catalogue gives the probable error of 100 μ_α and 100 μ_δ. The mean of the two was combined to represent 100 times the probable error of the proper motion in any co-ordinate, hence also of 100 τ. This is given in Table XXXIX under the heading 100 r. I have further disregarded the stars within 20° of the adopted antivertex (24), which excludes the Nebula-group. The results of the countings are given in Table XII.

---

[1] *Skew Curves*, art. 18, p. 34.

TABLE XI

Distribution of the Values of v

(Theoretical Values are for $r_u = \pm 2.5$)

λ	$\lambda=150°$			$\bar{\lambda}=154°$			$\bar{\lambda}=157°.5$		
	Obs.	Theor.	O−C	Obs.	Theor.	O−C	Obs.	Theor.	O−C
+0″.055	0.5	0.4	+0.1	0.3	0.3	0.0	1.1	0.9	+0.2
.050	0.5	0.5	0.0	0.5	0.4	+0.1	0.7	0.7	0.0
.045	0.9	0.9	0.0	0.8	0.7	+0.1	1.1	1.0	+0.1
.040	1.6	1.7	−0.1	1.6	1.4	+0.2	1.6	1.6	0.0
.035	2.6	2.8	−0.2	2.7	2.3	+0.4	2.5	2.4	+0.1
.030	4.0	4.3	−0.3	4.4	3.9	+0.5	3.6	3.4	+0.2
.025	6.1	6.2	−0.1	6.5	5.9	+0.6	5.1	4.8	+0.3
.020	7.9	8.3	−0.4	8.4	8.1	+0.3	6.8	6.6	+0.2
.015	9.2	9.8	−0.6	9.9	10.0	−0.1	8.6	8.8	−0.2
.010	10.2	10.0	+0.2	10.2	10.8	−0.6	10.0	10.7	−0.7
+0.005	9.2	8.8	+0.4	9.0	9.8	−0.8	10.5	11.5	−1.0
0.000	6.7	6.3	+0.4	6.7	7.4	−0.7	9.7	10.2	−0.5
−0.005	4.1	3.6	+0.5	4.2	4.4	−0.2	7.3	7.1	+0.2
−0.010	1.8	1.6	+0.2	2.1	2.0	+0.1	4.5	3.8	+0.7
−0.015	0.6	0.7	0.0	0.8	1.0	+0.1	1.9	1.5	+0.4
−0.020	0.1			0.3			0.5	0.6	−0.1
Total	66.0	65.9	......	68.4	68.4	......	75.5	75.6	.....

TABLE XII

Number of Values of τ

τ	Observed Number	τ	Observed Number
<−0″.025	0.5	+0.005 to + .010........	9.0
−0″.020 to −0″.025........	0.5	+ .010 " + .015........	8.5
− .015 " − .020........	2.0	+ .015 " + .020........	1.0
− .010 " − .015........	8.5	+0.020 " +0.025........	0.0
−0.005 " − .010........	13.5	>+0″.025	1.0
.000 " − .005........	12.0		
.000 " + .005........	15.5	Total................	72.0

The numbers fit very well an error-curve with the probable error ±0."0061.

11. PROBABLE AMOUNT OF r_u AND DISTRIBUTION OF THE COMPONENTS OF THE PECULIAR MOTION

Let u and t[1] represent the components of the linear peculiar motion at right angles to the line of sight, one toward the antivertex, the other at right angles thereto; u and t subtend the angles v and τ; $\bar{u}$ and $\bar{t}$ will denote the average values, all taken positively.

Since we suppose the directions of the peculiar motions to be distributed at random,

$$\bar{u}=\bar{t}=\text{average peculiar radial motion.} \tag{38}$$

This peculiar radial motion is the radial motion freed from stream-motion. We thus have to find[2]

$$\text{Observed radial motion}=-V\cos\lambda, \tag{39}$$

V and λ being in accordance with (33). The average of these values, all taken positively, will be $\bar{u}=t$. Outside the Nebula-region there are 45 stars for which we have radial velocities. Of these, I exclude Boss 1761, 1817, 1935. The velocity of the first rests on measures of the bright H line, a determination, there is reason to think, not quite comparable with the others. The second is a spectroscopic binary; the velocity of the center of mass is a simple estimate which may prove to be largely in error. The velocity of the third is quite abnormal. Unless a spectroscopic binary, the star cannot belong to the same system as the other stars. For the remaining 42 stars

$$\bar{u}=5.78\text{ km.} \tag{40}$$

Treating the stars of region (30) as a separate local group, this becomes 5.36. In *Mount Wilson Contribution* No. 82, p. 28, the corresponding value was found to be

$$\bar{u}=3.5\text{ km}\quad\text{(61 full-weight stars)} \tag{41}$$

---

[1] t is the quantity for which in *Mount Wilson Contribution* No. 82 was used the somewhat less obvious notation v.

[2] The correction −4.3 km is first to be applied to the observed radial velocities.

Since the values of $\bar{u}$ depend partly on real peculiar motions and partly on observational errors, either one or the other or both of these factors must be greater now than in the earlier investigation.

The following considerations show that the difference is due to both causes. First, all results were included in (40), whereas in (41) the less reliable values were either excluded or admitted with diminished weight; secondly, (41) rests exclusively on Lick Observatory results, which do not include stars whose spectra are not susceptible of at least fairly good measurement, whereas the Mount Wilson observations, upon which (40) is partly based, include all objects on the original program, irrespective of their difficulty. If, to secure homogeneity, we limit ourselves to the values obtained by the Lick observers, and if further we exclude all values marked as uncertain, or given without any decimal, or as the estimated velocity of a spectroscopic binary, we find

$$\bar{u}=4.24\text{ km} \qquad r_u=\pm 3.6\text{ km} \qquad (16\text{ stars}) \qquad (42)$$

We thus approach the value (41), but the number of stars has become so small that little reliance can be put on the result.

Fortunately we can derive a much more reliable value in another way; but this requires a knowledge of the parallaxes, so that we shall have to anticipate to some extent results obtained later. With known parallaxes we can transform the τ components into linear motions by

$$t=\frac{\tau}{0.212\,\pi} \qquad (t \text{ in km per second}) \qquad (43)$$

In order to exclude completely the Nebula-group I use only stars for which $\lambda < 160°$. Since for objects of small parallax observational errors in τ appear much magnified in t, I include only stars for which $\pi \geqq 0\overset{''}{.}0070$. Finally, I exclude Boss 1517, for which the parallax is exceptionally large and uncertain.[1] For comparison the same computation was made for the stars in *Mount Wilson Contribution* No. 82. In this I avoided practically all exceptional cases by limiting myself to the stars for which $\lambda \leqq 120°$ and galactic longitude $< 320°$, and I tried to improve the results by omitting badly observed stars for which $100\,r > 0''.80$.

---

[1] The value of τ, consequently of t, is quite normal for this star. Stars in our tables considered as not belonging to the system were, of course, also omitted; only one object, Boss 1944, was excluded on this account.

Before deriving averages I tried to find the frequency-curve of t freed from observational error. For the observed values[1] the distribution is at once given by counts, but we cannot hope to pass with any precision to the distribution of the true values as long as the observational errors predominate in the observed values of τ. This is the case if we treat all the stars, but it is no longer so if we confine ourselves to the best observed stars, those for which $100\,r \leqq 0''.40$. By this limitation the number of available objects becomes small, so that a very reliable result is not to be expected, but as a roughly approximate determination is to be preferred to none at all, or to a mere supposition, I do not hesitate to communicate my results.

We may safely assume, I think, that the frequency-curves, both of the observed and of the true values of t, are symmetrical. On this assumption we find, by counting, for the stars having $100\,r \leqq 0''.40$, the results in Table XIII. For both the Orion and the Scorpius-Centaurus region the observed distributions differ little from the normal error-law, as appears if we compare them with curves having probable errors of 2.32 and 1.83 km, respectively (third and sixth columns of Table XIII). The residuals show little that is systematic; they are mostly of different sign for the two regions. We thus conclude that the observed values of t are distributed closely in accordance with the error-law.

For the stars of other types, in particular for those of type K, there appears to be a deviation from this law in the direction of an excess of large motions.[2] We do not find much evidence of such an excess here, especially if we consider that the one star in the Scorpius-Centaurus region with a large value of t, namely, Boss 3115, has a very abnormal radial velocity. Should this be confirmed by later observations, the star should be excluded from the group.

---

[1] By *observed* values of t, I mean the values computed by (43) with the aid of the *observed* values of τ.

[2] *Proc. Nat. Acad. Sci.*, 1, 17–18, 1915.

Admitting, therefore, a distribution of the observed values of t according to the law of error, we should infer at once a similar distribution of the true values, could we assume that the observational errors affecting t also followed that law. Now this is certainly not rigorously the case. We may assume that the observational errors of τ—consequently, by (43), those of t—follow the error-law *for stars of the same* π. For different values of π, however, the probable value of the observational error in t will be quite different; in fact, inversely proportional to π. Nevertheless, I convinced myself that the observational errors in t follow the error-law with sufficient approximation for our present purpose, and that the corresponding probable error is ±1.47 km for the Orion region and ±1.50 km for the Scorpius-Centaurus stars. Consequently, the distribution of the true values of t must also follow approximately the error-law, and the probable value r_t which equals r_u will be

TABLE XIII

DISTRIBUTION OF $t_{\text{obs.}}$ $(100\, r \leqq 0''.40)$

$t_{\text{obs.}}$	ORION			SCORPIUS-CENTAURUS		
	No.	Normal $r=\pm 2.32$	O−C	No.	Normal $r=\pm 1.83$	O−C
0 to ±1km......	9	6.4	+2.6	6	7.2	−1.2
±1 " ±2	6	6.0	0.0	7.5	6.3	+1.2
±2 " ±3	4	5.0	−1.0	6	4.8	+1.2
±3 " ±4	1	3.8	−2.8	3.5	3.2	+0.3
±4 " ±5	2	2.7	−0.7	1	1.9	−0.9
±5 " ±6	3	1.9	+1.1	....	0.9	−0.6
±6 " ±7	1	1.0	0.0	....	0.4	
±7 " ±8	0.5	0.6	−0.1	....	0.2	
±8	1.5	0.6	+0.9	1	0.1	
Totals........	28	28.0	....	25	25.0	....

$$\left.\begin{aligned} r_t=r_u&=\pm\sqrt{2.32^2-1.47^2}=\pm 1.80 \text{ (28 stars) Orion region}\\ r_t=r_u&=\pm\sqrt{1.83^2-1.45^2}=\pm 1.12 \text{ (25 stars) Scorpius-Centaurus}\end{aligned}\right\} \quad (44)$$

The smallness of these values is the most surprising and promising fact brought to light by the present investigation. The B stars of *Mount Wilson Contribution* No. 82 with those of the present paper comprise about 65 per cent of all the B stars. With a value of r_u as small as those just found, the determination of accurate parallaxes of all these stars becomes merely a question of securing more accurate proper motions, which is only a matter of time; and with the powerful aid of photography the interval need not be so very long.

Further, preliminary investigation has shown that a similar parallelism exists for the B stars in the Perseus region and that at least a good part of the A stars share in the motion of the helium stars.[1] It thus seems not unlikely that further investigation by these methods will give *good determinations of the parallaxes of all the B stars and of a large number of the A stars.*

For the later types the beautiful method proposed by Adams and Kohlschütter[2] and developed in detail by Adams[3] has recently opened the prospect of extensive determination of parallax by spectroscopic means. All this awakens the hope that we are at last on the way toward a wholesale determination of the third co-ordinate—distance—the lack of which has been the main obstacle in the way of substantial knowledge of the structure of the stellar system.

The extreme importance of the matter makes it desirable to obtain for the B stars the most reliable values of the parallax possible. I therefore give another solution for r_u in which the stars less satisfactorily observed are not altogether neglected.

For the Scorpius-Centaurus region all the stars were used, whatever their parallaxes; for the Orion region the stars with parallaxes $<0''.0070$ were neglected, because it was feared that the remaining errors in the very small parallaxes would influence too greatly the values for t obtained by (43). For the first region the stars were subdivided into six groups,[4] the limits of the parallax being respectively: $100\pi \leqq 0''.49$; $0''.50$–$0''.69$; $0''.70$–$0''.86$; $0''.87$–$1''.04$; $1''.05$–$1''.27$; $1''.28$–$2''.24$. For the Orion region the limits were the same, but the first two groups are wanting. The first four columns of Tables XIV and XV contain, respectively, the averages of 100 π, 100 τ, 100 r, and of t computed from τ and π by (43). The fifth column contains the probable amount of 100 τ freed from observational error, as follows: Admitting that the values of τ are distributed substantially according to an error-curve (see Table XII) the probable amount 100 r_τ corresponding to 100 τ was found by multiplying the average amount by the factor 0.845. Freed from observational error we therefore evidently have

---

[1] *Trans. Internat. Solar Union*, **3**, 220, 1911.

[2] *Mt. Wilson Contr.*, No. 89; *Astrophysical Journal*, **40**, 385, 1914.

[3] *Mt. Wilson Comm.*, Nos. 23–25; *Proc. Nat. Acad. Sci.*, **2**, 143, 147, 152, 1916.

[4] In Table XV the first two had to be combined.

$$100\, r_\tau = 100\sqrt{(0.845\,\bar{\tau})^2 - \bar{r}^2}. \tag{45}$$

TABLE XIV

AVERAGE VALUES OF t, ETC.

ORION REGION							SCORPIUS-CENTAURUS REGION						
$100\,\bar{\pi}$	$100\,\bar{\tau}$	$100\,\bar{r}$	$\bar{t}$	$100\,r_\tau$	r_t	No.	$100\,\bar{\pi}$	$100\,\bar{\tau}$	$100\,\bar{r}$	$\bar{t}$	$100\,r_\tau$	r_t	No.
							(0″.32)	(0″.61)	(0″.62)	(7.66)	(0″.000)	(0.0)	(8)
							0.62	0.44	0.55	3.32	0.000	0.0	14
0″.77	0″.62	0″.48	3.70	0″.210	1.3	21	0.78	0.57	0.51	3.50	0.000	0.0	19
0.94	1.04	0.56	5.17	0.677	3.4	23	0.96	0.61	0.48	3.02	0.187	0.9	16
1.13	0.55	0.58	2.32	0.000	0.0	21	1.15	0.76	0.50	3.11	0.403	1.65	20
1.52	0.83	0.44	2.88	0.546	1.7	12	1.59	0.83	0.59	2.55	0.379	1.1	22
1.04	0.761	0.526	3.63	0.370	1.68 1.64	77	1.07	0.662	0.529	3.07	0.181	0.80 0.79	91

TABLE XV

SAME AS TABLE XIV BUT FOR 100 $r \leqq 0''.40$

ORION REGION							SCORPIUS-CENTAURUS REGION						
$100\,\bar{\pi}$	$100\,\bar{\tau}$	$100\,\bar{r}$	$\bar{t}$	$100\,r_\tau$	r_t	No.	$100\,\bar{\pi}$	$100\,\bar{\tau}$	$100\,\bar{r}$	$\bar{t}$	$100\,r_\tau$	r_t	No.
							0″.45	0″.33	0″.35	2.40	0″.000	0.0	2
0″.77	0″.58	0″.35	3.62	0″.343	2.1	10	0.79	0.28	0.31	1.72	0.000	0.0	5
0.91	0.50	0.26	2.40	0.332	1.7	5	0.96	0.30	0.32	1.45	0.000	0.0	8
1.12	0.32	0.33	1.35	neg.	0.0	6	1.13	0.53	0.32	2.22	0.314	1.3	6
1.57	0.87	0.31	2.90	0.666	2.0	7	1.89	1.45	0.37	4.02	1.168	2.9	4
1.07	0.582	0.321	2.74	0.373	1.64 1.55	28	1.07	0.538	0.329	2.18	0.314	1.38 0.78	25

In a few cases, the quantity under the radical being negative, r_τ was assumed to be zero. With the aid of r_τ we find the probable amount, $r_t = r_u$ of t, freed from observational error by

$$r_t = \frac{r_\tau}{0.212\,\pi}, \tag{46}$$

which evidently follows from (43). These quantities are given in the sixth column. In the seventh are the numbers of stars included in each average. The last line of each table shows the total averages; for r_t two values are given, the first, from the total averages of r_τ and π by (46), the second, from the separately computed values of r_t with weights proportional to the number of stars. Except for the last value in Table XV, the agreement is almost exact; I adopt the means.

Supplementing these results with those obtained by the same method when we limit ourselves still more closely to the best-observed stars, we have the following values for $r_t = r_u$:

ORION				SCORPIUS-CENTAURUS			
100 r	Reference	r_t	No.	100 r	Reference	r_t	No.
		km				km	
All values..	Table XIV	1.66	77	$\leqq 0''.80$..	Table XIV	0.80	91
$\leqq 0''.40$....	(44)	1.80	28	$\leqq 0.40$..	(44)	1.12	25
$\leqq 0''.40$....	Table XV	1.60	28	$\leqq 0''.40$..	Table XV	1.08	25
$\leqq 0.30$....	....	1.56	9	$\leqq 0.30$..	....	0.75	7

from which finally the *adopted values*

$$\left.\begin{array}{ll} \text{Orion region} & r_u = \pm 1.67 \text{ km} \\ \text{Scorpius-Centaurus region} & r_u = \pm 1.00 \text{ km} \end{array}\right\} \tag{47}$$

12. REMARKS

Remark 1.—It has been implicitly assumed in what precedes that the errors in the parallaxes do not sensibly influence the results for r_u. I have convinced myself that such is really the case.

Remark 2.—The accuracy of the determination of r_u certainly is still of a rather low order. I have refrained from computing probable errors, because the data are hardly adequate for a good determination. It is easy to obtain an upper limit for r_u by neglecting the observational errors altogether. From Table XV we find, since $r_t = 0.845\,\bar{t}$,

$$\text{Upper limit for } r_u \left\{ \begin{array}{ll} \text{Orion region} & = \pm 2.3 \text{ km} \\ \text{Scorpius-Centaurus region} & = \pm 1.8 \text{ km} \end{array} \right\} \qquad (48)$$

With these numbers before us it cannot be doubted that the real values of r_u do not materially exceed the adopted values (47); the chances are that the latter are somewhat too high.

In consideration of the remaining uncertainty, however, I have carried through the computations that follow on the two extreme suppositions

$$r_u = \pm 2.5 \text{ km and } r_u = 0.0 \text{ km}. \qquad (49)$$

This will make a subsequent correction easy, if we find means of improving our values by the addition of well-observed fainter stars, by the inclusion of later observations, or by the discovery that the A stars for the region under consideration show the same motions, etc. For the present we shall definitely adopt the parallaxes corresponding to the first of (47); these will be obtained by interpolating between the two solutions based on (49).

Remark 3.—The value now derived for the Scorpius-Centaurus region is considerably smaller than $r_u = \pm 2.1$ found in *Mount Wilson Contribution* No. 82, where fortunately it does not play nearly as conspicuous a part as it will here. This was obtained in a less direct way. As far as I can see, there are two causes for the divergence, both of which tend to give too large a value: First, in *Mount Wilson Contribution* No. 82, all stars for which the probable error of the position angle of the proper motion, due to observational error, exceeds 10°, have been omitted. It can be shown that a small systematic error was thus introduced, the effect of which is an increase in the value for r_u. Secondly, in that same paper there was no limitation to stars below galactic longitude 320°. The consequence must be the introduction of a relatively larger number of stars not belonging to the group. Avoiding the first source of error by not limiting the values of r_p and excluding only the four extreme values,[1] I find by the method of *Mount Wilson Contribution* No. 82, $r_u = \pm 1.3$ km (135 stars), which is in fairly good agreement with (47). By eliminating the second source of error as well, we should no doubt find the agreement quite satisfactory.

Remark 4.—The value (42) obtained from the best radial velocities gives for the probable amount of u, including errors of observation, ± 3.6 km. Since we adopt $r_u = 1.67$ km, the probable observational error of the radial velocities is ± 3.2 km. For the Scorpius-Centaurus region the corresponding quantity is ± 2.8 km.

13. RANGE IN DISTANCE OR PARALLAX AS A FUNCTION OF λ AND v

The principle of the method followed is in the main that given by Eddington,[2] but the divergence from his treatment is sufficiently important to make a full explanation necessary. The parallaxes are derived from a comparison of the observed distribution of the v (given in Section 10) with the theoretical distribution obtained from the known distribution of u given in the preceding section.

We have (see *Mount Wilson Contribution* No. 82, p. 35)

$$v = 0.212\,\pi(V \sin \lambda + u), \tag{50}$$

v and π being expressed in seconds of arc, V and u in km per second. Now, according to the preceding section, u is distributed about the central value $u=0$ in a normal error-curve having a probable error r_u. Therefore, if we consider only stars for which π and λ are practically constant, v will be distributed according to a normal curve about the central value

$$v = 0.212\,\pi V \sin \lambda \tag{51}$$

with a probable error

$$r_v = \pm 0.212\,\pi r_u . \tag{52}$$

This, however, supposes that we disregard the observational errors. In the present case, where the proper motions are so very small, this is by no means permissible. But as the observational errors presumably are also distributed in a normal curve, the observed values of v will have a similar distribution about the central value (51), only, instead of (52) we shall have to use

---

[1] If we do not exclude these, the value of r becomes still smaller.

[2] *Stellar Movements and the Structure of the Universe*, p. 218.

$$r_v=\pm\sqrt{(0.212\ \pi r_u)^2+r^2} \tag{53}$$

where r is the probable observational error of a component of the proper motion in Boss's catalogue. I have used

$$r=0''.0056 \tag{54}$$

which is the mean of the probable errors of the motions in α and δ, as given for all our stars in Boss's catalogue. Hence, finally,

$$r_v=\pm\sqrt{(0.212\ \pi r_u)^2+0.0056^2}. \tag{55}$$

The computations were first carried through with the first value of (49), namely,

$$r_u=\pm 2.5. \tag{56}$$

Table XVI gives the theoretical distribution for v derived in accordance with (51) and (55) for $\lambda=150°$, $V=20.0$ km,[1] on the supposition that the constant parallax has, successively, the values 0″.0015,

TABLE XVI

DISTRIBUTION OF v ($\lambda=150°$, $r_u=\pm 2.5$)

v	π							
	0″.0015	0″.0045	0″.0075	0″.0105	0″.0135	0″.0165	0″.0195	0″.0225
	0.000	0.000	0.000	0.003	0.025	0.097	0.216	0.355
+0″.0550.......								
	.000	.000	.000	.006	.031	.069	.092	.098
.0500.......								
	.000	.000	.002	.017	.056	.092	.108	.102
.0450.......								
	.000	.000	.007	.039	.087	.114	.114	.099
.0400.......								
	.000	.002	.021	.074	.118	.128	.111	.088
.0350.......								
	.001	.010	.053	.117	.142	.128	.101	.075
.0300.......								
	.004	.031	.102	.152	.146	.114	.084	.061
.0250.......								
	.017	.079	.159	.170	.134	.092	.064	.044
.0200.......								
	.058	.150	.191	.155	.105	.069	.045	.031
.0150.......								
	.129	.206	.183	.120	.072	.045	.029	.020
.0100.......								
	.206	.213	.140	.077	.044	.027	.017	.013
+0.0050.......								
	.234	.163	.083	.041	.023	.014	.010	.007
0.0000.......								
	.186	.092	.039	.019	.011	.006	.005	.004
−0.0050.......								
	.107	.039	.015	.007	.004	.004	.003	.002
−0.0100.......								
	0.058	0.015	0.005	0.003	0.002	0.001	0.001	0.001

---

[1] In accordance with the definitive elements (33).

0".0045, 0".0075, 0".0105, ... 0".0225.[1] As a matter of fact, the computation was made for all the following values of π: 0".0005, 0".0015, 0".0025, ... 0".0235, and the totals in Table XVIII are the values obtained by this more elaborate computation. Indeed it is only in order to avoid typographical difficulties that the abridgment has been made. The abridged calculation is hardly less accurate, however, as will be seen if, in Table XVIII, the totals are formed for each line. Multiplied by 3, these differ but little from the totals obtained by the more elaborate computation.

Fig. 1 gives a comparison of the observed (see Table XI for $\lambda = 150$) and theoretical distribution of v for $\pi = 0''.0077$, which, according to Table IX, is the mean parallax of the stars at $\lambda = 150°$. It shows clearly that the observations are not represented at all. We conclude that the assumption of a constant π for all the stars must be abandoned. The deficiency of the theoretical curve in large values of v can evidently be remedied only by the addition of stars having larger parallaxes, while the deficiency in small values of v calls for stars of smaller parallax. Let us suppose, therefore, that there are (in fractions of the whole) n_5 stars of

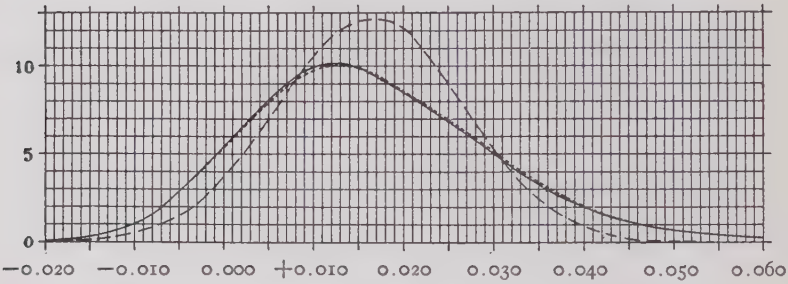

FIG. 1.—Distribution of the values of v for $\lambda = 150°$

———— Observation

— — — — Theory, constant parallax, $\pi = 0''.0081$

············ Definitive theory, interpolation from Tables XI and XXII

---

[1] Stated as a formula, the tabulated quantity is

$$\text{Prob. } v_1 \text{ to } v_2 = \frac{1}{\sqrt{3.141}} \int_{H(v_1 - 0.212\,\pi V \sin\lambda)}^{H(v_2 - 0.212\,\pi V \sin\lambda)} e^{-z^2} dz$$

where $H = 0.4769/r_v$ and r_v has the value given by (55).

parallax $0''.0005$; n_{15} stars of parallax $0''.0015$, etc. We must find n for different values of the parallax, that is, we must determine $n = \phi(\pi)$ in such a way that the mixture of all these stars gives a distribution for v agreeing with the observed distribution.[1]

Thus we might imagine each column of Table XVI to be multiplied by an indeterminate factor and then find the numerical values of these factors by equating the sums of the several horizontal lines to the corresponding numbers of the observed distribution. For instance, the sixth line of Table XVI, compared with the observed number from Table XI, would give:

$$0.001\, n_{15} + 0.010\, n_{45} + 0.053\, n_{75} + \; . \; . \; . \; . \; + 0.075\, n_{225} = \frac{4.0}{66.0} = 0.061 .$$

We could thus determine all the constants, provided they were not more numerous than the equations of condition; but the solution would be neither complete—on account of the restricted number of constants—nor satisfactory. There are conditions which certainly, or at least very probably, must be satisfied if the solution is to be acceptable. As such we may specify:

$$\left.\begin{array}{l} \phi(0) = 0 \qquad \phi(\infty) = 0 \\ \phi(\pi) \text{ shall have but one maximum and vary continuously;} \\ \quad \bar{\pi} = \text{known value}^{2} \end{array}\right\} \qquad \text{(B)}$$

I therefore proceeded somewhat differently. Starting from a first approximation[3] for $\phi(\pi)$, which satisfies the conditions (B), I computed the theoretical distribution. The divergences of this from

---

[1] Put in the form of an integral equation: if $\psi(v)\delta v$ represent the fraction of the stars having their v between v and $v + \delta v$, we have

$$\psi(v) = \frac{1}{\sqrt{3.1416}} \int_0^\infty H\phi(\pi) e^{-H^2(v - 0.212\pi V \sin\lambda)^2} \delta\pi$$

where

$$H = \frac{0.4769 \ldots .}{\sqrt{(0.212\, \pi r u)^2 + r^2}} . \qquad \text{In this equation: given } \psi(v), \text{ required } \phi(\pi).$$

[2] This condition might have been omitted. The method will itself furnish the value of $\bar{\pi}$. I have preferred, however, to use the values already found.

[3] It is not of much importance what form we choose as a first approximation for $\phi(\pi)$. Still it will shorten matters not a little if it is not too far in error, and it is not difficult to find a fairly plausible beginning. Let $\psi(M)\delta M$ be the fraction of all the stars having absolute magnitude between M and $M + \delta M$; $D(\pi)$ = star density =

the observed distribution were then diminished by a local correction of $\phi(\pi)$, in which I took pains to keep (B) always satisfied. The process requires some care; but I was not long in obtaining a solution,[1] which, if it is not the best that can be obtained, meets the requirements in a very satisfactory manner. The solutions for $\lambda=154^\circ$ and $\lambda=157^\circ\!.5$ were carried through in exactly the same manner. The results for $\phi(\pi)$ are in Table XVII. The computation of the theoretical distribution for v with the help of these values $\phi(\pi)$ is shown for $\lambda=150^\circ$ in Table XVIII. The second column is obtained by multiplying the second column of Table XVI by 0.027, i.e. (see Table XVII), by the value of $\phi(\pi)$ for $\pi=0''\!.0015$, and similarly for the other columns. These values of $\phi(\pi)$ are entered in the last line of the heading of Table XVIII. The theoretical distribution of v is given in the column headed Σ, which is the sum of all the numbers (for all the parallaxes $0''\!.0005$, $0''\!.0015$, $0''\!.0025$ . . . .) in the several horizontal lines. The last two

---

total number of stars per unit of volume at parallax π; m=apparent magnitude. Then it is easily found that

$$\phi(\pi)=\frac{A}{\pi^4}D(\pi)\psi(m+5+5\log\pi). \qquad (a)$$

It seems probable that we shall obtain a fair approximation if we assume the star-density to be constant, and if for $\psi(M)$ we use

$$\psi(M)=\frac{h}{\sqrt{\pi}}e^{-h^2(M-K)^2}$$

which was found for all the stars (see *Groningen Publication*, No. 11), and if finally for m we adopt the mean apparent magnitude of the Boss stars. We thus find

$$\phi(\pi)=\frac{B}{\pi^4}e^{-\lambda^2(G+5\log\pi)^2} \qquad (b)$$

in which there are two relations between the three constants expressing

$$\int_0^\infty\phi(\pi)\delta\pi=1; \qquad \int_0^\infty\pi\phi(\pi)\delta\pi=\bar{\pi}=\text{known quantity.}$$

The third constant is easily obtained from the observed distribution for v by successive approximations. For stars of every spectrum considered together, *Groningen Publications*, No. 11, p. 11, gives in each column of Table II the $\phi(\pi)$ for a determined value of the apparent magnitude m. I find that these are in fact represented by formula (b) with surprising accuracy.

[1] It turns out that rather different solutions for π represent the distribution of v with almost equal precision; in other words, the solution for $\phi(\pi)$ is necessarily inaccurate. This does not mean that the determination of $\bar{\pi}$ as a function of v and λ, although based on $\phi(\pi)$, is not fairly reliable. In fact it is little affected by small changes in $\phi(\pi)$.

columns will be explained presently. Repeating the computation for λ = 154° and λ = 157°.5, and multiplying the frequencies into the totals of stars observed, we have, for comparison with the observed numbers, the theoretical values in Table XI. The agreement, I think, may be considered satisfactory. For λ = 150° the theoretical distribution is shown by the dotted line in Fig. 1.

TABLE XVII

$\phi(\pi)$ FOR $r_u = \pm 2.5$

π	λ			Mean
	150°	154°	157°.5	
0".0005	0.015	0.011	0.052	0.026
.0015	.027	.026	.087	.047
.0025	.044	.043	.087	.058
.0035	.066	.062	.079	.069
.0045	.084	.075	.071	.077
.0055	.093	.084	.063	.080
.0065	.095	.091	.056	.081
.0075	.096	.095	.053	.081
.0085	.093	.094	.050	.079
.0095	.087	.090	.047	.075
.0105	.078	.082	.044	.068
.0115	.066	.072	.042	.060
.0125	.054	.059	.040	.051
.0135	.041	.045	.037	.041
.0145	.028	.032	.033	.031
.0155	.019	.020	.031	.023
.0165	.010	.010	.028	.016
.0175	.003	.005	.024	.011
.0185	0.001	.003	.021	.008
.0195	....	0.001	.018	.006
.0205	....	....	.015	.005
.0215	....	....	.011	.004
.0225	....	....	.008	.003
0.0235	....	....	0.003	0.001
$\bar{\pi}$	0".0079	0".0083	0".0083	....

The values of $\phi(\pi)$ having thus been found, the derivation of the average parallax of all the stars having the same v and λ offers no difficulty.[1] Take for instance λ = 150°. From Table XVIII we

---

[1] We have:

$$\bar{\pi}_{v,\,\lambda}=\frac{\int_0^\infty H\pi\phi(\pi)e^{-H^2(v-0.212\,\pi V\sin\lambda)^2}\delta\pi}{\int_0^\infty H\;\phi(\pi)e^{-H^2(v-0.212\,\pi V\sin\lambda)^2}\delta\pi}$$

where

$$H=\frac{0.4769\ldots}{\sqrt{(0.212\,\pi r_u)^2+r^2}}\,,\quad r=0''.0056\,.$$

find for the interval $v=0''.0350$ to $0''.0300$, that is, practically for $v=0''.0325$,

$$\bar{\pi}=\frac{0''.0045\times 0.0008+0''.0075\times 0.0051+\ldots.+0''.0165\times 0.0013}{0.0008+\qquad 0.0051+\ldots.\qquad +0.0013}=0''.0116.$$

The more complete computation, carried through with three times the number of parallaxes, furnishes the more accurate value $\bar{\pi}=0''.0107$ entered in the last column of Table XVIII. All other cases were treated in the same way.

TABLE XVIII

THEORETICAL DISTRIBUTION OF v TOGETHER WITH VALUES OF $\bar{\pi}$
(All Numbers in Units of the Fourth Decimal)

v	π AND ϕ (π)							Σ	Σ (π+tab.)	$\bar{\pi}$
	15	45	75	105	135	165	195			
	270	840	960	780	410	100	0			
	0	0	0	2	10	10	0	65	0.95	146
+550..										
	0	0	0	5	13	7	0	74	1.01	136
500..										
	0	0	2	13	23	9	0	140	1.81	129
450..										
	0	0	7	30	36	11	0	250	3.08	123
400..										
	0	2	20	58	48	13	0	420	4.85	115
350..										
	0	8	51	91	58	13	0	659	7.05	107
300..										
	1	26	98	119	60	11	0	943	9.27	98
250..										
	5	66	153	133	55	9	0	1,253	11.14	89
200..										
	16	126	183	121	43	7	0	1,484	11.79	79
150..										
	35	173	176	94	30	5	0	1,523	10.76	71
100..										
	56	179	134	60	18	3	0	1,335	8.36	63
+ 50..										
	63	137	80	32	9	1	0	953	5.27	55
0..										
	50	77	37	15	5	1	0	548	2.82	51
− 50..										
	29	33	14	5	2	0	0	244	1.11	46
−100..										
	16	13	5	2	1	0	0	110	0.46	42
Totals	271	840	960	780	411	100	0	10,001	79.73	79

Table XIX gives the complete results for λ=150°, λ=154°, and λ=157°.5. For convenience I have added the values for $v=-0''.0125$, as found by extrapolation.

The argument of this table is the *observed* value of v, which of course is the argument needed for the computation of the parallaxes. For certain purposes, however, another table is desirable with the *true* value of v (freed of observational errors) as argument. This for instance would be useful for stars whose proper motions are known with extreme precision. To calculate it we have only to use formula (52) instead of (53).[1] The results are given in Table XX.

TABLE XIX

$\bar{\pi}=F(v, \lambda)$ ($r_u=\pm 2.5$) OBSERVED VALUES OF v

v obs.	λ		
	150°	154°	157°.5
+0″.0525	0″.0135	0″.0142	0″.0180
.0475	.0129	.0134	.0170
.0425	.0122	.0127	.0160
.0375	.0115	.0119	.0150
.0325	.0107	.0112	.0139
.0275	.0098	.0103	.0124
.0225	.0089	.0094	.0107
.0175	.0079	.0085	.0090
.0125	.0071	.0076	.0073
.0075	.0063	.0068	.0061
+0.0025	.0055	.0062	.0052
−0.0025	.0051	.0057	.0045
0.0075	.0046	.0053	.0042
−0.0125	0.0042	0.0050	0.0042

TABLE XX

$\bar{\pi}=F(v, \lambda)$ ($r=\pm 2.5$) TRUE VALUES OF v

True v	λ		
	150°	154°	157°.5
+0″.070	0″.0171	0″.0187	0″.0199
.060	.0159	.0175	.0195
.050	.0146	.0161	.0187
.040	.0132	.0142	.0173
.030	.0115	.0121	.0151
.020	.0092	.0099	.0119
.010	.0061	.0069	.0076
+0.005	.0043	.0058	.0046
0.000	.0052	.0055	.0034
−0.005	.0104	.0083	.0125
−0.010	0.0136	.00124	0.0154

The divergences of Table XX from Table XIX are in a direction easy to foresee. The last shows the curious fact that, as v decreases beyond a certain value, $\bar{\pi}$ begins to increase, and soon increases at a rapid rate. This, too, is in accordance with what might have been expected, as is perhaps best seen by comparing the mean parallax of stars (all at the same distance λ from the vertex) having $v = 0''.000$ with that of stars having a definite negative value of v. For stars at all distances, the probability of the value $v = 0''.000$ is the same, for it is simply the probability that the linear velocity component u is equal, but opposite in sign, to the stream-velocity component $V \sin \lambda$. In order that v shall be negative, the linear velocity component u must be greater than (and opposite to) the stream component $V \sin \lambda$. In addition, the more distant stars, in order to show the same negative value of v, must have the greater negative value of u. A greater negative value of u, however, means a less probable one. Consequently, whereas near and distant stars contribute equally in the production of $v = 0''.000$, the nearer stars predominate in the formation of a negative value of v. Therefore, the mean parallax will be greater in the latter case.[1] This assumes that there are no observational errors. That Table XIX, in which these errors are taken into account, must show quite another behavior is clear. Indeed it is easily seen that, without such errors, practically no negative values of v would occur, at least for stars at some distance from the vertices.

---

[1] The substitution in the denominator of H of the value (52) for that of (53) is the only change in the formulae in the footnotes.

We now return to the parallaxes obtained by taking the observational errors into account. In Section 17 (*a*) evidence is given which indicates that it would have been preferable to have adopted the *same* values of $\phi(\pi)$ for all values of λ. I accordingly repeated the computation of the theoretical distribution of v and of the parallaxes, using in each case the mean values of $\phi(\pi)$ in the last column of Table XVII. These are direct means, notwithstanding the fact that the values for $\lambda = 154^\circ$ depend partly on stars also

---

[1] In order to show more in detail the way in which $\bar{\pi}$ varies with v, I computed the following table on the supposition that half the stars have $\pi = 0''.0000$, the other half $\pi = 0''.0100$, and further that $V = 20.0$ km, $\lambda = 150^\circ$, $r_u = \pm 2.5$ km.

v	$\bar{\pi}$	v	$\bar{\pi}$
$+0''.030$	$0''.0100$	$+0.005$	0.0073
0.025	0.0099	0.000	0.0080
0.020	0.0091	-0.005	0.0092
0.015	0.0078	-0.010	0.0099
$+0.010$	0.0072		

used for $\lambda = 150°$ and $\lambda = 157°.5$. The weight of the determination for $\lambda = 150°$ is undoubtedly considerably greater than that for $\lambda = 157°.5$. As the values for $\lambda = 154°$ are practically identical with those for $\lambda = 150°$, the manner of forming the means is sensibly equivalent to giving double weight to $\lambda = 150°$, which cannot be far wrong. Since the differences between the observed and the theoretical distribution were increased in every case by this procedure, the indication alluded to is not confirmed by the observed distribution of v. The safest course seems to be to adopt the arithmetic means of the parallaxes obtained on the two hypotheses, (*a*), $\phi(\pi)$ different for λ different; (*b*), $\phi(\pi)$ constant for all λ.

Having thus obtained the definitive parallaxes (for $r_u = \pm 2.5$) for $\lambda = 150°$, $154°$, and $157°.5$, we consider less frequently occurring values of λ. For $\lambda = 140°$, $145°$, $165°$, $180°$ I adopted the mean $\phi(\pi)$ in Table XVII and derived Table XXI, from which the individual parallaxes for $r_u = \pm 2.5$ were obtained by simple interpolation.

TABLE XXI

$\pi_{2.5} = \phi(v, \lambda)$ ADOPTED, FOR $r_u = \pm 2.5$ KM

v	λ							
	140°	145°	150°	154°	157°.5	160°	165°	180°
+0″.0525	0″.0143	0″.0144	0″.0145	0″.0151	0″.0172	0″.0171	0″.0170	....
.0475	.0133	.0135	.0137	.0142	.0162	.0161	.0160	....
.0425	.0124	.0126	.0128	.0133	.0151	.0151	.0150	....
.0375	.0114	.0116	.0119	.0123	.0141	.0140	.0139	....
.0325	.0104	.0107	.0110	.0115	.0130	.0129	.0127	0″.0139
.0275	.0093	.0097	.0100	.0105	.0117	.0116	.0115	.0123
.0225	.0082	.0086	.0090	.0094	.0103	.0103	.0103	.0108
.0175	.0071	.0075	.0079	.0085	.0089	.0090	.0092	.0094
.0125	.0060	.0065	.0070	.0075	.0074	.0077	.0083	.0084
.0075	.0051	.0056	.0061	.0066	.0064	.0068	.0075	.0077
+0.0025	.0043	.0048	.0053	.0060	.0056	.0060	.0069	.0074
−0.0025	0.0035	.0042	.0048	.0054	.0050	.0055	.0065	.0074
0.0075	....	0.0038	.0043	.0049	.0047	.0053	.0065	.0077
0.0125	....	....	0.0038	0.0046	0.0046	0.0052	0.0065	.0084
−0.0175	....	....	....	....	....	....	....	0.0094

14. CASE $r_u = 0.0$

According to Section 12, Remark 2, the calculations have now to be repeated for the value $r_u = 0.0$. Tables XXII, XXIII, and XXIV, corresponding to Tables XI, XVII, and XXI, unchanged but for the value of r_u, embody the results. Comparison of Tables XI and XXII shows that the observed distribution of v is about equally well represented in the two cases. The values of $\phi(\pi)$ in Tables XVII and XXIII show large differences. The remarks in the footnotes of Section 13 also hold here.

TABLE XXII*

DISTRIBUTION OF v (THEORETICAL NUMBERS ARE FOR r_u=0.0)

v	$\bar{\lambda}=150°$			$\bar{\lambda}=154°$			$\bar{\lambda}=157°.5$		
	Obs.	Theor.	O.−C.	Obs.	Theor.	O.−C.	Obs.	Theor.	O.−C.
	0.5	0.3	+0.2	0.3	0.2	+0.1	1.1	0.1	+1.0
+0″.055									
	0.5	0.5	0.0	0.5	0.3	+0.2	0.7	0.5	+0.2
.050									
	0.9	0.9	0.0	0.8	0.5	+0.3	1.1	0.8	+0.3
.045									
	1.6	1.8	−0.2	1.6	1.5	+0.1	1.6	1.9	−0.3
.040									
	2.6	2.9	−0.3	2.7	2.7	0.0	2.5	3.0	−0.5
.035									
	4.0	4.6	−0.6	4.4	4.4	0.0	3.6	4.4	−0.8
.030									
	6.1	6.4	−0.3	6.5	6.4	+0.1	5.1	5.6	−0.5
.025									
	7.9	8.1	−0.2	8.4	8.4	0.0	6.8	6.9	−0.1
.020									
	9.2	9.4	−0.2	9.9	10.1	−0.2	8.6	8.4	+0.2
.015									
	10.2	9.6	+0.6	10.2	10.5	−0.3	10.0	10.0	0.0
.010									
	9.2	8.6	+0.6	9.0	9.4	−0.4	10.5	10.9	−0.4
+0.005									
	6.7	6.4	+0.3	6.7	7.0	−0.3	9.7	10.0	−0.3
0.000									
	4.1	3.8	+0.3	4.2	4.2	0.0	7.3	7.2	+0.1
−0.005									
	1.8	1.8	0.0	2.1	1.9	+0.2	4.5	3.8	+0.7
0.010									
	0.6	0.8	−0.1	0.8	0.9	+0.2	1.9	1.7	+0.2
0.015									
	0.1			0.3			0.5	0.4	+0.1
−0.020									
Totals	66.0	66.0	....	68.4	68.4	....	75.5	75.6	....

* Same as Table XI except that r_u=0.0 instead of ±2.5.

The parallaxes obtained by interpolation from Table XXI ($r_u=\pm 2.5$) appear in Table XXXIX under the head $\pi_{2.5}$; those from Table XXIV ($r_u=0.0$), under the head $\pi_{0.0}$. Finally the adopted π, corresponding to the adopted value $r_u=\pm 1.67$ (47), was obtained from

$$\pi=\frac{2\pi_{2.5}+\pi_{0.0}}{3}. \qquad (57)$$

TABLE XXIII*

$\phi(\pi)$ FOR $r_u=0.0$

π	λ			Mean
	150°	154°	157°.5	
0″.0005.....	0″.040	0″.032	0″.119	0″.064
.0015.....	.066	.058	.115	.080
.0025.....	.074	.066	.094	.078
.0035.....	.077	.069	.072	.073
.0045.....	.077	.073	.054	.068
.0055.....	.075	.075	.043	.064
.0065.....	.072	.072	.039	.061
.0075.....	.070	.070	.036	.059
.0085.....	.067	.067	.035	.056
.0095.....	.063	.063	.034	.053
.0105.....	.058	.058	.033	.050
.0115.....	.052	.052	.032	.045
.0125.....	.046	.046	.030	.041
.0135.....	.039	.039	.028	.035
.0145.....	.032	.032	.027	.030
.0155.....	.023	.029	.026	.026
.0165.....	.018	.024	.025	.022
.0175.....	.013	.019	.024	.019
.0185.....	.010	.016	.023	.016
.0195.....	.009	.013	.022	.015
.0205.....	.007	.011	.020	.013
.0215.....	.006	.008	.019	.011
.0225.....	.004	.006	.016	.009
.0235.....	0.002	0.002	.014	.006
.0245.....	....	....	.010	.003
.0255.....	....	....	.007	.002
0.0265.....	....	....	0.003	0.001
π	0″.0079	0″.0085	0″.0083	

* Same as Table XVII except $r_u=0.0$ instead of ± 2.5.

For Boss 1517, for which v is far beyond the limits of the tables, see the footnote to Table XXXIX. For one or two stars there has been a slight extrapolation. For all stars outside the Nebula-group within 15° of the antivertex the values of π have been marked uncertain (:).

TABLE XXIV*

$\pi_{0.0}=\phi(v, \lambda)$ ADOPTED, FOR $r_u=0.0$

v	λ							
	140°	145°	150°	154°	157°.5	160°	165°	180°
+0″.0525	0″.0176	0″.0186	0″.0197	0″.0203	0″.0224	0″.0226	0″.0226	0″.0081
.0475	.0160	.0171	.0182	.0191	.0212	0214	.0216	.0081
.0425	.0142	.0153	.0165	.0177	.0199	.0200	.0202	.0081
.0375	.0126	.0136	.0148	.0162	.0183	.0184	.0186	.0081
.0325	.0109	.0119	.0130	.0143	.0165	.0166	.0169	.0081
.0275	.0093	.0102	.0111	.0122	.0142	.0145	.0151	.0081
.0225	.0077	.0085	.0093	.0102	.0116	.0120	.0129	.0081
.0175	.0062	.0069	.0076	.0084	.0091	.0097	.0109	.0081
.0125	.0049	.0055	.0061	.0068	.0068	.0075	.0089	.0081
.0075	.0038	.0043	.0048	.0053	.0051	.0058	.0072	.0081
+0.0025	.0029	.0033	.0037	.0043	.0039	.0045	.0059	.0081
−0.0025	0.0026	0.0026	.0030	.0034	.0032	.0037	.0048	.0081
0.0075	....	....	.0025	.0027	.0028	.0034	.0045	.0081
−0.0125	....	....	0.0022	0.0023	0.0026	0.0032	0.0043	0.0081

* Same as Table XXI except $r_u=0.0$ instead of ± 2.5.

15. PROBABLE ERRORS OF THE PARALLAXES

We again consider separately the two cases $r_u=\pm 2.5$ km and $r_u=0.0$ km, beginning with $r_u=\pm 2.5$. The value of π adopted for any one star is really the mean $\bar{\pi}$ of the parallaxes of all stars having the same v and λ. Let π_t be the true parallax. It is easy to find the probable value of the deviations $\pi_t-\bar{\pi}$, if for the moment we assume that they follow the error-law. Take for instance a star for which $\lambda=150°$, $v=0''.0325$. Table XVIII shows that for $r=\pm 2.5$ the adopted value of $\bar{\pi}$ $(=0''.0107)$ is the mean built up from

0.0008 stars having $\pi=0''.0045$, therefore $\pi_t-\bar{\pi}=-0''.0062$
0.0051 “ “ “$=0.0075$, “ “ $=-0.0032$
0.0091 “ “ “$=0.0105$, “ “ $=-0.0002$
0.0058 “ “ “$=0.0135$, “ “ $=+0.0028$
0.0013 “ “ “$=0.0165$, “ “ $=+0.0058$

Hence, for a total of 0.0221 stars, the sum of the residuals, all taken positively, is

$$0.0008\times 0.0062+0.0051\times 0.0032+\ .\ .\ .\ .\ =0.00004688.$$

Therefore

$$\text{Average value of } \pi_t-\bar{\pi}=0''.00212$$
$$\text{Probable value of } \pi_t-\bar{\pi}=0''.00179$$

The more refined computation, based on a table such as Table XVIII, but extended to all the parallaxes, 0″.0005, 0″.0015, 0″.0025, ... gives

$$\text{Probable value of } \pi_t - \bar{\pi} = \pm 0''.00191.$$

With similar computations for other values of v and λ, and a repetition for $r=0.0$, I find finally, interpolating for $r_u = \pm 1.67$, the results in Table XXV, which include the effect of observational errors in the proper motions. Roughly speaking, we may say that for $\lambda < 156°$

$$r_\pi = \pm 0''.0021. \tag{58}$$

For $\lambda > 156°$ the error rapidly increases.

TABLE XXV

PROBABLE ERRORS OF π

v	$\lambda=150°$	$\lambda=154°$	$\lambda=157°.5$
+0″.0325	0″.0020	0″.0021	0″.0029
0.0225	0.0021	0.0022	0.0030
0.0125	0.0020	0.0022	0.0029
+0.0025	0.0019	0.0021	0.0025
−0.0075	....	....	0.0022

But these probable errors have been computed on the supposition that the deviations follow the error-law. This may answer for the larger values of v, but it gives only a rough idea of the deviations for the smaller values of v. Indeed it is seen from Table XVIII, in which each horizontal line gives the frequency of the various values of π for stars of the same λ and v, that the distribution becomes very skew indeed for the vanishing values of v. The skewness is still more marked for the higher values of λ, the tables for which are not given here.

It is evident that this must be so. None of the parallaxes is negative; therefore, as an example, in the case of $\lambda = 150°$, $v = 0''.0025$, where Table XVIII gives $\bar{\pi} = 0''.0055$, deviations below $-0''.0055$ are impossible, whereas no such impossibility exists for deviations greater than $+0''.0055$. In fact, according to Table XVIII, the number of such deviations is by no means negligible.

In *Groningen Publications*, No. 8, p. 21, I assumed—in a very similar case and for quite the same reason—that not π but $\log \pi$ is distributed according to a normal error-curve. Schwarzschild[1] demonstrated theoretically that this must really be so, or rather that it is consistent with what we know or accept in connection with the distribution of the stars in space.

Table XVIII and others similar to it for the case of vanishing observational errors seem to offer an opportunity for testing the validity of the assumption directly by what we know from observation, for these tables are really derived from the observed distribution of v. It may be sufficient to state that, on trial, I found the result somewhat inconclusive. For $\lambda = 157\overset{\circ}{.}5$ the representation of the difficult cases by the logarithmic curve is satisfactory; for $\lambda = 150°$ it is not. More extensive data, less strongly influenced by observational errors, are required to make the test decisive.

16. APPLICATION OF THE METHOD TO THE VALUES OF τ

It seems natural to attempt to use the component τ of the proper motion as we have used v in what precedes. Since τ is independent of the stream-velocity, we avoid all the difficulties presented by this motion. We need not consider groups within narrow limits of λ; errors in its velocity V are of no consequence, etc.

We compare the observed distribution, which has been given in Table XII, with the theoretical distribution. To determine the latter we have, as before,

$$\tau = 0.212 \pi t \tag{59}$$

(τ and π in seconds of arc; t in km per second). The distribution of t (Section 11) is practically according to an error-curve, the central value being $t = 0$, with a probable error

$$r_t = r_u = \pm 1.67 \text{ km} \tag{60}$$

Hence, the values of τ for stars of the same parallax will also be distributed according to the error-law. The central value will be zero, and the probable error $\pm 0.212 \pi r_u$. The observational errors will not disturb the distribution in an error-curve; the only effect will be to increase the probable error to

---

[1] *Astronomische Nachrichten*, **190**, 361, 1912.

$$R=\pm\sqrt{(0.212\,\pi r_u)^2+r^2}$$

In Section 10 values of τ with probable errors exceeding $0''.0069$ were neglected. Consequently r is now found to be smaller than in the preceding section, namely,

$$r=\pm 0''.0047. \tag{61}$$

Hence

$$R=\pm\sqrt{(0.354\pi)^2+(0''.0047)^2}\,. \tag{62}$$

In analogy with Section 13, we might now compute the distribution of τ for a series of consecutive values of π and then try to find the relative numbers of stars with these parallaxes necessary to produce a distribution of τ agreeing with that observed—in other words, find values of $n=\phi(\pi)$ which will harmonize theory with observation.[1] But it appears that such an attempt is doomed to failure, for, whether we assume all the stars to have the same parallax, or whether we assume π to be distributed according to $\phi(\pi)$ in Tables XVII and XXIII, we find practically the same distribution for τ. The solution is so little sensitive to changes in $\phi(\pi)$ that the determination of this function in the manner proposed is hopeless.

For example, let I represent the distribution of τ resulting from the known distribution of t, when we adopt for all the stars the parallax $0''.0081$. The distribution of τ then follows an error-curve with a probable error found by (62) to be $R=\pm 0''.0055$. Similarly let II represent the distribution of τ, resulting when we assume for $\phi(\pi)$ the values found for $\lambda=150°$ by interpolation between Tables XVII and XXIII. Finally let III represent the same distribution, when for $\phi(\pi)$ we adopt the result of interpolating between the

---

[1] This would be equivalent to finding the solution of the integral equation:

$$\text{Prob.}\,{}_{\tau}^{\tau+\delta t}=\frac{1}{3.14\ldots\ldots}\delta\tau\int_0^\infty H\phi(\pi)e^{-H^2\tau^2}\delta\pi$$

where

$$H=\frac{0.4769\ldots\ldots}{\sqrt{(0.212\,\pi r_u)^2+r^2}}\,.$$

The first member being given, we would have to find $\phi(\pi)$.

mean values of Tables XVII and XXIII. The method of obtaining II and III is so analogous to that followed for v in Section 13 that it need not be described. The results (total number of stars 72) are given in Table XXVI. They are so nearly identical that, whatever the observed distribution, a choice between the three solutions is impossible. All three agree equally well or equally badly.[1] Actually the agreement is in no case perfect, for solution I (therefore also II and III) represents the distribution in an error-curve with probable error 0″.0055, while the observed distribution is sen-

TABLE XXVI

τ	Frequencies			No. of Stars		
	I	II	III	I	II	III
> ±0″.025.....	0.002	0.000	0.006	0.1	0.0	0.4
±0″.025 to ±0.020.	.012	.014	.018	0.9	1.0	1.3
±0.020 " ±0.015.	.052	.052	.056	3.7	3.7	4.0
±0.015 " ±0.010.	.154	.152	.154	11.1	10.9	11.1
±0.010 " ±0.005.	.320	.318	.314	23.0	22.9	22.6
±0.005 " ±0.000.	0.460	0.464	0.454	33.1	33.4	32.7
Totals........	1.000	1.000	1.002	71.9	71.9	72.1

---

[1] In the case of data a hundred times richer, such differences as we find between the several solutions might lie well outside the limits of uncertainty of the observed numbers. But even then the solution for $\phi(\pi)$ would have to be considered illusory, at least in the present state of science. To show this clearly, let us assume our data to be so numerous that the frequencies could be considered reliable to the third decimal inclusive, and further, that the observed frequencies agreed absolutely with the theoretical frequencies of solution II. Would this prove that solution II for $\phi(\pi)$ would be the correct one? By no means, for we are far from certain that the linear motion t for the distribution of which we assumed the error-law, really follows this law with a precision of a few thousandths in the frequencies. Indeed we know that, at least for a mixture of stars of all spectra, there are very appreciable deviations from this law (see Schwarzschild, *Astronomische Nachrichten*, **190**, 376, 1912; Kapteyn and Adams, *Proc. Nat. Acad. Sci.*, **1**, 18, 1915). It even seems questionable whether the accidental observational errors in t follow the error-law with such nicety. The real frequency law of the linear velocities might therefore be such that if we reduce to angular motion on the assumption of the same parallax for all stars, and add the effect of the accidental errors of observation, we would find, instead of I, such a distribution as II or III or any other distribution diverging from I by quantities of the same order. In case we found exactly the distribution II we should of course conclude, instead of inferring that $\phi(\pi)$ had the values given above for II, that all the stars had the same parallax.

sibly in an error-curve with the probable error ±0".0061 (Section 10). Were the difference well established it would have to be interpreted, either (*a*) as an error in the adopted mean parallax 0".0081, or (*b*) as an error in the adopted probable amount ±1.67 km for *t*, or (*c*) as a combination of both (*a*) and (*b*). On the first hypothesis the mean parallax should be 0".0110; but the evidence for the change is almost negligible.

17. ADDITIONAL EVIDENCE AS TO THE VALUES OF THE PARALLAXES

The difficulty of the question and particularly the relative crudeness of the data seem to justify the accumulation of as many checks as can be obtained. I have therefore brought together whatever further evidence I have been able to find, not hesitating to include some which is only partly independent of what precedes.

a) *The range in parallax.*—Though the values of τ do not afford a useful determination of the parallaxes, they may serve indirectly by rendering possible the elimination of observational errors. For this purpose I will compare the components υ and τ for stars at the same, or nearly the same, distance λ from the vertex. The values of υ contain the component of the stream-motion (in angular measure) and the peculiar proper motion; τ contains only the latter. If all the stars had the same parallax, the angular stream-motion in υ would be the same for all. As the peculiar motions are supposed to be random in direction, the common angular stream-motion would be the arithmetic mean $\bar{\upsilon}$ of υ. Hence $\upsilon-\bar{\upsilon}$, as well as τ, would include only the peculiar motion. Both would have all sorts of values, but the average amounts (all taken positively) and similarly the probable amounts would be equal.

If, on the contrary, the parallaxes are unequal, the stream-motion involved in the υ will not be the same for all stars. The quantities $\upsilon-\bar{\upsilon}$ will include the peculiar motions, and also an element dependent on the stream-motion, which will be the greater the greater the diversity of parallaxes.

The average value of $\upsilon-\bar{\upsilon}$ (disregarding signs) and its probable value will now be greater than the corresponding values for τ. The difference will be a measure of the diversity of the parallaxes, that is, of the range in distance.

In the elaboration of this idea we must consider the observational errors. Since the component of the stream-motion at right angles to the line of sight for stars at the distance λ from the vertex is $V \sin\lambda$ km per second, or $0.212\, V \sin\lambda$ astronomical units per year, we shall have, if we call α and β the peculiar angular motions in the direction of υ and τ respectively,

$$\left.\begin{aligned} \upsilon &= 0.212\, \pi V \sin\lambda + \alpha + \text{obs. err. in } \upsilon \\ \tau &= \beta + \text{obs. err. in } \tau \end{aligned}\right\}. \qquad (63)$$

For a great number of stars the arithmetic means of α, of β, and of the observational errors in υ and τ will be zero. Hence

$$\left.\begin{aligned} \upsilon - \bar{\upsilon} &= 0.212\, V \sin\lambda\, (\pi - \bar{\pi}) + \alpha + \text{obs. err. in } \upsilon \\ \tau &= \beta + \text{obs. err. in } \tau^{1} \end{aligned}\right\}. \qquad (64)$$

Squaring and forming the means for all available stars, we find, putting

$$\pi - \bar{\pi} = \Delta\pi \qquad (65)$$

$$\left.\begin{aligned} \frac{1}{n}\Sigma(\upsilon - \bar{\upsilon})^2 &= (0.212\, V \sin\lambda)^2 \overline{(\Delta\pi)^2} + \frac{1}{n}\Sigma\alpha^2 + \frac{1}{n}\Sigma(\text{obs. err. in } \upsilon)^2 \\ &\qquad + \text{double products} \\ \frac{1}{n}\Sigma\tau^2 &= \frac{1}{n}\Sigma\beta^2 + \frac{1}{n}\Sigma(\text{obs. err. in } \tau)^2 \\ &\qquad + \text{double products} \end{aligned}\right\} \qquad (66)$$

The double products will nearly disappear, because the factors are as frequently positive as negative. Further, $\Sigma\beta^2$ will approximately equal $\Sigma\alpha^2$. The terms depending on observational errors may differ slightly on account of possible differences of accuracy in the proper motions for α and δ; but as these differences are generally small, and greatly diminished in υ and τ, we assume these terms also to be equal. Hence, if we write

$$S^2 = \frac{1}{n}\Sigma(\upsilon - \bar{\upsilon})^2 - \frac{1}{n}\Sigma\tau^2 \qquad (67)$$

we obtain

$$(0.212\, V \sin\lambda)^2\, \overline{(\Delta\pi)^2} = S^2 \qquad (68)$$

where S is a quantity given by the observations.

---

[1] It is slightly more correct to use $\tau - \bar{\tau}$ than τ. This refinement was indeed introduced; $\bar{\tau}$, however, is so small that the correction is without influence.

Applying this formula to narrow zones of λ, I find

λ		No. Stars	Weight	
145° to 149°	$\overline{(\Delta\pi)^2}=+0.000011$	26	15	(69)
150 " 154	$+\ .000042$	40	12	
155 " 159	$+\ .000025$	28	4	
160 " 164	$+0.000017$	17	1	

from which

$$\overline{(\Delta\pi)^2}=+0.000024\pm0.000005 \quad (111 \text{ stars}). \tag{70}$$

From the preceding section, for $\lambda=150^\circ$ and $\lambda=157^\circ\!.5$, the two being practically independent,

$\lambda=150^\circ\!.0$	$\overline{(\Delta\pi)^2}=0.0000135$
$\lambda=157.5$	0.0000337
Mean	0.000024

The agreement of the two mean values is beyond expectation. As $\overline{(\Delta\pi)^2}$ is preponderatingly dependent on the extreme parallaxes, both large and small, I see in this agreement a good test of the correctness of the total range in distance. On the other hand, we here find a difference for high and low λ which is not confirmed by (69). As this difference is due to the differences shown in Tables XVII and XXIII between the values $\phi(\pi)$ for different values of λ, we obtain an indication that it would have been preferable to adopt for the different zones of λ values for $\phi(\pi)$ which more nearly agree. This is the reason why I definitively adopted in the preceding section, for $\lambda=150^\circ$, 154°, and $157^\circ\!.5$, values of $\phi(\pi)$ intermediate between those found directly and the mean of all.

b) *Test of the moderate and large parallaxes.*—Since v is the angle subtended at the earth by the projection on the sphere of the stream-velocity increased by the component u (u counted positively in the sense of the stream-motion), it will, on the whole, be somewhat greater for the stars having positive values of u, and smaller for those having negative values of u. In other words, there must be a certain degree of correlation between v and u. The coefficient of this correlation ρ necessarily lies between zero and unity, $\rho=0$ corresponding to an absence of correlation. For this case the average of the several u's corresponding to any given v would be zero; for $\rho=1$, u is a pure function of v alone, and a value of v fully determines u, which I will call u_v. According to (50) the two extreme cases give

$$\rho=0; \qquad \bar{\pi}_0=\frac{v}{0.212\, V \sin\lambda}\ ^{*} \tag{71}$$

$$\rho=1; \qquad \bar{\pi}_1=\frac{v}{0.212\,(V \sin\lambda+u_v)}\,. \tag{72}$$

As the truth lies between the two, we thus obtain two limits for $\bar{\pi}$.

The value of u_v for any value of v is easily obtained. It will be necessary, however, first to derive from Table XI, which gives the distribution of the observed v, one giving the distribution of the true v (free from observational error). Professor Eddington[1] has given an extremely elegant and convenient method, but the observed frequency-curves are here so nearly error-curves that an even more convenient method is available.

Thus, for instance, the observed frequency-curve of Table XI for $\lambda=150°$ is represented approximately by an error-curve with the central value 0″.0162 and the probable error 0″.00917. As the probable error of observation is ±0″.0056 (54), the frequency-curve of the v, freed from observational error, will evidently be an error-curve with the same central value, $\nu=0''.0162$, and the probable error $\sqrt{0.00917^2-0.0056^2}=\pm0''.00725$. Proceeding in the same way for the other values of λ we have:

	Central Value	P.E. Free from Obs. Error
$\lambda=150°$	0″.0162	±0″.00725
$\lambda=154$	0.0159	0.00705
$\lambda=157.5$	0.0135	±0.00693

---

* This is only approximately true and assumes that (with the exception of a vanishingly small number of extreme values of u) u is small as compared with $V \sin\lambda$. For in this case we may write, neglecting squares of small quantities,

$$\pi=\frac{v}{0.212\,(V\sin\lambda+u)}=\frac{v}{0.212\,V\sin\lambda}\left(1-\frac{u}{V\sin\lambda}\right)$$

from which, because $\bar{u}=0$,

$$\bar{\pi}=\frac{v}{0.212\,V\sin\lambda}\,.$$

[1] *Monthly Notices*, **73**, 359, 1913.

With the aid of these numbers we find by the ordinary theory of the distribution of observational errors that the following fractions of all the stars entered in Table XXVII have values of v exceeding given limits.

TABLE XXVII

FREQUENCY OF v EXCEEDING CERTAIN LIMITS

v	$\lambda = 150°$	$\lambda = 154°$	$\lambda = 157°.5$
$>0''.030$	0″.100	0″.089	0″.054
.025	.206	.192	.132
.020	.362	.347	.263
.015	.544	.535	.442
.010	.718	.714	.633
0.005	0.851	0.851	0.906

Now it is evident that if u is a function of v alone, as it is in the extreme case under consideration, it increases and diminishes with v, and the number of values of v and of u exceeding specified corresponding limits must be the same, and conversely. That is, the value u corresponding to any particular value of v will be that value of u which is as frequently exceeded as is the particular value of v. Therefore, to take an instance, since by Table XXVII, for $\lambda = 150°$, v exceeds $0''.030$ in 0.100 of all the cases, and since in the theory of observational errors we find that an error exceeding $+1.90$ times the probable error (which for u is ± 1.67) occurs in just 0.100 of all the cases, therefore $u_{0''.030} = +1.90 \times 1.67 = +3.2$, and similarly in other cases, thus giving the results in Table XXVIII. With the aid of these data, (71) and (72) lead to Table XXIX.

TABLE XXVIII

u_v $(r_u = \pm 1.67)$

v	λ		
	150°	154°	157°.5
	km	km	km
0″.030	+3.2	+3.4	+4.0
.025	+2.0	+2.2	+2.8
.020	+0.9	+1.0	+1.6
.015	−0.3	−0.2	+0.4
.010	−1.4	−1.4	−0.85
0.005	−2.6	−2.6	−3.3

TABLE XXIX

LIMITS FOR π

v	$\lambda=150°$			$\lambda=154°$			$\lambda=157°.5$		
	$\bar{\pi}_0$	π	$\bar{\pi}_1$	π_0	π	$\bar{\pi}_1$	$\bar{\pi}_0$	π	$\bar{\pi}_1$
0″.030...	0″.0141	0″.0124	0″.0107	0″.0161	0″.0134	0″.0116	0″.0185	0″.0162	0″.0121
.025...	.0118	.0109	.0098	.0134	.0119	.0108	.0154	.0142	.0113
.020...	.0094	.0093	.0087	.0107	.0102	.0097	.0124	.0120	.0103
.015...	.0071	.0076	.0073	.0081	.0084	.0082	.0093	.0097	.0088
.010...	.0047	.0056	.0055	.0054	.0064	.0064	.0062	.0071	.0069
0.005...	0.0024	0.0037	0.0032	0.0027	0.0048	0.0038	0.0031	0.0041	0.0054

With these limits we have to compare the values of $\bar{\pi}$ corresponding to the true values of v as argument. For $r_u=\pm 2.5$ km, $\bar{\pi}$ has been given in Table XX; for $r=0.0$ it is to be computed by

$$\bar{\pi}=\frac{v}{0.212\,V\sin\lambda}=\frac{v}{4.24\sin\lambda}\,.$$

Interpolating for $r_u=\pm 1.67$, we find the values in Table XXIX under the heading π. Our test is that π ought to be included between the limits $\bar{\pi}_0$ and $\bar{\pi}_1$.

In making the comparison we must consider that the values of u_v in Table XXVIII depend in the last instance on observations, and as such are liable to error. The limit $\bar{\pi}$, itself, is therefore liable to such error. Further, from (72) we see that for values of u_v not too far from $-V\sin\lambda$ any error in u_v appears in $\bar{\pi}$ enormously exaggerated. For this reason it is not surprising that for values of v as small as 0″.015 or 0″.010 the values of π in Table XXIX are sometimes slightly beyond the limit $\bar{\pi}_1$. For v still smaller, the present test of the parallaxes is, I think, of little value. Taking all this into consideration there seems to me every reason to be satisfied.

c) *Test for the distant stars.*—I will here use only the B0–B5 stars and will consider that fifth of them for which v is smallest—on the whole, the more distant objects. They are

for $\lambda=145°$ to $154°$ those for which $v<+0''.0048$
for $\lambda=155$ to 165 those for which $v<+0.0015$.

Stars still nearer to the antivertex will be disregarded, as will also the few stars for which $\lambda<145°$. It is my aim to find something like a lower limit for the parallax π_d of these stars which for brevity will be called the great-distance stars.

For this purpose I will make use of the luminosity-curve of the B0–B5 stars, for which a fairly reliable curve has been found in *Mount Wilson Contribution* No. 82. A formula was also derived (*op. cit.*, p. 64) by which the mean parallax can be found for a group of stars which is complete down to a specified magnitude m_0, when the average apparent magnitude $\overline{m}$ of the whole group has been observed. For $m_0=5.81$, which is the Harvard magnitude limit to which Boss's catalogue is complete, the formula becomes

$$\overline{m}=-4.115-5\log\pi-0.691\frac{e^{-P^2}}{\frac{1}{\sqrt{\pi}}\int_{-\infty}^{P}e^{-z^2}\delta z} \qquad (73)$$

where[1]

$$P=+4.055+2.045\log\pi. \qquad (74)$$

In order to eliminate to a great extent the errors of the adopted luminosity-curve, I will apply the formula not only to the great-distance stars but also, for comparison, to the entire group of B0–B5 stars, adopting for the mean parallax of the latter $\overline{\pi}=0\overset{''}{.}0081$. The method thus becomes a more or less differential one.

If to the limit 5.81 mag.

$\overline{m}_1$ = average mag. of all the stars

$\overline{m}_2$ = average mag. of the great-distance stars

then (73) and (74) show that

if $\overline{m}_2-\overline{m}_1=$ $0\overset{m}{.}00$ then $\pi_d=0\overset{''}{.}0081$

" " $+0.10$ " " 0.0069

" " $+0.20$ " " 0.0057

" " $+0.30$ " " 0.0046

" " $+0.40$ " " 0.0036

From Table XXXIX I find that in reality

$\overline{m}_1=4.78\pm0.06$ (86 stars)

$\overline{m}_2=4.81\pm0.14$ (14 stars)

---

[1] The formula supposes that the range in π is not excessive. I feel confident that we may safely apply it in the present case. But, in case of doubt, the method which is fully explained in *Mount Wilson Contribution* No. 82, pp. 65–68, can be applied.

Therefore $m_2-m_1=+0.03\pm0.15$, and according to the preceding table

$$\pi_d=0''.0077\pm0''.0018. \tag{75}$$

Since the average value of υ for the stars of great distance is found to be $-0''.0016$, interpolation between Tables XXI and XXIV gives for the mean of $\lambda=150°$, $154°$, and $157°.5$

$$\pi_d=0''.0046. \tag{76}$$

The difference is considerable, but so also is the probable error in (75). In fact the difference is 1.7 times the probable error.

The conclusion from this test would seem to be that the number of stars is too small to lead to any well-founded result. The result as it stands would indicate that the adopted parallaxes of the distant stars are too low rather than too high. Any material change in this direction seems pretty well excluded, however, by the more reliable tests (*a*) and (*b*).

d) *Test by binary systems.*—Professor Hertzsprung courteously furnished me with the following hypothetical parallaxes, derived by a method which allows of a fairly good determination of parallax for any double star as soon as it shows sensible orbital motion. He will no doubt soon publish his method. In addition I quote the parallax of δ Orionis according to Stebbins.[1] For comparison the parallaxes obtained in the present paper are added.

	Hertzsprung and Stebbins	Kapteyn
ζ Orionis =Boss 1398..	0″.0082	0″.0057 neb.
σ " = " 1389..	0.0060	0.0057 neb.
15 Monocerotis= " 1706..	0.0089	0.0057
32 Orionis = " 1331..	0.0138	0.0156
8 " = " 1339..	0.0032	0.0057 neb.
Mean................	0.0080	0.0077

18. THE NEBULA-GROUP. ITS PARALLAX

In this group the proper motions are so exceedingly small that the method for finding the stream-elements and the parallax used above fails altogether. Fortunately I had at my disposal for this region and its surroundings, namely,

---

[1] *Astrophysical Journal*, **42**, 145, 1915.

$$\text{R.A. } 5^h0^m \text{ to } 6^h0^m, \quad \text{Dec. } -10^\circ \text{ to } +20^\circ, \qquad (77)$$

the spectra for the A and B stars obtained by Miss Cannon for the *Revised Draper Catalogue.* In Table XXX the numbers of these spectra have been summarized. In order to be sure of including only the densest part of the Nebula-group, I narrowed the limits (2) of this group[1] to

$$\text{R.A. } 5^h20^m \text{ to } 5^h40^m, \quad \text{Dec. } -7^\circ \text{ to } +2^\circ, \qquad (78)$$

an area of 45 square degrees.[1] For comparison I included the stars of region (77) well outside the Nebula-group. For these I adopted the limits:

$$\left.\begin{array}{llllll} 5^h\ 0^m & \text{to} & 5^h20^m & +3^\circ & \text{to} & +20^\circ \\ 5\ 20 & \text{“} & 5\ 60 & +5 & \text{“} & +20 \\ 5\ \ 0 & \text{“} & 5\ 10 & -10 & \text{“} & +3 \\ 5\ 50 & \text{“} & 5\ 60 & -10 & \text{“} & +5 \end{array}\right\} \qquad (79)$$

containing in all 305 square degrees. The space between these regions was not used in order to be independent of any uncertainty in the exact limits of the Nebula-group.

The last line but one in Table XXX gives the mean of the observed magnitudes. The last line gives the ratio of star density in nebula region to star density outside this region. We thus find that the nebula region is fully twelve times richer in B0–B5 stars than are the surroundings. For later types this ratio rapidly diminishes. The Nebula-group thus contains both B and A stars, but, as compared with the surrounding sky, it is very much richer in spectra of the former class.

The striking fact in the numbers of Table XXX is that the magnitude of greatest frequency is different for the nebula and the region outside. This at once promises a determination of the ratio of the parallaxes of the two groups of stars. For the absolute magnitudes of stars which are practically at the same distance

---

[1] This narrowing of the limits is the reason why the number of bright B stars in the Nebula-group, as shown by Table XXX, is smaller than that in Table XXXIX. Moreover the Oe5 stars have been omitted from Table XXX.

TABLE XXX

NUMBER OF STARS IN "REVISED DRAPER CATALOGUE"

MAGNITUDE LIMITS	MEAN MAG.	B3		B5		B0–B5		B5–B9		B8–B9		A	
		Neb.	Outside	Neb.	Outside	Neb.	Outside	Neb.	Outside	Neb.	Outside	Neb.	Outside
9.05–9.55.....	9.3	0	0	0	0	0	0	12	7	12	7	48	87
8.55–9.05.....	8.8	0	0	2	0	2	0	52	31	50	31	43	207
8.05–8.55.....	8.3	3	0	3	3	6	3	26	45	23	42	21	99
7.55–8.05.....	7.8	3	3	3	2	6	6	18	31	15	29	6	35
7.05–7.55.....	7.3	3	0	1	0	4	0	5	9	4	9	2	13
6.55–7.05.....	6.8	1	1	2	2	3	3	4	11	2	9	4	8
6.05–6.55.....	6.3	4	3	4	....	11	4	7	4	3	4	0	13
5.55–6.05.....	5.8	4	1	....	....	6	3	....	7	....	7	2	2
5.05–5.55.....	5.3	0	1	....	....	3	2	....	3	....	3	....	8
4.55–5.05.....	4.8	2	2	....	....	3	2	....	1	....	1	....	0
4.05–4.55.....	4.3	....	1	....	....	0	3	....	....	....	....	....	1
3.55–4.05.....	3.8	....	....	....	....	1	0	....	....	....	....	....	0
3.05–3.55.....	3.3	....	....	....	....	0	0	....	....	....	....	....	0
2.55–3.05.....	2.8	....	....	....	....	0	0	....	....	....	....	....	1
2.05–2.55.....	2.3	....	....	....	....	2	0	....	....	....	....	....	....
1.55–2.05.....	1.8	....	....	....	....	1	1	....	....	....	....	....	....
1.05–1.55.....	1.3	....	....	....	....	....	....	....	....	....	....	....	....
0.55–1.05.....	0.8	....	....	....	....	....	....	....	....	....	....	....	....
0.05–0.55.....	0.3	....	....	....	....	....	....	....	1	....	1	....	....
Total no	......	20	12	15	7	48	27	124	150	109	143	126	474
Mean mags..	......	6.79	6.17	7.50	7.73	6.42	6.06	....	....	....	....	....	....
$\frac{\text{Density Nebula}}{\text{Density outside}}$	......	11.3		14.5		12.0		5.6		5.2		1.83	

differ from the apparent magnitudes by a constant, $5+5\log\pi$.[1] Consequently the frequency-curve of the apparent magnitudes differs from the luminosity-curve (which is the frequency-curve of the absolute magnitudes) merely in that there is a displacement of $5+5\log\pi$ mags. between the two. For two groups with parallaxes π_1 and π_2 the frequency-curves of the apparent magnitudes will thus be the same, with the exception of the displacement

$$5\log\frac{\pi_2}{\pi_1}\text{ magnitudes.} \tag{80}$$

Consider the region of the nebula and that defined by (79) lying outside the nebula. As to the former, the lateral dimensions being small, it is all but certain that the depth also will be small. For the outside stars the distances must vary to a much greater extent, and the frequency-curve of the apparent magnitudes will here consist of the superposed frequency-curves for the different distances. If we suppose the curve of the absolute magnitudes to be an error-curve (see Section 27), the frequency-curve of the apparent magnitudes for stars at the average distance will be an error-curve with its maximum at a certain magnitude. For the stars of smaller parallax the curve will be shifted to the fainter magnitudes; for the stars with greater parallax, to the brighter magnitudes. As long as the range in distance for the great majority of the stars is moderate, as is here the case, the superposition of all these curves will still be practically an error-curve, with its maximum at nearly the same magnitude as for the stars of average parallax. Only the probable error of the curve will have increased.

---

[1] See, for instance, *Groningen Publications*, No. 11, p. 12.

This is just what is seen in Table XXX. Take first the B0–B5 stars. Owing to the limited data the numbers run very irregularly. There is, however, the fortunate circumstance that for both regions the number of stars fainter than 9.0 is zero; for the outside stars there is none fainter than 8.5. I conclude that, in the latter case at least, we have before us the *complete* frequency-curve. In the nebula region this is less certain; still the number of stars fainter than 9.0 is certainly small. It seems reasonable to assume that the true number of stars fainter than 9.05 (adopted average magnitude 9.3) is between zero and six. Now, if the luminosity-curve is an error-curve, or any symmetrical curve, the lateral shift will be that of the center of gravity or of the arithmetic mean. The mean of the magnitudes for the outside stars is 6.06. For the Nebula-group it is 6.42 and 6.74, respectively, for the two limits adopted. The displacement therefore lies between 0.36 and 0.68 mags. As the whole difference corresponds to only 0".0010 in the parallax we may adopt

$$\text{B0–B5 stars} \qquad \text{Displacement} = 0.52 \text{ mag.} \tag{81}$$

For the B8–B9 stars the matter is more difficult. But I think we may assume with some confidence that the numbers for magnitudes 9.0 and brighter are complete: for, (*a*) the whole number of stars for which Miss Cannon has determined the spectrum is 240,000,[1] which, according to *Groningen Publications*, No. 18, involves average completeness to magnitude 9.5 (Harvard Scale); (*b*) the B and A stars, being very white, must in general have been observed to a fainter limit (visually) than the others; (*c*) according to Table XXX so many stars fainter than 9.05 have been observed in the regions now under consideration that it is improbable that the brighter stars should be seriously incomplete.

---

[1] *Vierteljahrsschrift der Astronomischen Gesellschaft*, 51, 85, 1916.

On the contrary, the numbers between 9.05 and 9.55 in Table XXX are almost certainly incomplete. To be comparable with the rest they must be multiplied by a factor ϵ, greater than unity. For the nebula region, ϵ cannot well exceed 2, as is shown by the A stars, which at magnitude 9.3 must be near the maximum of their frequency-curve of apparent magnitude; the total number, therefore, from 9.05 to 9.55 can scarcely be more than double that between 8.55 and 9.05. If we admit this the uncertainty about the true value of ϵ is of little consequence, for in attempting to fit an error-curve to the observed number of the B8–B9 stars in the nebula region, we find the maximum at practically 8.8, both for $\epsilon=1$ and $\epsilon=2$.

For the outside region it seems better to ignore the stars fainter than 9.05 altogether. From the others it appears that the maximum cannot lie far from 8.30. We are thus led to a displacement of 0.50 mag. Another estimate of this quantity made in a somewhat different way gave 0.37 mag.[1] I finally adopt:

B8–B9 stars Displacement = 0.44 mag. (82)

The displacements (81) and (82) require a correction. In the case of types B0–B5, the stars within the limits (78) of the Nebula-group are twelve times more crowded than those in the surrounding regions. We conclude that a twelfth part of the B0–B5 stars within these limits do not belong to the group, but are merely seen projected on it. These can have no displacement relative to the outside stars, to which they really belong. For the others, it must be increased by an eleventh in order to correct the displacement (81). For similar reasons the displacement (82) must be increased by $\frac{1}{4.2}$ its amount.

---

[1] In the countings of the Pickering-Cannon stars, there is, as in other investigations of the kind, an obvious excess of stars of magnitude 9.0, 8.5, 8.0, and a deficiency for magnitudes 9.1, 8.9, 8.1, 7.9. I also carried through a computation in which this error was corrected; as the corrections for the numbers of stars within the half-magnitude intervals of Table XXX are insignificant, I will not burden this paper with the computation.

Hence:

B0–B5 stars: corrected displacement = 0.57 mag. (weight 2)
B8–B9 stars: corrected displacement = 0.54 mag. (weight 3)

The weights are estimates; the weighted mean is

$$\text{Displacement} = 0.55 \text{ mag.} \tag{83}$$

and by (80)

$$\frac{\bar{\pi} \text{ Outside Stars}}{\bar{\pi} \text{ Nebula-group}} = 1.288 \tag{84}$$

It remains to find $\bar{\pi}$ for the stars of magnitude 7.8, which is the average of the Cannon stars. For the Boss stars, of average magnitude 4.7, $\pi = 0''.0081$. From the Table XXXIX I find[1]

Average Mag.	$\bar{\pi}$	No.
2.73	0''.0075	7
4.16	0.0083	14
5.04	0.0086	43
5.81	0.0083	38

Apparently there is no change with the magnitude; but, as it is improbable that there should be no change at all, I adopt as a conservative estimate,

$$\bar{\pi} = 0''.0077 \; (\bar{m} = 7.8, \text{ outside stars}), \tag{85}$$

with the aid of which by (84)

$$\pi \text{ (Nebula-group)} = 0''.0060. \tag{86}$$

I think that the error of the displacement (83) cannot well be greater than half its amount and that its probable amount will not exceed a fourth of the whole. The probable error of the difference of the average parallaxes of the two groups of stars here considered ought not, therefore, to exceed $0''.0005$ and, as the probable error of the average parallax of the outside Boss stars is, by (33), $\pm 0''.0007$, the probable error of (86) may be estimated at $\pm 0''.0009$. It is found in Section 26, however, from a discussion of the luminosity-curve of the A stars, that the value (86) is very probably somewhat high, and I finally adopted

---

[1] Preliminary values of the parallaxes were used. For the present purpose these are sufficient.

$$\bar{\pi}\text{ (Nebula-group)} = 0''.0054 \pm 0''.0009. \tag{87}$$

The lateral dimensions of the Nebula-group, according to Section 3, are about 7° in right ascension and 14° in declination. If, as a crude approximation, we suppose that the group is roughly spherical with a diameter of $10^\circ.5$, the parallaxes will range from $0''.0049$ to $0''.0060$. For that half of the stars for which the proper motions are smallest I assume the parallax to be $0''.0051$, and for the others, $0''.0057$; that is,

$$\left.\begin{array}{ll} \text{for } 100\,\mu \geqq 0''.8 & \pi = 0''.0057 \\ \text{for } 100\,\mu < 0''.8 & \pi = 0''.0051 \end{array}\right\} \tag{88}$$

As already mentioned, one-twelfth of the B0–B5 stars within the limits (2) do not belong to the physical group. Within these limits there are in Table XXXIX 26 stars, practically all B0–B5 stars. Two or three are, therefore, probably outside the group, but I have assumed that the four, Boss 1302, 1343, 1376, and 1382, the only ones having $\mu \geqq 0''.020$, are in this class. The last has a large negative value of v and perhaps ought to be excluded altogether. The motions of the others can be satisfactorily explained as the result of traces of stream-motion, peculiar motion, and observational error.

Five stars, Boss 1454, 1277, 1435, 1512, and 1297, having spectra B0–B5, are within 5° of the adopted limits (2) of the Nebula-group. Their proper motions are nearly vanishing. It is doubtful whether they belong to the Nebula-group. As their parallaxes computed on the hypothesis that they are group stars differ in no case more than 30 per cent from those obtained on the assumption that they are outside stars, I adopt the means for the two suppositions.

19. TESTS FOR THE PARALLAX OF THE NEBULA-GROUP

a) By the luminosity-curve of the B0–B5 stars.—From the third column of Table XXX we have concluded that the maximum of the frequency-curve for the B0–B5 stars in the Nebula-group lies between

$$m=6.42 \quad \text{and} \quad m=6.74. \tag{89}$$

In *Mount Wilson Contribution* No. 82, p. 43, the absolute magnitude corresponding to this maximum was found to be

$$M=0.885. \tag{90}$$

If, therefore, we adopt the mean of (89) we find from

$$M=m+5+5 \log \pi, \tag{91}$$

$$\pi=0\overset{''}{.}0072. \tag{92}$$

I have not used this for the improvement of the parallax (87) because it is preferable to follow the inverse course, that is, use (87) for converting the apparent magnitudes of Table XXX into absolute magnitudes, which will be employed to improve the luminosity-curve.

b) Binary systems.—Among the binaries of Section 17, the three marked "neb." belong to the Nebula-group. In the mean they give $\pi=+0\overset{''}{.}0058$, agreeing almost perfectly with the value $0\overset{''}{.}0057$ derived from (87). That these binaries were also used in the test of the parallax of the outside stars is justified by the fact that our determination of the parallax of the Nebula-group is based on that of the outside stars.

20. MOTION OF THE NEBULA-GROUP

Considering only the best-observed stars ($100\, r<0\overset{''}{.}040$) within the limits (2) of the Nebula-group, we derive from 17 stars the averages:

$$\bar{\alpha}=5^{h}25^{m}; \quad \bar{\delta}=-1\overset{\circ}{.}4; \quad 100\,\bar{\tau}=+0\overset{''}{.}03; \quad 100\,\bar{\upsilon}=+0\overset{''}{.}02. \tag{93}$$

Including further all the stars of known radial velocity, we find from 13 stars:

$$\bar{\alpha}=5^{\mathrm{h}}26^{\mathrm{m}}; \quad \bar{\delta}=-2^{\circ}\!.2; \quad \bar{\rho}_{\mathrm{corr.}}=\bar{\rho}-4.3=18.46 \text{ km.} \tag{94}$$

The value (93) of $\bar{v}$ being absolutely insensible, I conclude that the antivertex must be not far from the point

$$5^{\mathrm{h}}25^{\mathrm{m}}, \qquad -1^{\circ}\!.4. \tag{95}$$

How far away can it be placed without conflicting with the observations? I think it can safely be said that, in an average of 17 well-observed stars, a value of $100\,\bar{v}$ as high as $0''\!.5$ is irreconcilable with (93). It seems worth while in this connection to remark that the 12 outside stars, for λ between 170° and 178°, give

$$100\,\bar{v}=+0''\!.46, \text{ from which } \bar{\pi}=0''\!.0083. \tag{96}$$

Notwithstanding the extremely unfavorable circumstances we still find a parallax agreeing perfectly with the final result (33). Now, from (51) and (16), eliminating V,

$$\tan\lambda=\frac{v}{0.212\,\rho\pi}, \tag{97}$$

from which, if we put $\pi=0''\!.0054$; $v=+0''\!.0050$; $\rho=+18.46$, we obtain

$$\lambda=13^{\circ}. \tag{98}$$

It is to be considered extremely probable, therefore, that the antivertex of the Nebula-group lies within 13° of (95). The antivertex of the outside stars is at

$$5^{\mathrm{h}}44^{\mathrm{m}}, \qquad -11^{\circ} \tag{99}$$

which is $10^{\circ}\!.7$ from (95). The radial velocity of the outside stars at the point (94), which is $9^{\circ}\!.9$ from (99), is $20.0 \cos 9^{\circ}\!.9=19.7$, which differs only 1.24 km from (94). It is very possible, therefore, that both the direction and the velocity of the Nebula-group are identical with those of the outside stars. At all events the difference must be relatively small.

21. LUMINOSITY-CURVE OF THE Bo–B5 STARS

In accordance with earlier results, I will assume that the luminosity-curves are Gaussian error-curves, with the equation

$$y=\frac{h}{\sqrt{\pi}}e^{-h^2(M-k)^2}. \qquad (100)$$

Care will, of course, be taken to note any indicated deviations from this form, particularly for the fainter half of the curve, for which we have scarcely any data from direct observations.

First solution: from the Cannon stars in the Nebula-group.—Since it was assumed that the number of Bo–B5 stars fainter than 9.05 necessary to complete the quantities in the third column of Table XXX probably lies between 0 and 6, I will assume for this number the value 3. Any error thus committed will be of little importance. The arithmetic mean of the magnitudes thus becomes 6.58, and the median magnitude 6.48. If the luminosity-curve is an error-curve, or even a symmetrical curve, both the arithmetic mean and the median will coincide with the maximum. I thus adopt for the maximum of the frequency-curve of the apparent magnitudes $m_{max}=6.53$. As one-twelfth of the stars in this region belong to the outside stars (see Section 18) whose maximum (arithmetic mean) lies at $m=6.06$, we have

$$\text{Corrected } m_{max}=6.57. \qquad (101)$$

For the determination of the probable amount of deviation (probable error) we have from the seventh column of Table XXX

$\frac{1}{4}$ of the stars are fainter than 7.90. Therefore $r=7.90-6.57=1.33$

$\frac{1}{4}$ of the stars are brighter than 5.78. Therefore $r=6.57-5.78=0.79$,

so that in the mean we have $r=1.06$. Further, the parallax of the group being 0″.0054,

$$M=m-6.34. \qquad (102)$$

We thus have for the constants of the luminosity-curve (100)

$$\left.\begin{aligned} K&=6.57-6.34=+0.23 \\ h&=\frac{0.4769\ldots}{r}=0.450 \end{aligned}\right\} \qquad (103)$$

Second solution: from the outside Cannon stars.—Treating the numbers of the eighth column of Table XXX in the same way, we find, as remarked in Section 18, a value of K which must be substantially correct and a value of h which must be too low. Noting that for the mean parallax 0".0081 of the outside stars

$$M=m-5.46 \qquad (104)$$

we find (27 stars)

$$K=+0.60 \qquad h>0.40 \qquad r<1.19. \qquad (105)$$

Third solution: from the bright stars in Table XXXIX.—Arranging the stars for which $\lambda<165°$ according to absolute magnitude, M, and parallax, we obtain the summary[1] given in Table XXXI.

Treating the numbers in Table XXXI exactly as was done in the similar case of *Mount Wilson Contribution* No. 82, pp. 41 and 42, I find for the luminosity-curve the results shown in Table XXXII.

The third column of Table XXXII gives the numbers corresponding to the observed luminosity-curve, the number of stars on which each value rests being added in parentheses. The extreme values are thus seen to be very uncertain. It seems impossible to determine from these data the values of both K and h in (100). I therefore adopted $K=+0.36$, which is the weighted mean of the values obtained in the first and second solutions, and found

$$h=0.50. \qquad (106)$$

---

[1] The absolute magnitudes were obtained by using the values of $\pi_{2.5}$ instead of the finally adopted π. For the luminosity-curve the difference is immaterial.

The theoretical curve computed with these values of h and K is in the fourth column of Table XXXII. The enormous residual for $M=+0.5$ is not to be taken too seriously. It corresponds to an irregularity in the actually observed numbers of less than three stars.

TABLE XXXI

NUMBER OF B0–B5 STARS

M	$\overline{M}$	π									
		0″0194	0″0154	0″0122	0″0097	0″0077	0″0061	0″00485	0″00385	0″00305	
+1.75 to +2.25	+2.0				Domain of the stars apparently fainter than 5.80 (Harvard) and part of the stars 5.31 to 5.80						
+1.25 " +1.75	+1.5	.....	.....	1							
+0.75 " +1.25	+1.0	.....	.....	0.5	3.5						
+0.25 " +0.75	+0.5	.....	.....	1.0	4.5	4.5	1				
−0.25 " +0.25	0.0	.....	.....	2.0	4.0	4.0	3				
−0.75 " −0.25	−0.5	.....	.....	.....	1.0	0.5	5.5	1.5	0.5		
−1.25 " −0.75	−1.0	.....	.....	.....	1.0	4.0	3.0	1.0	1.0		
−1.75 " −1.25	−1.5	.....	.....	.....	.....	.....	5.0	2.0	0.5	0.5	
−2.25 " −1.75	−2.0	.....	.....	.....	1.0	.....	1.5	2.5	1.0	.....	.....
−2.75 " −2.25	−2.5	.....	.....	.....	.....	.....	.....	2.0	.....	.....	.....
−3.25 " −2.75	−3.0	.....	.....	.....	.....	.....	3.0	.....	.....	.....	.....
−3.75 " −3.25	−3.5	.....	.....	.....	.....	1.0	.....	.....	.....	.....	.....
−4.25 " −3.75	−4.0	.....	.....	.....	.....	.....	.....	.....	.....	.....	.....
−4.75 " −4.25	−4.5	.....	.....	.....	.....	.....	0.5	0.5	.....	.....	.....
−5.25 " −4.75	−5.0	.....	.....	.....	.....	.....	.....	.....	.....	.....	.....
Total below cross-lines	.....	.....	.....	3.5	11.5	9.5	18.5	8.0	1.5	.....	.....

TABLE XXXII

LUMINOSITY-CURVE B0–B5 STARS

M	$\overline{M}$	Number	Comp.	O.−C.
+1.25 to +0.75	+1.0	17.0 (0.5)	17.3	− 0.3
+0.75 " +0.25	+0.5	38.6 (5.5)	18.8	+19.8
+0.25 " −0.25	0.0	23.9 (10)	18.2	+ 5.7
−0.25 " −0.75	−0.5	10.2 (7)	15.9	− 5.7
−0.75 " −1.25	−1.0	9.0 (9)	11.9	− 2.9
−1.25 " −1.75	−1.5	7.0 (7)	8.1	− 1.1
−1.75 " −2.25	−2.0	6.0 (6)	4.9	+ 1.1
−2.25 " −2.75	−2.5	2.0 (2)	2.4	− 0.4
−2.75 " −3.25	−3.0	3.0 (3)	1.2	+ 1.8
−3.25 " −3.75	−3.5	1.0 (1)	0.7	+ 1.3
−3.75 " −4.25	−4.0	0.0 (0)		
−4.25 " −4.75	−4.5	1.0 (1)		

Collecting these results, including the solution of *Mount Wilson Contribution* No. 82, p. 43, with weights according to a rough estimate of the reliability, we have:

CONSTANTS LUMINOSITY-CURVE B0–B5 STARS

	No. of Stars	K	Weight	h	Weight
First solution.........	48.0	+0.23	1.8	0.450	1
Second "	27.0	+0.60	1.0	(>0.400)	0
Third "	69.0	....	....	0.500	1
Mt. Wilson Contr. No. 82	142.5	+0.885	1.0	0.409	2
Adopted means....	....	+0.500	....	0.442	......

(107)

To this value of h corresponds the value $r=\pm 1.01$ mag., that is, the B0–B5 stars are distributed according to an error-curve about the central value $M=+0.50$, with a probable error of about one magnitude.

22. LUMINOSITY-CURVE OF THE B8–B9 STARS

First solution: from the Cannon stars in the Nebula-group.—In Section 18 reasons were given for the assumption that, for the nebula region, the number of stars from 9.05 to 9.55 in Table XXX, in order to become complete, must be multiplied by a factor not exceeding 2. This being admitted, it is evident that the maximum of the frequency-curve of the apparent magnitudes must lie at about

$$m=8.80. \qquad (108)$$

Fitting an error-curve having this central value to the observed numbers, I find

$$h=0.90. \qquad (109)$$

The correction required for the position of the maximum on account of the admixture of stars not belonging to the group is $+0.10$ mag. Consequently, by (102), the elements of the luminosity-curve are

$$\left.\begin{aligned} K&=8.80+0.10-6.34=+2.56\\ h&=\qquad\qquad\qquad\quad\; 0.90\end{aligned}\right\}\quad \text{(109 stars)} \qquad (110)$$

Second solution: from the outside stars.—Neglecting the stars fainter than 9.05, the maximum is located somewhere near $m=8.30$.

The value of h found by fitting an error-curve to all data is 0.78, but, for reasons already given, this value must be too small. Hence, by (104),

$$\left.\begin{array}{l} K=8.30-5.46=+2.84 \\ h>0.78 \end{array}\right\} \qquad \text{(143 stars)} \qquad (111)$$

The bright B8–B9 stars are too few in number to yield any reliable result. The same holds for the stars in *Mount Wilson Contribution* No. 82. Finally, therefore, we have from (110) and (111), giving equal weight to the two values of K,

$$K=+2.70 \qquad h=+0.90 \qquad \text{(B8–B9 stars)} \qquad (112)$$

23. LUMINOSITY-CURVE OF THE B3 STARS

In passing from the B0–B5 stars to the B8–B9 stars, the change in the value of K is so considerable that it becomes highly important to attempt a still further subdivision. For the B3 and B5 stars the data are still fairly adequate to such a determination. For the former I use the Cannon stars, both for the nebula and the outside region and further the data contained in *Mount Wilson Contribution* No. 82, discussed in the same way as the bright B0–B5 stars in the third solution of Section 21.

In the case of the outside stars there is no objection to the value for K. The result for h is really (see Section 18) a lower limit. However, in the cases already treated, this value differs so little from that for the nebula region that in the present instance—for which only a rough result is all that can be hoped—I have no hesitation in using the h furnished by outside stars on the assumption that they are all at the same distance. The reduction to absolute magnitude is of course made with the mean parallax (33). Table XXXIII summarizes all the data. The apparent magnitudes corresponding to the values of M in the table were obtained by (102) and (104). The numbers from *Mount Wilson Contribution* No. 82 were multiplied by a factor such that the total brighter than $M=+1.75$ becomes equal to that for the stars in the nebula region increased by those outside. They thus become comparable with the sums of the two preceding columns. This reduction is necessary because only that part of the curve which corresponds to the stars brighter than $M=+2.25$ is given. The sudden breaking off of the curve at this point by no means implies the non-existence of fainter stars. In parentheses are added the observed numbers of stars on which the results of *Mount Wilson Contribution* No. 82 rest. They determine the weight with which these values are to be combined with the totals of the two preceding columns. The results of the combination are given in the column headed "adopted," and are fairly well represented by an error-curve for which

TABLE XXXIII

LUMINOSITY-CURVE B3 STARS

M	NUMBER OF STARS					
	Neb.	Outside	*Contr.* 82	Adopted	Comp.	O−C
>+2.75......	0	0.0	....	0.0	1.7	−1.7
+2.25 to +2.75..	0	0.0	....	0.0	1.7	−1.7
+1.75 " +2.25..	3	0.0	9.0 (1)	3.0	2.7	+0.3
+1.25 " +1.75..	3	4.0	5.0 (2)	6.0	3.7	+2.3
+0.75 " +1.25..	3	0.0	5.0 (5)	4.0	4.5	−0.5
+0.25 " +0.75..	1	0.0	4.5 (9)	3.0	4.8	−1.8
−0.25 " +0.25..	4	2.5	3.1 (11)	4.8	4.4	+0.4
−0.75 " −0.25..	4	0.5	2.8 (13)	3.7	3.5	+0.2
−1.25 " −0.75..	0	2.0	2.7 (12.5)	2.4	2.7	−0.3
−1.75 " −1.25..	2	2.0	1.2 (5.5)	2.1	1.6	+0.5
−2.25 " −1.75..	....	1.0	1.3 (6)	1.2	0.9	+0.3
−2.75 " −2.25..	....	....	0.4 (2)	0.4	0.4	0.0
<−2.75......	....	....	....	....	0.3	−0.3

$$K=+0.53 \qquad h=+0.52 \qquad \text{(B3 stars)} \qquad (113)$$

24. LUMINOSITY-CURVE OF THE B5 STARS

It is seen that among the outside B5 stars in Table XXX there is none fainter than 8.5. We may conclude, I think, that we have before us the complete frequency-curve. According to the last line but one we have for the maximum, $m_{max}=7.73$ (outside stars). In the nebula region two of the observed stars are fainter than 8.5, but none fainter than 9.0. It seems hardly safe to suppose that here, too, we have the whole of the frequency-curve before us. If we assume (*a*) that the frequency-curve is complete, (*b*) that there are two stars of magnitude 9.1 really existing but not observed, the probability is that the truth lies between the two. Corresponding to supposition (*a*) we find $m_{max}=7.50$, and to (*b*) $m_{max}=7.69$. The difference is not very material and I adopt

$$m_{max}=7.60 \quad \text{(neb. region)} \tag{114}$$

Transferring to absolute magnitudes by (104) and (102) we have

$$\left.\begin{array}{lll} \text{for the outside stars} & K=2.27 & (7\ \text{stars}) \\ \text{for the Nebula-group} & K=1.26 & (15\ \text{stars}) \\ \hline \text{Weighted mean} & K=1.58 & (22\ \text{stars}) \end{array}\right\} \tag{115}$$

The agreement is poor. For the derivation of h I added the data of *Mount Wilson Contribution* No. 82 to those of Table XXXIII, just as was done for the B3 stars, and found

$$h=0.50. \tag{116}$$

25. FURTHER LUMINOSITY-CURVES AND SUMMARY OF RESULTS

By the combination of the results (112) with (115) and (116) we obtain for the B5–B9 stars

$$K=+2.61 \qquad h=0.87 \qquad (274\ \text{stars}) \tag{117}$$

There is further the determination of *Mount Wilson Contribution* No. 82, p. 45,

$$K=+2.00 \qquad h=+0.508 \qquad (69\ \text{stars}) \tag{118}$$

which is confessedly poor; the solution (117), too, is not of high weight, but doubtless much better. Combining with the respective weights 4 and 1, I find

$$K=+2.49 \qquad h=+0.80 \qquad (\text{B5–B9 stars}) \tag{119}$$

For the B0, B0–B2, and B1–B2 stars, the value of K was obtained by taking the arithmetic means of the apparent magnitudes of the Cannon stars in the nebula region and reducing to absolute magnitudes by subtracting 6.34 according to (102). Further, in the case of the B0–B2 stars, I derived a very crude value of h. For the B0–B9 stars a good result could not be obtained. All the results are summarized in Table XXXIV, in which, for convenience, I also insert the constants for the A0–A9 stars, which will be obtained presently.

In the fifth column have been inserted the numbers of stars on which the several determinations rest. These give a very imperfect idea of the reliability of the corresponding luminosity-curve, not only because the absolute magnitudes are wholly dependent on the accuracy of a few parallaxes, but mainly because the observations embrace very different fractions of the whole curve. For this reason the part of the curve covered by observations has been roughly indicated in the sixth column. When the fraction is less than 0.50, the maximum is not included, and its determination becomes more or less precarious. As a consequence, the elements for the stars of type B3, resting on 99 stars, must be far better than those for the B5–B9 stars, for which 343 stars were available. Even the values of *K* for the B0, B0–B2, B1–B2 stars, though poor, deserve more confidence than we might at first sight be willing to concede on account of the extremely small numbers of stars on which they rest, simply because practically the whole of the curve is covered by observation. A crude estimate of the reliability of the elements has been given in the last column.

TABLE XXXIV

CONSTANTS OF LUMINOSITY-CURVES

	K	*h*	*r*	No. of Stars	Fraction of Curve	Quality
B0..............	−2.5	?	?	6	1.00	Poor
B3..............	+0.5	0.52	0.92	99	0.95	Good
B5..............	+1.6	0.50	0.95	22, 49*	0.81	Fair
B0–B2..........	−1.6	0.43:	1.11:	13	1.00	Poor
B0–B3..........	−0.4	0.52	0.92	33	1.00	Fair
B1–B2..........	−0.9	?	?	7	1.00	Poor
B0–B5..........	+0.5	0.442	1.01	286	0.96	Good
B5–B9..........	+2.5	0.80	0.60	343	0.50	Fair
B8–B9..........	+2.7	0.90	0.53	252	0.50	Fair
A0–A9..........	+3.4	0.80	0.60	474, 601†	0.50	Fair

* Twenty-two stars used for the derivation of *K*; 49 for *h*.

† 474 stars used for the derivation of *K*; 601 for *h*.

I have computed these numerous luminosity-curves in the hope that they might help materially in obtaining good parallax estimates when other means are defective or wanting.

Remark.—There are a few exceptionally bright stars in our lists, such as ϵ and ζ Orionis and ϵ Canis Majoris.[1] For all three the absolute magnitudes are brighter than -4.0. Since the spectrum of the last is B1, and the others are probably B1 or B0, the magnitudes do not seem irreconcilable with the luminosity-curves of Table XXXIV. The case of β Orionis (Boss 1250) is different. It is the brightest star in our lists, $M=-5.5$, whereas the spectrum is B8; hence it is more than 8 mags. brighter than the mean for stars of the same spectrum, and seems to deserve particular attention.

26. LUMINOSITY-CURVE OF THE A STARS

The value of K was determined from the outside stars. The main difficulty was the probable incompleteness of the numbers of stars between magnitude limits 9.05 and 9.55. We are not altogether without means for overcoming the difficulty, however.

We can make a rough determination of ϵ, the factor by which the observed number must be multiplied to make it complete, with the aid of the B5–B9 stars, by comparing the observed and the theoretical numbers obtained with the constants of Table XXXIV. We find

	No. Obs.	No. Theor.	ϵ
Nebula region.......	12	30.5	2.5
Outside stars........	7	11.2	1.6
Total...........	19	41.7	2.2

As already remarked, the A stars in the nebula region scarcely admit of a value of ϵ as high as 2.0. The theoretical number for the nebula region, therefore, and hence also for the outside stars, must be too high. I assume

$$1.0<\epsilon<2.4. \qquad (120)$$

If we try to represent the numbers of the last column of Table XXX by an error-curve on the two hypotheses $\epsilon=1$ and

---

[1] The Boss numbers are respectively 1370, 1398, 1804.

$\epsilon=2.4$, we find maxima at $m=8.80$ and 9.05, respectively, so that we cannot greatly err if we write $m=8.93$. We thus get, by (104),

$$K=3.47. \tag{121}$$

Adopting this value, the maximum in the Nebula-group, according to (102), must lie at $m=9.81$, and, corrected for the large admixture of external stars projected on the group, for all the A stars within the limits (78) $m=9.29$. From both regions together I then obtain the best representation by assuming

$$h=0.80. \tag{122}$$

As there may still remain some doubt as to the correctness of K, particularly because the preceding determination tacitly assumes that for the region considered the parallax of the bright A stars agrees with that of the bright B0–B9 stars, I have tried to find some verification by entirely independent data. The most suitable for the purpose is that furnished by the Pleiades and the Hyades.

If the stars in these groups be arranged in order of magnitude, they will also be arranged nearly in the order of spectrum. This remark is not new, but Table XXXV, which brings the fact clearly into view, may not be unwelcome.

a) *The Pleiades.*—The brighter stars are all B5–B9. For stars of magnitude 6.59 and fainter, with relatively few exceptions down to 9.05, the spectrum is A. Stars still fainter show an F spectrum. Outside the limits 6.5 and 9.1 no A stars occur, though we should expect a few to appear were the number of stars a hundred times greater. It is evident that we have before us the entire luminosity-curve and that the absolute magnitudes of the bulk of the A stars lie within a range of 2.6 mags. If we assume that the luminosity-curve is an error-curve, its maximum must coincide with the arithmetic mean. From the photographic magnitudes determined at Potsdam I find from 23 A stars

$$m_{max}=7.70 \qquad h=0.82 \tag{123}$$

and for 8 B5 stars

$$m_{max}=4.49. \tag{124}$$

It thus appears that the maximum of the frequency-curve for the A stars is 3.21 magnitudes fainter than that for the B5 stars.

TABLE XXXV

DISTRIBUTION OF SPECTRA

Mag.	Hyades*	Pleiades†
3.41	...	B5
3.62	A5	...
3.63 to 4.10	K, K, K, K	B8, B5
4.10 " 4.55	A, A3, A3, A5	B5, B5
4.55 " 5.05	A5, A5, A2, A5, A3	B5
5.05 " 5.55	A5, A8, A5, A, A2, A2, A, A5, A5	B8
5.55 " 6.05	A, A5, A5, G, A2, A9, F, A, F, A4, A9, F, A5, A9	B5, B8, B8, B8
6.05 " 6.55	A9, A8, A8	B8
6.55 " 7.05	F2, F5, F2, G0	A, B8, A, A, A
7.05 " 7.55	G0	A, A, A, A, A
7.55 " 8.05	G0, G0, G, G0, F8	A, A, A, A, A5
8.05 " 8.55	G0, G0, G0, G5	A2, A3, A5, A2, A2, A5, A5
8.55 " 9.05	G5, F8, K0, K0, K2, G0, K0, K0, G5	F, F, A5, A
9.05 " 9.55	...	F2, F, F2, F
10.45	...	F5

The same must also be true for the luminosity-curves, and since by (115) the maximum of the luminosity-curve for the B5 stars lies at absolute magnitude $K=+1.58$, we find

$$\text{A stars} \qquad K=4.79, \tag{125}$$

a determination which is independent of the parallax of the Pleiades.

b) *The Hyades.*—Table XXXV contains all the stars of determined spectrum which are known to belong to the group.

We here meet with the curious fact that four of the five brightest stars have K spectra, a type not again appearing until we reach stars fainter than 8.5. If I am not mistaken this fact first gave rise to the general[1] theory of giant and dwarf stars.

---

* The stars belonging to the Hyades were taken from the preface to *Groningen Publications*, No. 23, the data for spectrum being largely supplemented by private letters from the Harvard Observatory and by plates taken at Potsdam by Dr. Zernike. The list contains all the stars of determined spectrum known to belong to the group.

† The photographic magnitudes for the Pleiades are by Hertzsprung, *Pub. Astr. Obs. Potsdam*, **22**, No. 63, p. 21. It would have been preferable to use the visual magnitudes by Müller and Kempf (*Astronomische Nachrichten*, **150**, 193, 1899), but I have not deemed it important to make the change. The brighter stars have been reduced to the Harvard scale by subtracting 0.24 mag. The spectra for the brighter stars are from Miss Maury (*Harvard Annals*, **28**, Part I); for the fainter stars they are from Tikhoff (*Mitteilungen Pulkowo*, No. 40, Tableau II). The proper motions necessary for determining whether a star belongs to the physical group are from the following sources: Lagrula or Elkin (weight 1), Boss (weight 1), and Stratton (weight ½).

For the determination of the luminosity-curve we cannot use all the objects in Table XXXV, for it is evidently necessary to know *all* the stars belonging to the group, together with their spectra, down to a specified and rather faint limit, a condition satisfied only for that part of the group for which proper motion plates have been measured at Groningen.

As the spectra are still rather uncertain, I give in full all the A stars which, according to the data at my disposal, occur in the restricted area. It will thus be easy to improve the results as soon as better data are available.

No. *Gron.* 23	Harv. Mag.	Spectrum	No. *Gron.* 23	Harv. Mag.	Spectrum
227	3.62	A5	87	5.68	A2
143	4.24	A	245	5.70	A9
170	4.60	A5	64	5.76	A4
315	4.75	A5	371	5.80	A6
107	4.84	A2	222	5.97	A5
251	4.84	A5	282	6.04	A9
385	4.85	A3	44	6.14	A9
38	5.27	A5	1	6.35	A8
255	5.49	A5	150	6.39	A8
34	5.59	A5			

Among the stars fainter than 6.39 there is not a single A star.

The mean magnitude

$$m=5.36 \quad (19 \text{ stars}) \qquad (126)$$

is the apparent magnitude corresponding to the maximum of the frequency-curve. For the best-fitting modulus of precision I find

$$h=0.88. \qquad (127)$$

For the conversion into absolute magnitudes we require the parallax of the group, which, according to *Groningen Publications*, No. 23, p. 4, is

$$\pi=0''.024, \text{ therefore } M=m-3.10. \qquad (128)$$

---

[1] General in the sense that the theory applies not only to certain clusters but to the whole of the stellar system.

Finally, for the elements of the luminosity-curve

$$K=5.36-3.10=2.26 \qquad h=0.88. \qquad (129)$$

The agreement of the values for h in (129) and (123) *inter se* and with (122) is good. The agreement of (125), (129), and (121) for K is surprisingly bad.

I think that one of the causes must be an error in the value (129) furnished by the Hyades. For, adopting $K=+2.26$, we find by (102) and (104) that the maximum in the Nebula-group is at $m=8.60$ and in the outside group at $m=7.72$. A glance at Table XXX shows that such values are not to be thought of. After mature consideration I believe that the error must in great part be attributed to the parallax. We have two excellently agreeing values, one by Boss from the convergent of the proper motions and some measures of radial velocity; the other a direct determination of parallax made at Groningen. The following criticisms may, however, be made.

In the Groningen determination the magnitude error offered considerable difficulty and it does not seem impossible that, notwithstanding all our care, an error of 0.″01, though four times the probable error, may have crept into the result.

In Boss's determination,[1] the small extent of the group makes the evaluation of the convergent precarious. In order to estimate the possible error of his parallax, I made the following redetermination, first condensing his data into the four normals in Table XXXVI, chosen to give the most favorable determination of the convergent.

TABLE XXXVI

NORMAL PLACES

	$\bar{\alpha}$	$\bar{\delta}$	$100\bar{\mu}$	$\bar{p}$	No.	p COMP.		(O−C) SIN λ	
						Boss	Kapt.	Boss	Kapt.
$\delta>+18°$	4^h19^m	+20.°5	11.″6	113.°6	9	113.°6	116.°1	0.0	−1.1
$\delta<+13$	4 27	+ 9.5	11.0	92.8	7	94.0	90.8	−0.5	+0.7
Rest, α small	4 11	+15.9	12.2	104.7	13	104.1	104.5	+0.3	+0.1
Rest, α great	4 27	+15.3	10.5	104.3	12	106.1	106.6	−0.8	−0.8
Weighted mean	4 20	+15.6	11.35	......	....	......	......	......	......

---

[1] *Astronomical Journal*, **26**, 31, 1911.

According to Boss the convergent lies at

$$6^{\mathrm{h}}7^{\mathrm{m}}.2 \qquad +6°56' \tag{130}$$

which indeed satisfies the observations excellently (last column but one); but

$$5^{\mathrm{h}}46^{\mathrm{m}} \qquad +8°40' \tag{131}$$

satisfies them almost equally well (last column). For the stream-velocity Boss used only three stars, while we now have the nine objects in Table XXXVII. The values $\rho_{\mathrm{corr.}}$ were obtained by reducing Küstner's results to those of the Lick observers by applying the systematic corrections found by Küstner himself and then adding the constant corrections found by Campbell (*Lick Bulletin*, **6**, 127); λ is the angular distance from the point (131).

TABLE XXXVII

RADIAL VELOCITIES, HYADES

α	δ	ρ	Sp	ρ corr.	λ	Authority
$3^{\mathrm{h}}.8$	+17°	+25.7	F	+25.7	149°	Küstner, *A.N.*, **198**, 409
[4.0	+19	+21.6	K	+19.1	151]	" *A.N.*, **198**, 409
4.2	+15	+39.6	K	+37.1	155	" *Ap.J.*, **27**, 301
4.3	+17	+40.8	K	+38.3	156	" *Ap.J.*, **27**, 301
4.3	+22	+40.0	A3	+39.0	155	*Lick Bull.*, **7**, 20
4.3	+18	+36.4	A	+35.4	156	" " **7**, 20
4.4	+19	+39.4	K	+36.9	157	Küstner, *Ap.J.*, **27**, 301
4.4	+16	+39.4	K	+36.9	157	" *A.N.*, **198**, 409
4.9	+21	+42.0	A5	+41.0	161	*Lick Bull.*, **7**, 20
Mean 4.3..	+18	....	......	+36.3	155.8	

The second star was excluded on account of its great divergence. Forming for the others the equations of condition

$$V \cos \lambda = \rho_{\mathrm{corr.}}$$

and solving by least squares,

$$V = 40.0 \text{ km} \quad \text{(8 stars).} \tag{132}$$

This and $100\upsilon = 100\mu = 11''.35$ (Table XXXVI) give by (51)

$$\pi = 0''.033; \text{ therefore } M = m - 2.41. \tag{133}$$

The maximum at apparent magnitude 5.36 (126) thus entails

$$K = +2.95. \tag{134}$$

The value (125) furnished by the Pleiades is open to the criticism that it rests on (124), determined from only eight B5 stars. We may obtain a result based on a greater number of stars if we adopt the parallax[1] derived on the hypothesis that the motion of the group in space, referred to the center of gravity of the whole system, is parallel to the Milky Way. The parallax thus found is

$$\pi=0''.018, \text{ therefore } M=m-3.72. \tag{135}$$

The value (123), first reduced to the Harvard scale by subtracting 0.24 (see footnote to Table XXXV), thus leads to

$$K=3.74 \quad (23 \text{ A stars}). \tag{136}$$

Collecting results, we thus have, the adopted weights being in parentheses:

	K		h
	First Solution	Second Solution	
Pleiades (125), (136)..	4.79 (0.5)	3.74 (1)	(123) 0.82
Hyades (129), (134)...	2.26 (1)	2.95 (1)	(129) 0.88
Mean...........	3.10	3.34	0.85

The values of K, which in the first solution were extremely divergent, have come very much nearer together. The mean values for both solutions agree well with (121). The value of h is surprisingly close to that of (122). In conclusion, therefore, the Pleiades and the Hyades furnish values of K which leave much to be desired; still, as far as they go, they decidedly confirm the value (121). I finally adopt

$$K=+3.4. \tag{137}$$

27. REMARKS ON THE GEOMETRICAL FORM OF THE LUMINOSITY-CURVES

a) In what precedes we have assumed that the luminosity-curves are error-curves. In how far is this assumption justified? For stars of all spectra together the form was very decisively indicated by the results in *Groningen Publications*, No. 11, though the representation by an error-curve was not there given. This was first done in *Astronomical Journal*, **24,** 115, 1904. The representation over a range of 16 magnitudes leaves little to be desired. For spectra of the first and second types separately, luminosity-curves were also given in *Publication*, No. 11. These, too, are well represented by error-curves. But the data available for these investigations established the curve only as far as the maximum, or nearly so; the fainter branch is altogether wanting. What will be the form for the fainter magnitudes?

---

[1] *Proceedings Amsterdam Academy of Sciences*, 14, Part 2, 909, 1912.

The question was considered in *Mount Wilson Contribution* No. 82, p. 43, but could be answered only very imperfectly. Even now the data are scanty, though somewhat improved, especially for types B and A. They lead to the conclusion that for these spectra the whole curve, both ascending and descending branches, can be represented—with some rough approximation at least—by an error-curve.

Take, for instance, the stars of spectrum B3 for which the whole curve is pretty well covered by observations. In Table XXXIII a comparison is made between the observed numbers (adopted) and the best-fitting error-curve (computed). The divergences O.−C. for the fainter part of the curve are admittedly large, but they can hardly be qualified as systematic or as greater than can be explained by the scarcity of stars.

In order to obtain more material, I proceeded as follows. The *whole* curve is covered by observation for:

B5–B9	13	stars	in the	Pleiades
A	26	“	“	“
A	19	“	“	Hyades
B3	20	“	“	Nebula-group
	78			

Since, by Table XXXIV, the best-fitting error-curves do not differ excessively in their values of h, I formed the deviations from the separate means for each of these four groups. The question is whether the positive and negative deviations for all these 78 stars are symmetrical and in accordance with an error-curve. The result is as follows:

Deviations	Observed	Smoothed	Computed	O.−C.
<−2.25	0.0	1.0	1.0	0.0
−2.25 to −1.75	3.0	1.3	2.2	−0.9
−1.75 " −1.25	1.0	6.0	5.2	+0.8
−1.25 " −0.75	14.0	10.0	9.5	+0.5
−0.75 " −0.25	15.0	12.8	13.5	−0.7
−0.25 " +0.25	9.5	14.5	15.2	−0.7
+0.25 " +0.75	19.0	13.3	13.5	−0.2
+0.75 " +1.25	11.5	11.8	9.5	+2.3
+1.25 " +1.75	5.0	5.5	5.2	+0.3
+1.75 " +2.25	0.0	1.7	2.2	−0.5
>+2.25	0.0	0.0	1.0	−1.0

The theoretical curve has been computed with $h=0.70$. The last column shows the divergence of the observations (smoothed by taking means of three consecutive values) from the theoretical curve. The conclusion is as before: the representation by an error-curve is fairly satisfactory for the entire curve.

b) But this resemblance of the luminosity-curve to an error-curve must not be taken too literally. With our present data it is impossible to investigate the matter very closely. Still it may be well to call attention to the fact that even now there are signs indicating that the agreement probably is by no means absolute. Thus the representation for the A stars in Table XXX is defective. As compared with an error-curve, there is a decided excess of very large and very small deviations, and the same thing is indicated in other ways. Hertzsprung[1] has derived the absolute magnitudes of 15 stars belonging to the Ursa Major group. Twelve of these have A spectra, and their absolute magnitudes (increased by 5 mags. to reduce to our scale) range from −1.03 to +2.20;[2] they are accordingly, by Table XXXIV, from −4.4 to −1.2 mags. brighter than the average A star.

It is not at all surprising that the deviations are all on the bright side. Hertzsprung confined himself to Bradley stars and has, by this choice, given strong preference to very luminous stars. In fact, we may say that such catalogues as those of Bradley and Boss are really catalogues of exceptionally luminous stars. It is just this absence of stars of mean and faint absolute magnitude from our catalogues which makes the determination of the luminosity-curves so difficult. Nevertheless, in the case of the Ursa Major stars, the deviations seem to be somewhat excessive for a curve whose probable error is ±0.60 mag.[1] There is accordingly a strong indication of an excess of very luminous stars.

---

[1] *Astrophysical Journal*, **30**, 139, 1909.

[2] There seems to be a mistake in the parallax computed for β Aurigae. I have used the correct value. Without the correction the range would be −0.53 to +2.20.

Similarly there seems to be an excess of stars which are absolutely very faint. The companion to *o* Eridani, which shows an A spectrum, has absolute magnitude +10.3, which is 6.9 mags. fainter than the average A star. Other examples might also be given. As already remarked at the end of Section 25 we have, among the B8 stars, such an exceptional object as β Orionis, which is 8.2 mags. brighter than the average B8–B9 stars.

With more extensive data it may become necessary to give up the error-curve as the best representation of the frequencies of the absolute magnitudes. The most convenient form for trial will then probably be the sum of two error-curves having the same maximum but different moduli.

c) I have taken much trouble in deriving what in many cases can be considered only as first approximations to the luminosity-curves in the conviction that such curves form one of the most important elements in attempting to learn the structure of the universe. Scarcity of data is responsible for the fact that in former endeavors stars of all spectra have been grouped together or that, at most, a separation into only two types has been attempted. The results of the present paper will illustrate how crude is such a procedure, for it involves the combination of stars having −2.5 as a mean absolute magnitude (B0 stars) with others for which the mean magnitude is +10.3 (second-type stars). The corresponding ratio of intensities is more than 100,000 to 1.

---

[1] More important than the size of the deviations is the conclusion that the Ursa Major group must contain many more members than those we know, the bulk of which are among the fainter stars. Even now I think we can specify a great number of stars that belong to the group. There is, however, a great difficulty in the way of deciding with certainty, owing to the similarity of the elements of this group (vertex $20^{h}31^{m}$, −40°2; velocity, −18.4 km) with those of the second star-stream, especially the A stars of this stream (vertex $19^{h}12^{m}$, −47°; velocity, −18.5 km). For instance, the brightest of Hertzsprung's stars, β Aurigae, fits practically as well in the second stream as in the Ursa Major group. If we assign it to the former, its absolute magnitude changes from −1.03 to +0.49.

To secure entirely reliable results we must attack the spectral classes separately. This will be an immense task, for it involves obtaining the numbers, magnitudes, spectra, and proper motions of a suitable fraction of the faint and very faint stars. In fact the best of the results given in the present paper are due to the invaluable data for stars to magnitudes 9.0 or 9.5 placed at my disposal by Professor Pickering and Miss Cannon.

The requirements for a solid foundation in deriving the luminosity-curves are perhaps best seen from Table XXXVIII, which shows the mean absolute magnitudes for stars of given apparent magnitude and proper motion. It was computed with the data for all stars in *Groningen Publications*, No. 8. To all appearances the parallax for any specified magnitude and proper motion does not differ very markedly for stars of different spectra, so that for a rough estimate a single table can be used. The table shows, what of course is evident, that for the absolutely brightest stars we are dependent on the apparently bright stars of small proper motion. As these stars have been observed more completely and accurately than any others, the conditions are favorable for the brighter end of the luminosity-curve. The faint absolute magnitudes, on the contrary, are to be found among the apparently faint stars of large proper motion. The conditions here are nearly as unfavorable as possible. The table indicates, roughly, how far

TABLE XXXVIII

ABSOLUTE MAGNITUDES M

μ	m		
	6.0	9.0	12.0
0″05	+1.2	+3.6	+ 5.9
0.10	+2.3	+4.6	+ 7.0
0.20	+3.4	+5.7	+ 8.1
0.40	+4.4	+6.8	+ 9.2
0.80	+5.5	+7.9	+10.2

we may hope to go with the available data and what will be required for further progress.

Since we have found the mean absolute magnitude of the B5 stars to be +1.6, and of the A stars to be +3.4, whereas for the second-type stars it is +10.3,[1] it is rather more than a guess if we assign the following series of values:

B5 stars at + 1.6
A5 " " + 3.4
F5 " " + 7
G5 " " +10
K5 " " +13
M " " +15

Assuming that the luminosity-curves are error-curves and that for a satisfactory determination of their constants we must possess reliable observational data, at least to a magnitude well past the maximum, we see from Table XXXVIII that Boss's *Catalogue* and the *Revised Harvard Photometry* (*Harvard Annals*, 50), which are complete to magnitudes 5.8 and 6.5, respectively, may be considered as perhaps just sufficient for the derivation of the curve for the A5 stars. For the F stars we cannot expect altogether reliable results until the stars to 9.0 or somewhat beyond can be included. The *Revised Draper Catalogue* will furnish the required data for the spectra. For the large proper motions (which are the more important) we shall probably be able to manage with what is known, especially when the much-longed-for determinations of proper motion, now in preparation at Albany, have been placed in the hands of astronomers. For the G stars even these data will be inadequate, and we shall have for them no thoroughly sound determination until the data for the Selected Areas become available.

For the K and M stars the outlook might seem to be nearly hopeless. But there is one circumstance which probably will bring success along as soon as the definitive luminosity-curve for the G stars is found. It has long been known that the stars of very large proper motion, almost without exception, are of the second type.

---

[1] This value was obtained by representing the numbers of *Groningen Publications*, No. 11, p. 31, Type II, Solution B, by an error-curve.

We further find that the larger the proper motion and the fainter the apparent magnitude, the more do the K5–M stars begin to predominate. From van Maanen's table of large proper motions (*Mount Wilson Contribution* No. 96), I find that among the stars fainter than magnitude 6.0, with proper motion ≧ 1″.0, 60 per cent are of type K5–M. For still fainter stars we must expect that this percentage will increase largely, so that finally a limit of faintness will be reached for which practically all the stars of large proper motion will be K5–M. Not only must this be so theoretically, but there is a strong indication of its confirmation by observed color indices such as those of Seares and Hertzsprung (*Mount Wilson Contributions*, Nos. 81, 100, and 102).

We therefore expect that beyond the magnitude for which we can determine spectra we shall be justified in including with the K5–M stars all swiftly moving objects, instead of limiting ourselves to those for which the spectra have been ascertained. Perhaps we shall have to multiply our numbers by a certain fraction, slightly less than unity, but it seems probable that this fraction will be capable of a sufficiently accurate determination with the aid of the somewhat brighter stars. Consequently, as soon as the data now under observation for the Selected Areas have become available, we shall probably be able to complete the investigation down to the faintest stars observed for the *Durchmusterung* of the Selected Areas, that is, approximately to:

Mag. 16.0 in the Northern Hemisphere (Harvard plates)
" 18.2 " " " (Mount Wilson plates)
" 16.8 " Southern " (Harvard Arequipa plates)

Of course there will remain the necessity of finding all the stars having large proper motions. This, however, will present no real difficulty. A repetition of the plates, even if made at the present moment, would be sufficient for the purpose. If photographed through the glass and superposed on the originals for differential measurement, or if taken as usual and carefully measured with the stereocomparator, the labor of finding all the proper motions exceeding 0″.10 would not be very trying. We may thus hope to secure the data necessary for a thorough study of the arrangement in space of all the stars, including even those, thousands of times fainter than the sun, which are barely visible in our largest telescopes when near, and escape all observation[1] when situated in the remoter regions of space.

28. SUMMARY

1. The bulk of the B stars within the limits (2) form a local group. The great Orion nebula lies within these limits, and I have therefore called this group the *Nebula-group.*

2. Boss's proper motions in declination, for the stars in the region of the sky considered in the present paper, require the corrections (13) of Section 4.

3. Of the stars outside the Nebula-group, those within the limits $l=180°$ to $216°$, $b=-30°$ to $+4°$ *may* form a local group. It seems more probable, however, that they all have the same systematic motion. I have assumed this to be the case. If later investigation should confirm the existence of the local group, relatively little will be changed in the conclusions of the present paper (Section 7).

4. The definitive elements of the motion of the helium stars outside the nebula region are given in (33), Section 8. The vertex nearly coincides with the vertex of the first stream of the non-helium stars.

5. The mean parallaxes for three separate groups of these stars are given in Table IX (Section 7), the average parallax for all being $0\overset{''}{.}0081 \pm 0\overset{''}{.}0007$.

6. The error in the position of the vertex due to remaining systematic errors in the proper motions cannot exceed 3° or 4°, and the remaining uncertainties in V and π from this source must be negligible (Section 8).

7. The components u and t of the peculiar motion are distributed approximately in accordance with error-curves. The probable amount of these components is:

for region of present paper (outside stars) $r_u = \pm 1.67$ km
for region of *Mount Wilson Contribution* No. 82 $r_u = \pm 1.0$ km

---

[1] I do not mean that we must be idle until the Selected Areas are completed. On the contrary, I believe that even now we can find very useful representations of the most urgently needed portions of the luminosity-curves.

The smallness of these values is probably the most important fact brought to light by the present investigation.

8. The distribution of u being found, we can derive the distribution of v as soon as we know the fraction of the stars $\phi(\pi)$ having any given parallax π; $\phi(\pi)$ is determined by the condition that the theoretical distribution of v shall agree with the observed distribution (Section 13).

9. $\phi(\pi)$ being known, it becomes easy to determine the mean parallax of all the stars having given values of v and λ. These mean parallaxes have been adopted as the individual parallaxes of stars having the same v and λ. They have been tabulated for $r_u = \pm 2.5$ in Table XXI, for $r_u = 0.0$ in Table XXIV, and the definitive values, corresponding to $r_u = \pm 1.67$, have finally been obtained by interpolation between these tables.

10. The same method applied to τ does not lead to valuable results (Section 16).

11. The parallax of any star more than 24° from the antivertex, derived in the manner described, is, roughly speaking, $\pm 0''.0021$. This includes the effect of the observational errors in the proper motions (Section 15).

12. The parallax of the Nebula-group, $\pi = 0''.0054 \pm 0''.0009$, has been found by a consideration of the luminosity-curves (Section 18).

13. To the parallaxes various tests have been applied. In general they are strongly confirmatory, both for the outside stars and for the Nebula-group (Sections 17 and 19).

14. The systematic motion of the Nebula-group can differ but little from the motion of the outside stars (Section 20).

15. Luminosity-curves have been determined for many subdivisions of the B stars. Further, a curve was also derived for the A stars. All the results are summarized in Table XXXIV.

16. The frequency-curve of the absolute magnitudes (luminosity-curve) has in former publications been found to coincide nearly with a normal error-curve; in consequence of a lack of data, in particular for the faint stars, the agreement could not be established beyond a point near the maximum. In the present paper occur several cases for which the descending branch could also be included more or less completely. From all available material it appears that the

TABLE XXXIX

B STARS, GAL. LONG. 150° TO 216°

BOSS No.	SP.	HARV. MAG.	1900		GAL. LONG.	GAL. LAT.	CORRECTION (13) APPLIED		VERT. 17h48m, +9°		100 τ	100 υ	100 r	ρ−4.3	ρ comp.	UNIT 0″.0001			
			α	δ			100 μ	ρ	ρ comp.	λ						$\pi_{2.5}$	$\pi_{0.0}$	Adopted π	Adopted M
a) LAT. 0° TO +30°; 100 μ ≧ 1″.7																			
														km	km				
1635....	B5	4.06	6h 23m	+20°.3	160°	+ 5°	2″.2	201°	198°	149°	−0″.1	+2″.2	0″.23	....	......	88	90	89	−1.19
1550....	B3	4.92	6 6	+16.2	161	0	2.4	165	190	154	+1.0	+2.2	0.44	....	......	94	101	96	−0.17
1568....	B9	5.28	6 10	+16.2	161	+ 1	2.1	163	192	153	+1.0	+1.8	0.36	+25.2W	+17.8	85	84	85	−0.07
1751....	B8	5.69	6 44	+16.3	166	+ 8	2.3	236	210	151	−1.0	+2.1	0.52	+ 8.5W	+17.5	88	91	89	+0.44
1788....	B8	5.88	6 51	+10.1	172	+ 7	2.7	246	220	155	−1.2	+2.4	0.69	+28.7W	+18.1	101	113	105	+0.99
1944....	B8	3.09	7 22	+ 8.5	177	+13	6.6	229	233	150	+0.5	+6.6	0.18	....	......	163	240	189	−0.53
2071....	B8	5.11	7 47	+ 2.0	186	+15	2.5	256	249	148	−0.3	+2.5	0.36	....	......	94	99	96	+0.02
2330....	B3	4.32	8 38	+ 3.8	191	+28	2.2	265	253	136	−0.5	+2.2	0.40	....	......	79	70	76	−1.28
2365....	B9	5.19	8 44	− 3.1	198	+25	2.9	226	260	136	+1.6	+2.4	0.40	....	......	82	77	80	−0.29
1935....	B8	5.20	7 20	−16.0	199	+ 1	3.4	260	285	156	+1.4	+3.1	0.74	−11.9W	+18.3	118	149	126	+0.70
2451....	B8	5.50	9 4	− 8.2	206	+27	3.0	245	265	132	+1.0	+2.8	0.40	....	......	87	82	85	+0.15
2492....	B9	5.54	9 12	− 8.3	207	+28	4.0	274	265	130	−0.6	+4.0	0.46	+ 6.7W	+12.8	115	114	115	+0.84
2042....	B3	5.53	7 40	−24.4	208	+ 1	3.9	301	294	148	−0.5	+3.9	0.70	....	......	121	147	130	+1.10
b) LAT. 0° TO −30°; 100μ ≧ 1″.7																			
975....	B8	5.15	4 9	+ 9.8	151	−27	4.2	170	128	149	−2.8	+3.1	0.72	....	......	105	122	111	+0.38
1315....	B3	4.83	5 22	+21.9	151	− 6	1.7	140	168	148	+0.8	+1.5	0.32	+12.2	+17.0	72	66	70	−0.94
1354....	B3	5.28	5 29	+24.0	151	− 4	3.2	167	171	146	+0.2	+3.2	0.43	+18.9W	+16.6	106	119	110	+0.49
981....	B3	4.32	4 10	+ 8.6	152	−28	3.4	126	127	149	+0.1	+3.4	0.34	+13.7	+17.1	112	132	119	−0.30
1097....	B9	5.37	4 34	+12.0	153	−21	2.7	165	138	152	−1.2	+2.4	0.44	+13.8W	+17.7	95	103	98	+0.33
1165....	B8	5.74	4 50	+14.9	153	−16	2.4	145	147	152	+0.1	+2.4	0.74	+ 4.7W	+17.7	95	103	98	+0.70
1375....	B3	3.00	5 32	+21.1	153	− 5	2.8	174	172	149	−0.1	+2.8	0.18	+12.1	+17.1	100	112	104	−1.92
1203....	B9	4.65	4 59	+15.3	154	−14	4.1	152	152	153	0.0	+4.1	0.28	....	......	128	168	141	+0.39
1464....	B2	5.89	5 49	+19.7	157	− 2	2.2	177	180	151	+0.1	+2.2	0.34	....	......	90	94	91	+0.69
1504....	B8	5.17	5 58	+19.7	158	0	2.8	172	185	150	+0.6	+2.7	0.44	....	......	99	110	103	+0.23
1396....	B3	4.87	5 36	+16.5	159	− 6	3.1	155	173	154	+1.0	+2.9	0.40	+27.7	+18.0	108	129	115	+0.17
1048....	B8	5.50	4 23	+ 1.2	161	−30	3.5	141	117	157	−1.4	+3.2	0.48	....	......	124	158	135	+1.15
1448....	B9	6.61	5 45	+14.4	161	− 6	2.8	172	178	157	+0.3	+2.8	0.38	....	......	116	141	124	+2.08
1455....	B9	5.57	5 47	+14.1	161	− 5	1.7	230	179	157	−1.3	+1.1	0.38	....	......	72	64	69	−0.24
1084....	B5	5.32	4 32	+ 0.8	162	−28	1.8	220	119	158	−1.8	−0.3	0.45	+18.3W	+18.5	51:	29:	44:	−1.46:
1438....	B9	4.92	5 44	+12.6	162	− 6	2.9	207	178	158	−1.4	+2.5	0.44	+16.8	+18.5	110	133	118	+0.28

TABLE XXXIX—*Continued*

1525....	B3	4.40	6	2	+14.8	162	− 2	3.7	166	188	155	+1.4	+ 3.4	0.20	....	....	121	153	132	0.00
1548....	B3	4.35	6	6	+14.2	164	− 1	3.5	165	191	156	+1.5	+ 3.2	0.38	....	....	121	152	131	−0.06
1567....	B2	5.81	6	9	+13.9	164	− 1	4.1	74	193	155	+3.6	− 2.0	0.66	....	....	44::	28::	39::	−1.23::
1303....	B2	1.70	5	20	+ 6.3	165	−15	2.0	200	158	162	−1.3	+ 1.5	0.16	+13.7:	+19.0	85	90	87	−3.60
1572....	B9	5.36	6	10	+12.6	165	− 1	1.7	135	193	156	+1.4	+ 0.9	0.36	+ 8.3W	+18.3	68	57	64	−0.61
1331....	B3	4.32	5	25	+ 5.9	166	−14	3.8	162	162	163	0.0	+ 3.8	0.36	....	....	141	187	156	+0.28
1123....	B5	4.18	4	41	− 3.4	168	−28	1.8	112	110	162	−0.1	+ 1.8	0.22	....	....	92	104	96	−0.91
1302....	B3	4.73	5	20	+ 1.8	168	−17	2.1	209	154	166	−1.7	+ 1.2	0.62	....	....	83:	83:	83:	−0.67:
1343....	B2	5.30	5	28	− 1.7	174	−17	2.4	182	134	170	−1.8	+ 1.6	0.74	....	....	90:	89:	90:	+0.07:
1262....	B5	3.68	5	13	− 7.0	176	−23	1.6	259	80	169	0.0	− 1.6	0.22	+13.7:	+19.6	57n	57n	57n	−2.54
1376....	B2	5.62	5	32	− 6.1	178	−18	2.0	192	80	172	−1.9	− 0.7	0.65	....	....	71:	60:	67:	−0.25:
1382....	B1	5.75	5	33	− 6.0	178	−18	2.4	272	80	174	+0.5	− 2.4	1.06	....	....	93::	65::	84::	+0.37::
1666....	B3	5.02	6	29	− 1.1	180	− 3	4.7	226	229	166	+0.2	+ 4.7	0.66	....	....	158:	200:	172:	+1.20:
1239....	B8	4.54	5	8	−12.0	181	−26	3.2	108	55	168	−2.6	+ 1.9	0.39	....	....	95:	105:	98:	−0.50:
1625....	B5	6.88	6	22	− 4.3	181	− 6	2.0	84	252	168	+0.4	− 2.0	0.57	....	....	71::	40::	61::	+0.81::
1242....	B8	4.46	5	9	−13.1	182	−26	2.0	246	52	169	+0.5	− 1.9	0.45	....	....	73::	40::	62::	−1.58::
1639....	B3p	4.73	6	24	− 7.0	184	− 7	3.7	278	279	169	+0.1	+ 3.7	0.39	+16.3	+19.6	143:	167:	151:	+0.62:
1640....	B3	5.22												0.84						+1.11:
1603....	B2	5.49	6	17	−11.7	188	−11	2.7	251	319	170	+2.5	+ 1.0	0.82	....	....	79:	78:	79:	−0.02
1831....	B3	5.28	7	2	−11.1	192	0	2.2	236	274	161	+1.4	+ 1.7	0.52	....	....	89	97	92	+0.10
1754....	B5	5.29	6	44	−15.0	194	− 6	1.6	195	290	164	+1.6	− 0.1	0.80	....	....	65:	47:	59:	−0.86:
1792....	B3	5.26	6	52	−22.8	202	− 8	2.7	306	308	159	+0.1	+ 2.7	1.00	....	....	115	144	125	+0.74
1802....	B3	5.66	6	55	−25.3	203	− 8	2.8	321	311	157	−0.5	+ 2.7	0.58	....	....	113	138	121	+1.08
1807....	B3	5.80	6	57	−25.1	204	− 8	3.6	318	310	156	−0.5	+ 3.6	0.78	....	....	129	167	142	+1.56
1838....	B3	5.75	7	3	−23.7	204	− 6	2.3	310	306	157	−0.2	+ 2.3	0.96	....	....	103	118	108	+0.92
1847....	B3	5.76	7	6	−25.1	205	− 6	2.3	280	307	156	+1.0	+ 2.0	0.59	....	....	93	100	95	+0.65
1958....	B8	5.69	7	23	−22.7	206	− 2	2.2	43	298	153	−2.1	− 0.6	1.14	....	....	50:	28:	43:	−1.14:
1517....	B	5.64	6	1	−32.2	206	−22	13.1	359	353	156	−1.3	+13.0	1.66	....	....	300:*	400:*	333:	+3.25:
1401....	B5	2.75	5	36	−34.1	207	−28	2.7	172	7	154	−0.7	− 2.6	0.24	....	....	excl.	....	....	....
1467....	B5	4.89	5	49	−33.8	207	−25	3.6	2	0	155	−0.1	+ 3.6	0.74	+20.7	+18.1	125	160	137	+0.57
1642....	B3	5.80	6	25	−32.3	208	−17	2.2	321	339	155	+0.7	+ 2.1	0.70	....	....	94	100	96	+0.71
1641....	B5	4.48	6	24	−32.5	209	−18	3.7	311	339	155	+1.7	+ 3.3	0.44	+20.7(1)	+18.1	119	150	129	+0.03
2011....	B8	4.50	7	35	−26.6	210	− 1	3.4	341	300	148	−2.2	+ 2.6	0.61	+18.7	+17.0	96	103	98	−0.54
1961....	B9	5.52	7	24	−29.0	210	− 5	2.7	304	307	149	+0.1	+ 2.7	0.54	....	....	98	108	101	+0.54
2012....	B3	4.62	7	35	−26.6	210	− 1	3.6	307	300	148	−0.4	+ 3.6	0.60	....	....	115	137	122	+0.05
1605....	B2	5.60	6	17	−34.1	210	−19	3.3	358	344	153	−0.8	+ 3.2	0.74	....	....	112	137	120	+1.00
1882....	B5	5.31	7	11	−30.5	211	− 8	3.2	300	314	151	+0.8	+ 3.1	0.85	....	....	107	127	114	+0.60
1994....	B8	4.55	7	31	−28.1	211	− 3	7.1	255	303	149	+5.3	+ 4.8	0.60	....	....	excl.	....	....	....
1805....	B5	5.07	6	55	−34.0	213	−12	3.7	327	325	150	−0.1	+ 3.7	0.66	....	....	118	145	127	+0.59
1967....	B3	5.80	7	25	−31.2	213	− 5	2.8	278	310	148	+1.5	+ 2.4	0.68	....	....	92	95	93	+0.64
1955....	B	5.98	7	23	−33.9	215	− 7	4.1	270	313	146	+2.8	+ 3.0	0.76	....	....	102	113	106	+1.11
2004....	B8	4.62	7	34	−34.7	216	− 6	4.2	302	310	144	+0.6	+ 4.2	0.71	....	....	124	149	132	+0.22

*By extrapolation of the value for $\frac{\pi}{v}$, guiding ourselves by the way in which $\frac{\pi}{\mu}$ changes in *Gron. Publ.* No. 8, p. 31.

TABLE XXXIX—*Continued*

Boss No.	Sp.	Harv. Mag.	1900		Gal. Long.	Gal. Lat.	Correction (13) Applied		Vert. 17^h48^m, $+9°$		100 τ	100 ν	100 r	$\rho-4.3$	ρ comp.	Unit 0″0001			
			α	δ			100 μ	ρ	ρ comp.	λ						$\pi_{2.5}$	$\pi_{0.0}$	Adopted π	Adopted M
c) LAT. −30° TO +30°; 100 μ ≦ 1″6																			
1475....	B2	4.90	5 52	+25.9	151	+ 2	0.4	194	182	145	−0.1	+0.4	0.40	....	....	50	36	45	−1.83
1313....	B3	5.31	5 21	+17.9	154	− 8	1.6	150	166	152	+0.4	+1.5	0.54	....	....	77	73	76	−0.29
1307....	B3	6.18	5 20	+16.6	155	− 9	0.9	207	165	152	−0.6	+0.7	0.37	....	....	63	50	59	+0.03
1578....	B5	6.26	6 11	+23.8	155	+ 5	1.3	108	190	146	+1.3	+0.2	0.36	+ 7.3W	+16.6	48	32	43	−0.57
1345....	B3	5.50	5 28	+18.5	156	− 7	1.2	121	169	152	+0.9	+0.8	0.40	....	....	65	52	61	−0.57
1336...}	B9	{6.07	5 26	+17.0	156	− 8	0.9	198	168	152	−0.4	+0.8	0.46	....	....	65	52	61	0.00
1337...}		{6.44	5 26	+17.0	156	− 8	0.9	320	168	152	−0.4	−0.8	0.80	....	....	46:	26:	39:	−0.60:
1507....	B2	4.71 c	5 58	+20.1	158	0	1.5	148	185	150	+0.9	+1.2	0.39	+16.7	+17.3	69	60	66	−1.19
1346....	B3	5.58	5 28	+14.2	159	− 9	0.6	189	168	156	−0.2	+0.6	0.43	....	....	63	49	58	−0.60
1147....	B3	3.78	4 46	+ 5.4	161	−23	0.7	214	130	160	−0.7	+0.1	0.28	+19.0 orb.	+18.8	59	40	53	−2.60
1357....	Oe5	3.66	5 30	+ 9.9	163	−11	1.1	175	168	160	−0.1	+1.1	0.27	....	....	74	69	72	−2.05
1353....	B	4.53	5 29	+ 9.4	164	−12	0.8	187	167	160	−0.3	+0.8	0.32	....	....	69	59	66	−1.37
1159....	B3	3.87	4 49	+ 2.3	164	−24	0.4	225	126	162	−0.4	−0.1	0.25	+13.7	+19.0	61	42	55	−2.43
1314....	B2	4.66	5 22	+ 3.0	168	−16	1.4	197	157	165	−0.9	+1.1	0.32	+ 7.7 orb.	+19.3	57n	57n	57n	−1.56
1312....	B9	(7.7)	5 21	+ 2.8	168	−16	0.2	297	156	165	−0.1	−0.2	0.40	....	....	51n	51n	51n	(+1.2)
1391....	B3	4.54	5 34	+ 4.1	168	−13	0.6	72	168	166	+0.6	−0.1	0.36	....	....	51n	51n	51n	−1.92
1289....	B3	4.99	5 18	+ 3.4	168	−17	0.7	180	153	164	−0.3	+0.6	0.36	....	....	51n	51n	51n	−1.47
1332....	B3	5.52	5 26	+ 3.2	169	−15	0.9	140	160	165	+0.3	+0.8	0.31	+17.3W	+19.3	57n	57n	57n	−0.70
1295....	B3	5.64	5 19	− 0.3	170	−18	1.5	341	151	167	+0.3	−1.5	1.02	+18.1W	+19.5	57n	57n	57n	−0.58
1284....	B3	4.65	5 17	− 0.5	170	−19	0.5	281	149	167	−0.4	−0.3	0.33	+23.7 est.	+19.5	51n	51n	51n	−1.81
1339....	B	2.48	5 27	− 0.4	171	−16	0.1	45	159	166	+0.1	0.0	0.14	+18.8 orb.	+19.4	51n	51n	51n	−3.98
1706....	Oe5	4.68	6 35	+10.0	171	+ 3	0.8	157	211	157	+0.6	+0.5	0.26	....	....	62	46	57	−1.54
1283....	B3	5.65	5 16	− 0.5	171	−19	1.2	306	148	167	−0.4	−1.1	0.39	....	....	57n	57n	57n	−0.57
1301....	B1	3.44	5 19	− 2.5	172	−19	0.8	50	130	168	+0.8	+0.1	0.28	+31.2 orb.	+19.6	57n	57n	57n	−2.78
1370....	B	1.75	5 31	− 1.3	173	−16	0.2	0	149	169	+0.1	−0.2	0.15	+20.1 est.	+19.6	51n	51n	51n	−4.71
1349....	B2	5.37	5 28	− 1.2	173	−17	0.3	180	147	169	−0.3	+0.2	0.64	S.B.	....	51n	51n	51n	−1.09
1399....	B3	5.00	5 36	− 1.2	174	−15	1.3	252	153	170	−1.3	−0.2	0.64	+21.8 orb.	+19.7	57n	57n	57n	−1.22
1192....	B8	4.81	4 57	− 7.3	174	−26	1.4	0	92	166	+1.4	0.0	0.32	....	....	67:	55:	63:	−1.19:
1398....	B	2.05	5 36	− 2.0	175	−15	0.8	114	138	171	+0.3	+0.7	0.16	+13.2	+19.8	57n	57n	57n	−4.17
1389....	B	3.78	5 34	− 2.7	175	−16	0.5	0	123	171	+0.4	−0.3	0.23	....	....	51n	51n	51n	−2.68
1363....	Oe5	5.36	5 30	− 5.5	177	−18	0.9	20	81	172	+0.8	+0.4	0.31	....	....	57n	57n	57n	−0.86
1364....	B2	4.65	5 30	− 4.9	177	−18	0.2	26	94	172	+0.2	+0.1	0.36	....	....	51n	51n	51n	−1.81
1250....	B8pc	0.34	5 10	− 8.3	177	−24	0.3	19	74	170	+0.2	+0.2	0.12	+18.3 orb.	+19.7	71:	64:	69:	−5.47:
1231....	B2	4.34	5 4	− 8.9	177	−26	0.5	143	73	169	−0.5	+0.2	0.28	....	....	71:	63:	68:	−1.50:
1223....	B8	5.67	5 4	− 8.8	177	−26	1.0	180	73	169	−1.0	−0.3	0.56	....	....	67:	58:	64:	−0.30:
1366....	Oe5	2.87	5 31	− 6.0	178	−18	0.3	90	80	172	−0.1	+0.3	0.26	+17.0 orb.	+19.8	51n	51n	51n	−3.59
1361....	B1	5.58	5 30	− 6.1	178	−19	0.8	7	81	172	+0.8	+0.2	0.64	....	....	57n	57n	57n	−0.64
1362....	B1	4.67	5 30	− 6.1	178	−19	1.0	16	81	172	+0.9	+0.4	0.54	+24.7	+19.8	57n	57n	57n	−1.55
1340....	B3	4.64	5 27	− 7.4	178	−20	0.9	159	70	172	−0.9	0.0	0.40	+12.7	+19.8	57n	57n	57n	−1.58
1523....	B3	5.37	6 2	− 4.2	179	−11	0.5	116	252	172	+0.3	−0.4	0.72	+11.8W	+19.8	69:	62:	67:	−0.50:
1454....	B3	5.32	5 47	− 7.5	181	−16	1.2	90	37	177	−1.0	+0.7	0.41	....	....	67::	68::	67::	−0.55::
1277....	B1	4.29	5 15	−13.3	182	−25	0.7	0	45	170	+0.5	+0.5	0.32	+16.7	+19.7	62:	60:	61:	−1.78:
1435....	B	2.20	5 43	− 9.7	182	−17	0.3	108	8	178	−0.3	−0.1	0.20	+16.7	+20.0	62::	65::	63::	−3.80:
1512....	B3	5.12	5 59	− 6.7	182	−13	1.0	241	297	174	+0.8	+0.6	0.71	....	....	66:	67:	66:	−0.78:
1634....	B3	4.98	6 23	− 4.7	183	− 6	1.8	350	261	168	−1.8	0.0	0.41	+23.7	+19.6	68:	57:	64:	−0.99:
1598....	B3	5.13	6 15	− 7.8	183	− 9	0.7	286	297	171	+0.1	+0.7	0.44	....	....	76:	73:	75:	−0.49:

TABLE XXXIX—*Continued*

1554....	B3	5.09	6 7	− 6.5	183	−11	1.1	236	278	172	+0.7	+0.8	0.60	....	....	76:	75:	76:	−0.51:
1686....	B9	5.48	6 32	− 5.1	184	− 4	0.8	157	259	167	+0.8	−0.2	0.74	....	....	66:	53:	62:	−0.56:
1297....	B3	5.17	5 19	−14.0	184	−24	0.8	0	37	170	+0.5	+0.6	0.52	....	....	66:	64:	65:	−0.77:
1503....	B8	4.97	5 57	−10.6	185	−15	1.0	5	347	175	−0.3	+1.0	0.48	....	....	80::	79::	80::	−0.51::
1812....	B3	4.89	6 58	− 4.1	186	+ 2	1.2	355	254	161	−1.2	−0.2	0.37	....	....	58:	38:	51:	−1.57:
1580....	B9	4.99	6 11	−13.7	189	−13	0.8	66	330	171	−0.8	−0.1	0.95	....	....	69:	64:	67:	−0.88:
1739....	B8	5.19	6 42	−14.3	193	− 6	1.5	42	292	165	−1.4	−0.5	0.50	+13.0W	+19.3	65:	47:	59:	−0.96:
1609....	B1	1.99	6 18	−17.9	194	−13	0.8	300	329	167	+0.4	+0.7	0.22	+29.4 est.	+19.5	74:	70:	73:	−3.69:
1594....	B3	5.31	6 14	−19.9	195	−15	1.7	287	336	166	+1.3	+1.1	1.12	....	....	81:	80:	81:	−0.15:
1819....	B5	4.07	6 59	−15.5	196	− 3	1.0	185	289	160	+1.0	−0.2	0.24	+24.2	+18.8	56:	36:	49:	−2.48:
1793....	B5	4.39	6 52	−16.9	196	− 5	1.5	356	294	162	−1.3	+0.7	0.36	+35.7	+19.0	70	61	67	−1.48
1597....	B5	5.66	6 15	−20.9	196	−15	1.5	318	336	165	+0.5	+1.4	1.08	....	....	86:	90:	87:	+0.36:
1781....	B1	4.66	6 49	−20.1	199	− 7	1.5	12	305	162	−1.4	+0.6	0.46	....	....	69	58	65	−1.28
1660....	B1	4.35	6 28	−23.3	200	−13	1.2	42	327	162	−1.2	+0.3	0.56	+25.7 est.	+19.0	64	50	59	−1.80
1924....	B8	4.87	7 18	−18.8	201	− 1	0.7	270	292	156	+0.3	+0.7	1.03	+12.7	+18.3	65	52	61	−1.20
1998....	B3	5.66	7 32	−19.5	203	+ 2	1.8	315	291	153	−0.7	+1.6	1.06	....	....	81	77	80	+0.18
1652....	B8	5.81	6 27	−27.7	204	−15	1.1	26	334	158	−0.9	+0.7	0.63	....	....	64	51	60	−0.30
1817....	B5pc	3.12	6 59	−23.7	204	− 7	0.6	288	308	157	+0.2	+0.6	0.32	+44.7 est.	+18.4	63	48	58	−3.06
2159....	B3	5.54	8 5	−16.0	204	+10	1.1	138	277	145	+0.7	−0.8	0.78	+28.4W	+16.4	38:	20:	32:	−1.93:
1899....	Oe	4.90	7 15	−24.4	205	− 4	1.4	270	302	154	+0.7	+1.2	0.44	....	....	74	66	71	−0.84
2158....	B3	4.34	8 5	−19.0	206	+ 9	1.5	254	281	145	+0.7	+1.3	0.40	....	....	67	56	63	−1.66
1954....	B2	5.48	7 23	−22.9	206	− 2	1.5	11	298	152	−1.4	+0.4	0.99	....	....	59	43	54	−0.86
1901....	Oe5	4.40	7 15	−24.8	206	− 4	1.6	330	304	154	−0.7	+1.4	0.50	....	....	78	73	76	−1.20
1872....	B5p	4.66	7 10	−26.2	206	− 6	1.6	334	307	154	−0.7	+1.4	0.35	....	....	78	73	76	−0.94
1858....	B5	5.86	7 8	−25.8	206	− 6	1.3	321	308	154	−0.3	+1.3	0.50	....	....	76	70	74	+0.21
1601....	B3	3.10	6 16	−30.0	206	−18	1.2	42	342	157	−1.0	+0.6	0.29	+19.7 est.	+18.4	63	48	58	−3.08
1877....	B3	3.83	7 11	−26.6	207	− 6	0.4	270	309	153	+.03	+0.3	0.51	+24.7 est.	+17.8	59	42	52	−2.59
2009....	B8	4.64	7 34	−25.1	208	− 1	1.4	270	298	149	+0.7	+1.2	0.62	....	....	68	58	65	−1.30
1804....	B1ac	1.63	6 55	−28.8	208	−10	0.7	8	318	155	−0.5	+0.4	0.22	+24.9	+18.1	61	45	56	−4.63
1736....	B	5.91	6 42	−30.8	208	−14	1.5	53	328	154	−1.5	+0.1	0.69	....	....	58:	40:	52:	−0.51:
1731....	B	5.16	6 41	−31.0	208	−14	2.3	347	328	154	−0.8	+2.2	0.66	....	....	94	101	96	+0.07
1669....	B3	5.70	6 29	−32.0	208	−16	0.9	18	336	154	−0.6	+0.7	0.70	....	....	66	53	62	−0.34
1532....	B5	5.93	6 3	−34.3	208	−22	0.9	333	353	154	+0.3	+0.8	0.72	....	....	67	55	63	−0.07
1490....	B3	4.36	5 54	−35.3	208	−24	1.1	338	357	154	+0.4	+1.0	0.38	+18.7	+18.0	70	60	67	−1.51
2061....	B2	4.59	7 44	−25.7	210	+ 1	1.2	275	295	148	+0.4	+1.1	0.56	....	....	66	54	62	−1.45
1934....	B5pc	2.43	7 20	−29.1	210	− 5	1.5	323	308	150	−0.4	+1.5	0.26	+36.0	+17.3	74	69	72	−3.28
1761....	B2	3.78	6 46	−32.4	210	−13	1.3	312	325	153	+0.3	+1.3	0.38	+ 3.7:*	+17.8	75	68	73	−1.90
1600....	B8	5.83	6 16	−34.4	210	−20	0.7	63	344	153	−0.7	+0.1	0.74	....	....	56	38	50	−0.68
1870....	B	6.53	7 10	−30.9	211	− 8	1.3	293	315	150	+0.5	+1.2	0.67	....	....	69	60	66	+0.63
1946....	B	6.20	7 22	−31.5	213	− 6	1.3	4	311	148	−1.0	+0.8	0.68	....	....	60	47	56	−0.06
1932....	B	5.47	7 20	−32.0	213	− 7	1.6	346	314	148	−0.8	+1.4	0.59	....	....	70	63	68	−0.37
1929....	B	5.43	7 19	−31.7	213	− 7	0.5	12	314	148	−0.4	+0.3	0.66	....	....	52	36	47	−1.21
1966....	B	6.51	7 25	−31.6	214	− 6	0.3	252	311	148	+0.3	+0.2	0.70	....	....	51	34	45	−0.22
1891....	B3	5.01	7 13	−36.4	215	−10	0.8	220	320	146	+0.8	−0.1	0.70	....	....	44:	28:	39:	−2.03:

d) SUPPLEMENTARY LIST

857....	B8	5.09	3 39	− 1.5	156	−40	1.7	123	104	146	−0.6	+1.6	0.46	....	....	73	66	71	−0.65
926....	B5	5.25	3 56	− 1.8	160	−37	2.4	100	106	150	+0.2	+2.4	0.36	....	....	93	99	95	+0.14
893....	B8	5.49	3 48	− 5.7	163	−41	1.2	228	98	150	−0.9	−0.8	0.38	....	....	43:	24:	37:	−1.67:
1079....	B2	4.12	4 31	− 3.6	167	−31	0.2	180	105	160	−0.2	+0.1	0.26	+ 9.7 est.	+18.8	59:	40	53:	−2.26:
1123....	B5	4.18	4 41	− 3.4	168	−28	2.2	117	110	162	−0.3	+2.2	0.22	....	....	102	123	109	−0.63
1010....	B8	5.72	4 16	− 7.8	169	−36	2.4	86	95	158	+0.4	+2.4	0.67	....	....	108	128	115	+1.02
1052....	B3	5.50	4 24	−13.3	176	−36	0.7	98	81	158	−0.2	+0.7	0.92	....	....	64	51	60	−0.61
956....	B3	5.45	4 5	−16.6	178	−42	1.3	48	76	153	+0.6	+1.1	1.00	+ 9.0W	+17.8	71	62	68	−0.39

* Mean of two components of bright Hγ excluded.

agreement with an error-curve extends, with some rough approximation, over the whole curve, though there are signs indicating some excess of extreme luminosities in the case of the B8–B9 and A stars.

29. NOTATION

The notation used is the same as in *Mount Wilson Contribution* No. 82, except that t has been substituted for v (Section 11). Only what is necessary for the understanding of Table XXXIX is repeated here.

v, τ	components of the angular proper motion μ along the great circle toward the antivertex, and at right angles thereto, respectively.	
$100\,r$	100 times probable error in the proper motion of any co-ordinate (Section 10).	
$\rho-4.3$	the observed radial velocity corrected by the constant amount -4.3 km, in accordance with *Mount Wilson Contribution* No. 82, p. 28.	
W	observed at Mount Wilson.	
:	observation uncertain.	
orb.	spectroscopic binary, radial velocity of system obtained from determination of orbit.	
est.	spectroscopic binary, radial velocity of system estimated.	
(1)	only one observation.	
$\pi_{2.5}$	parallax on the supposition that $r_u=\pm 2.5$	See (47) and Section 12, Remark 2.
$\pi_{0.0}$	" " " " $r_u=0.0$	
π adopted	" " " " $r_u=\pm 1.67$	
n	when the parallax is marked with n the star has been assumed to belong to the Nebula-group.	

GRONINGEN
January 1917

END OF VOL. VII

INDEX TO VOLUME VII

Nos. 124 to 147

AUTHORS

PAGE

ADAMS, WALTER S., AND ALFRED H. JOY—
  The Luminosities and Parallaxes of Five Hundred Stars . . . 299

ADAMS, WALTER S., AND HARLOW SHAPLEY—
  Note on the Cepheid Variable SU Cassiopeiae 365

ADAMS, WALTER S., AND GUSTAF STRÖMBERG—
  Radial Velocity and Absolute Magnitude: Comments on Professor Perrine's Article 371
  The Relationship of Stellar Motions to Absolute Magnitude . . 95

ANDERSON, JOHN A.—
  A Method of Investigating the Stark Effect for Metals, with Results for Chromium 153

BABCOCK, HAROLD D. *See* St. John, Charles E.

CARTER, EDNA. *See* King, Arthur S.

ELLERMAN, FERDINAND—
  Solar Hydrogen "Bombs" 295

HALE, GEORGE E.—
  Baxandall's Explanation of an "Abnormal" Solar Spectrum . . 327

JOY, ALFRED H. *See* Adams, Walter S.

KAPTEYN, J. C.—
  On the Parallaxes and the Motion of the Brighter Galactic Helium Stars between Galactic Longitudes 150° and 216° . . . 375

KING, ARTHUR S.—
  A Study with the Electric Furnace of the Anomalous Dispersion of Metallic Vapors 79

KING, ARTHUR S., AND EDNA CARTER—
  Preliminary Observations of the Spectra of Calcium and Iron When Produced by Cathodo-Luminescence 21

PEASE, FRANCIS G.—
  Hind's Variable Nebula N.G.C. 1555 47
  Photographs of Nebulae with the 60-Inch Reflector 1911–1916 . 109

PAGE

Pease, Francis G., and Harlow Shapley—
  On the Distribution of Stars in Twelve Globular Clusters . . . 59

St. John, Charles E.—
  The Principle of Generalized Relativity and the Displacement of Fraunhofer Lines toward the Red 261

St. John, Charles E., and Harold D. Babcock—
  The Elimination of Pole-Effect from the Source for Secondary Standards of Wave-Length 231

Seares, Frederick H.—
  A Determination of the Galactic Condensation from Certain Zones of the *Astrographic Catalogue* 167
  The Spiral of Obscuration 279

Shapley, Harlow—
  Studies Based on the Colors and Magnitudes in Stellar Clusters.
    Fourth Paper: The Galactic Cluster Messier 11 29
    Fifth Paper: Color-Indices of Stars in the Galactic Clouds . 141
  The Variations in Spectral Type of Twenty Cepheid Variables . 1

Shapley, Harlow, and J. van der Bilt—
  Notes on the Color-Curve and Light-Elements of W Ursae Majoris 285

Shapley, Harlow. *See also* Adams, Walter S.; Pease, Francis G.

Shapley, Martha Betz—
  The Color-Curve of XZ Cygni 51

Strömberg, Gustaf—
  A Determination of the Solar Motion and the Stream-Motion from Radial Velocities and Absolute Magnitudes of Stars of Late Spectral Types 333

Strömberg, Gustaf. *See also* Adams, Walter S.

van der Bilt, J. *See* Shapley, Harlow.

van Maanen, Adriaan—
  The Photographic Determination of Stellar Parallaxes with the 60-Inch Reflector. Second Series 189

SUBJECTS

Absolute magnitude and radial velocity, 371
Absolute magnitude, relation to stellar motions, 95
Anomalous dispersion of metallic vapors, studied with the electric furnace, 79
Bombs, solar hydrogen, 295
Calcium, observations of spectra produced by cathodo-luminescence, 21
Cepheid variable SU Cassiopeiae, 365
Cepheid variables, variations in spectral type, 1
Chromium, Stark effect, 153
Clusters, galactic, Messier 11, 29
———, globular, distribution of stars in, 59
———, studies based on colors and magnitudes in, 29, 141
Color-curve and light-elements of W Ursae Majoris, 285
Color-curve of XZ Cygni, 51
Color-indices of stars in the galactic clouds, 141
Colors and magnitudes in stellar clusters, 29, 141
Electric furnace, anomalous dispersion of metallic vapors, 79
Furnace. *See* Electric furnace
Galactic condensation, determination from zones of *Astrographic Catalogue*, 167
Globular clusters. *See* Clusters
Hind's variable nebula N.G.C. 1555, 47
Hydrogen bombs, 295
Iron spectra, observations when produced by cathodo-luminescence, 21
Light-elements and color-curve of W Ursae Majoris, 285
Luminosities and parallaxes of 500 stars, 299
Magnitudes in stellar clusters, 29, 141
Messier 11, 29
Metallic vapors, anomalous dispersion, 79
Nebulae, Hind's variable N.G.C. 1555, 47
———, photographed with 60-inch reflector, 109
Parallax, photographic determination with the 60-inch reflector, 189
Parallaxes and motion of brighter galactic helium stars, 375
Parallaxes of 500 stars, 299
Pole-effect, elimination from source for secondary standards, 231
Radial velocity and absolute magnitude, 371
Relativity, generalized, and displacement of Fraunhofer lines toward red, 261
Solar motion and stream-motion, determined from radial velocities and absolute magnitudes of stars of late spectral types, 333
Solar spectrum. *See* Spectrum
Spectra of calcium and iron produced by cathodo-luminescence, 21

Spectral type of twenty Cepheid variables, variations in, 1
Spectrum, abnormal solar, Baxandall's explanation, 327
Spiral of obscuration, 279
Stark effect for metals, method of investigating, 153
Stars, brighter galactic helium, parallaxes and motion, 375
———, distribution in twelve globular clusters, 59
———, in the galactic clouds, color-indices, 141
———, luminosities and parallaxes, 299
Stellar clusters. *See* Clusters
Stellar motions and absolute magnitude, 95
Stellar parallax. *See* Parallax
Stream-motion, determined from radial velocities and absolute magnitudes of stars of late spectral types, 333
Vapors, metallic, anomalous dispersion, 79
Variable nebula N.G.C. 1555, 47
Variable stars, Cepheid SU Cassiopeiae, 365
———, variations in spectral type of twenty Cepheids, 1
———, W Ursae Majoris, color-curve and light-elements, 285
———, XZ Cygni, color-curve, 51
Wave-length, elimination of pole-effect from the source for secondary standards, 231

522.19 C28 V07

a39001 006937190b

522 19 C28 V07
MOUNT WILSON OBSERVATORY CONTRIBUTION

INSERT BOOK
MASTER CARD
FACE UP IN
FRONT SLOT
OF S.R. PUNCH

MASTER CARD

UNIVERSITY OF ARIZON
LIBRARY

GLOBE 901149-0